University of Alberta Library
0 1620 2666917 4

Ex libris
universitatis
albertaensis

QUAECUMQUE VERA

BRUCE PEEL SPECIAL COLLECTIONS LIBRARY

UNIVERSITY OF ALBERTA

REQUEST FOR DUPLICATION

I wish a photocopy of the thesis by Andrew J. Willis

entitled Sedimentology and stratigraphic framework of the . . .

The copy is for the sole purpose of private scholarly or scientific study and research. I will not reproduce, sell or distribute the copy I request, and I will not copy any substantial part of it in my own work without permission of the copyright owner. I understand that the Library performs the service of copying at my request, and I assume all copyright responsibility for the item requested.

Pages copied _____

Date _____ Signature _____

Name and address _____

Pages copied _____

Date _____ Signature _____

Name and address _____

Pages copied _____

Date _____ Signature _____

Name and address _____

Pages copied _____

Date _____ Signature _____

UNIVERSITY OF ALBERTA

RELEASE FORM

Name of Author: ANDREW JOHN WILLIS

Title of Thesis: SEDIMENTOLOGY AND STRATIGRAPHIC FRAMEWORK OF THE MIDDLE TRIASSIC HALFWAY FORMATION, WEMBLEY OILFIELD, ALBERTA.

Degree: MASTER OF SCIENCE.

Year This Degree Granted: 1992.

Permission is hereby granted to the University of Alberta Library to reproduce single copies of this thesis and to lend or sell such copies for private, scholarly or scientific research purposes only.

The author reserves all other publication and other rights in association with the copyright in the thesis, and except as hereinbefore provided neither the thesis nor any substantial portion thereof may be printed or otherwise reproduced in any material form whatever without the author's prior written permission.

Date: July 2nd, 1992.

UNIVERSITY OF ALBERTA

SEDIMENTOLOGY AND STRATIGRAPHIC FRAMEWORK OF THE MIDDLE TRIASSIC HALFWAY FORMATION, WEMBLEY OILFIELD, ALBERTA.

By

ANDREW JOHN WILLIS

©

A thesis submitted to the Faculty of Graduate Studies and Research in partial fulfillment of the requirements for the degree of Master of Science.

Department of Geology

Edmonton, Alberta

Fall 1992

UNIVERSITY OF ALBERTA

FACULTY OF GRADUATE STUDIES AND RESEARCH

The undersigned certify that they have read, and recommend to the Faculty of Graduate Studies and Research for acceptance, a thesis entitled Sedimentology and Stratigraphic Framework of the Middle Triassic Halfway Formation, Wembley Oilfield, Alberta submitted by Andrew John Willis in partial fulfillment of the requirements for the degree of Master of Science.

Date: May 10/92

ABSTRACT.

148 cores cut from the Middle Triassic Halfway Formation have been described from the Wembley oilfield of west-central Alberta and supplemented with a further 156 well logs. Five parasequences are identified in the Middle Triassic interval, each representing southwesterly progradation of a barrier island shoreface.

Facies patterns within each parasequence indicate that the Middle-Upper Triassic Doig, Halfway and lower Charlie Lake Formations are time-equivalent parts of the same depositional system. The shales of the Doig Formation represent deposition in the offshore shelf environment and the coarser-grained Halfway Formation the laterally equivalent barrier island shoreface, while the lower part of the Charlie Lake Formation consists of associated backbarrier and coastal plain deposits. The Wembley oil field is located in barrier island shoreface and tidal inlet sandstones of parasequence 4. The up-dip margin of the field is defined by the depositional pinchout of this parasequence, not post-Halfway erosion.

Halfway barrier island shorelines were deposited in a mesotidal regime comparable to the Holocene shoreline of South Carolina. The up-dip pinchout of active tidal inlet and ebb-delta sandstones against fine grained abandoned inlet fill creates two potential stratigraphic hydrocarbon traps in Halfway mesotidal inlet channel fills. This facies heterogeneity in the Halfway Formation sandstone in the Wembley oilfield makes it unlikely that any field-scale water-flooding program would be successful in enhancing recovery. Infill drilling is recommended.

The proportion of the Halfway Formation barrier island lithosome consisting of tidal inlet sediments (90%) is much greater than that found in Holocene barrier island systems (35-40%). The explanation for this discrepancy is the geologically short time period over which tidal inlet channels have had the opportunity to rework Holocene coastlines. This restricted temporal evolution of Holocene coastlines severely limits their usefulness as models for predicting the three-dimensional facies architecture of ancient coastal lithosomes.

ACKNOWLEDGEMENTS

Financial support for this study was generously provided by Total Petroleum Canada Ltd., PanCanadian Petroleum Ltd., Union Pacific Resources and an N.S.E.R.C. award to T. F. Moslow.

I would also like to acknowledge personal financial support during the completion of this thesis from Amoco Canada Petroleum Co. Ltd in the form of an Amoco Canada Graduate Fellowship in Geology; The American Association of Petroleum Geologists in the form of a Grant-in-Aid; The Society of Professional Well Log Analysts for a Graduate Scholarship; and the Department of Geology, University of Alberta, for a Graduate Research Assistantship.

Esso Resources Canada Ltd. kindly made available biostratigraphic data from the Wembley field, and Tony Jenkins of Associated Biostratigraphic Consultants provided much useful discussion. Doug Glass of Unocal Canada Exploration Ltd. provided ongoing database and mapping support.

Finally, to Dr. Thomas Moslow for his supervision of this study and for the warm welcome and continuing friendship and support he and Maxine Moslow have provided during my stay in Canada.

TABLE OF CONTENTS.

		Page
1.0.0	**INTRODUCTION**	1
1.1.0	Economic Significance	1
1.2.0	Previous Work	1
1.3.0	Unresolved Problems	10
1.4.0	Objectives	13
1.5.0	Study Area	13
1.6.0	Methods	14
1.6.1.	Core Description	14
1.6.2	Process Sedimentology	17
1.6.3	Genetic Units	17
1.6.4	Sampling and Photography	18
2.0.0	**REGIONAL STRATIGRAPHY**	19
2.1.0	Schooler Creek Group	19
2.1.1	Halfway Formation	22
2.1.2	Charlie Lake Formation	25
2.2.0	Daiber Group	27
2.2.1	Montney Formation	27
2.2.2	Doig Formation	29
2.3.0	Discussion of Regional Stratigraphy	29
3.0.0	**DEPOSITIONAL SETTING**	31
3.1.0	Sediment Source	33
3.2.0	Palaeoclimate	33
4.0.0	**SEDIMENTARY FACIES**	36
4.1.0	Facies A. Bioclastic Sandstone	36
4.2.0	Facies B. Laminated Black Silty Shale	40
4.3.0	Facies C. Interlaminated Green Shale and Siltstone	46
4.4.0	Facies D. Oscillation Ripple Cross-Laminated Sandstone	51
4.5.0	Facies E. Cross-Bedded Sandstone	54
4.6.0	Facies F. Plane Laminated Chert Sandstone	57
4.7.0	Facies G. Laminated Anhydrite and Dolomite Mudstone	57
4.7.1	Facies G1. Crypt-algal Laminites	59

4.7.2 Facies G2. Dolomite Mudstone..... 63
4.8.0 Facies H. Red Beds and Nodular Anhydrite..... 67
4.8.1 Red Beds..... 67
4.8.2 Anhydrites..... 69
4.9.0 Facies I. Sandy Dolomite Coquina..... 74
4.10.0 Facies J. Cross-Bedded Sandstone with Mudstone Laminae..... 80
4.11.0 Facies K. Interlaminated Sandstone and Siltstone..... 83
4.12.0 Facies L.Cross-Bedded and Plane Laminated Sandstone..... 86
4.13.0 Facies M. Plane Laminated Granular Sandstone..... 97

5.0.0 **FACIES ASSOCIATIONS**..... 108
5.1.0 Facies Association 1: Regressive Shoreface..... 109
5.2.0 Facies Association 2: Tidal Inlet Channel Fill..... 116
5.2.1 Tidal Inlet Sequence..... 118
5.2.2 Variations in Modern Tidal Inlet Fill Sequences..... 121
5.2.3 MicrotidalWave-Dominated Coastlines..... 121
5.2.4 Mesotidal Mixed-Energy Coastlines..... 125
5.2.5 Halfway Tidal Inlet Sequences..... 128
5.3.0 Lateral Facies Relationships..... 132

6.0.0 **CORE-TO-WELL LOG CORRELATION**..... 141
6.1.0 Method..... 141
6.2.0 Facies Association 1: Regressive Shoreface..... 142
6.3.0 Facies Association 2: Tidal Inlet Channel Fill..... 148
6.3.1 Single Tidal Inlet Cycle..... 149
6.3.2 Tidal Inlet Mouth: Welded Ebb-Tidal Delta..... 151
6.3.3 Stacked Tidal Inlet Cycles..... 151
6.4.0 Facies M Washover Sandstones..... 153
6.5.0 Summary..... 153

7.0.0 **LOCAL STRATIGRAPHIC FRAMEWORK**..... 156
7.1.0 Discussion..... 156
7.2.0 Origin of the Erosion Surface..... 159
7.3.0 Shoreface Retreat..... 159
7.4.0 Relationship Between Ravinement and Facies M Distribution..... 165
7.5.0 Preservation of Transgressive Deposits..... 169

7.6.0 Summary of Local Stratigraphy 171

8.0.0 **SEQUENCE STRATIGRAPHY** 173
8.1.0 Discussion 173
8.2.0 Parasequence Stacking in the Study Area 174
8.3.0 Comparison of Middle Triassic Sequence and Lithostratigraphy 175
8.4.0 Middle Triassic Sequence Stratigraphic Model 178

9.0.0 **HALFWAY PARASEQUENCE GEOMETRY** 181
9.1.0 Structure of Bounding Flooding Surfaces 181
9.2.0 Parasequence Isopachs 181
9.3.0 Parasequence Controls on Hydrocarbon Distribution 184
9.4.0 Parasequence Continuity along Strike 186

10.0.0 **DISCUSSION** 189
10.1.0 Halfway Tidal Inlet Reservoir Model 189
10.2.0 Shortcomings of Holocene Analogues 190
10.3.0 Halfway Reservoir Heterogeneity 191
10.4.0 Stratigraphy 192
10.5.0 Implications for Halfway-Doig Exploration 194

11.0.0 **CONCLUSIONS** 196

12.0.0 **REFERENCES CITED** 199

APPENDIX A (Core Descriptions) 221

APPENDIX B (Stratigraphic Database) 402

LIST OF TABLES.

		Page
Table 1.	Oil reserves in Middle Triassic reservoirs of west-central Alberta.....	4
Table 2.	Summary of Halfway Formation sedimentary facies.....	37
Table 3.	Halfway Formation facies associations.....	108
Table 4.	Location of wells containing Halfway facies association 1.....	133
Table 5.	Radioactive mineral content of shales.....	145
Table 6.	Location of wells containing two Halfway shoreface facies associations.....	160

LIST OF FIGURES.

		Page
Figure 1.	Location map of the study area	2
Figure 2.	Subsurface Triassic stratigraphy of the Western Canada Sedimentary Basin (after Podruski et al., 1988)	3
Figure 3.	Triassic Stratigraphy of the Spirit River Area (after Aukes and Webb, 1986)	7
Figure 4.	Schematic stratigraphic cross-section through the Triassic strata of west-central Alberta (after Campbell et al., 1989)	8
Figure 5.	Lithostratigraphic correlation of Triassic formations between surface exposures and the adjacent subsurface of the Peace River Plains (after Gibson and Edwards, 1990)	12
Figure 6.	Location map of wells in the study area which penetrate the Halfway Formation, showing those cores examined during this study	15
Figure 7.	Isopach map of Triassic strata in the Western Canada Sedimentary Basin (after Gibson and Barclay, 1989)	20
Figure 8.	Table of outcrop and subsurface Triassic formations in the Western Canada Sedimentary Basin (after Podruski et al., 1988)	21
Figure 9.	Schematic cross-section illustrating stratigraphic relationships and depositional environments of Triassic formations between the Foothills outcrop belt and the subsurface plains (after Gibson and Edwards, 1990)	21
Figure 10.	Table of Triassic formations showing the faunal zones used in outcrop-to-subsurface correlations (after Armitage, 1962)	23

Figure 11. Type section of the Halfway Formation in the Southern Production well B-14-I (1-12-84-23-W6) (after Hunt and Ratcliffe, 1959)..... 24

Figure 12. The currently accepted lithostratigraphic definition of the Halfway Formation showing (a) the origin of sharp-based Halfway sandstones as tidal inlet channel fills, and (b) the gradational relationship of the Halfway sandstone interval with the underlying shales in regressive shoreface facies successions (after Campbell and Horne, 1986)..... 26

Figure 13. Type section of the Montney and Doig Formations in the Texaco N.F.A. Buick Creek No. 7 well (6-26-87-21-W6) (after Armitage, 1962)..... 28

Figure 14. Location map of late Triassic and earliest Jurassic arc-related igneous rocks in the North American Cordillera (after Mortimer, 1986)..... 32

Figure 15. Schematic plate tectonic reconstructions of the western margin of North America from the Carboniferous to Middle Jurassic, based on data from the Yukon (after Tempelmann-Kluit, 1979)..... 34

Figure 16. Schematic diagram illustrating the possible consequences of compaction upon a normal algal mat accumulation, and its possible fossil equivalent (after Park, 1976)..... 62

Figure 17. Schematic block diagram showing the distribution of sediment and evaporite in the Abu Dhabi Sabkha (after Schreiber, 1986)..... 71

Figure 18. An example of a complete sabkha cycle in the Cretaceous Lower Purbeck Beds of the Warlingham Borehole, southern England (after Schreiber, 1986)..... 73

Figure 19. Schematic diagram showing the morphology of ebb-tidal deltas, based on examples from the tidal inlets of the West Frisian Islands in the Netherlands (after Sha, 1990)..... 91

Figure 20. Hypothetical vertical sedimentary sequence of ebb-tidal delta sediments based on observations of surface bedforms and processes (after Hayes, 1980) 92

Figure 21. Shore-parallel vibracore cross-section through the ebb-tidal delta of North Edisto Inlet, South Carolina (after Imperato et al., 1988) 94

Figure 22. Vibracore cross-section through an abandoned marginal flood channel on the ebb-tidal delta of North Edisto Inlet, South Carolina (after Imperato et al., 1988) 96

Figure 23. Schematic diagram illustrating the sedimentary structures associated with washover fans (after Schwartz, 1982) 104

Figure 24. Example of a thick washover sandstone above lagoonal mudstones from the Pleistocene Port Durnford Formation of Zululand (after Hobday and Jackson, 1979) 107

Figure 25. An example of the upward-coarsening Halfway vertical facies association 1 (regressive shoreface) cored in well 5-24-74-9-W6 110

Figure 26. Shoreface sub-environments, processes and facies (after Elliott, 1986) 115

Figure 27. An example of Halfway vertical facies association 2 (tidal inlet channel fill) cored in well 6-31-72-7-W6 117

Figure 28. Tidal inlet channel sequence cored at Fire Island Inlet, New York (after Kumar and Sanders, 1974) 121

Figure 29. Average wave heights and tidal ranges along the Georgia Embayment of the southeastern United States (after Moslow and Tye, 1985) 122

Figure 30. Wave- and tide-dominated barrier island/ tidal inlet geomorphological models for the Georgia Embayment of the southeastern United States (after Moslow and Tye, 1985)..... 123

Figure 31 Geomorphological evolution of wave-dominated inlet-related sand-bodies (after Moslow and Tye, 1985)..... 124

Figure 32 Wave-dominated tidal inlet sequence deposited by the lateral migration of Captain Sam's inlet, South Carolina (after Moslow and Tye, 1985)..... 124

Figure 33. Four stages of the tidal inlet migration and abandonment mechanism in a mesotidal setting, based on coastal charts and aerial photos of Price and Capers Inlets, South Carolina (after Tye, 1984)..... 126

Figure 34. Tidal inlet / ebb-delta sequence cored at Stono Inlet, South Carolina. The vertical sequence represents preservation of the seaward-most inlet deposits in a tide-dominated setting (after Moslow and Tye, 1985)..... 127

Figure 35. Mud-rich, fining-upward sequence deposited by the channel migration and abandonment of Capers Inlet, South Carolina (after Moslow and Tye, 1985)..... 129

Figure 36. Schematic block diagram illustrating the barrier island depositional model and corresponding facies envisioned for the Halfway Formation..... 131

Figure 37. Dip-oriented vibracore cross-section through the abandoned channel of Price Inlet, South Carolina, showing the landward-thickening of fine grained abandoned inlet fill (after Tye and Moslow, in press)..... 135

Figure 38. Dip-oriented core correlation of Halfway tidal inlet sequences in the Wembley oilfield showing the palaeolandward-thickening of fine grained abandoned inlet fill..... 139

Figure 39. Strike-oriented core correlation of Halfway tidal inlet sequences in the Wembley oilfield illustrating the absence of intervening regressive shoreface deposits..... 141

Figure 40. Schematic representation of the use of the gamma ray log in facies analysis (after Rider, 1990)..... 143

Figure 41. Core-well log correlation of facies association 1 regressive shoreface sequence in well 16-26-72-8-W6..... 144

Figure 42 Spectral gamma ray log run over the Middle Triassic interval in well 8-21-73-9-W6 showing the presence of uraniferous condensed sections..... 146

Figure 43. Core-well log correlation of facies association 2 tidal inlet channel fill sequence in well 6-31-72-7-W6. A single upward-fining inlet sequence is present..... 150

Figure 44. Core-well log correlation of facies association 2 tidal inlet channel fill sequence in well 14-16-72-7-W6. The sequence represents a welded ebb-delta from the seaward mouth of the inlet channel..... 152

Figure 45. Core-well log correlation of facies association 2 in well 6-27-728-W6. The well contains two amalgamated tidal inlet channel fill sequences and an example of Facies M washover sandstone..... 154

Figure 46. Dip-oriented stratigraphic correlation of cored Halfway facies through the Wembley oilfield illustrating the intra-Halfway ravinement surface..... 158

Figure 47. Cross-section through the Holocene coastal deposits north of Bethany Beach, Delaware showing a transgressive barrier island truncated by a ravinement surface (after Kraft, 1971)..... 161

Figure 48. The Bruun model of shoreface erosion during rising sea level (after Suter et al., 1987)..... 163

Figure 49. Variations in shoreface erosion during storm and fairweather conditions (after Penland et al., 1985)..... 164

Figure 50. Isopach map of Halway Facies M washover sandstones..... 167

Figure 51. Cross-section through Pleistocene transgressive shoreline deposits near Bethany Beach, Delaware, showing the relationship between a ravinement surface and the distribution of transgressive washover sandstones (after Demarest and Kraft, 1987)..... 168

Figure 52. Complete vertical sedimentary sequence produced by a transgressive washover-dominated barrier island coastline, showing the abrupt change in palaeowater depth commonly found across a ravinement surface (after Demarest and Kraft, 1987)..... 170

Figure 53. Dip-oriented well log stratigraphic cross-section showing the Middle Triassic parasequences identified in the Wembley area (Pocket)

Figure 54. Gamma ray log and inferred lithology of the Middle Triassic section in well 16-23-72-8-W6 comparing lithostratigraphic formations with the informal sequence stratigraphic framework developed in this study..... 177

Figure 55. Schematic sequence stratigraphic model of the Middle Triassic section in west-central Alberta..... 179

Figure 56. Structure contour map drawn on the marine flooding surface at the base of parasequence 4 (Wembley Halfway Formation)..... 182

Figure 57. Structure contour map drawn on the marine flooding surface at the base of parasequence 5. A correlative flooding surface at the base of transgressive washover sandstones has allowed the contouring to be extended into the coastal plain deposits of the Charlie Lake Formation..... 183

Figure 58. Isopach map of parasequence 4 (approximates to the Wembley Halfway Formation). Contouring only extends to the down-dip (southwestern) limit of shoreface sandstones; isopach values beyond this are posted but not contoured..... 185

Figure 59. Strike-oriented well log stratigraphic cross-section through the study area showing the lateral continuity of Middle Triassic parasequences (Pocket)

LIST OF PLATES

		Page
Plate 1.	Core photograph Facies A	39
Plate 2.	Core photograph Facies B	42
Plate 3.	Core photograph Facies B	42
Plate 4.	Core photograph Facies B	43
Plate 5.	Core photograph Facies C	47
Plate 6.	Core photograph Facies C	47
Plate 7.	Core photograph Facies C	49
Plate 8	Core photograph Facies C	49
Plate 9.	Core photograph Facies D	52
Plate 10.	Core photograph Facies D	52
Plate 11.	Core photograph Facies D	53
Plate 12	Core photograph Facies D	53
Plate 13.	Core photograph Facies E	55
Plate 14.	Core photograph Facies E	55
Plate 15.	Core photograph Facies F	58
Plate 16.	Core photograph Facies F	58
Plate 17.	Core photograph Facies G1	60
Plate 18.	Core photograph Facies G1	60
Plate 19.	Photomicrograph Facies G1	61
Plate 20.	Core photograph Facies G2	64
Plate 21.	Core photograph Facies G2	64
Plate 22.	Core Photograph Facies G2	66
Plate 23.	Core photograph Facies H	68
Plate 24.	Core photograph Facies H	68
Plate 25.	Core photograph Facies H	70
Plate 26.	Core photograph Facies H	70
Plate 27.	Core photograph Facies I	75
Plate 29.	Core photograph Facies I	77
Plate 30.	Core photograph Facies I	77
Plate 31.	Core photograph Facies I	78
Plate 32.	Core photograph Facies I	78
Plate 33.	Core photograph Facies J	81
Plate 34.	Core photograph Facies J	81
Plate 35.	Core photograph Facies K	84

Plate 36. Core photograph Facies K..... 84
Plate 37. Core photograph Facies K..... 85
Plate 38. Core photograph Facies K..... 85
Plate 39. Core photograph Facies L..... 87
Plate 40. Core photograph Facies L..... 87
Plate 41. Core photograph Facies L..... 89
Plate 42. Core photograph Facies L..... 89
Plate 43. Core photograph Facies M..... 98
Plate 44. Core photograph Facies M..... 98
Plate 45. Core photograph Facies M..... 99
Plate 46. Core photograph Facies M..... 99
Plate 47. Core photograph Facies M..... 101
Plate 48. Core photograph Facies M..... 102
Plate 49. Core photograph Facies M..... 102
Plate 50. Core photograph Facies G1..... 113
Plate 51. Core photograph Facies M..... 113

1.0.0 INTRODUCTION.

This study describes the sedimentology and stratigraphic relationships of the upper-Middle Triassic (Ladinian-Carnian) Halfway Formation in the Wembley oilfied, west-central Alberta (Figure1).

The Halfway Formation is a siliciclastic unit restricted to the subsurface of the Western Canada Sedimentary Basin (Figure 2). Like all subsurface Triassic units in the basin, the Halfway Formation is a lithostratigraphic entity, defined as the first marine sandstone encountered beneath the red beds of the Upper Triassic Charlie Lake Formation (Hunt and Ratcliffe, 1959). The Halfway has previously been interpreted as both a transgressive (Hunt and Ratcliffe, 1959; Clark, 1961; Armitage, 1962) and more recently a regressive (Harrington, 1984; Barclay and Leckie, 1986; Campbell and Horne, 1986; Cant, 1986) marine sandstone.

1.1.0 Economic Significance

The Triassic strata of west-central Alberta and northeastern British Columbia account for approximately 4% of the in-place and recoverable conventional oil reserves in the Western Canada Sedimentary Basin (Podruski et al., 1988). To date, 23 stratigraphically trapped hydrocarbon pools containing 24 million cubic metres of oil-in-place have been discovered in the Halfway Formation in west-central Alberta (Table 1). The undiscovered potential for this Halfway stratigraphic play was estimated by Podruski et al. (1988) at 22 million cubic metres of oil-in-place, distributed in 67 new pools. This suggests that to date only about 50% of the Halfway oil in west-central Alberta has been found. There is therefore an obvious need for models to aid exploration for new Halfway pools and also to assist in the successful development of existing reservoirs.

1.2.0 Previous Work.

The Triassic rocks exposed in the Foothills of northeastern British Columbia were recognized as long ago as 1875 by A.R.C. Selwyn of the Geological Survey of Canada in the upper Peace River and later described by Dawson (1886) and McConnell (1891) from the Pine and Liard River valleys respectively. Since 1917, F.H. McLearn made numerous contributions to the study of Triassic stratigraphy, summarized by him and his colleague E.D. Kindle in a Geological Survey of Canada report on the geology of northeastern British Columbia (McLearn and Kindle, 1950) and in McLearn (1953). Subsequent studies of Triassic outcrops in northeastern British Columbia and western Alberta include Colquhoun (1962), Pelletier (1963, 65) and Gibson (1975). Warren (1945), Tozer (1961,

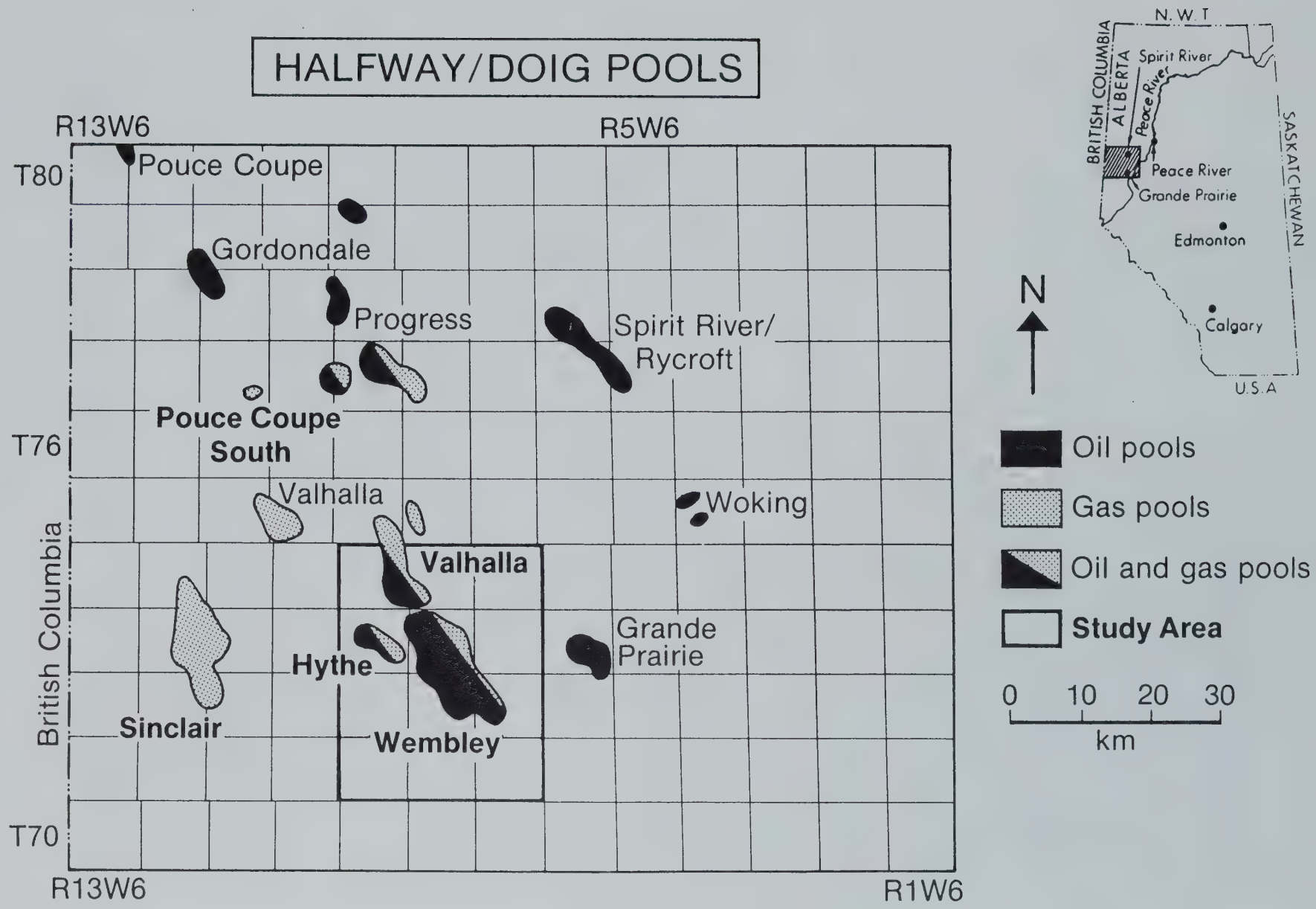

Figure 1. Location of the study area showing major Middle Triassic hydrocarbon pools in west-central Alberta (after Wittenberg, 1992).

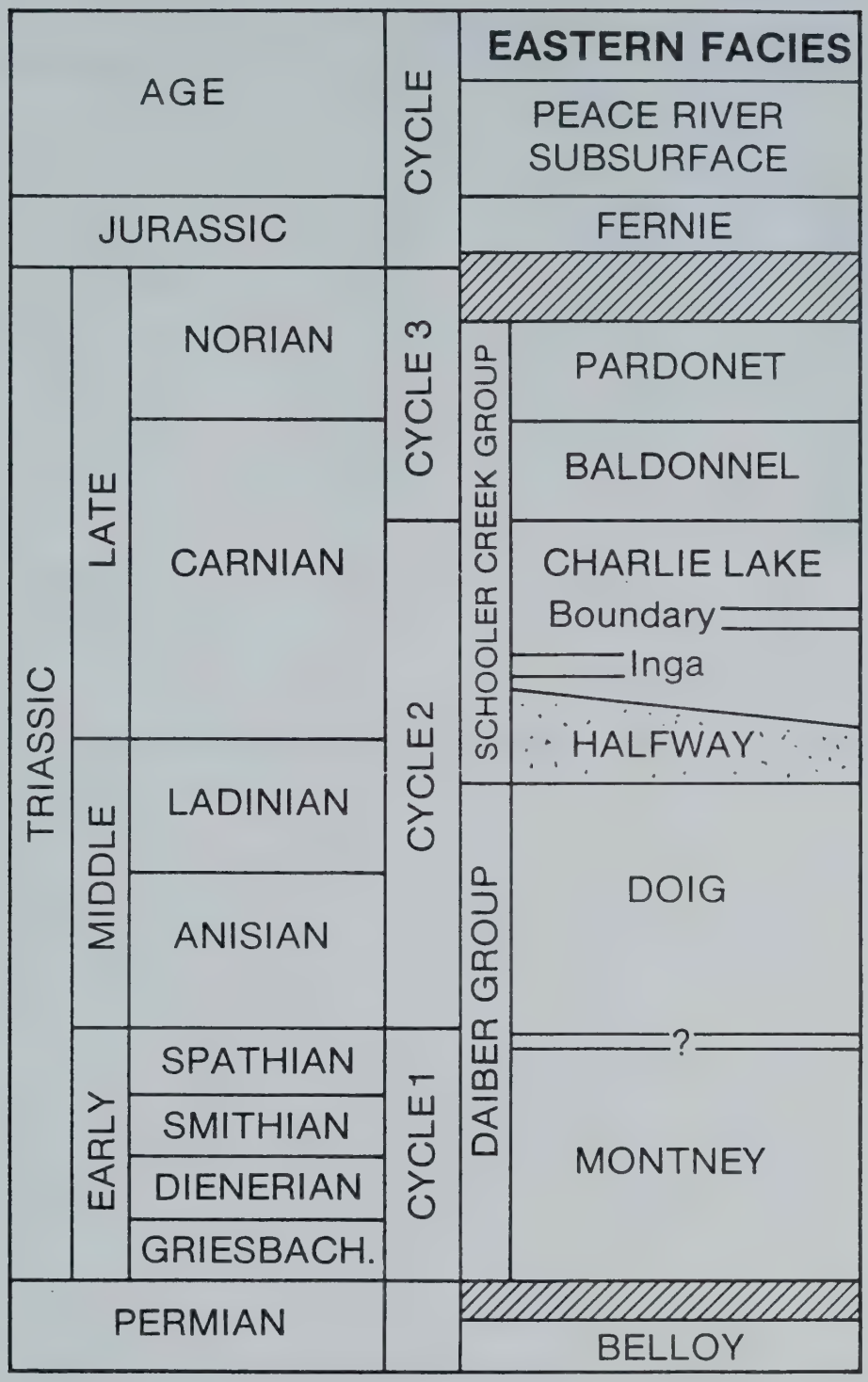

Figure 2. Subsurface Triassic Stratigraphy of the Western Canada Sedimentary Basin (after Podruski et al., 1988).

Pool Name	In-Place Pool Volume		Discovery Year
	10^6 m^3	10^6bbl	
Spirit River Doig A	7.20	60.38	1983
Wembley Halfway B	5.73	48.05	1978
Grande Prairie Halfway A	4.00	33.55	1982
Progress Halfway B	2.35	19.71	1982
Spirit River Halfway D	0.72	6.04	1983
Gordondale Halfway B	0.69	5.79	1979
Wembley Doig A	0.60	5.03	1982
Wembley Halfway E	0.49	4.11	1983
Wembley Halfway D	0.45	3.77	1983
Hythe Halfway A	0.41	3.44	1981
Total Oil In-Place	22.64	189.87	
Wembley Halfway Total	6.67	55.94	

Table 1. Oil reserves of Middle Triassic hydrocarbon pools in west-central Alberta. (After Podruski et al., 1988).

67) and Silberling and Tozer (1968) provide details of western Canadian Triassic biostratigraphy.

The Halfway Formation itself was first defined by Hunt and Ratcliffe (1959) in a paper discussing the correlation of these Triassic outcrops in the Rocky Mountain Foothills of northeastern British Columbia to the adjacent subsurface of the Peace River area, where hydrocarbons had recently been discovered in Triassic strata. They defined the unit as a marine sandstone occurring between siltstones of the Middle Triassic Toad-Grayling Formations and red beds of the Upper Triassic Charlie Lake Formation in a type well (01-12-84-23 W6) located near the confluence of the Halfway and Peace Rivers. No such sandstone occurs at this stratigraphic level in the outcrops to the west. They carried the name Toad Formation (Doig Formation of current subsurface terminology) directly from the outcrop stratigraphy and did not erect a subsurface type section for it. The Halfway Formation and all younger subsurface Triassic strata were included in their Schooler Creek Group, a name that had previously been used to describe the Middle-to-Upper Triassic sedimentary succession in the Foothills (McLearn and Kindle, 1950).

Armitage (1962), in a review of Triassic hydrocarbon occurrences in northeastern British Columbia, defined a type section (06-26-87-21 W6) for the Triassic succession beneath the Schooler Creek Group in the subsurface, discarding the use of the Toad-Grayling Formations taken from the outcrop nomenclature. He named this sequence between the Palaeozoic unconformity and the Schooler Creek Group the Daiber Group and subdivided it into the Montney and Doig Formations. This nomenclature persists to the present (Figure 2). Hydrocarbon occurrences in the Halfway Formation of northeastern British Columbia are also described by Clark (1961), Mothersill (1968) and Chunta (1969).

The discovery of oil in the Halfway Formation at Wembley in west-central Alberta in 1978 lead to a resurgence of interest in this unit. A brief description of typical Halfway lithologies in the Wembley field can be found in an abstract by Halton (1981), but otherwise this goes no further than saying "the Halfway Formation was deposited in near-shore shallow marine environments" (Halton, 1981).

The unpublished work of Harrington (1984) is the first study dealing at length with the Halfway Formation in the Wembley oil field and was undertaken at an early stage of the field's development. The main focus of this thesis was "to describe the diagenetic history

of the reservoir rocks of the Halfway Formation in the Wembley Field" (Harrington, 1984), largely through petrographic study but also employing scanning electron microscopy, x-ray diffraction and cathodoluminescence. Harrington (1984) interpreted the Halfway Formation in the Wembley field to be a regressive barrier island sequence. This marked a departure from the earlier belief expressed by Hunt and Ratcliffe (1959), Clark (1961) and Armitage (1962) that the Halfway Formation was the deposit of a transgressive sea. Subsequent papers by Cant (1986), Campbell and Horne (1986) and Barclay and Leckie (1986) broadly agree with Harrington's (1984) interpretation.

Cant (1986) details the conditions responsible for hydrocarbon trapping at the Wembley field, gives an overview of reservoir sedimentology and diagenesis and discusses the relationship of the Halfway to the under- and overlying Doig and Charlie Lake Formations.

Campbell and Horne (1986) provide the most comprehensive discussion of regional Halfway deposition in the Western Canada Sedimentary Basin to date, including the first explicit recognition of the genetic relationship of the Halfway sandstone interval to the underlying shales, which had previously been considered part of the Doig Formation (in line with the original Halfway type section of Hunt and Ratcliffe (1959)).

Barclay and Leckie (1986) provide a brief description of a typical cored Halfway sequence from the Progress field some 40km to the north of Wembley and of their interpreted depositional model. A more recent discussion of the same area is presented by Styan and Shaw (1991). Aukes and Webb (1986) describe the Triassic Spirit River oilfield 45km northeast of Wembley, which they consider to be in the Doig Formation, although the sedimentary succession described is very similar to the Halfway Formation at Wembley. They also state that more than one regressive sequence is present in the Middle Triassic section in the Spirit River area and question the validity of separating the Halfway and Doig Formations (Figure 3).

Although interest in the hydrocarbon potential of the Halfway Formation has continued, subsequent published work has been mainly in the form of abstracts from oral presentations. Campbell and Hassler (1989) and Campbell et al. (1989) discuss a model for hydrocarbon entrapment in the Halfway and Doig Formations of west-central Alberta (Figure 4). They recognized six upward-coarsening depositional cycles (parasequences)

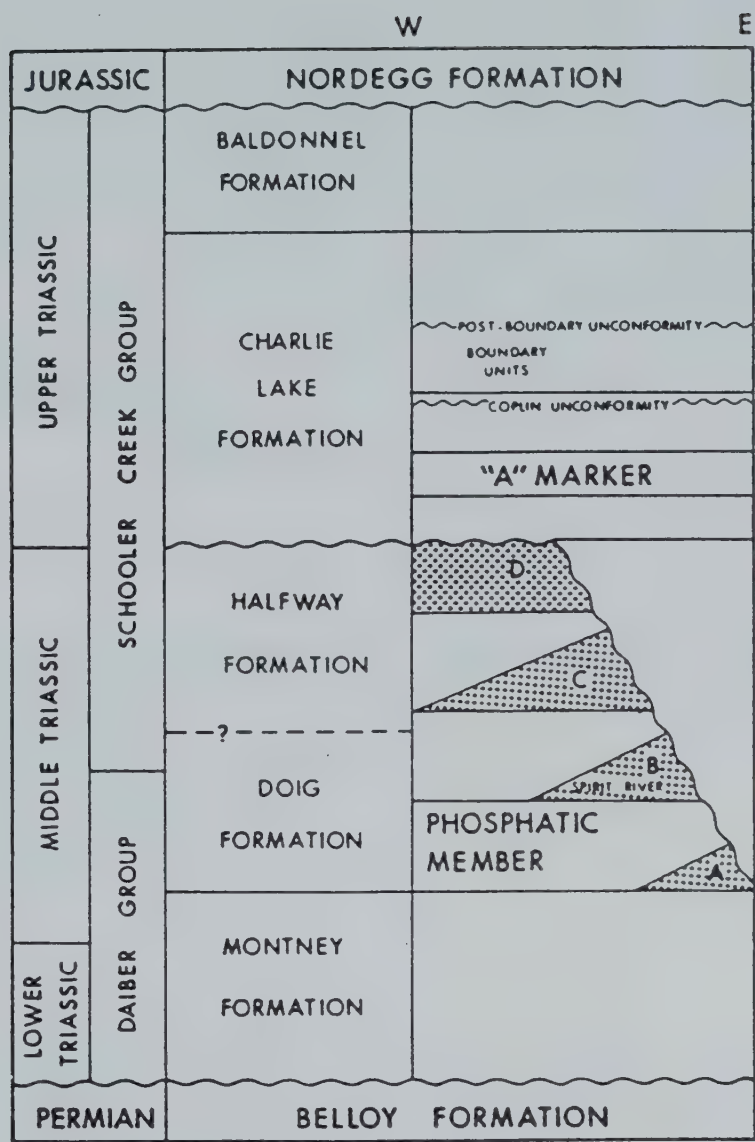

Figure 3. Triassic stratigraphy of the Spirit River area. Note recognition of several sandstone units (stippled) in the Halfway-Doig interval. "Spirit River" in the sandstone labelled "B" refers to the location of the Spirit River oilfield (after Aukes and Webb, 1986).

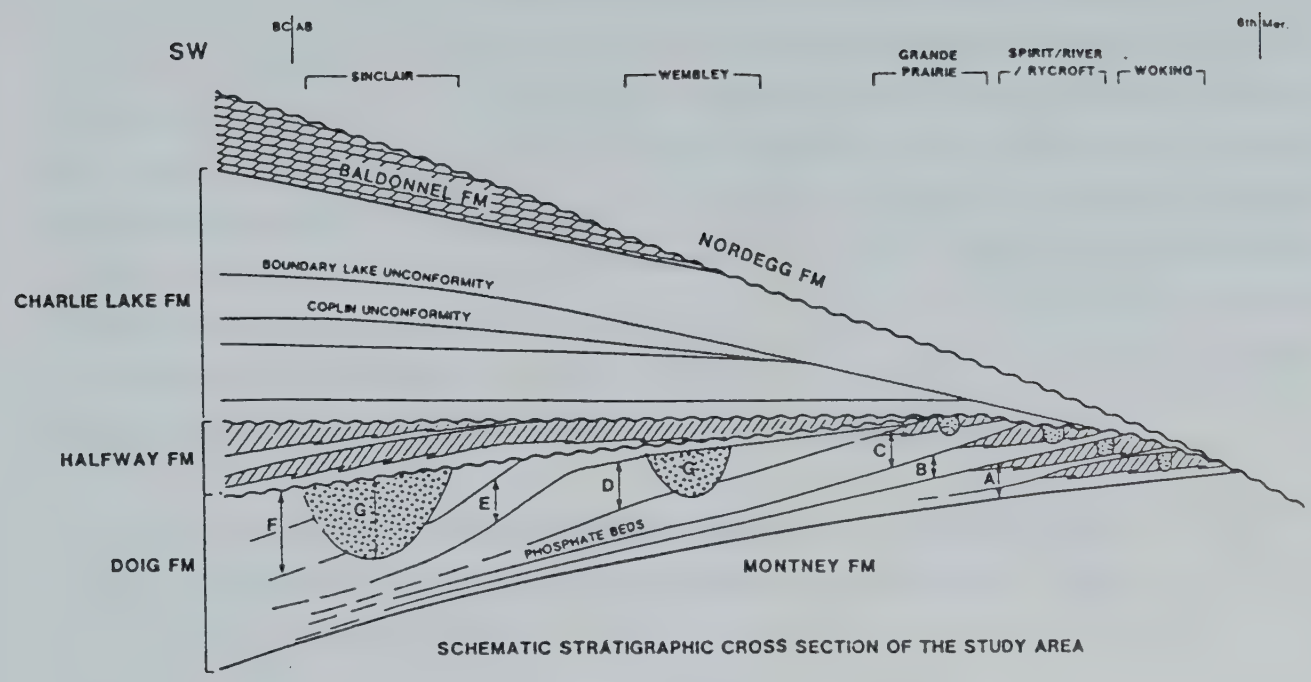

Figure 4. Schematic stratigraphic cross-section through the Triassic strata of west-central Alberta. Note the presence of several sedimentary cycles (A, B, C etc.) and unconformities within the Doig Formation and at the top and base of the Halfway Formation (after Campbell et al, 1989).

within the Doig Formation and two within the Halfway Formation, similar to those recognised by Aukes and Webb (1986). These workers however, placed an unconformity between the Halfway and Doig Formations. The fall in sea level associated with this unconformity was also considered responsible for the incision of a series of deep fluvial valleys into the exposed Doig siltstones, producing thick linear sandbodies. Uplift and erosion prior to deposition of the Charlie Lake Formation was envisioned to have truncated progressively older Halfway shoreline cycles eastward, creating a series of shoreline-parallel subcrop belts. Hydrocarbon pools were interpreted to be located at the updip erosional pinchout of each shoreline sandstone and in erosional outliers further to the east. This interpretation of the Halfway-Charlie Lake contact as a regional unconformity and the controlling factor on hydrocarbon trapping is in contrast to previous studies, which have consistently maintained that this contact is a facies transition between shoreline sandstones and back-barrier evaporites and red beds. Unfortunately, the data Campbell et al. (1989) used to construct this model is a confidential consultants' report to the petroleum industry and is therefore not available for public scrutiny.

Abstracts by Horne et al. (1985), Munroe and Moslow (1990) and Caplan and Moslow (1991) briefly describe tidal inlet-fill sequences from the Halfway Formation of Alberta and northeastern British Columbia.

Two broadly similar concise summaries of the Triassic strata of western Canada are given by Gibson and Barclay (1989) and Gibson and Edwards (1990), based largely on the previously discussed studies. Older regional reviews of Triassic strata in western Canada are given by Barss et al. (1964), Carlson (1968) and Torrie (1973).

Miscellaneous other related work includes Riediger et al. (1990), who provide a review of Middle Triassic hydrocarbon source-rocks in the Peace River area of western Canada. This study concludes that most of the oil which has accumulated in the Halfway and Doig Formations was generated by adjacent Middle Triassic shales, particularly the Phosphate Zone of the lower Doig Formation. In a review of western Canada's conventional hydrocarbon resources, Podruski et al. (1988) describe the major Halfway play types in the Western Canada Sedimentary Basin, together with estimates of the proven and as yet undiscovered reserves in the formation. Dudley et al. (1989) describe the effects of Halfway mineralogy on the acidization treatment commonly used in completing oilwells in the unit, and Sharma (1969) addresses aspects of Halfway diagenesis in the Peejay oilfield of northeastern British Columbia.

Wittenberg (1992) studied the Doig Formation of west-central Alberta and recognized that each of the progradational cycles (parasequences) noted by Aukes and Webb (1986) and Campbell et al. (1989) in the Middle Triassic section are bounded by radioactive phosphatic shale beds. He interpreted these regionally correlatable marker beds as condensed horizons associated with times of maximum transgression, each pair bounding a progradational sediment package. Facies correlations within each progradational cycle lead him to deduce: (a) that the Halfway shoreline sandstones and the Doig shelf mudstones are in fact time-equivalent parts of the same depositional system, and: (b) that the linear Doig sandbodies were deposited as shelf slump features contemporaneously with the surrounding mudstones and not as a later valley incision associated with a drop in sea level as suggested by Campbell et al. (1989).

1.3.0 Unresolved Problems.

Previous studies of Halfway Formation sedimentology (Horne et al., 1985; Barclay and Leckie, 1986; Campbell and Horne, 1986; Cant, 1986; Munroe and Moslow, 1990) have broadly agreed on the depositional origin of the unit as a regressive barrier island shoreface deposit and emphasized the importance of tidal inlet channel fill sequences as hydrocarbon reservoirs. However, studies of modern barrier island coastlines, particularly along the Georgia embayment of the southeastern United States, have demonstrated great variability of tidal inlet sequences, geometries and distribution as a function of palaeotopography, hydrographic regime, and sediment supply (Tye and Moslow, in press). This interaction of dynamic physical processes results in the formation of distinct inlet types and stratigraphic sequences on wave-dominated versus tide-dominated mixed-energy coasts (eg. Moslow and Tye, 1985). These marked differences in tidal inlet stratigraphy, geometry and distribution in wave versus tide-dominated settings mean that a more precise knowledge of the hydrographic regime which shaped an ancient deposit is required to predict its reservoir distribution and heterogeneity in the subsurface. This information is presently lacking for the Halfway Formation and can only come from a rigorous process sedimentological study.

The original definition of the Halfway Formation as the first marine sandstone encountered in the subsurface type-well beneath the thick red beds and evaporites of the Charlie Lake Formation (Hunt and Ratcliffe, 1959) has subsequently lead to every such sandstone being lithostratigraphically correlated across the basin as a single regressive sheet sandstone (Figure 5). However, lithologically similar sandstones discovered within

the *pre-existing* Doig and Montney Formations, and not therefore subject to this lithostratigraphic "straightjacket", were recognised as a series of progradational shoreline cycles and correlated as separate entities (Miall, 1976; Aukes and Webb, 1986; Wittenberg, 1992).

Studies of sediment budgets along modern coastlines (e.g. Pierce, 1969; Armon and McCann, 1977) suggest that it is unlikely that longshore drift and shelf sources of sediment could be maintained at sufficient magnitude to allow extensive progradation of the shoreface. Heward (1981) calculated that assuming no sand loss beyond the delta front, it would still take a river the size of the Mississippi (supplying some 9.4 x 10^{10} kg of sand to the sea annually) 14,000 years to build a 126 km x 104 km x 51 m "average" ancient regressive sheet sandstone. No significant fluvial deposits have been documented in Middle Triassic strata of western Canada and therefore most sediment for the Halfway coastline is assumed to have been supplied by longshore drift from some unknown depocentre to the north (Campbell and Horne, 1986). It would therefore seem theoretically unlikely that the Halfway coastline could possibly have prograded in a single episode from its present subcrop edge to its westernmost extent, a distance greater than 300 km. This suggests that some doubt should be cast on lithostratigraphic correlations such as that shown in Figure 5, depicting the Halfway as a single sandbody throughout the Western Canada Basin.

At a more practical level, the lithostratigraphically-induced interpretation of the Halfway Formation as a single regressive sheet sandstone presents serious problems when trying to explain the location of separate hydrocarbon pools in the unit. Halfway hydrocarbon pools in west-central Alberta show no structural closure and must therefore be stratigraphically separated. However, it is difficult to reconcile the occurrence of numerous stratigraphically-trapped hydrocarbon pools in what is commonly believed to be a single sheet sandstone. The traditional solution to this problem has been to invoke either (a) a "permeability barrier", presumably diagenetic cementation, between pools (Brack et al., 1989), or (b) that the reservoirs have been separated by post-Halfway erosion (Campbell et al., 1989). There are no reports in the literature of significant permeability barriers in the Halfway Formation, and there is some debate as to whether a regional unconformity is present at the top of the formation.

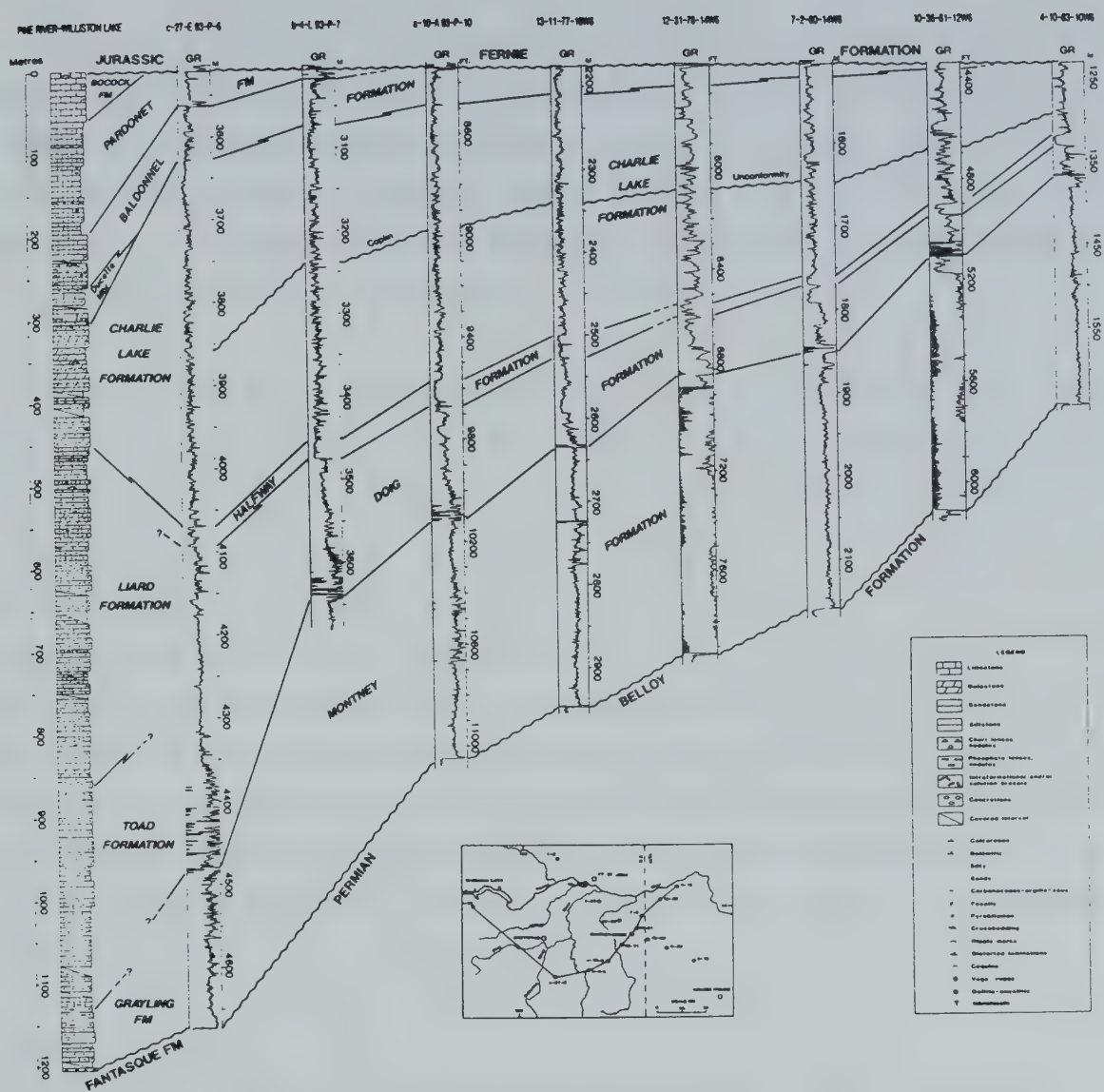

Figure 5. Lithostratigraphic correlation of Triassic formations between surface exposures in the Foothills and the adjacent subsurface Peace River Plains. Note that the line of section crosses the Peace River Arch (after Gibson and Edwards, 1990).

1.4.0 Objectives.

The goals of this study are therefore to:

1) Conduct a detailed sedimentological study of the Halfway Formation in a geographically restricted area of abundant data (core and well logs). The observed physical processes of deposition in cored sequences would provide a better understanding of the prevalent hydrographic regime during Halfway time and thus allow more accurate prediction of subsurface reservoir geometry, heterogeneity and distribution using the insights gained from studies of modern coastlines.

2) Use the observed sedimentary facies relationships in the Doig-Halfway-Charlie Lake interval to determine the stratigraphic relationships of the three formations. In light of the theoretical and practical problems associated with the traditional Middle Triassic lithostratigraphy outlined above, and the insights gained from the studies of Aukes and Webb (1986) and Wittenberg (1992), it was anticipated that several shoreline sedimentation cycles (parasequences) would be present in the Halfway Formation. The recognition of such flooding surface-bounded depositional episodes offers the possibility of erecting a chronostratigraphic framework which truly depicts the relationship of successive sedimentary events (Galloway, 1989; Van Waggoner et al., 1990). The paucity of biostratigraphic data suggests that this may be the only method of improving our understanding of subsurface Triassic stratigraphy and its controls on hydrocarbon pool distribution.

1.5.0 Study Area.

The Wembley oilfield is located approximately 19 km northwest of the town of Grande Prairie in west-central Alberta (Figure 1). It is 24 km long by 8 km wide and is the largest oil accumulation in the Halfway Formation in the Alberta portion of the Western Canada Sedimentary Basin, containing primary recoverable reserves of 5083.1 x 10^3 m^3 (43 million barrels) of oil and 8956 x 10^6 m^3 (316 BCF) of solution and associated gas (Alberta E.R.C.B., 1989).

The Wembley field has a large subsurface database of some 300 well logs and over 150 cores cut from the Halfway Formation, making it an ideal area to undertake a detailed study of the unit. A study area was therefore selected around the Wembley field, consisting of Townships 71 to 74, Ranges 7 to 9, west of the Sixth Meridian (Figure 1). This covers an area of approximately 1200 km^2. Within the main field area, wells may be

as closely spaced as 500m, giving a high degree of confidence in correlations of both sedimentary facies and stratigraphically significant surfaces. It has the added advantage that as the field was only discovered in 1978, most of the wells have a full suite of good quality wireline logs of similar vintage. In addition, the fact that the underlying Doig Formation is also a potential hydrocarbon reservoir in this area means that most wells are drilled into the "Phosphate Zone" of the Doig Formation, giving complete coverage of the Middle Triassic section.

1.6.0 Methods.

The basis of this thesis involved the sedimentological description of cores cut from the Halfway Formation in the Wembley field. As a first step to identifying which cores would be suitable for the study, geophysical well logs (gamma-ray, sonic, resistivity, formation density, compensated neutron and where available spectral gamma-ray and dip-meter) were obtained for the interval from the base of the Jurassic system ("Nordegg Member") to the base of the Triassic (Permian Belloy Formation or T.D.) for all 304 wells within the study area which were available to the general public as of December 31st, 1990. Using depths given on standard petroleum industry and Energy Resources Conservation Board well data sheets, cored intervals in the Triassic were then marked on each well log and the approximate boundaries of the lithostratigraphic Montney, Doig and Halfway Formations added. Each well was then allocated a study priority according to the degree of core coverage in the Halfway interval, bearing in mind the need to assemble an adequate database both in terms of areal spacing and coverage of important stratigraphic intervals such as formation contacts. This resulted in a list of approximately 100 cores. Ninety two of these cores were examined at the Alberta Energy Resources Conservation Board Core Research Facility in Calgary between June and August 1990. A further 56 cores were described throughout 1991 to address specific points raised by the study of the earlier data. This resulted in a total of some 2800m of core being described from 148 wells. The distribution of wells penetrating the Halfway formation within the study area together with the location of the 148 cores examined in the study are shown in Figure 6.

1.6.1 Core Description.

The procedure for measuring and describing a cored sequence is essentially similar to studying a stratigraphic section in outcrop, except that the amount of material available for study is considerably more limited in core and it is not possible to examine lateral changes in lithology and sediment body geometry. When attempting to make a

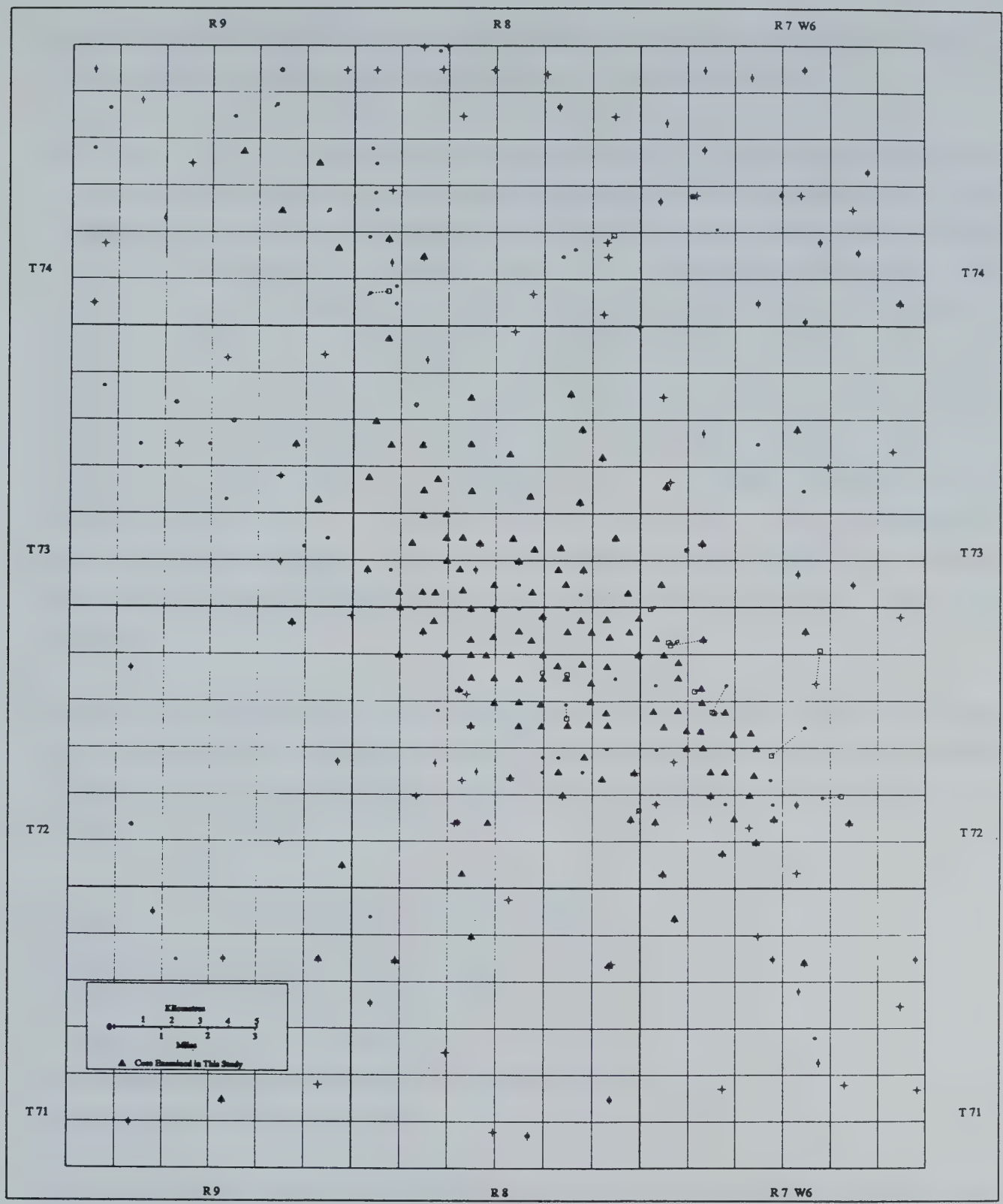

Figure 6. Location of all 304 wells in the study area which penetrate the Halfway Formation, highlighting the 148 cored intervals examined during this study.

sedimentological interpretation of a cored sequence, it is therefore important to utilize all available information and to make maximum use of the vertical sequence.

This reliance on the vertical sedimentary sequence to develop three-dimensional models of depositional complexes makes it critically important to have an understanding of the relationship of vertical facies successions seen in core to the lateral facies relationships of a variety of depositional complexes. The most general statement of such facies relationships is that of Walther's Law of Correlation of Facies, reviewed by Middleton (1973). This has been simply stated in the form "facies that occur in a conformable vertical core sequence were formed in laterally adjacent depositional environments; or, conformably vertically adjacent lithofacies represent laterally adjacent depositional (environmental) facies" (Siemers and Tillman, 1981). It is especially important to note, as Middleton (1973) pointed out, that Walther's Law applies only to conformable successions without major erosional or non-depositional breaks. It is therefore extremely important to recognize such erosional or non-depositional breaks in a vertical core sequence.

The first step in describing a core was to ensure that all the pieces were in the correct order and measure the re-assembled core to assess the degree of core loss. One could then make an accurate record of the characteristics that are critical to a correct interpretation of the lithological sequence:

(a) primary (depositional) sediment composition
(b) grain texture (size and sorting)
(c) primary physical sedimentary structures
(d) biogenic sedimentary structures
(e) secondary (e.g. deformational) sedimentary structures
(f) macroscopic diagenetic features.

The use of such a checklist format ensures that specific aspects of core description are not overlooked and that successive descriptions are consistent. The information was recorded on a core description sheet at a scale of 1:50. This provides a visual summary of the core and also shows the vertical distribution and variation of the above parameters and the contact relationships between vertically adjacent lithological units. The completed core description sheets used in this study are contained in Appendix A.

1.6.2 Process Sedimentology.

Following the method outlined by Siemers and Tillman (1981), a process sedimentological approach was taken in describing the cored Halfway Formation sequences. In general, the process approach attempts to understand the origin of a sedimentary deposit through the careful observation of details and recognition of genetic units (see below) in the vertical sequence. It delineates the physical, biological and chemical processes that must have occurred to generate the sedimentary product. Important aspects include the separation of current and wave-formed sedimentary structures, differentiation of suspension, density and traction deposits, and sediments deposited in upper- or lower-flow regimes. A knowledge of the processes, combined with other information such as regional lithofacies distribution, can be used to generate a predictive sedimentary model that accounts for all of the data and therefore best fits the particular sedimentary sequence of interest.

This is in contrast to the widespread model approach to the interpretation of sedimentary sequences, which involves comparison of the sequence of interest with pre-existing depositional models constructed from the study of modern depositional systems or other ancient sedimentary sequences. While such models are extremely useful in sedimentology, they must be applied with the knowledge that no one model can adequately describe all of the characteristics of other less well studied sedimentary sequences; a common misuse of the model approach involves the elimination or modification of data from a stratigraphic sequence in order to better fit the depositional model. As succinctly stated by Siemers and Tillman (1981), "The goal of sedimentology is to delineate and interpret what depositional system actually exists, not to document a depositional model that someone wants to exist.".

1.6.3 Genetic Units.

Once a process-oriented description has been made of the sedimentary features in a core, it is then possible to delineate a series of genetic units. Genetic units are "lithological units that display features which originated from processes that were relatively constant, or that varied in a uniform manner, throughout the formation of these lithologic units." (Siemers and Tillman, 1981). It is usually possible to delineate genetic units during the process of describing the core, such that for whatever reason each unit is identified as having an origin that was significantly different from units below and above. Several forms of genetic unit are recognised by Siemers and Tillman (1981), depending on the dominant process which shaped the deposit: sedimentation unit, ichnogenetic unit, soft

sediment deformation unit, and diagenetic unit. The vertical profile of genetic units and the nature of the contacts between them can then be used to interpret depositional environment.

1.6.4 Sampling and Photography.

While each core was being described, it was extensively photographed both to provide a final set of prints for the thesis and to allow later comparison of units and features seen in different cores. In addition, small samples of rock were collected from each facies to facilitate biostratigraphic and petrographic study. Unfortunately, due to the fact that many of the reservoir intervals had been subject to whole diameter core analysis, samples could not always be obtained from the most ideal location.

2.0.0 REGIONAL STRATIGRAPHY.

Triassic strata of the Western Canada Sedimentary Basin form a westward-thickening wedge of sediment, reaching up to 1200m in the western-most outcrops in the Rocky Mountain Foothills (Figure 7). Beyond the eastern limit of the Foothills, Triassic strata are encountered only in the subsurface, extending over some 142,000 km^2 (55,000 sq. miles) of the northeastern British Columbia and west-central Alberta portions of the Western Canada Sedimentary Basin.

In general, the Triassic strata of the Western Canada Sedimentary Basin rest unconformably on Permian rocks in the west and onlap Mississippian carbonates eastward. Throughout most of the basin they are unconformably overlain by shales of the Lower Jurassic Fernie Group (Nordegg Member), but in parts of northeastern British Columbia the Lower Cretaceous Gething or Bluesky Formations rest directly on the Triassic.

Assemblages of Triassic volcanic and carbonate rocks which crop out in the western part of the Rocky Mountains are considered to be part of various allochthonous terranes, having originated elsewhere and accreted onto the western margin of the North American craton from the late Triassic onward (Tozer, 1982; Mortimer, 1986; Monger, 1989).

Investigation of the outcrop sections in the Foothills was accompanied by documentation of faunas ranging in age from early Triassic Griesbachian to late Triassic Norian, a period of some 37 million years (Tozer, 1961, 67). This sequence forms what is probably the most complete described Triassic biostratigraphic succession in the world (Harland et al., 1989). The stratigraphic terminology which has grown up around the subsurface Triassic strata to the east however, is based mainly on the lithostratigraphic units which form hydrocarbon reservoirs. Correlation between the two areas has been hampered by the lack of biostratigraphic data from the subsurface and the absence of widespread lithological marker beds. A summary of the present correlation of Triassic outcrop and subsurface sections is given in Figure 8 and shown schematically in Figure 9.

2.1.0 Schooler Creek Group.

The Halfway Formation forms the lowest unit of the Schooler Creek Group and is thought to be of upper-Middle Triassic (Ladinian-Carnian) age. The name "Schooler Creek" was first applied by McLearn (1921) to a series of Middle and Upper Triassic sedimentary rocks in the Foothills of northeastern British Columbia. These were

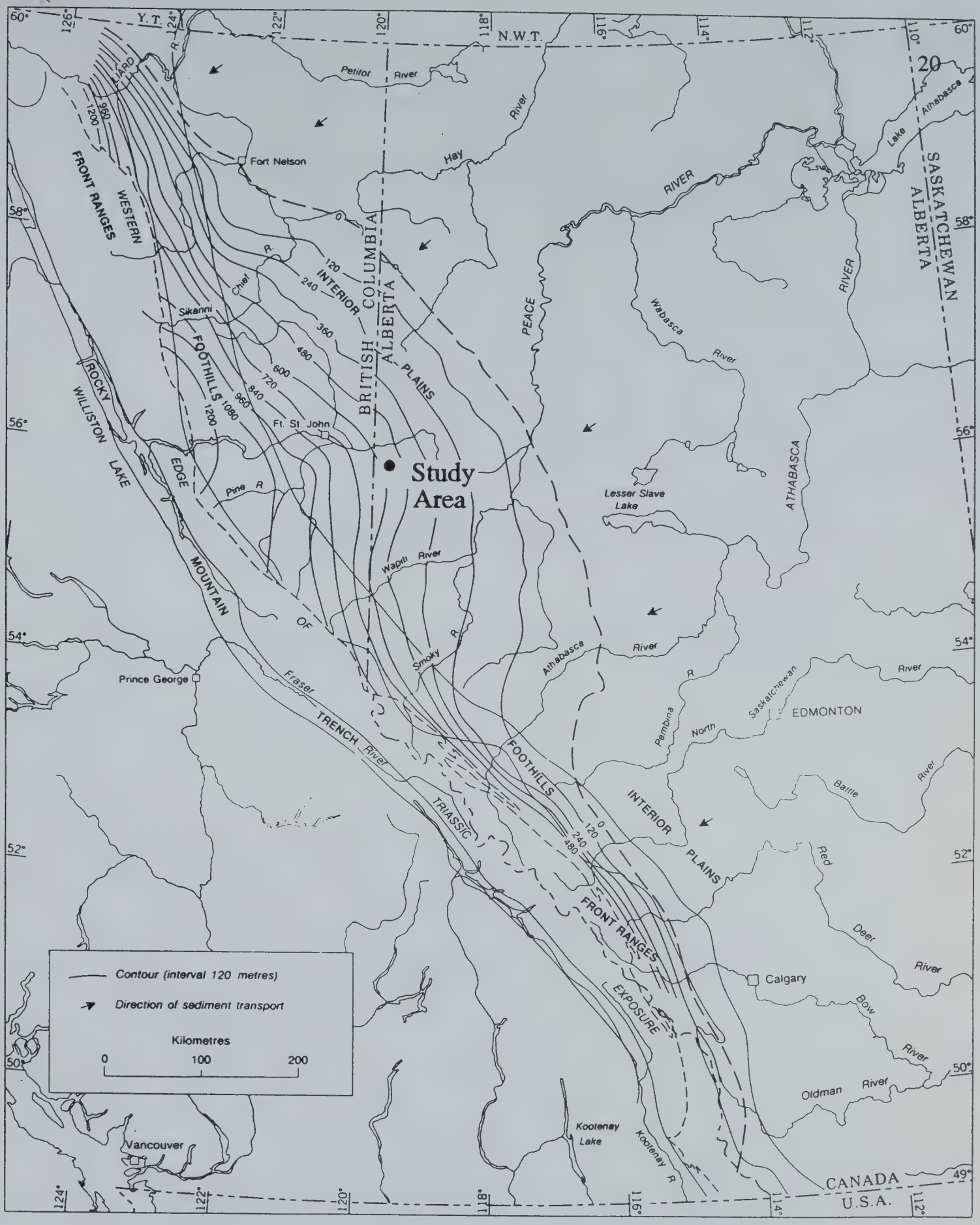

Figure 7. Isopach map of Triassic strata in the Western Canada Sedimentary Basin (after Gibson and Barclay, 1989).

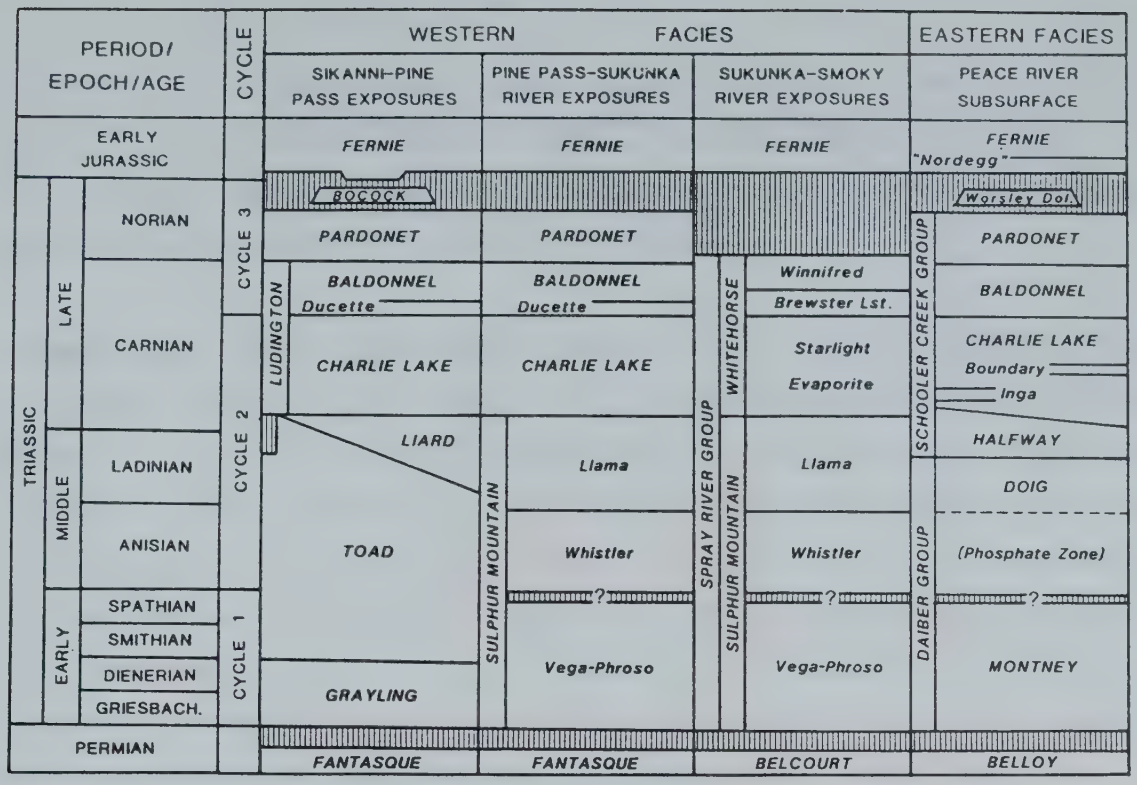

Figure 8. Correlation of outcrop and subsurface Triassic stratigraphy in the Western Canada Sedimentary Basin (after Podruski et al., 1988; Riediger et al., 1990).

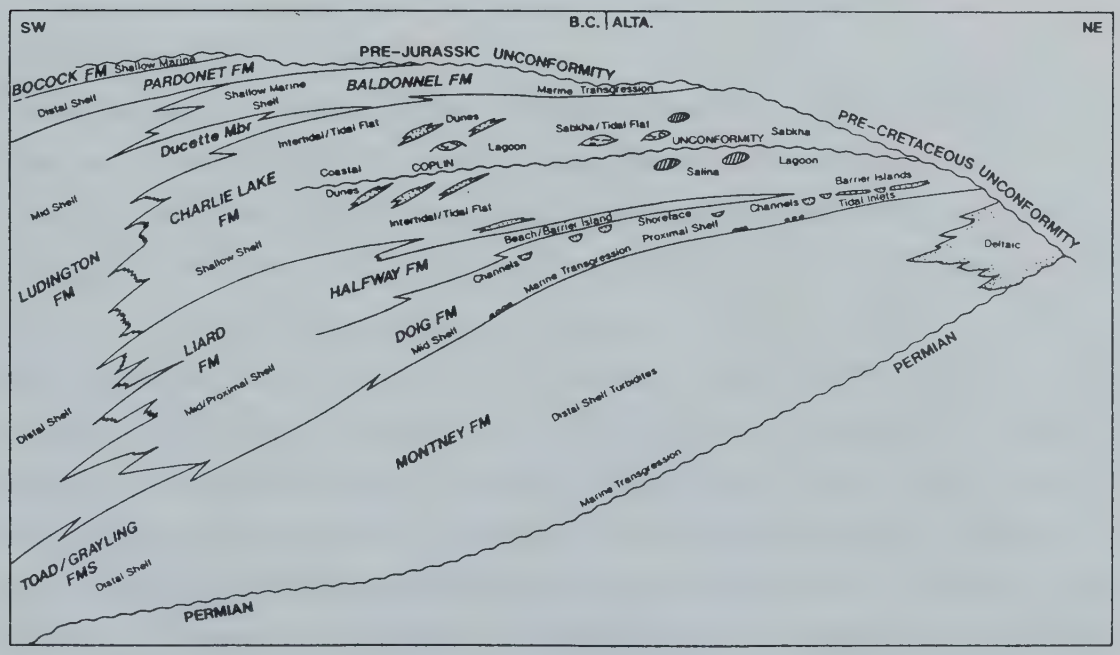

Figure 9. Schematic cross-section illustrating stratigraphic relationships and depositional environments of Triassic formations between the Foothills outcrop belt (SW) and the subsurface plains (NE) (after Gibson and Edwards, 1990).

subsequently subdivided into a number of units by both McLearn himself (1947) and Kindle (1944). The term "Schooler Creek" was later redefined by Hunt and Ratcliffe (1959) who erected the Schooler Creek Group for subsurface Middle-to-Upper Triassic strata including and overlying their Halfway Formation.

The lowermost units of McLearn's "Schooler Creek", which he named the "Flagstones" and "Dark Siltstones" in the Peace River Foothills (McLearn, 1947), are lithologically similar to and contain the same ammonite species of the *Nathorstites* fauna as the Liard Formation of the Liard River area to the north described by Kindle (1944) (Figure 10). Hunt and Ratcliffe (1959) recommended retaining the name Liard Formation in preference to the two descriptive terms. Conformably underlying the Schooler Creek / Liard beds are a section of Lower-to-Middle Triassic siltstones and shales named the Toad and Grayling Formations by Kindle (1944), which in turn rest unconformably on Palaeozoic strata. Overlying McLearn's "Dark Siltstones" are his "Grey Beds", consisting of fine-grained sandstones and limestones and containing three fairly well defined faunas: the *Nathorstites* fauna in the lower part; the Mahaffy Cliffs fauna near the middle; and the *Lima poyana* fauna near the top. These "Grey Beds" pass conformably upward into the finer-grained Pardonet Beds, the uppermost unit of his Schooler Creek, which are unconformably overlain by shales of the Jurassic Fernie Group (McLearn and Kindle, 1950).

2.1.1 Halfway Formation.

In their attempt to correlate these outcrop sections to the adjacent Peace River subsurface, Hunt and Ratcliffe (1959) defined the Halfway Formation as a marine sandstone overlying the Toad-Grayling Formations in their type section, the Southern Production well B-14-1 (01-12-84-23 W6) located at the confluence of the Halfway and Peace Rivers (Figure 11). They state that in the eastern part of the Peace River area the Halfway lies disconformably on the Toad, but to the west this contact becomes conformable and transitional (Hunt and Ratcliffe, 1959). The top of the formation is marked by the passage into the red beds and evaporites of their newly-defined Charlie Lake Formation, but to the west this again merges into a completely marine sequence which is difficult to subdivide. On the basis of the identification of the brachiopod *Lingula selwyni* in cores from the Halfway in the type area, Hunt and Ratcliffe (1959) correlated their Halfway Formation with the upper part of the *Nathorstites* zone in the lower part of the Grey Beds of the outcrop section.

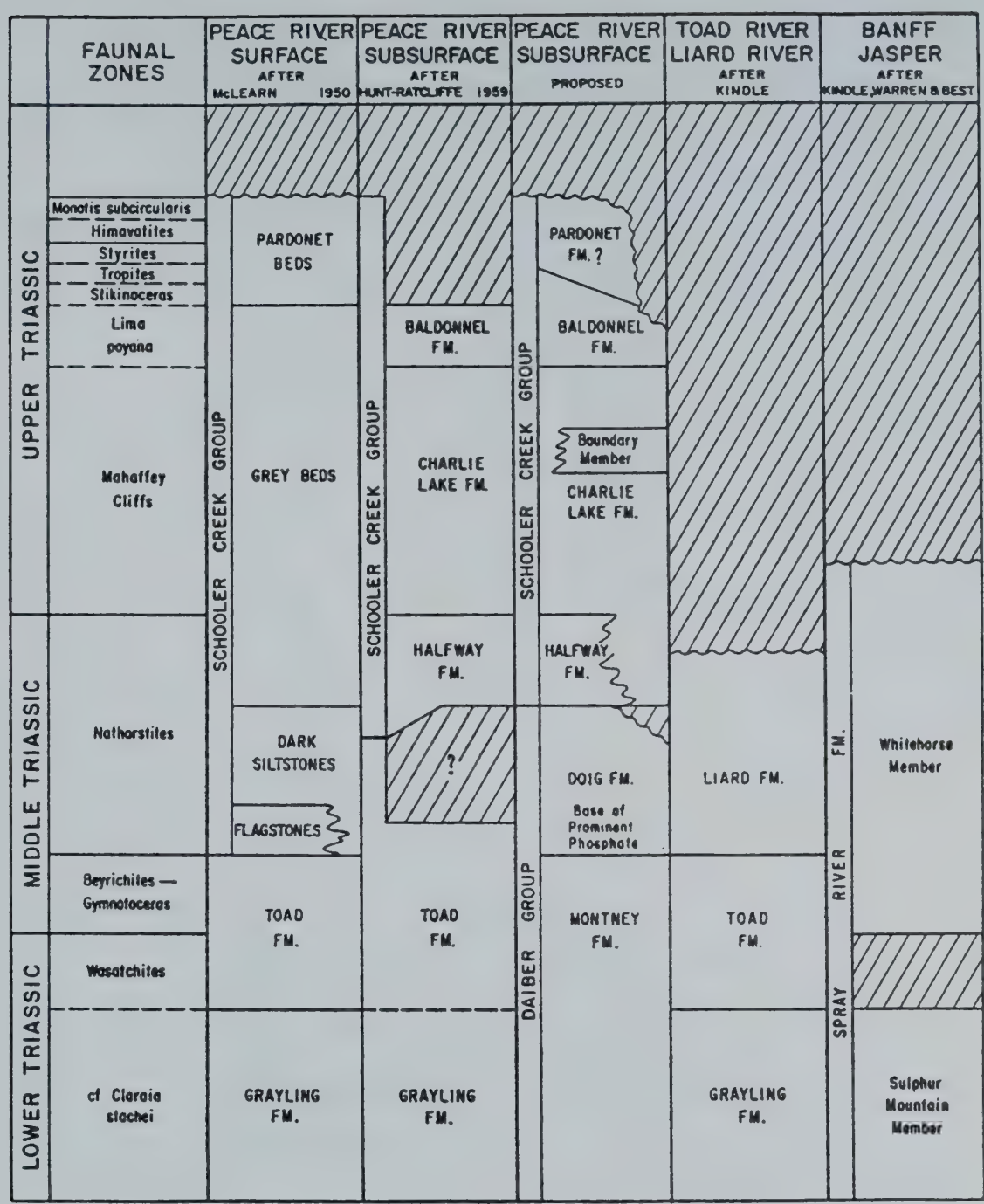

Figure 10. Table of Triassic formations showing the faunal zones used in outcrop-to-subsurface correlations (after Armitage, 1962).

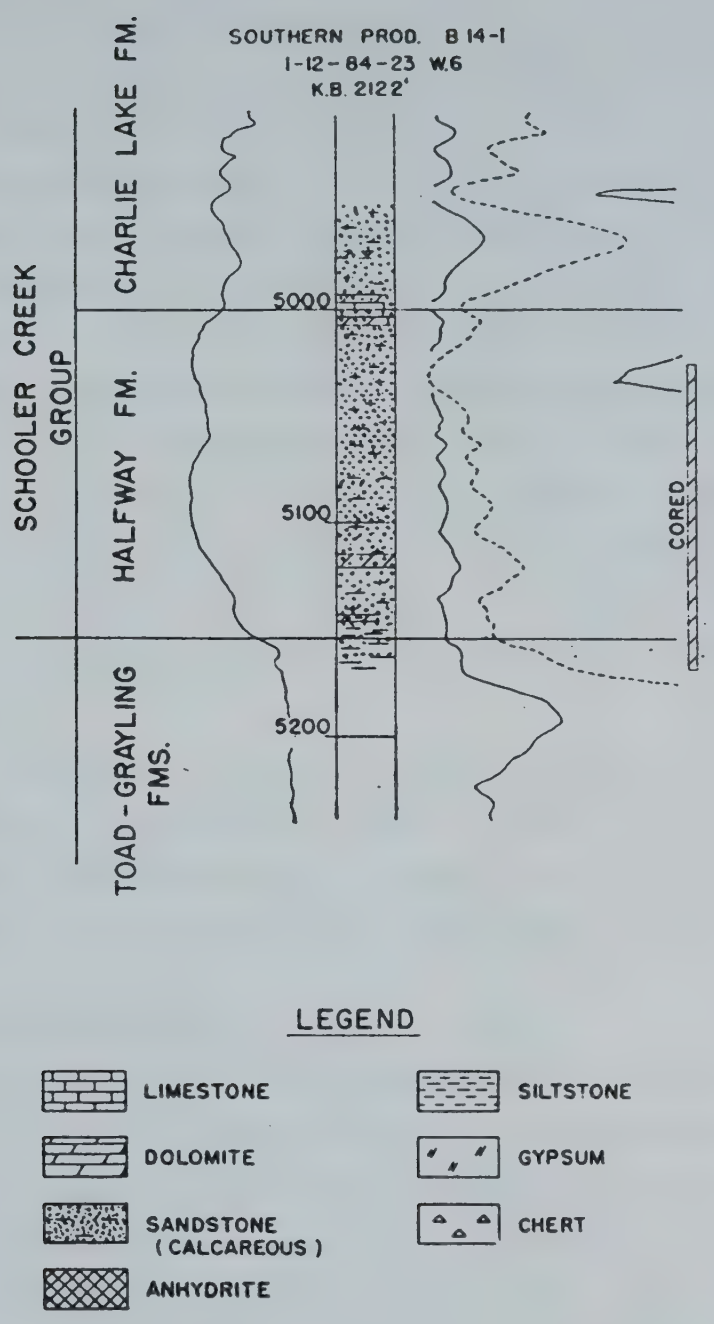

Figure 11. Type section of the Halfway Formation. The Halfway is defined in this well as the sandstone overlying siltstones of the Toad-Grayling Formations and overlain by red beds and evaporites of the Charlie Lake Formation (after Hunt and Ratcliffe, 1959).

Some confusion still results from the original designation by Hunt and Ratcliffe (1959) of the base of the Halfway sandstone interval as the base of the Halfway Formation. The base of this Halfway sandstone interval is commonly erosive and was originally interpreted by Hunt and Ratcliffe (1959), Clark (1961) and Armitage (1962) as representing a marine transgression over the underlying shales. However, more recent studies which have placed a greater emphasis on sedimentology (Campbell and Horne, 1986; Cant, 1986; Munroe and Moslow, 1990) have consistently interpreted this contact as the scoured base of a tidal inlet fill sequence (Figure 12a). This interpretation is in agreement with the results of this study and is supported by the occurrence of numerous cored intervals in which the Halfway sandstone interval is entirely gradational with the underlying shales and siltstones, interpreted as the offshore component of a regressive shoreface sequence (Figure 12b). Following the recognition of this fact by Campbell and Horne (1986), it has become accepted practice to include these shales in the Halfway Formation, rather than in the Doig Formation as in the original definition.

The Halfway Formation, in its present lithostratigraphic definition, is simply the uppermost shallow marine sandstone beneath the Charlie Lake Formation red beds and evaporites, and is lithologically similar to sandstones in both the Doig and Montney Formations (Miall, 1976; Aukes and Webb, 1986; Wittenberg, 1992).

2.1.2 Charlie Lake Formation.

As mentioned above, the upper boundary of the Halfway Formation in the type well was defined as the point where the Halfway sandstone passed upward into a thick sequence of red beds and evaporites named the Charlie Lake Formation (Hunt and Ratcliffe, 1959). The Charlie Lake Formation contains no fauna and because of marked facies changes cannot be correlated directly with the outcrops to the west. However, the overlying Baldonnel Formation is demonstrably the equivalent of the uppermost *Lima poyana* zone of the Grey Beds, and as the lower faunal zone of the Grey Beds (*Nathorstites*) has been correlated with the Halfway Formation, Hunt and Ratcliffe (1959) infer that the beds of the intermediate Mahaffy Cliffs fauna are equivalent to the Charlie Lake Formation, adding that "the reddish nature of the (marine) Mahaffy Cliffs Beds may be indicative of some similarity" (Hunt and Ratcliffe, 1959).

Hunt and Ratcliffe (1959) and subsequent workers (Armitage, 1962; Barclay and Leckie, 1986; Cant, 1986; Campbell and Horne, 1986) regarded the Halfway-Charlie Lake contact as conformable and representing a facies transition from the shoreline deposits of

B

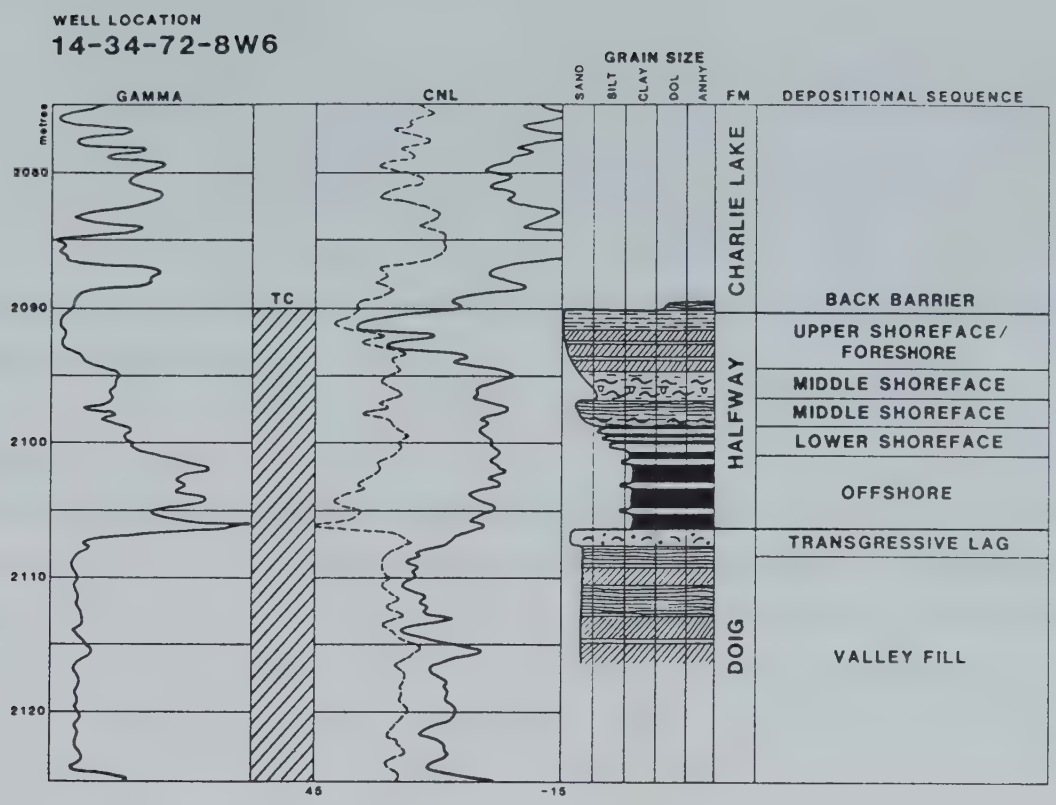

A

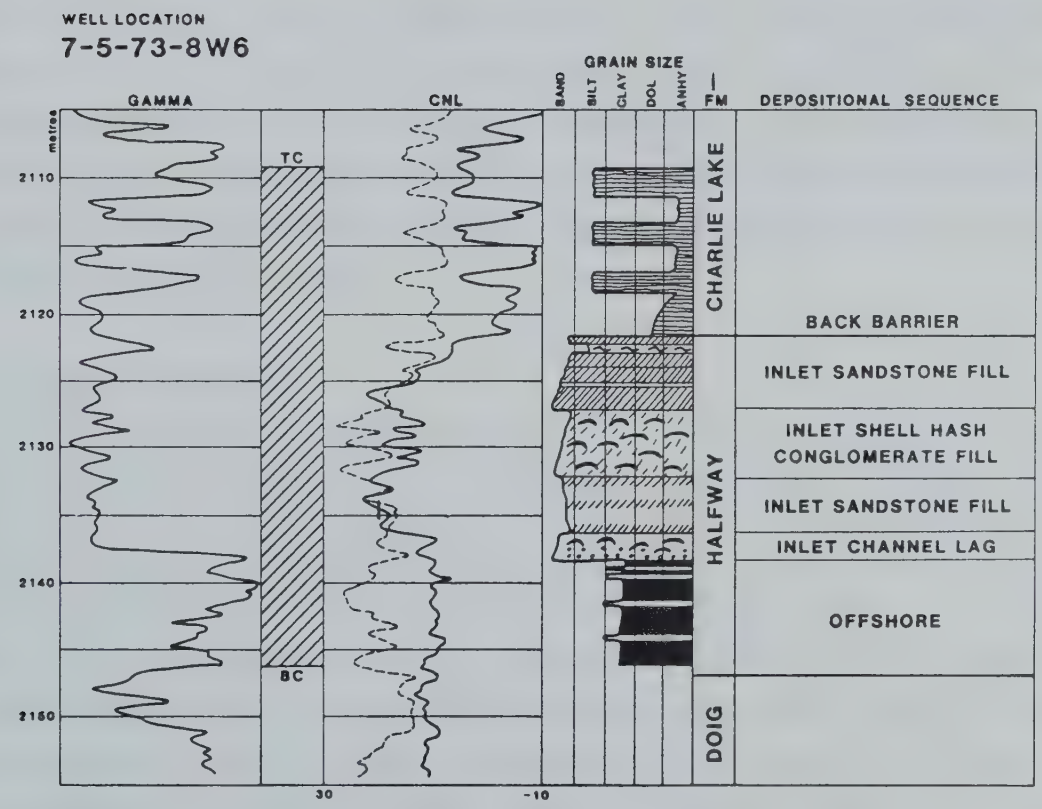

Figure 12. Currently accepted lithostratigraphic definition of the Halfway Formation showing (a) origin of sharp-based Halfway sandstones as tidal inlet channel fills, and (b) the gradational relationship of the Halfway sandstone interval with the underlying shales in shoreface sequences (after Campbell and Horne, 1986).

the Halfway Formation to time-equivalent arid coastal plain deposits of the Charlie Lake Formation. However, Campbell et al. (1989) and Campbell and Hassler (1989) state that the contact with the Charlie Lake is a major regional unconformity which progressively truncates the Halfway Formation eastward. Beyond their Halfway "subcrop edge" Campbell et al. (1989) show the Charlie Lake Formation resting unconformably on the Doig Formation (Figure 4).

2.2.0 Daiber Group.

A further modification to Middle Triassic stratigraphy in the Peace River area was made by Armitage (1962) in his discussion of oil and gas occurrences in northeastern British Columbia. He proposed that the use of the term Toad-Grayling Formations for the sequence below the Halfway Formation in the subsurface be discontinued and these Triassic beds below the Schooler Creek Group in the subsurface be raised to group status and called the Daiber Group, with the Texaco NFA Buick Creek No.7 well (06-26-87-21 W6) as the type section (Figure 13).

The top of the Daiber Group was taken at the base of the Halfway Formation as defined by Hunt and Ratcliffe (1959), ie. the base of the Halfway sandstone, and its base at the unconformity on top of the Permian or Mississippian. He subdivided it into two lithological units: a lower argillaceous siltstone which he called the Montney Formation, and an upper siltstone which he termed the Doig Formation, their boundary being marked by a prominent phosphatic zone.

2.2.1 Montney Formation.

The Montney Formation is typically a fine-grained clastic unit consisting mainly of shales (Gibson and Edwards, 1990). Its base is marked by a major unconformity on the the underlying Palaeozoic section which in the study area is the Permian Belloy Formation. A series of glauconitic sandstone units are developed at the base of the Montney Formation across west-central Alberta, probably representing successive shoreline positions as the Palaeozoic surface was transgressed (Gibson and Barclay, 1989). In some areas along its eastern erosional margin, up to four progradational cycles capped by shallow marine or deltaic sandstones are present in the Montney Formation (Miall, 1976; Gibson and Barclay, 1989). Within the shaly section to the west, several highly radioactive zones are apparent on gamma ray logs, probably representing condensed horizons associated with minor transgressions between these progradational episodes (Gibson and Edwards, 1990).

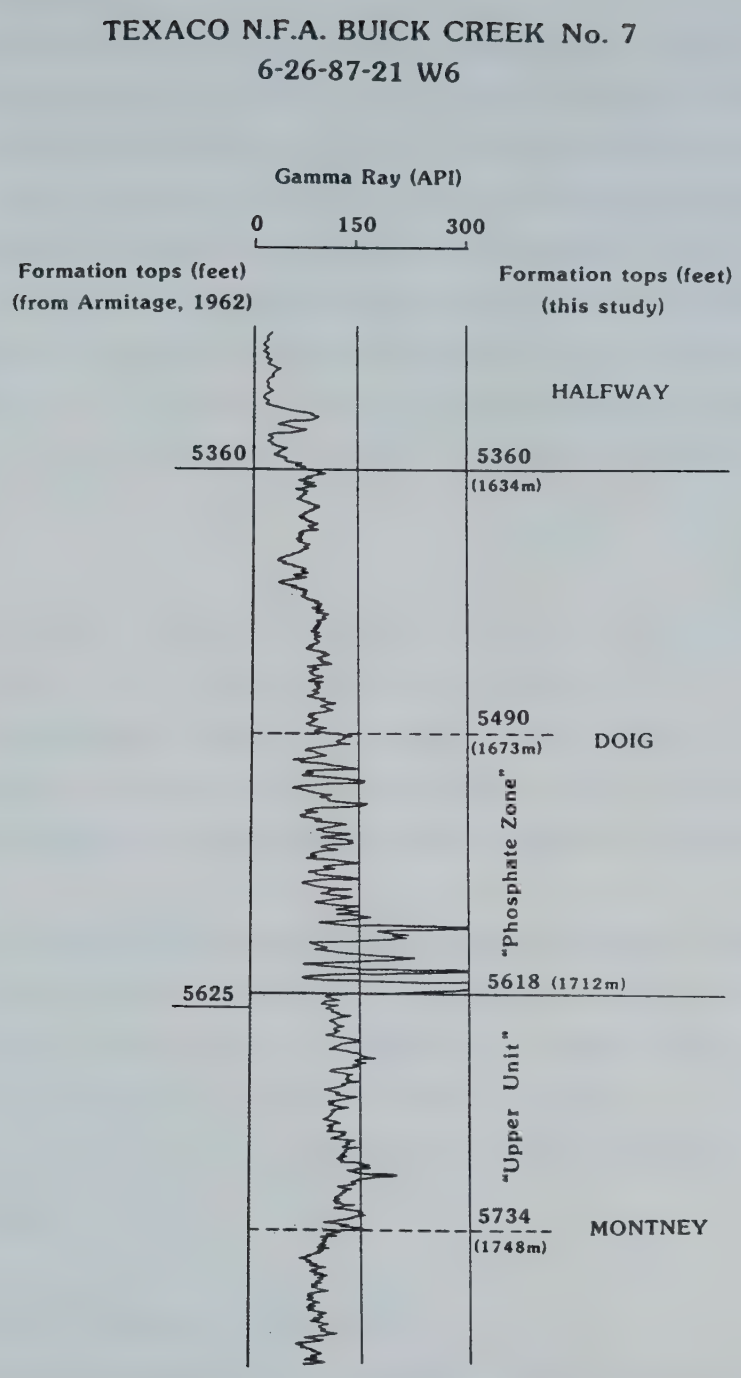

Figure 13. Type section of the Doig and Montney Formations (after Armitage, 1962; Riediger et al., 1990).

2.2.2 Doig Formation.

The Doig Formation of the lithostratigraphic nomenclature comprises a sequence of dark grey siltstone and shale. The base of the Doig Formation is characterized by a thin phosphatic sandstone or pebble conglomerate containing fish scales and bone fragments (Wittenberg, 1992), overlain by highly radioactive phosphatic shale throughout most areas of the Western Canada Basin (Gibson and Edwards, 1990). This contact has been interpreted by Gibson and Barclay (1989) as representing a major transgressive event over the Montney Formation, followed by marine shale accumulation. Gibson (1975) noted the presence of a phosphatic pebble conglomerate at this stratigraphic level in the Foothills outcrops and cited it as evidence of a hiatus associated with a transgressive disconformity.

The lower radioactive part of Doig shale section is informally referred to as the "Phosphate Zone" of the Doig Formation (Armitage, 1962). Above the "Phosphate Zone", several fine-grained upward-coarsening cycles are present in the Doig Formation. These were interpreted by Aukes and Webb (1986) and Wittenberg (1992) as regressive shoreface cycles, similar to those described above from the Montney Formation.

The upper part of the Doig Formation contains isolated linear sandstone bodies 30 m to 55m thick in certain areas, including the Wembley Field. These have variously been ascribed to incised valley systems cut following a relative drop in sea level (Campbell and Horne, 1986; Campbell and Hassler, 1989; Campbell et al., 1989) and small shelf slump features produced by slope instability (Wittenberg and Moslow, 1991; Munroe 1991; Wittenberg, 1992).

2.3.0 Discussion of Regional Stratigraphy.

The stratigraphic subdivision of the subsurface Triassic strata shown in Figure 8 is based on two type-wells located some 200 km to the northwest of the present study area. Extrapolation of the units defined in these type-wells to other areas is based largely on lithological similarity, since biostratigaphic data from the subsurface is sparse. Interpretations based on such lithostratigraphic correlations have commonly overlooked the probability that these lithologically similar units are diachronous at the scale of the basin. Studies which have placed greater emphasis on the depositional origin of the units have indicated that several depositional cycles are present in each of the Montney, Doig and Halfway Formations. Similarly, difficulties arising from purely lithostratigraphic

correlation, such as the inexplicable pinchout of sandstone units, have resulted in unconformities being placed at almost every stratigraphic level in the Triassic section.

3.0.0 DEPOSITIONAL SETTING.

Triassic strata of the Western Canada Sedimentary Basin accumulated along the western margin of the North American craton facing an ancestral Pacific oceanic area to the west known as Panthalassa (Tozer, 1982; Monger, 1989). The tectonic setting of this western continental margin during Triassic time is not well understood. Gibson and Edwards (1990) suggest it to have been "passive", implying a trailing edge similar to modern Atlantic-type continental margins. However, there are several features present in the Triassic section which suggest that the cratonic margin was not passive at this time. Dr. T. Moslow (personal communication, 1991) observed bentonite clay beds in certain cores from the Lower Triassic Montney Formation of the Ring-Border area of northeastern British Columbia which would suggest active volcanism along the continental margin during at least early Triassic time. Large shelf margin slump deposits have been identified in the Doig Formation by Munroe (1991), Wittenberg and Moslow (1991) and Wittenberg (1992) and interpreted as seismically-triggered features similar to those on the modern tectonically active Alaskan shelf. In addition, there is abundant evidence in the underlying Carboniferous to Permian sequence and Triassic of the Canadian and American Cordillera to suggest that the margin was tectonically active and probably destructive (Richards, 1989; Barclay et al., 1990).

Igneous and carbonate rocks of Triassic and early Jurassic age are widespread in the western Cordillera of North America (Figure 14). These are interpreted as island arc volcanics and associated fringing reefs which accreted to the cratonic margin during eastward subduction of the Panthalassan ocean and now form a number of fault-bounded tectono-stratigraphic terranes (Monger et al., 1982; Tozer, 1982; Mortimer, 1986; Monger, 1989). Faunal evidence suggests that the present distribution of terranes reflects considerable post-accretion northward displacement by faulting Tozer (1982), Monger et al., 1982). Northward terrane displacement is supported by the palaeomagnetic data of Irving et al. (1985), which suggests that the terranes of British Columbia were at Baja California palaeolatitudes in Cretaceous time, and presumably still further south during the Triassic. However, there is evidence of Carboniferous to Permian subduction and arc accretion along this margin (Richards, 1989), and Triassic subduction along the western United States cratonic margin (Davis et al., 1978). It is thus probable that subduction was occurring along the western Canadian cratonic margin during the Triassic, but that direct evidence of this has subsequently been displaced northward.

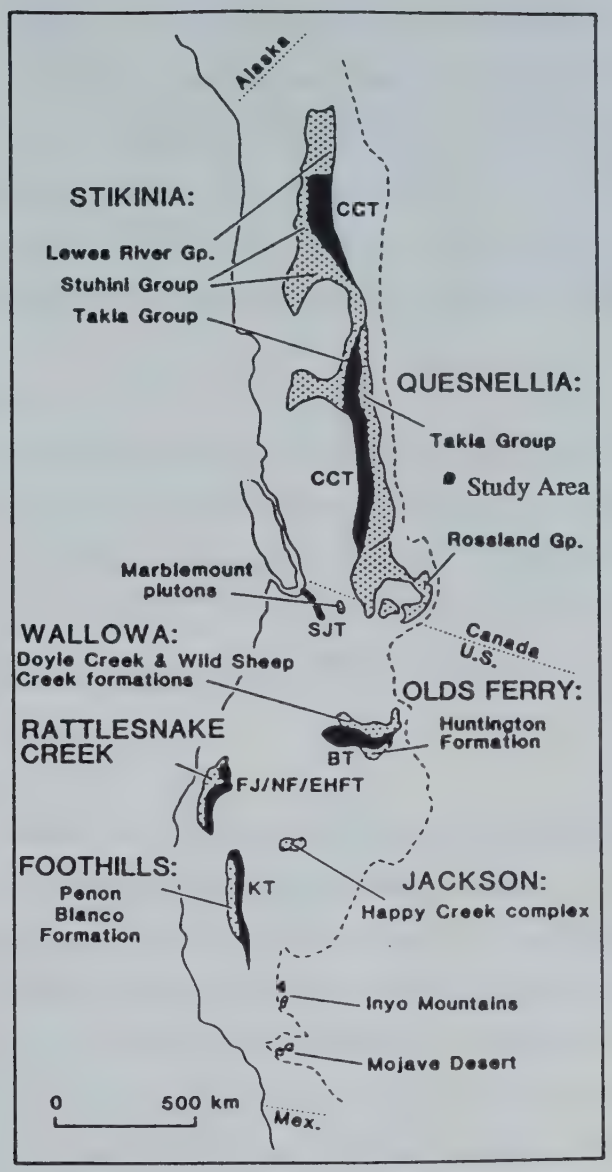

Figure 14. Map showing location of late Triassic and earliest Jurassic arc-related igneous rocks in the North American Cordillera. Stippled areas are terranes in which these rocks occur. Black areas are melange terranes containing Permian Tethyan faunas. Dashed line indicates eastern limit of Cordilleran suspect terranes (after Mortimer, 1986).

Recent plate tectonic reconstructions of western Canada during late Triassic time (Figure 15) show the cratonic margin separated from an offshore island arc by a back-arc basin, but again make no estimate as to the width of this separation. Monger (1989) states that by the late Triassic, a relatively continuous west-facing arc extended from the Yukon to southern California. Most of this arc was built on earlier deformed Palaeozoic arc and marginal basin deposits, but in the southwestern United States it formed on the continental margin. Monger (1989) describes the setting on the cratonic margin itself as "a complex passive margin, with varying rates of extension, subsidence and flexure".

3.1.0 Sediment Source.

Palaeocurrent and provenance studies of Triassic sediments in outcrop (Pelletier, 1963; Gibson, 1975) indicate that they were sourced largely from Permian and Carboniferous sedimentary rocks exposed on the craton to the east. The lack of westerly-derived clastic sediments further suggests that if a volcanic island arc was present along the cratonic margin during the Triassic, it was too far offshore to shed any clastic detritus eastwards onto the continental margin.

Most of the clastic Triassic sediments are at least second cycle deposits and generally tend to be texturally and mineralogically mature. They are also typically very fine grained, suggesting that the source area to the east was of relatively low relief. While deltaic deposits have been described from the Montney and Doig Formations of west-central Alberta, none are presently known from the Halfway Formation. Campbell and Horne (1986) therefore speculate that the only significant area of clastic input into the basin during middle Triassic time was in northeastern British Columbia, with the sediment transported along the coastline by longshore currents. Bioclastic sediment is also an important component of Middle Triassic deposits and tends to be concentrated as lags in reworked shelf sandstones and tidal inlet channel fills.

3.2.0 Palaeoclimate.

Palaeomagnetic data (Habicht, 1979; Irving et al., 1985) places the study area at approximately 30° N of the palaeoequator during early and middle Triassic time. At present, above 30° N latitude winds blow from west-to-east (westerlies). Campbell and Horne (1986) have inferred from this that Triassic winds in the study area would have been dominantly from the west. These onshore westerly winds would have generated a wave regime resulting in southeasterly longshore currents, carrying sediment down-drift to the southeast from areas of sediment influx. To support his hypothesis, they produce a

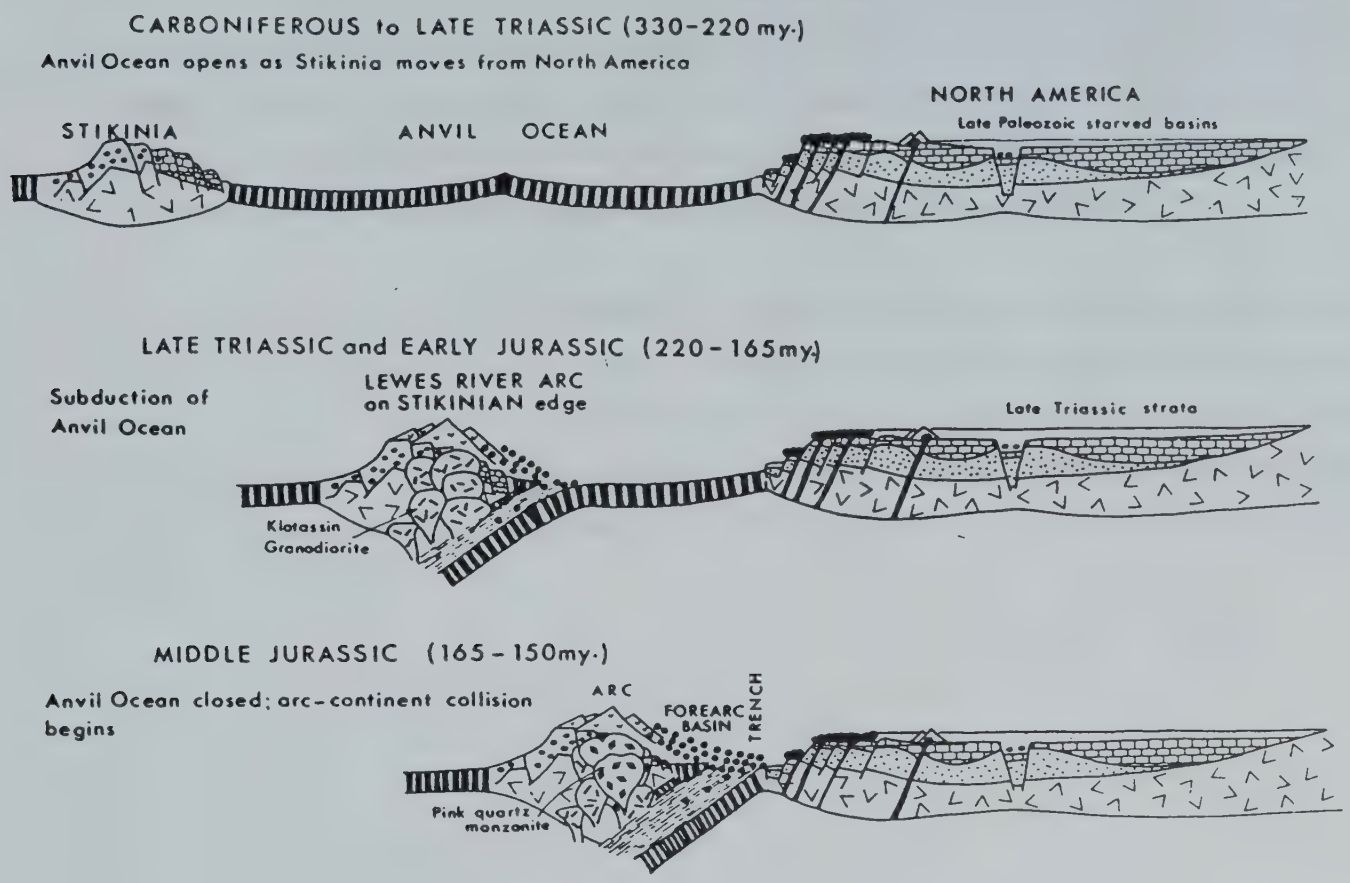

Figure 15. Schematic plate tectonic reconstructions of the western margin of North America from the Carboniferous to Middle Jurassic, based on data from the Yukon. The width of the subducting ocean during late Triassic time is not known (after Tempelman-Kluit, 1979).

graph showing a progressive decrease in Halfway Formation sandstone grainsize from north-to-south over some 200 km. It is not clear whether this represents data from a single facies such as beach sands, or is collected from random stratigraphic intervals within the Halfway. If the latter, the variation in grainsizes between facies noted in this study makes the plot meaningless. In addition, samples were probably collected from a number of different Halfway progradational cycles. Any variation in sediment supply between successive progradational events would tend to defeat the object of demonstrating a progressive fining of grainsize along any one particular Halfway coastline.

Less tenuous sedimentological climatic indicators associated with the Halfway and Charlie Lake Formations, such as sabkha anhydrites, crypt-algal-laminated dolomites and red beds (Roy, 1972; Barclay and Leckie, 1986; Campbell and Horne, 1986; this study), are found today in arid to semi-arid climatic zones within about 35° north or south of the equator. This is consistent with the 30° N middle Triassic palaeolatitude derived from palaeomagnetic data.

4.0.0 SEDIMENTARY FACIES.

The following pages contain descriptions and sedimentological interpretations of the thirteen facies identified in this study. These facies are labelled A to M and are summarised in Table 2. Facies B to F and I to M would be included in the lithostratigraphic Halfway Formation in the sense of Campbell and Horne (1986). Facies A would lithostratigraphically be referred to the Doig Formation in the Wembley area, and Facies G and H to the lower part of the Charlie Lake Formation.

Following the process sedimentological approach of Siemers and Tillman (1981) outlined in section 1.6.1, each facies was established on the basis that its internal features characterised it as having been formed by significantly different sedimentary processes than units above and below it. These internal features consisted of lithology, bounding contacts, primary physical and biogenic sedimentary structures, secondary soft-sediment deformation features, and later diagenetic overprinting.

There is some degree of overlap between different facies in certain instances due to their having been deposited in adjacent depositional environments. While the end members of such gradational facies are readily distinguished, intermediate examples may be more difficult to classify. In such cases, the vertical facies succession was used to assign the facies to one of the end members for the purpose of labelling the core descriptions in Appendix A.

The scale bar in all photographic plates is in centimetres.

4.1.0 Facies A. Bioclastic Sandstone.

The stratigraphically lowest facies identified in cores cut from the Halfway Formation is a thin (0.3-2m) bioclastic sandstone herein referred to as Facies A. Facies A sandstone rests erosively or abruptly on sandstone and siltstone referred to as the lithostratigraphic Doig Formation in the Wembley field. Where the Doig Formation is developed as a siltstone, this contact is readily apparent, but in areas where sandstone is present at the top of the Doig, the sand-on-sand contact is often obscure. In the southwestern part of the study area, Facies A is also present <u>within</u> the Halfway Formation and rests sharply on Facies C (offshore-shoreface transition) or D (lower shoreface). The Facies A of this study corresponds to the Facies C2 of Wittenberg (1992).

Facies	Lithology	Thickness	Bedding Features	Physical Sedimentary Structures	Biogenic Sedimentary Structures	Depositional Environment
A	Bioclastic Sandstone	0.3-2m	Erosional base	Oscillation ripple cross-lamination Thin HCS beds	*Planolites* *Skolithos*	Transgressive Shoreface
B	Black shale	2-4m	Thin normally graded siltstone beds	Horizontal lamination	*Palaeophycus* *Chondrites* (Both rare)	Offshore
C	Interlaminated green shale, siltstone and very fine sandstone	3-5m	Sharp-based HCS beds	Horizontal and lenticular laminae Oscillation ripple cross-lamination	*Planolites* *Palaeophycus* Escape Traces	Offshore - Shoreface Transition
D	Burrowed Silty Sandstone	2-4m	Biogenic sedimentary structures may dominate physical ones	Oscillation ripple cross-lamination. Amalgamated HCS beds	*Planolites* *Palaeophycus* *Terebellina* *Teichichnus* *Asterosoma* *Rosselia* *Skolithos* *Monocraterion* *Thalassinoides*	Lower Shoreface
E	Clean Sandstone	2-4m	Scour surfaces	Cross-bedding Plane lamination	*Skolithos* Escape Traces	Upper Shoreface
F	Black and White Chert Sandstone	0.5m	Rarely present	Sub-horizontal plane lamination. Inversely graded laminae.	None	Foreshore
G1	Interlaminated anhydrite and dolomite mudstone	0.3-1m	Crypt-algal lamination	Dessication cracks	None	Evaporitic Intertidal flats
G2	Grey dolomite mudstone	0.3-1m	Stylolites	Massive. Solution-collapse breccias.	Bioturbation.	Hypersaline lagoon
H	Red mudstone, siltstone, and anhydrite	> 4m	Chaotic mudstone-evaporite mixture	Mud-chip-conglomerates Nodular anhydrite	Bioturbation	Supratidal flat (Sabkha)
I	Sandy dolomitic coquina with mud clasts	0.2-2m	Erosional base	Massive Cross-bedding Mudstone laminae	*Glossifungites* assemblage at erosional base	Tidal inlet channel lag and active inlet fill
J	Slightly bioclastic sandstone	0-6m	Gradational and interbedded with Facies I and K.	Cross-bedding Current ripple cross-lamination. Mudstone laminae	*Skolithos* *Terebellina*	Active tidal inlet channel fill
K	Interlaminated sandstone and mudstone	0-5m	Frequent alternation between traction and suspension deposition	Current ripple cross-lamination, flaser and wavy bedding, load casts	*Planolites* *Palaeophycus* *Terebellina* *Skolithos* *Teichichnus* Escape Traces	Abandoned tidal inlet channel fill
L	Clean sandstone	2-9m	Erosional or loaded base Scour surfaces with coarse lags	Cross-bedding Gently inclined plane lamination Adhesion lamination	Escape traces	Ebb tidal delta
M	Granular cherty Sandstone	0.5-6m	Amalgamated sharp-based beds with lags	Sub-horizontal plane lamination with minor cross-bedding Adhesion lamination	None	Washover

Table 2. Summary of Halfway Formation sedimentary facies identified in this study.

The upper contact of Facies A is typically sharp and overlain by black shale of Facies B (Plate 1). In some instances *Skolithos* and *Planolites* burrows were observed to extend down into Facies A from this contact suggesting a hiatus or very slow rate of deposition (eg. well 6-8-74-8-W6; Appendix A). In some cored sequences however, Facies A sandstone grades up into Facies B black shale via 10-20cm of interlaminated shale and lenticular-bedded silty sandstone.

Facies A sandstone is generally poorly sorted and contains small siltstone clasts, quartz granules, bioclastic debris (bivalves and inarticulate brachiopods) and commonly brown phosphatic coatings on many of the grains. This coarse-grained sandstone is typically massive, but oscillation ripple cross-lamination and hummocky cross-stratification were observed in several cores.

The constituent grains of Facies A represent the coarsest fragments seen in the underlying Doig Formation sediments. Their concentration in one bed suggests a period of winnowing of the substrate, leaving a coarse lag. This is supported by the typically erosive base of Facies A. The rare occurrence of oscillation ripple cross-lamination suggests that this winnowing was performed by oscillatory waves and therefore occurred in a shallow marine setting, probably above mean fairweather wavebase. The common phosphate coatings on many of the grains tends to suggest that net sedimentation rate was very low. Taken together, these features suggest that Facies A was formed by a prolonged period of wave-reworking of the seafloor, producing a thin, coarse-grained lag. Beds within Facies A displaying hummocky cross-stratification probably represent episodic storm deposits which were not entirely reworked by fairweather wave action. Such beds of wave-reworked sandstone displaying hummocky cross-stratification are commonly associated with deposition during a marine transgression (eg. Swift, 1975; Winn, 1991).

If Facies A is to be interpreted as a transgressive shoreface deposit, then the erosion surface beneath Facies A sandstone would represent the actual shoreface erosion surface (or "ravinement surface" of Swift (1968)), and the burrowed upper surface a condensed horizon prior to deposition of the overlying Facies B regressive marine black shales (Loutit et al., 1988). However, Kumar and Sanders (1970) suggest that many "transgressive sands" may in fact be the basal lag of tidal inlet channel fill sequences, the upper part of which was removed by transgressive shoreface erosion. In this situation, the erosion surface beneath Facies A would represent the basal scour of the tidal inlet

Plate 1. Sharp contact between Facies A bioclastic sandstone below and Facies B black shale above. Well 6-31-72-7-W6. 2054 m.

channel, and the upper surface of Facies A would be the shoreface erosion surface. The simple transgressive lag interpretation is favoured for Halfway Facies A for three reasons:

1) Although Facies A bioclastic sandstone does bear some similarity to the bioclastic sandstone of Facies I, interpreted as a tidal inlet channel lag, there are significant differences. Firstly, Facies A was never observed to contain clasts of lagoonal dolomitic mudstone, which are ubiquitous in Facies I. Secondly, Facies A does contain abundant grain-coating phosphate, which is not common in Facies I. These observations suggest that Facies A and I have different origins.

2) Facies A is present throughout the study area, which would not be expected of remnant tidal inlet deposits.

3) Occurrences of hummocky cross-stratification in Facies A are difficult to reconcile with an origin as a tidal inlet channel lag. This structure is common however, in transgressive shelf sediments affected by storms (Elliot, 1986).

Facies A is therefore interpreted as a thin shoreface deposit produced by wave reworking of the seafloor during a marine transgression. Rare interbedded hummocky cross-stratified sandstone beds were deposited during storms and escaped extensive fairweather reworking.

4.2.0 Facies B. Laminated Black Silty Shale.

Facies B is a unit of finely laminated black shale which rests abruptly on the bioclastic sandstone of Facies A (Plate 1). Facies B shales range from 2-4m in thickness and grade upward into the interlaminated siltstone and green shale of Facies C.

In a few cored sequences, irregular sandstone laminae were observed in the black shales directly above the contact with Facies A. These sandstone laminae are generally conformable to bedding and associated with microfaulting, but in some instances are highly contorted and cross-cut the shale laminae (eg. wells 8-9-72-8-W6 and 7-5-73-8-W6; Appendix A). This feature was probably caused by injection of the Facies A sandstone into the shales during burial compaction.

The lower 10-20cm of Facies B consists of finely laminated black shale or massive mudstone. Using the simple test outlined by Swanson (1981), it was found that the shale

had a measurable phosphate content. Spectral gamma-ray log readings show that uranium radioactivity levels over this lower unit of Facies B are higher than the rest of the interval, suggesting that uranium may be bound up in the phosphate.

The finely laminated phosphatic shale at the base of Facies B grades upward into more fissile black shale with an increasing silt content. Siltstone is present as both millimetre-thick pale grey laminae which give the rock a "pinstriped" appearance, and thicker, lenticular silt laminae (Plate 2). The frequency and thickness of these siltier laminations increases upward through Facies B to 4cm toward the top of the unit. The thicker siltstone laminae have sharp bases and display subtle normal grading from silt to clay (Plate 3). Although typically separated by several centimetres of laminated silty shale in the lower part of the section, toward the top of the Facies these siltstone laminae are sometimes amalgamated. A few of the thicker siltstone beds in the upper part of the facies also display sub-horizontal and divergent laminae arranged in erosive sets (Plate 4). This is interpreted as hummocky cross-stratification.

Trace fossils are very rare in Facies B. *Palaeophycus* burrows 3mm in diameter were observed in the upper part of the facies, together with one occurrence of *Chondrites* (well 6-32-72-7-W6; Appendix A). No body fossils were found in Facies B during the course of this study. Cant (1986) reports the presence of acritarchs, a strictly marine group. Gallagher and Jenkins (1988) examined samples of Facies B from the Wembley area for their microfaunal content. They recovered only badly corroded and unidentifiable agglutinated foraminifera.

Pyrite in the form of nodules 5mm to 1cm in diameter and impregnations of siltstone laminae are common in Facies B, as are anhydrite nodules up to 5cm in diameter. In many cases these anhydrite nodules can be seen to cut across lamination and are clearly a later diagenetic feature, but in some instances laminae in the shale were observed to deflect around the nodules, indicating that they grew within the sediment while it was still soft.

The finely laminated mud and silt characteristic of Facies B was produced by deposition of the fine-grained sediment from suspension. The documentation of acritarchs by Cant (1986) indicates that these shales were deposited in a marine environment. This is consistent with the stratigraphic position of Facies B at the base of a conformable upward-coarsening vertical facies association interpreted as a regressive marine shoreface

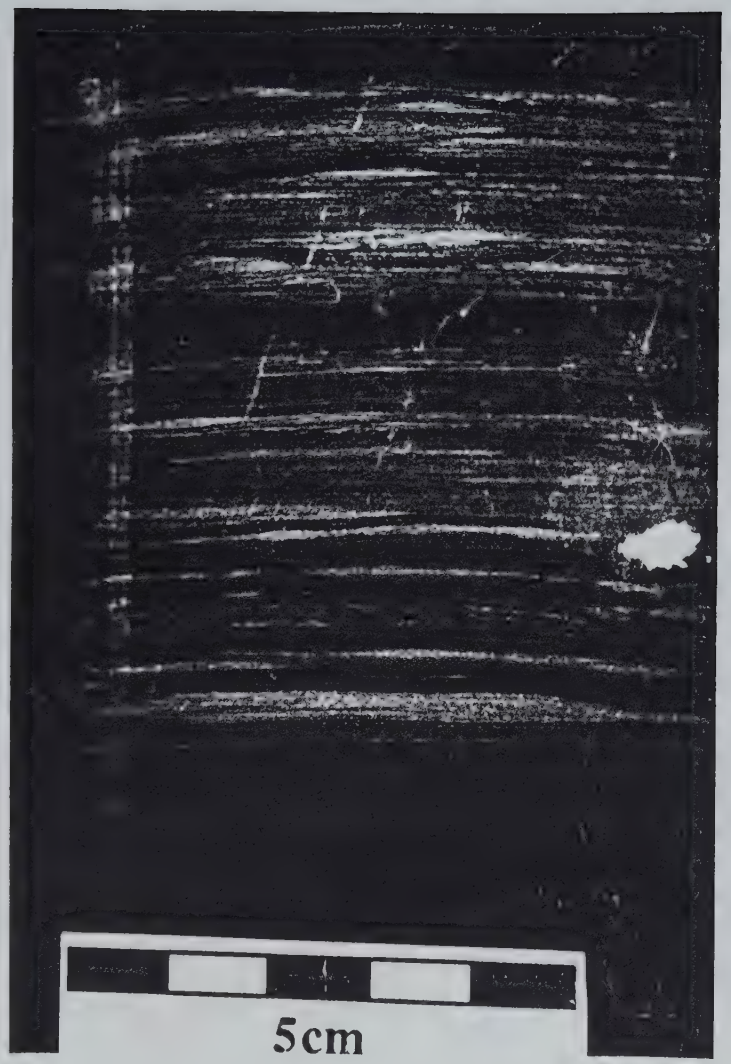

Plate 2. Lenticular siltstone laminae in the upper part of Facies B shale. Well 14-22-73-7-W6. 2015 m.

Plate 3. Sharp based and normally graded siltstone beds in Facies B shale. Well 6-22-72-8-W6. 2215 m.

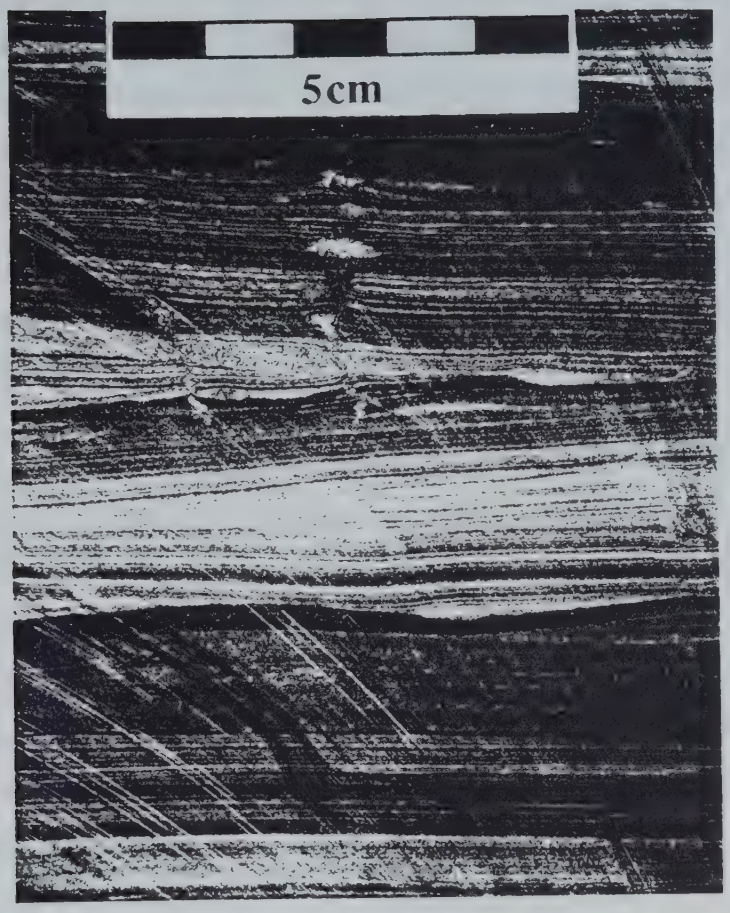

Plate 4. Hummocky cross-stratified siltstone beds in the upper part of Facies B shale. Note small escape trace in upper-centreof view. Well 8-9-72-8-W6. 2298 m.

deposit. The rarity of current-formed sedimentary structures in Facies B indicates that deposition took place mainly below mean stormweather wavebase, with only a few waves feeling the bottom to produce the lenticular siltstone laminae. The normally graded siltstone beds probably represent settling out of slightly coarser-grained sediment entrained by storm waves and carried offshore in the manner described by Reineck and Singh (1972). The rarer siltstone laminae at the top of Facies B which display hummocky cross-stratification were deposited by oscillatory storm waves at approximately stormweather wavebase. The observed upward increase in thickness and frequency of these storm-generated beds within Facies B is consistent with an increasing influence of storm-generated currents in a prograding marine shoreface (Aigner and Reineck, 1982). Facies B is therefore interpreted as a product of suspension deposition in the marine offshore at depths below mean stormweather wave base.

The thin, radioactive, phosphate-rich interval at the base of Facies B probably represents a condensed section. Condensed sections are thin marine beds consisting of pelagic or hemipelagic sediments which accumulate during periods of very low sedimentation, commonly facilitating the concentration of authigenic minerals such as glauconite, phosphate, and siderite (Loutit et al., 1988). They tend to be most widespread at times of maximum regional transgression of the shoreline, when landward movement of depositional loci effectively starves shelf areas of terrigenous material. This is consistent with the position of the phosphatic bed immediately above the Facies A transgressive sandstone.

The lack of bioturbation and benthic microfossils and the presence of early diagenetic pyrite and anhydrite nodules indicate that Facies B is not a typical marine shale. The virtual absence of any bottom-living macro- or microfauna and the restricted trace fossil assemblage suggest that the substrate was probably strongly dysaerobic. Cant (1986) suggests that this oxygen deficiency may have been due to a salinity-stratified water column (halocline). Although the sedimentological evidence from the Charlie Lake Formation that Cant invokes does indicate that the necessary evaporative conditions were prevalent during late Triassic time, there is presently no conclusive evidence to support the presence of an offshore island arc to effectively restrict circulation with the open Panthalassan ocean to the west (Gibson and Barclay, 1990). Such restricted oceanic circulation is necessary to maintain a halocline. In addition, Heckel (1977) in a review of similar Pennsylvanian phosphatic black shales in the eastern United States pointed out that if such a barrier "were effective enough to cut off bottom circulation with the more

open sea during maximum transgression, then later shallowing should cause the sill to become increasingly effective and eventually to isolate the sea completely". As with Heckel's example, regressive strata conformably overlying the Halfway black shale do not show any evidence of increasing restriction, such as the presence of halite pseudomorphs. It is therefore felt that the development of a halocline in a restricted basin is not a suitable explanation of the anoxic conditions recorded in the Halfway shale.

Vertical density stratification can also result from an abrupt temperature difference (thermocline) between warm surface water and significantly colder bottom water. In this case, a barrier to restrict bottom water circulation and maintain anoxic conditions is necessary only if the water available to circulate into the basin at depth is rich in oxygen. In modern oceans, the base of the warm upper photic zone is marked by an oxygen-minimum zone resulting from decay of organic matter that settles below the level of net oxygen replenishment by photosynthesis. In the eastern Pacific this zone is nearly depleted in oxygen and extends from about 80m to 800m in depth (Heckel, 1977 and references therein). Therefore, any bottom circulation in from the open ocean below the thermocline would supply colder water from the oxygen-minimum zone and not significantly replenish bottom oxygen. Along the western coasts of southern Africa, Peru, Morocco and Australia, cold deeper water rises along the continental margin. This deeper water is not only poor in oxygen, but also rich in phosphate which has been concentrated in the oxygen-minimum zone from the decay of settling organic matter. As this deeper water upwells, it replenishes phosphate in the oxygenated sunlit surface waters and supports an enormous population of phytoplankton. Much of the organic matter from these phytoplankton blooms eventually settles into the oxygen-minimum water moving shoreward at depth below the thermocline, where it decays and further depletes what little oxygen is there. Thus where the upwelling waters are moving up onto a relatively shallow body of water such as the continental shelf, anoxic bottom waters are produced.

This model for producing anoxic conditions is considered a better analogy for the Halfway Formation for two reasons other than the lack of a demonstrable circulation barrier during the Middle Triassic. Firstly, the absence in Middle Triassic strata of western Canada of corals and other warm water faunas such as megalodont bivalves and sponges found in similar aged deposits elsewhere lead Tozer (1982) to infer that the basin waters were cold. Secondly, phosphate, which is a prominent feature of sediments accumulating in the above-mentioned areas of cold coastal upwelling, is abundant

throughout the marine Triassic section, particularly those shale sections of the Montney and Doig Formations interpreted as outer shelf deposits (Wittenberg, 1992).

Along the continental margin of South West Africa, the upwelling Benguela Current has produced a belt of anoxic sediment close to shore. Siesser and Rogers (1976) have documented authigenic pyrite and gypsum from these shelf mudstones which maybe analogous to the pyrite and anhydrite nodules observed in the Facies B shales. The model they propose for the formation of these minerals involves the reduction of sulphate in seawater by the anaerobic bacteria which thrive in the anoxic substrate. This initiates the formation of hydrogen sulphide and the reaction of this compound with iron minerals present in the sediment eventually forms pyrite. This strongly reducing, low pH environment has the effect of dissolving the tests of calcareous plankton and saturating the sediment with calcium. The abundance of dissolved calcium combined with sulphate in the seawater leads to the precipitation of gypsum, which upon later burial would convert to anhydrite. Similar authigenic gypsum occurrences in marine mudstones are described by Briskin and Schreiber (1978) and Muza and Wise (1983). However, in none of the examples they discuss do authigenic gypsum crystals appear larger than several millimetres in length, an order of magnitude smaller than the nodules observed in the Facies B shales. It may be that later remobilization of calcium sulphate produced the larger nodules seen in the Halfway and Doig Formation shales.

This dissolution of calcareous microorganisms along the South West African coast during gypsum formation means that despite their abundance in the water column, they have low preservation potential. This process was investigated by Schnitker et al (1980) who found that virtually all calcareous microfossils in their samples were destroyed during the course of gypsum formation in a matter of a few months. This may explain the paucity of microfossils in the Halfway shales, where only a few corroded agglutinated forms can be identified (Gallagher and Jenkins, 1988).

4.3.0 Facies C. Interlaminated Green Shale and Siltstone.

Facies C grades upward from a silty shale where it is completely gradational with Facies B to a sandy siltstone at its upper gradational contact with Facies D. The facies is typically an olive green silty shale interlaminated with grey siltstone (Plates 5 and 6).

The lower part of the facies is similar to the laminated shale of Facies B, but distinguished by the appearance of current formed sedimentary structures. This is also

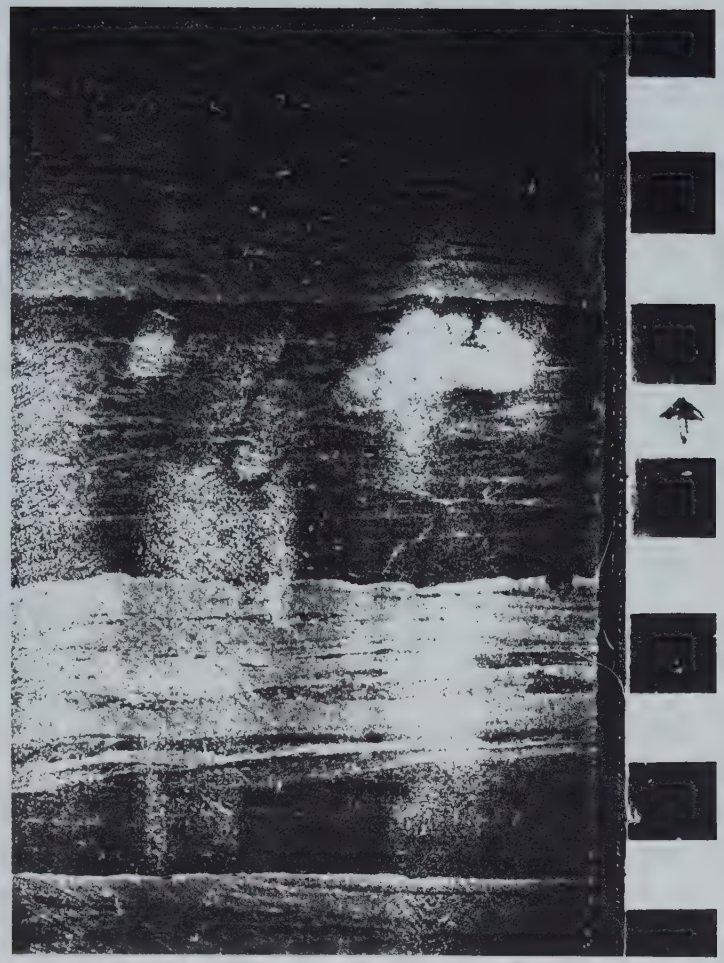

Plate 5. Interlaminated silty shale (pale) and siltstone (dark) from the lower part of Facies C. Well 14-17-72-7-W6. 2116 m.

Plate 6. Interlaminated siltstone (dark) and combined-flow ripple-bedded very-fine grained sandstone (pale) from the upper part of Facies C. Well 14-3-73-8-W6. 2090 m.

commonly associated with a colour change from black to olive green silty shale and the appearance of some trace fossils. Traces of pyrite are present in the green shales but in much lesser quantities than Facies B. Together these observations suggest that the substrate was better oxygenated than in areas where Facies B accumulated, probably as a direct result of the currents which formed the sedimentary structures.

The green silty shale units are typically 1-2 cm thick and are horizontally laminated similar to the underlying Facies B shales. The intervening siltstone laminae are more variable, but generally less than 2 cm thick. Most have sharp (possibly erosional) or loaded bases with flame structures, and internally may be massive, plane laminated or display oscillation ripple cross-lamination. Syneresis cracks are particularly abundant in the green shale laminae of Facies C.

Trace fossils are relatively rare in the lower part of Facies C and consist of *Planolites* and *Palaeophycus* burrows with a few small escape traces. They become more abundant upward but no more diverse.

Silty sandstone beds up to 10cm thick with sharp, erosional, or loaded bases are also present in this facies. These sandstone beds commonly contain concentrations of thin black phosphatic shell valves and fragments at the base (Plate 7) and are subtley normally graded. The dominant sedimentary structure displayed is sub-horizontal lamination, which was observed to either converge or diverge slightly across the width of the core (Plate 8). The laminae are grouped into sets ranging from 2-5cm in thickness in which the set boundaries are defined by low angle truncation of the laminae. Individual escape traces were observed to cut through successive lamina sets, indicating that they were deposited by a single rapid sedimentation event. The sub-horizontal laminations are interpreted as hummocky cross-stratification. In many of the sandstone beds this hummocky cross-stratification is seen to grade upward into oscillation or combined-flow ripple cross-laminated sandy siltstone and then horizontally laminated muddy siltstone. In other cases however, the upper part of the bed is not present, either due to subsequent burrowing activity or truncation beneath another such bed.

Similar sharp-based and normally graded sandstone beds in sections of otherwise muddy shelf sediments have been described by Hayes (1967), Reineck and Singh (1972), Kumar and Saunders (1976), Kreisa (1981) and Nelson (1982) among others. All agree that the beds have an origin in storm activity, but disagree on the exact relationship between

Plate 7. Sandstone bed of storm origin with basal lag of black phosphatic shell fragments. Facies C. Well 8-1-72-9-W6. 2401 m.

Plate 8. Hummocky cross-stratification in storm-generated sandstone bed, Facies C. Note divergence of laminae (arrowed). Well 14-22-73-7-W6. 2011 m.

storm activity and sedimentary processes which shaped the final sedimentary structures. Hayes (1967) noted the appearance of such a bed on the central Texas continental shelf following the passage of Hurricane Carla in 1961. He believed that the coastal set-up created during the storm subsequently ebbed offshore and entrained sediment as a bottom-flowing turbidity current. Waning of this storm-generated turbidity current was envisioned to be responsible for deposition of the graded sand layer.

However, Reineck and Singh (1972) and Kumar and Saunders (1976) both noted the common report from ships that stormy seas are frequently sediment-laden and therefore questioned the need to invoke a turbidity current to suspend and transport the sand. They suggested that sand was thrown into suspension by the scouring action of large oscillatory storm waves and later settled out as the storm subsided. This deposition from suspension during the waning of a storm accounted for the apparently horizontally laminated and normally graded sand layers that they observed in their piston cores. It has subsequently been recognised, particularly in ancient examples (eg. Kreisa, 1981), that the "horizontal" lamination observed in many of these storm sand layers is in fact hummocky cross-stratification. Despite numerous experimental studies (eg. Duke et al., 1991) and measurements of storm weather shelf currents (Morton, 1981; Snedden et al., 1988), the exact physical processes responsible for the formation of hummocky cross-stratification are presently not fully agreed upon. In a synthesis of palaeocurrent data from many ancient shoreface sequences, Leckie and Krystinik (1989) suggest that the structure is formed by high-energy oscillatory waves of storm origin with a weak, shore-normal, combined flow component.

In conclusion, Facies C is dominated by horizontal lamination produced by deposition of fine-grained sediment from suspension, but with an increasing proportion of siltstone than in the underlying Facies B. Many of the thicker siltstone laminae in Facies C also show evidence of deposition from traction currents in the form of oscillation and combined-flow ripple cross-lamination. The oscillation ripple cross-lamination indicates that these traction currents were oscillatory and thus wave-generated. However, the lack of <u>persistent</u> background current activity suggests that Facies C accumulated below mean fairweather wave base, so the ripple cross-laminated siltstone beds are probably the result of larger episodic storm waves feeling the bottom further offshore. More intense storms generated thicker silty sandstone beds displaying hummocky cross-stratification. Facies C is therefore interpreted to have accumulated largely in the marine offshore-shoreface transition zone between mean storm-weather and fair-weather wavebase.

4.4.0 Facies D. Oscillation Ripple Cross-Laminated Sandstone.

Facies D typically consists of oscillation ripple cross-laminated very-fine grained sandstone with an upwardly decreasing silt and clay content. It is transitional with Facies C below, but its upper contact with Facies E is commonly sharp.

Distinct siltstone and silty mudstone laminae similar to those in Facies C persist in the lower part of this facies, but tend to become subordinate to oscillation and combined-flow ripple cross-laminated siltstone and very fine grained sandstone upward (Plate 9). Units of wavy and flaser bedding do, however, occur throughout the facies. These features indicate an upward increase in the dominance of persistent traction current transport processes over the deposition from suspension characteristic of Facies B and C. The common oscillation ripple cross-lamination indicates that these traction currents were oscillatory and thus wave generated. Facies D is therefore interpreted to have accumulated largely above mean fair-weather wavebase, a bathymetric zone termed the lower shoreface (Elliot, 1986).

There is a marked increase in the number, size and diversity of trace fossils observed in Facies D compared to the lower units and in many cases the unit is well burrowed (Plate 10). The assemblage is dominated by infaunal dwelling and feeding traces. Most common are *Planolites* and *Palaeophycus*, both more robust than seen in Facies C. Other ichnogenera include *Teichichnus, Terebellina, Rosselia, Asterosoma, Monocraterion, Skolithos* and *Thalassinoides* in order of decreasing importance.

Within Facies D, there are beds of very fine sandstone up to 30 cm thick similar to those described from Facies C. These sandstone beds typically have erosional or loaded bases with a lag of shell fragments, quartz granules and small mudstone clasts (Plate 11). Whole valves of the inarticulate brachiopod genus *Lingula* were observed in one of these beds in the well 16-29-72-8-W6 (Appendix A). An idealized sequence of sedimentary structures in one of the beds consists of: hummocky cross-stratification, combined-flow ripple cross-lamination, and at the top horizontally laminated siltstone. Not all of these features are seen in every such bed, especially the upper portion which is commonly destroyed either by later burrowing activity or normal fairweather wave processes (Plate 12). In several cored sequences (eg. well 11-25-72-8-W6; Appendix A), Facies D is dominated by amalgamated units of these sandstone beds. These hummocky cross-stratified sandstone beds are interpreted as the more proximal parts of the storm-

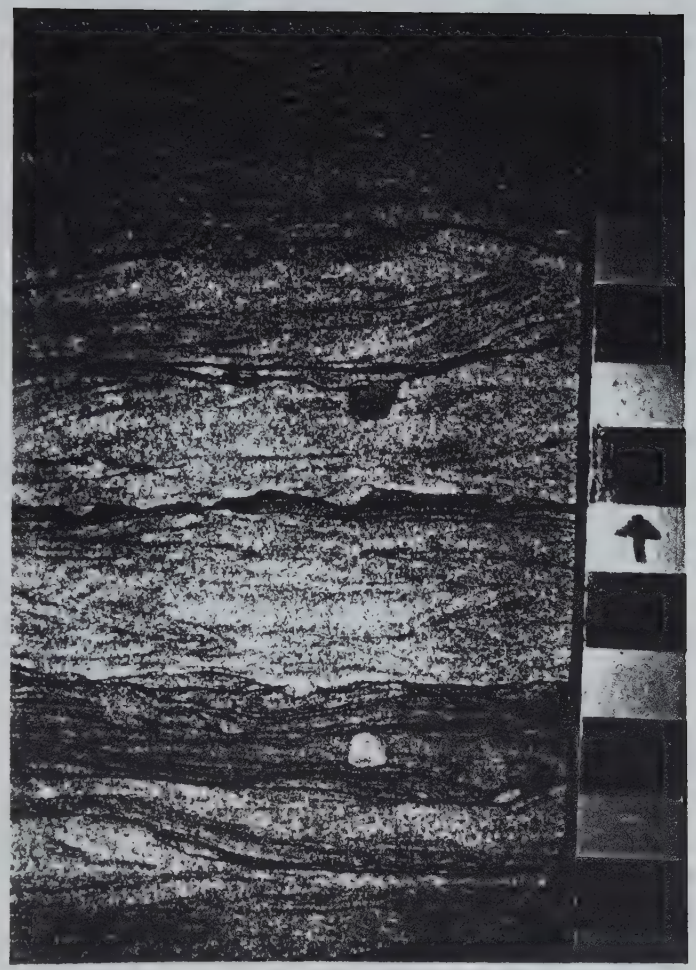

Plate 9. Facies D oscillation ripple cross-laminated very-fine grained sandstone with some burrows. Well 16-8-73-8-W6. 2138 m.

Plate 10. Well burrowed very-fine grained sandstone. Almost all physical sedimentary structures have been destroyed. Facies D. Well 16-23-72-8-W6. 2144 m.

Plate 11. Storm-generated sandstone bed, Facies D. Note basal lag of mudstone clasts and escape trace at upper-right, indicating rapid deposition of the bed. Well 11-25-72-8-W6. 2126 m.

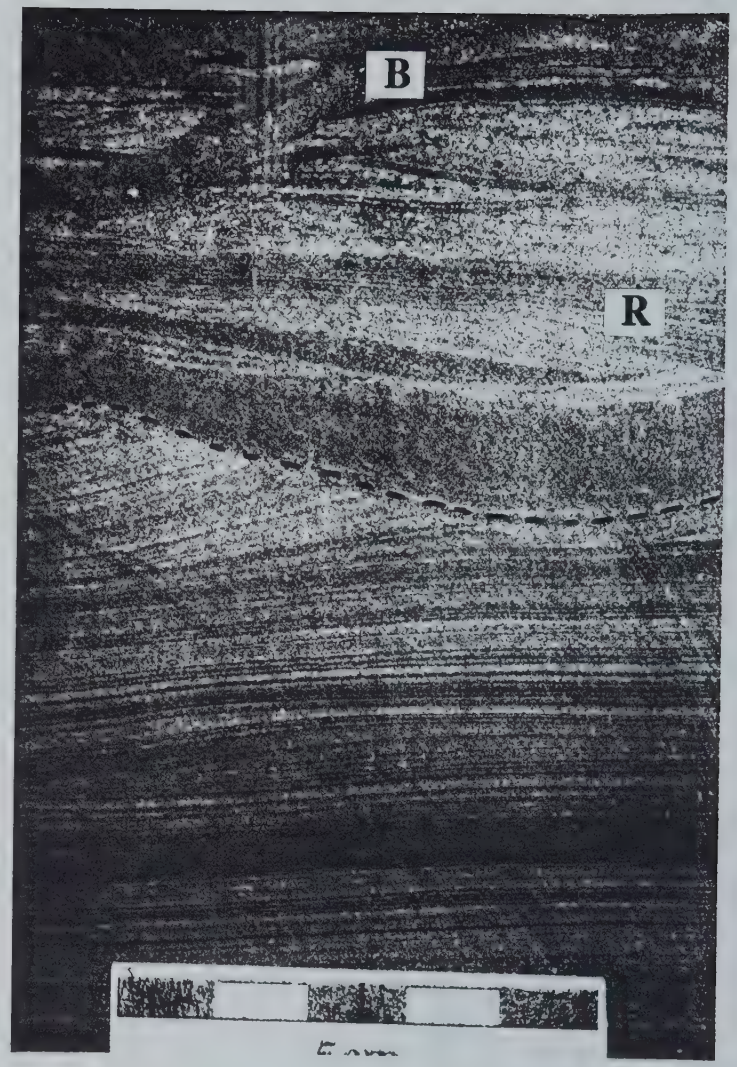

Plate 12. Hummocky cross-stratified sandstone bed in Facies D. Note that upper contact of bed (dashed line) has been modified by fairweather combined-flow ripple cross-lamination (R) and burrowing (B). Well 10-35-72-9-W6. 2256 m.

generated beds (tempestites) observed in Facies B and C. The upward change from hummocky cross-stratification to ripple cross-lamination to horizontal lamination within an individual bed reflects the decreasing current strengths as the storm waned (Kreisa, 1981).

In a number of examples of Facies D, thin erosively-based bioclastic sandstone beds containing small dolomitic mudstone clasts were observed (eg. well 16-26-72-8-W6; Appendix A). These beds do not display hummocky cross-stratification and are therefore not thought to be of storm origin. Their similarity to Facies I, interpreted as tidal inlet channel fill, suggests that they may indicate deposition close to the seaward mouth of a tidal inlet channel.

Facies D is thus interpreted to have accumulated in the lower shoreface environment above mean fairweather wavebase. The substrate was subject to persistent agitation by oscillatory wave currents which formed oscillation ripple cross-lamination and sufficiently aerated the bottom waters to allow a diverse fauna to become established. Periodic storms generated hummocky cross-stratified sandstone beds. These are thicker than those found in Facies B and C, reflecting the increasing strength of oscillatory storm waves above fairweather wavebase.

4.5.0 Facies E. Cross-Bedded Sandstone.

Facies E is a fine-grained and well sorted sandstone which lies above facies D. Although beds of Facies D and E may be interbedded over a thickness of a metre or so, the base of each bed of Facies E is always sharp and in many instances loaded. The upper contact of facies E is typically erosional and overlain by either a thin bed of Facies M washover sandstone or Facies G lagoonal / tidal flat deposits. Rarely however, a thin bed of Facies F sandstone is present between Facies E and this erosion surface.

There is a slight upward increase in grainsize through Facies E from very-fine to fine sand; rarely is it medium grained. Physical sedimentary structures are dominated by gently inclined plane lamination and trough cross-bedding (Plate 13). Thin beds of oscillation ripple cross-lamination occur in the lower part of the facies. Planar tabular cross-bedding and rare silt laminae were also observed (Plate 14). The uniform grainsize of Facies E can, however, make sedimentary structures difficult to see. Trough cross-bed sets are 5-25cm thick and many have a scoured base with a thin lag of lower-coarse-grained black and white chert and clear quartz. Concentrations of these coarse sand grains

Plate 13. Trough cross-bedding in Facies E fine grained sandstone. Darker coloured areas are dolomite cemented, foreset laminae are picked out by white anhydrite cement. Well 5-24-74-9-W6. 2015 m.

Plate 14. Planar-tabular cross-bedding in Facies E fine grained sandstone. Cements as in Plate 13. Well 16-20-72-7-W6. 2098 m.

also occur along foreset laminae. Foreset laminae are commonly picked out by a concentration of white anhydrite cement, which contrasts with the pale brown colour imparted to the bulk of the facies by dolomite cement (Plates 13 and 14). Anhydrite cement also occurs as circular patches up to 1 cm in diameter.

Trace fossils observed in Facies E were limited to a few *Skolithos* burrows and some escape traces. This however, could be a function of the difficulty in distinguishing any traces in the uniform grainsize. Thin sections cut through the circular anhydrite cement patches mentioned above reveal that they are are composed of slightly finer-grained sandstone than the surrounding sediment. Such grainsize segregation in this cylindrical pattern is presumably the work of deposit feeding organisms who ingested only grains of a certain size.

Facies E is interpreted as being deposited in an environment where currents were persistent and strong enough to winnow out all silt and clay and form large three dimensional ripples in fine-grained sand. The presence of oscillation ripple cross-lamination indicates that these currents had an oscillatory component and were therefore wave generated. The numerous scour surfaces, shell and chert grain lags and the presence of only a few vertical burrows also suggest a highly mobile substrate. This is characteristic of the upper shoreface environment above mean fair-weather wave base where waves begin to shoal and break. Studies of this high energy nearshore environment have been made by Clifton et al. (1971) and Howard and Reineck (1981). Both describe the dominant sedimentary structures as trough cross-bedding produced by the migration of megaripples, and planar bedding. Scour surfaces and thin, coarse grained lags were abundant. The observed dominance of bedforms produced by strong unidirectional rather than oscillatory flows can be explained by the modifications waves experience as they travel into shoaling water, which results in a strongly asymmetric landward-directed flow (Clifton et al., 1971). Planar bedding is produced by upper flow regime sheet flow induced by the strong landward component of the shoaling waves. Waning of each landward surge allows ripple bedforms to develop, but these tend to be obliterated by the passage of the next wave crest (Clifton et al., 1971). Shore-parallel sections cut through megaripples also produces sets of gently inclined planar laminae (Clifton et al., 1971). Megaripple migration may be either landward or seaward, but tends to show a dominance of one direction over the other in any given location (Howard and Reineck, 1981). Clifton et al. (1971) also noted that the various subenvironments of the nearshore enviroment tended to migrate back and forth in response to fluctuating tidal and wave conditions. A

similar situation may have been responsible for the common interbedding of Facies E and D across the facies boundary.

4.6.0 Facies F. Plane Laminated Chert Sandstone.

Facies F is a rarely preserved sandstone unit containing a high proportion of lower coarse-grained black and white chert. This gives the facies a distinctive "salt and pepper" appearance (Plate 15). The facies rests abruptly on either Facies E (upper shoreface) or Facies L (ebb-tidal delta). Where seen, Facies F is only 10-50 cm thick and overlain erosionally by either a thin unit of Facies M washover sandstone or Facies G lagoonal mudstones.

The characteristic sedimentary structure of Facies F is gently inclined planar stratification (Plate 16). Individual laminae are 0.5-1.5 cm in thickness and may taper across the width of the core. In addition, some laminae were observed to display inverse size grading, with a greater concentration of the coarse-grained chert toward the top. This is emphasized by the black colour of much of the chert as compared to the clear fine-grained quartz which characterise the lower part of each lamina (Plate 16). In several examples, the well-sorted nature of Facies F made it difficult to determine any stratification and the unit had a massive appearance. No trace fossils were observed in this facies.

Gently inclined, sub-parallel lamination defined by alternating layers of different grainsize or heavy mineral content is considered characteristic of beach foreshore deposits (Clifton, 1969). This distinctive lamination with its common inverse size grading results from grain segregation within bed flow during wave backwash (Clifton, 1969). A foreshore interpretation for Facies F is consistent with its occurrence above Facies E upper shoreface deposits in an overall upward-shallowing sequence. Such a high energy setting subject to constant wave swash and backwash would also explain the absence of any evidence of burrowing activity.

4.7.0 Facies G. Laminated Anhydrite and Dolomite Mudstone.

Facies G consists of two distinctive but intimately associated lithologies: interlaminated anhydrite and dolomite (Facies G1) and pale brownish-grey dolomite mudstone (Facies G2). Facies G typically gradationally overlies a thin (50 cm) bed of Facies M washover sandstone, but may also be found resting abruptly on Facies E, F or L. As it lies above the "Halfway sandstone", Facies G would lithostratigraphically be placed in the lower part of the Charlie Lake Formation.

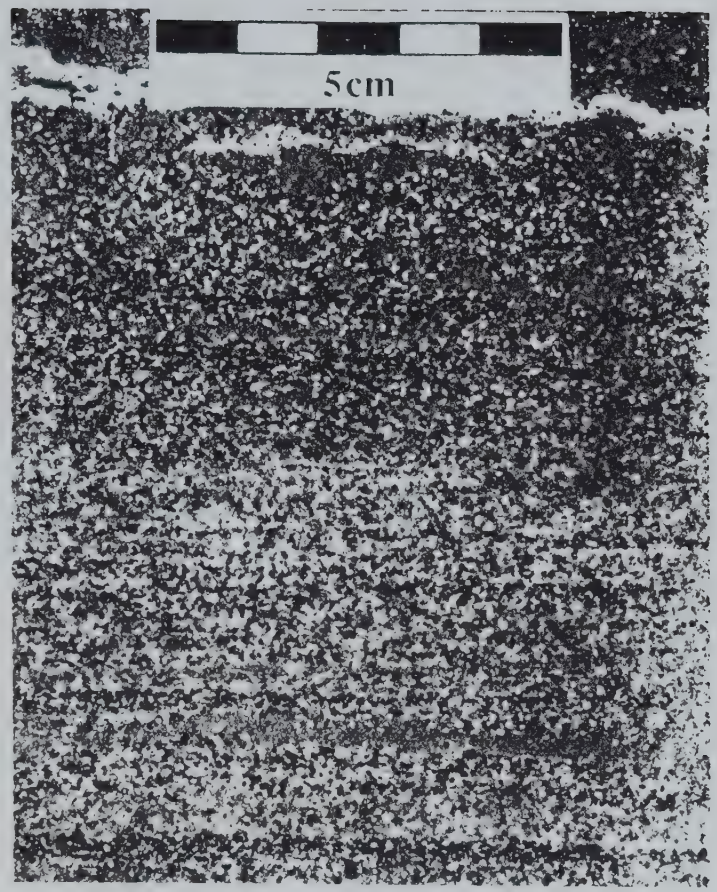

Plate 15. Facies F plane laminated sandstone. Note the abundance of coarse black and white chert grains. Well 16-15-72-8-W6. 2211 m.

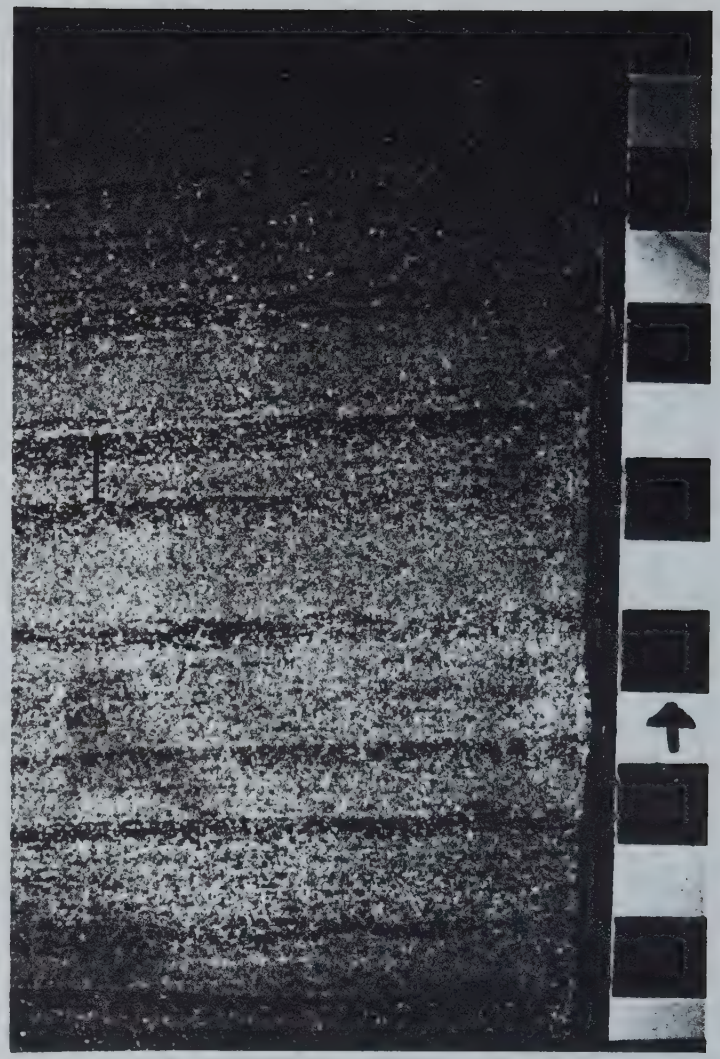

Plate 16. Inclined plane lamination characteristic of Facies F sandstone. Note inverse grading of laminae (arrowed) marked by concentration of darker-coloured coarse chert grains toward top. Well 16-18-72-7-W6. 2131 m.

The typical vertical succession of lithologies in Facies G consists of: (a) 30 cm -1 m of Facies G1 laminated anhydrite and dolomite; (b) a similar thickness of Facies G2 pale brownish-grey dolomite mudstone; and (c) a further metre of Facies G1. This sequence is overlain abruptly by Facies H red mudstones.

4.7.1 Facies G1.

Facies G1 laminated anhydritic dolomite consists of alternating millimetre-thick laminae of white anhydrite and grey dolomite mudstone (Plates 17 and 19). The laminae are generally slightly irregular and in some cases markedly arched (Plate 18). Fenestral porosity was observed in the dolomite mudstone laminae. Interbedded units 1-2 cm thick of sand-sized bioclastic fragments were also observed. As it is so intimately associated with the laminations, it seems reasonable to assume that the anhydrite (or its gypsum precursor) is primary in origin. This would imply that deposition occurred in an evaporative environment.

The irregular millimetre laminae of alternating mineralogy, domal structures and fenestral porosity observed in Facies G1 are all features commonly described from sediments bound by algal mats (Shinn et al., 1969; Davies, 1970; Park, 1976). Along the modern Trucial Coast of the Persian Gulf, algal mats are largely restricted to the mid- to high-intertidal zones where they are beyond the reach of predatory organisms such as gastropods, but still wetted by each high tide (Park, 1976). However, in cases where lagoonal waters are hypersaline, such as Shark Bay, Western Australia (Davies, 1970), predatory gastropods are unable to survive, thereby allowing the algal mats to extend down into lower intertidal and possibly subtidal zones. Such algal mats trap wind- and water-driven particles, and in order to keep photosynthesising the algae must grow up through the sediment cover, so binding it (Park, 1976). The older buried portions of the algal mat dehydrate, decay and flatten down to simple layers of algal peat, producing alternating sediment-rich and organic laminae (Figure 16). Park (1976) noted that most of the sediment bound by the algal mats along the Trucial Coast consisted of carbonate mud from the adjacent lagoons carried onto the intertidal flats at high tide and deposited from suspension. Minor amounts of wind-blown quartz silt were introduced from the hinterland at low tide. Thicker laminae (up to 1 cm) of bioclastic fragments and faecal pellets were swept onto the intertidal flats during storms. These may be analogous to the thicker bioclastic laminae observed in Facies G1.

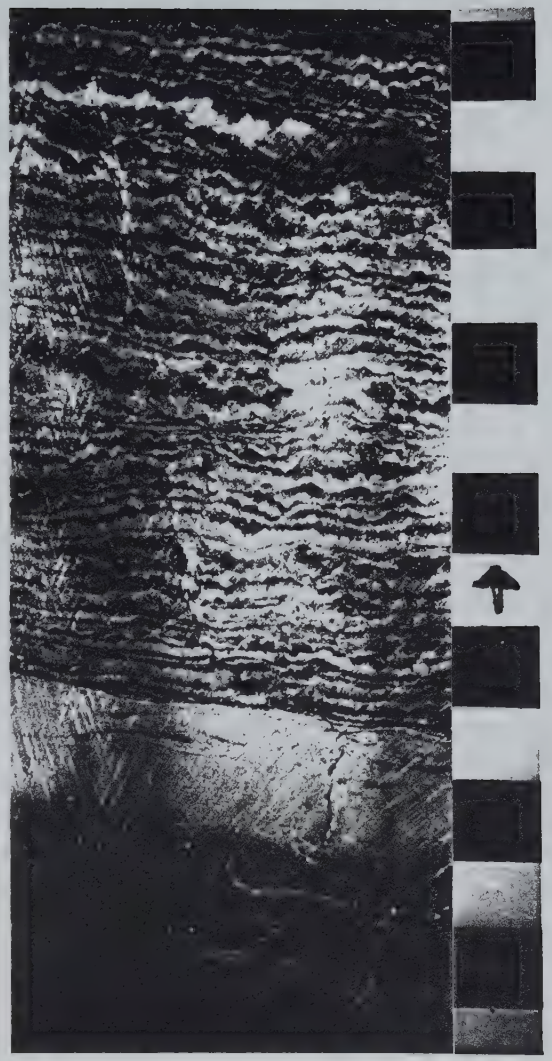

Plate 17. Facies G1 crypt-algal laminite composed of alternating laminae of anhydrite (dark) and dolomite mud (light). Well 8-19-72-7-W6. 2107 m.

Plate 18. Irregular arched laminae in Facies G1 crypt-algal laminite. Well 14-11-72-8-W6. 2180 m.

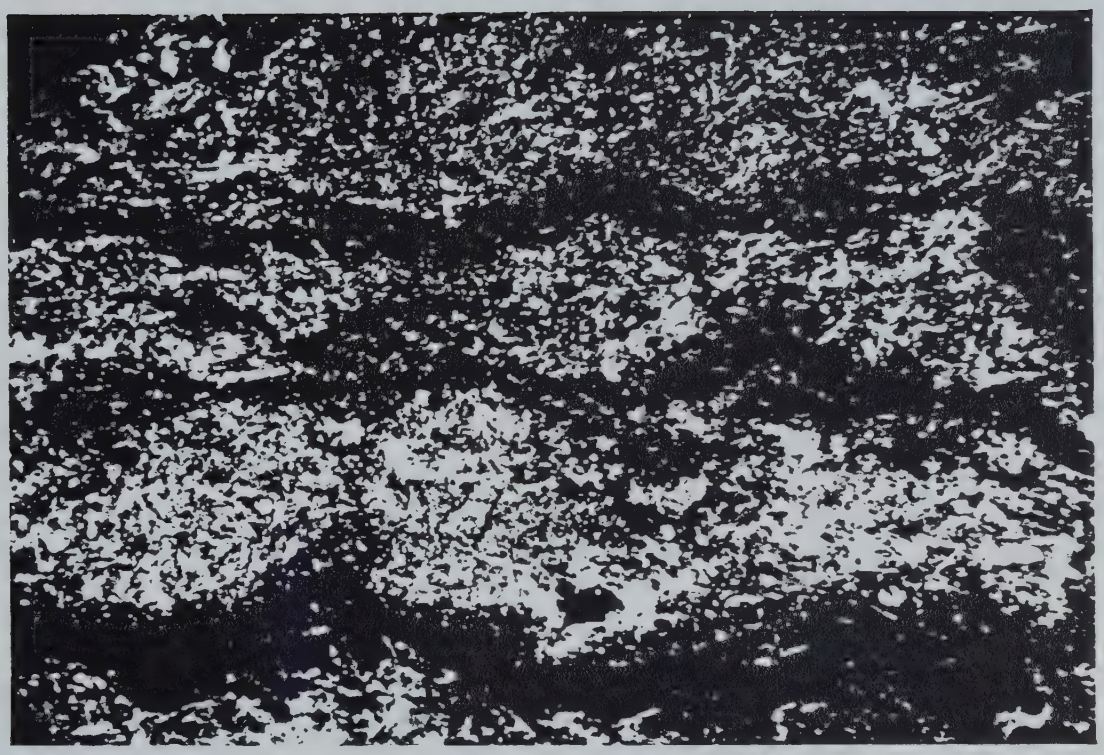

Plate 19. Photomicrograph of Facies G1 crypt-algal laminite. Note alternating anhydrite (light coloured) and dolomite mud rich (darker) laminae. XPL. Field of view 4 mm. Well 6-8-73-7-W6. 1974 m.

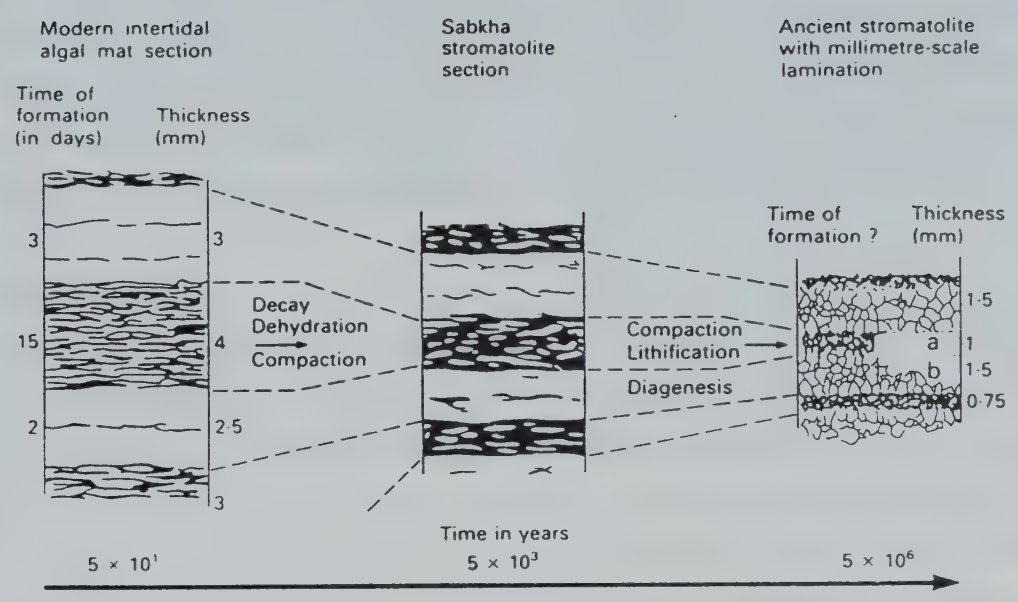

Figure 16. Schematic diagram illustrating the possible consequences of compaction upon a normal algal mat accumulation, and its possible fossil equivalent. (a) Micrite, commonly dolomite; (b) spar, commonly calcite (after Park, 1976).

The laminated anhydritic dolomite of Facies G1 is therefore interpreted as crypt-algal lamination, produced by algal mats binding fine-grained carbonate sediment deposited from suspension at high tide. This may have occurred in either an intertidal or shallow subtidal setting. The association of anhydrite with the laminae indicates that these Facies G algal mats grew in an evaporative climate. It is unlikely that the gypsum precipitation occurred at the surface and was bound within the algal mats, as studies of modern evaporative tidal flats (eg. Miller, 1975; Schreiber, 1986) indicate that such evaporites are highly ephemeral and do not survive shallow burial. It is more likely that the irregularly laminated anhydrite in Facies G1 represents the early stages of sabkha gypsum growth in the shallow subsurface of the high intertidal zone (see Facies H discussion).

4.7.2 Facies G2.

The frequency of the anhydritic laminae in Facies G1 decreases upward and the laminated unit grades into massive dolomite mudstone of Facies G2. Thin sections show that this dolomite mudstone is microcrystalline and contains numerous silt-sized quartz grains. It is generally massive in appearance, with only a few thin darker clastic mud and silt laminae (Plate 20). However, in a few instances centimetre-thick slightly brecciated beds were observed in the mudstone (Plate 21). These are interpreted as evaporite solution-collapse breccias. Stylolites are common in Facies G2 and their relief suggests that considerable pressure solution has occurred in the unit. Irregular micro-fissures were observed extending down from several apparent bedding plane surfaces in these mudstones and are tentatively interpreted as desiccation cracks. The Facies G1 dolomite mudstones pass conformably back up into Facies G1 laminated anhydritic dolomite in a "mirror image" of the lower half of Facies G.

Carbonate mud in modern environments is known to be largely the product of the decay of calcareous green algae such as *Penicillus* (Neumann and Land, 1975) and bioerosion of skeletal material (Reid et al., 1992). Accumulation of this carbonate mud is dependent on a lack of coarser-grained material to dilute it; this is usually found in lagoonal environments away from strong wave and tidal currents. A protected lagoonal environment of deposition for the Facies G2 dolomite mudstones is compatible with the lack of current-formed sedimentary structures, its association with intertidal flat deposits (Facies G1) and its stratigraphic position between an interpreted regressive shoreface sequence below (Facies B-F) and supratidal deposits (Facies H) above.

Plate 20. Facies G2 massive dolomite mudstone, with stylolite toward top of view. Well 5-13-72-8-W6. 2152 m.

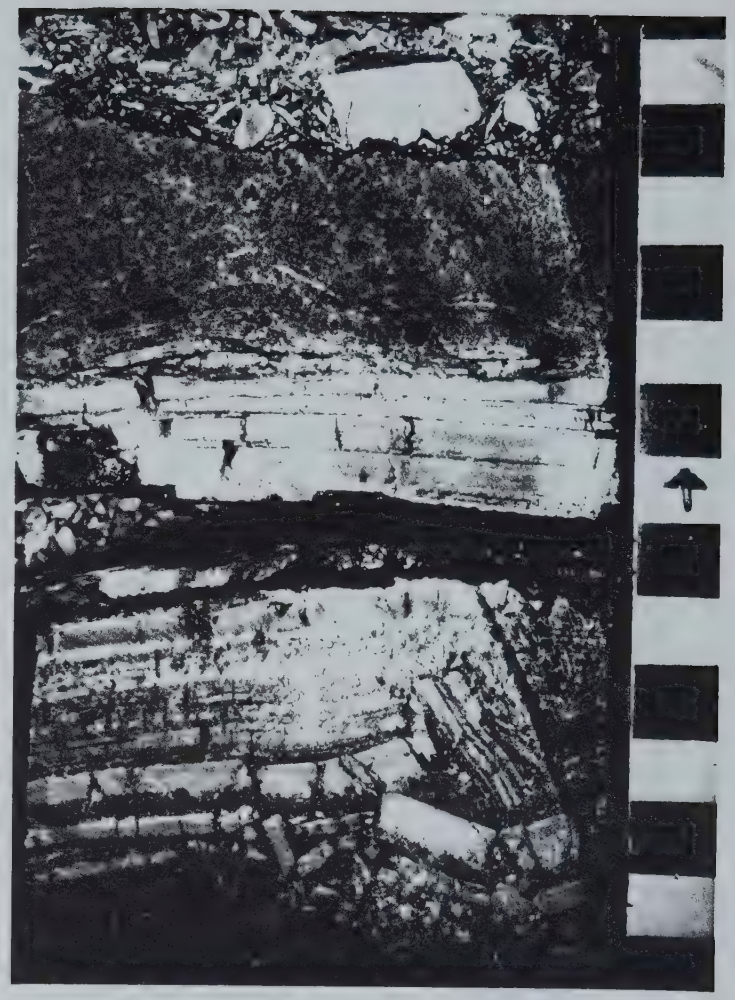

Plate 21. Evaporite solution-collapse breccia within Facies G2 dolomite mudstone. Well 10-32-72-8-W6.

In some cores, Facies G2 dolomite mudstone is not present between the upper and lower units of Facies G1. In such cases this interval is occupied by interlaminated clastic mudstone and siltstone displaying horizontal lamination, wavy bedding and rarely ripple cross-lamination (Plate 22). In several cases this clastic sediment was bioturbated, but no specific trace fossils were identified in this or any other part of Facies G. The horizontal lamination indicates that these fine-grained sediments were deposited from suspension, with periodic traction current action producing the ripple cross-lamination. Similar sediments have been described from Ordovician tidally-influenced backbarrier deposits by Tankard and Hobday (1977).The sediment closely resembles Facies K, interpreted as abandoned tidal inlet channel fill. It is suggested that in certain areas of the Facies G lagoon, clastic sediment input diluted the carbonate mud accumulating elsewhere. The similarity between this lagoonal clastic sediment and that found in Facies K suggests that this local clastic dominance may be related to the position of tidal inlet channels. This communication between Facies G2 lagoonal environment and Facies K abandoned tidal inlet channel fill is further demonstrated by the presence of Facies G2 pale grey dolomite mudstone laminae in Facies K. Such a close relationship between facies belonging to both the Halfway and Charlie Lake Formations make it difficult to uphold the presence of an unconformity between the two formations.

Thin (<10 cm) silty sandstone beds are rarely present in both the dolomitic mudstone and the interbedded siltstone and mudstone of Facies G. These sandstone beds have an indistinct base and are internally structureless and mottled, suggesting bioturbation. Several examples contain scattered lower-coarse-grained black, white and red chert grains. The beds are interpreted as storm washover sands, the chert grains having been derived from upper shoreface and foreshore deposits (Facies E and F).

The typical Facies G sequence is therefore envisioned as a product of seaward progradation of sub-tidal lagoonal environments (Facies G2 dolomite mudstone) over inter-tidal flats established on the back of a barrier island, followed by further progradation of intertidal flats from the landward side of the lagoon (upper laminated anhydritic dolomite) over the infilled lagoon. With continued regression, supratidal red muds and silts (Facies H) prograded seaward over these backbarrier deposits. Similar progradational backbarrier sequences have been noted from the New Jersey coastal plain by Fischer (1961). Complications of this ideal sequence, such as thin beds of Facies G1 within the lagoonal mud, may be explained by there having been intertidal areas present within the lagoonal area and not just around its margins. Such intertidal areas are

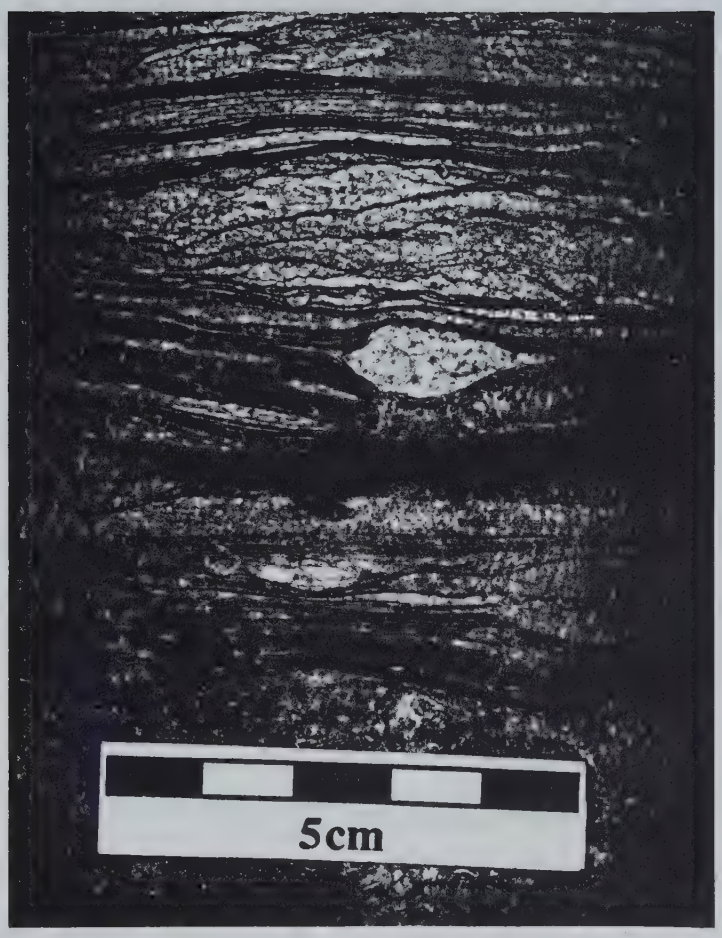

Plate 22. Facies G2 wavy-bedded siltstone and mudstone.
Well 16-22-72-8-W6. 2157 m.

common in modern backbarrier environments (eg. Wojtal-Duc and Tye, 1987). The relatively greater thickness of intertidal sediments compared to lagoonal deposits in Facies G suggests that the environment was dominated by intertidal flats rather than a large, permanently submerged lagoon. This is characteristic of mesotidal (tidal range 2-4 m) coastlines, but may also occur in microtidal (0-2 m) settings (Hayes, 1975).

4.8.0 Facies H. Red Beds and Nodular Anhydrite.

Facies H is typically found conformably overlying Facies G1 crypt-algal laminites, but may rest on Facies M sandstone where this is present. The facies consists of red mudstone, siltstone and some sandstone with beds of massive, nodular or rarely laminated white anhydrite. Beds of laminated anhydritic dolomite similar to those described from Facies G1 also occur. Facies H, like Facies G, would lithostratigraphically be included in the lower part of the Charlie Lake Formation.

4.8.1 Red Beds.

Sedimentary structures are rare in the red mudstones of Facies H. Much of the sediment consists of a chaotic mixture of small mudstone clasts in a clay or silt matrix with no discernable bedding features (Plate 23). Where sedimentary structures were observed, they consisted of horizontally laminated red mudstone and rare current ripple cross-laminated lenticular siltstone laminae (Plate 24). Most examples of these structures have been modified to some extent by scouring, bioturbation or anhydrite-filled fractures.

Scour surfaces truncate laminae in the mudstones and are often associated with thin (1-10 cm) silty sandstone beds containing coarse chert grains similar to those observed in Facies E, F and M. Centimetre-sized clasts of anhydrite, crypt-algal laminated anhydritic dolomite, and various clastic sediments are also commonly associated with these scour surfaces. The anhydrite-filled fractures are typically 1-2 cm deep but may range up to a metre in length (eg. well 16-29-72-8-W6; Appendix A). Since such fractures are absent in the underlying facies, it would appear that they are not of tectonic origin, but due to dessication. In many instances the sediment looks bioturbated, but no trace fossils could be specifically identified to confirm this. One possible exception is a tenuous *Monocraterion* burrow in well 7-36-72-8-W6 (Appendix A).

The evidence available would thus suggest that the red mudstones of Facies H were deposited from suspension in an environment where they were subject to intense dessication, producing the anhydrite-filled vertical cracks. The abundant small mud clasts

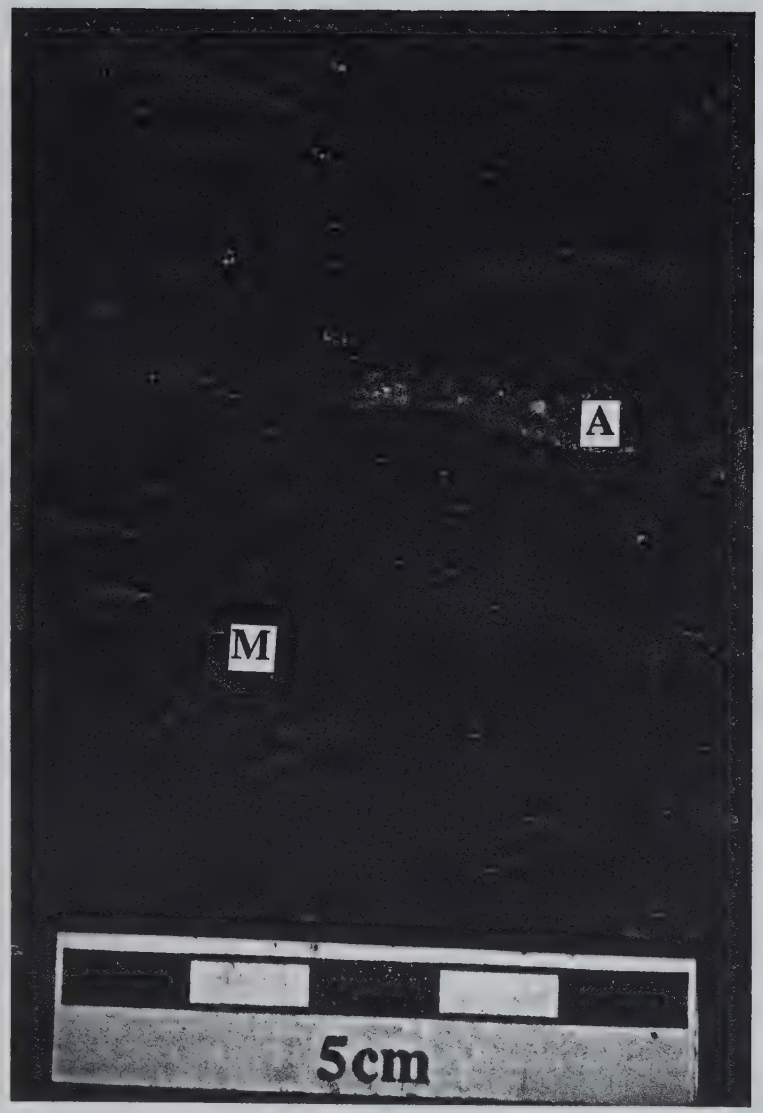

Plate 23. Facies H composed of small mudstone (M) and anhydrite (A) clasts in a silty clay matrix. Well 14-22-72-8-W6. 2150 m.

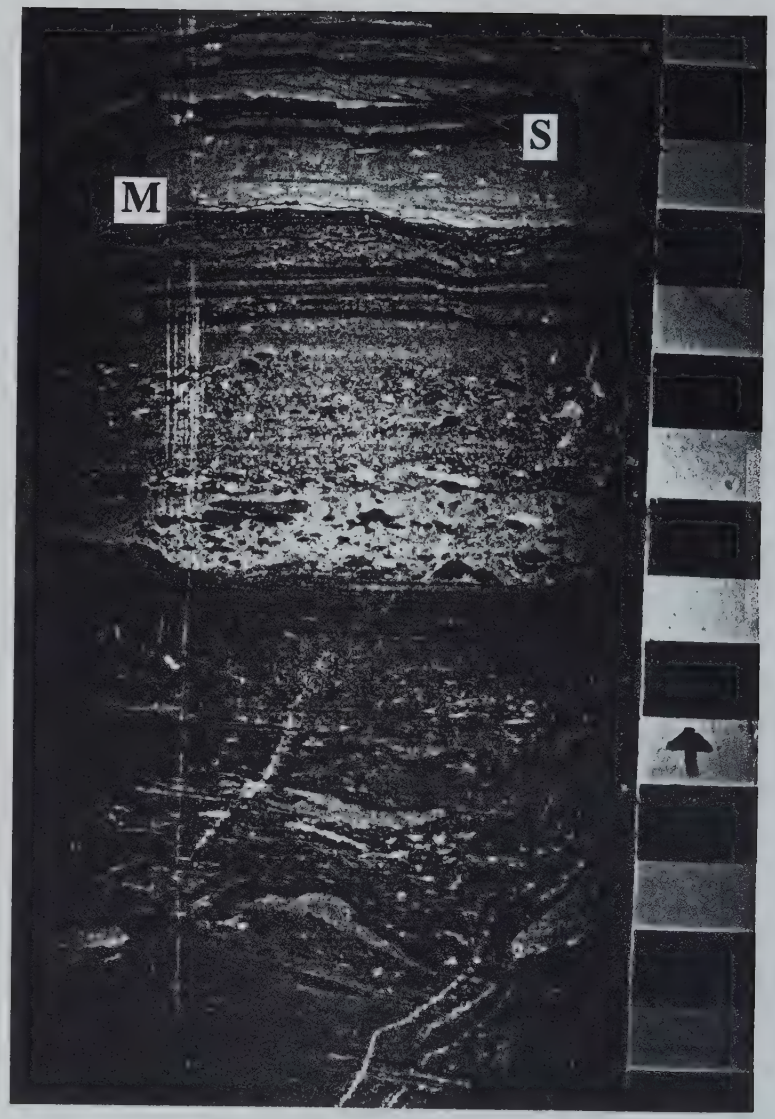

Plate 24. Facies H red beds. Note horizontally laminated mudstone (M) and current ripple cross-laminated siltstone (S) cut by microfaults. Well 6-4-73-8-W6. 2103 m.

may therefore be analogous to the "mud-chip conglomerates" produced by dessication and wind-deflation of muddy supratidal flats in arid climates (Thompson, 1968; Kinsman, 1969). Sediment accumulating on such supratidal flats is mainly in the form of wind-blown silt and material deposited by episodic tidal and storm flooding. Along the arid northern coast of the Gulf of California, the expansive supratidal mud flats of the Colorado River delta consist of finely laminated muds and silts deposited by infrequent tidal floodings (Thompson, 1968). Intervals between flooding are marked by evaporation and the formation of gypsum and halite in the near-surface muds. Crystal growth of these minerals, along with shrinkage and mud-crack formation, combine to totally destroy any lamination and yield a chaotic mud-evaporite mixture that caps the tidal flat accumulation. Similar sediments have been interpreted as muddy tidal flat deposits in the Triassic red bed section of the southwestern United States (Reif and Slatt, 1979). In the Colorado River delta, periodic storms transport shell debris from the foreshore environment landward over the muddy supratidal flats (Thompson, 1968). These shell beds may be analogous to the erosionally-based thin sandstone beds present in Facies H, which contain chert grains similar to those concentrated in Facies F foreshore sandstone, and clasts of intertidal flat crypt-algal laminites.

4.8.2 Anhydrites.

White-to-pale green anhydrite occurs in the red mudstones of Facies H both as nodules and beds ranging from a few centimetres to three metres in thickness. The beds of anhydrite are typically massive (Plate 25), but faint lamination is present in some examples. The anhydrite nodules are commonly closely spaced and in some instances linked to form irregular laminae (Plate 26). This has the appearance of the "chicken wire" anhydrite texture described by Kinsman (1969) from the supratidal sabkha of the Trucial Coast.

In the Trucial Coast sabkha, high evaporation rates (150 cm/yr) combined with low, sporadic rainfall (5 cm/yr) results in groundwater salinities up to ten times that of normal seawater (Kinsman, 1969; Schreiber, 1986). In the seaward-most part of the sabkha, this groundwater concentration causes lenticular gypsum to precipitate within the shallow surface sediments, usually older intertidal algal mats buried beneath the prograding supratidal flat (Figure 17). Preservation of precipitated halite is usually prevented by humidities being greater than 76% and dissolution by episodic storm flooding, so in arid coastlines gypsum-anhydrite are the principle precipitates (Schreiber, 1986). In supratidal flats in more humid settings such as the Texas coast, <u>all</u> evaporite minerals are highly

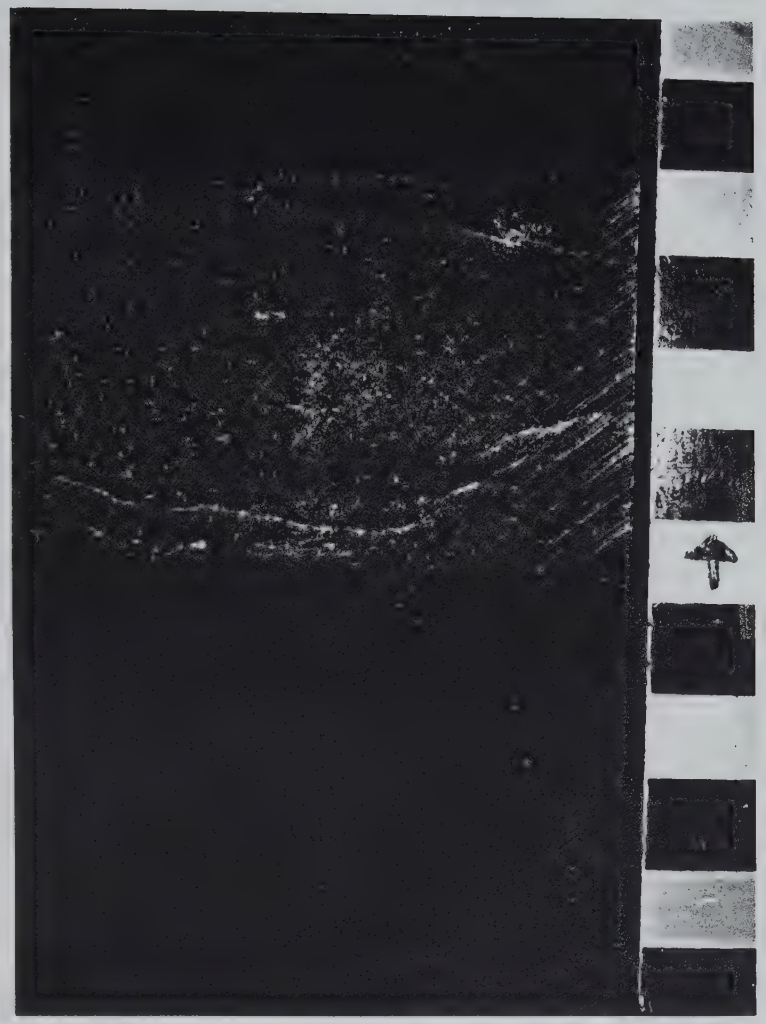

Plate 25. Massive white anhydrite bed between red mudstones of Facies H. Well 8-17-72-7-W6. 2022 m.

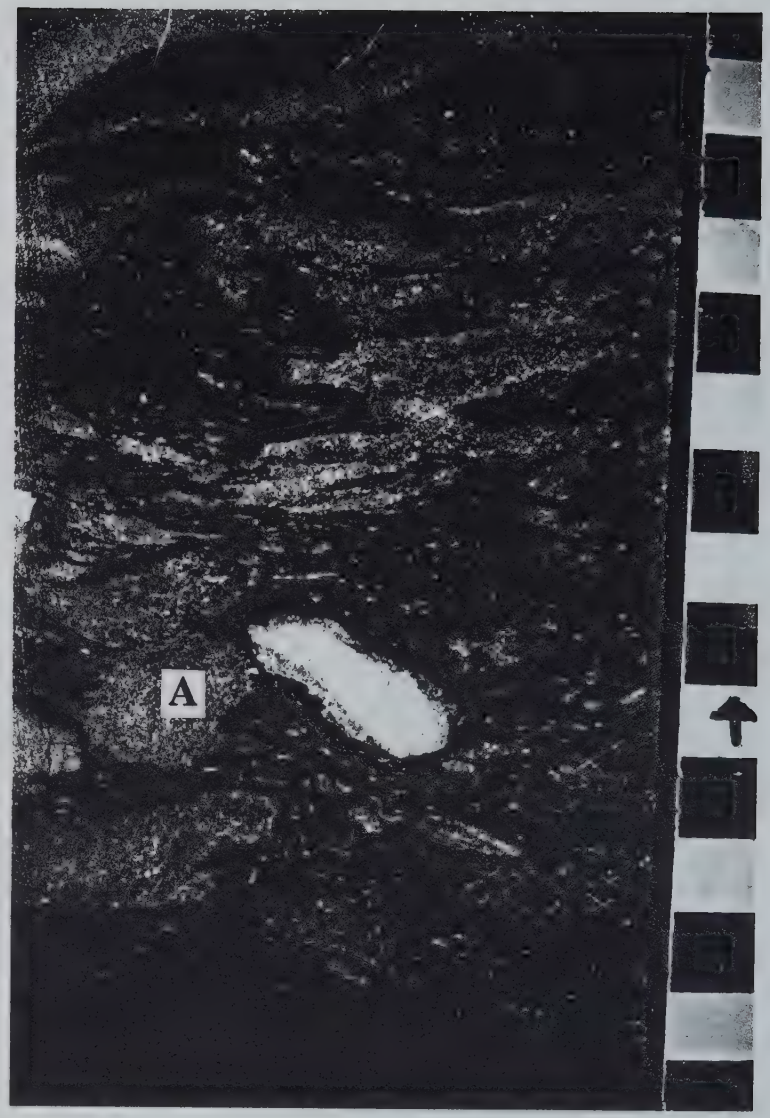

Plate 26. Diagenetic anhydrite nodules (A) characteristic of sabkha sediments in Facies H red chaotic mudstones. Well 16-2-73-8-W6. 2022 m.

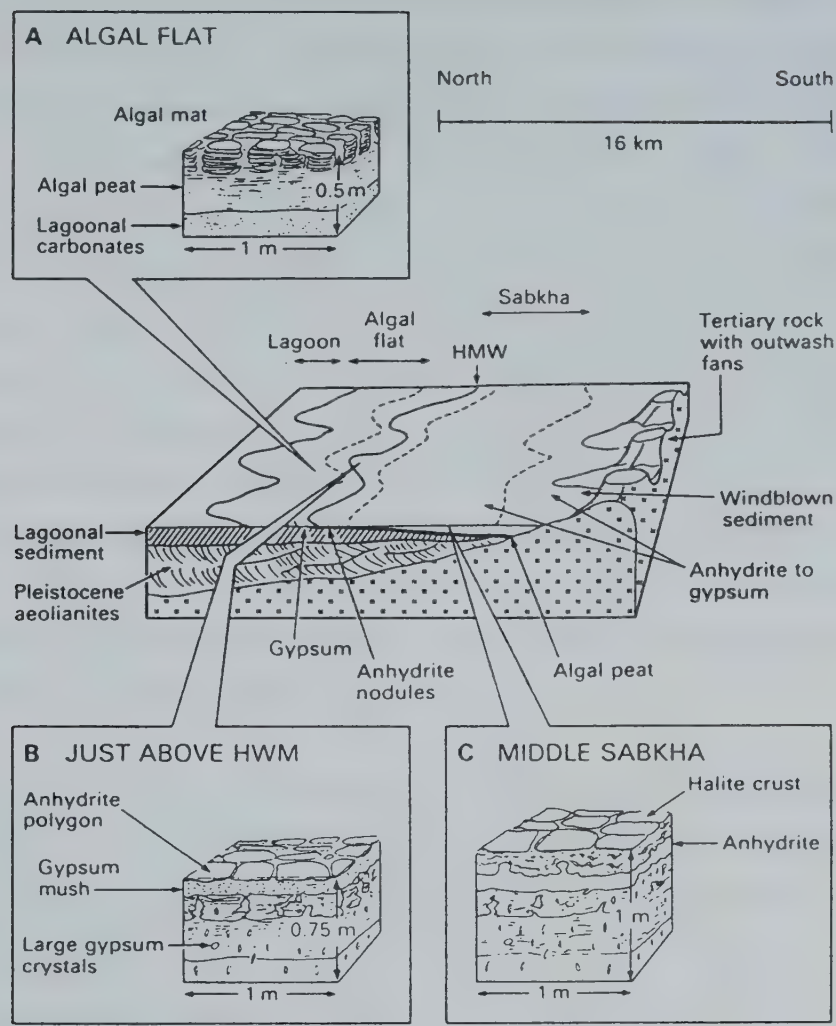

Figure 17. Schematic block diagrams showing the distribution of sediment and evaporite in the Abu Dhabi Sabkha (after Schreiber, 1986).

ephemeral and do not survive shallow burial (Miller, 1975). In the sabkha, gypsum precipitation continues higher in the supratidal zone, commonly forming a discrete layer up to 30 cm thick of gypsum crystal mush. This tends to obscure the original algal lamination of the sediment. In addition, many of the faster-growing gypsum crystals envelope and include patches of the host sediment (Kinsman, 1969). In the mid-supratidal zone, where storm flood replenishment of groundwaters is rare, a marked increase in salinity causes a change in the earlier formed gypsum to amorphous and nodular anhydrite through dehydration (Shearman, 1985). Further concentration of porewaters causes primary diagenetic anhydrite (anhydrite with no gypsum precursor) to be precipitated upon and between the older nodules, producing a characteristic "chicken wire" texture of closely-spaced nodules. The precipitation of evaporites within the sediment causes it to expand and raises the sediment surface, but this is typically planed off by wind deflation and storm-driven floods. Gypsum and halite beds are also formed by evaporation of surficial ponds and restricted parts of the lagoon and then incorporated into the sabkha complex (Kinsman, 1969). These may be analogous to the thicker beds of anhydrite found in Facies H (Plate 25).

The idealized vertical through a sabkha is shown in Figure 18. It is typically in the order of a metre thick and truncated by an erosion surface overlain by either aeolian dunes or alluvial fans which encroach the landward edge of the supratidal flat and reflect prolonged emergence of the coastline, or else lagoonal deposits reflecting renewed transgression. Cored sections of Facies H are generally restricted to the few metres directly above the Halfway sandstone, so the vertical thickness of the sabkha sediments cannot be measured. Roy (1972) has identified sabkha deposits from a stratigraphically higher level in the Charlie Lake Formation in the Boundary Lake oilfield to the nothwest of the study area. Higgs (1990) and Kelly Arnold (personal communication, 1992) have identified aeolian dune sandstones within Facies H equivalent strata in northeastern British Columbia. It would thus appear that Facies H supratidal deposits pass upward into a continental sequence.

Facies H is therefore envisaged to have accumulated landward of the Halfway backbarrier environments on an arid, low-relief supratidal flat. Sediment accumulation was probably limited to deposition from exceptionally high tides and storm-driven floods. In between these inundations, the muddy flat was subject to very high rates of evaporation, resulting in the formation of desiccation cracks and mud-chip conglomerates. Gypsum and anhydrite precipitated in the shallow subsurface in the manner seen in the modern Trucial

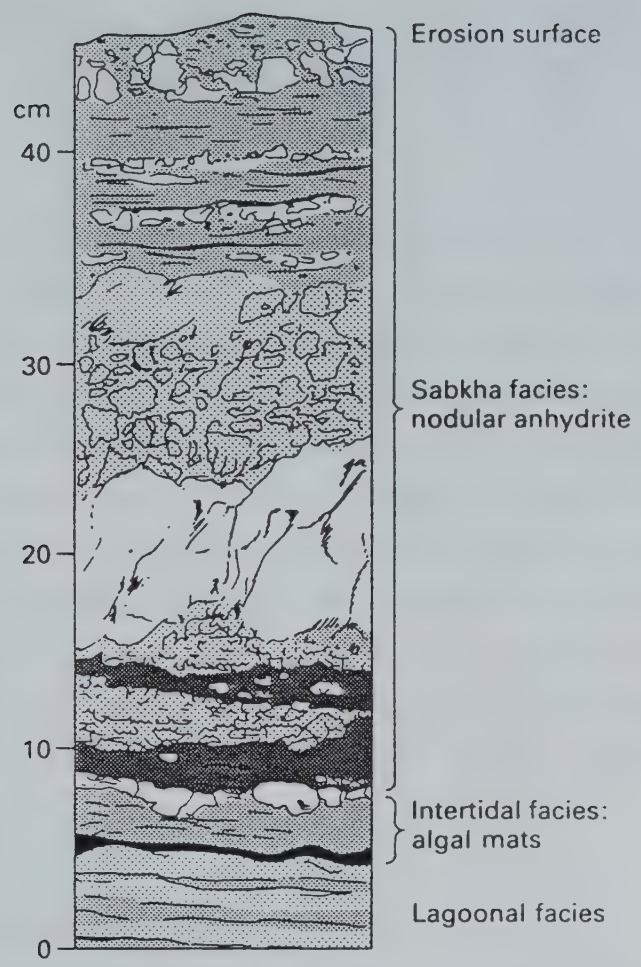

Figure 18. A complete sabkha cycle in the Cretaceous Lower Purbeck Beds of the Warlingham Borehole, southern England. Note that the sabkha deposits overlie lagoonal and intertidal facies and are capped by an erosion surface (after Schreiber, 1986).

Coast sabkhas and the Colorado River delta, producing a chaotic mud-evaporite mixture and leaving little trace of the original lamination. The thicker beds of anhydrite probably precipitated directly from larger bodies of water ponded on the mudflat. However, the fact that the Halfway sabkha was dominantly siliciclastic means that certain differences would be expected from the Trucial Coast carbonate model of Kinsman (1969) described above.

Since most of the porewater in a sabkha is marine in origin and therefore contains more sulphate than it does calcium, the precipitation of calcium sulphate (gypsum) rapidly depletes the available calcium but leaves a good deal of sulphate still in solution. The lack of calcium prevents more gypsum from forming. Within a carbonate matrix the process of dolomitization frees additional calcium which can then combine with the remaining sulphate, but in siliciclastic sediments this extra supply of calcium is absent (Schreiber, 1986). Therefore, a siliciclastic sabkha has a far lower quantity of calcium sulphate than the Trucial Coast example cited. This seems compatible with the high proportion of undisturbed clastic sediment relative to anhydrite in Facies H. Examples of ancient siliciclastic sabkha sediments bearing strong similarity to Facies H have been described from the Permian Basin of Texas by Handford (1981) and Mazullo et al. (1991), and the Lower Triassic of Nevada by Reif and Slatt (1979).

4.9.0 Facies I. Sandy Dolomite Coquina.

Facies I is typically a pale pinkish-grey sandy dolomite coquina ranging from 0.5 m to 2 m in thickness (Plate 27). The bioclastic material is highly variable in terms of abundance, fragment size and preservation state. Shell material belongs to bivalves, brachiopods, gastropods and rarely crinoids and ranges from whole disarticulated valves up to 2 cm in length to finely comminuted fragments; the modal size is 2-4 mm. Most fragments have been leached, producing extensive biomoldic porosity, but in many cases this has been infilled by later anhydrite cement. Numerous phosphatic shell fragments can be observed in thin section. Pelletier (1965) and Gibson (1975) identified shell fragments in Halfway-equivalent strata in outcrop as being spirifers, terabratulids, gryphaeids and lingulids.

In most examples of Facies I the bioclastic fragments form the framework of the sediment, with a matrix of dolomite mud (micrite) and poorly sorted quartz sand. In some cases however, the proportion of bioclastic fragments is much smaller and they are scattered in the sandstone. This variability in the proportion of carbonate and clastic

Plate 27. Facies I massive coquina containing large anhydrite-filled shell moulds in a sandy dolomite matrix. Well 8-9-72-7-W6. 2092 m.

grains in Facies I, coupled with the diagenetic modification, make it difficult to name the rock using accepted classification schemes. The use of "sandy dolomite coquina" seems to best fit the typical appearance of the facies. Scattered throughout the facies are clasts of grey dolomitic mudstone ranging in size from a few millimetres to greater than the width of the core (>15 cm), as well as pyritic black shale fragments similar to Facies B lithology, and coarse grains of chert.

The lower contact of Facies I is always sharp, in most cases erosional, and commonly overlain by large (up to 15 cm) clasts of both the underlying lithology and pale grey dolomitic mudstone similar to that seen in Facies G2 (Plates 29 and 30). This erosional base of Facies I rests most commonly on Facies C (marine offshore-transition), but also Facies D (lower shoreface) and Facies B (marine offshore). In one instance (well 14-33-72-08-W6; Appendix A) Facies I rests directly on the "regional Doig sandstone" (Facies A). Repeated units of Facies I within a single cored sequence were also observed to rest erosively on Facies J and K. Facies I may also be stacked vertically, although this is not easy to demonstrate conclusively as the basal erosional surface is difficult to differentiate from erosive cross-bed set boundaries found within the unit. Immediately beneath the scoured base of the facies, the coarse sediment of Facies I is sometimes observed to infill *Skolithos* and *Thalassinoides* burrows in the underlying sediment (Plate 31). In addition, the rock immediately beneath the scour commonly exhibits unusual diagenetic cementation suggesting that the more porous bioclastic sandstone has acted as a conduit for diagenetic fluids.

The upper contact of Facies I is always gradational with the cross-bedded sandstone of Facies J.

In the more bioclastic examples of Facies I it is rare to see any sedimentary structures, although crude horizontal lamination, planar and trough cross-bedding have been observed (Plate 32). The same sedimentary structures were observed (more commonly) in the less bioclastic units of the facies. This generally massive appearance of the bioclastic units might be partly due to the extensive pressure solution and diagenetic alteration evidenced by stylolites and shell moulds. Beds of dolomitic mudstone up to 1 m thick and of similar lithology to Facies G2 were observed in Facies I in wells 16-36-72-8-W6 and 16-5-73-8-W6 (Appendix A). The bases of these beds and their internal sedimentary structures are discordant to the bedding observed in vertically adjacent beds. Thin (<1 cm) laminae of dolomitic mudstone are also commonly interbedded with the bioclastic

Plate 29. Erosional base of Facies I overlain by cross-bedded bioclastic sandstone containing intraformational mudstone clasts. Well 16-18-72-7-W6. 2135 m.

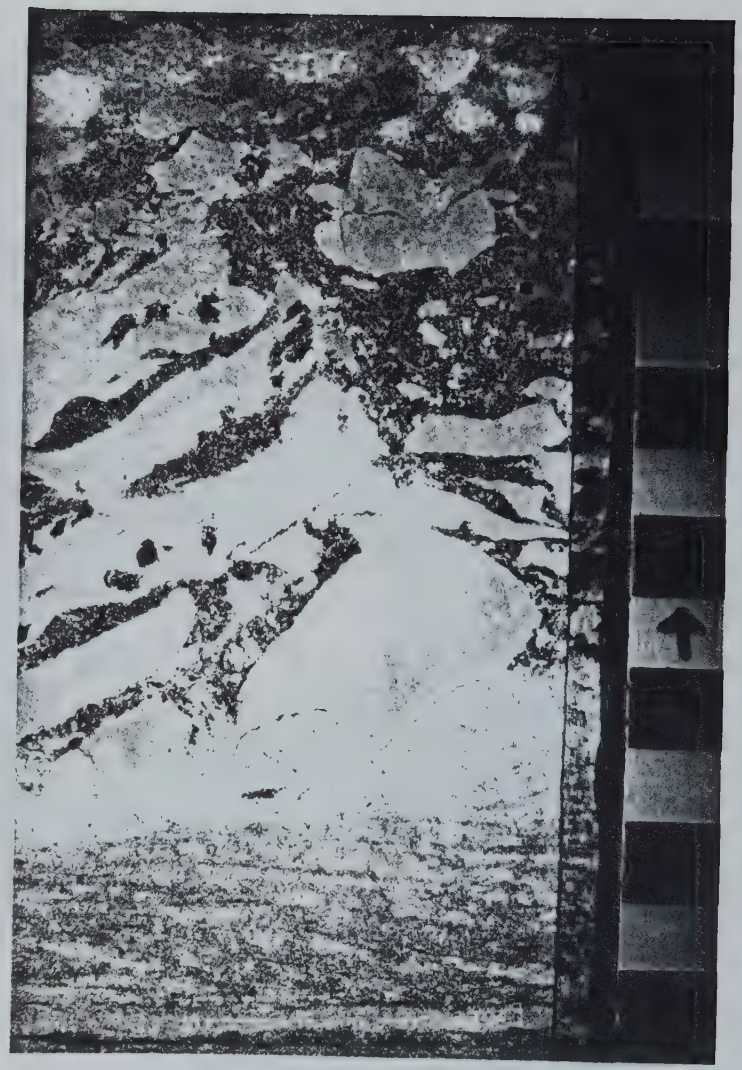

Plate 30. Facies I bioclastic sandstone with mudstone clasts resting erosively on Facies D ripple cross-laminated sandstone. Well 1-10-73-8-W6. 2071 m.

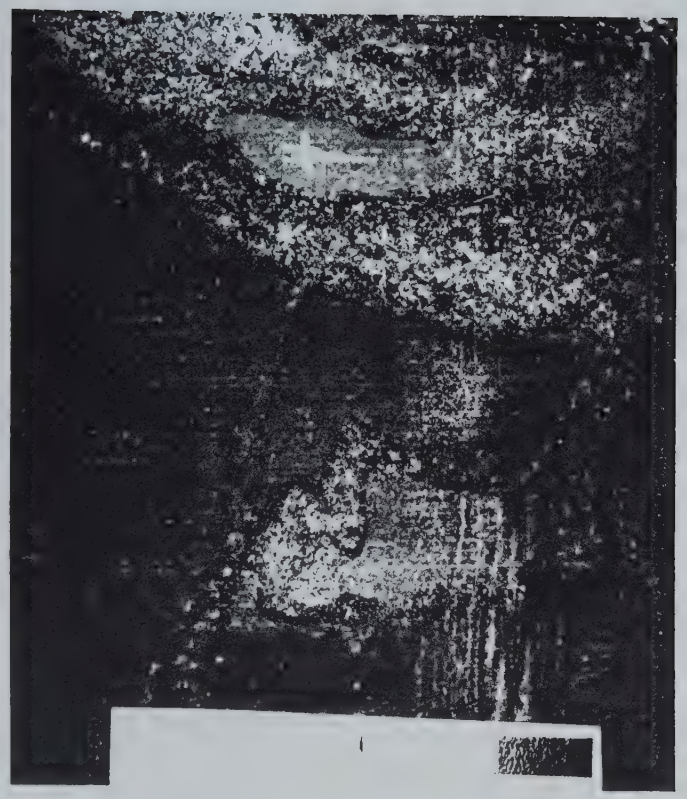

Plate 31. Erosional contact between Facies I bioclastic sandstone above and Facies B shale below. Note vertical burrows extending down from contact, interpreted as the *Glossifungites* ichnofacies. Well 6-27-72-8-W6. 2157 m.

Plate 32. Cross-bedding in Facies I coquina. Note abundance of shell moulds and small mudstone clasts. Well 6-4-73-8-W6.

sandstone. These laminae indicate that the currents which formed the cross-bedded bioclastic sandstone of Facies I were subject to frequent changes in flow strength and interspersed with periods of fallout of finer-grained sediment from suspension. This is strongly suggestive of the presence of tidal currents during Facies I (Oertel, 1973; Nio and Yang, 1991).

The erosive base of Facies I and the commonly associated intraformational conglomerate above it indicates that the facies was scoured into the underlying deposits. The variation in the stratigraphic depth of this scoured base, in the order of several metres, suggests that Facies I probably forms the base of a channel feature, rather than a laterally continuous scour surface as might be expected at the base of a turbidite or storm bed. The stacked sets of cross-bedding found above the erosional base also point to ongoing rather than episodic sedimentation for Facies I. The dominant sedimentary process during Facies I accumulation was migration of large sandwaves and megaripples formed of coarse-grained sand and bioclastic fragments, producing planar and trough cross-bedding. However, it is evident that there were frequent breaks in this current flow, during which fine-grained dolomitic mud fell out of suspension. Such repeated alternations of strong unidirectional current flow with fallout of finer-grained material from suspension are commonly reported from tidally influenced environments (eg. Oertel, 1973). It would appear then that Facies I was deposited in a tidally influenced channel. In view of the similarity between the composition of the dolomitic mudstone laminae in Facies I and the lagoonal dolomitic mudstone of Facies G2, it is suggested that the mud layers formed in the slack water after the ebb tide.

Shell beds of similar composition to Facies I are commonly reported from the bases of tidal channels in estuaries (Klein, 1963), barrier island systems (Kumar and Sanders, 1974; Barwis and Makurath, 1978; Hubbard et al., 1979; Moslow and Tye, 1985; Henderson and Frey, 1986; Uhlir et al., 1988; Davies et al., 1989), and tidal creeks (Van Straaten, 1956; Tye, 1984). Their common interpretation is as a lag too coarse for the tidal currents in even the deepest part of the channel to move. The mud clasts commonly found in these channel lags are derived from scouring of the substrate and slumping from the cut bank as the channel migrates. Slumped blocks up to one metre in size were observed on the floor of Murrels Inlet, South Carolina by Hubbard et al. (1979), and in Price and Capers inlets by Tye (1984); these may be analogous to the thick discordant beds of dolomitic mudstone in Facies I in wells 16-36-72-8-W6 and 6-5-73-8-W6 mentioned above.

The presence of infilled burrows in facies B, C, and D beneath the scoured base of these Facies I tidal channels can be explained in two ways: 1) the burrows were already present in facies B, C, and D and exhumed by Facies I erosion, or 2) they were formed after the scoured surface was cut but before it was covered by the channel lag. As large *Skolithos* and *Thalassinoides* burrow traces were never observed in facies B, C, or D except in conjunction with the base of Facies I, it is considered probable that they are associated with this erosional event. The fact that the tracefossil assemblage consists solely of unlined vertical burrows suggests that they were burrowed into a cohesive substrate, which would be expected of the exhumed, partially-dewatered mudstones of facies B, C and D. This assemblage is similar to the *Glossifungites* ichnofacies of Pemberton and Frey (1985), which they describe as being "typical of firm but unlithified substrates, whether intertidal to subtidal omission surfaces or stable, cohesive sediments either in protected, low-energy settings or in places of somewhat higher energy where the semiconsolidated substrate offers resistance to erosion. Most such substrates consist of dewatered muds." The *Glossifungites* assemblage beneath Facies I is therefore interpreted to be the result of burrowing into a cohesive substrate exhumed by the scouring action of a tidal channel. Later migration of coarse lag material across this surface infilled the burrows. Pemberton and Frey (1985) give as one example of the *Glossifungites* ichnofacies the burrowed cohesive mud bank of a tidal channel, in which some of the abandoned burrows have been infilled with sand.

Facies I is therefore interpreted as the lag and deep channel deposits from the base of a tidally-influenced channel. Whether this channel was a tidal inlet, tidal creek, or estuarine cannot be determined without consideration of the overlying deposits.

4.10.0 Facies J. Cross-Bedded Sandstone with Mudstone Laminae.

Facies J consists of slightly bioclastic silty sandstone with small dolomitic mudstone clasts similar to those in the underlying Facies I. Facies J gradationally overlies the more bioclastic Facies I and grades upward into Facies K. It reaches up to 6 m in thickness, and like Facies I, two or more units of Facies J may be repeated in any one Halfway core.

The dominant sedimentary structures of Facies J are planar tabular and trough cross-bedding (Plate 33). Beds of horizontal lamination are abundant in some cores, particularly

Plate 33. Facies J planar-tabular cross-bedded sandstone containing small mudstone clasts. Well 16-2-73-8-W6. 2037 m.

Plate 34. Vertical burrow (escape trace) in Facies J plane laminated sandstone. Well 16-5-73-8-W6. 2128 m.

toward the top of the facies. Cross-bed sets are 5-20 cm thick and many contain small mudstone clasts at their bases and along foreset laminae. In several instances (eg. well 14-2-73-8-W6), vertically adjacent cross-bed sets appear to have opposing palaeocurrent directions. As the cores were not oriented however, it was not possible to determine the actual palaeocurrent azimuths. If these cross-bed sets are truly bipolar and occur commonly in Facies J, it would suggest some tidal current influence on deposition.

Intercalated with the cross-bedding are beds of current ripple cross-laminated silty sandstone. The presence of current ripple cross-lamination indicates that the currents which deposited Facies J were predominantly unidirectional, rather than oscillatory as observed in other Halfway facies. Several examples of climbing ripple cross-lamination were observed, suggesting periods of very rapid sedimentation. Many of the laminae of current ripple cross-lamination however, contain thin siltstone drapes over foreset laminae. This indicates that traction transport of sand sized sediment which produced the ripple cross-lamination alternated with slack water periods when finer-grained material was able to fall from suspension. Thicker laminae of green shale and grey dolomitic mudstone are also found in Facies J between ripple cross-laminated and cross-bedded units. These mudstone laminae are commonly brecciated, both by fluid escape and scour and probably form the source of many of the small mudstone clasts scattered through the facies.

The proportion of ripple cross-laminated silty sandstone increses upward in many cored examples of Facies J and the unit grades into Facies K, characterised by interlaminated sandstone and mudstone. In many examples however, the upper part of Facies J is dominated by horizontally laminated sandstone. This represents deposition under upper flow regime plane bed conditions, probably in very shallow water.

Trace fossils in the cross-bedded sandstone units of Facies J are dominated by simple vertical forms such as *Skolithos*, and escape traces (Plate 34). Other forms such as *Asterosoma*, *Terebellina*, *Planolites* and *Palaeophycus* were also observed, most commonly in the silty rippled sandstone intervals. This probably reflects the more hospitable nature of a substrate subject to lower rather than upper flow regime current strengths. In some instances these burrow traces have almost destroyed the primary physical sedimentary structures.

4.11.0 Facies K. Interlaminated Sandstone and Siltstone.

Facies K consists of pale brown-grey current ripple cross-laminated very fine grained sandstone and siltstone interlaminated with green shale and grey dolomitic mudstone (Plate 35). It is always gradational with the underlying Facies J sandstone and is typically overlain abruptly by Facies L. The facies ranges from less than one metre to 5 m in thickness, with the mode being about 2 m.

The lower part of Facies K in most sections consists of current ripple cross-laminated fine grained sandstone which is gradational with the cross-bedded and current ripple cross-laminated Facies J sandstone below. Small scattered clasts of dolomitic mudstone persist into this facies. Many of the Facies K current ripples also have mud-draped foresets. Distinct mudstone laminae become abundant upward (Plate 35), such that the upper part of the facies is characterized by wavy and lenticular bedding. In some cases the top of Facies K consists entirely of horizontally laminated shale (Plate 36). Such fine-grained laminae in Facies K may be of either green silty shale or pale grey dolomitic mudstone identical to that in Facies G2. Where sandstone and mudstone are interbedded, sandstone dykes and other fluid escape structures are common (Plate 37), many superficially resembling erosionally ripped-up beds. In addition, many of the ripple cross-laminated sandstone beds have loaded bases. Thin horizontally laminated sandstone beds similar to Facies M may also be present within Facies K.

Trace fossils are relatively abundant but not particularly diverse in Facies K, consisting of robust examples of the horizontal burrow forms *Planolites* and *Palaeophycus*, with some examples of *Skolithos*, *Teichichnus*, *Terebellina*, and escape traces (Plate 38).

The interbedding of thin sandstone and mudstone laminae characteristic of Facies K represents the same repeated alternation of deposition from current traction and suspension observed in Facies I and J, and is similarly interpreted as being tidally-generated. In Facies I and J, fine grained sediment deposited from suspension during slack water is markedly subordinate to coarser-grained sand transported by ebb- or flood-tidal currents, whereas in Facies K the reverse is true. This suggests that Facies K accumulated in a part of the tidal channel where tidal current flow was more restricted and intermittent than the areas where Facies I and J formed. A lower-energy setting for Facies K is also suggested by the high degree of burrowing and the trace fossil assemblage, which consists dominantly of horizontal forms. Despite the evidence of an overall lower-energy environment, the presence of loaded sandstone laminae, current

Plate 35. Facies K interlaminated silty shale (dark) and current ripple cross-laminated sandstone (pale). Well 8-23-73-9-W6. 2150 m.

Plate 36. Horizontally laminated shale from the upper part of Facies K. Note lenticular, ripple cross-laminated sandstone in centre of view. Well 6-23-72-8-W6. 2179 m.

Plate 37. Small sandstone dyke in Facies K interlaminated sandstone (with white anhydrite nodules) and dolomite mudstone. Well 6-22-72-8-W6. 2208 m.

Plate 38. Moderately burrowed sandstone-shale from the upper part of Facies K. Well 16-2-73-8-W6. 2031 m.

ripple cross-lamination, escape traces and fluid escape structures all point to periods of rapid sedimentation. Facies K is therefore interpreted to have accumulated in a tidal channel environment where tidal current flow was relatively weak and infrequent, allowing large amounts of fine grained sediment to fall out of suspension. The presence of thin sandstone beds similar to Facies M suggests that rapid sedimentation of the sandstone laminae may have been associated with higher than normal tides or storm activity.

Similar sequences of interlaminated rippled sandstone and mud have been described from the upper part of tidal inlet fill sequences in Price and Capers inlets, South Carolina, by Tye (1984). Historical records allowed Tye (1984) to interpret this muddy unit as representing a decrease in tidal flow through the inlets as the channels were abandoned. Following channel abandonment, the old ebb-tidal channels of Price and Capers inlets became sealed by wave-reworked ebb-tidal delta sands, restricting tidal flow through them. The abandoned tidal inlet channels were therefore protected from wave action and strong tidal currents, allowing fine grained sediments to accumulate from suspension. This is somewhat analogous to the formation of a clay-filled oxbow lake in a fluvial environment. Tye (1984) also reported the presence of thin coarser-grained sand and shell laminae transported into the abandoned inlet channel by high tides and storm washover.

The evidence of deposition under relatively low-energy tidal conditions displayed in Facies K could also have been produced in a tidal flat setting as described by Evans (1965), as process-wise there is little difference between the two environments. However, the association of Facies K with the active tidal channel fill deposits of Facies I and J suggest that an origin as abandoned tidal channel fill similar to that described by Tye (1984) is more likely.

4.12.0 Facies L. Cross-Bedded and Plane Laminated Sandstone

Facies L consists of very-fine grained and well sorted pale brown sandstone and typically rests abruptly (with load casts) or erosively (with rip-up clasts) on Facies K abandoned tidal inlet channel fill (Plate 39). In some instances however, this contact is gradational. The facies is typically 2-4 m thick, but examples up to 6 m thick were measured in several wells (eg. well 8-26-72-8-W6; Appendix A). In these thicker examples, Facies L was observed to rest gradationally on Facies J active tidal channel deposits. The upper contact, like that of Facies E, is always sharp and overlain by either Facies F (foreshore) or Facies G (lagoon).

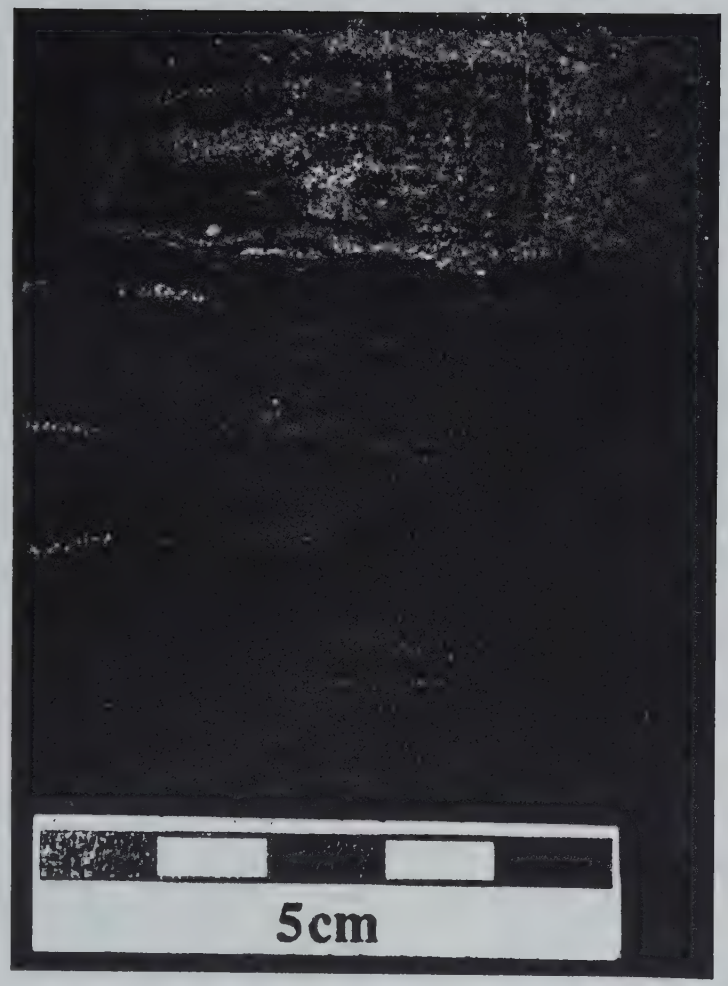

Plate 39. Facies L sandstone above resting abruptly on Facies K siltstone below. Well 7-5-73-8-W6. 2125 m.

Plate 40. Facies L sandstone. Note inclined planar laminae with concentrations of chert grains. Well 6-22-72-8-W6. 2200 m.

The dominant sedimentary structures of Facies L are interbedded units of cross-bedding and horizontal or gently inclined plane lamination. Individual horizontal laminae range in thickness from 5 mm to 2 cm and in several cases displayed normal grading (eg. well 16-30-72-7-W6; Appendix A). Beds of this plane lamination are variable in thickness and bounded by cross-cutting discontinuity planes, commonly marked by thin laminae of chert grains or bioclastic fragments (Plate 40). In view of the well sorted nature of the sandstone and its association with cross-bedding and scour planes, this horizontal lamination is interpreted as upper flow regime plane bedding. This would suggest that Facies L accumulated in very shallow water.

Interbedded with the plane lamination are units of planar-tabular and trough cross-bedding (Plates 40 and 41). Cross-bed sets range from 5-30 cm in thickness and are bounded by scour planes with coarse chert grain lags. Thin beds of oscillation and current ripple cross-lamination were also observed in Facies L. The occurrence of oscillation ripple cross-lamination indicates that the Facies L depositional environment was subject to at least periodic influence from oscillatory wave currents, but the other bedforms indicate the dominance of strong unidirectional currents.

Mud-draped foreset laminae (eg. well 16-2-73-8-W6; Appendix A) and flaser beds (eg. well 16-19-72-7-W6; Appendix A) were observed in a few of the cross-bedded sandstone units of Facies L. These indicate periodic breaks in deposition of sand from currents and fallout of finer-grained material from suspension. As mentioned in discussions of Facies I, J, and K, such alternations of strong unidirectional current flow and still water are commonly associated with tidal environments, where flood- or ebb-oriented bedforms are draped with thin mud layers which fall out of suspension at slack tide (Visser, 1980; Nio and Yang, 1991).

An unusual sedimentary structure was observed in many cored intervals of Facies L. This consists of 1-2 cm of crinkly, white coloured sub-millimetre laminated sandstone (Plate 42). The lamination is not caused by any grainsize or mineralogical variation in the sediment and appears to be similar to the adhesion lamination described by Kocurek and Fielder (1982). This is produced by the adhesion of wind-blown grains to a damp surface and implies that the Facies L depositional surface must have been periodically subaerially exposed.

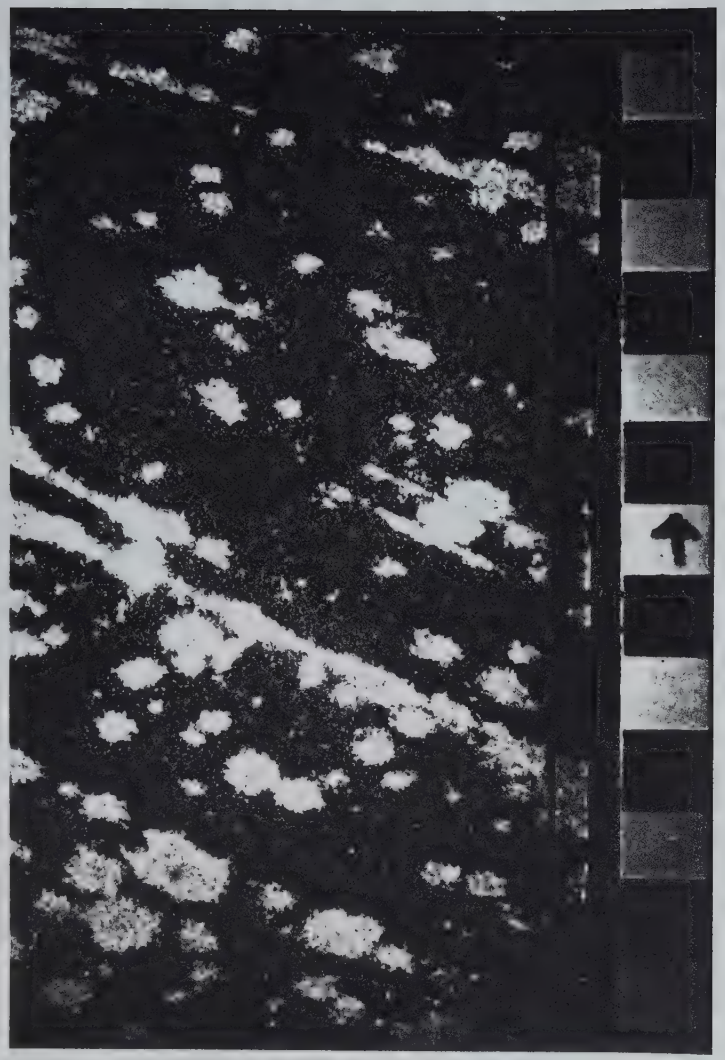

Plate 41. Planar-tabular cross-bedding in Facies L sandstone. Darker areas are dolomite cemented, white ones anhydrite. Well 10-35-72-8-W6. 2072 m.

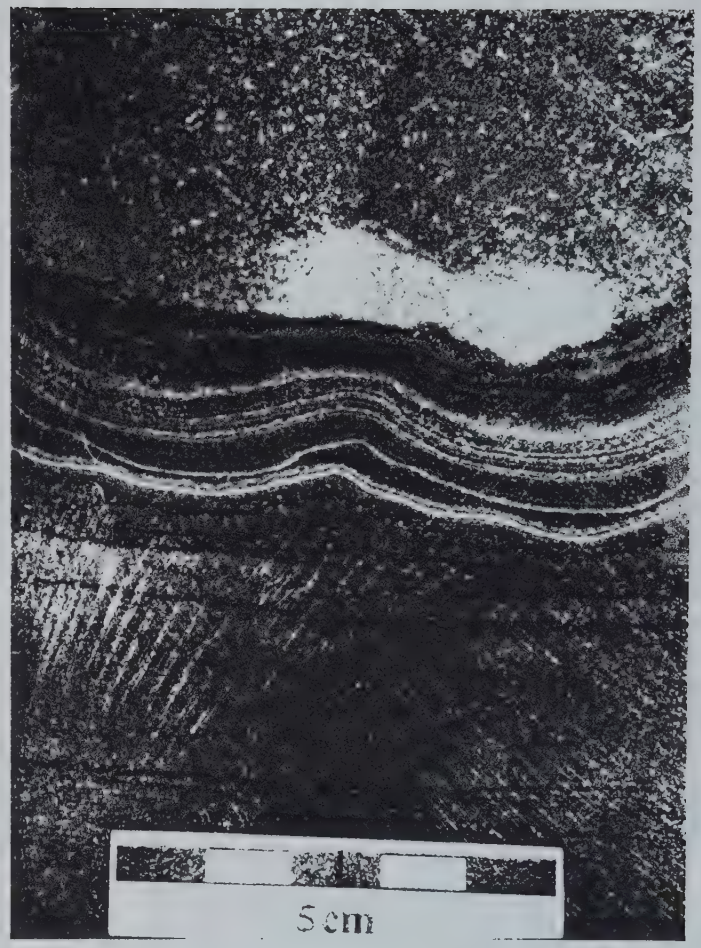

Plate 42. Undulatory white laminae in Facies L sandstone, interpreted as adhesion lamination. Well 5-13-72-8-W6. 2154 m.

Trace fossils were rarely observed in Facies L, and where present consisted solely of escape traces (eg. well 16-21-72-8-W6; Appendix A). This is consistent with the highly mobile substrate indicated by the physical sedimentary structures.

The occurrence of both wave and tidally influenced sedimentary structures in Facies L place some constraints on its depositional environment. The interaction between wave-generated processes and tidal processes is typically restricted to the mouths of estuaries and tidal inlet channels (Oertel, 1972; Greer, 1975; Davis and Fox, 1981). The almost ubiquitous occurrence of Facies L above facies I, J, and K, interpreted as a tidal inlet channel fill sequence, suggests that it was deposited at the mouth of a tidal inlet channel rather than in an estuary. The lobate sandbodies which accumulate at the seaward mouth of such tidal inlet channels on microtidal and mesotidal coastlines through the interaction of waves and tidal inlet currents are referred to as ebb-tidal deltas (Hayes, 1980).

The components of a typical ebb-tidal delta are illustrated in Figure 19. Field studies of this ebb-tidal delta depositional environment are relatively few owing to the difficult working conditions resulting from strong tidal currents, large waves, and mostly subtidal conditions. Hayes (1980) produced a hypothetical ebb-tidal delta sequence based on his and other workers observations of surficial ebb-tidal delta processes and bedforms (Figure 20). Imperato et al. (1988) describe the mesotidal ebb-tidal delta associated with North Edisto Inlet, South Carolina, and Sha (1990) that of the microtidal Texel Inlet in the Netherlands. The sequences of sedimentary structures described in both papers are similar to Hayes (1980) model and contain many of the features observed in Facies L.

Interpreted ancient ebb-tidal delta sequences are limited to an example from the Eocene of Spain by Yang and Nio (1989) and a brief mention in a paper on Carboniferous barrier island deposits by Hobday and Horne (1977). Similar sandstones above ancient tidal inlet fill sequences have, however, been referred to as "spit platform" deposits by Barwis and Makurath (1978) and Uhlir et al. (1988). This paucity of ancient examples may be in part due to the lack of modern analogues to aid their interpretation, and also the apparent poor preservation potential of ebb-tidal deltas. Periodic ebb-tidal channel avulsion allows waves to rework and destroy much of the sedimentary record of ebb-delta deposits (Oertel, 1977; Moslow and Tye, 1985).

Imperato et al. (1988) observed ebb-tidal delta sands of North Edisto Inlet to overlay interlaminated sands and muds of abandoned tidal inlet ebb-channel fill (Figure 21). This

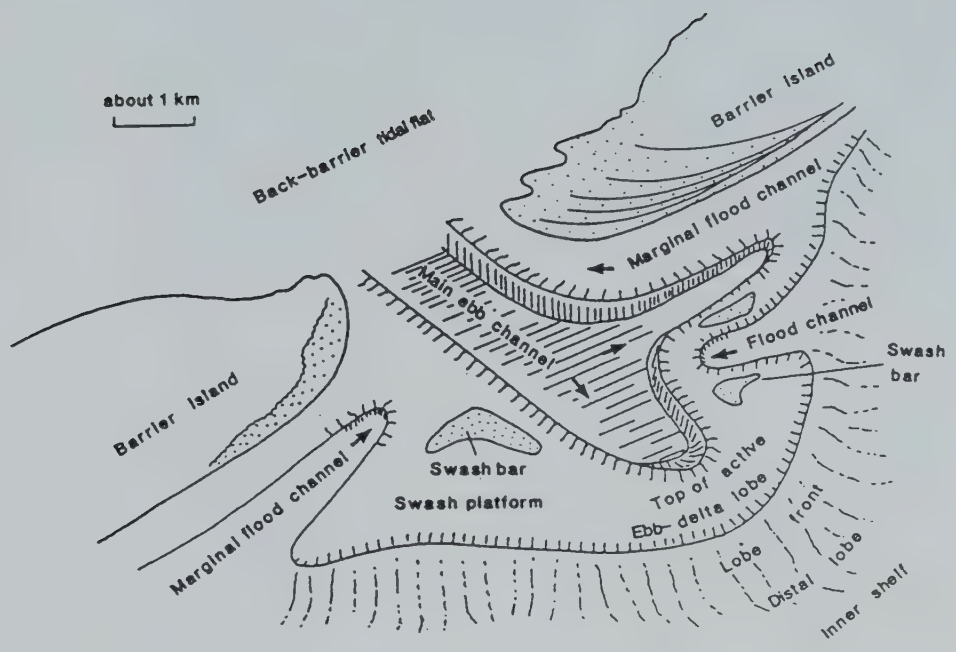

Figure 19. Schematic diagram showing the morphology of ebb-tidal deltas, based on examples from the tidal inlets of the West Frisian Islands in the Netherlands (after Sha, 1990).

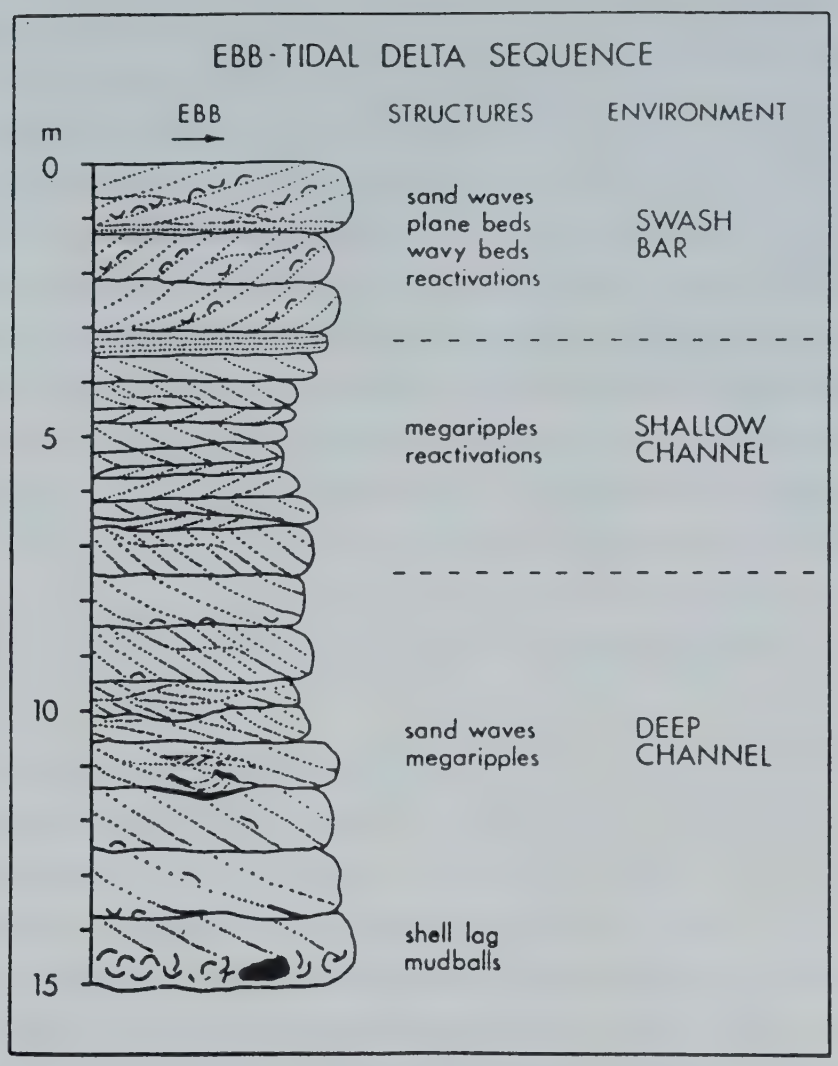

Figure 20. Hypothetical vertical stratigraphic sequence of ebb-tidal delta sediments based on observation of surface bedforms and processes (after Hayes, 1980).

is analogous to the common occurrence of Facies L resting on Facies K abandoned tidal inlet channel fill. The North Edisto ebb-delta sands were characterised by either horizontal plane lamination or were massive, the latter attributed to the uniform grainsize of the sand. This plane lamination was interpreted by Imperato et al. (1988) as upper flow regime plane bedding, representing continuing shallowing of the abandoned inlet channel. Their field observations suggested that the lamination was produced on the swash platform of the ebb-tidal delta (Figure 19) by the landward-directed bore of spilling breakers in the shallow (<5 m) water. Upper flow regime plane bedding generated in this way was also the dominant structure recorded in the Texel inlet ebb-tidal delta by Sha (1990). The measured thickness of the ebb-tidal delta sands in these studies were 5-8 m in the case of North Edisto Inlet, and 20 m for Texel Inlet. Both are capped by units of gently inclined plane bedding deposited in the foreshore of the barrier/spit beach, analogous to the thin unit of Facies F sandstone sometimes preserved above Facies L. Sha (1990) also noted the presence of thin beds of oscillation ripple cross-lamination in the slightly deeper water, more distal parts of the Texel ebb-tidal delta.

The shallow swash platform of the ebb-tidal delta is typically covered by large isolated bedforms termed swash bars (Figure 19). These bedforms form as a result of the swash action of waves (Oertel, 1972; Hubbard et al., 1979; Hayes, 1980; Davis and Fox, 1981). The swash bars of North Edisto Inlet are composed almost exclusively of very well sorted, fine grained sand and consist of a scoured base with a course grained lag overlain by large landward-dipping planar-tabular cross-bedding with numerous reactivation surfaces (Imperato et al., 1988). Onshore swash bar migration often completely reworks deposits from the preceding swash bar, so the most commonly preserved portion is the basal coarse-grained shelly lag. Cross-bed sets are also commonly reworked by spilling breakers into plane beds, making this the most common bedding type preserved in the subsurface of the swash platform (Imperato et al., 1988). This accounts for the abundance of plane lamination and thin, coarse-grained chert lags in Facies L.

Swash bars also create a relatively sheltered area in their lee, as the bar blocks wave energy for most of the tidal cycle. Imperato et al. (1988) recorded *Callianassa major* burrows in these areas as the only evidence of biogenic activity on the otherwise inhospitable swash platform. In addition, Sha (1990) observed mud drapes forming at slack water in areas behind large bedforms sheltered from wave action on the Texel ebb-tidal delta. He did not find mud drapes elsewhere on the ebb-tidal delta due to the constant strong wave influence and short duration of slack water, and also found them to

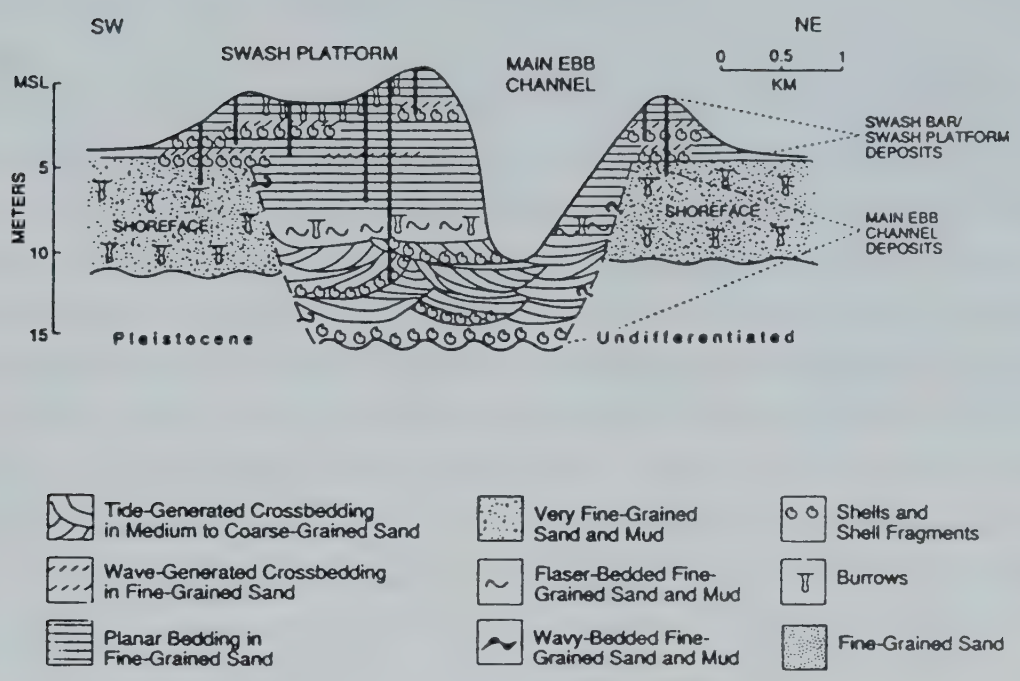

Figure 21. Shore-parallel vibracore cross-section through the ebb-tidal delta of North Edisto Inlet, South Carolina. Tidal inlet ebb-channel deposits rest disconformably on Pleistocene sediments and are overlain by ebb-tidal delta swash platform deposits (after Imperato et al., 1988).

be rarely preserved in the flood- and ebb-tidal channels. Oertel (1973) ascribed the origin of mud laminae in sands at the mouth of Doboy Sound, Georgia to (a) suspension fallout of mud at slack tide, (b) accumulation of faecal pellets of *Callianassa major*, and (c) bedload deposition of eroded mud pebbles. It is suggested that the rare mud drapes and flaser bedding in Facies L originated in a similar manner.

As shown in Figure 19, the areas between the swash platform of an ebb-tidal delta and the adjacent updrift and downdrift beaches are usually occupied by marginal flood channels. This is a result of the time-velocity asymmetry of the tidal currents (Hayes, 1980), whereby at low water as the tide turns, strong ebb-currents are still flowing out of the main ebb-channel. This forces incoming flood-currents to seek paths of least resistance around the margins of the delta. Marginal flood-channel deposits were noted by Imperato et al. (1988) and Sha (1990) to consist of an erosional base with coarse-grained shelly lag overlain by flood-oriented cross-bedded sand. Similar erosively-based cross-bedded sandstones occur in Facies L (eg. well 16-22-72-8-W6; Appendix A) and have been described from Carboniferous barrier island deposits by Hobday and Horne (1977). Switching of the marginal flood-channels on both The North Edisto and Texel ebb-tidal deltas due to hydraulic inefficiently caused new channels to be cut into swash platform sands and the abandoned channels to infill with burrowed flaser bedded sand and mud (Figure 22). Imperato et al. (1988) therefore suggested that in some cases much of the record of ebb-tidal delta sedimentation may consist of active and inactive channel fill produced by the migration of the main ebb-channel and marginal flood-channels.

The plane laminated and cross-bedded sandstone of Facies L is interpreted to have been produced by wave swash and migration of large swash bars on an ebb-tidal delta at the seaward mouth of a tidal inlet channel. Reworking of these deposits by marginal flood channels is also recorded by erosively-based cross-bedded sandstones. Preservation was probably related to the mechanism of bar-bypassing, where the ebb-tidal delta sands were welded onto the front of the abandoned tidal inlet channel. Wave reworking of the sediment and landward-directed washover into the inlet channel during abandonment has resulted in some examples of Facies L being similar to Facies E (upper shoreface) and M (washover) respectively.

Thicker examples of Facies L overlying Facies I and J active inlet deposits represent deposition in the seaward mouth of the inlet channel. Thinner examples which overly and

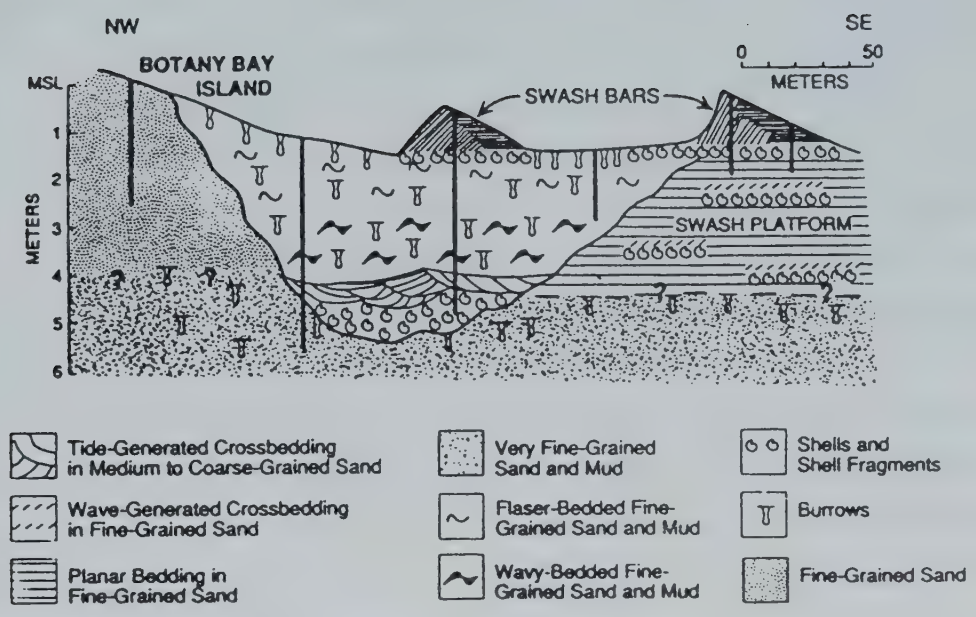

Figure 22. Vibracore cross-section through an abandoned marginal flood channel on the ebb-tidal delta of North Edisto Inlet, South Carolina. The channel sequence is approximately 5 m thick and is capped by swash-bar deposits (after Imperato et al., 1988).

are interbedded with Facies K fine-grained inlet fill probably represent ebb-tidal delta sand washed further back into the abandoned channel.

As discussed under Facies D, some Halfway lower shoreface deposits contain scour surfaces similar to those commonly associated with Facies I inlet channel lags. In such cases, the lower shoreface sediments are noticeably different, containing small dolomitic mudstone clasts, bioclastic fragments and mud laminae. These features suggest that such sequences represent establishment of an ebb-tidal delta in the lower shoreface environment seaward of a tidal inlet mouth. Strong ebb-currents flowing out of the inlet channel resulted in scours, introduction of bioclastic material and mudstone clasts and tidal influence in the lower shoreface deposits. Where the inlet remained stable, continued progradation of the coastline would result in the sequence coarsening-upward into sandstones which display characteristics of both Facies E and L. These sequences thus display features of both tidal inlet and shoreface environments and are intermediate between the two. In cases where the tidal inlet has migrated laterally, the distal interfingering ebb-tidal delta and lower shoreface deposits may be preserved immediately beneath the basal inlet scour (Greer, 1975). This can be seen in several Halfway tidal inlet sequences (eg. 8-28-72-8-W6; Appendix A).

Thus a whole spectrum of ebb-tidal delta deposits are preserved within the Halfway Formation, representing both establishment and eventual abandonment of the sandbody. This has resulted in a variety of preserved sedimentary structures which in many cases mimic other facies deposited under similar conditions.

4.13.0 Facies M. Plane Laminated Granular Sandstone.

Facies M consists of up to 6 m of very-fine-to-fine grained chert-rich sandstone, but tapers rapidly northeastward into a thin, discontinuous, mottled silty sandstone. The base of the facies is usually erosional on Facies G2 lagoonal mudstones, with a thin lag of rip-up clasts and chert granules (Plates 43 and 44). In some instances however (eg. well 10-32-72-8-W6; Appendix A), Facies M appears to be gradational with 1-2 m of the silty washover sandstones observed in Facies G. The upper contact of the facies is typically abrupt and overlain by either Facies G1 crypt-algal laminites, or red beds of Facies H. In some cases however, the upper part of Facies M is distinctly interbedded with Facies G, providing evidence for the time-equivalence of the Halfway and Charlie Lake Formations (Plate 45).

Plate 43. Facies M plane laminated granular sandstone above resting abruptly on Facies G2 mudstones below. Well 6-14-72-8-W6. 2196 m.

Plate 44. Facies M sandstone resting erosively on Facies G2 dolomite mudstone. Note small rip-up clasts above contact (arrowed) and graded laminae within Facies M. Well 16-15-72-8-W6. 2210 m.

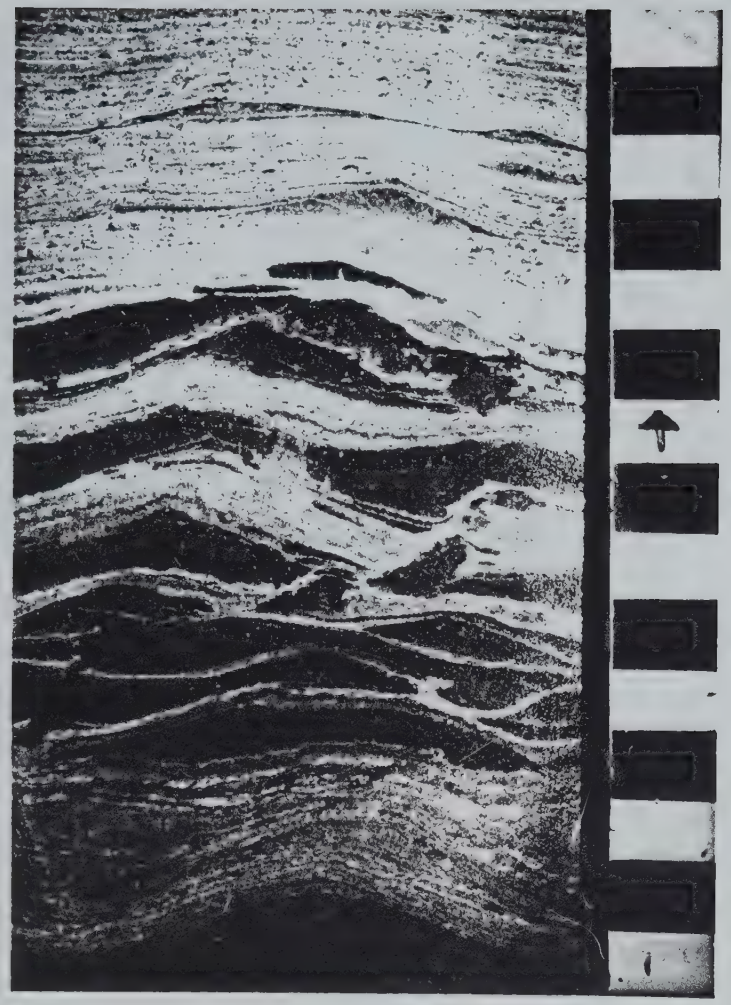

Plate 45. Facies M sandstone of the Halfway Formation (dark) interbedded with Facies G1 crypt-algal laminites of the Charlie Lake Formation (pale). Well 6-4-73-8-W6. 2103 m.

Plate 46. Facies M plane laminated granular sandstone. Well 8-22-72-8-W6. 2179 m.

Additionally, in most Halfway sequences, a thin (<50 cm) bed of Facies M is commonly found erosionally overlying Facies E and L, in which case it is overlain by Facies G.

The dominant sedimentary structure of Facies M is sub-horizontal plane lamination, commonly with concentrations of coarse grains of black and white chert as seen in Facies E, F and L (Plate 46). Individual laminae are 1-2 cm thick and may show slight normal or inverse grading. These laminae are grouped into beds up to 50 cm thick separated by cross-cutting discontinuity surfaces marked by concentrations of coarse chert grains. The abundance of scour features in the sandstone suggests that this lamination is upper flow regime plane bedding generated by high velocity sheet flow in shallow water depths.

Intercalated with this plane lamination are sets of planar-tabular and trough-cross-bedding (Plate 47) and some current ripple cross-lamination. Mud-draped ripple bedforms were observed in Facies M in several cores (eg. well 6-23-72-8-W6; Appendix A), suggesting that there were periodic breaks in current flow, allowing finer-grained sediment to fall out of suspension. In addition, thin beds (1-5 cm) of the millimetre-scale crinkly adhesion lamination described in Facies L are common in Facies M sandstone. This implies that the Facies M depositional surface was periodically subaerially exposed, providing further evidence for the intermittent nature of Facies M current flow.

Syn-sedimentary microfaulting (eg. well 6-9-73-8-W6; Appendix A) and small slump structures (well 6-4-73-8-W6; Appendix A) are common features in Facies M sandstone, as well as loading of the underlying mudstones (Plates 48 and 49). These features suggest that the Facies M sandstone was rapidly deposited and subsequently unstable.

No specific biogenic sedimentary structures were recorded from Facies M during this study. This is probably related more to preservation difficulty in the uniform grainsize than a primary absence of burrowing activity, since bioturbation is inferred in the mottled distal units of Facies M and biogenic activity is common in other Halfway facies.

The stratigraphic position of Facies M, encased in backbarrier deposits (Facies G), is one commonly associated with washover fans and flood-tidal deltas (eg. Hennessy and Zarillo, 1987). Facies M however, contains none of the evidence of tidal influence common to published descriptions of flood-tidal delta sequences (Hayes, 1980; Donselaar, 1984; Berelson and Heron, 1985; Israel et al., 1987; Murakoshi and Masuda, 1991; Boersma, 1991). The physical sedimentary structures observed in Facies M,

Plate 47. Trough cross-bedding (at bottom of view) intercalated with horizontal lamination in Facies M granular sandstone. Well 6-14-72-8-W6. 2192 m.

Plate 48. Soft-sediment deformation (slump) feature in Facies M sandstone. Well 6-4-73-8-W6. 2105 m.

Plate 49. Sand volcano (arrowed) in Facies G2 lagoonal mudstones produced by loading of overlying Facies M sandstone (dark coloured). Well 6-33-72-8-W6. 2134 m.

consisting dominantly of upper flow regime plane beds with minor cross-laminated units, suggest deposition in a very shallow water environment from fast-flowing currents. The presence of adhesion lamination indicates that the depositional surface was frequently subaerially exposed and that the fast-flowing currents which produced the plane lamination must therefore have been episodic. These features are characteristic of washover deposits produced by storm breaching of a strandplain (Hayes, 1967; Andrews, 1970; Deery and Howard, 1977; Leatherman and Williams, 1977; Schwartz, 1975, 82; Donselaar and Nio, 1982).

Washover (or overwash) is the continuation of the foreshore swash over the crest of the barrier platform, typically in response to higher energy conditions produced by storms (Leatherman and Williams, 1977). Washover surges cut narrow channels through the subaerial portion of the strandplain, allowing the sediment-laden water to spill out onto the backbarrier flats, marsh or lagoon, depending on the magnitude of the surge and the width of the island. Here the flow can expand and decelerate as it leaves the horizontal confines of the channel. Multiple washover events may be produced during a single storm in response to repeated surges (Leatherman and Williams, 1977). Repeated breaching of the same stretch of the strandplain by washover surges leads to the amalgamation of washover deposits into lobate washover fans, which may themselves coalesce through time to form a more linear washover terrace (Schwartz, 1982).

Basal contacts of washover deposits tend to be sharp, commonly with a thin lag of pebbles, plant and shell fragments (Donselaar and Nio, 1982). This is produced by the initial scouring action of the washover surge as it crosses the barrier crest and backbarrier environments and is analogous to the thin lag present at the base of Facies M in Plate 25.

Internally, the deposit of a single washover event consists mainly of sub-horizontal to very low angle landward-dipping planar laminae reflecting sedimentation during high velocity flow across the fan's surface (Leatherman and Williams, 1977; Schwartz, 1982). These laminae may exhibit both normal and inverse grading, but Leatherman and Williams (1977) found inverse grading to be predominant. Heavy mineral-rich laminae are also common in washover deposits (Schwartz, 1982) and may be analogous to the laminae of coarse chert grains present in Facies M.

As an overwash enters a body of water, such as a lagoon, flow expansion and deceleration results in the development of "microdelta" high-angle tabular foreset strata (Figure 23).

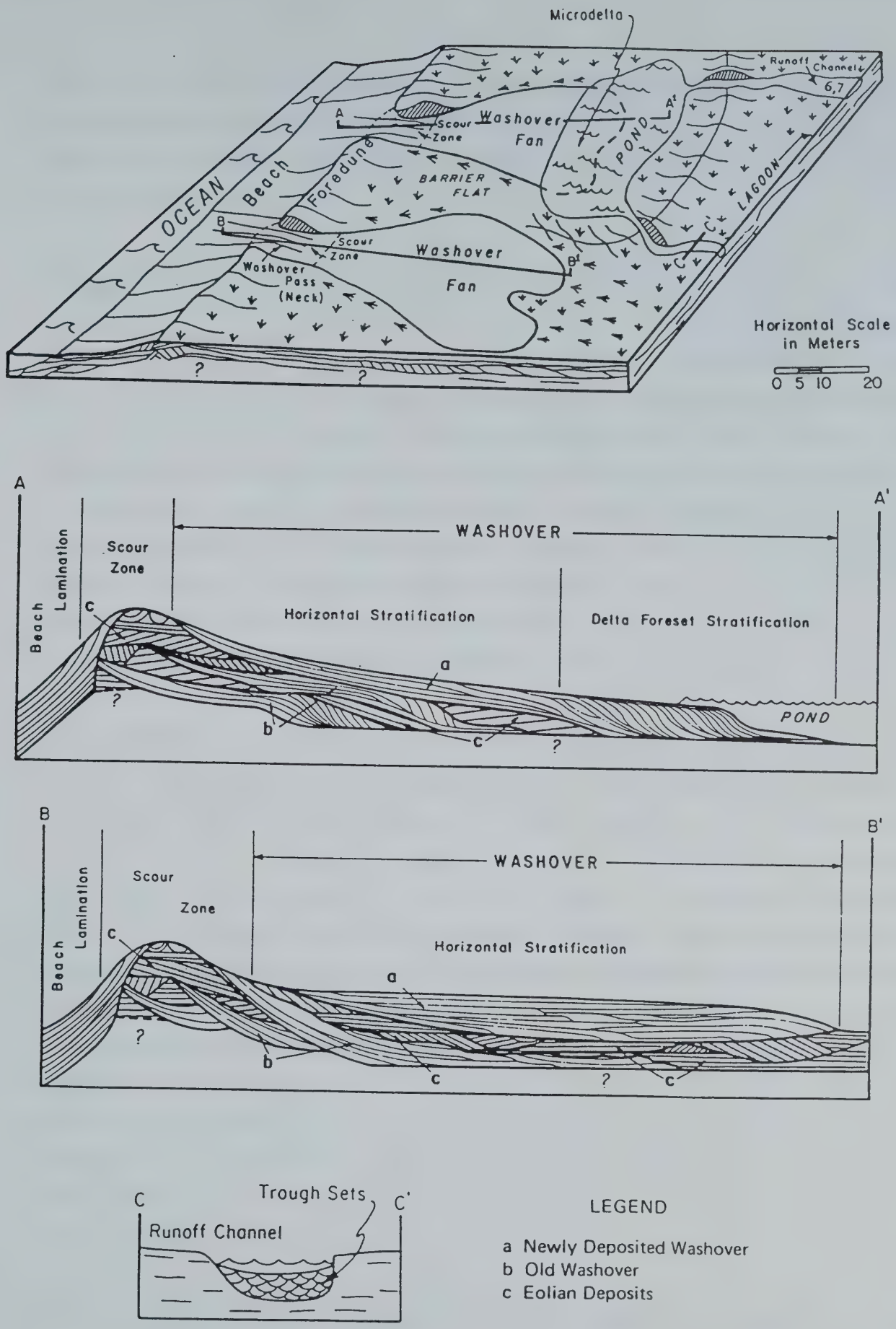

Figure 23. Schematic diagram illustrating the sedimentary structures associated with small-scale washover fans. The sectional views represent the upper metre or less of the sandbody complex (after Schwartz, 1982).

Minor current ripple cross-lamination or cross-bedding may also develop where the washover event crosses slight irregularities in the fan's surface, or where flow becomes channelised (Schwartz, 1982). This is considered responsible for the cross-lamination present in Facies M sandstone.

Individual washover deposits tend to be relatively thin (5 cm to about 1 m; eg. Bridges, 1976) and isolated within backbarrier lagoonal deposits, reflecting the intermittent nature of their storm genesis. This is in contrast to the thick (6 m) Facies M sandbody. Extended periods between storm overwash events can also lead to their extensive modification by wind, wave and tidal currents, burrowing organisms and plant rooting. Aeolian modification of Facies M is evidenced by the presence of adhesion ripple lamination, and it is possible that some of the cross-stratification observed in the facies is in fact aeolian in origin. Prominent scour surfaces and chert grain lags within Facies M sandstone may represent the bases of successive periods of overwash, but no evidence of any hiatus (such as a palaeosol) was found between them. This would suggest that the thick Facies M washover sandbody accumulated in a relatively short period of time.

Under conditions of persistent overwash sedimentation, particularly when a barrier island coastline is undergoing transgression, much thicker amalgamated washover deposits can accumulate (Leatherman and Williams, 1977; Kraft and John, 1979). Kraft and John (1979) describe the transgressive barrier islands of the Delaware coast as consisting dominantly of washover sands 4 to 8 m thick. These rest on lagoonal deposits, either abruptly or gradationally as with the contact between Halfway Facies M and G. Continuing transgression along the Delaware coastline has resulted in the washover fans migrating landward, such that the distal silty sandstones are covered by coarser sands of the proximal fan. This is similar to the gradational upward-coarsening sequence of lagoonal mudstones through mottled silty sandstones to clean sandstone seen in many cored examples of Facies M (eg. well 10-32-72-8-W6; Appendix A). An identical sequence was also noted from a Pleistocene transgressive barrier island by Demarest and Kraft (1987), who commented on the unusual formation of an upward-coarsening sequence during a transgression.

Other examples of washover deposits of similar thickness to Facies M have been described from the Eocene of Spain by Donselaar and Nio (1982) and from the Pleistocene Port Durnford Formation of Zululand, South Africa by Hobday and Orme (1974) and Hobday and Jackson (1979). In the Port Durnford Formation, lagoonal clays

and peat are overlain by 5.5 m of well-sorted, fine grained quartz sand (Figure 24). Physical sedimentary structures are dominated by landward-dipping, sub-horizontal planar laminae with heavy minerals and intercalated sets of high-angle planar tabular cross-bedding and some adhesion ripple lamination. The authors interpret this sandbody as washover fan deposit associated with barrier island destruction following a rise in sea level during the Sangamon (Eem) transgression.

Examples of soft sediment deformation features similar to those noted in Facies M are commonly reported in washover deposits (Hobday and Jackson, 1979; Donselaar and Nio, 1982; Murakoshi and Masuda, 1991). Convoluted laminae result from pore fluid escape in the rapidly deposited washovers in subaqueous settings such as a lagoon (Lowe, 1975). In subaerial portions of washover fans, pore water is lost through percolation and such features do not develop (Schwartz, 1975). Rapid deposition of washover sands also compacts underlying sediment and can result in expulsion of their pore fluids. This can be seen in the large sand volcano shown in Plate 45 and an identical example in the Figure 10 of Murakoshi and Masuda (1991). Hobday and Jackson (1979) consider the numerous syn-sedimentary faults and folds in the Pleistocene Port Durnford Formation of Zululand to be the result of gravity gliding and loading following thick washover sand deposition on lagoonal mudstones. Similar processes may be responsible for the Facies M slump structure shown in Plate 27.

The plane laminated sandstones of Facies M are therefore interpreted as the product of washover sedimentation into the Halfway backbarrier environment. The subaerially exposed washover deposits were subsequently subjected to modification by aeolian processes.

The great thickness (6 m) of amalgamated washover deposits in Facies M suggests that the unit accumulated under conditions of persistent overwash. Documented examples of such thicknesses of washover deposits are restricted to transgressive shorelines. It is therefore felt that Facies M accumulated during a period of persistent overwash along the Halfway coastline, probably associated with a transgression.

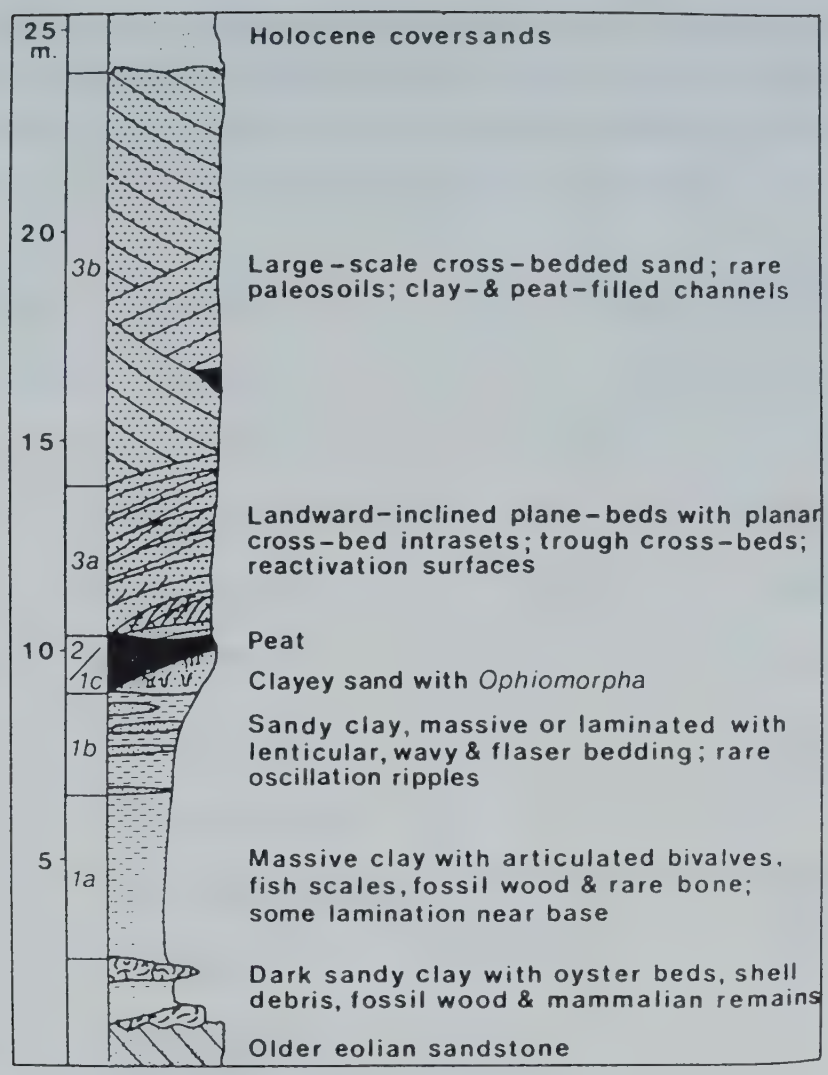

Figure 24. An example of a thick sandbody of washover origin resting on lagoonal mudstones in the Pleistocene Port Durnford Formation of South Africa (after Hobday and Jackson, 1979).

5.0.0 FACIES ASSOCIATIONS.

Two recurring vertical facies associations were identified in this study (Table 3). Facies association 1 consists of a gradational upward-coarsening sequence displaying an upward increase in the influence of oscillatory current action and is interpreted as a regressive shoreface deposit. Facies association 2 is an upward-fining sequence which truncates facies association 1 and is interpreted as a tidal inlet channel fill.

Facies Association 1 Regressive Shoreface		**Facies Association 2** Tidal Inlet Channel Fill	
Facies	Environment	Facies	Environment
H	Supratidal	H	Supratidal
G	Backbarrier	G	Backbarrier
F	Foreshore	L	Ebb-tidal delta
E	Upper shoreface	K	Abandoned tidal inlet fill
D	Lower shoreface	J	Active tidal inlet fill
C	Offshore- transition	I	Tidal inlet channel lag
B	Offshore		
A	Transgressive sandsheet		

Table 3. Halfway Formation Facies Associations.

The following chapter describes the depositional origin of these facies associations and compares them to modern and ancient analogues. Vertical and lateral variation of the facies associations and their relationships to each other are also discussed.

Facies M occurs above both facies associations and is not intimately associated with either. Its origin is discussed in section 7.4.0.

5.1.0 Facies Association 1: Regressive Shoreface.

Facies association 1 consists of a conformable upward-coarsening sequence comprising Facies B to H (Figure 25). The upper part of the sequence (Facies G and H) is common to facies association 2.

The base of facies association 1 is picked at the base of Facies A. This facies is interpreted as a thin shoreface deposit formed during transgression over the underlying Doig Formation. It consists largely of reworked Doig sediments and contains rip-up clasts. Sedimentary structures in Facies A indicate that it was deposited within wave base, probably during the initial stages of transgression before water depths increased. Phosphate-coated grains are common in Facies A, suggesting slow rates of deposition during the transgression. The upper contact of the transgressive unit is typically sharp and overlain by Facies B black shales deposited in the marine offshore, indicating a significant increase in palaeowater depth. The lower-most few centimetres of these black shales are rich in phosphate and probably represent a condensed section deposited on the continental shelf immediately following transgression, when clastic sediment input was limited.

Facies B shales represent the initial stages of renewed regressive sedimentation in the study area following transgression of the Doig Formation. The finely laminated shales were deposited mainly by mud and silt falling out of suspension in the water column and accumulating on the sea floor at depths below storm wave base. The lack of burrowing activity in this quiescent environment is ascribed to the formation of anoxic bottom conditions in an area of coastal upwelling, similar to the modern Namibian coastline. Toward the top of Facies B, lenticular siltstone laminae and scour surfaces indicate that the substrate had shallowed to approximately storm weather wave base. Normally graded siltstone laminae in this interval represent the suspension fallout of sediment entrained in the water column during these storm events.

Facies B grades upward into Facies C interlaminated shale and siltstone, representing deposition in the offshore-shoreface transition zone between storm and fairweather wave bases. This interval is characterised by fairweather deposition of fine grained sediment from suspension, similar to Facies B, but punctuated by beds of slightly coarser siltstone and sandstone deposited by large oscillatory waves feeling the substrate during storm events. These coarser-grained beds display hummocky cross-stratification and oscillation ripple cross-lamination. Facies C is also marked by the appearance of burrow traces,

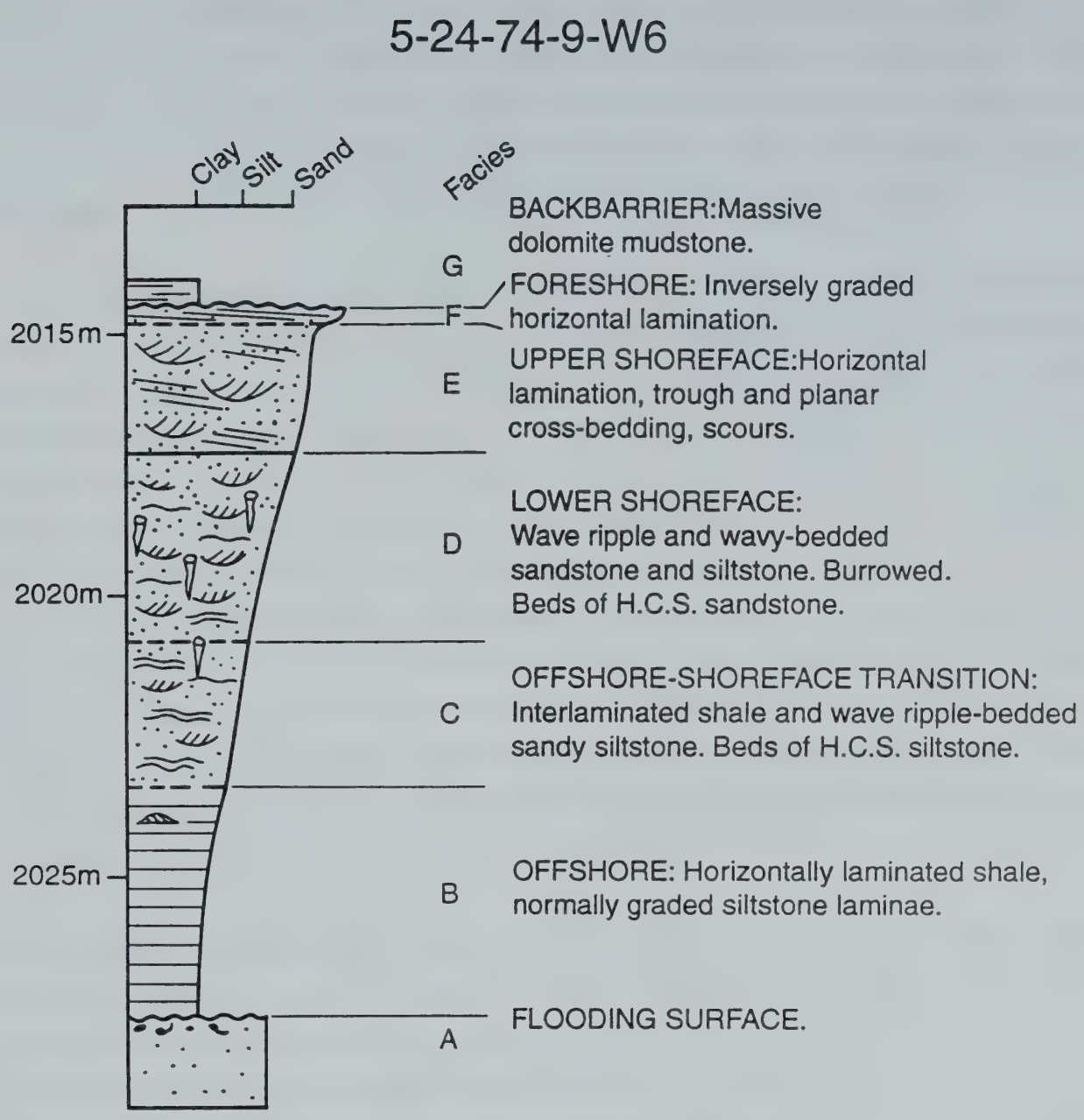

Figure 25. An example of the upward-coarsening Halfway vertical facies association 1(regressive shoreface sequence) cored in well 5-24-74-9-W6.

suggesting that these storm generated currents were sufficient to aerate the substrate. Toward the top of Facies C, thicker beds of oscillation ripple cross-laminated silty sandstone were observed. These were deposited under fairweather conditions by waves feeling the sea bottom for extended periods of time. The point at which the sedimentary sequence continuously shows such evidence of deposition above fairweather wave base marks the start of the lower shoreface and the contact between Facies C and D.

Facies D consists of oscillation ripple cross-laminated siltstone and very fine grained sandstone deposited on the sea floor above fairweather wave base. In many instances this interval of Facies Association 1 has been heavily burrowed, suggesting that bottom waters were fully aerated at this shallower depth. Thin shale laminae are present within some examples of Facies D, indicating periods when fairweather waves were not winnowing the substrate. Facies D and E, the section of Facies Association 1 deposited above fairweather wave base, have a combined thickness of six to eight metres. Allowing for the effects of compaction of the sediment during burial, this would suggest that fairweather wave base was approximately eight metres in the study area during Halfway deposition. The upper part of Facies D is commonly interbedded with the well-winnowed sandstone of Facies E, deposited in the upper shoreface zone where waves begin to shoal and break on the substrate. In several cases however, this contact is sharp and loaded, suggesting very rapid seaward progradation of the upper shoreface.

Facies E displays all the typical features of sediment deposited in the high energy upper shoreface: truncated sets of trough and planar tabular cross-bedding produced by migrating dunes and sandwaves, gently-inclined lamination generated by landward-directed wave swash and abundant scour surfaces with thin lags of chert grains and bioclastic fragments. Such a high energy, shifting substrate is inhospitable to most organisms, with the result that trace fossils are uncommon in Facies E. Facies E is seen in some cored sequences to pass upward into a thin unit of horizontally laminated chert sandstone, which may display inversely graded laminae (Facies F). These are interpreted as foreshore deposits from the inter-tidal zone of the shoreface, the lamination having been generated by the swash and backwash of breaking waves.

In most modern shorefaces, the foreshore passes landward into backshore and subaerial aeolian dune deposits and then into lagoonal, tidal flat or delta plain deposits, depending on the morphology of the coastline (eg. Frey and Howard, 1988). Application of Walther's Law would indicate that in a regressive shoreface setting such as facies

association 1, one would expect to find these backshore deposits preserved between the foreshore and more landward deposits. In the case of Halfway Facies Association 1 however, fine-grained deposits of lagoonal origin (Facies G) are commonly found resting directly on the foreshore and even upper shoreface deposits (Plate 50). This indicates that some erosion must have occurred at this stratigraphic level to remove foreshore, backbarrier and aeolian dune deposits prior to the lagoonal sedimentation. This erosional contact is commonly marked by a bed of Facies M chert-rich sandstone (Plate 51). As this bed corresponds to the contact between the lithostratigraphic Halfway and Charlie Lake Formations, it has commonly been cited as evidence of a regional unconformity between the two units (eg. Halton, 1981). However, in many sequences observed in this study units which would be variously assigned to the Halfway and Charlie Lake Formations are interbedded, indicating that the two formations were deposited contemporaneously (Plate 45). This indicates that within the study area this lithostratigraphic boundary does not represent a regional unconformity.

The origin of this erosion surface can be found in many recent and ancient shoreface sequences, rather than observations of present shoreface morphologies. Continued regression of the shoreface results in lagoonal or tidal flat deposits prograding seaward over the shoreface sequence. During this process, the subaerial portions of the shoreface sequence tend to be deflated by wind and storm washover processes, so removing them from the stratigraphic record (Reinson, 1984). The result is a disconformable contact at which fine grained lagoonal deposits abruptly overlie upper shoreface sandstones. This is marked by a bed of Facies M washover sandstone in Halfway facies association 1.

The erosion surface is overlain by Facies G1 inter-tidal flat deposits and then Facies G2 subtidal lagoonal mudstones. This interval is capped by a second unit of Facies G1, interpreted as the seaward progradation of tidal flats developed around the landward edge of the lagoon. The abundant dolomite and anhydrite in these deposits and the absence of any plant material suggest that they were deposited in an arid, hypersaline lagoonal environment as opposed to a humid setting. Facies association 1 is capped by red mudstones and anhydrite beds of Facies H, interpreted to have been deposited in an arid supratidal flat setting similar to the modern Colorado River delta plain (Thompson, 1968).

Facies association 1 thus records an increasing influence of wave current activity on a progressively shallowing and eventually emergent substrate, followed by lagoonal and

Plate 50. Facies G1 crypt-algal laminites of backbarrier origin resting sharply on Facies E upper shoreface sandstone. The contact is marked by a concentration of chert granules. Well 16-23-72-8-W6. 2137 m.

Plate 51. Bed of Facies M horizontally laminated chert-rich sandstone resting erosively on Facies E upper shoreface sandstone. Facies M grades upward into Facies G backbarrier deposits. Well 14-27-72-8-W6. 2124 m.

supratidal flat sedimentation. This is indicative of deposition in a regressive shoreface setting (Figure 26). Such sequences are known to be generated by prograding strandplains, barrier island shorelines and wave-dominated deltas (Heward, 1981).

While the interpretation of facies association 2 as tidal inlet fill deposits might suggest a barrier island setting, such inlets are also common features along wave-dominated deltas (eg. Oomkens, 1974). The presence of tidal inlet sequences in the Halfway of the study area does, however, rule out deposition in a simple strandplain setting. The dolomitic mudstones, algal laminites and anhydrite (Facies G) which cap Halfway regressive shoreface sequences are interpreted as being of lagoonal and intertidal flat origin. Lagoons are uncommon features of recent wave-dominated deltas, with the exception of those formed during temporary destructive episodes (Heward, 1981), but delta plain deposits may appear similar to lagoonal deposits (Oomkens, 1974). Delta plain sequences however, tend to contain fluvial distributary channel deposits, which are not found in the Halfway-Charlie Lake sequence. It would therefore seem that within the study area, the Halfway Formation regressive shoreface sequences were deposited by a prograding barrier island chain backed by lagoons and tidal flats rather than a delta plain crossed by distributary channels.

The thickness and sequence of sedimentary structures observed in Halfway facies association 1 is comparable to many published examples of ancient regressive shoreface sequences (eg. Davies et al., 1971; Roep et al., 1979; Heward, 1981; Taverner-Smith, 1982; Howard and Scott, 1983; Moslow and Pemberton, 1988; and summaries in Reinson, 1984; Elliott, 1986). Observation of modern shoreface depositional structures and sequences is hampered by difficult working conditions and only three examples have been documented (Clifton et al., 1971; Davidson-Arnott and Greenwood, 1976; Howard and Reineck, 1981). This limited number of examples has, however, served to highlight the possible variation in regressive shoreface sequences produced by differences in shoreface profile, wave energy, tidal current strength and frequency of storms. Summaries of shoreface sequences (eg. Elliott, 1986) have thus attempted to categorize them as wave-dominated, storm-dominated, etc. Facies association 1 does contain beds of inferred storm origin in Facies B, C and D, but these are widely spaced and too few in number compared to the example given by Hamblin and Walker (1979) to classify the Halfway sequence as storm-dominated. The effect of tidal current action on shoreface sequences is poorly understood, since most studies appear to have concentrated on the tidal inlet and backbarrier deposits associated with such shorelines rather than the

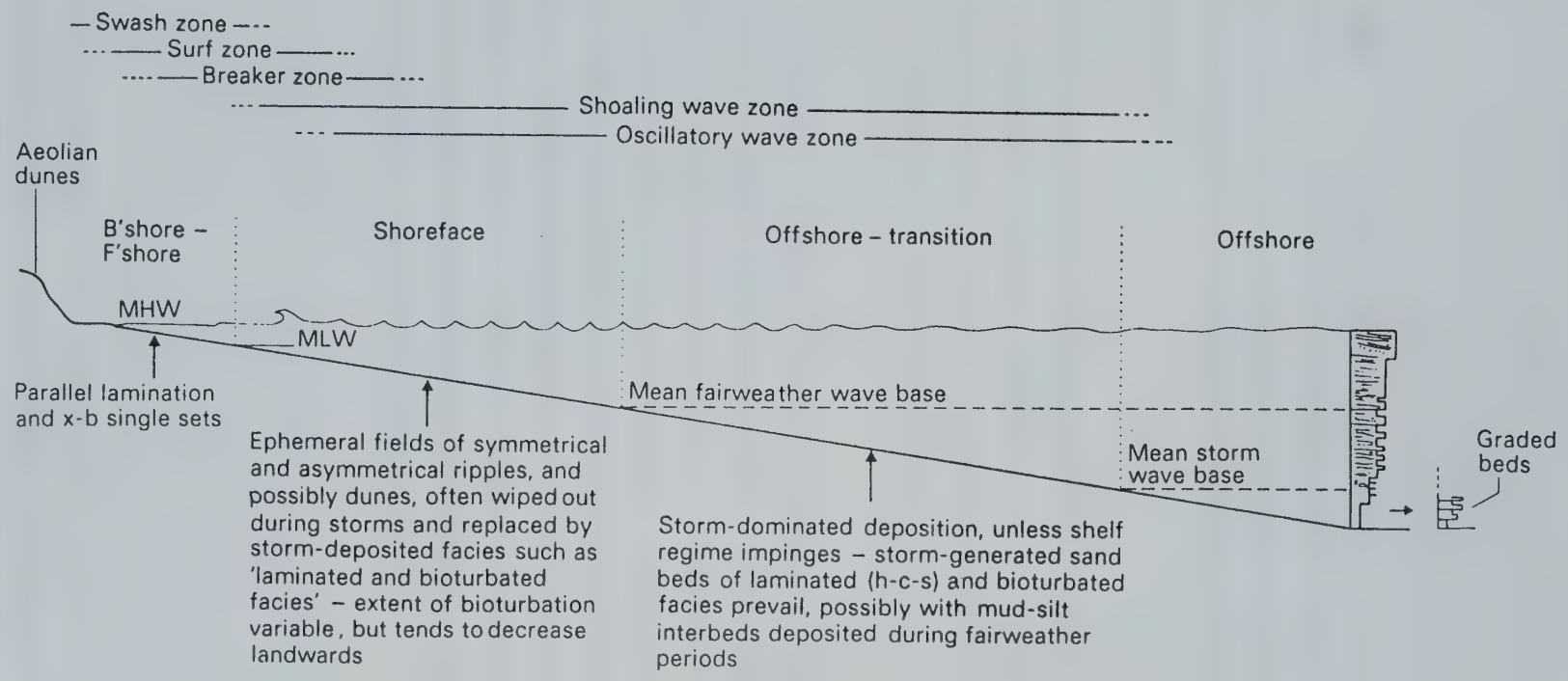

Figure 26. Shoreface sub-environments, processes and facies, illustrating the upward-coarsening sedimentary sequence generated by progradation (after Elliott, 1986).

shoreface sequence itself (eg. Hobday and Horne, 1977). The presence of ebb-tidal delta deposits in several facies association 1 shoreface sequences (eg. 16-26-72-8-W6; Appendix A) and the interpretation of facies association 2 as a tidal inlet channel fill sequence suggest that the Halfway shoreface was strongly affected by tidal currents. This tidal influence may be reflected in the shale laminae commonly observed in Facies D lower shoreface deposits; such fine grained material is not common above inferred fairweather wave base in wave-dominated shoreface sequences such as that described by Roep et al. (1979). Halfway facies association is therefore interpreted as having been deposited by a regressive barrier island shoreface under the mixed influence of waves and tidal currents.

5.2.0 Facies Association 2: Tidal Inlet Channel Fill.

Facies association 2 consists of Facies I, J, K, and L. These facies always rest erosionally on facies association 1 and form a gradational upward-fining sequence (Figure 27). One or more upward-fining cycles may be present in a single cored sequence.

The erosional base, upward-fining nature, and decrease in bedform thickness of facies association 2 suggest deposition within a channel setting. The highly variable rate of sediment deposition from both traction and suspension described from Facies I, J and K rules out an origin as a fluvial point bar, where deposition tends to be dominated by steady unidirectional flow. In addition, strong marine influence is suggested by the abundance of shell material and the trace fossil assemblage. More specifically, many of the features of Facies I, J and K are interpreted to have formed under tidal conditions. Tidally-influenced channel deposits are found in estuarine systems, tidal creek point bars, and tidal inlet channels in barrier island systems.

Estuarine channel-fill deposits do not display the consistent upward-fining sequence of facies association 2, but a tripartite arrangement of: fluvial sands - estuarine sands and muds - shallow marine sands (eg. Nichols et al., 1991). In addition, estuarine channels are located between estuarine shoals, rather than between barrier islands; no evidence was found of any such estuarine shoal deposits in the Halfway Formation in this study. Tidal creek deposits, while displaying an upward-fining grain size trend, are of a much smaller scale (2 m) than the thicknesses recorded from facies association 2 (10-20 m). In addition, in regressive shoreface sequences, tidal creek channel fill deposits are commonly observed encased in lagoonal and tidal flat sediments at the very top of the sequence (eg. Wojtal-Duc and Tye, 1987), as opposed to the much deeper incision observed in facies

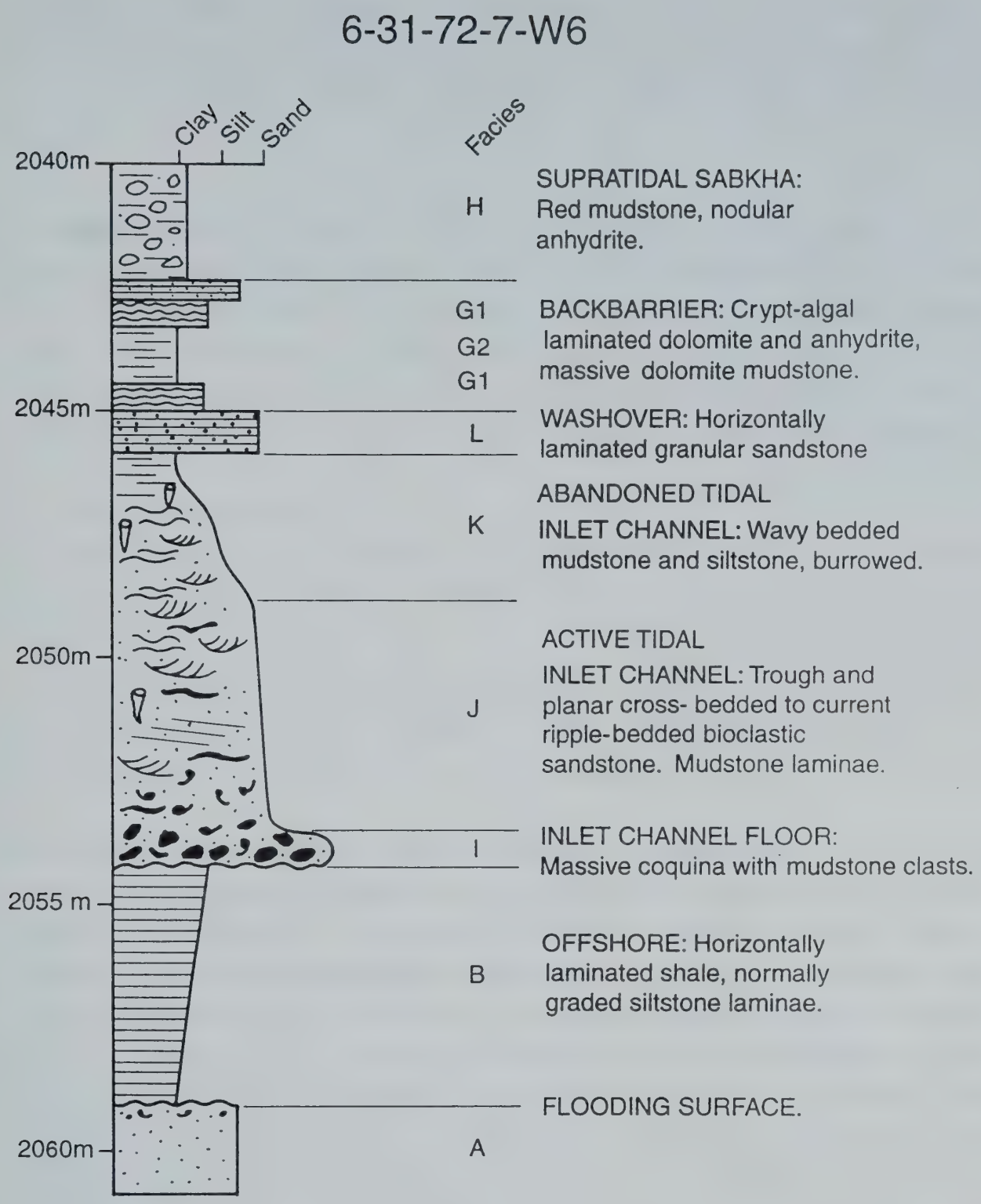

Figure 27. Halfway vertical facies association 2, interpreted as a tidal inlet channel fill sequence. Note the erosional base of the inlet channel on offshore shales of facies association 1 and the upward-fining grainsize trend. Cored in well 6-31-72-7-W6.

association 2. This deep erosion of facies association 2 into the regressive shoreface sequence of facies association 1, coupled with its apparent gradational relationship with the lagoonal dolomitic mudstones of Facies G1, suggest deposition in a tidal inlet channel.

This interpretation is supported by the close similarity of facies association 2 to descriptions of modern and ancient tidal inlet channel fill sequences given by Terwindt (1971), Kumar and Sanders (1974), Oomkens (1974), Hayes (1975), Hobday and Horne (1977), Barwis and Makurath (1978), Moslow and Heron (1978), Hubbard et al. (1979), Hayes (1980), Reddering (1983), Tye (1984), Moslow and Tye (1985), Uhlir et al. (1988), Leckie et al. (1989), Cheel and Leckie (1990) and Tye and Moslow (in press).

5.2.1 Tidal Inlet Sequence.

The first vertical sequence of tidal inlet sedimentary structures to be carefully described was that by Kumar and Sanders (1974) from Fire Island Inlet, New York. Their interpretations of this sequence were aided by being able to observe processes in the adjacent still active inlet channel. While subsequent studies have noted some variation in inlet sequences, the Fire Island example serves as a well documented example of the basic processes and products found in a tidal inlet channel (Figure 28).

The erosional base of the Fire Island inlet channel is overlain by a lag of shells and pebbles. These represent fragments too coarse for the tidal currents flowing in the inlet channel to transport and are analogous to the Facies I bioclastic sandstone with mud clasts at the base of facies association 2. Bioclastic material in tidal inlet channel lags is commonly reported as being a mixture of lagoonal and open-ocean species (Henderson and Frey, 1986; Davies et al., 1989), the mix being a result of the alternating tidal cycle. Shells may also be reworked from the older sediments beneath the channel floor. Facies I bioclastic material has undergone too much diagenetic alteration to specifically identify any of the fauna, but the rare occurrence of crinoid ossicles does indicate that fully open marine forms were transported into the inlet.

Intraclasts and pebbles derived from the underlying deposits are ubiquitous in all published examples of tidal inlet sequences and cored intervals of Facies I. Large blocks of mud which slumped from the cut bank were observed in the base of Murrels Inlet, South Carolina by Hubbard et al. (1979). These are considered analogous to the discordant beds of mudstone described from Facies I.

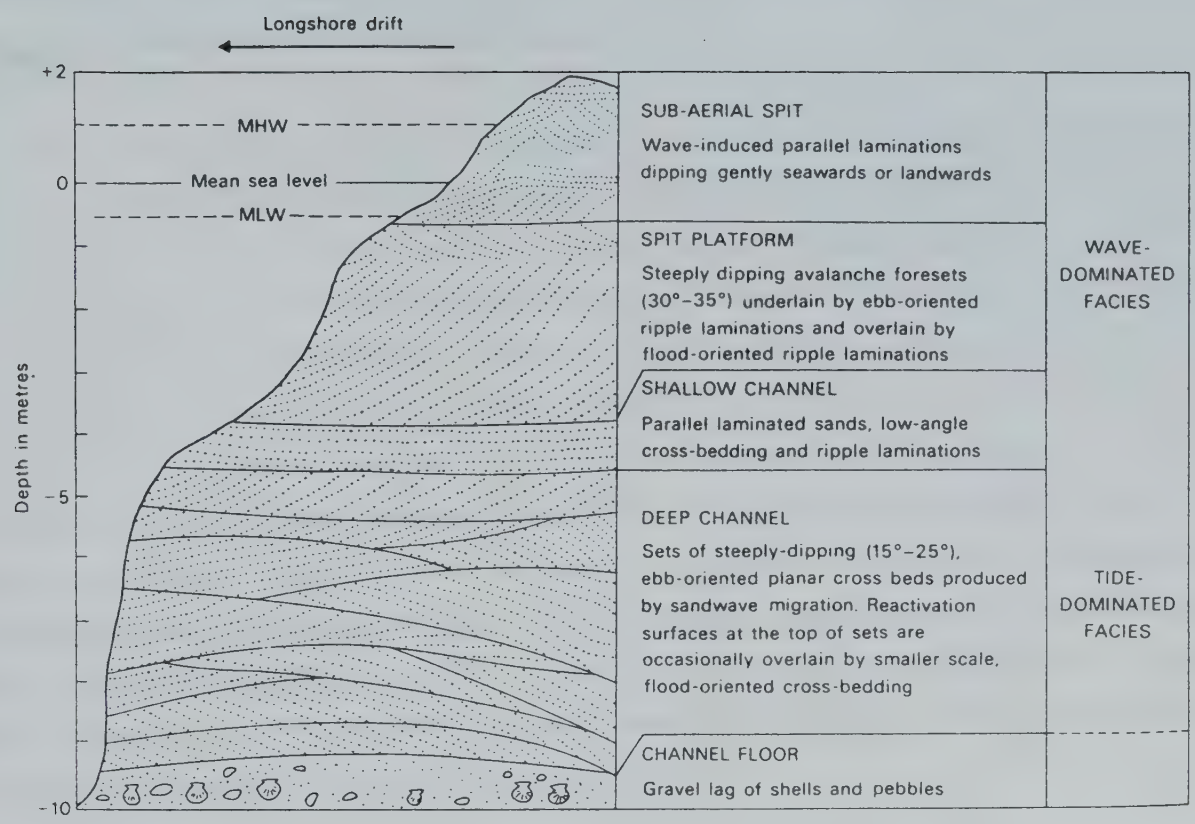

Figure 28. Tidal inlet channel fill sequence cored at Fire Island Inlet, New York (after Kumar and Sanders, 1974; Elliott, 1986).

The thickness of the Fire Island channel lag could not be determined due to the difficulties of coring coarse fragments. Coquina at the base of an inlet sequence described by Uhlir et al. (1988) is 1-3 m thick, similar to Facies I. Due to the lack of core recovery, no sedimentary structures were observed in the Fire Island inlet lag, but those described by Uhlir et al. (1988), consisting of large-scale planar and trough cross-bedding produced by migrating sandwaves, are similar to Facies I.

The coarse grained lag in the Fire Island sequence grades up into medium to coarse sand containing some pebbles and shell fragments. This sand was deposited in the deepest part of the active tidal inlet channel (4.5-10 m below MSL) by large migrating sandwaves. The sedimentary structures observed by Kumar and Sanders (1974) consist of dominantly ebb-oriented planar cross-bedding. These sets are truncated by reactivation surfaces representing a reversal of the tide. During the flood-tide, oppositely oriented cross-strata did form in the Fire Island channel, but most of the laminae were subsequently eroded by the next ebb tide, leaving the reactivation surface. Sets of bidirectional, planar cross-beds formed by ebb and flood sandwave migration are also the major physical sedimentary structures described from most other active inlet channel deposits (eg. Moslow and Tye, 1985). Smaller-scale sets of trough cross-bedding and ripple cross lamination are also common, and represent lower flow regime megaripple migration on the stoss slopes of sandwaves. These are all features of Halfway Facies J.

Although not observed by Kumar and Sanders (1974), mud drapes and flaser beds formed during slack water are commonly incorporated in these cross-bedded sandstones (Moslow and Tye, 1985). In some cases, preservation of mud drapes deposited at each slack tide results in the formation of "tidal bundles" (eg. Uhlir et al., 1988; Leckie et al., 1989). These are beds which contain approximately 28 alternating thick-thin sandstone-mudstone couplets deposited during by ebb- and flood-tides over a complete neap-spring tidal cycle of 14 days (Visser, 1980). While alternating sandstone-mudstone laminae were observed in several examples of Facies J cross-bedded sandstone, no units regular enough to warrant the description of tidal bundle were seen.

While the physical processes and sedimentary products of active tidal inlet channels described above are relatively similar in most examples, studies of modern tidal inlets, particularly along the Georgia embayment of the southeastern United States, have shown that differences in hydrographic regime (wave energy and tidal range) result in distinct

variations in the upper part of the inlet sequence. This is a reflection of the different ways in which inlets in wave- and tide-dominated settings behave after channel abandonment.

5.2.2 Variations in Modern Tidal Inlet Fill Sequences.

The arcuate shape of the Georgia embayment and the increasing width of the continental shelf toward the centre of the arc have opposing effects on wave height and tidal range (Figure 29). The flanks of this arc (North Carolina and Florida) have a narrow continental shelf, which results in high wave energy and a low tidal range. Conversely, the wider shelf at the apex of the embayment (South Carolina and Georgia) amplifies the tidal range while attenuating wave energy. Using the tidal ranges of Davis and Hayes (1984), this change in shelf bathymetry produces microtidal, wave-dominated shorelines on the flanks of the embayment and a mesotidal mixed-energy (both tides and waves are important) shoreline at the apex (Hayes, 1979).

5.2.3 Microtidal, Wave-Dominated Coastlines.

Microtidal wave-dominated regimes (tidal range <2 m) are typified by long, linear, narrow barrier islands extending for tens of kilometres and backed by broad, open lagoons (Figure 30). The islands are separated by widely-spaced, ephemeral, rapidly migrating tidal inlets with associated flood-tidal deltas. Extratropical storms and hurricanes can lead to the development of the tidal inlets by cutting channels through the narrow barrier islands (Hayes, 1967; Pierce, 1970; Davis et al., 1989). Most of these breaches are stranded above high water mark or are healed by post-storm conditions, but the deeper, more efficient channels are tidally maintained and form new inlets. These wave-dominated tidal inlets tend to migrate rapidly downdrift due to: 1) high rates of longshore sediment transport associated with a wave-dominated environment, 2) the fact that the inlets tend to be shallow and therefore not anchored in a cohesive substrate, and 3) the barrier islands are narrow (Tye and Moslow, 1991). The associated flood-tidal deltas, deposited by waves and tidal currents, form large, lobate sandbodies in the lagoon. Wave energy and flood-tidal currents exert more influence on sedimentation than ebb currents, so ebb-tidal delta development is poor. Downdrift extension of the inlet channel results in hydraulic inefficiency and induces channel abandonment. Landward sand transport by the dominant wave action closes the former channel mouth (Figure 31). In a wave-dominated setting then, tidal inlet sequences are generally thin, and both active and abandoned channel fill are composed of cross-bedded sand (Figure 32).

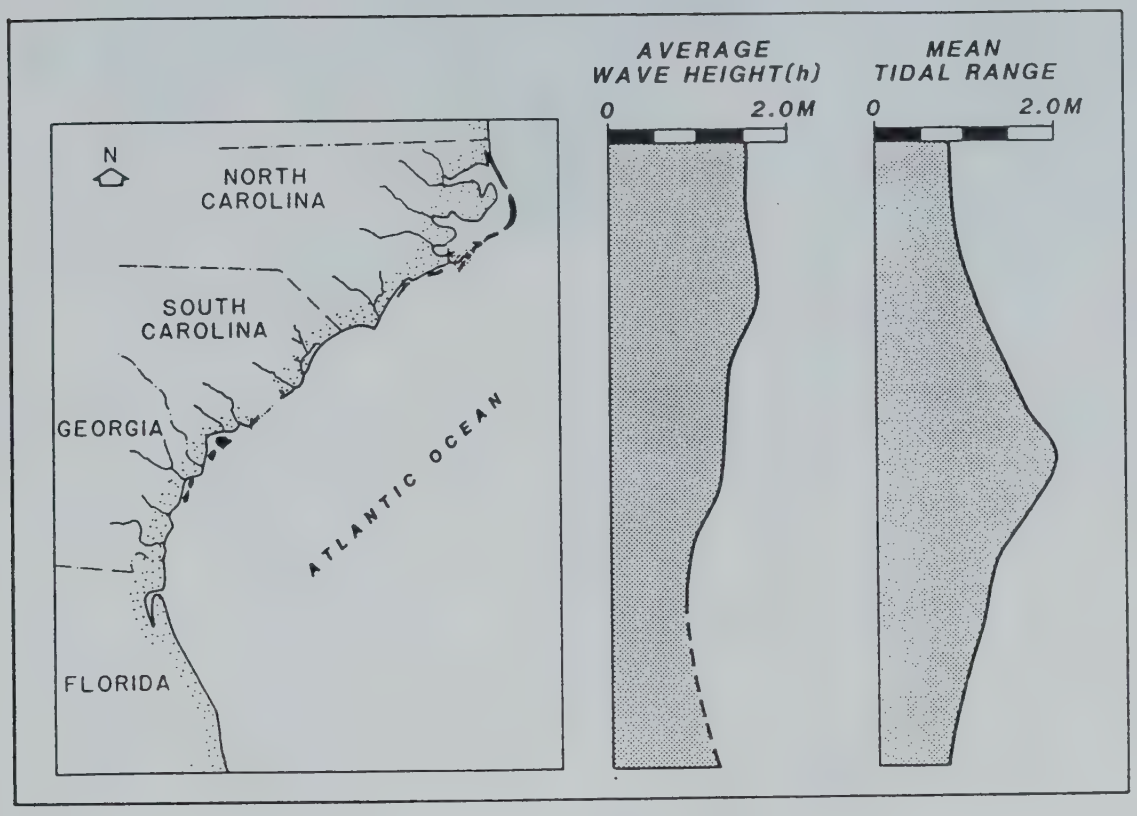

Figure 29. Average wave heights and tidal ranges along the Georgia Embayment of the southeastern United States. Note the antipathetic relationship between wave height and tidal range, indicating a wave-dominated North Carolina/Florida and tide-dominated South Carolina/Georgia coastal setting (after Moslow and Tye, 1985).

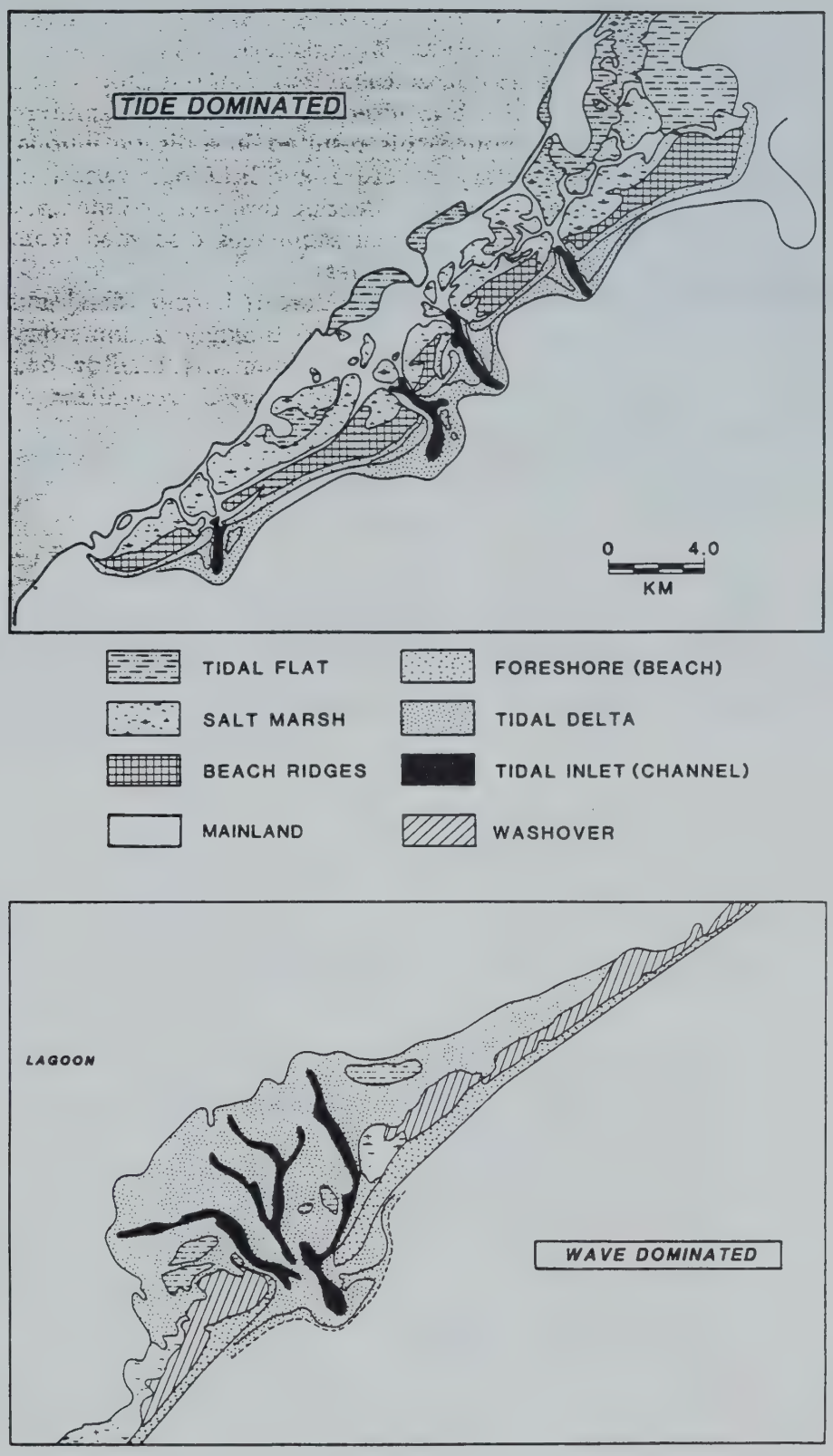

Figure 30. Wave- and tide-dominated tidal inlet geomorphological models for the Georgia Embayment of the southeastern United States. Long, narrow wave-dominated barriers are separated by a few tidal inlets with well developed flood-tidal deltas. Shorter, tide-dominated barriers are separated by numerous inlets. Flood-tidal deltas in wave-dominated settings are replaced by salt marsh and large ebb-deltas in tide-dominated coastlines. (After Moslow and Tye, 1985).

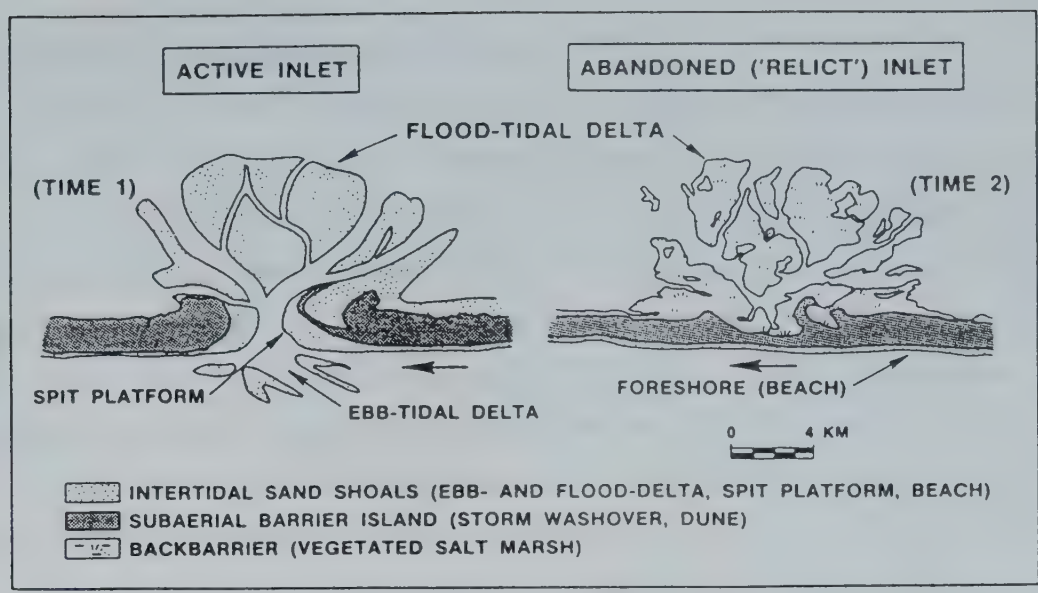

Figure 31. Morphological evolution of wave-dominated inlet-related sandbodies. Downdrift migration over-extends the inlet channel and landward swash bar migration closes the inlet mouth. Flood-tidal delta remnants are vegetated by salt marsh. Horizontal arrows indicate direction of longshore sediment transport (after Moslow and Tye, 1985).

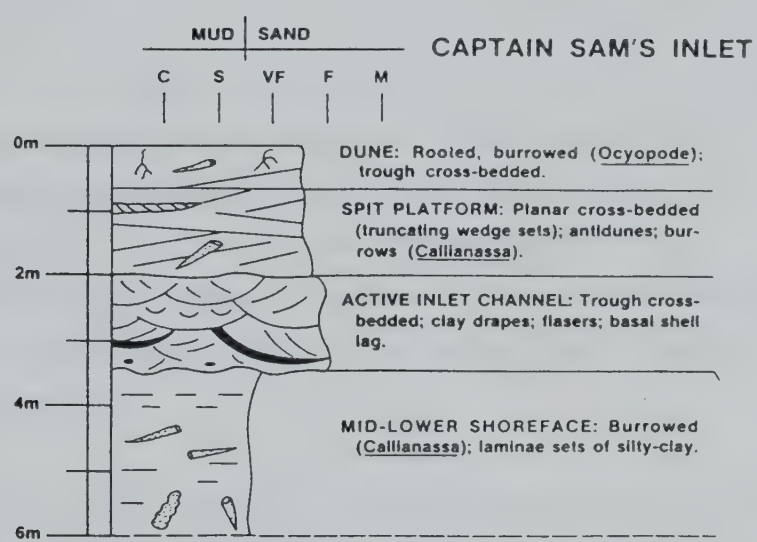

Figure 32. Wave-dominated tidal inlet sequence deposited by the lateral migration of Captain Sam's inlet, South Carolina. Note that both active inlet channel and abandoned fill (spit platform) consist of cross-bedded sand (after Moslow and Tye, 1985).

5.2.4 Mesotidal, Mixed-Energy Coastlines.

Along mesotidal coastlines (tidal range 2-4 m) where both tidal and wave action are important, barrier islands tend to assume as stunted, drumstick-shaped configuration (Figure 30). The barriers are wider than those in wave-dominated settings, extend only a few kilometres along the coast and are separated by numerous, more stable inlets. Strong ebb currents along tidally-influenced shorelines result in well developed ebb-tidal deltas (Hayes, 1975). The backbarrier lagoon and flood-tidal delta of the wave-dominated microtidal shoreline are replaced by intertidal flats and tidal creeks (Wojtal-Duc and Tye, 1984; Howard and Frey, 1985). The dominance of tidal currents over wave energy results in the inlet channels cutting deep into the underlying cohesive substrate; this and the greater width of the barrier islands inhibits the channels from extensive lateral migration.

The seaward portion of the main ebb channel does migrate downdrift by the preferential addition of sand to the updrift lobe of the ebb-tidal delta, but these channels lose hydraulic efficiency and breach the ebb-tidal delta to form a shorter updrift channel (Figure 33). Former ebb-tidal delta sand lobes are then reworked by waves, forming a large ridge which migrates landward. Landward migration of the ridge further restricts flow through the abandoned inlet channel, resulting in a change from lateral accretion to vertical channel aggradation. Complete welding of the ridge to the barrier seals the mouth of the abandoned channel, creating a shallow bay (Figure 33.4). This process of inlet channel migration and ultimate closure by wave-reworked, ebb-tidal delta sand is called bar bypassing. Bar bypassing occurs rapidly at small inlets, but one cycle of inlet channel migration and abandonment took more than 100 years at Capers, Price, and Stono Inlets in South Carolina (Tye, 1984). Repeated bar bypassing events can lead to the same stretch of coastline being reworked by successive inlet ebb channels. Two or more fining-upward cycles of active and abandoned channel-fill may then be found in a single sequence (Tye, 1984).

The seaward portion of the abandoned ebb-tidal channel is filled by wave-reworked ebb-tidal delta sands, producing a thick sand wedge. Figure 34 shows a core taken from the seaward mouth of the tide-dominated Stono Inlet in South Carolina after the ebb-tidal delta welded onto the barrier island. Landward, away from wave influence, a low-energy shallow body of water (similar to an oxbow lake) forms in the abandoned channel. This landward part of the abandoned channel then tends to fill with fine-grained sediment and some coarser washover deposits, eventually being incorporated into the backbarrier tidal flats (Figure 35).

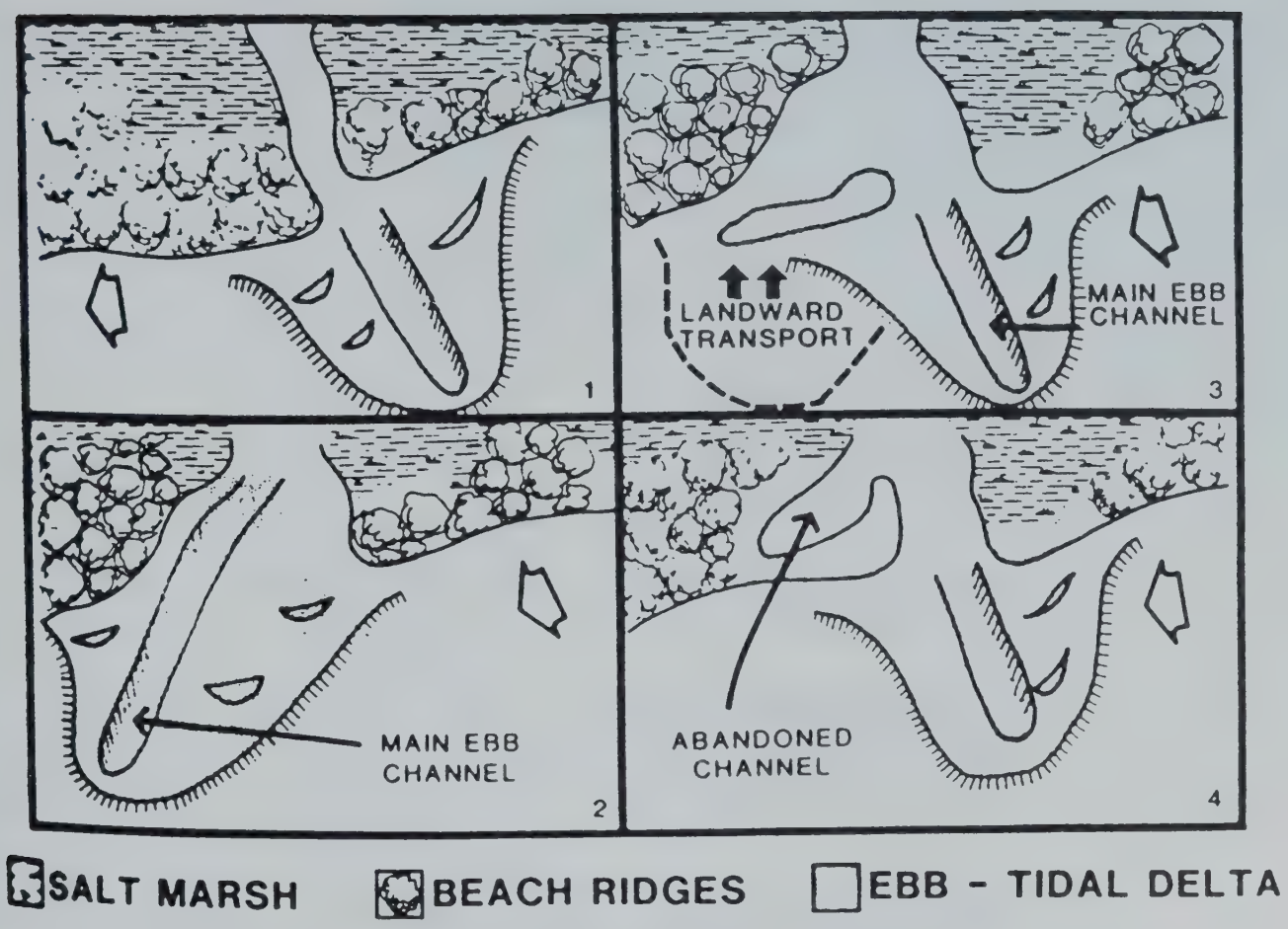

Figure 33. Four stages of the inlet migration and abandonment mechanism in a mesotidal setting, based on coastal charts and aerial photos of Price and Capers Inlets, South Carolina. (1) Formation of a straight inlet channel; (2) Downdrift inlet migration and erosion of barrier island; (3) Shorter, updrift channel causes earlier channel to become a marginal flood channel which is subsequently closed by a landward migrating swash bar; (4) Swash bar welds to barrier and sediment is trapped, filling the former inlet channel. Arrows indicate direction of longshore sediment transport (after Tye, 1984).

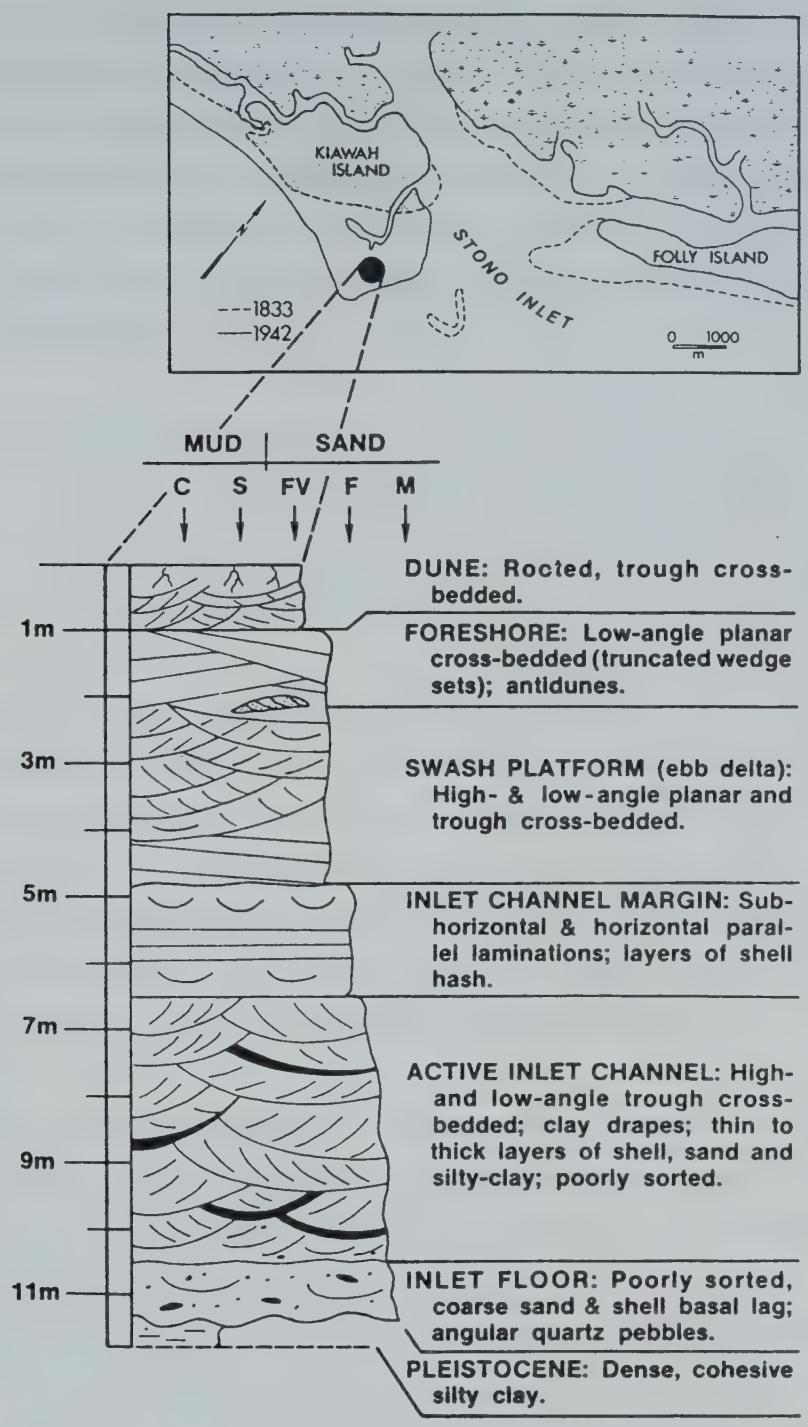

Figure 34. Tidal inlet sequence cored at Stono Inlet, South Carolina. The vertical sequence represents preservation of the seaward-most inlet deposits in a tide-dominated setting, where the Stono Inlet ebb-tidal delta has welded onto the adjacent barrier island by the bar bypassing mechanism (after Moslow and Tye, 1985).

The landward part of a plugged tide-dominated inlet sequence therefore generally consists of burrowed fine-grained sediment representing vertical aggradation from suspension fallout. In the seaward part of the channel fill, cross-bedded ebb-tidal delta and foreshore sand overlies the inlet deposits (Figure 34). Landward, the sand interfingers with fine-grained abandoned inlet fill and marsh deposits. This is in marked contrtast to inlet fill sequences in wave-dominated settings which tend to be entirely plugged by clean sand after channel abandonment.

5.2.5 Halfway Tidal Inlet Sequences.

Although it is not possible to reconstruct the geometry of the Halfway barrier islands themselves due to extensive reworking by tidal inlets, other observations can be used to determine the prevalent hydrographic regime:

1) Facies association 2 tidal inlet fill sequences typically consist of a lower unit of active inlet channel fill (Facies I and J) overlain by interbedded siltstone and mudstone of Facies K, interpreted as abandoned inlet fill. As mentioned above, abandoned inlet fills consisting predominantly of fine-grained sediment are characteristic of tide-dominated settings. In wave-dominated shorelines, abandoned inlets are typically filled with sand reworked by wave action. In addition, the mud laminae observed throughout facies association 2 are more compatible with a strong tidal influence.

2) The Halfway tidal inlet channel fill sequences are typically 10-15 m thick and cut down into the offshore shales of the barrier island shoreface sequence (Figure 27). Using the table of dimensions of modern inlet fill sequences in Tye and Moslow (in press), it is apparent that wave-dominated tidal inlets typically have a depth of 3-10 m, and would therefore rarely be expected to erode deeper than the lower shoreface deposits of facies association 1. Tide-dominated channels however, are commonly in the range 10-15 m. It is this deeper channel cut into cohesive muddy substrates like the Halfway offshore shales which helps limit the lateral migration of tide-dominated inlets.

3) More than one upward-fining cycle of active and abandoned channel fill is commonly present in a single Halfway inlet sequence. This is typically associated with tide-dominated inlets, where throat stability results in the same stretch of shoreline being reworked by successive ebb-channels as a result of bar bypassing. The more widely-spaced, ephemeral inlets of wave-dominated coastlines tend to be more random in their distribution.

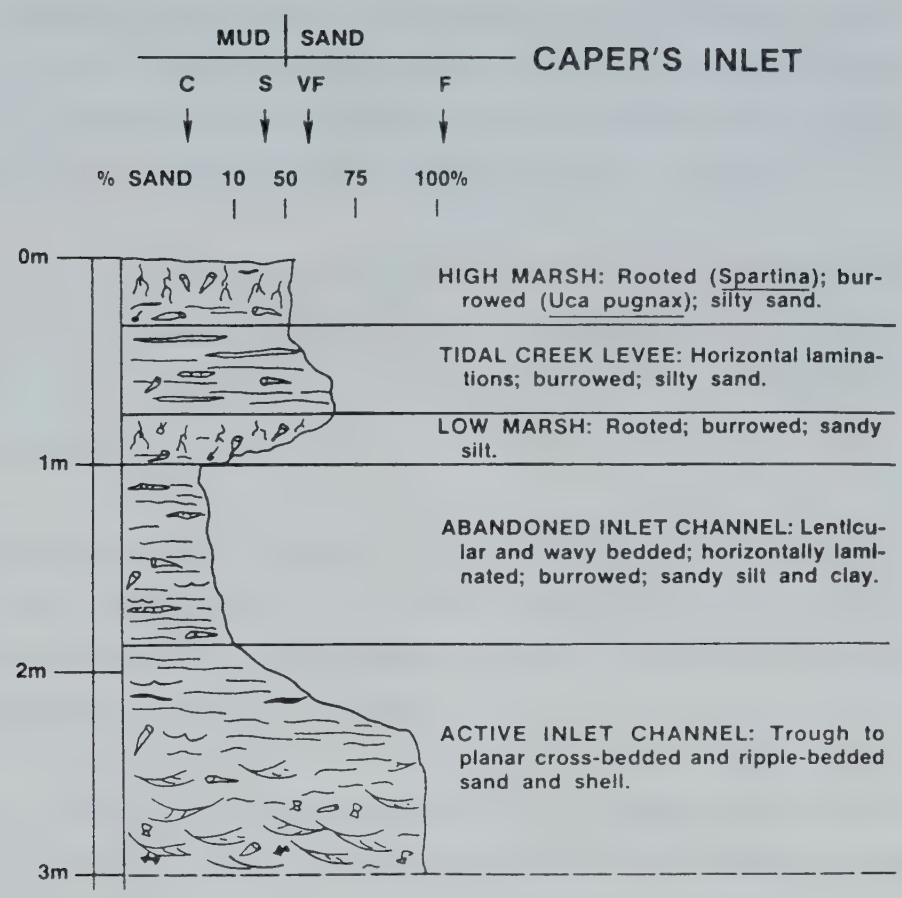

Figure 35. Mud-rich, fining-upward sequence deposited by the channel migration and abandonment of Capers Inlet, South Carolina. Note the fine grained abandoned channel fill grading up into backbarrier marsh deposits, in contrast to the sand-rich wave-dominated inlet sequence shown in Figure 32b (after Moslow and Tye, 1985).

4) Facies association 2 is commonly capped by a unit of clean sandstone (Facies L) interpreted as an ebb-tidal delta deposit. Ebb-tidal deltas are more commonly associated with tide-dominated than wave-dominated tidal inlets. In some cases this ebb-tidal delta sandstone forms the greater part of the inlet channel fill (eg. well 8-26-72-8-W6; Appendix A). This probably represents preservation of the seaward-most inlet deposits where the inlet mouth has been blocked by a welded swash bar following bar bypassing, similar to the cored example from Stono Inlet shown in Figure 34.

5) No significant flood-tidal delta deposits were identified in this study. These are more commonly associated with microtidal, wave-dominated barrier island systems (Hubbard et al., 1979; Tye and Moslow, in press) and their absence supports a more tidally-influenced setting.

6) Halfway shoreface and tidal inlet fill sequences are capped by backbarrier deposits containing a high proportion of tidal flat sediments (Facies G1). This abundance of intertidal deposits implies a significant tidal range during Halfway deposition and is therefore suggestive of a mesotidal setting.

7) Washover sands in the Halfway Formation are largely associated with periods of transgressive shoreface erosion and occur as thick, linear washover terraces. Individual thin washover sands characteristic of wave-dominated shorelines are not abundant in Halfway backbarrier deposits.

On the basis of these observations, the Halfway barrier island coastline in the study area is interpreted to have been subject to a mesotidal range (2 to 4 m) similar to the examples from South Carolina documented by Tye (1984). A schematic representation of this Halfway depositional model is shown in Figure 36.

Halfway Formation
Mesotidal Barrier Island System
Depositional Model

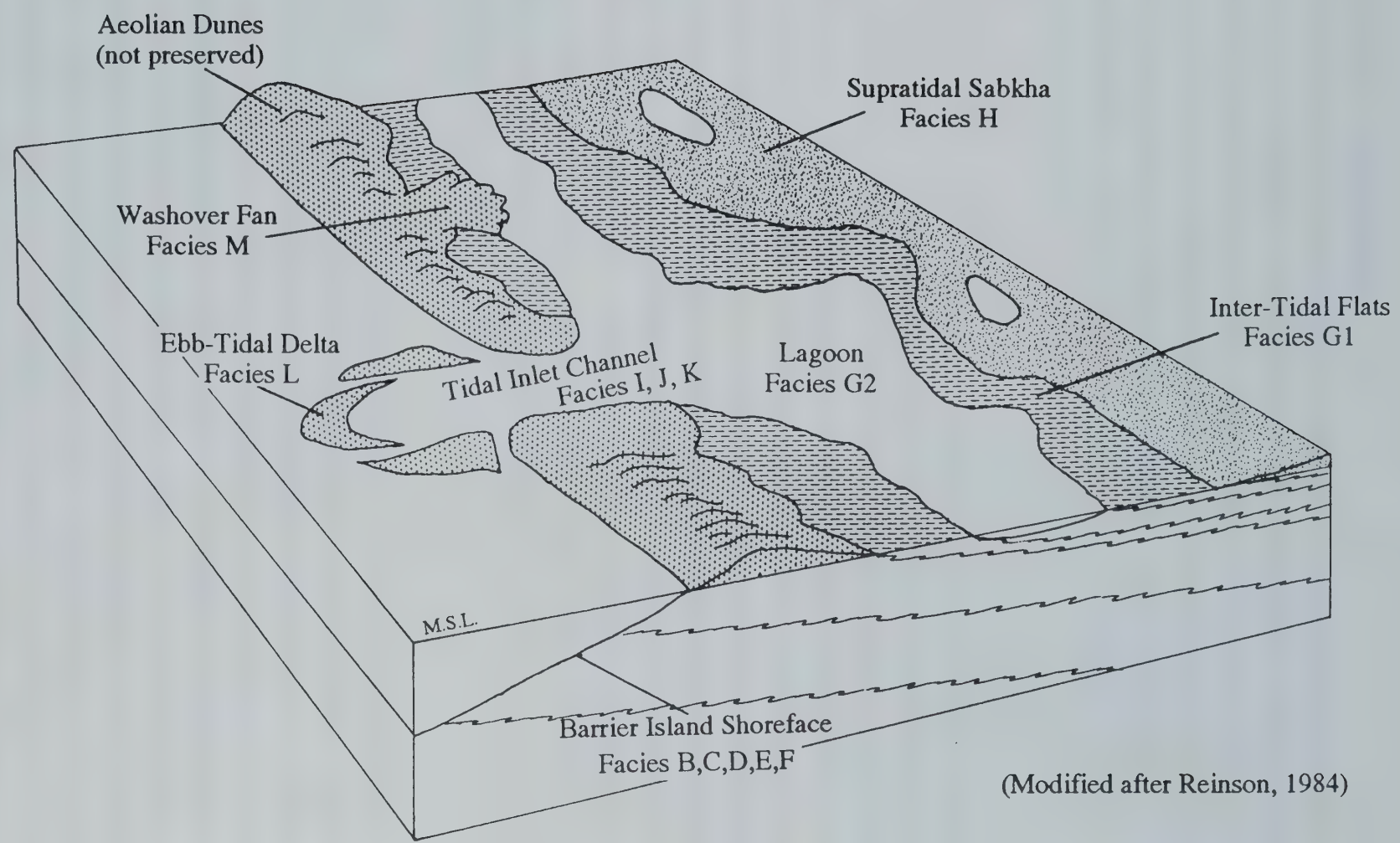

Figure 36. Schematic block diagram illustrating the barrier island depositional system and corresponding Halfway facies.

5.3.0 Lateral Facies Relationships.

Vertical facies associations 1 and 2 allow the Halfway Formation in the Wembley area to be interpreted as a progradational mesotidal barrier island system. With this information is it possible to compare the lateral facies relationships in the Halfway Formation with those that have been documented from Holocene mesotidal barrier island systems. Integration of these modern analogues with Halfway data will highlight the three-dimensional distribution of facies in the formation and their influence on the reservoir heterogeneity of the unit.

Continuity of shoreface facies associations along both strike and dip is probable in a lithosome deposited by a prograding shoreface as depositional processes do not vary markedly either along the length of the coastline or through time as the system progrades. This would result in a relatively homogeneous sandbody that would behave as a single hydrocarbon pool. The presence of tidal inlet channels along barrier island coastlines complicates this model and results in a complex sandbody containing both shoreface and tidal inlet sequences (eg. Tye, 1984; Galloway, 1986). The juxtaposition of sandstone and shale units in both a strike and dip direction in such a composite sandbody can have a serious effect on its behaviour as a hydrocarbon reservoir and must therefore be fully understood to effectively exploit it. For this reason, many studies of Holocene barrier island systems have determined the spacing of tidal inlet channels and the percentage of the barrier underlain by inlet fill.

Tye and Moslow (in press) tabulate percentages of Holocene tidal inlet fill and active tidal inlets for both wave- and tide-dominated barrier island shorelines. The average percentage of tide-dominated shorelines represented by active tidal inlets is 20% and the average percentage of of subsurface inlet fill sediments per barrier island is 15%. Adding the two figures suggests that the total proportion of Holocene tide-dominated barrier island systems occupied by tidal inlet sediments is around 35%. Wave-dominated barrier island systems contain a nearly equal proportion of inlet sediments (40%). Table 4 shows all wells in the study area in which the Halfway has been identified as a facies association 1 regressive shoreface sequence. The total is 27 wells. The remaining 277 of the 304 wells studied contain tidal inlet sequences. Since wells in the Wembley field are largely drilled on a grid spacing and therefore unlikely to be geologically biased, it can be concluded that approximately 90% of the Halfway Formation in this area consists of tidal inlet sediments. This is obviously a much higher proportion than the 35-40% documented in Holocene barrier island systems.

Well Location	Core	Thickness
10-08-71-07-W6		16 m
06-27-71-07-W6		14 m
16-08-72-07-W6		15 m
16-09-72-07-W6	•	11 m
06-11-72-07-W6	•	4 m
07-16-72-07-W6		10 m
10-18-72-07-W6		15 m
14-18-72-07-W6	•	13 m
06-04-72-08-W6	•	8 m
14-08-72-08-W6		9 m
08-13-72-08-W6		13 m
06-21-72-08-W6	•	7 m
14-23-72-08-W6		17 m
16-23-72-08-W6		18 m
11-24-72-08-W6	•	14 m
06-25-72-08-W6		16 m
11-26-72-08-W6	•	21 m
16-26-72-08-W6	•	17 m
16-34-72-08-W6	•	15 m
14-03-73-08-W6	•	15 m
11-06-74-08-W6		17 m
06-08-74-08-W6	•	11 m
10-12-74-09-W6	•	16 m
06-13-74-09-W6	•	16 m
05-24-74-09-W6	•	13 m
11-26-74-09-W6		14 m

Table 4. Location, thickness and core coverage of Halfway facies association 1 regressive shoreface sequences.

It is considered that this discrepancy is a result of the different time-scales under which Holocene and Halfway deposits formed. Studies of Holocene barrier island systems represent only the present configuration of the coastline and cannot consider its future modification. It is, however, the final product of this ongoing coastal evolution that we see in the stratigraphic record of units such as the Halfway Formation. Most Holocene regressive shorelines have been prograding for no more than about 7, 000 years. During this time, approximately 35-40% of the coastline has been reworked by migrating tidal inlet channels. Continued progradation coupled with lateral tidal inlet migration will presumably result in an ultimately greater proportion of inlet sediments in Holocene coastal lithosomes, since the rate at which tidal inlet channels migrate laterally along the shoreline tends to be greater than the rate at which the shoreline progrades. This is considered to be the cause of the high proportion of tidal inlet sediments in the Halfway Formation.

Lateral distribution of tidal inlet deposits has only been documented in two studies of ancient strata. Uhlir et al. (1988) describe tidal inlet deposits as being present in outcrops of the Jurassic Sundance Formation throughout most of the Bighorn Basin of Wyoming, a distance of greater than 200 km. Shoreface sequences which have not been reworked by migrating tidal inlets are only present in the extreme south of the Sundance Formation outcrop. Leckie et al. (1989) and Cheel and Leckie (1990) interpret the Virgille Member of the Upper Cretaceous Milk River Formation in southern Alberta as a tidal inlet deposit. The Virgille Member rests erosively on the underlying Telegraph Creek Member shoreface deposits throughout the 4 km length of the outcrop. From the limited data available, it would thus seem that a predominance of tidal inlet deposits is common in ancient barrier island lithosomes. This has previously been overlooked due to the influence of models based on Holocene examples.

The fact that tidal inlet channel fill sequences form approximately 90% of the Halfway Formation in the study area suggests that inlet facies relationships are the major cause of heterogeneity within the Halfway sandbody. Tye (1984) and Tye and Moslow (in press) document the lateral facies relationships in mesotidal inlet fill sequences from South Carolina, which would appear to be analogous to the mesotidal Halfway tidal inlet sequences. Figure 37 shows a dip-oriented vibracore profile through an abandoned part of Price Inlet, South Carolina. Two cycles of tidal inlet abandonment are present in this section. The lower active channel fill rests erosively on the Pleistocene surface and

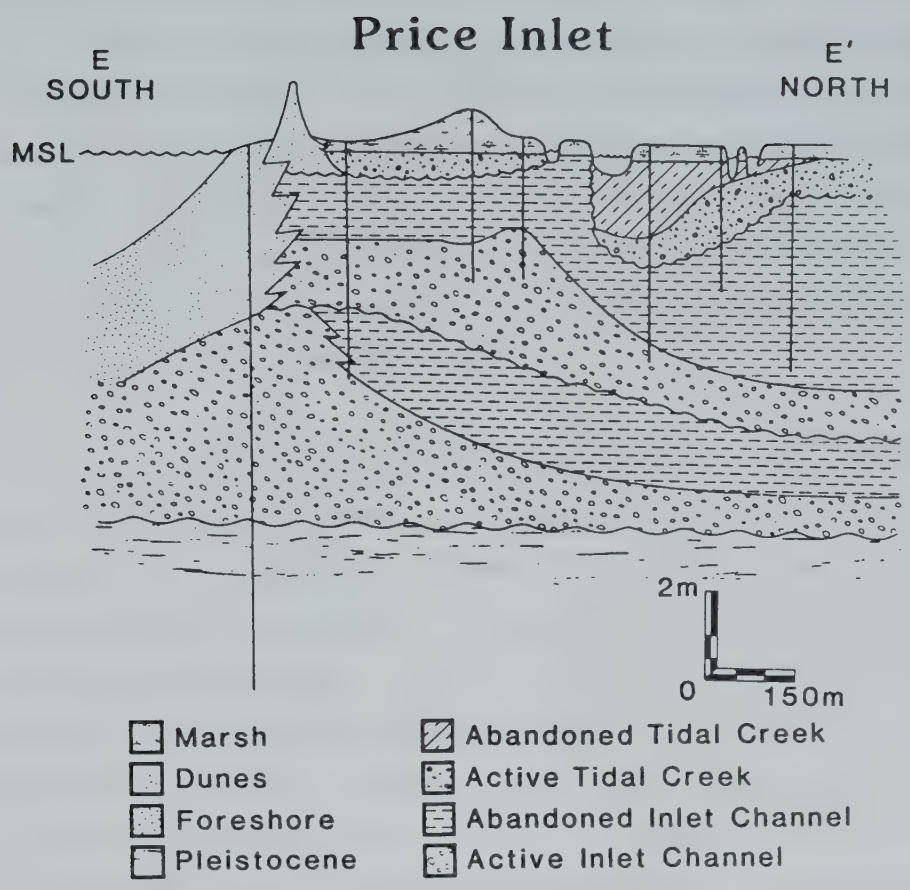

Figure 37. Dip-oriented vibracore cross-section through the abandoned part of Price Inlet, South Carolina showing the landward thickening of fine grained abandoned inlet fill and its seaward pinchout (after Tye and Moslow, in press).

interfingers landward (north) with fine-grained abandoned inlet deposits. The marked landward-thickening of these fine-grained abandoned inlet deposits can be seen in the upper inlet fill sequence. The foreshore sandstone at the southern end of the profile represents the welded ebb-tidal delta which sealed the upper tidal inlet channel and caused it to fill with fine-grained sediment. These foreshore sands interfinger landward with the fine-grained sediment. Tye (1984) states that abandoned inlet fill clay plugs underlie large portions of the adjacent barrier islands and form permeability barriers between shoreface sandstones. These clay plugs also form up-dip seals to the active channel bioclastic sandstones. The resulting lithosome would consist of a staggered distribution of shoreface sands, active channel sands and abandoned channel clay plugs and form a heterogeneous hydrocarbon reservoir.

Figure 38 is a dip-oriented core cross-section illustrating the facies relationships within a Halfway tidal inlet channel fill sequence. All wells on this section (except 16-23) display a basal inlet scour with associated lag (Facies I) and active channel deposits (Facies J). Well 6-36 represents the deepest part, or throat, of the inlet channel. The depth to which the inlet channel scours decreases both to the northeast (palaeo-landward) and southwest (palaeoseaward). This is consistent with axial bathymetric profiles of modern tidal inlet channels (Hubbard et al., 1979; Imperato et al., 1984) and observations of other ancient inlet fill sequences (Galloway, 1986). The cored sequence in well 6-36 records one complete upward-fining cycle of inlet channel abandonment. To the northeast (wells 7-36 and 16-36), the active channel deposits thin and are interbedded with dolomitic lagoonal mudstones (Facies G), representing deposition at the distal landward end of the inlet channel. In this distal area, the unequivocal identification of active inlet channel deposits becomes difficult; the erosive-based sandstone bodies may actually represent poorly developed flood-tidal delta or tidal creek deposits. Whatever their specific origin, they mark the up-dip stratigraphic pinchout of the coarse-grained tidal inlet deposits in finer-grained lagoonal sediments.

Southwest of the inlet throat, well 8-26 represents deposition at a site close to the seaward mouth of the inlet. The cored sequence consists solely of active channel deposits (Facies I and J) overlain by ebb-tidal delta sandstones (Facies L). The occurrence of these thick ebb-tidal delta sandstones above active inlet channel deposits represents welding of the ebb-delta to the shoreface following abandonment of the ebb-channel. This is analogous to the core from the mouth of Stono Inlet, South Carolina, shown in Figure 34. These welded ebb-delta sandstones extend back into the inlet channel and can be seen

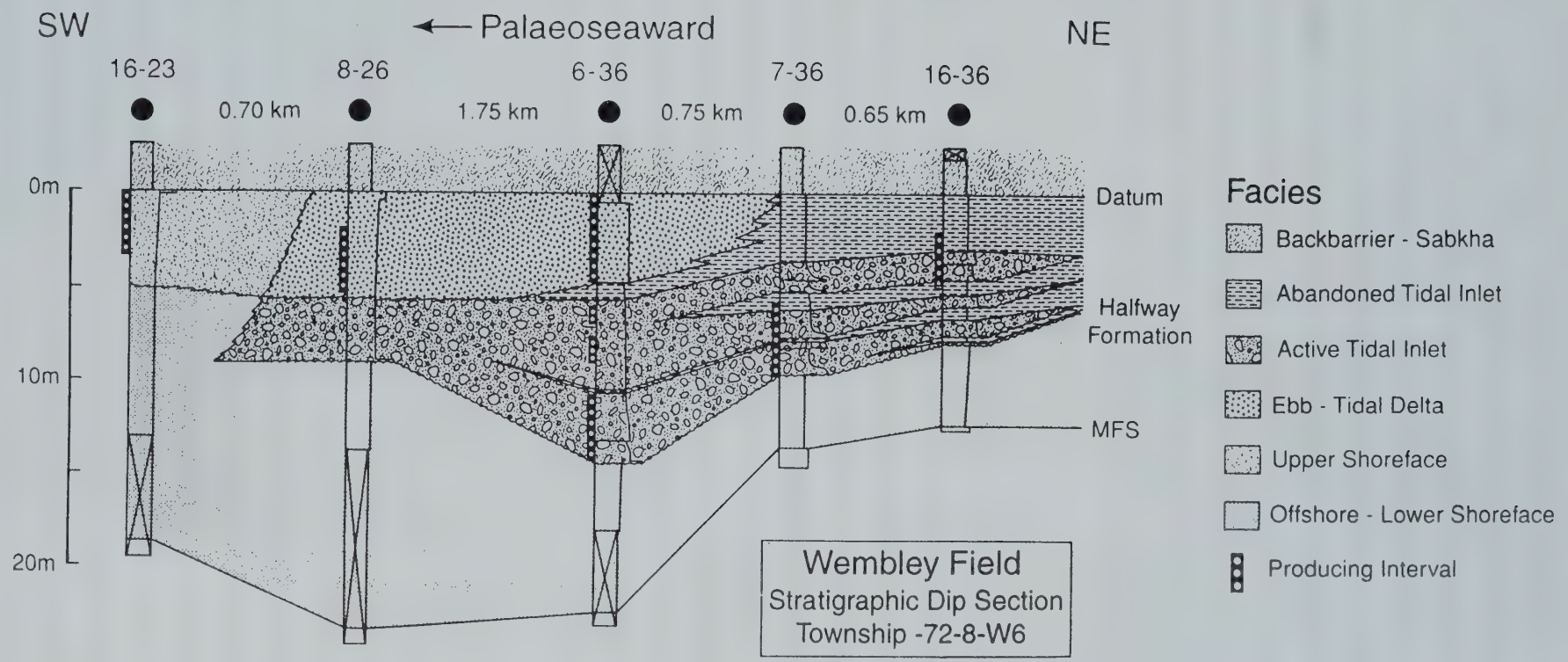

Figure 38. Dip-oriented core correlation of Halfway tidal inlet fill sequences in the Wembley oilfield. Note landward thickening of fine grained abandoned inlet fill and its seaward pinchout, similar to that shown in Figure 37. Both active tidal inlet sandstones and ebb-delta sandstones pinchout up-dip (northeast) against this fine-grained abandoned inlet fill, creating potential stratigraphic hydrocarbon traps. MFS= marine flooding surface over the Doig Formation.

overlaying fine-grained abandoned channel deposits in well 6-36. This represents landward transfer of the ebb-delta sand into the abandoned inlet channel, probably by washover events. For this reason, it is difficult in many cored sequences to distinguish Facies L ebb-delta sandstones from the plane laminated washover sandstones of Facies M. In the more landward parts of the abandoned inlet channel (well 7-36) these overwashed ebb-delta sandstones interfinger with fine-grained deposits (Facies K). At the landward-most end of the abandoned channel (16-36), which was presumably beyond the reach of overwash events, only fine grained material aggraded. This up-dip pinchout of welded ebb-delta sandstones in fine-grained abandoned inlet channel deposits creates a second potential stratigraphic hydrocarbon trap in the Halfway mesotidal inlet fill deposits.

The area between the inlet mouth cored in well 8-26, and well 16-23 immediately to the southeast in which there are no tidal inlet deposits, marks the point at which the main inlet channel was plugged and a new one established up-drift to the northwest, out of the plane of the cross-section. Facies relationships in this transitional area, where a welded ebb-tidal delta in effect becomes the shoreface, are poorly understood in modern environments. The ebb-delta sands would presumably be so modified by shoreface processes during the welding process that there would be little to distinguish the two in an ancient sequence other than their stratigraphic relationships to adjacent facies. For this reason, the contact between the reworked ebb-tidal delta sandstone in well 8-26 and the upper shoreface sandstone in well 16-23 is shown as completely gradational.

The systematic variation in tidal inlet fill sequences along the axis of the Halfway mesotidal inlet channel described above is similar to that recorded in modern mesotidal inlet fill sequences by Tye (1984), shown in Figure 37. Distribution of Halfway tidal inlet channel sandbodies along strike however, does not resemble that described from Holocene barrier islands. Figure 39 is a strike-oriented core cross-section through a series of tidal inlet channels in the Wembley Field. It is evident that the Halfway tidal inlet channel bodies are not separated along strike by barrier island shoreface deposits, as observed in the Holocene barrier island system of South Carolina by Tye (1984). Two of the wells in Figure 39 (6-31 and 14-30) represent facies successions deposited in the throat of a mesotidal inlet and consist of a single upward-fining cycle capped by welded ebb-tidal delta sandstones, or in the case of 14-30 a marginal flood channel or tidal creek. To the southeast, well 8-30 contains a thick welded ebb-tidal delta sandbody, representing

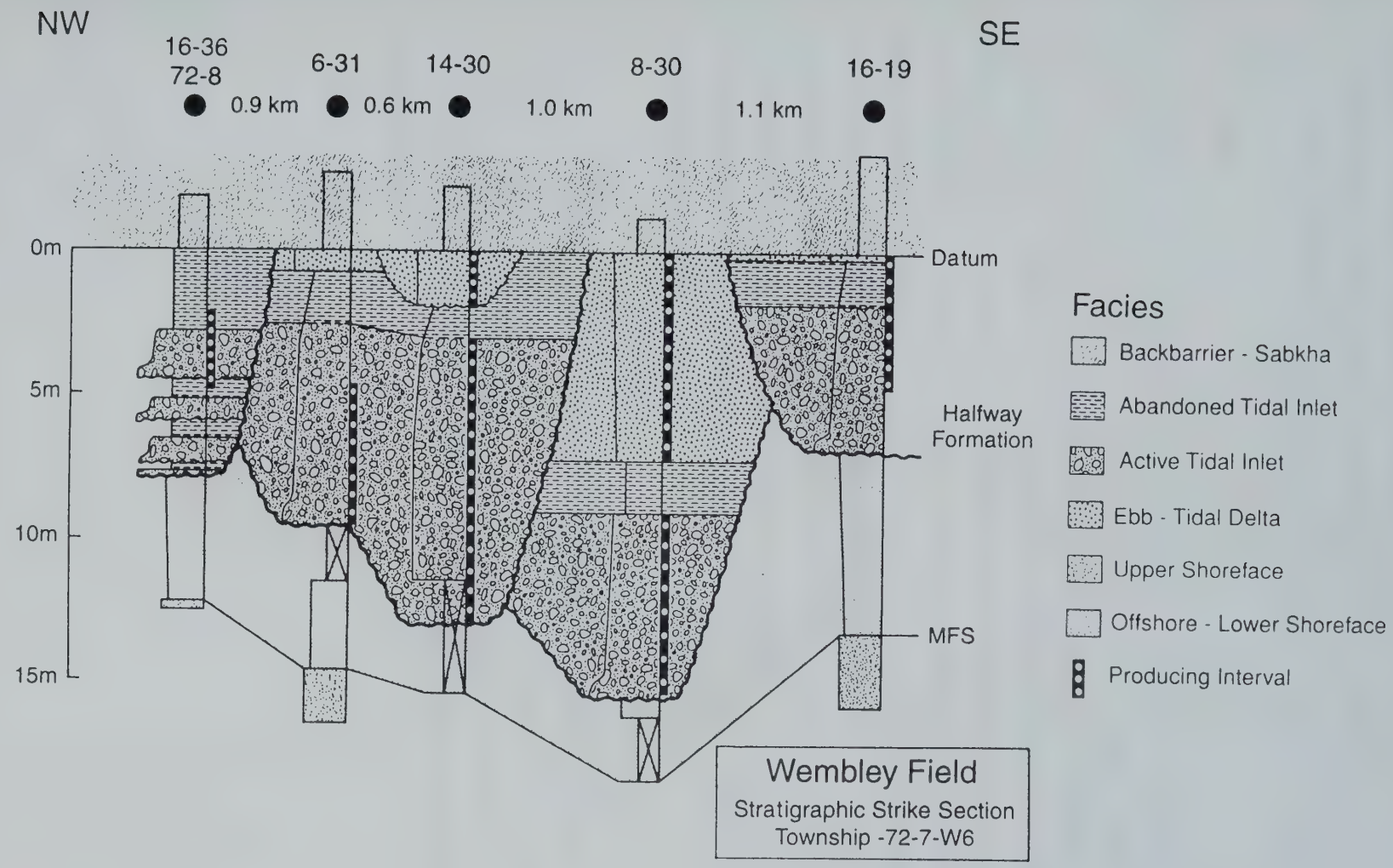

Figure 39 Strike-oriented core correlation of Halfway tidal inlet fill sequences in the Wembley oilfield. Note the lack of intervening barrier island shoreface sequences and the lateral juxtaposition of coarse grained active tidal inlet and ebb-delta sandstones against fine grained abandoned inlet fill. This results in a very heterogeneous hydrocarbon reservoir. MFS= marine flooding surface over the Doig Formation,

deposition near an inlet mouth, and to the northwest in well 16-36, a predominantly fine-grained sequence deposited toward the back of the inlet channel was cored. These laterally adjacent sequences represent deposition in different parts of an inlet channel axis and cannot therefore be explained by the simple down-drift migration of a single tidal inlet.

This preservation pattern can be explained by taking into consideration the fact that the Halfway coastline prograded southwestward through time. Inlet ebb-channel switching (bar bypassing) superimposed on overall coastal progradation would result in progressively landward parts of successive inlet channels occupying any given point through time. In Figure 39 this would suggest that the inlet mouth sequence in well 8-30 was deposited at a time when the Halfway shoreline was in this position. Continued progradation to the southwest meant that this area now lay slightly inland from the shoreline, such that when a new ebb-channel was incised it was in the throat position. The inlet throat sequences from wells 6-31 and 14-30 can thus be inferred as younger than that in well 8-30. Similarly, a third inlet channel incision when the shoreline had prograded even further to the southwest is recorded in well 16-36, which consists of interbedded inlet and lagoonal deposits.

Thus an understanding of the facies relationships within different parts of a single inlet channel (Figure 38) coupled with the evolution of the coastline through time is paramount to unravelling the ultimate facies architecture. In understanding the architecture of clastic reservoirs this critical element of time and temporal facies relationships has previously been ignored.

6.0.0 CORE-TO-WELL LOG CORRELATION.

An important aim in the description of cores is the correlation of genetic units, sedimentary facies and important stratigraphic surfaces to downhole wireline logs, as the establishment of the typical log responses to these features will help in their recognition in adjacent uncored wells. This is a relatively simple process involving matching variations in log response to vertical variation in core lithology. In the early stages of the study, all logs (gamma-ray, sonic, resistivity, formation density, compensated neutron) were compared to each core described to determine which were potentially most useful in establishing such correlations. It was found that a combination of the gamma-ray and formation density-compensated neutron logs represented most features adequately.

6.1.0 Method.

The first step in matching the wireline logs to the core was to establish a core-to-log depth correction. As core gamma-ray logs were not available, downhole gamma-ray and density-neutron logs were used. As many prominant lithological breaks (such as sandstone-shale, sandstone-anhydrite) as possible were identified in each core and tied to their log depth. This helped to identify any areas of core loss within the cored interval, rather than using a single marker and assuming all loss to be from the base of the core. Calculated core-to-log depth corrections were typically in the range of plus or minus 1 to 5 m.

Once core-to-log depth correction was established, an attempt could be made at identifying lithological units and important stratigraphic horizons on the logs. The precision to which this could be achieved was largely a function of the bed resolution of the wireline logs. While most of the gamma-ray logs had a resolution sufficient to delineate genetic units in the order of a metre thick, a few older logs (pre-1970's) were too crude to make any reliable correlations.

Since many of the Halfway facies are of similar lithology (eg. facies E, L and M), it is generally not possible to identify each solely on the basis of its log response. However, it is possible to characterize the two Halfway facies associations. By using the predictable facies patterns within these associations described in Chapter 5, it is possible to distinguish lithologically similar facies on the basis of their position in the overall sequence.

Cored facies associations are shown here correlated to their gamma ray log responses. This commonly-used method of identifying depositional facies in siliciclastic sequences assumes that there is a consistent relationship between gamma ray log values and clay content and between clay content and grainsize (Figure 40). The elements which contribute to a rock's radioactivity (potassium, thorium and uranium) generally have a far greater concentration in shales than in most other sedimentary rocks. Conversely, quartz, the principle component of sandstones, does not contain any of these three radioactive elements. Therefore, in siliciclastic rock sequences, high gamma ray readings are usually taken to indicate high clay content.

However, Rider (1990) has pointed out several pitfalls in the universal application of this methodology. For example, arkosic sandstones produce a high gamma ray response due to the potassium content of feldspar, invalidating the simple correlation of radioactivity with clay content. Similarly, highly radioactive mica tends to accumulate hydrodynamically with fine-grained sandstones rather than clay-sized grains. Consequently, Rider (1990) stresses the need to establish a definite correlation between log shape, grain size trend and clay content in a formation of interest before proceeding with this method.

Comparison of gamma ray log profiles to cored sequences during this study suggested that in the case of the Halfway, radioactivity was indeed reflecting its clay mineral content. Later petrographic study also found feldspars and micas to be a negligable component of Halfway sandstones. It is therefore considered that a semi-quantitative correlation between gamma ray response and clay volume is justified in the case of the Halfway. Certain exceptions, such as the presence of radioactive phosphatic material in Halfway sandstones, will be discussed below.

6.2.0 Facies Association 1: Regressive Shoreface.

Figure 41 illustrates a cored example of a regressive shoreface facies association and its corresponding the log suite over the Halfway interval from a typical well (16-26-72-8-W6) in the study area. The base of the Halfway Formation is picked at the base of the Facies B black shale, since it is impossible to distinguish the thin Facies A sandstone from the underlying Doig sandstone on well logs.

The gamma ray log in Figure 41 shows the basal Halfway shales to be highly radioactive, reading about 130 API units. In many cases the reading is over 150 API. A typical

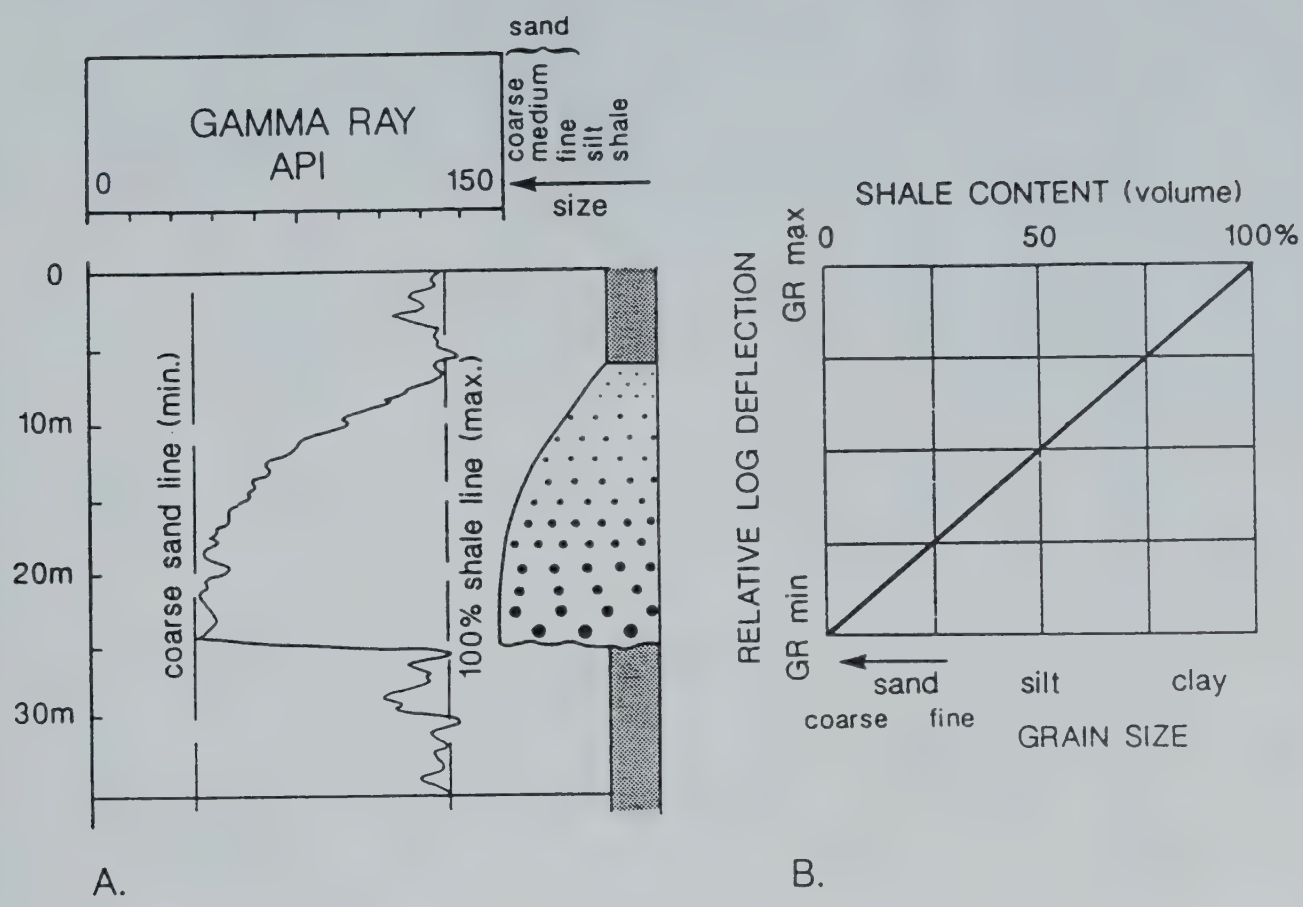

Figure 40. Schematic representation of the use of the gamma ray log in facies analysis. A. Grain size changes reflected in the gamma ray log. B. Graphical presentation of the semi-quantitative relationships implied (after Rider, 1990).

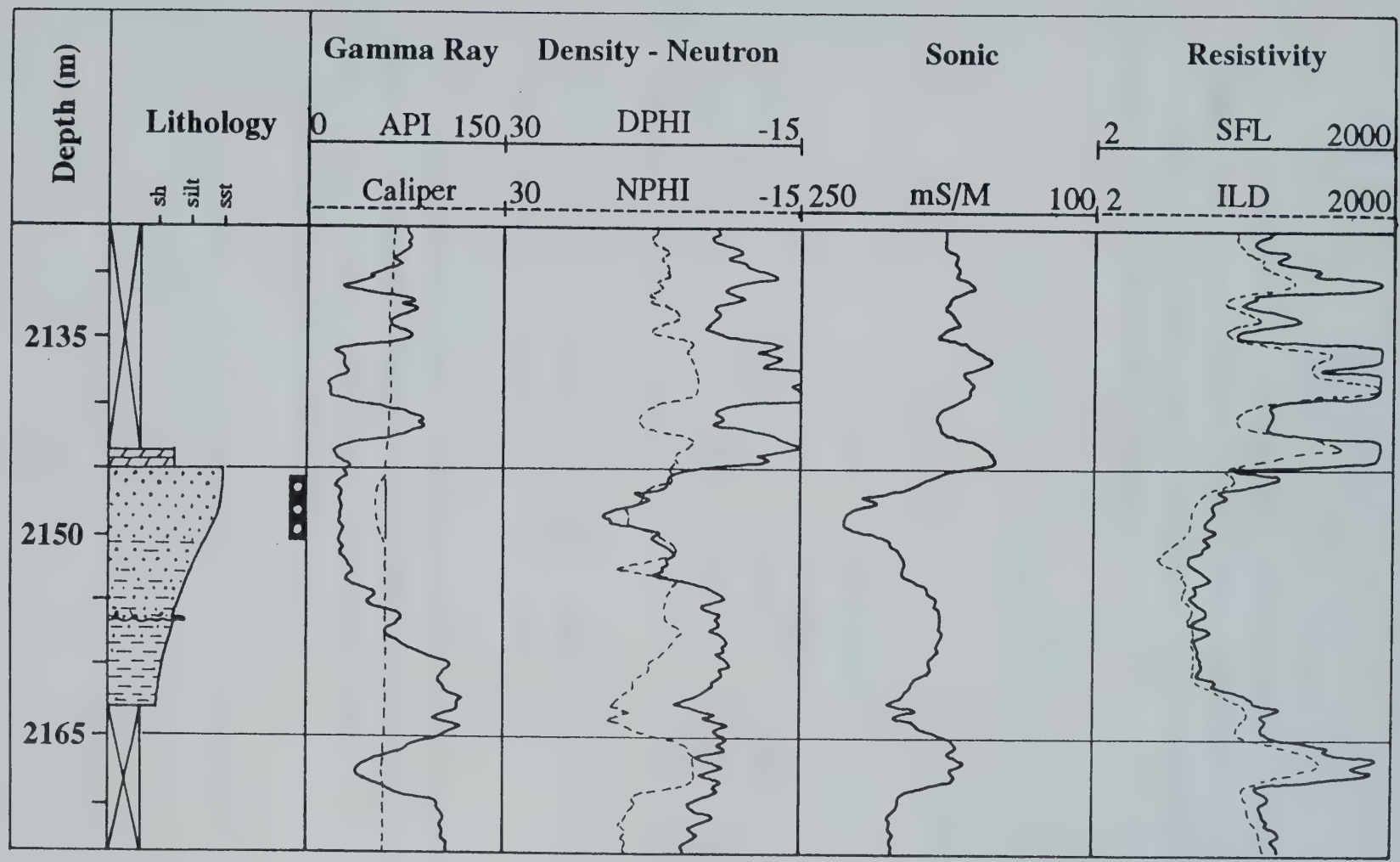

Figure 41. Well log suite correlated to a facies association 1 regressive shoreface sequence cored in well 16-26-72-8-W6.

gamma ray response in a shale interval is around 80-100 API, therefore the basal Halfway shales might be considered unusually radioactive. The gamma ray log reading reflects the total radioactivity of the rock. Natural radiation in rocks comes essentially from three sources: the elements potassium, thorium and uranium (Rider, 1986). Quantitatively, potassium is by far the most abundant of the three elements, forming 2.7% of the average shale. However, its contribution to the overall radioactivity in relation to its weight is small (Table 5). In reality, the contribution to the overall radioactivity of the three elements is of the same order of magnitude.

Element	Gamma rays per unit weight	Average Shale		Radioactive black shale	
		Content	Contribution to total GR	Content	Contribution to total GR
Potassium	1	2.7%	35-45%	1.34%	6%
Thorium	1300	12 ppm	40-50%	10.46 ppm	33%
Uranium	3600	3 ppm	10-20%	5.27 ppm	61%

Table 5. Radioactive mineral content and contribution to total radioactivity of average and radioactive shales. Compiled from data in Rider (1986).

The relative contribution each radioactive element makes to the overall gamma ray reading of a particular lithology can be determined from a spectral gamma ray log. Spectral gamma ray logs could only be obtained for four wells in the study area. Figure 42 shows one of these from well 8-21-73-9-W6.

Potassium is part of the clay mineral structure and therefore has a fairly constant distribution through most shales, contributing 35-40% of the overall radioactivity (Table 5). In general, uranium does not form part of the chemical makeup of clay minerals like potassium, but is associated with secondary components in shales. Geologically, the most important way in which uranium finds its way into sediments is the absorbtion of uranium salts present in seawater by organic matter and phosphates (Rider, 1986). Both of these processes require stagnant water and a relatively slow rate of deposition, so uranium peaks are commonly associated with condensed sections (Rider, 1986). The relative

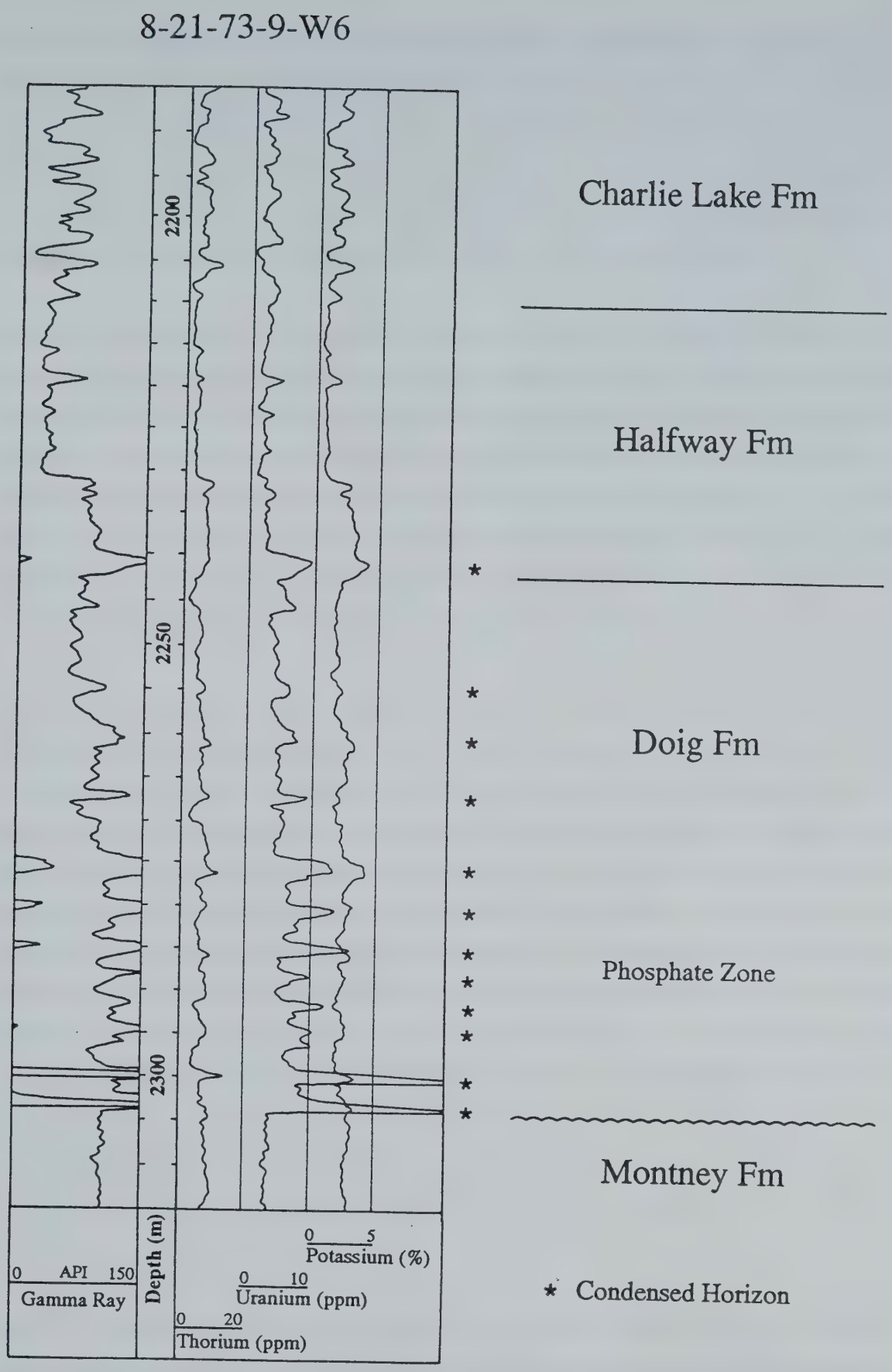

Figure 42. Spectral gamma ray log run over the Middle Triassic interval in well 8-21-73-9-W6. Note the numerous beds with high uranium concentrations, interpreted as condensed sections.

enrichment of uranium and its associated increase in contribution to the total gamma ray reading in a typical organic-rich black shale can be seen in Table 5. This affinity with secondary components and not the rock-forming minerals means that uranium distribution is generally not related to clay volume, and consequently uranium is a poor shale indicator. For this reason, on some spectral gamma-ray logs uranium is subtracted from the total gamma ray reading to give a better clay volume estimate.

Thorium, like uranium, is a detrital component derived from the breakdown of acid igneous rocks and does not form part of clay mineral structure. Unlike uranium however, thorium is extremely stable and will not generally pass into solution. Thorium therefore finds its way into sediments principally as detrital grains such as zircon, sphene, epidote and thorite (Rider, 1986). Studies have shown that thorium has a relatively constant value of about 12 ppm (range 5 to 20 ppm) in almost all shales (Rider, 1986), which contributes 40 to 50% of overall shale radioactivity. This consistent distribution and high contribution to overall radioactivity make thorium a very good shale indicator.

The spectral gamma ray log in Figure 42 shows that most of the Halfway shale interval (2231m - 2241m) is characterised by a "normal" shale gamma ray reading of 75-90 API and a uranium content of 2-4 ppm. However, the base of the Halfway shale at 2241m is associated with a total gamma ray reading of 165 API and a uranium content of about 9 ppm. The thorium content, considered the most reliable indicator of clay volume, remains constant at about 6 ppm across the uranium peak. This indicates that the total gamma ray peak is reflecting the high uranium content and not any variation in clay volume. Samples from the base of Facies B black shales have a high phosphate content, so it is inferred that the uranium anomaly is associated with uranium bound up in the phosphate. Similar high gamma ray readings and associated uranium peaks can be seen throughout the Middle Triassic section, particularly in the Phosphate Zone of the Doig Formation. These zones are interpreted as condensed sections, representing slow periods of sedimentation during which the proportion of phosphate (and consequently uranium) in the sediment was enriched.

Above the radioactive condensed horizon at the base of the Halfway in Figure 41, the overall sequence shows an upward decrease in gamma ray response. Examination of the corresponding cored interval shows this to reflect the upwardly-decreasing clay content produced by increasingly effective wave winnowing of the substrate through the lower and upper shoreface. The gradational contacts between the offshore (Facies B), offshore-

shoreface transition zone (Facies C) and the lower shoreface (Facies D) are difficult to pick on logs and can only be marked with confidence by reference to core. A thin bioclastic sandstone bed at 2157 m is interpreted as an incursion of ebb-tidal delta deposits onto the lower shoreface. Anomalous gamma ray peaks within the upwardly-decreasing shoreface profile were commonly observed to be caused by concentrations of phosphatic shell fragments, particularly lags at the base of storm beds. The upward increase in the proportion of more porous sandstone is also apparent on density and sonic logs.

The contact between the lower and upper shoreface (Facies D and E) tends to be more abrupt and therefore easier to identify on logs. This is seen at approximately 2151 m in Figure 41, where there is a marked flattening of the gamma ray profile through the 10-20 API upper shoreface sandstones of Facies E. This change is also apparent on density and sonic logs, particularly where the sandstone is hydrocarbon bearing. The porous nature of the sandstone also allows invasion of drilling fluids, producing a separation of deep and shallow resistivity logs and a build up of mud cake on the borehole wall visible on the caliper log.

The top of the Halfway sandstone is difficult to pick using only the gamma ray log, since it is commonly overlain by 1-2 m of Facies G anhydritic dolomites which also have a low gamma ray response. However, these laminites have low porosity, causing deflections of the sonic, density and resistivity logs. This can be seen at 2145 m in Figure 41. Use of the gamma ray log alone would result in an over-estimation of the thickness of Halfway sandstone. The first red bed unit (Facies H) above the anhydritic dolomites shows up as a high gamma ray response. Above this, the lower part of the Charlie Lake Formation consists of interbedded mudstones (high gamma ray, low density, low resistivity) and anhydrites (low gamma ray, high density, high resistivity with no separation of deep and shallow readings) deposited in an arid coastal plain setting.

6.3.0 Facies Association 2: Tidal Inlet Channel Fill.

As discussed in Chapter 5, tidal inlet fill sequences comprise the bulk of the Halfway Formation in the study area. These inlet sequences display a much greater variation in facies successions than shoreface sequences, reflecting deposition in landward and seaward parts of the tidal channel. This results in a wide variety of log shapes associated with Halfway tidal inlet fill sequences.

6.3.1 Single Tidal Inlet Cycle.

Figure 43 shows a complete log suite correlated to a tidal inlet fill sequence cored in well 6-31-72-7-W6. The inlet channel scour occurs at 2050 m, in this example cutting down into shales of the offshore-shoreface transition zone (Facies C). The abrupt upward change from shale to bioclastic sandstone is readily apparent on the gamma ray, density, sonic and resistivity logs. However, it was noted when correlating several inlet sequences to their log responses that this sharp lithological break is not always marked by a corresponding decrease in gamma ray response. This is due to the common occurrence of shale rip-up clasts at the base of the inlet fill sequence (Facies I), which mask the sandstone on the gamma ray log. The change from shale to porous sandstone is, however, readily apparent on the sonic, density and resistivity logs. This illustrates one of the pitfalls of relying solely on gamma ray profiles when making core-to-log correlations.

The lower part of the inlet fill sequence in Figure 43 is bioclastic sandstone (Facies I and J) deposited in the active inlet channel. This is the hydrocarbon producing interval in this well. This bioclastic sandstone unit has a low gamma ray response and its porous nature is indicated by the density, sonic and resistivity logs. It is difficult to distinguish these active inlet channel bioclastic sandstones and coquinas (Facies I and J) from other non-bioclastic sandstones (Facies E, L and M) on the basis of their log responses. Only their position at the base of an upward-fining facies succession allows their identification without core control. Above this clean sandstone unit, the inlet fill sequence displays an upwardly-increasing gamma ray response, reflecting the increasing shale content of sediment accumulating in the abandoned inlet channel. Corresponding decreases in porosity and hydrocarbon saturation are reflected in the sonic and resistivity log responses respectively. This upwardly-increasing, or "bell-shaped" gamma ray log profile typical of Halfway tidal inlet channel sequences is commonly considered diagnostic of sediments deposited in a channel setting (Rider, 1986). The inlet fill sequence in well 6-31-72-7-W6 is capped at 2040 m by a thin unit of Facies L sandstone washed into the abandoned channel from the welded ebb-tidal delta.

The upper contact of Halfway tidal inlet sequences is generally marked by the passage into anhydrites and dolomite similar to the shoreface sequence described above and has the same log response.

Wells penetrating the more landward part of an abandoned mesotidal inlet channel fill typically contain a greater proportion of shale (Chapter 5). In such cases, the bell-shaped

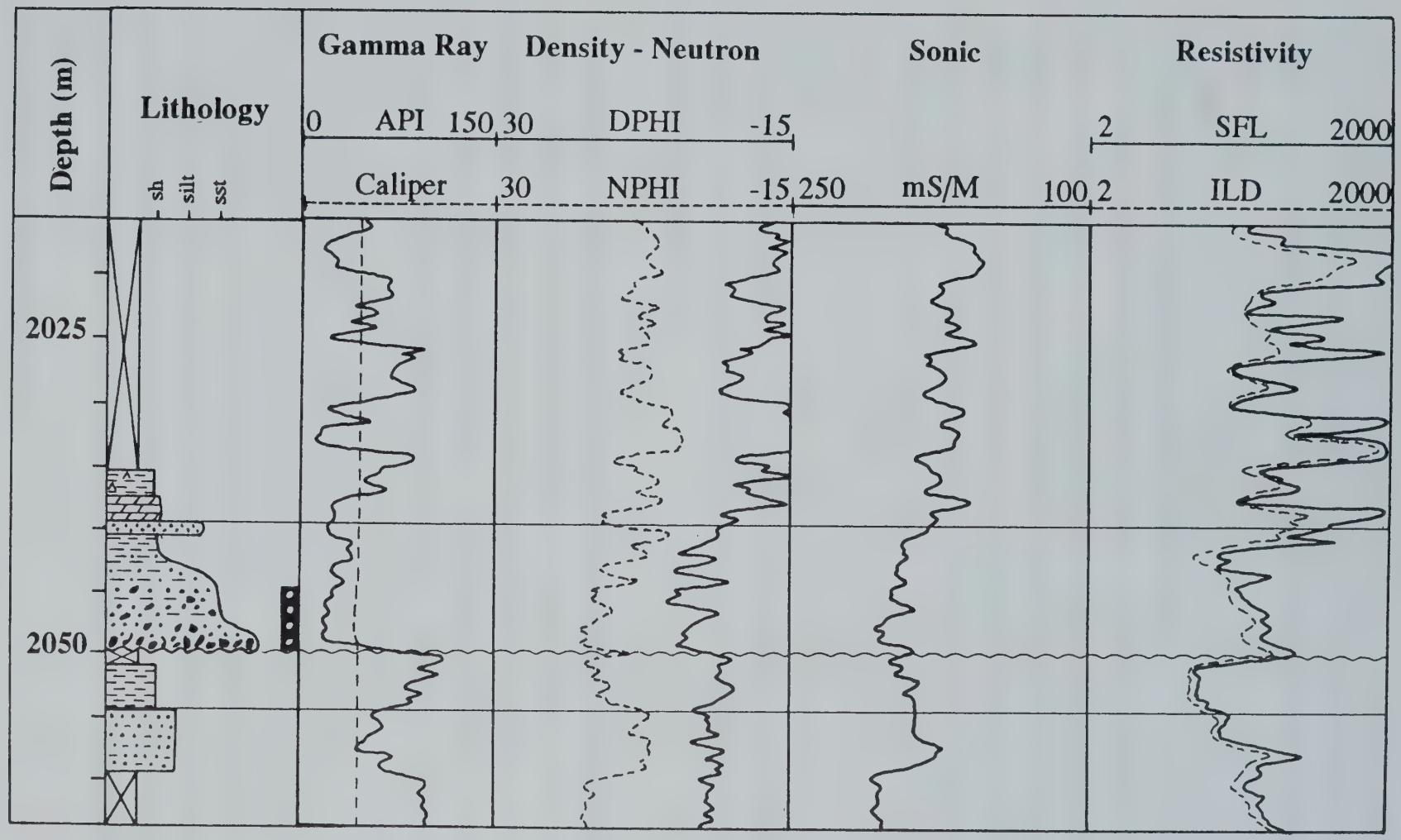

Figure 43. Well log suite correlated to a facies association 2 tidal inlet channel fill sequence in well 6-31-72-7-W6. In this case a single upward-fining inlet fill sequence is present, capped by a thin washover sandstone at 2040 m.

gamma ray profile described above is replaced by a sharper-based shale interval reflecting the rapid change from lateral accretion to vertical aggradation of the inlet channel. The fine-grained abandoned channel fill may be interbedded with coarser-grained active channel or flood-tidal delta deposits, giving a serrated gamma ray log profile.

6.3.2 Tidal Inlet Mouth: Welded Ebb-Tidal Delta.

In the case of inlet fill sequences from the seaward mouth of the inlet channel, abandonment causes the the channel to be filled with welded ebb-tidal delta sands. An example of such a sequence is shown in Figure 44. The base of the inlet channel can clearly be seen at 2054 m and shows a slight upward-fining trend to 2052 m. At 2052 m in the core there is an abrupt change from the active inlet channel bioclastic sandstone with silt laminae to clean sandstone of Facies L, representing welding of the ebb-tidal delta onto the inlet mouth. Although there is no apparent grainsize change in this example of Facies L in the core, the gamma ray log response does decrease upward. This may be reflecting removal of clay by more effective winnowing of the sediment in progressively shallower water. The ebb-tidal delta sandstone is overlain by impermeable backbarrier deposits as in Figure 41.

In some cases, even with the aid of core, it was difficult to differentiate welded ebb-tidal delta sequences from a simple regressive shoreface. This occurs where the basal inlet channel scour occurs within lower shoreface sandstones and does not mark a significant break in lithology. If this scour surface is not identified, then the overlying ebb-tidal delta sandstone can easily be mistaken for the upper shoreface sandstone of a regressive shoreface sequence. It is therefore critical to identify the basal inlet channel scour to correctly interpret such sequences. The scour is often marked by a concentration of small dolomitic mudstone clasts and bioclastic debris transported out of the inlet channel by ebb-tidal currents. Such clasts are not found in regressive shoreface deposits. At the seaward limit of the inlet channel however, this distinction between inlet and shoreface sequences becomes somewhat semantic since the two are entirely gradational, as seen in the thin bioclastic sandstone bed in the shoreface sequence depicted in Figure 41.

6.3.3 Stacked Tidal Inlet Cycles.

In many Halfway sequences, two or more amalgamated inlet cycles may be present. Downcutting of successive inlet channels results in variable preservation of the older channel sequences and difficulty in identifying one from another on logs. This alternation

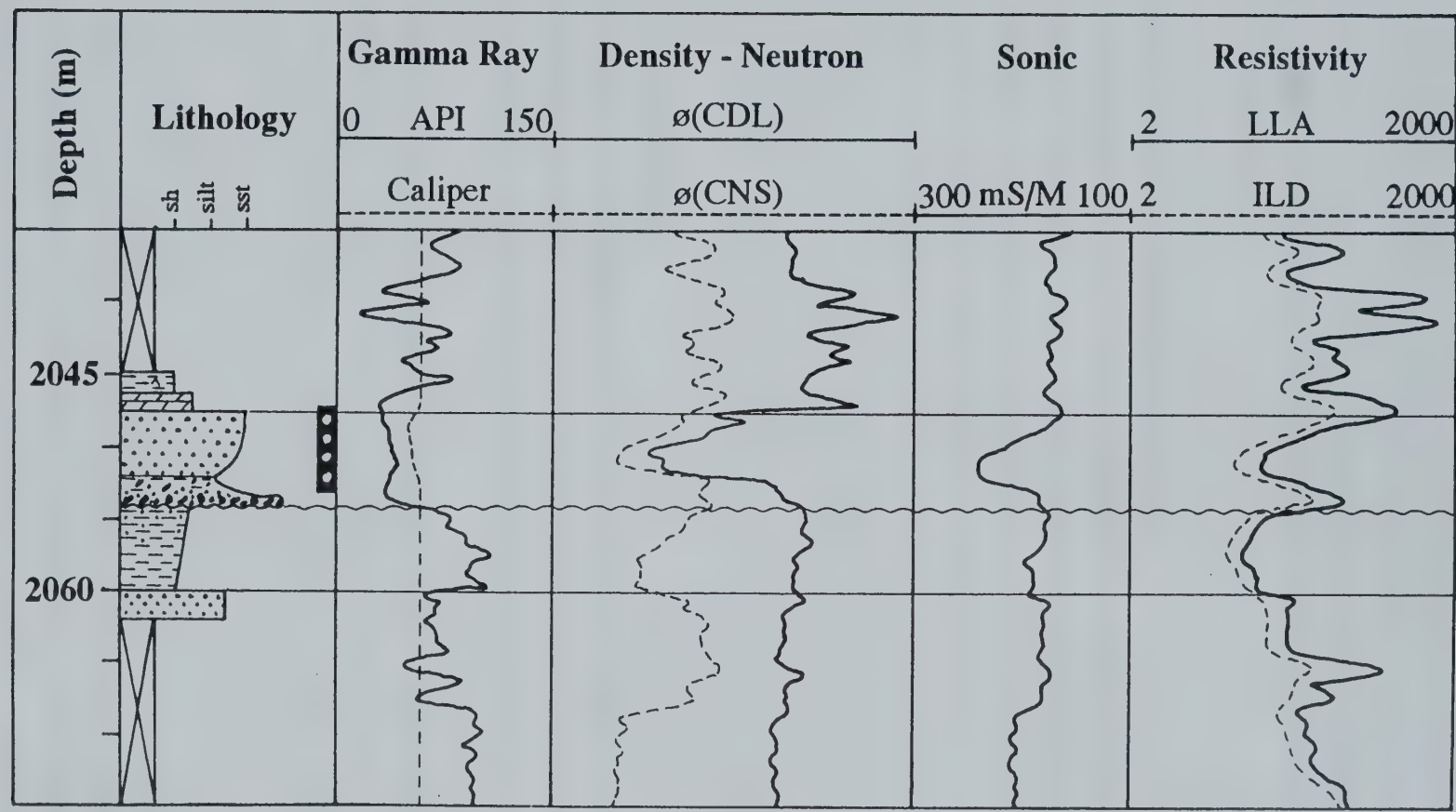

Figure 44. Well log suite correlated to a facies association 2 tidal inlet channel fill sequence in well 14-16-72-7-W6. This example represents a sequence from the seaward mouth of the tidal inlet channel, which was plugged by a welded ebb-tidal delta sandbody. No fine grained abandoned inlet channel deposits are present and the sequence does not therefore exhibit an upward-fining trend.

of active channel sandstones and fine-grained abandoned inlet fill results in a serrated, blocky gamma ray profile (Figure 45). While it may be possible to distinguish units of porous active channel sandstone from fine-grained abandoned channel fill on well logs, it is difficult to determine which belong to the same inlet cycle without reference to core. Therefore when a blocky, serrated gamma ray profile with no distinct upward-fining trend is encountered in the Halfway, it is likely to be the result of amalgamated inlet channel fill sequences.

6.4.0 Facies M Washover Sandstones.

Also present at the top of the Halfway Formation in Figure 45 is a unit of Facies M washover sandstone (2135-2140 m). Facies M is typically separated from the underlying shoreface or inlet facies succession by one metre of Facies G lagoonal mudstones, seen here at 2141-42 m. These mudstones produce a distinct gamma ray peak between the sandstones below and Facies M above and are useful in identifying Facies M in wells where core is not available. Sonic, density and resistivity logs show that the the lagoonal mudstones form a thin impermeable layer between the sandstones above and below, so separating the Facies M sandbody from the underlying reservoir sandstones.

6.5.0 Summary.

Well logs are useful in identifying Halfway facies successions. It is generally not possible to identify individual facies on well logs due to their lithological similarity, but they may be inferred from their position within the overall facies succession.

Halfway regressive shoreface sequences are characterized by a typical upwardly-decreasing, or "funnel-shaped" gamma ray profile. These are generally smooth, but anomalous peaks may result from concentrations of phosphatic shell material in storm beds.

Most Halfway tidal inlet sequences are recognisable as such on well logs by virtue of the sharp lithological break across the basal channel scour. Single inlet cycles display an upwardly-increasing "bell-shaped" gamma ray profile representing gradual channel filling by lateral accretion. The upper part of inlet fill sequences from the landward end of the inlet channel contain a higher proportion of fine-grained material and have a correspondingly higher gamma ray response. Sequences which accumulated at the inlet mouth however, contain little fine-grained material as a result of wave-reworking of the ebb-tidal delta and show an upward-coarsening profile. These three basic log responses

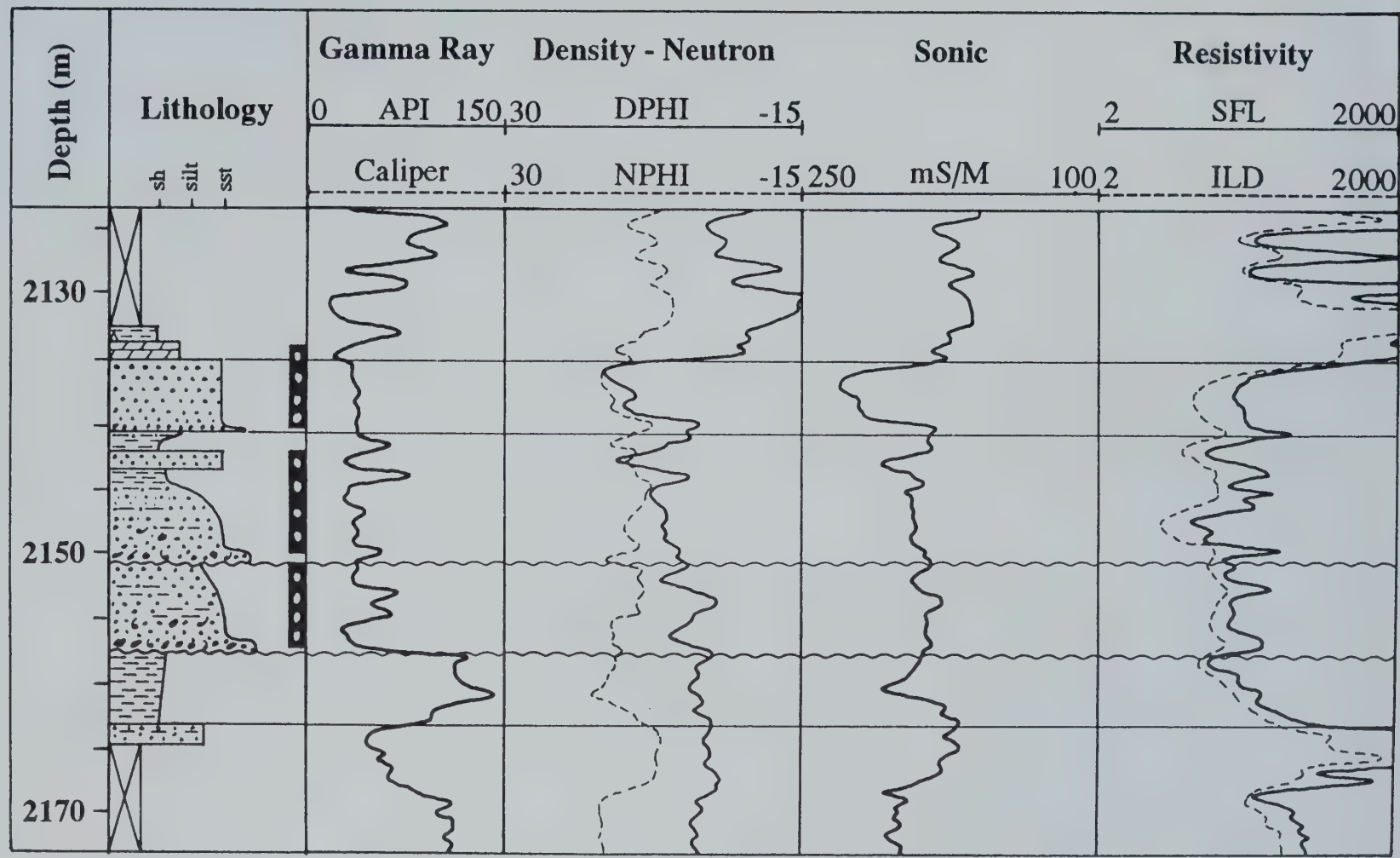

Figure 45. Well log suite correlated to a facies association 2 tidal inlet channel fill sequence in well 6-27-72-8-W6. This example contains two amalgamated tidal inlet channel sequences and has a serrated, blocky gamma ray profile with no overall grain size trend. The upper part of this sequence contains an example of a thick Facies M washover sandstone between 2135 m and 2140 m. Note the bed of Facies G backbarrier mudstones beneath this washover sandstone at 2140m.

represent a single cycle of inlet activation and abandonment at various positions along the channel axis. Amalgamation of successive inlet channels as a result of bar-bypassing superimposes these sequences and commonly results in a serrated, blocky gamma ray response.

7.0.0 LOCAL STRATIGRAPHIC FRAMEWORK.

The second major objective of this study was to use the facies associations described in Chapter 5 to clarify the local stratigraphic relationships of the Doig, Halfway and Charlie Lake Formations. This was achieved by constructing numerous core-based cross-sections showing the correlation of facies between adjacent wells. Figure 46 is a stratigraphic dip section through the Wembley field which summarises the findings of this work.

The large vertical exaggeration (x 200) of these core-based cross-sections produces a distortion of the facies relationships in the Halfway interval. This distortion is a result of differential compaction of sandstone and shale within the Halfway and also compactional drape over the underlying thick Doig Formation sandstones. The fact that all cored Halfway sequences in the study area show a complete upward-shallowing succession demonstrates that this thickness variability is not the result of post-Halfway erosion. If this was the case, then the upper part of thinner Halfway sequences would have been removed and the overlying Charlie Lake deposits would rest on units lower in the Halfway facies succession. This was never observed.

Using the base of the Halfway shale (Facies B) as a datum results in the differential compaction distorting the upper part of the Halfway section, making it difficult to depict depositional facies relationships in the area of greatest interest. Conversely, using a datum near the top of the Halfway results in the lower part of the section being irregular. The latter was felt to be the better compromise since it does not affect the reservoir interval. Therefore the datum chosen for facies correlations is the contact between the top of the Halfway sandstone interval (Facies E, F or L) and the overlying backbarrier deposits (Facies G). This datum is easily identified both in core and on well logs and corresponds in most wells to the lithostratigraphic Halfway-Charlie Lake contact. The absence of foreshore and backshore deposits in most cored facies successions indicate that some erosion has occurred at this stratigraphic level, superimposing backbarrier deposits directly upon upper shoreface sandstones. As discussed in section 5.1.0, the amount of erosion is considered to be limited and approximately equal throughout the study area.

7.1.0 Discussion.

In Figure 46 the Halfway Formation rests on sandstones referred to the Doig Formation. This contact is marked as the lower marine flooding surface (separating parasequences 3 and 4) on Figure 46 and has previously been interpreted as the product of a marine transgression over the shoreface deposits of the Doig Formation, followed by deposition

of the regressive Halfway Formation (Campbell and Horne, 1986; Cant, 1986). There is some disagreement as to whether this transgression occurred over a subaerially exposed surface (Campbell et al., 1989), or in the marine environment (Wittenberg, 1992).

Halfway Facies A, which is present as a thin veneer above the Doig Formation throughout the area, is interpreted as a shoreface deposit which accumulated during this transgression. Beyond the southwestern extent of Doig Formation shoreface sandstones, Halfway Facies A disappears and Facies B shales rest directly on Doig siltstones (eg. well 8-1-72-9-W6).

In the northeastern half of Figure 46, wells 6-6-73-7-W6 through 16-21 each display an upward-shallowing facies succession produced by southwesterly progradation of the Halfway barrier island shoreline. This progradational package of strata contains three tidal inlet channels separated by two shoreface sequences (wells 11-26 and 16-26) and thickens in a southwesterly direction. The sequence is capped by Facies G and H, representing coeval seaward progradation and aggradation of backbarrier and supratidal deposits.

Toward the southwestern end of Figure 46, two major changes are apparent in the Halfway facies relationships:

1) In wells 16-21, 14-22 and 6-27, Facies M washover sandstones are present within backbarrier-sabkha deposits above the datum. It should be noted that these washover sandstones thin northeastward and are not present throughout most of the width of the cross-section.

2) Immediately southwest of the Facies M sandbody, Halfway facies associations 1 and 2 are incomplete. For example, in well 8-9 facies association 1 coarsens upward into offshore-shoreface transition siltstones (Facies C) and is then capped by an erosion surface (marked R). This erosion surface is overlain by 0.5 m of Facies A bioclastic sandstone displaying oscillation ripple cross-lamination and hummocky cross-stratification. Above this unit of Facies A lies a second upward-coarsening facies association within the Halfway Formation (labelled parasequence 5 in Figure 46).

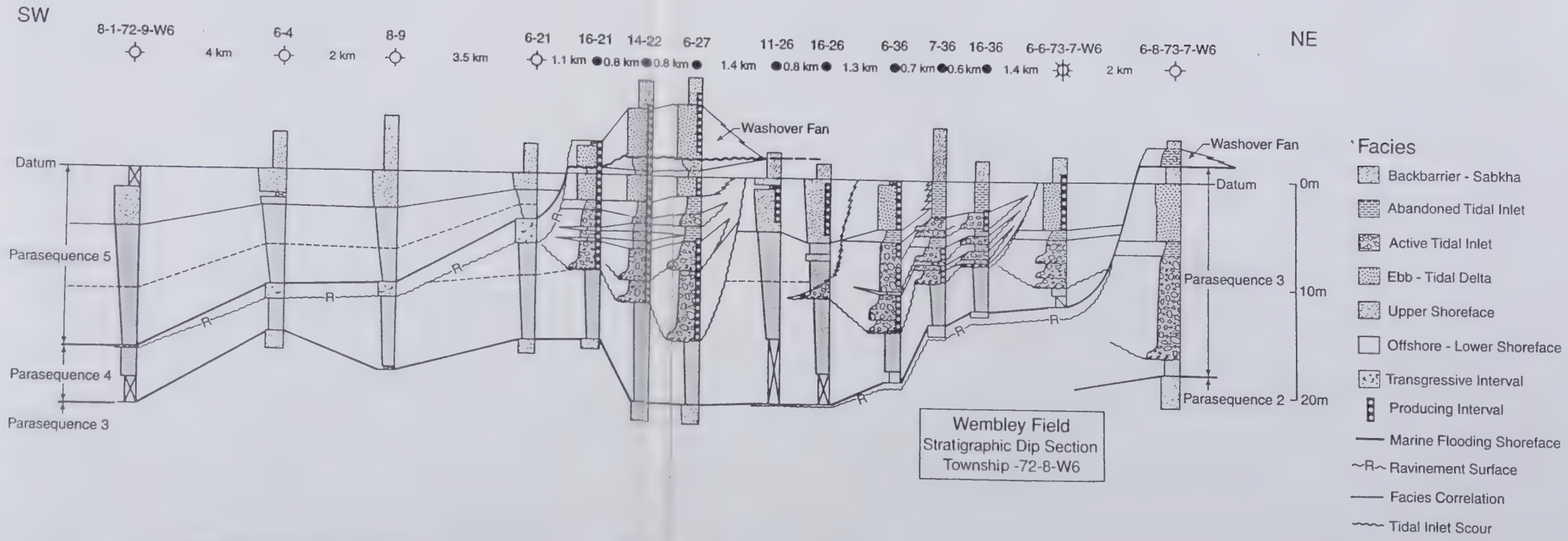

Figure 46. Dip oriented stratigraphic correlation of cored Halfway facies through the Wembley oilfield. Datum is the top of the Halfway sandstone interval. Parasequences 4 and 5 represent the Halfway Formation, and Parasequence 3 the Doig Formation. Two tidal inlet channel fills are present in the Halfway, separated along dip by shoreface sequences in wells 11-26 and 16-26. Note the ravinement surface within the Halfway Formation in the southwestern part of the section separating parasequences 4 and 5 and its northeastern termination at the thick washover sandstones in wells 16-21 to 6-27. A second ravinement surface and washover sandstone are present at the extreme northeastern end of the section and separate the Halfway and Doig formations.

Duplicated facies successions within the Halfway Formation similar to that in well 8-9 are present in a zone extending 3 km southwest of the Facies M sandbody and along strike throughout the study area (Table 6). In each example, the erosion surface (R) marks an abrupt change in lithofacies, palaeowater depth and palaeoenvironment. In well 8-9 for example, Facies C siltstones interpreted as deposits of the offshore-shoreface transition zone are overlain by Facies B black shales deposited in the offshore. The level of the erosion surface drops stratigraphically to the southwest: immediately adjacent to the position of Facies M it is found within Facies D lower shoreface deposits (e.g. well 6-21), but to the southwest occurs in Facies C offshore-shoreface transition deposits (e.g. well 8-9) and then Facies B offshore shales. Evidence of erosion at the surface also tends to decrease to the southwest, as does the thickness of the overlying unit of Facies A bioclastic sandstone. At its southwestern detectable limit, the surface appears entirely conformable and is represented by an abrupt change from siltstone to black shale (e.g. well 8-1-72-9-W6). This is strikingly similar to the occurrence of Facies A at the contact between the Halfway and Doig Formations.

7.2.0 Origin of the Erosion Surface

The erosion surface observed in cored intervals of Halfway shoreface deposits immediately southwest of the Facies M washover sandstones is interpreted as a ravinement surface. A ravinement surface is a submarine erosion surface produced by transgressive shoreface retreat (Swift, 1968). It does not represent a sudden shift in shoreline position, but is the product of gradual landward migration of a shoreface as a result of wave erosion, somewhat analogous to the surface produced at the cut bank of a meandering stream. This shoreface erosion may be in response to a rise in relative sea level or a decrease in sediment supply to the shoreface. Palaeowater depths can change from near sea level below the surface to lower shoreface or deeper above it, suggesting that a catastrophic transgression occurred. However, studies of Holocene shorelines have shown that gradual transgression associated with shoreface retreat produces the same result (Figure 47).

7.3.0 Shoreface Retreat.

The geometry of shoreface movement in response to rising sea-level was first described by Bruun (1962), who argued that if the coastal profile is an equilibrium response of the sea floor to the coastal fluid power expenditure, then the effect of sea-level rise must be a landward and upwards translation of the profile (Figure 48). This model predicts that the shoreface must retreat by erosion, while there is a site of potential aggradation under the

Well Location	Core	Log Depth
06-25-71-08-W6	•	2229m
06-04-72-08-W6	•	2305m
14-08-72-08-W6	•	2315m
05-08-72-08-W6		2320m
08-09-72-08-W6	•	2293m
06-15-72-08-W6		2258m
06-16-72-07-W6	•	2285m
07-16-72-08-W6		2261m
10-17-72-08-W6	•	2286m
16-20-72-08-W6	•	2225m
06-21-72-08-W6	•	2211m
04-28-72-08-W6	•	2180m
06-28-72-08-W6	•	2164m
14-28-72-08-W6	•	2146m
16-29-72-08-W6	•	2170m
16-30-72-08-W6	•	2211m
08-01-72-09-W6	•	2401m
06-14-74-09-W6	•	2050m
10-22-74-09-W6	•	2081m

Table 6. Location of wells in the southwestern part of the study area which contain two upward-coarsening facies associations within the Halfway Formation. The well log depth of the transgressive surface separating the two facies associations is shown, together with details of those wells which were cored over this interval.

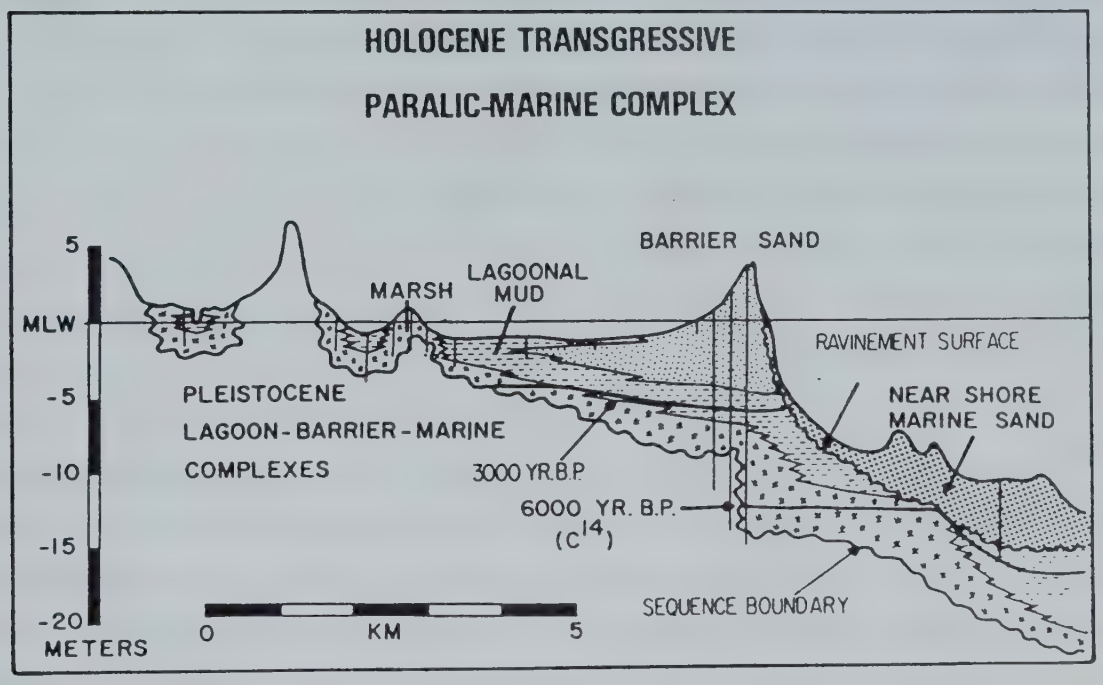

Figure 47. Cross-section through the Holocene coastal deposits north of Bethany Beach, Delaware. The Holocene sequence consists of a transgressive barrier island erosionally truncated to the east by a ravinement surface. Note the superposition of nearshore marine sand above the ravinement surface directly on lagoonal muds below (after Kraft, 1971).

rising seaward limb of the profile. Bruun suggested that if there were no net loss of sand alongshore, then there should be an equal-volume transfer of sediment from the eroding shoreface to the adjacent shelf floor.

Studies of the coastal processes affecting erosional shoreface retreat by Swift et al. (1985) and Niedoroda et al. (1985) have demonstrated that the process is far more complicated than that predicted by Bruun's model. A complex interplay between sediment accretion to and erosion from the shoreface during fairweather and storm conditions and variations in offshore and onshore transport of eroded sediment control the pattern of barrier retreat during a relative rise in sea-level (Figure 49). In particular, much of the sediment eroded from the shoreface is known to be washed over the barrier crest into the lagoon during storms, rather than being transported offshore in accordance with Bruun's model (Swift et al., 1985; Niedoroda et al., 1985; Kraft et al., 1987). This washover allows the barrier island to retreat landward over its associated lagoonal deposits, since it is recycled in tank-tread fashion as the eroding shoreface approaches (Niedoroda et al., 1985). Sand which is left behind on the shelf is lost to the barrier system. If the sediment lost offshore is considerable, it may reduce the sediment supply of the barrier to the point at which it cannot maintain its subaerial integrity. This situation is most common in more rapidly subsiding delta-destructive barriers which submerge to form a submarine shoal (Penland et al., 1985).

The deposits that become incorporated as part of the transgressive vertical sequence above the ravinement surface are dependent upon the width of the zone of net erosion, which in turn is a function of the depth of wave base and the gradient of the shoreface. Where the zone is narrow, shoreface deposits may be preserved, and where the zone is wider, sediments farther offshore will immediately overlie the ravinement surface (Demarest and Kraft, 1987). The wider the zone of net erosion, the farther offshore the first sediments above the ravinement will be deposited and the more dramatic the surface will appear in the geological record in terms of change in palaeoenvironment. Where preserved, transgressive shoreface deposits tend to be discontinuous and consist predominantly of lower shoreface sands directly above the ravinement (Kraft et al., 1987). These deposits consist of inner shelf sheet sands, storm-graded beds and silty shales, and may grade upward into outer-shelf shales if the transgression persists long enough (Demarest and Kraft, 1987). These transgressive shoreface deposits are analogous to the thin Facies A sandstones which occur above the ravinement capping Halfway shoreface successions in the southwestern part of the study area.

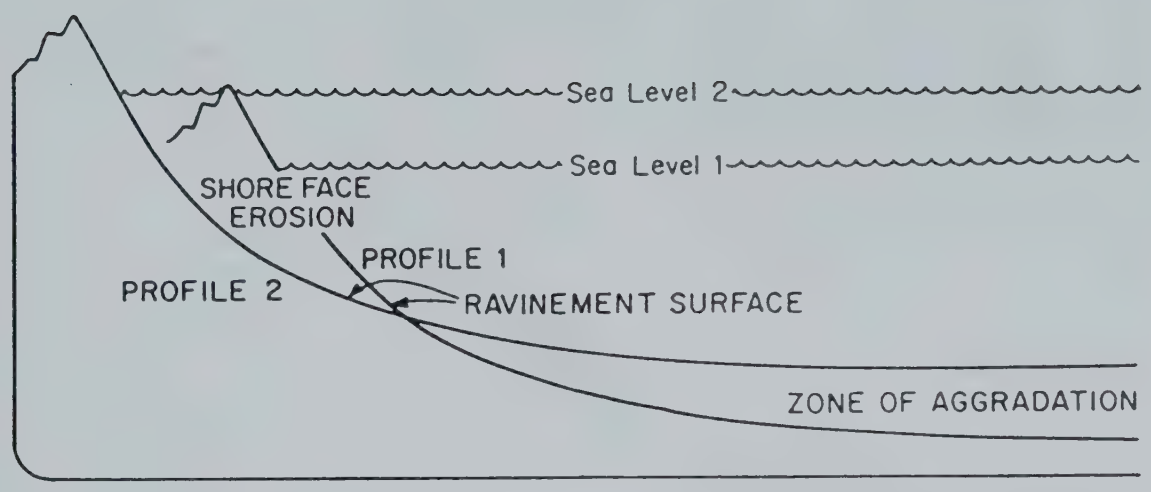

Figure 48. Bruun's model of shoreface erosion during rising sea level, resulting in the formation of a ravinement surface. If the coastal profile is in equilibrium with nearshore energy, sea level rise causes a landward and upward translation of the profile, resulting in shoreface erosion and potential aggradation offshore (after Suter et al., 1987).

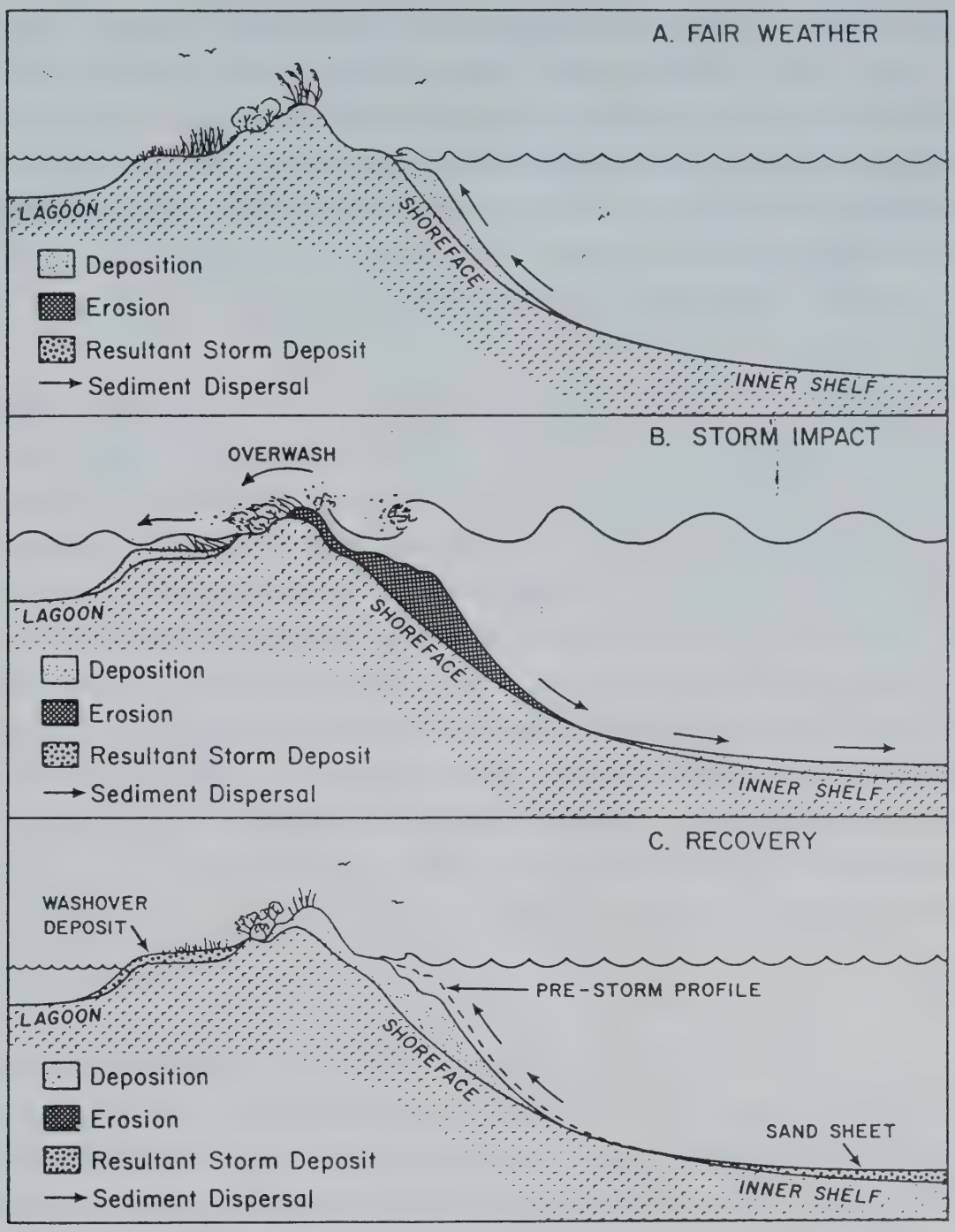

Figure 49. Variations in shoreface erosion during storm and fairweather conditions. (A) Under fairweather conditions sediment accumulates on the upper shoreface. (B) Under storm conditions, sediment is eroded from the foreshore and shoreface and deposited landward by overwash and seaward by bottom currents. (C) Under renewed fairweather conditions, the foreshore and upper shoreface recover but not to their original pre-storm profile. The result is a net landward migration of the shoreface and the accumulation of washover and inner-shelf sheet sands (after Penland et al., 1985).

Shoreface erosion on the modern Delaware transgressive coastline is operative to -10 m MSL and is eroding lagoonal and Pleistocene deposits beneath the barrier core (Figure 47). With continuing transgression the entire barrier sandbody will be lost. In places where the depth of shoreface erosion is not so deep however, the lower part of the barrier-lagoon sequence below the advancing ravinement surface may eventually be preserved on the inner shelf. This is observed in transgressive barrier islands on abandoned lobes of the Mississippi delta, where rapid compactional subsidence allows much of the barrier lithosome to sink below the depth of shoreface erosion (Penland et al., 1985).

Tidal inlet deposits have been noted as having a higher preservation potential beneath a ravinement surface due to the depth they cut down into the shoreface sequence (Kumar and Sanders, 1970; Hine and Snyder, 1985; Penland et al., 1985; Kraft et al., 1987). Such preserved inlet deposits will occur as isolated lenses of coarse grained sediment bounded both above and below by erosional surfaces. Kraft et al. (1987) also note that part of the ebb-tidal delta sandbody seaward of Indian River Inlet on the transgressive Delaware coast lies below the depth of shoreface erosion and will therefore be preserved as a lens of sand on the inner shelf beneath the ravinement surface. Both Kraft et al. (1987) and Hine and Snyder (1985) commented on the potential difficulty in interpreting such erosional remnants, particularly in ancient sequences. An isolated unit of bioclastic sandstone was noted beneath the Halfway ravinement surface in well 10-35-72-9-W6 (Appendix A) and may represent such preferential preservation of lower tidal inlet or ebb-tidal delta deposits.

7.4.0 Relationship Between Ravinement and Facies M Distribution.

During transgressive shoreface erosion, sediment eroded from the upper part of the shoreface profile is carried offshore to form a shelf sand veneer as described above, and also washed over the barrier crest into the lagoon. Studies of modern transgressive barrier islands have shown that many are dominated by washover deposits 3 to 10 m thick and a few hundred metres wide (Kraft and John, 1979; Leatherman, 1979; Heron et al., 1984; Kraft et al., 1987).

As can be seen from the cross-section in Figure 46, Facies M washover sands thin to the northeast and are not present in backbarrier deposits throughout most the study area. Figure 50 is an isopach map of Facies M washover sandstones. The facies is seen to occur as a series of elongate NW-SE trending sandbodies some 2 km wide and extending over 30 km along strike. The sandstone thins to the northeast and is not present throughout

most of the area crossed by the prograding Halfway shoreface. Washover fans are typically most common on microtidal, wave-dominated coastlines (Hayes, 1979; Davis and Hayes, 1984). Overwash in such settings is an episodic but ongoing process and would therefore be expected to leave some record throughout the area crossed by a prograding shoreline. The absence of Facies M washover sandstones in backbarrier deposits throughout most of the study area therefore suggests that overwash was not a significant ongoing process during the progradation of the Halfway shoreline and that their distribution is related to some short-lived period of washover sedimentation. It is apparent in Figure 50 that the southwestern margin of Facies M sandstones coincides with the northeastern limit of the ravinement surface discussed above. This indicates that Facies M washover sandstones may have been formed during the episode of shoreface erosion which produced the ravinement surface in a manner similar to that documented in many modern transgressive barrier islands.

In many cored examples of Facies M sandstone (eg. well 10-32-72-8-W6; Appendix A), the lagoonal mudstones capping the regressive Halfway shoreface facies association grade upward into Facies M through 1-2 m of silty sandstone identical to the more distal (northeasterly) parts of the Facies M sandbody. This suggests that the locus of Facies M deposition migrated to the northeast (palaeolandward) through time, so that coarser proximal washover sands overlie earlier distal silty sandstones, generating an upward-coarsening sequence. Kraft and John (1979) describe an identical sequence from washover deposits associated with the Holocene transgressive barrier islands of the Delaware coast. Demarest and Kraft (1987) consider such a sequence to be conclusive evidence of deposition during landward migration of the shoreline. They present a cored example of a Pleistocene transgressive barrier island shoreface deposit from Bethany Beach, Delaware (Figure 51). The upper sandy portion of this vertical sequence in core CNAA-03 was produced by overwash processes in a position proximal to the shoreline, similar to that envisaged for Facies M. Continued shoreface erosion has resulted in earlier-formed washover sands themselves being reworked, with the end result that their seaward (eastern) margin is truncated by the ravinement. This is identical to the southwestern (palaeoseaward) margin of Facies M in Figure 46.

It is therefore considered that Facies M washover sandstones were formed during shoreface erosion of the Halfway coastline in a manner similar to that documented from the Pleistocene of Delaware and many modern transgressive barrier island shorelines. Continued erosion and landward migration of the Halfway shoreface resulted in coarser-

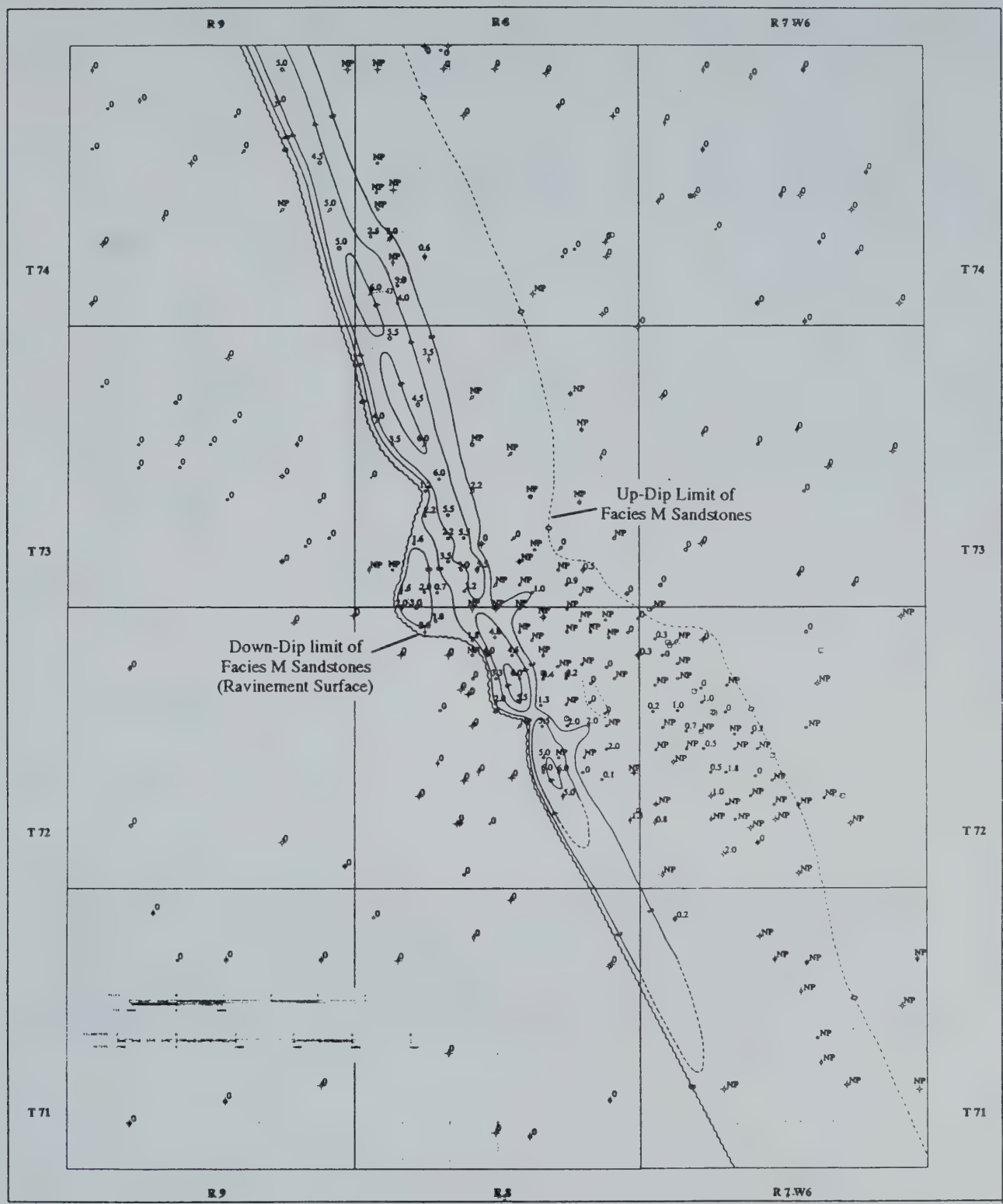

Figure 50. Isopach map of Facies M washover sandstones in the Wembley oilfield. Note the strike-linear nature of the sandbody and the ravinement surface immediately to the southwest (palaeoseaward). The northeastern edge of washover sand deposition is difficult to determine without core control as the thin silty sandstones are not easily identified on well logs.

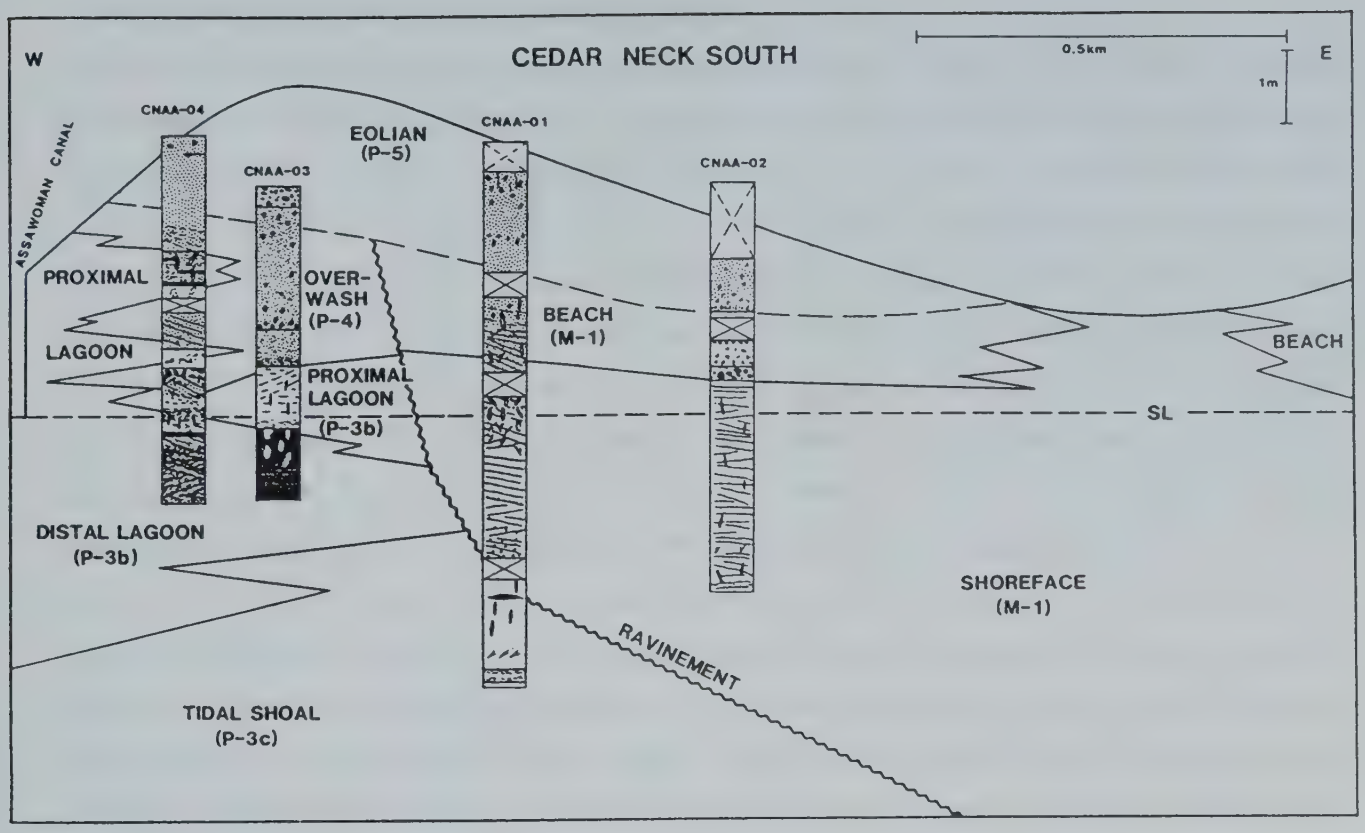

Figure 51. Cross-section through Pleistocene transgressive shoreline deposits near Bethany Beach, Delaware. The western end of the section is dominated by transgressive washover sands resting on lagoonal deposits and represents the most landward position of the shoreline prior to abandonment. Shoreface sands (labelled M-1) in cores CNAA-01 and CNAA-02 are deposits of renewed progradation of the shoreface during the initial stages of falling sea level after peak interglacial level between 5000 and 9000 years BP. The two units are

grained proximal washover sandstones being deposited on earlier distal silty washover sandstones, generating an upward-coarsening sequence.

7.5.0 Preservation of Transgressive Deposits.

Studies of the eastern United States continental shelf have shown that Holocene lagoonal deposits are widespread across much of the area, implying that barrier islands must have existed across much of the shelf (eg. Niedoroda et al., 1985). As these barrier island complexes migrated landward across the shelf during the Holocene transgression, shoreface erosion resulted in the loss of earlier-formed washover deposits, leaving behind backbarrier deposits capped by a ravinement surface and a thin surficial sandsheet (Kraft et al., 1987). Continuing transgression put marine deposits directly on top of the lagoonal sediments (Figure 52). Similar removal of coastal sandbodies during prolonged transgression has been described both from a variety of Holocene marginal marine settings and also the Cretaceous of the western interior of the United States by Nummedal and Swift (1987). These studies would therefore seem to suggest that preservation of washover deposits similar to Halfway Facies M would not be expected during a period of extensive transgression and landward retreat of the shoreface. However, the Holocene transgression is continuing in many parts of the eastern United States and the barrier islands which form the modern coastline mark the present landward limit of shoreface erosion. In several places, relative sea level rise has decreased to the point that sedimentation rate has overcome it and the transgression has therefore ceased. Subsequent progradation of these stretches of coastline would leave the ravinement surface marking the change from transgression to regression. Immediately landward of this ravinement limit an "abandoned" transgressive washover sandbody would be preserved.

Demarest et al. (1981) studied the Pleistocene deposits of the Delaware coast and identified at least four juxtaposed, transgressive barrier island sandbodies of different ages. The successive sandbodies become younger in the seaward direction, such that although each represents a transgressive deposit produced during a rise in relative sea level, the overall sequence is progradational. Dating of backbarrier peats in these paralic units allowed Demarest et al. (1981) to demonstrate that each transgressive sandbody originated during periods of rising sea level prior to a maximum interglacial high sea stand. Preservation of the sandbodies was due to regression of the shoreline forced by glacio-eustatic sea-level fall. Each preserved coastal unit formed in about 10, 000 years during the last stages of a glacio-eustatic transgression that traversed most of the

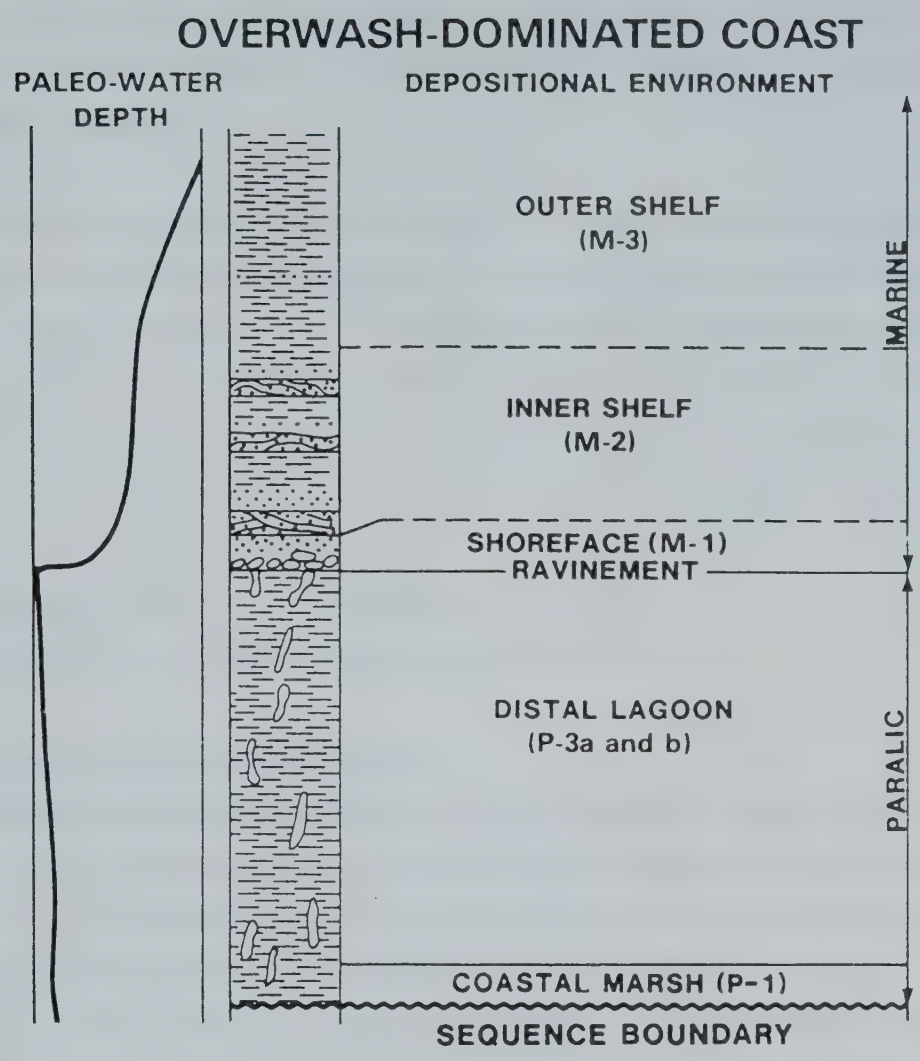

Figure 52. Complete vertical sequence produced by a transgressive washover-dominated barrier island coastline. The ravinement process has eroded the upper part of the paralic section such that marine deposits rest directly on lagoonal clays, suggesting a catastrophic increase in palaeowater depth. A deepening upward from ravinement through shoreface (M-1), inner shelf (M-2) and outer shelf (M-3) is shown, although such a complete marine succession would rarely be developed (after Demarest and Kraft, 1987).

continental shelf. The majority of the intervening regressive deposits as well as most of the transgressive deposits were lost to shoreface erosion during the transgressions. Most of the two million year timespan covering deposition of these Pleistocene deposits is therefore represented by hiatuses marked by the ravinement surfaces. Demarest et al. (1981) also noted that similar responses would be generated by variations in sediment supply to the shoreface.

The Bethany Beach section shown in Figure 51 is one of these "abandoned" Pleistocene transgressive shorelines from Delaware. Demarest and Kraft (1987) state that the Bethany Beach shoreline stabilized due to decreasing sea-level rise and then started to prograde seaward, leaving the ravinement surface and linear washover sands to mark the landward limit of shoreface erosion. Such preservation of transgressive deposits at the landward edge of a transgressive erosion surface has also been described by Heward (1981). The linear Facies M washover sandbody lies immediately northeast of a ravinement surface and is similarly interpreted as marking the landward limit of the transgression which interrupted Halfway shoreface progradation in the study area.

7.6.0 Summary of Local Stratigraphy.

The preservation pattern of Halfway Facies M washover sandstones in the study area, which are only found along a linear belt immediately landward of a ravinement surface, is analogous to the preservation of "abandoned" washover sandbodies at the turnaround point from transgression to regression seen in the Pleistocene of Delaware. The implication of this pattern of Facies M distribution is that overall progradation of the Halfway shoreline in the study area was punctuated by at least one period of transgression during which significant washover sandstones were deposited. This is supported by the presence of two upward-coarsening shoreface facies associations within the Halfway Formation throughout the southwestern part of the study area, representing two periods of shoreface progradation separated by a transgression.

Styan and Shaw (1991) describe sandstones similar to Facies M from the Halfway Formation of the Progress area north of Wembley as occurring as "elongate lenses" within backbarrier deposits, but make no interpretation of their origin. In their presentation these were shown as a series of regionally strike-parallel sandstone ribbons. It is felt that these probably represent washover deposits associated with a series of Halfway transgressive episodes punctuating an overall prograding sequence, similar to the example present within the Wembley field. If so, recognition of these washover

sandstones within backbarrier deposits above the Halfway Formation has important implications for mapping the regional distribution of transgressive-regressive depositional cycles in the Halfway Formation, which has previously been considered a single regressive episode.

8.0.0 SEQUENCE STRATIGRAPHY.

Having recognized that the Halfway Formation within the study area was deposited during more than one progradational episode (Chapter 7), several longer cross-sections were constructed to examine the distribution and relationships of these transgressive-regressive cycles. To make these longer cross-sections manageable, well logs rather than core descriptions were used as the display format, but core data was integrated into the interpretation. Figure 53 (in pocket) is an example of one of these longer dip sections.

As the vertical scale of the well logs is much smaller than the core descriptions used for facies correlations, the base of the Halfway shale could be used as a datum without introducing the severe compactional distortion discussed in Chapter 7. As will be discussed below, this datum does not represent a single surface throughout the length of the section, necessitating datum changes. The cross-section extends down into the Montney Formation, giving complete coverage of the Middle Triassic strata.

8.1.0 Discussion.

The intra-Halfway ravinement surface discussed in Chapter 7 can be identified to the southwest of the Wembley field in Figure 53 in wells 14-8-72-8-W6, 7-16-72-8-W6 and 6-15-72-8-W6. It separates the two Halfway progradational facies successions, here labelled PS 4 and PS 5. The ravinement surface is overlain by a thin unit of Facies A bioclastic sandstone deposited on the shelf during the transgression. If the ravinement surface is traced to the southwest, the thin unit of Facies A sandstone pinches out and the ravinement grades into a radioactive shale condensed section similar to that present at the base of the Halfway Formation. The conformable nature of this contact can be seen in cored sequences to the southwest of Wembley (eg. well 8-1-72-9-W6), where there is minimal erosion associated with the ravinement surface and the Halfway shoreface deposits are abruptly overlain by black shale. This condensed section probably formed on the shelf seaward of the retreating Halfway coastline as a result of decreased sediment influx. The ravinement surface is overlain by a second upward-coarsening facies succession representing renewed progradation of the Halfway shoreline.

Immediately to the northeast of the ravinement surface, in well 16-15-72-8-W6, a thick unit of Facies M washover sandstone is present. This washover sandstone thins to the northeast through wells 6-23-72-8-W6 and 8-23-72-8-W6 and then pinches out entirely. These washover sandstones are interpreted as being associated with the shoreface retreat which generated the ravinement surface, and thus form its time-equivalent landward

expression. Integration of core and well log data thus shows that the intra-Halfway ravinement surface grades seaward into a conformable condensed horizon and landward into a washover fan.

In the sequence stratigraphic terminology of Van Wagoner et al. (1988) and Van Wagoner et al. (1990), the intra-Halfway ravinement surface and its correlative offshore condensed sections and onshore washover fan would be called a marine flooding surface. Van Wagoner et al. (1990) define a marine flooding surface as "a surface separating younger from older strata across which there is evidence of an abrupt increase in water depth. This deepening commonly is accompanied by minor submarine erosion or nondeposition (but no subaerial exposure or basinward shift in facies), with a minor hiatus indicated. The marine flooding surface has a correlative surface in the coastal plain and a correlative surface on the shelf."

The package of progradational, upward-shoaling strata deposited after one transgressive (flooding) event and capped by a second is termed a parasequence by Van Wagoner et al. (1990). Similar flooding surface-bounded progradational packages have been described as "facies sequences" by Frazier (1974) and "depositional episodes" by Galloway (1989). Van Wagoner et al. (1990) define a parasequence is "a relatively conformable succession of genetically related beds or bedsets bounded by marine flooding surfaces or their correlative surfaces." In this context, the Halfway Formation of the Wembley field (labelled PS 4 in Figure 53), which consists of a progradational cycle bounded below by a marine flooding surface over the Doig Formation and above by the intra-Halfway marine flooding surface (ravinement surface) could be described as a parasequence.

8.2.0 Parasequence Stacking in the Study Area.

Even a cursory glance at the lower part of the Halfway-Doig interval in Figure 53 reveals the presence of several more radioactive shale beds. Closer inspection shows that each of these beds can be traced throughout the study area. By analogy with the log responses over cored intervals at the base of the Halfway Formation and the intra-Halfway flooding surface, these regionally persistent radioactive shale beds are interpreted to be phosphate-rich condensed sections associated with transgressive events (ie. marine flooding surfaces).

Five of these radioactive marker beds can be recognized and correlated in the Halfway and Doig Formations in the study area (Figure 53). Each pair of these radioactive beds

bound a package of strata that shows an upwardly-decreasing gamma ray response, commonly associated with progradational facies successions (Chapter 6). Each of these progradational packages of strata bounded above and below by marine flooding surfaces (or their correlative condensed sections) is interpreted as a parasequence. The five parasequences recognized within the Middle Triassic section are labelled (from the base upward) Parasequence 1 to 5 (PS 1 to PS 5) in Figure 53. The Halfway Formation in the Wembley oilfield is represented by Parasequence 4, and the Halfway of the Hythe field immediatelty to the southwest lies in Parasequence 5.

Each Middle Triassic parasequence tapers to the southwest and the bounding phosphatic condensed sections begin to merge into the "Phosphate Zone" of the lower Doig Formation. In his regional study of the Doig Formation, Wittenberg (1992) found that these phosphatic beds downlap to the southwest (basinward) into a thick radioactive shale interval above the Montney Formation. Four more-closely-spaced phosphatic beds are present in the "Phosphate Zone" below Parasequence 1 in Figure 53; these probably represent thin distal (basinward) parts of parasequences more fully developed to the northeast of the study area.

In any given location, each parasequence is thicker and is capped by coarser-grained sediment than the one below, suggesting deposition progressively nearer to the sediment source. Such deposition of successively younger and conformable parasequences further basinward is termed a progradational parasequence set by Van Wagoner et al. (1990) and implies a rate of deposition greater than the rate of accommodation. The result is an overall progradation of the shoreline through time punctuated by transgressive (flooding) events.

8.4.0 Comparison of Middle Triassic Sequence and Lithostratigraphy.

Close inspection of Figure 53 shows that the coarser-grained shoreface deposits capping the uppermost parasequence in any given well form what is lithostratigraphically termed the Halfway Formation, in line with the original definition of Hunt and Ratcliffe (1959). However, these shoreface deposits belong to progressively younger parasequences southwestward, separated by flooding surfaces, and do not form a continuous regressive sandsheet. For example, the Halfway Formation in well 7-27-72-7-W6 to the northeast of the Wembley field is part of parasequence 3, whereas that in well 8-29-72-7-W6 belongs to the younger parasequence 4.

Just as the lithostratigraphic Halfway Formation is seen to belong to successively younger parasequences southwestward, so is the Doig Formation. The upper part of the lithostratigraphic Doig Formation in the Wembley field in Figure 53 (eg. that in well 14-20-72-7-W6) is bounded by the same pair of marine flooding surfaces as the Halfway Formation in well 7-27-72-7-W6 to the northeast and must therefore have been deposited during the same period of time (parasequence 3). Each fine grained parasequence present in the Doig Formation can be traced up-dip (northeastward) into coarser-grained shoreface facies (Halfway Formation) bounded by the same pair of radioactive flooding surfaces. The lithostratigraphic Doig and Halfway Formations are therefore seen to be part of the same prograding depositional system. The "Doig" shales represent deposition in the offshore shelf environment and the "Halfway" sandstones the more proximal part of the same shoreface system.

Wittenberg (1992) used these radioactive shale beds to demonstrate that the thick sandbodies found within the Doig Formation were deposited coevally with the adjacent shales as slump features. Both shales and sandbody are bounded by the same pair of marine flooding surfaces and must therefore have formed during the same depositional episode. This can be seen in the case of the thick Doig sandbody and adjacent shales present in parasequence 3 at the western end of the cross-section in Figure 53. The Doig sandbody does not cut through the phosphatic marker beds, discrediting the suggestion of Campbell et al. (1989) that they represent infilling of valleys incised during a sea-level lowstand.

A comparison of the sequence stratigraphic subdivision of the Middle Triassic recognized in this study with the conventional lithostratigraphy is shown in Figure 54. In the well illustrated in Figure 54 the lithostratigraphic Halfway Formation belongs to parasequence 4. In wells to the southwest similar "Halfway" sandstones would be part of the younger parasequence 5, and to the north part of the older parasequence 3. The Doig Formation in Figure 53 contains the fine grained distal portions of parasequence 3 and several other older parasequences. These parasequences are bounded by radioactive condensed horizons deposited during marine flooding events. Interfingering facies relationships discussed in section 5.1.0 indicate that at least the lower part of the Charlie Lake Formation represents arid backbarrier and coastal plain sediments deposited coevally with the Halfway-Doig shoreface deposits. As discussed below, it is difficult to identify correlative marine flooding surfaces within the Charlie Lake coastal plain deposits, so the

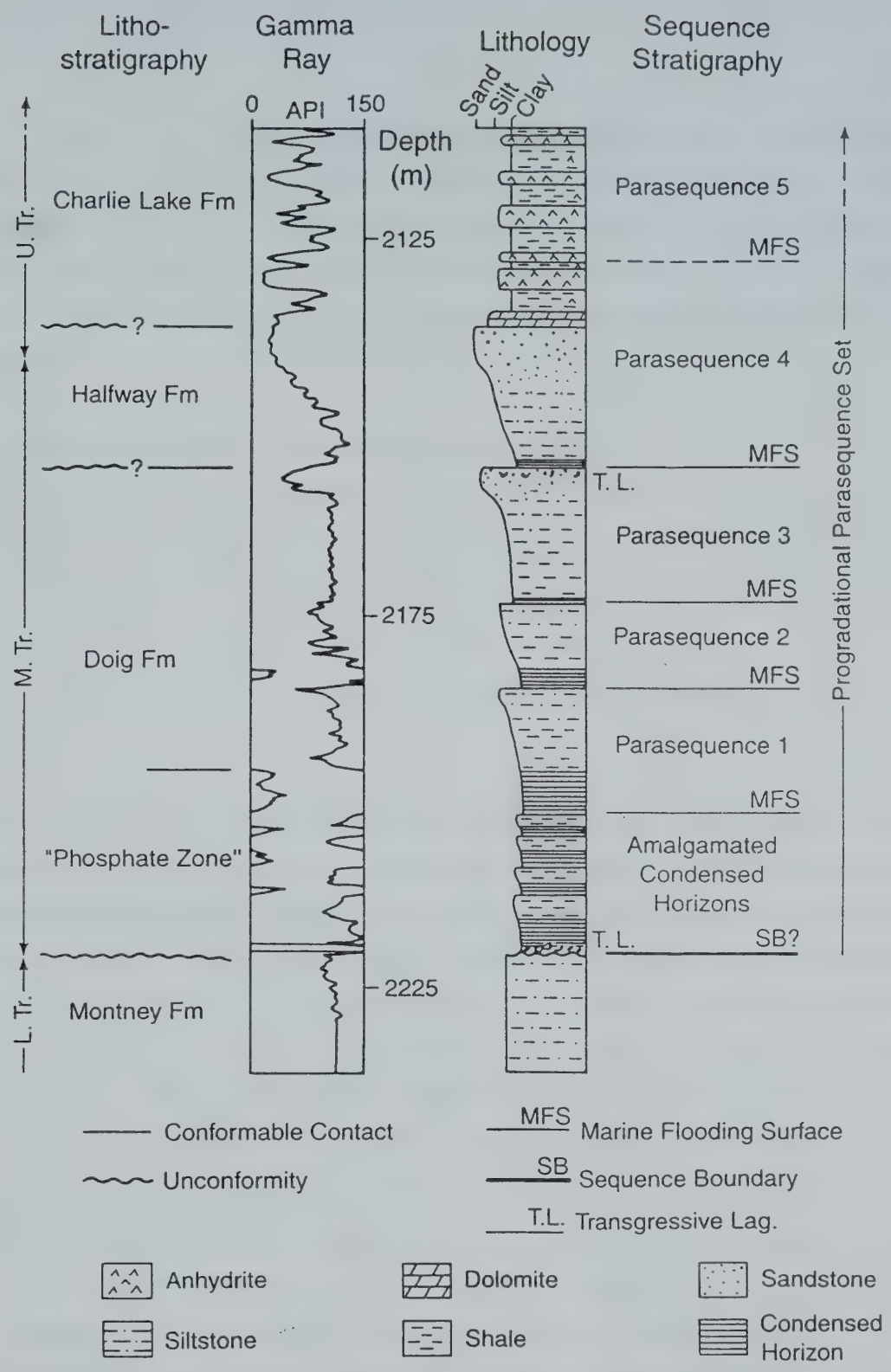

Figure 54. Gamma ray log and inferred lithology of the Middle Triassic section in well 16-23-72-8-W6 comparing lithostratigraphic formations with the informal sequence stratigraphic framework developed in this study. Note that the parasequences cut across formation contacts.

upper boundary of parasequence 4 in Figure 54 is shown as within the lower Charlie Lake Formation but uncertain.

Parasequences, which reflect depositional facies relationships, are observed to cut across Middle Triassic lithostratigraphic boundaries in Figures 53 and 54, indicating the diachronous nature of the Doig, Halfway and Charlie Lake Formations. For example, the Halfway-Doig interval at the northeastern end of Figure 53 (well 14-36-72-7-W6) consists of parasequences 1 to 3, but at the southwestern end (well 8-1-72-9-W6) parasequences 1 to 5.

8.4.0 Middle Triassic Sequence Stratigraphic Model.

A schematic sequence stratigraphic model for the Middle Triassic strata of west-central Alberta is shown in Figure 55. As far as can be determined from the present study and the work of Wittenberg (1992), the entire lower Charlie Lake-Halfway-Doig interval forms a progradational parasequence set. These parasequences downlap onto the unconformity surface at the top of the Montney Formation, which presumably forms a sequence boundary.

Identification of correlative flooding surfaces within the coastal plain deposits of the lower Charlie Lake Formation is hampered by the chaotic nature of much of the sabkha sediment and the limited amount of core available. In Figure 46 the marine flooding surface would be placed at the base of Facies M washover sandstones, which are interpreted as the time-equivalent product of transgressive shoreface erosion. In some cases is it possible to trace the thin distal parts of these washover sandstones some distance to the northeast, where they "climb" lithostratigraphically into the supratidal red beds of Facies H. This may allow the marine flooding surfaces identified within the Halfway-Doig interval to be extrapolated some distance into the coastal plain section. The Charlie Lake Formation also contains numerous anhydrite beds, some of which appear from well log cross-sections to be sub-regionally correlatable. It may be that some of these apparently extensive anhydrite beds formed as a result of flooding of the low relief coastal sabkha during times of transgression. If this is the case, then they might be of use in extending parasequence boundaries much further into the Charlie Lake Formation than has been attempted in this study.

The distribution of Middle Triassic parasequences in the study area has been determined by detailed well-to-well correlation of the radioactive marine flooding surfaces which

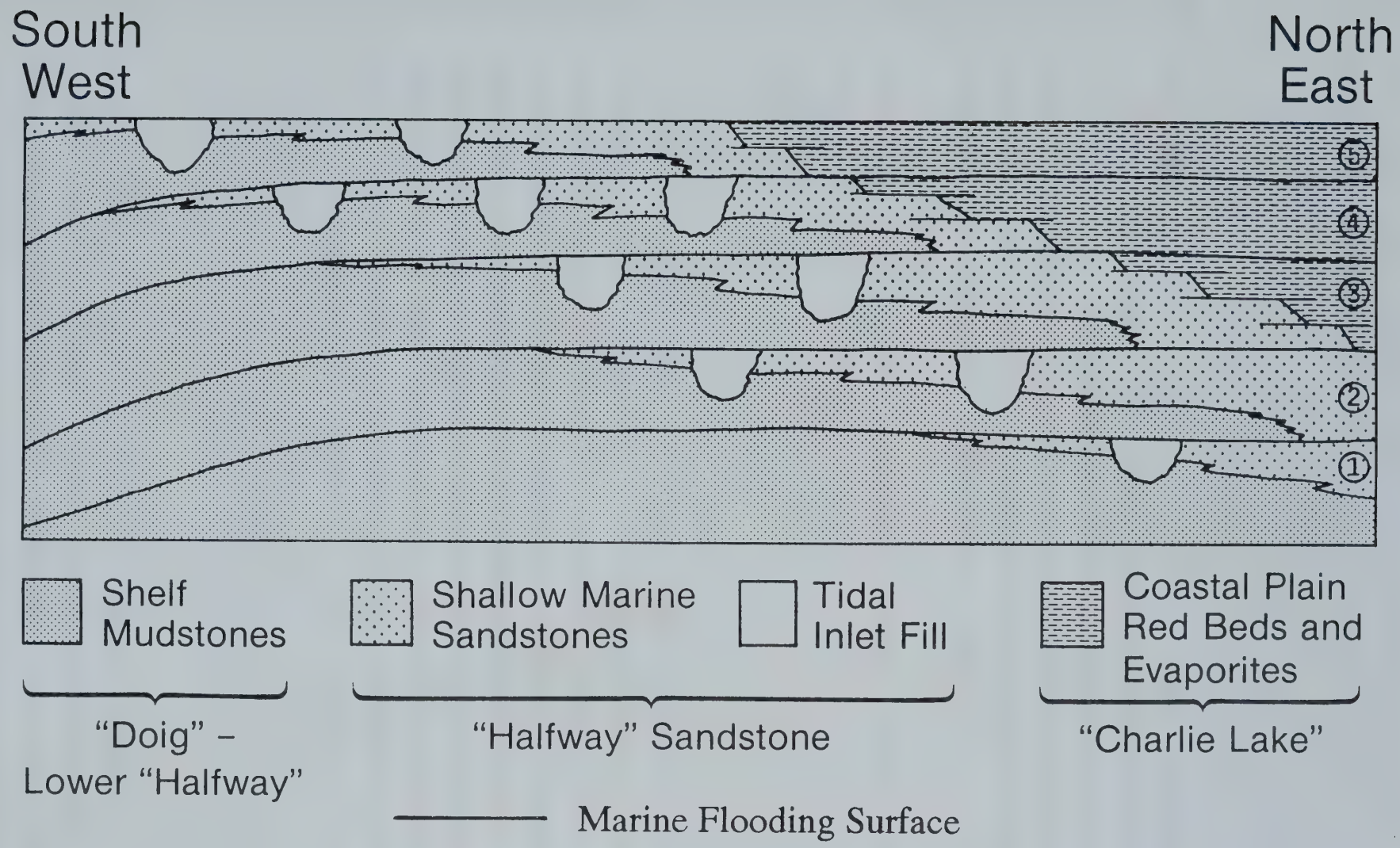

Figure 55. Schematic sequence stratigraphic model of the Middle Triassic section in west-central Alberta. The Doig-Halfway-Charlie Lake formations form a progradational parasequence set in which individual parasequences become progressively younger southwestward.

bound them. This sequence stratigraphic framework depicts the stacking pattern of successive depositional episodes and is thus a more realistic guide to facies relationships than correlations based on lithostratigraphic units, which are demonstrated to be diachronous even at the relatively small scale of the study area. However, the parasequences have not been dated relative to any absolute time scale and their correlation into adjacent areas of the Western Canda Sedimentary Basin therefore requires the same careful well-to-well correlation as has been undertaken in this study. This is obviously a time-consuming process for correlations over any great distance and somewhat speculative where wells are not closely-spaced. Dating of these parasequences by biostratigraphic, isotopic or radiometric methods would allow their rapid correlation with Middle Triassic sections in other parts of the basin.

Biostratigraphic dating of the condensed sections associated with marine flooding surfaces has been recognized by Loutit et al. (1988) as the key to tying a sequence stratigraphic framework to an absolute age which can be used for correlation purposes. The long period of time represented by a condensed section generally allows the accumulation of numerous palaeontological material and thus makes the bed a valuable sampling point for biostratigraphic analysis. Biostratigraphic sampling of the phosphatic condensed horizons in the Middle Triassic would therefore seem to be an ideal method of correlating them over large areas. The sequence of marine Triassic faunas in western Canada is detailed by Warren (1945) and Tozer (1961, 67). This sequence is, however, based largely on ammonoids, which are difficult to identify in the rock cuttings recovered from most subsurface boreholes and therefore of limited use in biostratigraphically dating subsurface Triassic strata. Microfossils are more easily recovered from rock cuttings, but apparently not common in the Middle Triassic of western Canada (Tony Jenkins, Associated Biostratigraphic Consultants, personal communication 1991), probably for reasons associated with coastal upwelling outlined in section 4.2.0. The solution might be to more intensively sample those Middle Triassic condensed sections thay have been cored for both macro and microfaunal content rather than rely on well cuttings.

It is also doubtful whether biostratigraphic dating of any kind in the Middle Triassic could be sufficiently accurate to resolve individual parasequences, which are commonly cited as representing durations of approximately 50,000 years (Van Wagoner et al., 1990). Such biostratigraphic studies may, however, highlight the diachronous nature of the lithostratigraphic formations at the regional scale, so reinforcing the interpretations made from a sequence stratigraphic viewpoint.

9.0.0 HALFWAY PARASEQUENCE GEOMETRY.

The marine flooding surfaces (or their correlative condensed section or washover fan) which bound the Middle Triassic parasequences were identified on gamma ray logs from each well in the study area and their depths assembled into a database. This database is presented in Appendix B. The five markers were coded A through E from the bottom up, such that parasequence 1 is bounded by markers A and B. Parasequence 5, the youngest, is not capped by a marine flooding surface within the study area.

9.1.0 Structure of Bounding Flooding Surfaces.

The stratigraphic database in Appendix B was used to generate structure maps of each of the five marine flooding surfaces. This was done to confirm that there is no structural control on hydrocarbon trapping in the Middle Triassic of west-central Alberta. Due to the difficulties in identifying marine flooding surfaces within the Charlie Lake Formation described in section 8.4.0, the structure maps terminate at the northeastern limit of the ravinement surface associated with the base of each parasequence. Figure 56 shows the structure on the base of parasequence 4 which contains the Wembley hydrocarbon pool. This and the other structure maps constructed show a uniformly southwesterly-dipping surface with no possible structural control on hydrocarbon trapping. The Wembley pool is therefore confirmed to be stratigraphically controlled. Apparent in Figure 56 is the compactional drape of the base of parasequence 4 over the thick north-south oriented Doig sandbody in township 72-8-W6. Figure 57 illustrates a similar structure map drawn on the base of parasequence 5. This has been included solely because in this case, it has been possible to extend marine flooding surface E (the base of parasequence 5) into the coastal plain deposits of the Charlie Lake Formation by virtue of the extensively cored washover sandstones northeastward of the ravinement surface limit.

9.2.0 Parasequence Isopachs.

The stratigraphic database in Appendix B was also used to construct isopach maps of each parasequence in the study area. However, the difficulty in recognizing flooding surfaces within the Charlie Lake Formation necessitated some modification in order to construct isopach maps northeast of the ravinement limit. The Halfway-Charlie Lake contact was used as the upper boundary of each parasequence for the purposes of the isopach maps. This horizon is listed in a separate column labelled "Top PS" in Appendix B. While this results in 2 to 3 m of the associated coastal plain deposits being omitted from the true parasequence thickness, it was the only way that a representative map could be constructed. Figure 58 is an isopach map of parasequence 4 constructed in this

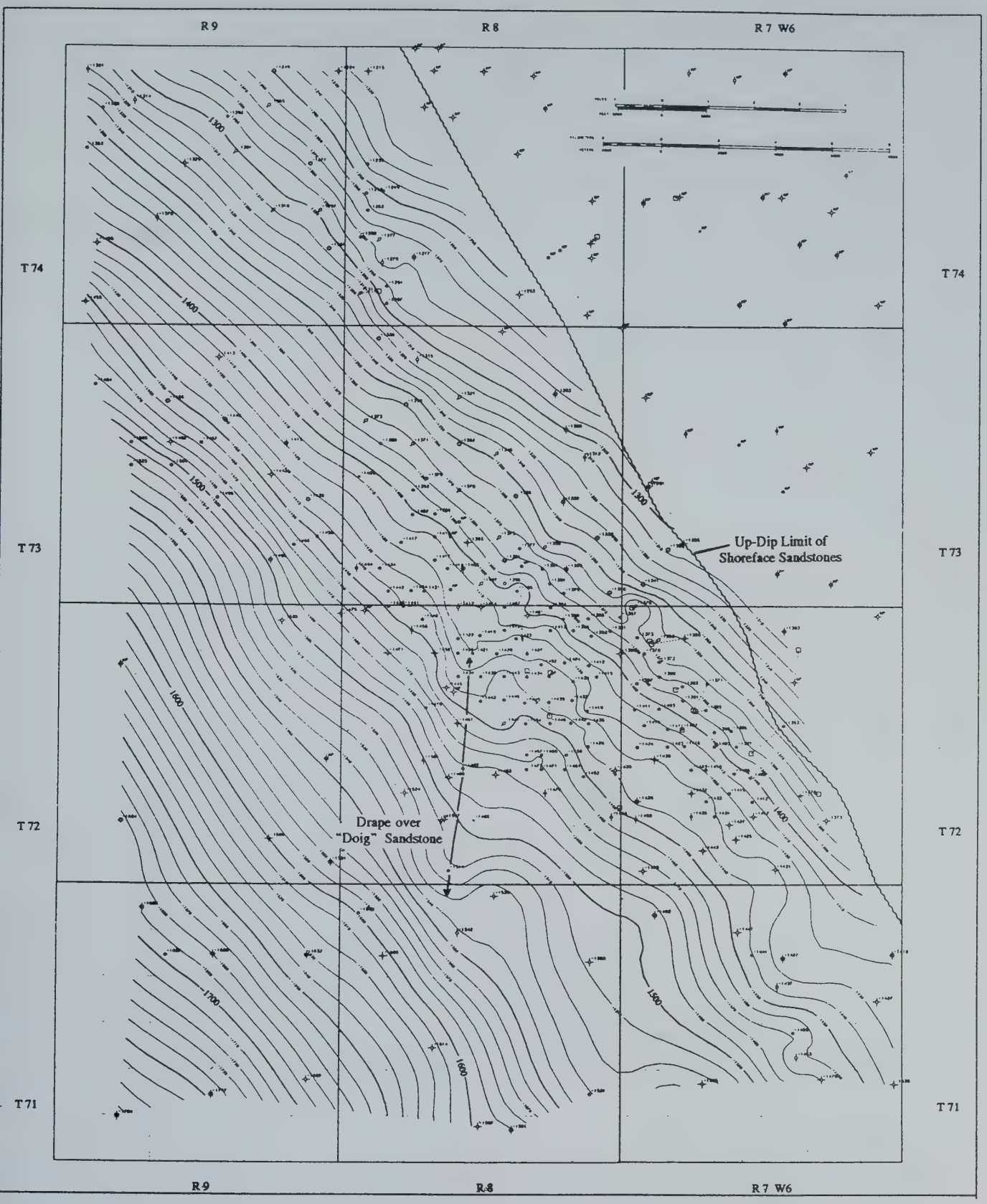

Figure 56. Structure map drawn on the base of parasequence 4 (the Wembley Halfway Formation). The northeastern depositional edge of the parasequence is marked by a ravinement surface (undulating line). Note the compactional drape over the Doig (parasequence 3) sandbody in Township 72-8-W6.

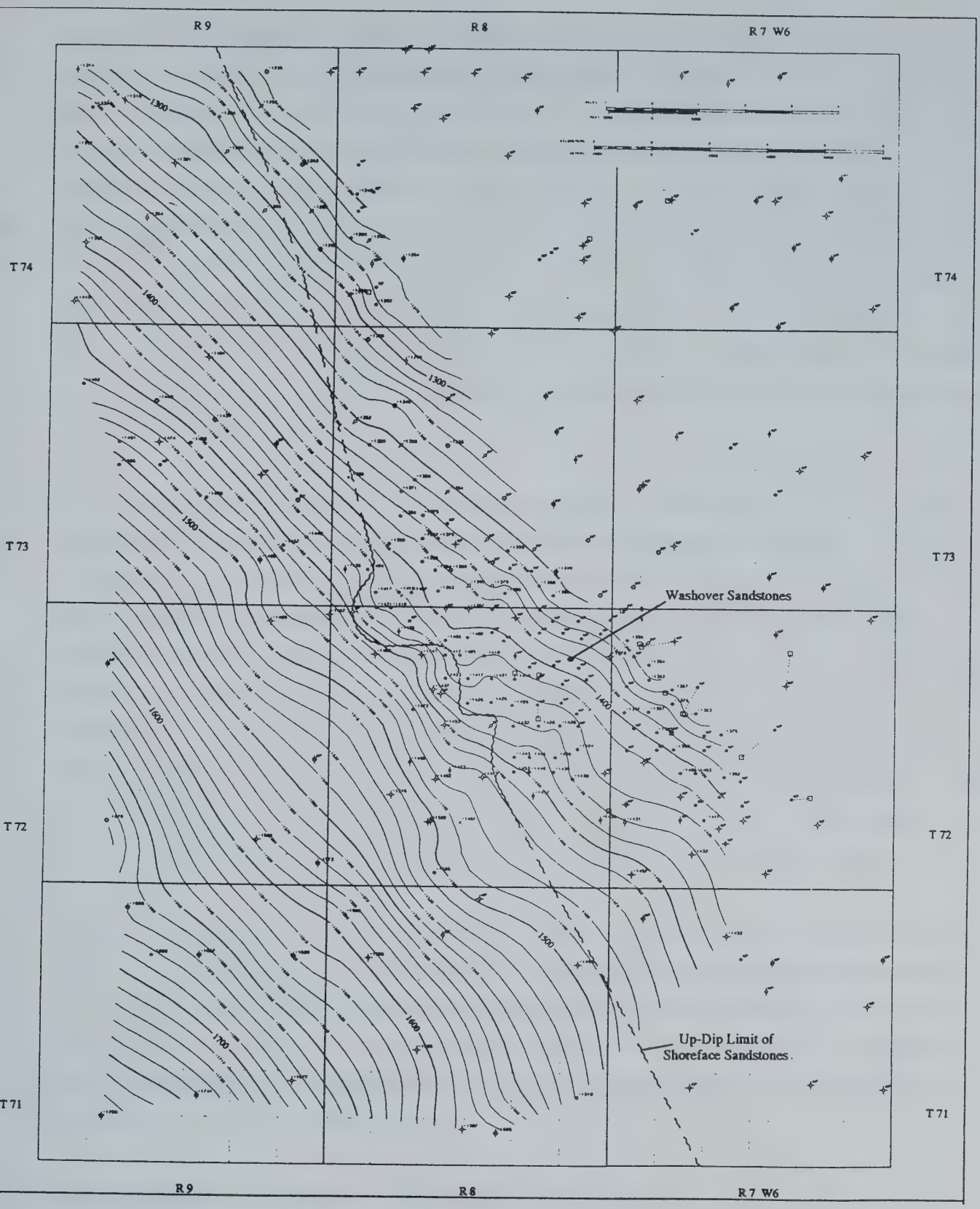

Figure 57. Structure map drawn on the base of parasequence 5. Contours to the southwest of the ravinement limit are drawn on the marine flooding surface itself, while those to the northeast are drawn on the base of Facies M transgressive washover sandstones, interpreted as the correlative flooding surface in the coastal plain deposits of the Charlie Lake Formation. The irregular trace of the ravinement surface in the centre of the study area is a result of the more closely-spaced data points in that area.

manner. The northeastern edge of parasequence 4 is the detectable limit of its basal ravinement surface over the underlying parasequence 3. Values are posted beyond this edge in wells 7-27-72-7-W6, 6-8-73-7-W6 and 10-18-73-7-W6. These represent washover sandstones associated with the shoreface erosion process, similar to those correlated to parasequence 5 shown in Figure 50. The washover sandstones in these three wells are thin, but two of the wells (7-27-72-7-W6 and 10-18-72-7-W6) were initially shut in as potential gas wells. Most of the area potentially covered with thicker washover sandstones associated with parasequence 4 lies beneath Bear Lake in Township 72-7-W6 and has not been extensively drilled. If of similar extent to the washover sands to the west associated with parasequence 5, these may represent a significant future hydrocarbon exploration target.

The contoured area southwest of the ravinement edge of parasequence 4 in Figure 58 represents the thickness of sediment deposited by the Halfway parasequence 4 shoreface as it prograded to the southwest. The parasequence thickens uniformly from its zero edge in the northeast to approximately 20 m at the southwestern limit of shoreface sandstones. The southwestern margin of the parasequence thins rapidly to around 10 m beneath the ravinement surface at the base of parasequence 5. Beyond this ravinement edge parasequence 4 is developed only as shale and has not been contoured. The anomolously thicker elliptical areas within this overall southwesterly-thickening sediment wedge represent tidal inlet channel fills. Each of these isopach thicks does not represent the depositional geometry of a single tidal inlet fill, but is the result of stacked inlet cycles.

The parasequence 4 shoreface presumably prograded some distance further to the southwest of its present extent in Figure 58, but evidence of this was largely removed by the shoreface erosion which terminated the parasequence 4 depositional episode. Possible ebb-tidal delta or tidal inlet sandstones associated with parasequence 4 are preserved some 4 km southwest of its present extent beneath the parasequence 5 ravinement surface in well 10-35-72-9-W6 (Appendix A).

9.3.0 Parasequence Controls on Hydrocarbon Distribution.

The contoured area of parasequence 4 in Figure 58, which is the area containing parasequence 4 shoreface and tidal inlet sandstones, is essentially the area occupied by the Wembley Halfway hydrocarbon pool. Figure 53 shows that shoreface sandstones belonging to parasequence 3 are present northeast (up-dip) of the Wembley pool but contain no hydrocarbons (wells 7-27-72-7-W6 and 14-36-72-7-W6 in Figure 53 are dry

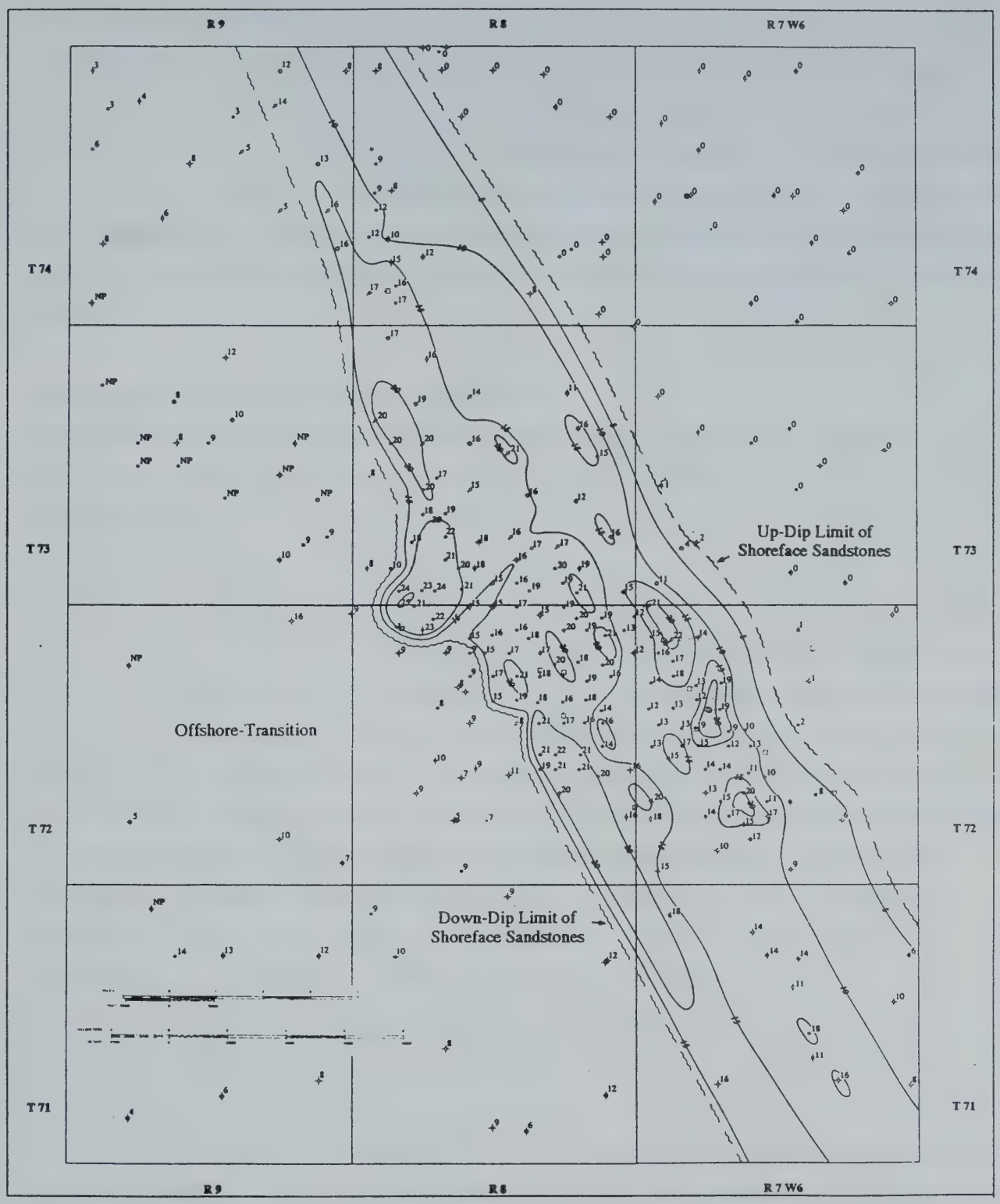

Figure 58. Isopach map of parasequence 4 (approximates to Wembley Halfway Formation). Contouring only extends to the down-dip (southwestern) limit of shoreface sandstones; isopach values beyond this are posted but not contoured and represent offshore-transition deposits. Elliptical isopach thicks represent amalgamated tidal inlet channel fills and their orientation does not reflect the depositional geometry of single inlet channels.

holes). This suggests that the ravinement surface which separates sandstones belonging to parasequences 3 and 4 is acting as a permeability barrier, preventing up-dip migration of oil out of parasequence 4 and therefore controlling the location of the Wembley oilfield. Similar up-dip pinchout of individual parasequences is probably the controlling factor in the location of other Halfway hydrocarbon pools in west-central Alberta. Locating these up-dip parasequence pinchouts would therefore seem to be a major objective in exploring for other stratigraphically trapped hydrocarbons in the Halfway Formation of west-central Alberta.

9.4.0 Parasequence Continuity along Strike.

Figure 59 (in pocket) is a northwest-southeast (strike) oriented cross-section through the study area showing the variations in thickness of individual parasequences along the palaeoshoreline. The "Phosphate Zone" and parasequences 1 and 2 thicken to the northwest, indicating that this area accommodated a greater proportion of sediment during the early part of the Middle Triassic than the southeastern part of the cross-section. Parasequences 3 and 4 on the other hand thicken to the southeast. This suggests that the locus of sediment input shifted southeastward along the shoreline during Middle Triassic time, possibly as a result avulsing delta distributary channels. Note that the thick Doig sandbody in the Valhalla oilfield at the northwestern end of the cross-section (eg. well 6-19-74-8-W6) is within parasequences 2 and 3; the marine flooding surface separating the two parasequences is present within the Valhalla Doig sandbody as a shale bed (Joerg Wittenberg, personal communication 1992). A similar thick Doig sandbody in the Wembley oilfield to the southwest (eg. well 8-33-72-8-W6) is developed only within parasequence 3. Wittenberg (1992) interpreted these thick sandstones to have been deposited in "hollows" created by rotational slump features on the continental shelf. This would suggest that slumping was initiated during parasequence 2 time in the northwest of the study area and continued into parasequence 3 time, but did not commence until parasequence 3 time to the southeast. The coincidence between this delay in the onset of rotational slumping and the apparent shift in sediment influx to the southeast at this time suggests that slumping may have been related to a large input of sediment into the shelf environment.

The Wembley hydrocarbon pool is located in shoreface and tidal inlet sandstones belonging to parasequence 4 and overlying washover sandstones associated with parasequence 5. The two wells at the southeastern end of the cross-section in Figure 59 are the structurally lowest and parasequence 4 sandstones lie below the Wembley pool

oil-water contact. The next well to the northwest, 14-11-72-8-W6, is a suspended oil well. The parasequence 4 sandstone in this well was initially above the oil-water contact, but production of oil from the field has caused the oil-water contact to rise through time to the point at which the well was producing a large volume of water and was suspended. The next ten wells structurally up-dip to the northwest (16-15-72-8-W6 through 9-17-73-8-W6) form the oil column of the Wembley hydrocarbon pool. The remaining wells to the northwest represent the gas cap of the pool.

Some idea of the lateral reservoir heterogeneity of the parasequence 4 barrier island lithosome can be deduced from noting the marked variation in gamma ray responses within the unit and difficulty in making any internal correlation of sandstone units. In contrast, the overlying washover sandstones associated with parasequence 5 have much greater continuity along strike (the one apparent break in the along-strike continuity of the washover sandstones in well 7-9-73-8-W6 is due to the line of section deviating slightly from true strike). This suggests that using waterflooding as a means of enhancing oil recovery from the Wembley Halfway pool would only be predictable in the upper washover sandstones.

Parasequence 4 thins markedly to the northwest in Figure 59 and probably pinches out just beyond the northern edge of the study area. This pinchout controls the lateral extent of the Wembley pool. The marked thinning and eventual pinchout of parasequences along strike displayed in Figure 59 is significant in determining the underlying controls on parasequence development during Middle Triassic time. Whether a shoreline progrades, aggrades vertically or undergoes transgression depends on the interplay between accommodation space for sediment and sediment supply. Accommodation space is in turn controlled by subsidence of the basin (either gradual or more actively tectonic) and eustatic sea level. Where sediment supply overcomes the accommodation space the shoreline will prograde, and where it cannot transgression will occur, generating a marine flooding surface. In the case where such transgression is a result of a eustatic rise in sea level, one would expect an entire stretch of coastline to be affected. The fact that Middle Triassic parasequences in the study area thin markedly along strike indicates that the controlling factor in their development was affecting relatively short (in the order of tens of kilometres) stretches of the coastline. This argues against a purely eustatic origin. In cases where transgression is the result of decreasing sediment supply however, the area affected may be as limited as a single abandoned delta lobe. This model is more compatible with the restricted lateral extent of Middle Triassic parasequences and the

evidence from the "Doig" sandbodies that the locus of sediment influx may have migrated through time. The effect of subsidence on parasequence development is more difficult to asses, but is is unlikely that fault-controlled subsidence would produce the observed lateral shift in accommodation space through time.

It is therefore felt that the shoreface erosion events which punctuate periods of Middle Triassic shoreface progradation were initiated largely by a decrease in sediment supply to a particular stretch of coastline. Other segments of the same coastline which were still receiving an adequate sediment supply would continue to prograde. The overall result is a complex of laterally discontinuous parasequences reflecting changes in the locus of sediment influx through time. This pattern of laterally discontinuous parasequences created by simultaneous progradation and transgression of different parts of the Halfway coastline creates the potential for a series of separate oil and gas pools along any one northwest-southeast oriented shoreline trend.

10.0.0 DISCUSSION.

Identification of upward-coarsening shoreface facies associations and upward-fining tidal inlet facies associations has provided for the interpretation of the Halfway Formation in the study area as the deposit of a prograding barrier island shoreline. This is in agreement with previous sedimentological studies of the Halfway in west-central Alberta by Harrington (1984), Horne et al. (1985), Campbell and Horne (1986), Barclay and Leckie (1986) and Cant (1986). However, detailed interpretation of sedimentary processes and comparison of vertical and lateral tidal inlet facies relationships with Holocene analogues in this study indicates that the Halfway barrier island system in the study area was subject to a mesotidal regime (tidal range 2-4 m). The marked differences in facies associations between micro- and mesotidal inlet fill sequences documented in Holocene barrier islands (Moslow and Tye, 1985; Tye and Moslow, in press) makes this an observation of paramount importance when attempting to predict the reservoir heterogeneity of the Halfway lithosome.

10.1.0 Halfway Tidal Inlet Reservoir Model.

Detailed correlation of facies between closely spaced wells has resulted in the construction of a predictive model of depositional facies distribution within a Halfway mesotidal inlet fill (Figure 38). The basal inlet channel scour is overlain by coarse grained bioclastic sandstone along the length of the northeast-southwest (dip) oriented channel axis, representing deposition in the deepest part of the active inlet channel. Palaeolandward (up-dip) this active inlet fill sediment interfingers with fine grained lagoonal sediment, possibly in association with poorly developed flood-tidal delta sandstones. This interfingering results in an up-dip deterioration of the reservoir quality of the inlet sandstones and creates a potential stratigraphic hydrocarbon trap. Palaeoseaward (down-dip) the inlet sandstones interfinger with silty sandstones in the lower shoreface and clean sandstones of the associated ebb-tidal delta. Bar-bypassing along the Halfway mesotidal coastline resulted in the abandonment of ebb-channels and their subsequent infilling. The nature of this abandoned channel fill is predictable along the dip-parallel length of the channel axis. The seaward (down-dip) mouth of the abandoned inlet channel is filled with clean sandstone washed in from the associated ebb-tidal delta. The plugged inlet mouth created a ponded body of water in the landward part of the inlet channel in which fine grained sediment accumulated. The thickness of this fine grained abandoned channel fill decreases seaward and interfingers with coarser grained sediment washed into the abandoned channel during storms and high tides. The up-dip pinchout of welded ebb-tidal delta sandstones against this fine grained abandoned

present day, not its future development. It is this ultimate evolution however, that is observed in ancient strata such as the Halfway Formation. Progradation of the Halfway barrier island over a longer time period than that recorded in Holocene examples allowed successive tidal inlet channels to rework most of the barrier lithosome as they migrated laterally along the coastline. This is in contrast to the 35-40% of most Holocene barrier lithosomes that has been reworked to date.

Consideration of this temporal component of coastal evolution has previously been overlooked by geologists studying facies relationships in ancient strata, who tend to rely heavily on Holocene analogues (eg. Galloway, 1986). While Holocene environments are a valuable tool for studying depositional processes and constructing vertical facies models, the relatively short time period over which they have evolved makes them unrealistic models for predicting the ultimate three-dimensional facies architecture of ancient lithosomes. To do this requires an understanding of the evolution of the depositional environment through time and the resulting modification of initial facies relationships and their preservation potential. In understanding the architecture of clastic reservoirs this critical element of time and temporal facies relationships has previously been ignored.

10.3.0 Halfway Reservoir Heterogeneity.

Tidal inlet ebb-channel switching during Halfway shoreface progradation has resulted in the complex three-dimensional juxtaposition of shoreface and tidal inlet facies associations rather than the simpler alternation of inlet and shoreface facies documented along Holocene coastlines. Modelling of depositional facies relationships within a single Halfway mesotidal inlet channel fill has allowed the determination of the relative age relationships of laterally juxtaposed tidal inlet facies successions (Figure 39). For example, where a fine grained facies sequence deposited in the landward part of the inlet channel is juxtaposed against a coarser-grained facies association from an inlet mouth, then it is likely that the more landward sequence is the later of the two, since any given geographical reference point would have become relatively more landward with respect to the Halfway shoreline as it prograded through time. By using these relationships it is possible to determine the chronological order of successive tidal inlet channels both along strike and dip.

With an understanding of the cross-cutting relationships between tidal inlet fill sequences it is possible to examine the lateral continuity of potential hydrocarbon reservoir facies

between adjacent inlet fills and therefore make some estimate of reservoir heterogeneity. For example, where ebb-tidal delta sandstones of one inlet sequence are juxtaposed against active inlet fill sandstones of a second it is likely that the two sandbodies will be in fluid communication. Where sandstones are laterally adjacent to fine grained abandoned inlet fill however, a permeability barrier would exist. Dip and strike oriented facies correlations through Halfway tidal inlet fills such as those shown in Figures 38 and 39 suggest that such permeability barriers are abundant in the Halfway lithosome. Fine grained abandoned tidal inlet deposits form lateral permeability barriers between shoreface, ebb-tidal delta and active inlet sandbodies, and may act as barriers to vertical communication between active tidal inlet sandstones below and ebb-tidal delta sandstones above.

This high degree of vertical and horizontal heterogeneity apparent in the Wembley Halfway parasequence 4 reservoir makes it unlikely that any field-scale water injection program to enhance recovery would be successful. One possible exception is the linear parasequence 5 washover sandbody above the main reservoir, which appears to be relatively homogeneous and continuous along strike (Figure 59). A more realistic approach to the development of the main part of the parasequence 4 reservoir would appear to be infill drilling to exploit presently untapped reservoir compartments. These would be identified by careful three-dimensional facies correlations covering the entire field.

10.4.0 Stratigraphy.

While the sedimentological study which forms the first part of this investigation highlights the high degree of heterogeneity within the Wembley Halfway hydrocarbon pool, it does not address the question of why the oil field is located where it is. There is no structural control on Halfway hydrocarbon accumulations in west-central Alberta, so the trapping mechanism must be stratigraphic. An understanding of the local stratigraphic relationship of the Halfway to the Doig and Charlie Lake Formations is therefore critical to determining the exact stratigraphic trapping mechanism in the Wembley oil field, and also important in further exploration for similar Halfway stratigraphic traps.

Campbell et al. (1989) have suggested that erosional truncation of the Halfway sandstone beneath impermeable Charlie Lake strata is the trapping mechanism in Halfway oil and gas fields of west-central Alberta. Such erosional isolation of Halfway-Doig sandstones has been documented in the Spirit River oil field to the northeast of the study area by

Aukes and Webb (1986) and in the Peejay oil field of northeastern British Columbia by Mark Caplan (personal communication, 1992). Both areas are adjacent to the present subcrop edge of Middle Triassic strata in western Canada. In the Spirit River area erosional outliers of Halfway-Doig sandstone are overlain by Charlie Lake dolomites and mudstones, indicating that erosion occurred prior to Charlie Lake deposition. However, there is no evidence of any erosional removal of the Halfway sandstone within the present study area. Indeed, the Halfway-Charlie Lake formation contact is observed to be gradational and is interpreted as a facies boundary, not an unconformity. Erosion is therefore not considered a plausible explanation for the isolation of the Wembley Halfway sandstones from other Halfway sandstones to the northeast.

Several unconformities have been documented *within* the lithostratigraphic Charlie Lake Formation by Hess (1968) and Torrie (1973). These unconformities can be seen in Figure 4. It is considered that the erosion surface at the top of the Halfway-Doig sandstone in the Spirit River area represents one of these intra-Charlie Lake unconformities and that the overlying deposits assigned to the Charlie Lake Formation are therefore younger than those seen at Wembley. Older Charlie Lake sediments originally present at Spirit River were eroded at the same time as the Halfway-Doig sandstone. This postulated difference in age of the strata assigned to the Charlie Lake Formation in the Wembley and Spirit River areas would be difficult to prove, since the unit is largely of continental origin and contains no fauna for biostratigraphic analysis.

Facies correlations across the Wembley oil field show that Halfway facies successions are truncated along the southwestern margin of the field. This truncation is interpreted to be the product of shoreface erosion of the Halfway coastline during a relative rise in sea level. The shoreface erosion (or ravinement) surface is overlain by a second upward-coarsening facies association within the lithostratigraphic Halfway Formation. This indicates that at least two distinct progradational episodes are present within the Halfway Formation in the study area. The ravinement (or flooding) surface separating these two progradational episodes can be traced down-dip (palaeoseaward) into a radioactive shale bed, interpreted as a condensed section, and has a correlative up-dip flooding surface within the backbarrier and coastal plain deposits of the lower Charlie Lake Formation.

Several other radioactive beds in the Middle Triassic section can be traced throughout the study area and are similarly interpreted as condensed sections associated with marine flooding events. Strata bounded by two such flooding surfaces were deposited during the

same interval of time. By correlating the radioactive flooding surfaces throughout the Wembley area it has been demonstrated that the lithostratigraphic Doig, Halfway and Charlie Lake formations are time-equivalent parts of the same depositional system; the shales of the Doig Formation represent deposition in the offshore shelf environment and the coarser-grained Halfway Formation the laterally equivalent shoreface, while the lower part of the Charlie Lake Formation consists of backbarrier and coastal plain deposits (Figure 55). In sequence stratigraphic terminology these flooding surface-bounded depositional episodes are parasequences. Each flooding surface-bounded parasequence in the lithostratigraphic Doig Formation can be correlated up-dip (northeast) to a coarser-grained Halfway shoreface facies association and some way into the lower Charlie Lake Formation where washover sandstones are present.

Five parasequences have been identified within the Middle Triassic strata of the study area and informally designated parasequence 1 through 5. The Wembley hydrocarbon pool lies in the shoreface and tidal inlet sandstones ("Halfway Formation") of parasequence 4. The up-dip margin of the pool is observed to coincide with the northeastern limit of the ravinement surface beneath parasequence 4 (Figure 58). It is therefore concluded that the ravinement surface forms a permeability barrier, preventing the up-dip migration of oil and gas into the "Halfway" sandstones of the adjacent parasequence 3. Similarly, the southwestern margin of the Wembley pool coincides with the ravinement surface at the base of the overlying parasequence 5. Parasequence 4 sandstones are largely absent southwest of this line, having presumably been removed during the ravinement process. It would appear then that stratigraphic trapping of oil and gas in the Halfway Formation of the Wembley oil field is related to the up-dip termination of an individual parasequence, not post-Halfway erosional isolation.

10.5.0 Implications for Halfway -Doig Exploration.

Future exploration for Wembley-style Halfway hydrocarbon accumulations in west-central Alberta should therefore concentrate on correlating Middle Triassic radioactive condensed sections (marine flooding surfaces) beyond the Wembley area with the aim of delineating parasequence distribution throughout the Western Canada Sedimentary Basin. Sampling of cored condensed sections for macro and microfossils may facilitate the more detailed biostratigraphic zonation of the subsurface Triassic strata in western Canada and allow the sequence stratigraphic framework to be more easily correlated to other areas. Potential Halfway oil and gas fields lie in strike-linear (northwest-southeast) trends along the up-dip (northeastern) pinchout of sandstones in each parasequence. The up-dip

pinchout of Middle Triassic parasequences is marked by the development of thick, strike-linear washover sandstones within the backbarrier and supratidal deposits of the lower Charlie Lake Formation. Identification of thin distal Facies M washover sandstones within the lower part of the Charlie Lake Formation indicates the proximity of a thicker washover sandbody immediately down-dip.

In addition to assisting in the mapping of parasequence pinchout trends, these washover sandstones also form a major potential hydrocarbon reservoir in their own right. Location of thick washover sandstones associated with parasequence 4 immediately to the northwest of the Wembley pool in Townships 72-7-W6, 73-7-W6 and 74-8-W6 would appear to be an important future exploration objective.

The lateral thickening of individual parasequences along strike observed in Figure 59 may also be useful in predicting the occurrence of thick "Doig" sandstones. The growth-faulting considered by Wittenberg (1992) to be responsible for development of thick sandstones in the "Doig" shales appears in Figure 59 to coincide with the areas of greatest sediment accumulation along the Middle Triassic shoreline (ie. within the thickest part of a particular parasequence). By noting the along-strike (northwest-southeast) thickening of individual parasequences within the shales of the "Doig" it may be possible to predict the general location of additional "Doig" thick sandstones. This lateral thickening of the "Doig" interval may be apparent on both cross-sections and isopach maps.

11.0.0 CONCLUSIONS.

1) Five distinct upward-coarsening cycles are identified in the Middle Triassic interval in the study area. Each cycle represents southwesterly progradation of a barrier island shoreface and is bounded by marine flooding surfaces. The flooding surfaces are expressed as a ravinement surface and associated bioclastic sandstone veneer in shoreface facies and can be traced down-dip into a phosphatic condensed section in offshore shales. A correlative flooding surface has been identified at the base of washover sandstones in the associated backbarrier and coastal plain deposits. In sequence stratigraphic terminology these flooding-surface-bounded progradational cycles would be called parasequences.

2) Facies patterns within each parasequence indicate that the Doig, Halfway and lower Charlie Lake Formations are time-equivalent parts of the same depositional system. The shales of the Doig Formation represent deposition in the offshore shelf environment and the coarser-grained Halfway Formation the laterally equivalent shoreface, while the lower part of the Charlie Lake Formation consists of associated backbarrier and coastal plain deposits. Each parasequence within the lithostratigraphic Doig Formation can be traced up-dip to a coarser-grained Halfway shoreface facies association and some way into the lower Charlie Lake Formation. The five parasequences identified in the Middle Triassic strata of the study area have informally been designated parasequence 1 through 5 and form part of a progradational parasequence set.

3) This study documents that in west-central Alberta the Doig, Halfway and Charlie Lake Formations form a westward-younging progradational parasequence set. Thus, while they might usefully be retained for describing the offshore, shoreface and backbarrier deposits of the Middle Triassic in individual well sections, these lithostratigraphic units should be discarded for correlation purposes. To accurately depict depositional facies relationships, future correlations of the Middle Triassic strata of western Canada should be based on a sequence stratigraphic framework and integrated with biostratigraphic data.

4) The Wembley oil field is located in shoreface and inlet sandstones of parasequence 4. The northeastern margin of the field is defined by the up-dip pinchout of parasequence 4 sandstones. This pinchout is related to the landward limit of the flooding event prior to parasequence 4 deposition and is not due to post-Halfway erosion. The northwestern limit of the field is caused by the lateral pinchout of parasequence 4.

5) Future exploration for Wembley-style Halfway hydrocarbon accumulations in west-central Alberta should concentrate on extending the sequence stratigraphic framework identified in this study with the objective of locating similar up-dip parasequence pinchout trends. These trends are marked by the development of thick, strike-linear washover sandstones within the backbarrier and supratidal deposits of the lower Charlie Lake Formation. Further to the east however (eg. at Spirit River), the Halfway-Doig interval has been affected by intra-Charlie Lake erosion and parasequence pinchout is unlikely to be the major control on pool distribution.

6) The Halfway Formation in the study area was deposited by a series of southwesterly prograding barrier island systems. The presence of ebb-tidal delta sandstones, stacked tidal inlet cycles and fine grained abandoned tidal inlet channel fill, coupled with the absence of washover- and flood-tidal delta sandstones indicates that these barrier island shorelines were deposited in a mesotidal regime. The marked differences between wave- and tide-dominated inlet fill sequences make such a knowledge of the prevalent hydrographic regime essential when attempting to predict the distribution of porous reservoir sandstones in an ancient barrier island lithosome.

7) Halfway tidal inlet facies patterns compare closely to those described from Holocene mesotidal inlet fill sequences along the South Carolina coast and are similarly interpreted to be the result of bar-bypassing and ebb-channel abandonment. The seaward (down-dip) mouth of Halfway tidal inlet channels are filled with clean sandstone swept in during welding of the ebb-tidal delta to the barrier system. The landward (up-dip) part of the abandoned inlet channel consists of fine grained sediment deposited from suspension. The up-dip pinchout of active tidal inlet and ebb-delta sandstones against this fine grained abandoned inlet fill creates two potential stratigraphic hydrocarbon traps in Halfway mesotidal inlet fills.

8) The proportion of the Halfway barrier island lithosome consisting of tidal inlet sediments (90%) is much greater than in Holocene barrier island examples (35-40%). This is apparently the case in other ancient examples of barrier island deposits. The explanation for this discrepancy between ancient lithosomes and Holocene analogues is the geologically short period over which tidal inlet channels have had the opportunity to rework Holocene coastlines. Much longer periods of coastal progradation recorded by ancient examples resulted in successive tidal inlet channels reworking most of the barrier island shoreface and earlier inlet deposits. The restricted temporal evolution of Holocene

coastlines severely limits their usefulness as models for predicting the three-dimensional facies architecture of ancient coastal lithosomes.

9) The combination of lateral tidal inlet migration and overall coastal progradation has resulted in the complex three-dimensional juxtaposition of shoreface and tidal inlet facies associations in the Halfway lithosome. Fine grained abandoned inlet fill deposits form lateral permeability barriers between shoreface, ebb-delta and active inlet sandstones, and may also act as barriers to vertical communication between active tidal inlet sandstones and overlying ebb-delta delta sandstones. This high degree of lateral and vertical heterogeneity in the Halfway sandstone of parasequence 4 makes it unlikely that any field-scale water-flooding program to enhance recovery would be successful. One possible exception is the parasequence 5 washover sandstone, which appears to be continuous along strike and is separated from the underlying parasequence 4 sandstones by lagoonal mudstones. Infill drilling to exploit presently untapped reservoir compartments would be a more realistic option in the parasequence 4 lithosome.

10) Listric normal faulting which controlled the development of "Doig" thick sandstones appears to coincide in the study area with areas of greatest sediment accumulation, marked by the lateral thickening of individual parasequences. Along-strike thickening of individual parasequences in the Middle Triassic may therefore be useful in predicting the general location of "Doig" thick sandstones.

REFERENCES CITED.

Aigner, T. and Reineck, H. E. (1982). Proximality trends in modern storm sands from the Helegoland Bight (North Sea) and their implications for basin analysis. Senckenbergiana Maritima, 14; 183-215.

Alberta Energy Resources Conservation Board. (1989). Alberta's reserves of crude oil, oilsands, gas, natural gas liquids, and sulphur. E.R.C.B. Report ST89-18. Calgary, Alberta.

Andrews, P. B. (1970). Facies and genesis of a hurricane-washover fan, St. Joseph Island, central Texas coast. Bureau of Economic Geology, University of Texas, Austin. Report of Investigation, 67. 147p.

Armitage, J. H. (1962). Triassic oil and gas occurrences in northeastern British Columbia, Canada. Journal of the Alberta Society of Petroleum Geologists, 10; 35-56.

Armon, J. W. and McCann, S. B. (1977). Longshore sediment transport and a sediment budget for the Malpeque barrier system, southern Gulf of St. Lawrence. Canadian Journal of Earth Science, 14; 2429-2439.

Aukes, P. G. and Webb, T. K. (1986). Triassic Spirit River Pool, Northwestern Alberta. In: Meijer Drees, N. C. (Ed.), 1986 Core Conference, Calgary, Canadian Society of Petroleum Geologists. p. 3.1-3.34.

Barclay, J. E. and Leckie, D. A. (1986). Tidal inlet reservoirs of the Triassic Halfway Formation, Wembley region, Alberta. In: Meijer Drees, N. C. (Ed.), 1986 Core Conference, Calgary, Canadian Society of Petroleum Geologists. p. 4.1-4.6.

Barclay, J. E., Krause, F.F., Campbell, R.I., and Utting, J. (1990). Dynamic casting and growth faulting: Dawson Creek graben complex, Carboniferous-Permian Peace River Embayment, western Canada. Bulletin of Canadian Petroleum Geology, 38A; 15-145.

Barss, D. L., Best, E. W. and Meyers, N. (1964). Triassic, Chapter 9. In: McCrossan, R. G. and Glaister, R. P. (Eds.), Geological History of Western Canada. Alberta Society of Petroleum Geologists, Calgary. p. 113-136.

Barwis, J. H., and Makurath, J. H. (1978). Recognition of ancient tidal inlet sequences: an example from the Upper Silurian Keyser Limestone in Virginia. Sedimentology, 25; 61-82.

Berelson, W. M. and Heron, S. D. (1985). Correlations between Holocene flood tidal delta and barrier island inlet fill sequences: Back Sound-Shackleford Banks, North Carolina. Sedimentology, 32; 215-222.

Boersma, J. R. (1991). A large flood-tidal delta and its successive spill-over apron: Detailed proximal-distal facies relationships (Miocene Lignite Suite, Lower Rhine Embayment, Germany). In: Smith, D. G., Reinson, G.E., Zaitlin, B.A., and Rahmani, R.A. (Eds.), Clastic Tidal Sedimentology. Canadian Society of Petroleum Geologists Memoir 16. p. 227-254.

Brack, L., Marshall-Abbott, G., Noble, I. A., and Tang, R.C.W. (1989). Triassic / Jurassic fields. In: Anderson, N.L., Hills, L.V. and Cedarwall, D.A. (Eds). Geophysical Atlas of Western Canadian Hydrocarbon Pools. Canadian Society of Exploration Geophysicists / Canadian Society of Petroleum Geologists, Calgary, Alberta. p. 207-211.

Bridges, P. H. (1976). Lower Silurian transgressive barrier islands, southwest Wales. Sedimentology, 23; 347-362.

Briskin, M. and Schreiber, B. C. (1978). Authigenic gypsum in marine sediments. Marine Geology, 28; 37-49.

Bruun, P. (1962). Sea level rise as a cause of shore erosion. American Society of Civil Engineers Proceedings, Journal of Waterways and Harbors Division, 88; 117-130.

Campbell, C. V. and Hassler, G. (1989). Stratigraphy and facies of the Triassic Halfway and Doig Formations in west-central Alberta (abstract). Canadian Society of Petroleum Geologists Reservoir., 16(2); 1-2.

Campbell, C. V., Dixon, R. J. and Forbes, D.M. (1989). Up-dip erosional truncation of Halfway and Doig shoreline sequences: A new model for exploration in west-central Alberta (abstract). Programs and Abstracts, Exploration Update '89, Canadian Society of Petroleum Geologists Convention, Calgary. p.138.

Campbell, C. V. and Horne, J. C. (1986). Depositional facies of the Middle Triassic Halfway Formation, Western Canada Basin. In: Moslow, T. F. and Rhodes, E. G. (Eds.), Modern and Ancient Shelf Clastics: A Core Workshop. Society of Economic Palaeontologists and Mineralogists Core Workshop No. 9; 413-459.

Cant, D. J. (1986). Hydrocarbon trapping in the Halfway Formation (Triassic), Wembley Field, Alberta. Bulletin of Canadian Petroleum Geology, 34; 329-338.

Caplan, M. L. and Moslow, T. F. (1991). Reservoir quality and characterization of the Halfway Formation. Peejay Field, northeastern British Columbia (abstract). Buletin of Canadian Petroleum Geology, 39; 207.

Carlson, C. E. (1968). Triassic-Jurassic of Alberta, Saskatchewan, Manitoba, Montana and North Dakota. American Association of Petroleum Geologists Bulletin, 52; 1969-1983.

Cheel, R. J. and Leckie, D. A. (1990). A tidal inlet complex in the Cretaceous epeiric sea of North America: Virgelle Member, Milk River Formation, southern Alberta, Canada. Sedimentology, 37; 67-81.

Chunta, A. (1969). The Halfway reservoir western portion, Peejay Field, British Columbia (abstract). Bulletin of Canadian Petroleum Geology, 17; 528.

Clark, D. A. (1961). Primary structures of the Halfway Sand in the Milligan Creek Oilfield, British Columbia. Journal of the Alberta Society of Petroleum Geologists, 9; 109-130.

Clifton, H. E. (1969). Beach lamination: nature and origin. Marine Geology, 7; 553-559.

Clifton, H. E., Hunter, R. E., and Phillips, R. L. (1971). Depositional structures and processes in the non-barred high-energy nearshore. Journal of Sedimentary Petrology, 41; 651-670.

Colquhoun, D. J. (1962). Triassic stratigraphy in the vicinity of Peace River Foothills, British Columbia. Edmonton Geological Society 4th Fieldtrip Guidebook. p. 57-88.

Davidson-Arnott, R. G. D., and Greenwood, B. (1976). Facies relationships on a barred coast, Kouchibouguac Bay, New Brunswick, Canada. In: Davis, R. A. and Ethington, R.L. (Eds.), Beach and Nearshore Sedimentation. Society of Economic Paleontologists and Mineralogists Special Publication No. 24; 149-168.

Davies, D. J, Powell, E. N., and Stanton, R. J. (1989). Taphonomic signature as a function of environmental process: shells and shell beds in a hurricane-influenced inlet on the Texas coast. Palaeogeography, Palaeoclimatology, Palaeoecology, 72; 317-356.

Davies, D. K., Ethridge, F. G., and Berg, R. R. (1971). Recognition of barrier environments. Bulletin of the American Association of Petroleum Geologists, 55; 550-565.

Davies, G. R. (1970). Algal-laminated sediments, Gladstone Embayment, Shark Bay, Western Australia. Memoir of the American Association of Petroleum Geologists 13; 169-205.

Davis, G. A., Monger, J.W.H., and Burchfield, B.C. (1978). Mesozoic construction of the Cordilleran "collage", central British Columbia to central California. In: D.G. Howell and K.A. McDougall (Eds), Mesozoic paleogeography of the western United States. Society of Economic Paleontologists and Mineralogists Pacific Section, Pacific Coast Paleogeography Symposium 2. p. 1-32.

Davis, R. A., and Fox, W. T. (1981). Interaction between wave and tide generated processes at the mouth of a microtidal estuary: Matanzas River, Florida (U.S.A.). Marine Geology, 40; 49-68.

Davis, R. A. and Hayes, M. O. (1984). What is a wave-dominated coast? Marine Geology, 60; 313-329.

Davis, R. A., Andronaco, M. A., and Gibeaut, J. C. (1989). Formation and development of a tidal inlet from a washover fan, west-central Florida coast, U.S.A. Sedimentary Geology, 65; 87-94.

Dawson, G. M. (1881). Report on an exploration from Port Simpson on the Pacific Coast to Edmonton on the Saskatchewan, embracing a portion of the Northern part of British Columbia and the Peace River Country. Geol. Nat. Hist. Surv., Canada, Report of Progress 1879-80, part B; 1-177.

Deery, J. R., and Howard, J. D. (1977). Origin and character of washover fans on the Georgia Coast, U.S.A. Gulf Coast Association, Geological Society Transactions, 27; 259-271.

Demarest, J. M., Biggs, R. B., and Kraft, J. C. (1981). Time-stratigraphic aspects of a formation: Interpretation of surficial Pleistocene deposits by analogy with Holocene paralic deposits, southeastern Delaware. Geology, 9; 360-365.

Demarest, J. M. and Kraft, J. C. (1987). Stratigraphic record of Quaternary sea levels: implications for more ancient strata. In: Nummedal, D., Pilkey, O. H., and Howard, J. D. (Eds), Sea level fluctuation and coastal evolution. Society of Economic Paleontologists and Mineralogists Special Publication No. 41. p. 223-239.

Donselaar, M. E. (1984). Flood tidal delta sedimentation in the late Cretaceous Menefee Formation (Mesaverde Group), San Juan Basin, northwest New Mexico. Geologie en Mijnbouw, 63; 323-331.

Donselaar, M. E. and Nio, S. D. (1982). An Eocene tidal inlet / washover type barrier island complex in the south Pyrenean marginal basin, Spain. Geologie en Mijnbouw, 61; 343-353.

Dudley, J. S., Haskin, H. K. and Moore, C. H. (1989). Effects of geological heterogeneity on acidization: Halfway Formation. 1989 Core Conference, Canadian Society of Petroleum Geologists, Calgary. p. 7.1-7.18.

Duke, W. L., Arnott, R. W. C. and Cheel, R. J. (1991). Shelf sandstones and hummocky cross-stratification: New insights on a stormy debate. Geology, 19; 625-628.

Elliot, T. (1986). Siliciclastic shorelines. In: H.G. Reading (Ed.), Sedimentary Environments and Facies (2nd Edn.). Blackwell. Oxford. p. 155-188.

Evans, G. (1965). Intertidal flat sediments and their environments of deposition in the Wash. Quarterly Journal of the Geological Society of London, 121; 209-245.

Fischer, A. G. (1961). Stratigraphic record of transgressing seas in light of sedimentation on Atlantic coast of New Jersey. Bulletin of the American Association of Petroleum Geologists, 45; 1656-1666.

Frazier, D. E. (1974). Depositional episodes: their relationship to the Quaternary stratigraphic framework in the northwestern portion of the Gulf basin. University of Texas at Austin, Bureau of Economic Geology Circular 74-1.

Frey, R. W. and Howard, J. D. (1988). Beaches and beach-related facies, Holocene barrier islands of Georgia. Geological Magazine, 125; 621-640.

Gallagher, M. T., and Jenkins, W. A. M. (1988). Micropalaeontological and palynological interpretations of depositional environments in Triassic rocks of the Wembley area. (Unpublished report for Esso Resources Canada Ltd.). 22 p

Galloway, W. E. (1986). Reservoir facies architecture of microtidal barrier systems. American Association of Petroleum Geologists Bulletin, 70; 787-808.

Galloway, W. E. (1989). Genetic stratigraphic sequences in basin analysis 1: architecture and genesis of flooding-surface bounded depositional units. American Association of Petroleum Geologists Bulletin, 73; 125-142.

Gibson, D. W. (1975). Triassic rocks of the Rocky Mountain Foothills and Front Ranges of northeastern British Columbia and west-central Alberta. Geological Survey of Canada Bulletin 247.

Gibson, D. W. and Barclay, J. E. (1989). Middle Absaroka Sequence- The Triassic stable craton. In: Ricketts, B. D. (Ed.), Western Canada Sedimentary Basin- A Case History. p. 219-231.

Gibson, D.W. and Edwards, D.E. (1990). An overview of Triassic stratigraphy and depositional environments in the Rocky Mountain Foothills and Western Interior Plains, Peace River Arch area, northeastern British Columbia. Bulletin of Canadian Petroleum Geology, 38A; 146-158.

Greer, S. A. (1975). Sandbody geometry and sedimentary facies at the estuary-marine transition zone. Senckenbergiana Maritima, 7; 105-136.

Habicht, J. K. A. (1979). Paleoclimate, paleomagnetism and continental drift. American Association of Petroleum Geologists Studies in Geology, No. 9. Tulsa, Oklahoma. 34 p.

Halton, E. (1981). Wembley Field- facies variations in the Halfway Formation (abst.). In: Stoakes, F. A. (Ed.), Environmental Analysis From Core and Field Sample Studies, 1981 Core Conference, Calgary, Canadian Society of Petroleum Geologists. p.9.

Hamblin, A. P. and Walker, R. G. (1979). Storm-dominated shallow marine deposits: the Fernie-Kootenay (Jurassic) transition, southern Rocky Mountains. Canadian Journal of Earth Sciences, 16; 1673-1690.

Handford, C. R. (1981). Coastal sabkha and salt pan deposition of the Lower Clear Fork Formation (Permian), Texas. Journal of Sedimentary Petrology, 51; 761-778.

Harland, W. B., R. L. Armstrong, A. V. Cox, L. E. Craig, A. G. Smith and D. G. Smith. (1989). A Geologic Time Scale 1989. Cambridge University Press. Cambridge. 263 p.

Harms, J. C., Southard, J. B., and Walker, R. G. (1982). Structures and sequences in clastic rocks. Society of Economic Paleontologists and Mineralogists Short Course No. 9. Tulsa.

Harrington, P. A. (1984). Subsurface geology and diagenetic history of the Halfway Formation (Middle Triassic), Wembley Field, Alberta. Unpublished B.Sc. Thesis, Carleton University, Ottawa. 98p.

Hayes, M. O. (1967). Hurricanes as geological agents, south Texas coast. American Association of Petroleum Geologists Bulletin, 51; 937-942.

Hayes, M. O. (1975). Morphology of sand accumulations in estuaries: an introduction to the symposium. In: Cronin, L.E. (Ed), Estuarine Research, V.2. Academic Press. London. pp 3-22.

Hayes, M. O. (1979). Barrier island morphology as a function of tidal and wave regime. In: Leatherman, S.P. (Ed.), Barrier islands from the Gulf of St. Lawrence to the Gulf of Mexico. Academic Press, New York. pp 1-27.

Hayes, M. O. (1980). General morphology and sediment patterns in tidal inlets. Sedimentary Geology, 26; 139-156.

Heckel, P. H. (1977). Origin of phosphatic black shale facies in Pennsylvanian cyclothems of mid-continent North America. Bulletin of the American Association of Petroleum Geologists, 61; 1045-1068.

Henderson, S. W., and Frey, R. W. (1986). Taphonomic redistribution of mollusk shells in a tidal inlet channel, Sapelo Island, Georgia. Palaios, 1; 3-16.

Hennessey, J. T. and Zarillo, G. A. (1987). The interrelation and distinction between flood-tidal delta and washover deposits in a transgressive barrier island. Marine Geology, 78; 35-56.

Heron, S. D., Moslow, T. F., Berelson, W. M., Herbert, J. R., Steele, G. A., and Susman, K. R. (1984). Holocene sedimentation of a wave-dominated barrier island shoreline: Cape Lookout, North Carolina. Marine Geology, 60; 413-434.

Hess, E. B. (1968). Subsurface stratigraphic correlations, Schooler Creek Group, northeast British Columbia. Pacific Petroleums report for British Columbia Bureau of Energy, Mines and Petroleum Resources. Unpublished.

Heward, A. P. (1981). A review of wave-dominated clastic shoreline deposits. Earth Science Review, 17; 223-276.

Higgs, R. (1990). Sedimentology and petroleum geology of the Artex Member (Charlie Lake Formation), northeast British Columbia (abstract). Bulletin of Canadian Petroleum Geology, 38; p.166.

Hine, A. C. and Snyder, S. W. (1985). Coastal lithosome preservation: Evidence from the shoreface and inner continental shelf off Bogue Banks, North Carolina. Marine Geology, 63; 307-330.

Hobday, D. K. and Horne, J. C. (1977). Tidally influenced barrier island and estuarine sedimentation in the Upper Carboniferous of southern West Virginia. Sedimentary Geology, 18; 97-122.

Hobday, D. K. and Jackson, M. P. A. (1979). Transgressive shore zone sedimentation and syndepositional deformation in the Pleistocene of Zululand, South Africa. Journal of Sedimentary Petrology, 49; 145-158.

Hobday, D. K. and Orme, A. R. (1974). The Port Durnford Formation: A major Pleistocene barrier-lagoon complex along the Zululand coast. Transactions of the Geological Society of South Africa, 77; 141-149.

Horne, J. C., Campbell, C. V. and Odland, S. K. (1985). Tidal inlet fills as hydrocarbon reservoirs: Examples from Halfway Formation, Alberta (abstract). American Association of Petroleum Geologists Bulletin, 69; p. 267.

Howard, J. D. and Reineck, H. E. (1981). Depositional facies of high-energy beach-to-offshore sequence: comparison with low-energy sequence. American Association of Petroleum Geologists Bulletin, 65; 807-830.

Howard, J. D. and Scott, R. M. (1983). Comparison of Pleistocene and Holocene barrier island beach-to-offshore sequences, Georgia and northeast Florida coasts, U.S.A. Sedimentary Geology, 34; 167-183.

Hoyt, J. H. and Henry, V. J. (1967). Influence of island migration on barrier island sedimentation. Geological Society of America Bulletin, 78; 77-86.

Hubbard, D. K., Oertel, G., and Nummedal, D. (1979). The role of waves and tidal currents in the development of tidal inlet sedimentary structures and sand body geometry: examples from North Carolina, South Carolina, and Georgia. Journal of Sedimentary Petrology, 49; 1073-1092.

Hunt, A. D. and Ratcliffe, J. D. (1959). Triassic stratigraphy, Peace River Area, Alberta and British Columbia, Canada. Bulletin of the American Association of Petroleum Geologists, 43; 563-589.

Imperato, D. P., Sexton, W. J., and Hayes, M. O. (1988). Stratigraphy and sediment characteristics of a mesotidal ebb-tidal delta, North Edisto Inlet, South Carolina. Journal of Sedimentary Petrology, 58; 950-958.

Irving, E., Woodsworth, G.J., Wynne, P.J., and Morrison, A. (1985). Paleomagnetic evidence for displacement from the south of the Coast Plutonic Complex, British Columbia. Canadian Journal of Earth Sciences, 22; 584-598.

Israel, A. M., Ethridge, F. G. and Estes, E. L. (1987). A sedimentologic description of a microtidal, flood-tidal delta, San Luis Pass, Texas. Journal of Sedimentary Petrology, 57; 288-300.

Kindle, E. D. (1944). Geological reconnaissance along Fort Nelson, Liard and Beaver Rivers, northeastern British Columbia and southeastern Yukon. Geological Survey of Canada Paper 44-16.

Kinsman, D. J. J. (1969). Modes of formation, sedimentary associations, and diagnostic features of shallow-water and supratidal evaporites. Bulletin of the American Association of Petroleum Geologists, 53; 830-840.

Klein, G. de V. (1963). Bay of Fundy intertidal zone sediments. Journal of Sedimentary Petrology, 33; 844-854.

Klein, G. de V. (1977). Clastic Tidal Facies. CEPCO. Illinois. 149 p.

Kocurek, G. and Fielder, G. (1982). Adhesion structures. Journal of Sedimentary Petrology, 52; 1229-1241.

Kraft, J. C. (1971). Sedimentary facies patterns and geologic history of a Holocene marine transgression. Geological Society of America Bulletin, 82; 2131-2158.

Kraft, J. C. and John, C. J. (1979). Lateral and vertical facies relations of a transgressive barrier. American Association of Petroleum Geologists Bulletin, 63; 2145-2163.

Kraft, J. C., Chrzastowski, M. J., Belknap, D. F., Toscano, M. A., and Fletcher, C. H. (1987). The transgressive barrier-lagoon coast of Delaware: morphostratigraphy, sedimentary sequences and responses to relative rise in sea level. In: Nummedal, D., Pilkey, O. H., and Howard, J. D. (Eds), Sea level fluctuation and coastal evolution. Society of Economic Paleontologists and Mineralogists Special Publication No. 41. p. 129-143

Kreisa, R. D. (1981). Storm-generated sedimentary structures in subtidal marine facies with examples from the Middle and Upper Ordovician of southwestern Virginia. Journal of Sedimentary Petrology, 51; 823-848.

Kumar, N., and Sanders, J. E. (1970). Are basal transgressive sands chiefly inlet-filling sands? Maritime sediments, 6; 12-14.

Kumar, N., and Sanders, J. E. (1974). Inlet sequence: a vertical succession of sedimentary structures and textures created by the lateral migration of tidal inlets. Sedimentology, 21; 491-532.

Kumar, N., and Sanders, J. E. (1976). Characteristics of shoreface storm deposits: modern and ancient examples. Journal of Sedimentary Petrology, 46; 145-162.

Leatherman, S. P. (1979). Migration of Assateague Island, Maryland, by tidal inlet and overwash processes. Geology, 7; 104-107.

Leatherman, S. P. and Williams, A. T. (1977). Lateral textural grading in overwash sediments. Earth Surface Processes, 2; 333-341.

Leckie, D. A. and Krystinik, L. F. (1989). Is there evidence for geostrophic currents preserved in the sedimentary record of inner to middle-shelf deposits? Journal of Sedimentary Petrology, 59; 862-870.

Leckie, D. A., Cheel, R. J., and Rosenthal, L. (1989). Sedimentology of the Upper Virgille Member (Upper Cretaceous Milk River Formation), Writing-on-Stone Provincial Park, Alberta. Field trip guide to the second international research symposium on clastic tidal deposits. Canadian Society of Petroluem Geologists, Calgary, Alberta.

Loutit, T. S., Hardenbol, J., Vail, P. R., and Baum, G. R. (1988). Condensed sections: the key to age determination and correlation of continental margin sequences. In: Wilgus, C. K., Hastings, B.S., Kendall, C.G., Posamentier, H.W., Ross, C.A., and Van Wagoner, J.C (Eds.). Sea-Level Changes- An Integrated Approach. Society of Economic Paleontologists and Mineralogists Special Publication No. 42. p. 183-213.

Lowe, D. R. (1975). Water escape structure in coarse-grained sediments. Sedimentology, 22; 157-204.

Mazullo, J., Malicse, A., and Siegel, J. (1991). Facies and depositional environments of the Shattuck Sandstone on the northwest shelf of the Permian Basin. Journal of Sedimentary Petrology, 61; 940-958.

McConnell, R. G. (1891). Report on a portion of the District of Athabaska comprising the country between Peace River and Athabaska River North of Lesser Slave Lake. Geological Survey of Canada, Annual Report. v. V, part I, part D.

McLearn, F. H. (1921). Mesozoic of upper Peace River, British Columbia. Geological Survey of Canada Summ. Rept. 1920, part B; p. 1-6.

McLearn, F. H. (1947). The Triassic Nathorstites fauna in northeastern British Columbia. Geological Survey of Canada Paper 47-24.

McLearn, F. H. (1953). Correlation of the Triassic formations of Canada. Bulletin of the Geological Society of America, 64; 1205-1228.

McLearn, F. H., and Kindle, E.D. (1950). Geology of northeastern British Columbia. Geological Survey of Canada Memoir 259.

Miall, A. D. (1976). The Triassic sediments of Sturgeon Lake south and surrounding areas. In: M. Lerand (Ed.), The Sedimentology of selected clastic oil and gas reservoirs in Alberta. Canadian Society of Petroleum Geologists, Calgary, Alberta. p. 25-93.

Middleton, G. V. (1973). Johannes Walther's law of correlation of facies. Bulletin of the Geological Society of America, 84; 979-988.

Miller, J. A. (1975). Facies characteristics of Laguna Madre wind-tidal flats. In: R. N. Ginsburg (Ed.), Tidal Deposits. Springer-Verlag. New York. p. 67-73.

Monger, J. W. H. (1989). Overview of Cordilleran geology. In B. D. Ricketts (Ed.), Western Canada Sedimentary Basin. A Case History. Canadian Society of Petroleum Geologists, Calgary, Alberta. p. 9-32.

Monger, J.W.H., Price, R.A., and Tempelman-Kluit, D.J. (1982). Tectonic accretion and the origin of two major metamorphic and plutonic welts in the Canadian Cordillera. Geology, 10; 70-75.

Mortimer, N. (1986). Late Triassic, arc-related, potassic igneous rocks in the North American Cordillera. Geology, 14; 1035-1038.

Morton, R. A. (1981). Formation of storm deposits by wind-forced currents in the Gulf of Mexico and the North Sea. In: Nio, S.D., Shuttenhelm, R.T.E., and Van Weering, T.C.E. (Eds), Holocene marine sedimentation in the North Sea basin. Special Publication of the International Association of Sedimentologists No. 5; 385-396.

Moslow, T. F. and Heron, S.D. (1978). Relict inlets: preservation and occurrence in the Holocene stratigraphy of southern Core Banks, North Carolina. Journal of Sedimentary Petrology, 48; 1275-1286.

Moslow, T. F. and Pemberton, S. G. (1988). An integrated approach to the sedimentological analysis of some Lower Cretaceous shoreface and delta front sandstone sequences. In: James, D. P. and Leckie, D. A. (Eds.), Sequences, Stratigraphy, Sedimentology: Surface and Subsurface. Canadian Society of Petroleum Geologists Memoir 15; 373-386.

Moslow, T. F., and Tye, R. S. (1985). Recognition and characterization of Holocene tidal inlet sequences. Marine Geology, 63; 129-151.

Mothersill, J. S. (1968). Environments of deposition of the Halfway Formation, Milligan Creek area, British Columbia. Bulletin of Canadian Petroleum Geology, 16; 180-199.

Munroe, H. D. (1991). Depositional models for the Doig Formation of northeastern British Columbia (abstract). Bulletin of Canadian Petroleum Geology, 39; 220.

Munroe, H. D. and Moslow, T. F. (1990). Reservoir quality and architecture of tidal inlet sandstones, Halfway Formation, northeastern British Columbia. Abstracts, Canadian Society of Petroleum Geologists Convention, Calgary, Alberta, 1990. Bulletin of Canadian Petroleum Geology, 38; p.174.

Murakoshi, N. and Masuda, F. (1991). A depositional model for a flood-tidal delta and washover sands in the late Pleistocene Paleo-Tokyo Bay, Japan. In: Smith, D. G., Reinson, G.E., Zaitlin, B.A., and Rahmani, R.A.(Eds.), Clastic Tidal Sedimentology. Canadian Society of Petroleum Geologists Memoir 16. p. 219-226.

Muza, J. P. and Wise, S. W. (1983). An authigenic gypsum, pyrite and glauconite association in a Miocene deep sea biogenic ooze from the Falkland Plateau, southwest Atlantic Ocean. Initial Reports of the Deep Sea Drilling Project, 71(Pt.1). Washington (U.S. Government Printing Office).

Nelson, C. H. (1982). Modern shallow-water graded sand layers from storm surges, Bering Shelf: a mimic of Bouma Sequences and turbidite systems. Journal of Sedimentary Petrology, 52; 537-545.

Neumann, A. C. and Land, L. S. (1975). Lime mud deposition and calcareous algae in the Bight of Abaco, Bahamas: a budget. Journal of Sedimentary Petrology, 45; 763-786.

Nichols, M. N., Johnson, G. H., and Peebles, P. C. (1991). Modern sediments and facies model for a microtidal coastal plain estuary, the James estuary, Virginia. Journal of Sedimentary Petrology, 61; 883-899.

Niedoroda, A. W., Swift, D. J. P., Figueiredo, A. G., and Freeland, G. F. (1985). Barrier island evolution, middle Atlantic shelf, U.S.A. Part 2: Evidence from the shelf floor. Marine Geology, 63; 363-396.

Nio, S. D., and Yang, C. S. (1991). Diagnostic attributes of clastic tidal deposits: a review. In: Smith, D. G., Reinson, G.E., Zaitlin, B.A., and Rahmani, R.A. (Eds.), Clastic Tidal Sedimentology. Canadian Society of Petroleum Geologists Memoir 16. p. 3-27.

Nummedal, D. and Swift, D. J. P. (1987). Transgressive stratigraphy at sequence-bounding unconformities: some principles derived from Holocene and Cretaceous examples. In: Nummedal, D., Pilkey, O. H., and Howard, J. D. (Eds), Sea level fluctuation and coastal evolution. Society of Economic Paleontologists and Mineralogists Special Publication No. 41. p. 241-260.

Oertel, G. F. (1972). Sediment transport of estuary entrance shoals and the formation of swash platforms. Journal of Sedimentary Petrology, 42; 857-863.

Oertel, G. J. (1973). Examination of textures and structures of mud in layered sediments at the entrance of a Georgia tidal inlet. Journal of Sedimentary Petrology, 43; 33-41.

Oomkens, E. (1974). Lithofacies relationships in the late Quaternary Niger Delta complex. Sedimentology, 21; 195-222.

Park, R. (1976). A note on the significance of lamination in stromatolites. Sedimentology, 23; 379-393.

Pelletier, B. R. (1963). Triassic stratigraphy of the Rocky Mountains and Foothills, Peace River District, British Columbia. Geological Survey of Canada Paper 62-26.

Pelletier, B. R. (1965). Palaeocurrents in the Triassic of northeastern British Columbia. In: Middleton, G. V. (Ed.), Primary sedimentary structures and their hydrodynamic interpretation. Society of Economic Palaeontologists and Mineralogists Special Publication No. 12. p. 233-245.

Pemberton, S. G. and Frey, R. W. (1985). The *Glossifungites* ichnofacies: modern examples from the Georgia coast, U.S.A. In: Curran, H. A. (Ed). Biogenic structures: their use in interpreting depositional environments. Society of Economic Paleontologists and Mineralogists Special Publication No.35. Tulsa. p. 237-259.

Penland, S., Suter, J. R., and Boyd, R. (1985). Barrier island arcs along abandoned Mississippi River deltas. Marine Geology, 63; 197-233.

Pierce, J. W. (1969). Sediment budget along a barrier island chain. Sedimentary Geology, 3; 5-16.

Pierce, J. W. (1970). Tidal inlets and washover fans. Journal of Geology, 78; 230-234.

Podruski, J. A., Barclay, J. E., Hamblin, A. P., Lee, P. J., Osadetz, K. G., Procter, R. M. and Taylor, G. C. (1988). Conventional oil resources of western Canada (light and medium). Geological Survey of Canada Paper 87-26.

Reddering, J. S. V. (1983). The sequence produced by migration of a small microtidal inlet against longshore drift: the Keurbooms Inlet, South Africa. Sedimentology, 30; 201-218.

Reid, P. R., Macintyre, I. G., and Post, J. E. (1992). Micritized skeletal grains in Northern Belize Lagoon: a major source of Mg-calcite mud. Journal of Sedimentary Petrology, 62; 145-156.

Reif, D. M. and Slatt, R. M. (1979). Red bed members of the Lower Triassic Moenkopi Formation, southern Nevada: sedimentology and paleogeography of a muddy tidal flat deposit. Journal of Sedimentary Petrology, 49; 869-890.

Reineck, H. E. and Singh, I. B. (1972). Genesis of laminated sand and graded rhythmites in storm-sand layers of shelf mud. Sedimentology, 18; 123-128.

Reinson, G. E. (1984). Barrier island and associated strandplain systems. In: Walker, R. G. (Ed.), Facies Models, 2nd Edition. Geoscience Canada. 119-140.

Richards, B. C. (1989). Upper Kaskaskia Sequence: Uppermost Devonian and Lower Carboniferous. In B. D. Ricketts (Ed.), Western Canada Sedimentary Basin. A Case History. Canadian Society of Petroleum Geologists, Calgary, Alberta. p. 165-201.

Rider, M. H. (1986). The geological interpretation of well logs. Blackie. London. 175pp.

Rider, M. H. (1990). Gamma ray log shape used as a facies indicator: critical analysis of an oversimplified methodology. In: Hurst, A., Lovell, M. A., and Morton, A. C. (Eds). Geological applications of wireline logs. Geological Society Special Publication No. 48, 27-37.

Riediger, C.L., Brooks, P.W., Fowler, M.G. and Snowdon, L.R. (1990). Lower and Middle Triassic source rocks, thermal maturation, and oil-source rock correlations in the Peace River Embayment area, Alberta and British Columbia. Bulletin of Canadian Petroleum Geology, 38A; 218-235.

Roep, T. B., Beets, D. J., Dronkert, H., and Pagnier, H. (1979). A prograding coastal sequence of wave-built structures of Messinian age, Sorbas, Almeria, Spain. Sedimentary Geology, 22; 135-163.

Roy, K. J. (1972). The Boundary Member: A buried erosional remnant of Triassic age in northeastern British Columbia. Bulletin of Canadian Petroleum Geology, 20; 27-57.

Schnitker, D., Mayer, L. M. and Norton, S. (1980). Loss of calcareous microfossils from sediments through gypsum formation. Marine Geology, 36; M35-M44.

Schreiber, B. C. (1986). Arid shorelines and evaporites. In: H.G. Reading (Ed.), Sedimentary Environments and Facies (2nd Edn.). Blackwell. Oxford. p. 189-228.

Schwartz, M. L. (1967). The Bruun theory of sea level rise as a cause of shore erosion. Journal of Geology, 75; 76-91.

Schwartz, R. K. (1975). Nature and genesis of some storm washover deposits. U. S. Army Corps of Engineers coastal engineering centre technical memoir 61. 69 p.

Schwartz, R. K. (1982). Bedform and stratification characteristics of some modern small-scale washover sand bodies. Sedimentology, 29; 835-849.

Sha, L. P. (1990). Surface sediments and sequence models in the ebb-tidal delta of Texel Inlet, Wadden Sea, the Netherlands. Sedimentary Geology, 68; 125-141.

Sharma, G. D. (1969). Paragenetic evolution in Peejay Field, British Columbia, Canada. Mineral. Deposita, 4; 346-354.

Shearman, D. J. (1985). Syndepositional and late diagenetic alteration of primary gypsum. In: Schreiber, B.C. (Ed.), Sixth Salt Symposium. Northern Ohio Geological Society, Cleveland.

Shinn, E. A., Lloyd, R. M., and Ginsburg, R. N. (1969). Anatomy of a modern carbonate tidal flat, Andros Island, Bahamas. Journal of Sedimentary Petrology, 39; 1202-1228.

Siemers, C. T. and Tillman, R. W. (1981). Recommendations for the proper handling of cores and sedimentological analysis of core sequences. In: Siemers, C. T., Tillman, R. W. and Williamson, C. R. (Eds.), Deep-water clastic sediments: A core workshop. S.E.P.M. Core Workshop No. 2. p. 20-44.

Siesser, W. G. and Rogers, J. (1976). Authigenic pyrite and gypsum in South West African continental slope sediments. Sedimentology, 23; 567-577.

Silberling, N. J. and Tozer, E. T. (1968). Biostratigraphic classification of the marine Triassic in North America. Geological Society of America Special Paper 110.

Smith, P. L., and Tipper, H. W. (1986). Plate tectonics and palaeobiogeography. Early Jurassic (Pliensbachian) endemism and diversity. Palaios, 1; 399-412.

Snedden, J. W., Nummedal, D., and Amos, A. (1988). Storm- and fairweather combined flow on the central Texas continental shelf. Journal of Sedimentary Petrology, 58; 580-595.

Styan, W. and Shaw, J. (1991). An overview of Triassic Halfway pools in the Progress area (abstract). Bulletin of Canadian Petroleum Geology, 39; 226.

Suter, J. R., Berryhill, H. L. and Penland, S. (1987). Late Quaternary sea-level fluctuations and depositional sequences, southwest Louisiana continental shelf. In: Nummedal, D., Pilkey, O. H., and Howard, J. D. (Eds), Sea level fluctuation and coastal evolution. Society of Economic Paleontologists and Mineralogists Special Publication No. 41. p. 199-219.

Swanson, R. G. (1981). Sample examination manual. Methods in Exploration series. American Association of Petroleum Geologists. Tulsa, Oklahoma.

Swift, D. J. P. (1968). Coastal erosion and transgressive stratigraphy. Journal of Geology, 76; 444-456.

Swift, D. J. P. (1975). Barrier island genesis: evidence from the Middle Atlantic Shelf of North America. Sedimentary Geology, 14; 1-43.

Swift, D. J. P., Niedoroda, A. W., Vincent, C. E., and Hopkins, T. S. (1985). Barrier island evolution, middle Atlantic shelf, U.S.A. Part 1: Shoreface dynamics. Marine Geology, 63; 331-361.

Tankard, A. J. and Hobday, D. K. (1977). Tide-dominated back-barrier sedimentation, early Ordovician Cape Basin, Cape Peninsula, South Africa. Sedimentary Geology, 18; 135-159.

Taverner-Smith, R. (1982). Prograding coastal facies associations in the Vryheid Formation (Permian) at Effingham Quarries near Durban, South Africa. Sedimentary Geology, 32; 111-140.

Tempelman-Kluit, D. J. (1979). Transported cataclasite, ophiolite and granodiorite in Yukon: evidence of arc-continent collision. Geological Survey of Canada Paper 79-14. 27 p.

Terwindt, J. H. J. (1971). Lithofacies of inshore estuarine and tidal inlet deposits. Geologie en Mijnbouw, 50; 515-526.

Thompson, R. W. (1968). Tidal flat sedimentation on the Colorado River delta, northwestern Gulf of California. Geological Society of America Memoir 107.

Torrie, J. E. (1973). Northeastern British Columbia. In: R. G. McCrossan (Ed.), Future petroleum provinces of Canada. Canadian Society of Petroleum Geologists Memoir 1. p. 151-186.

Tozer, E. T. (1961). The sequence of marine Triassic faunas in western Canada. Geological Survey of Canada Paper 61-6.

Tozer, E. T. (1967). A standard for Triassic time. Geological Survey of Canada Bulletin 156.

Tozer, E.T. (1982). Marine Triassic faunas of North America: Their significance for assessing plate and terrane movements. Geologische Rundschau, 71; 1077-1104.

Tye, R. S. (1984). Geomorphic evolution and stratigraphy of Price and Capers Inlets, South Carolina. Sedimentology, 31; 655-674.

Tye, R. S. and Moslow, T. F. (In press, 1992). Tidal inlet reservoirs: insights from modern examples. In: Rhodes, E. G. and Moslow, T. F. (Eds.), Marine Clastic Reservoirs. Springer-Verlag. New York, New York.

Uhlir, D. M., Akers, A., and Vondra, C. F. (1988). Tidal inlet sequence, Sundance Formation (Upper Jurassic), north-central Wyoming. Sedimentology, 35; 739-752.

Van Straaten, L.M.J.U. (1956). Composition of shell beds formed in tidal flat environments in the Netherlands and in the Bay of Arachon (France). Geologie en Mijnbouw, 18; 209-226.

Van Wagoner, J. C., Posamentier, H. W., Mitchum, R. M., Vail, P. R., Sarg, J. F., Loutit, T. S., and Hardenbol, J. (1988). An overview of the fundamentals of sequence stratigraphy and key definitions. In: Wilgus, C. K., Hastings, B.S., Kendall, C.G., Posamentier, H.W., Ross, C.A., and Van Wagoner, J.C (Eds.). Sea-Level Changes- An Integrated Approach. Society of Economic Paleontologists and Mineralogists Special Publication No. 42. p. 39-46.

Van Wagoner, J. C., Mitchum, R. M., Campion, K. M., and Rahmanian, V. D. (1990). Siliciclastic sequence stratigraphy in well logs, cores, and outcrops. A.A.P.G. Methods in Exploration Series, No. 7. Tulsa, Oklahoma. 55 p.

Visser, M. J. (1980). Neap-spring cycles reflected in Holocene subtidal large-scale bedform deposits: a preliminary note. Geology, 8; 543-546.

Warren, P. S. (1945). Triassic faunas in the Canadian Rockies. American Journal of Science, 243; 480-491.

Winn, R. D. (1991). Storm deposition in marine sand sheets: Wall Creek Member, Frontier Formation, Powder River Basin, Wyoming. Journal of Sedimentary Petrology, 61; 86-101.

Wittenberg, J. (1992). Origin and stratigraphic significance of anomalously thick sandstone trends in the Middle Triassic Doig Formation of west-central Alberta. Unpublished M.Sc. thesis, University of Alberta, Edmonton, Canada. 290 p.

Wittenberg, J. and Moslow, T.F. (1991). Origin and facies variability of overthickened sandstones in the Middle Triassic Doig Formation, west-central Alberta (abstract). Bulletin of Canadian Petroleum Geology. v.39; 228.

Wojtal-Duc, A. and Tye, R. S. (1987). Evolution and stratigraphy of a regressive barrier / backbarrier complex: Kiawah Island, South Carolina. Sedimentology, 34; 237-251.

Yang, C. S. and Nio, S. D. (1989). An ebb-tide delta depositional model-a comparison between the modern Eastern Scheldt tidal basin (southwest Netherlands) and the Lower Eocene Roda Sandstone in the southern Pyranees (Spain). Sedimentary Geology, 64; 175-196.

APPENDIX A.

Appendix A contains lithological descriptions of the cored Halfway intervals examined during this study.

Key to Symbols Used:

Lithology:

Claystone / Shale

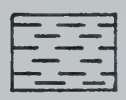
Siltstone

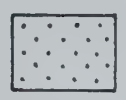
Sandstone

Limestone

Dolomite

Anhydrite

Conglomerate

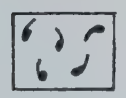
Bioclastic material

Lithological Contacts:

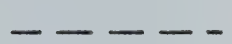
Gradational

Abrupt

Erosional

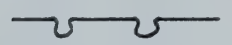
Loaded

Stylolitic

Desiccation Cracks

WELL NAME: Amoco Dunsmuir FORMATION: DATE:

LOCATION: 7-31-71-7-W6 CORE INTERVAL: KB:

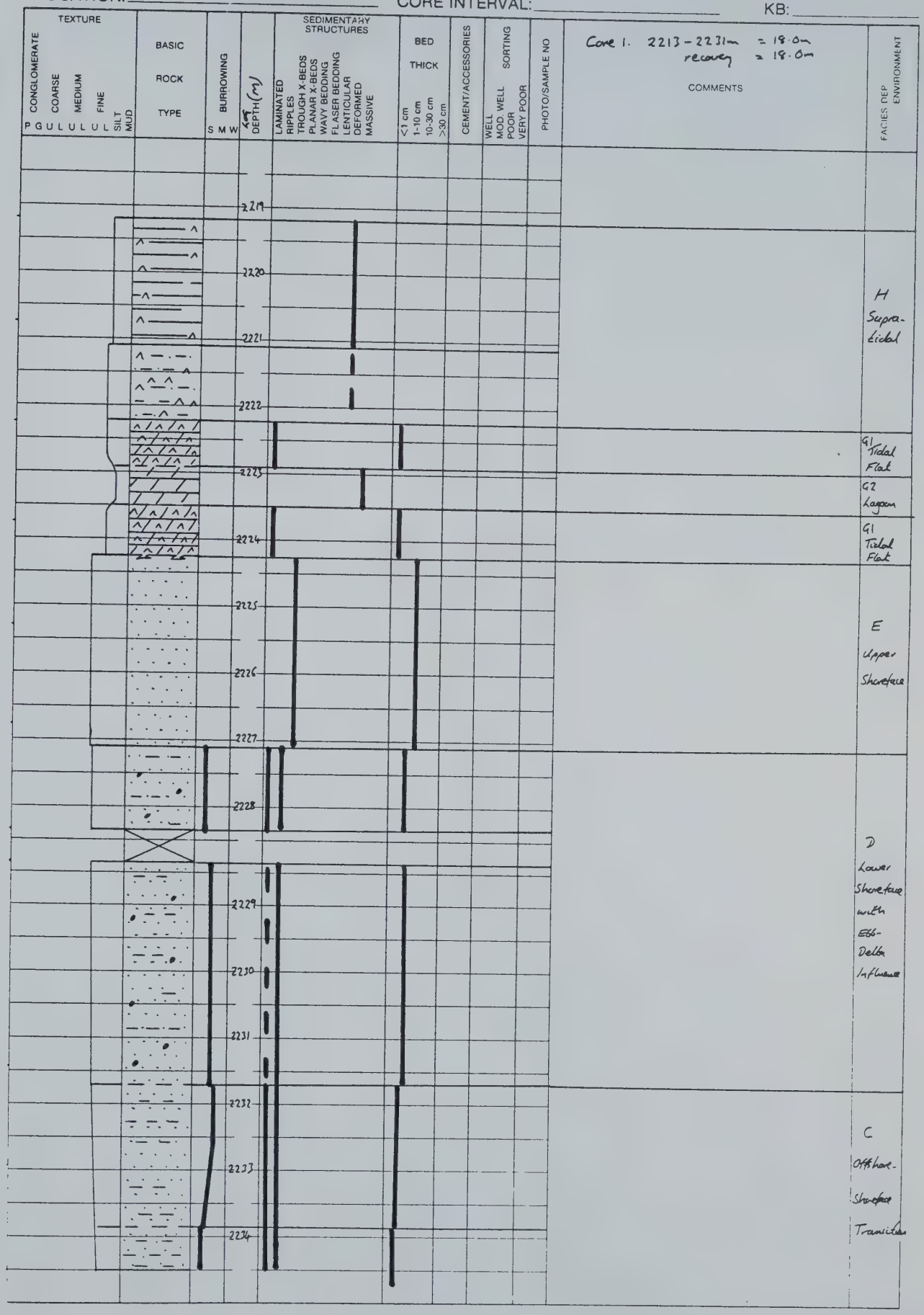

WELL NAME: (2/2) 7-31-71-7-W6 FORMATION: DATE:

LOCATION: CORE INTERVAL: KB:

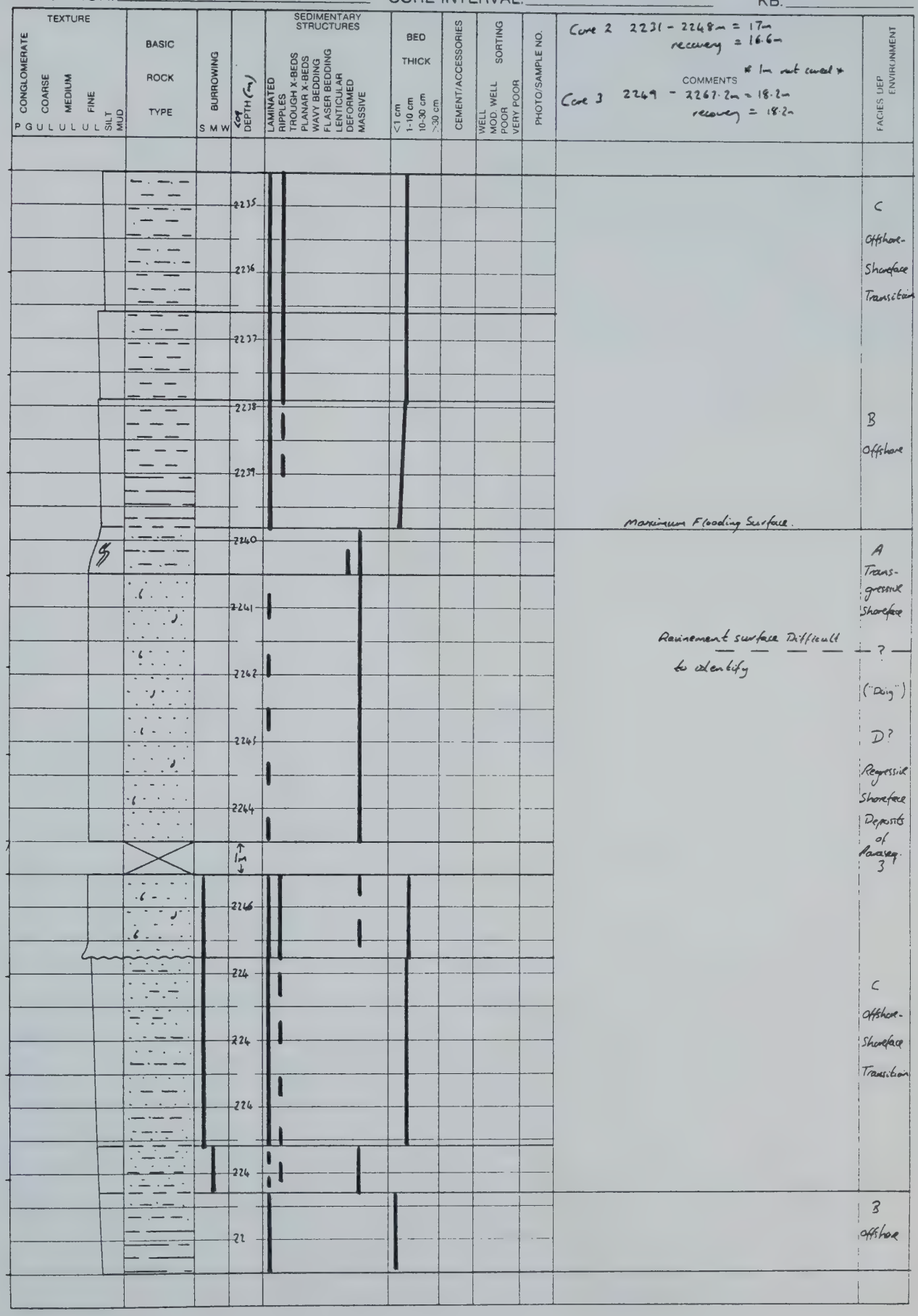

WELL NAME: Gulf et al Wembley 102/6-25-71-8-W6 FORMATION: DATE:

LOCATION: CORE INTERVAL: KB:

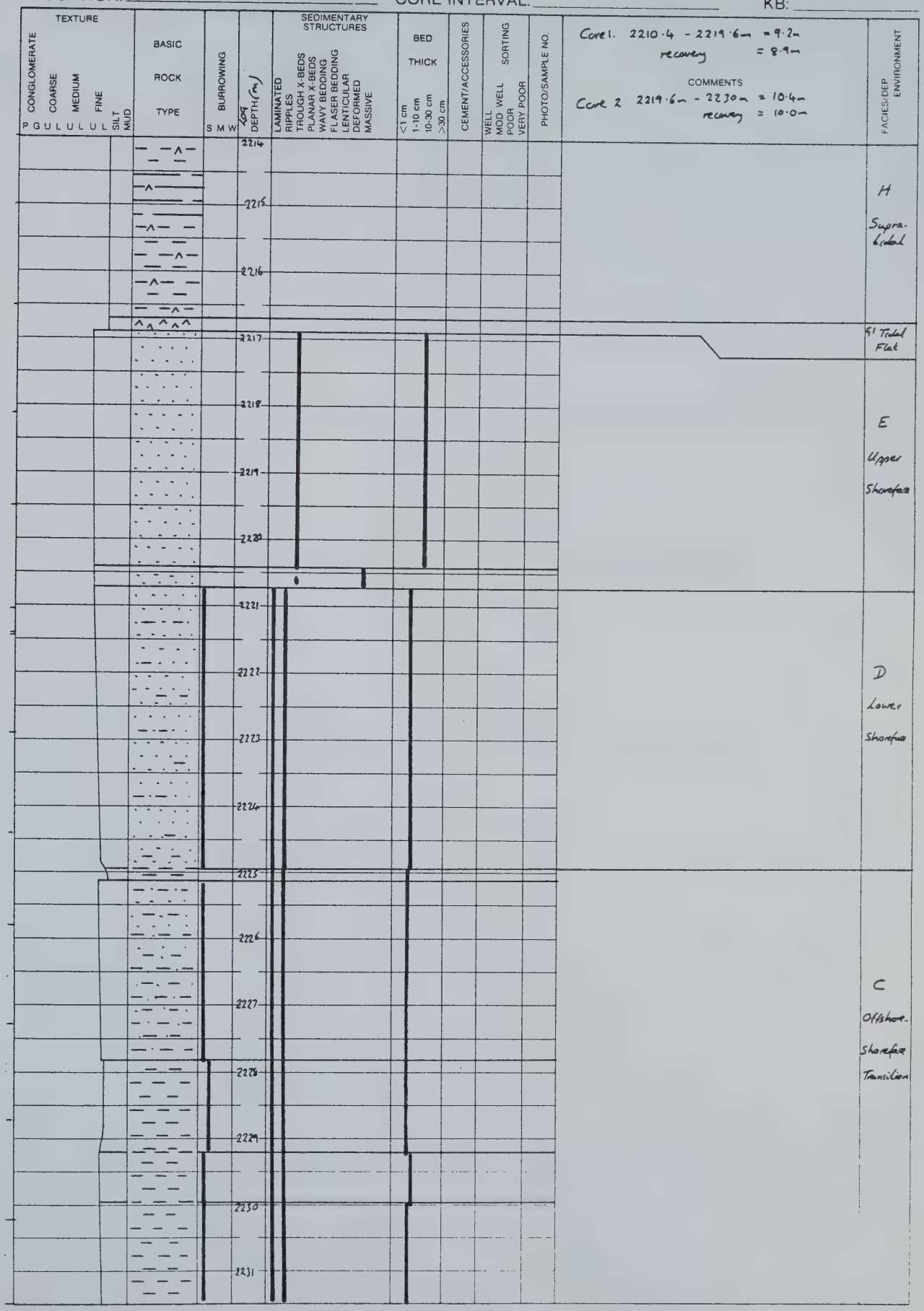

WELL NAME: Colonial Amoco Wembley 14-28-71-8-W6 FORMATION: DATE:

LOCATION: CORE INTERVAL: KB:

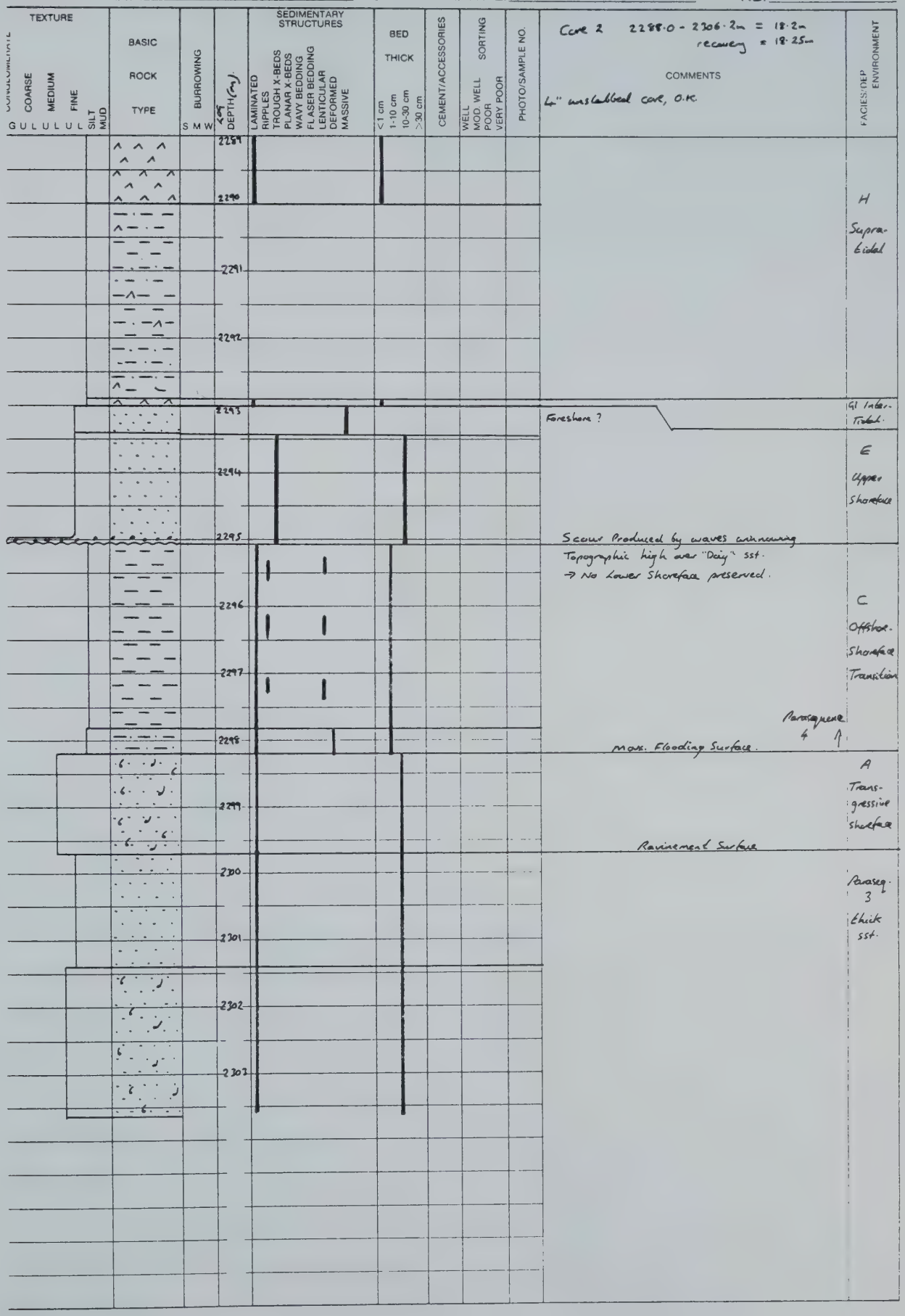

WELL NAME: Colonial Amoco Wembley 8-30-71-8-W6 FORMATION: _____ DATE: _____

LOCATION: _____ CORE INTERVAL: _____ KB: _____

TEXTURE (CONGLOMERATE, COARSE, MEDIUM, FINE, SILT, MUD)	BASIC ROCK TYPE	BURROWING (S M W)	DEPTH (m)	SEDIMENTARY STRUCTURES (LAMINATED, RIPPLES, TROUGH X-BEDS, PLANAR X-BEDS, WAVY BEDDING, FLASER BEDDING, LENTICULAR, DEFORMED, MASSIVE)	BED THICK (<1 cm, 1-10 cm, 10-30 cm, >30 cm)	CEMENT/ACCESSORIES	SORTING (WELL, MOD. WELL, POOR, VERY POOR)	PHOTO/SAMPLE NO.	COMMENTS	FACIES/DEP ENVIRONMENT
									Core 2 2350.0 - 2368.2m = 18.2m recovery = 17.9m	
									4" unslabbed core, OK.	
			2350						Black shale cavings?	
			2351							
			2352							J
			2353							Active
			2354							Tidal
			2355							Inlet
			2356							Fill
			2357							
			2358							
			2359							

WELL NAME: 2 FORMATION: DATE:

LOCATION: 8-30-71-8-W6 CORE INTERVAL: KB:

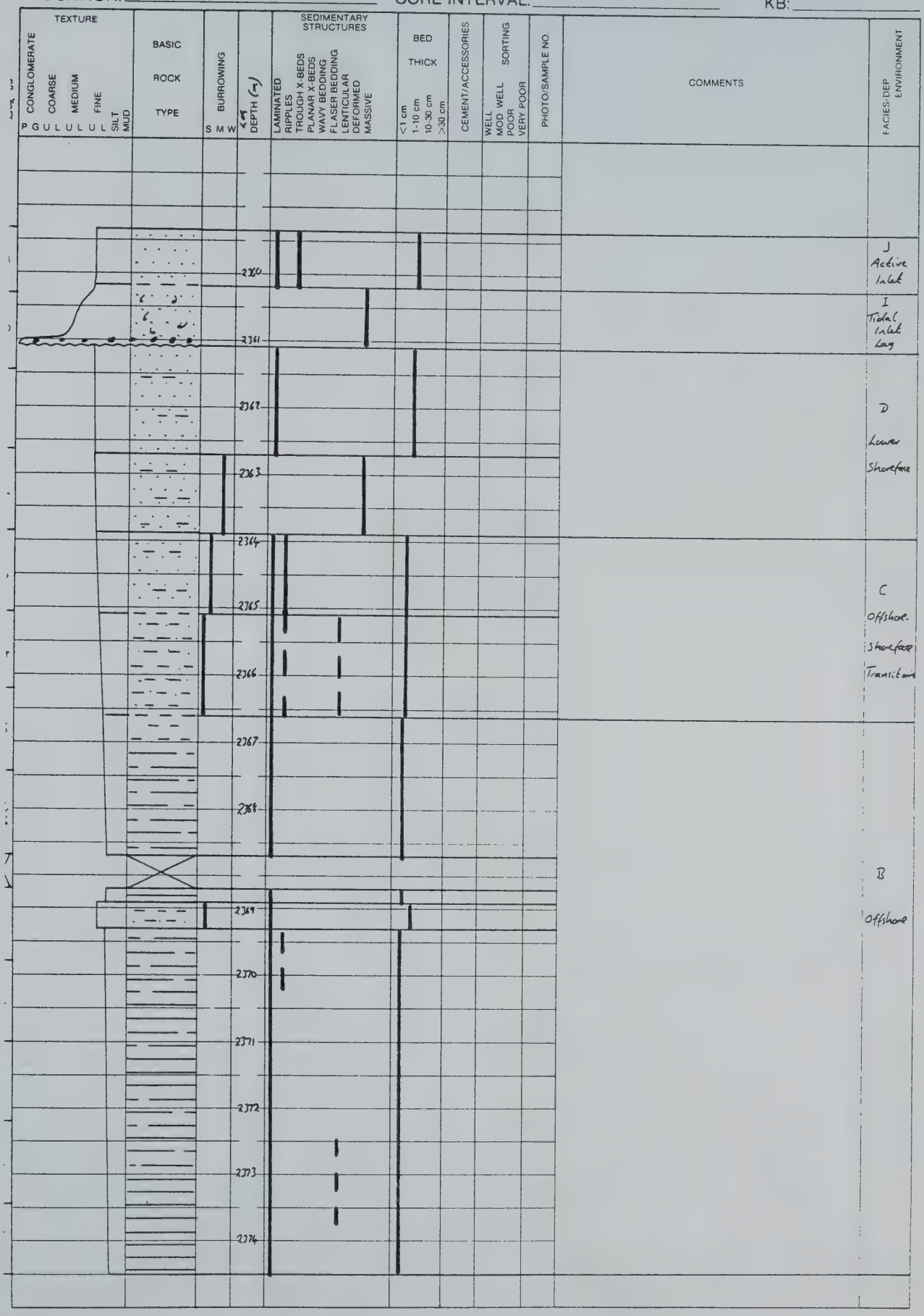

WELL NAME: Colonial Amoco Albright 6-10-71-9-W6 FORMATION: DATE:

LOCATION: CORE INTERVAL: KB:

TEXTURE (CONGLOMERATE, COARSE, MEDIUM, FINE, SILT, MUD)	BASIC ROCK TYPE	BURROWING (S M W)	DEPTH (m)	SEDIMENTARY STRUCTURES (LAMINATED, RIPPLES, TROUGH X-BEDS, PLANAR X-BEDS, WAVY BEDDING, FLASER BEDDING, LENTICULAR, DEFORMED, MASSIVE)	BED THICK (<1 cm, 1-10 cm, 10-30 cm, >30 cm)	CEMENT/ACCESSORIES	SORTING (WELL, MOD. WELL, POOR, VERY POOR)	PHOTO/SAMPLE NO	COMMENTS	FACIES/DEP ENVIRONMENT
									Core 4. 2414.0 - 2432.2m = 18.2m recovery = 16.4m measured 17.1m	
			2415							
			2416							
			2417							
			2418							H Supra-tidal flat
			2419							
			2420							
			2421							
			2422							
			2423							
			2424							
			2425							G? Lagoon
			2426							
			2427							J Active Tidal Inlet
			2428							
			2429							
			2430							I Inlet Lag.
			2431							

WELL NAME: (2/2) 6-10-71-9-W6 FORMATION: DATE:

LOCATION: CORE INTERVAL: KB:

TEXTURE (CONGLOMERATE, COARSE, MEDIUM, FINE, SILT, MUD)	BASIC ROCK TYPE	BURROWING (S M W)	DEPTH	SEDIMENTARY STRUCTURES (LAMINATED, RIPPLES, TROUGH X-BEDS, PLANAR X-BEDS, WAVY BEDDING, FLASER BEDDING, LENTICULAR, DEFORMED, MASSIVE)	BED THICK (<1 cm, 1-10 cm, 10-30 cm, >30 cm)	CEMENT/ACCESSORIES	SORTING (WELL, MOD. WELL, POOR, VERY POOR)	PHOTO/SAMPLE NO.	COMMENTS	FACIES/DEP ENVIRONMENT
									Core 5. 2432.2 - 2450.4m = 18.2m recovery = 18.2m measured 18.6m. 4" unslabbed core, o.k.	
			2432							
			2433							
			2434							
			2435							
			2436							
			2437							C Offshore-Shoreface Transition
			2438							
			2439							
			2440							
			2441							
			2442							
			2443							
			2444							B Offshore
			2445							
			2446							
			2447							
			2448							
			2449							

WELL NAME: Colonial Amoco Albright 6-25-71-9-W6 FORMATION: DATE:

LOCATION: CORE INTERVAL: KB:

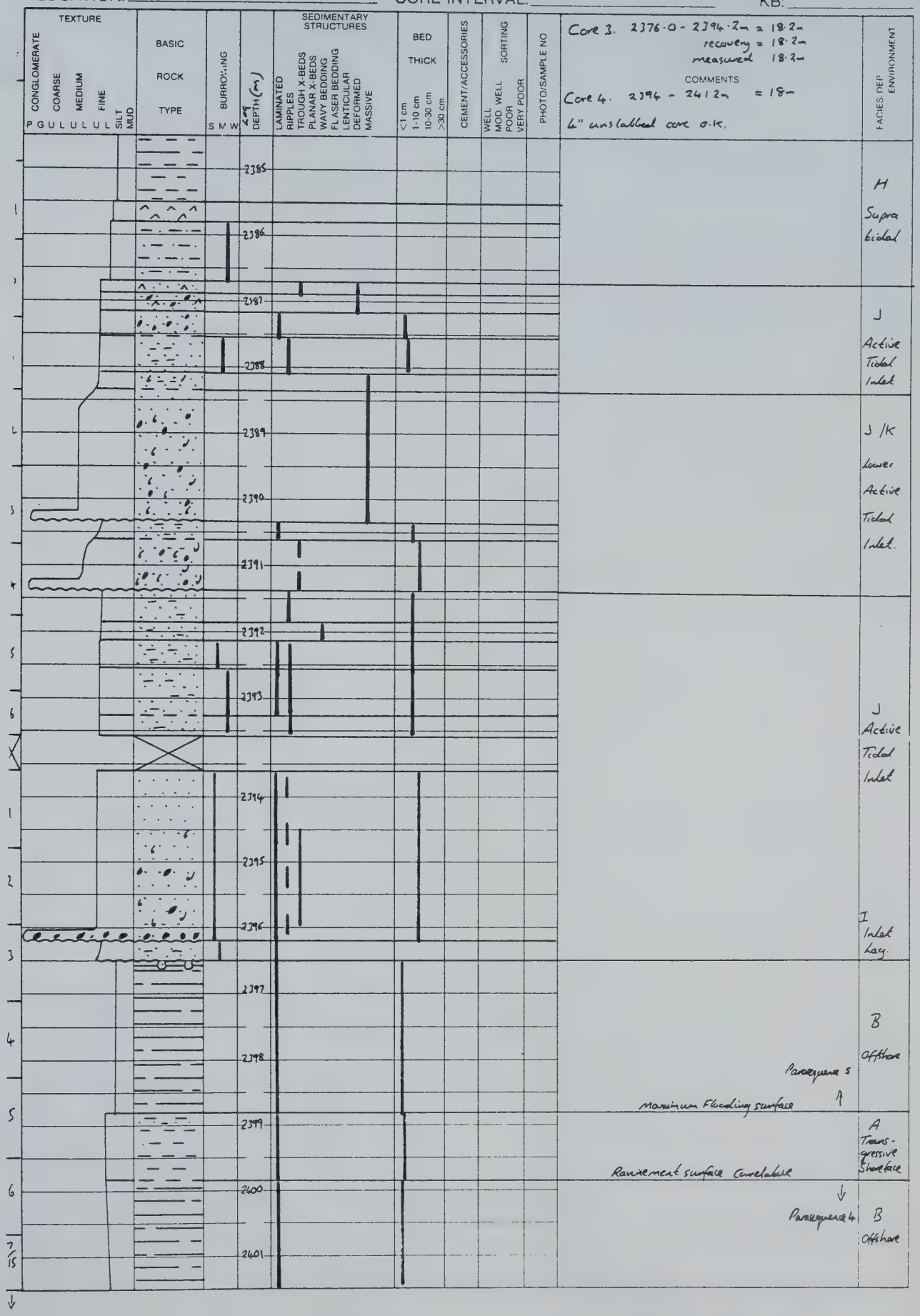

WELL NAME: Wincan et al Wembley

FORMATION:

DATE:

LOCATION: 14-4-72-7-W6

CORE INTERVAL:

KB:

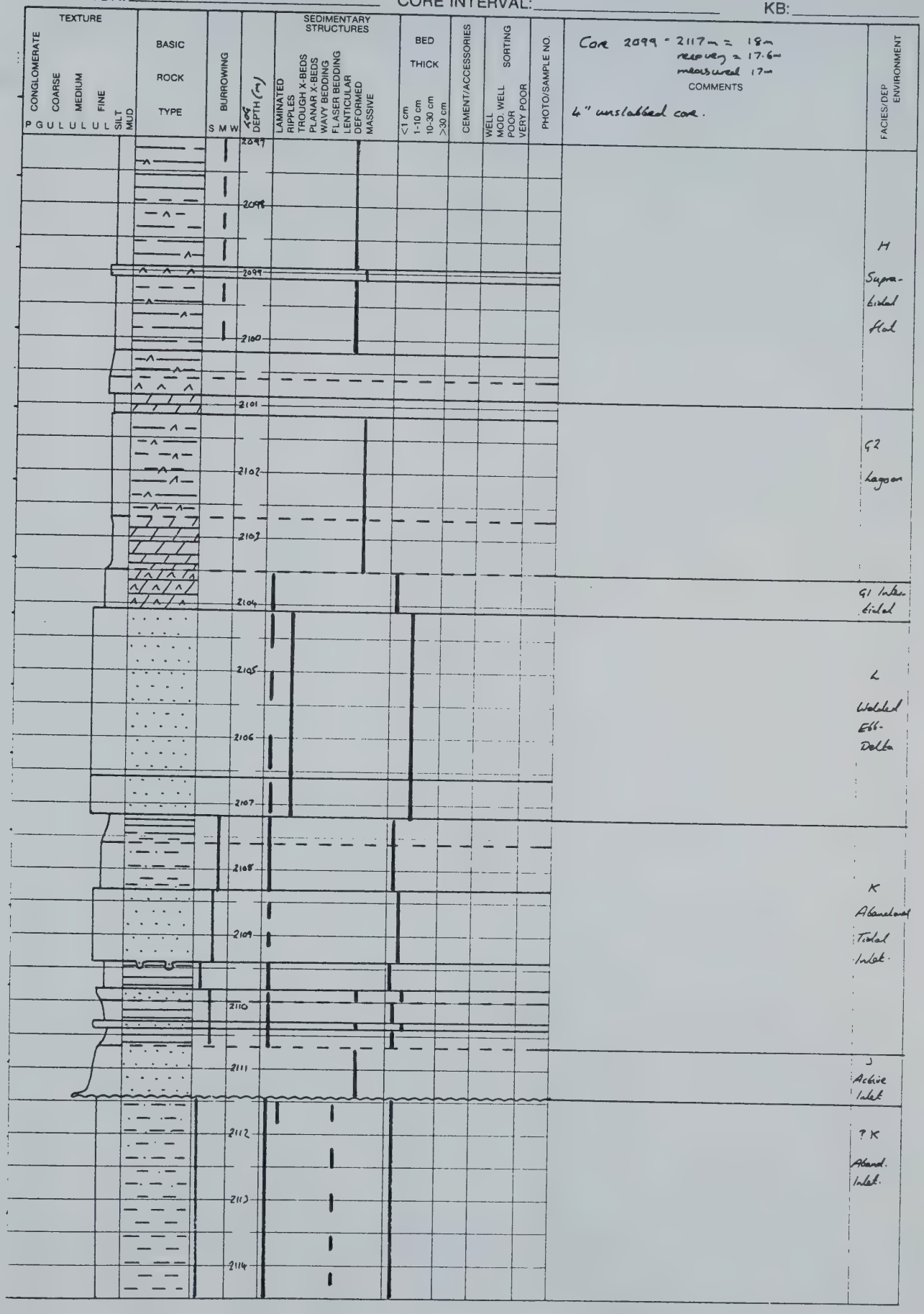

WELL NAME: PCP Wembley FORMATION: DATE:

LOCATION: 10-5-72-7-W6 CORE INTERVAL: KB:

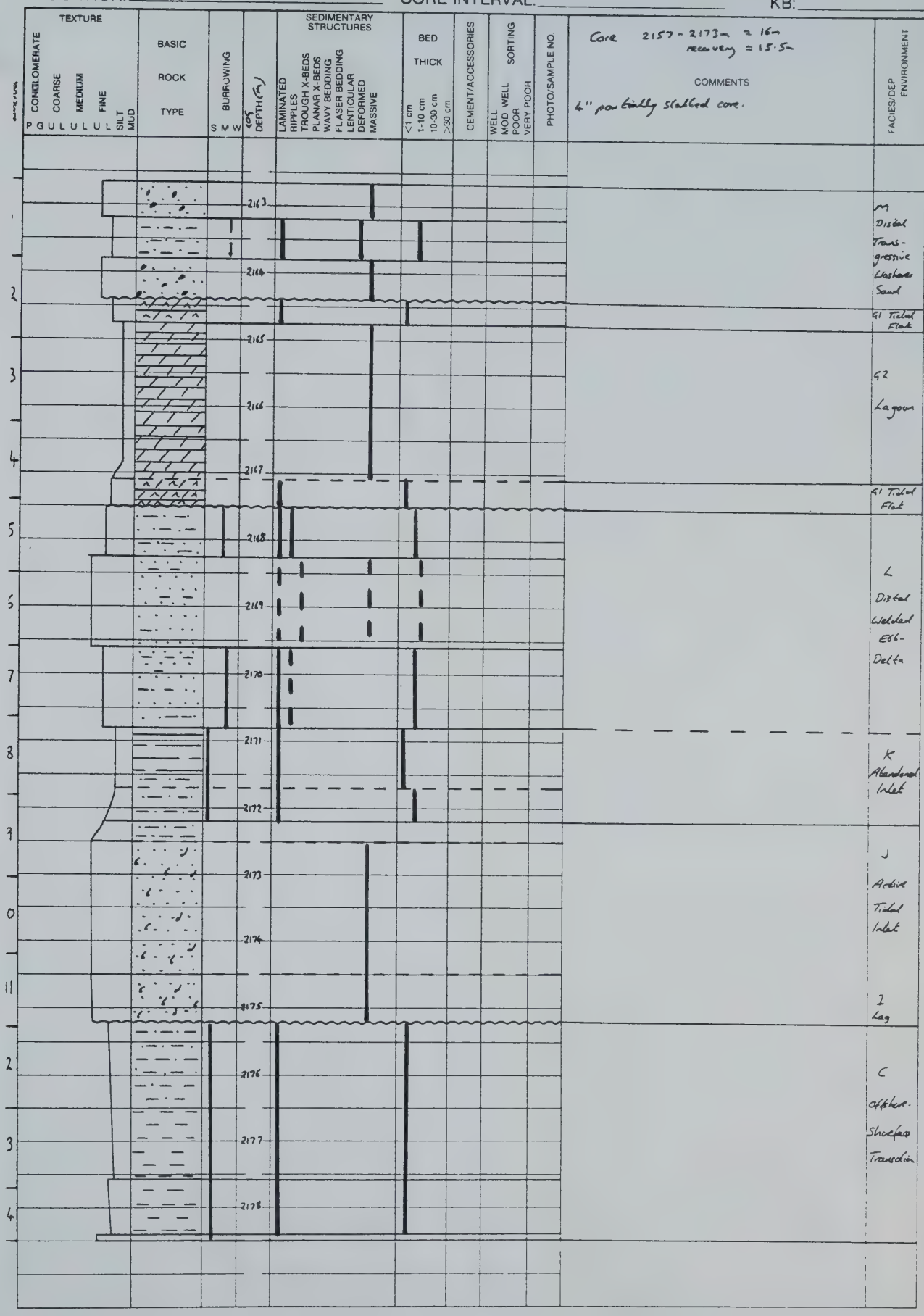

WELL NAME: Westburne et al Wembley FORMATION: DATE:

LOCATION: 6-6-72-7-W6 CORE INTERVAL: KB:

TEXTURE: CONGLOMERATE (P)	COARSE (G)	MEDIUM (U)	FINE (L)	SILT (U)	MUD (L)	BASIC ROCK TYPE	BURROWING S	M	W	DEPTH (m)	SEDIMENTARY STRUCTURES: LAMINATED	RIPPLES	TROUGH X-BEDS	PLANAR X-BEDS	WAVY BEDDING	FLASER BEDDING	LENTICULAR	DEFORMED	MASSIVE	BED THICK <1 cm	1-10 cm	10-30 cm	>30 cm	CEMENT/ACCESSORIES	SORTING WELL	MOD. WELL	POOR	VERY POOR	PHOTO/SAMPLE NO.	COMMENTS	FACIES/DEP ENVIRONMENT
																														Core. 2174.4 - 2183m = recovery = 6.0m Core 4m low.	
										2170																					
																															G1 Tidal Flat
										2171																					
										2172																					L
																															Welded
										2173																					E66-
																															Delta.
										2174																					
										2175																					
										2176																					

WELL NAME: Wesrburne et al Wembley

FORMATION:

DATE:

LOCATION: 6-7-72-7-W6

CORE INTERVAL:

KB:

Core 2143 - 2156 = 13.0m
recovery = 9.4m * core loss
measured 9.5m

3½" unslabbed core

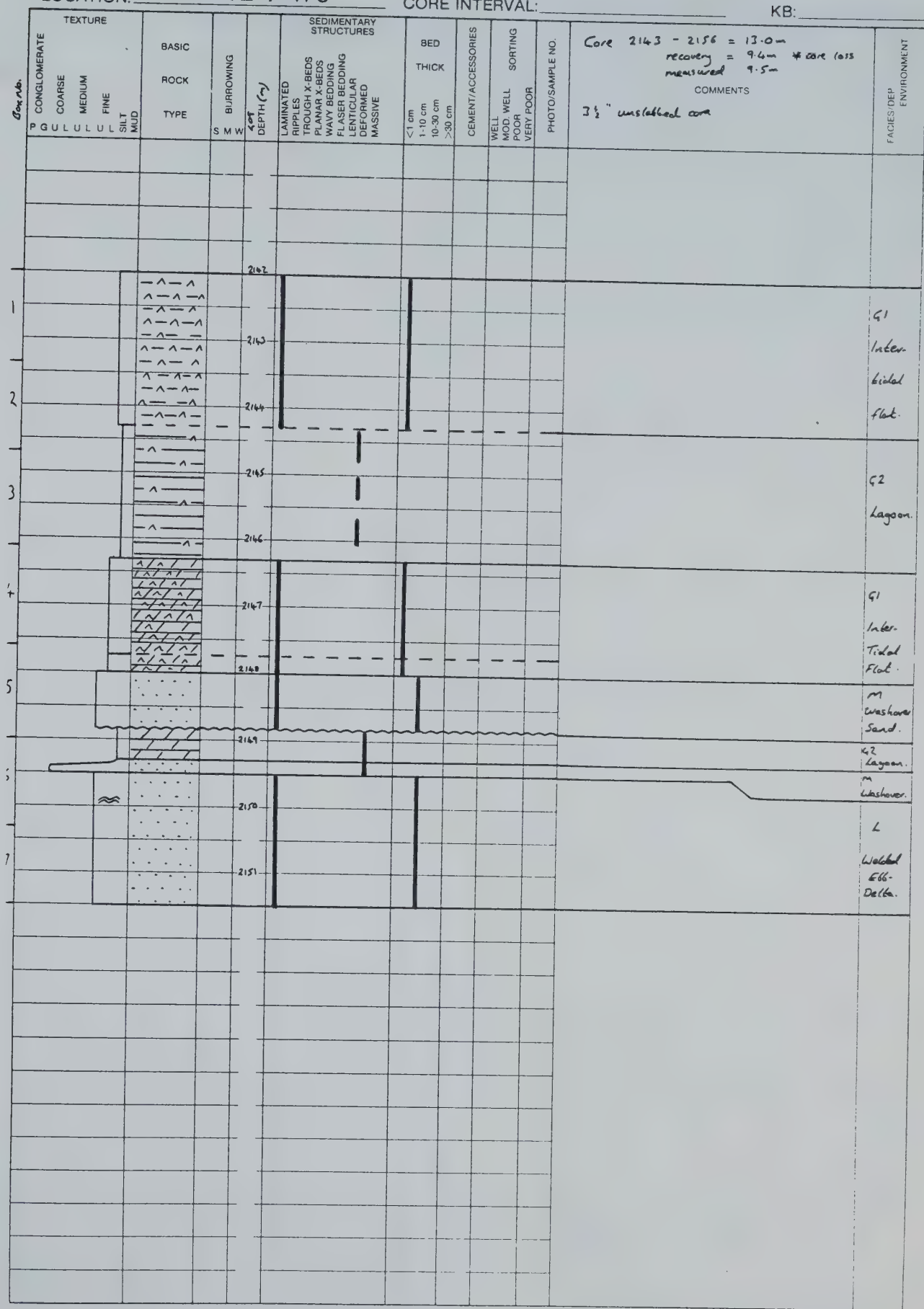

WELL NAME: Wincan Wembley FORMATION: DATE:

LOCATION: 8-8-72-7-W6 CORE INTERVAL: KB:

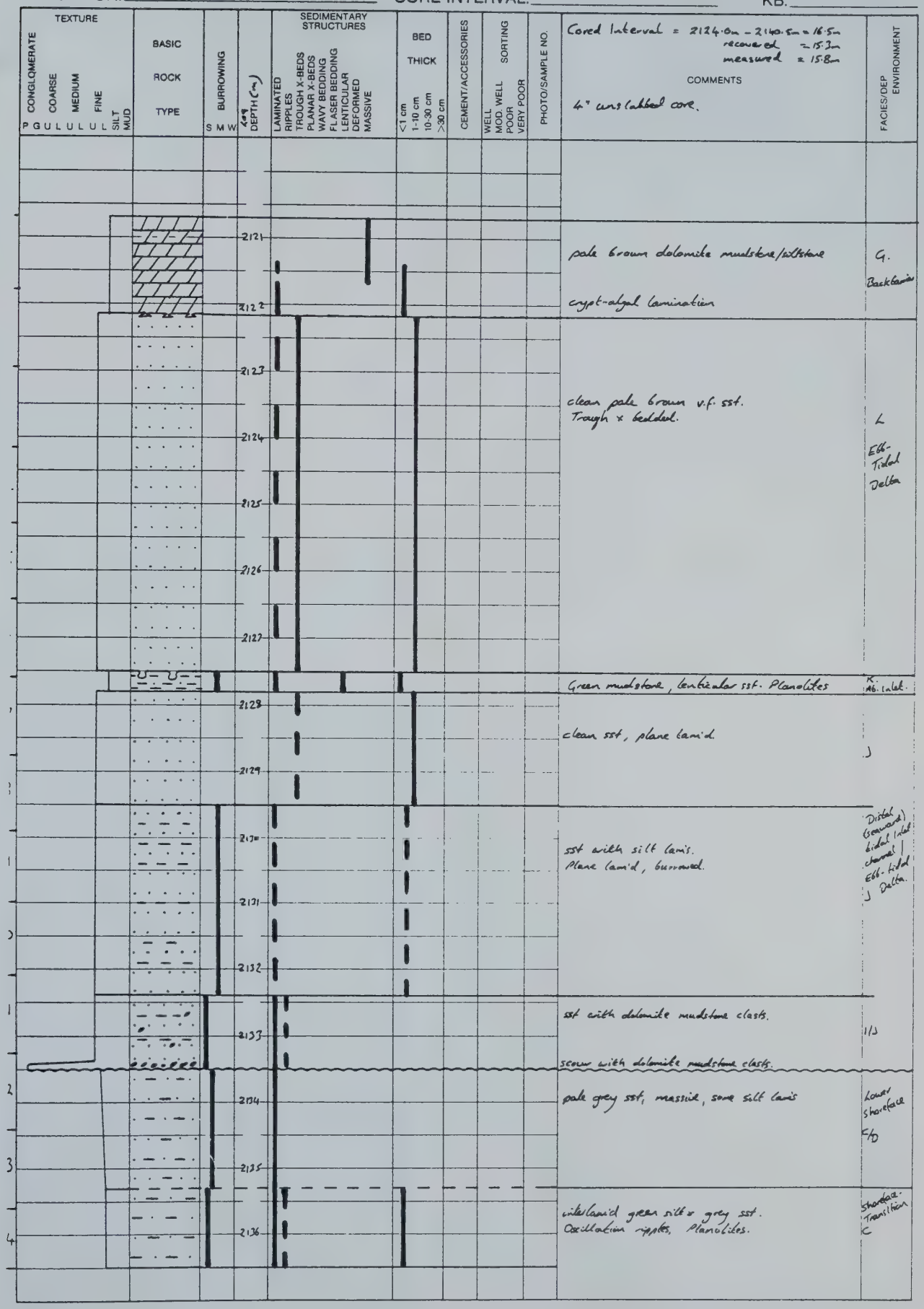

WELL NAME: Wincan et al Wembley FORMATION: DATE:

LOCATION: 14-8-72-7-W6 CORE INTERVAL: KB:

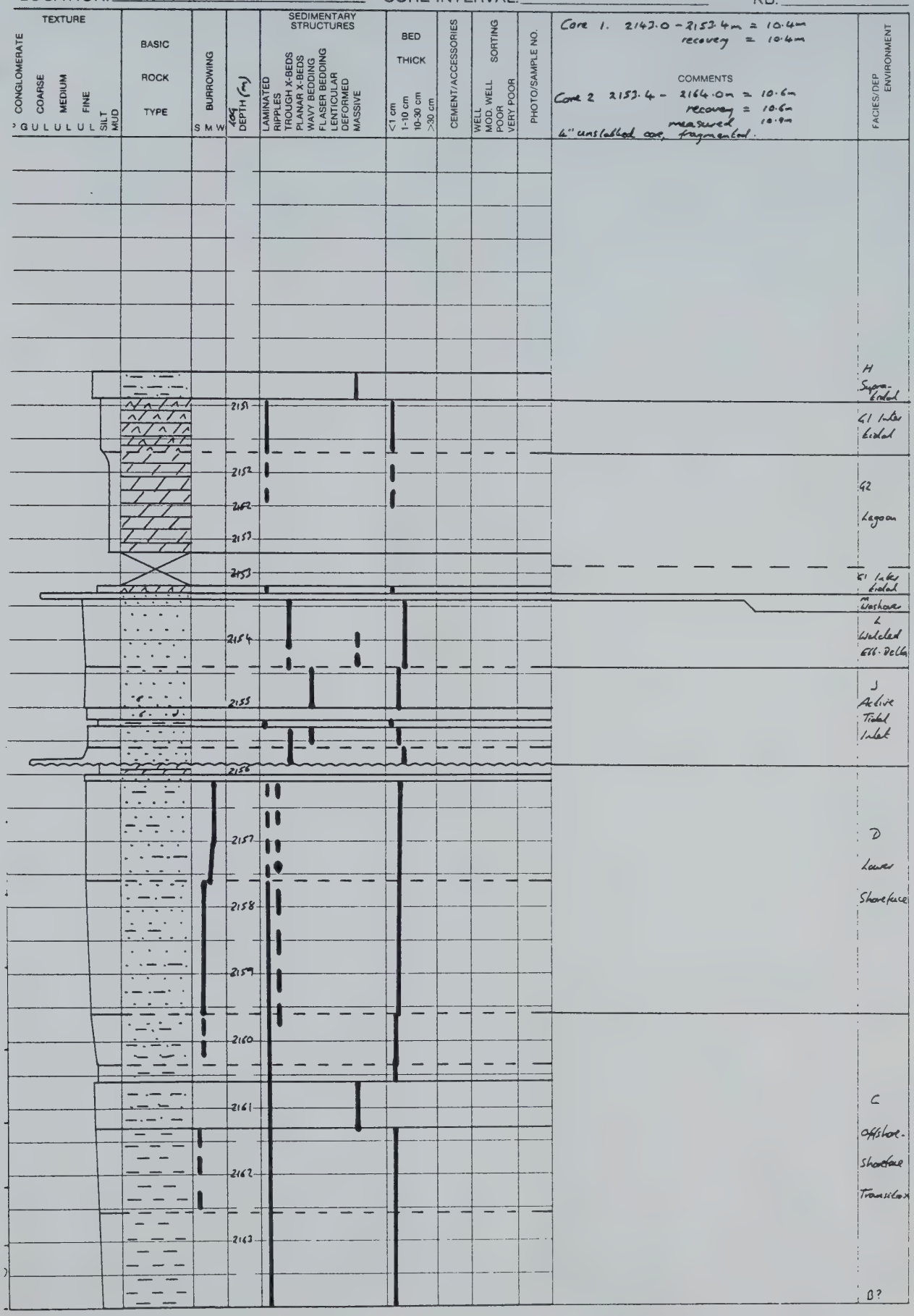

WELL NAME: Wincan et al Wembley FORMATION: DATE:

LOCATION: 8-9-72-7-W6 CORE INTERVAL: KB:

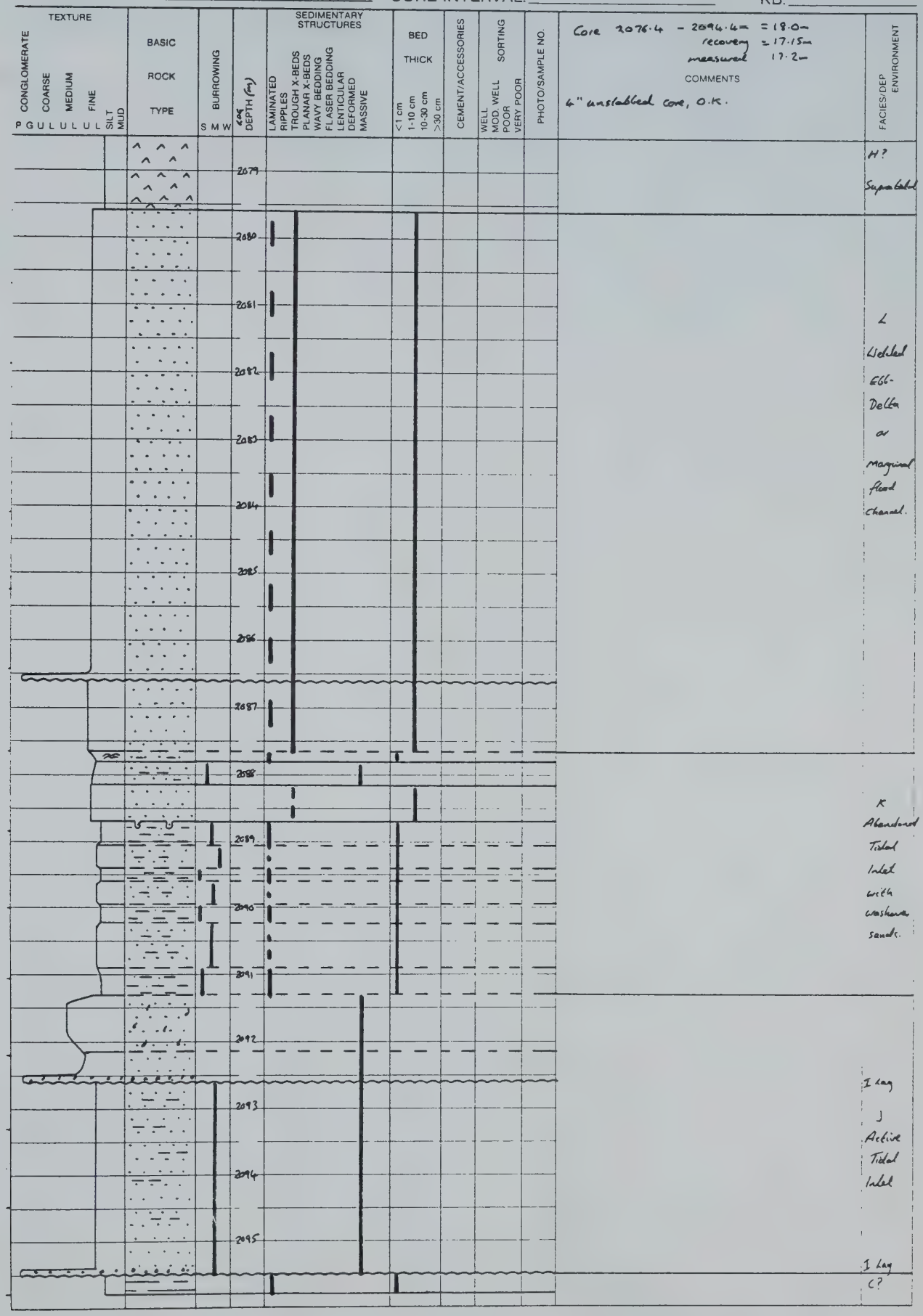

WELL NAME: Wincan et al Wembley FORMATION: DATE:

LOCATION: 14-9-72-7-W6 CORE INTERVAL: KB:

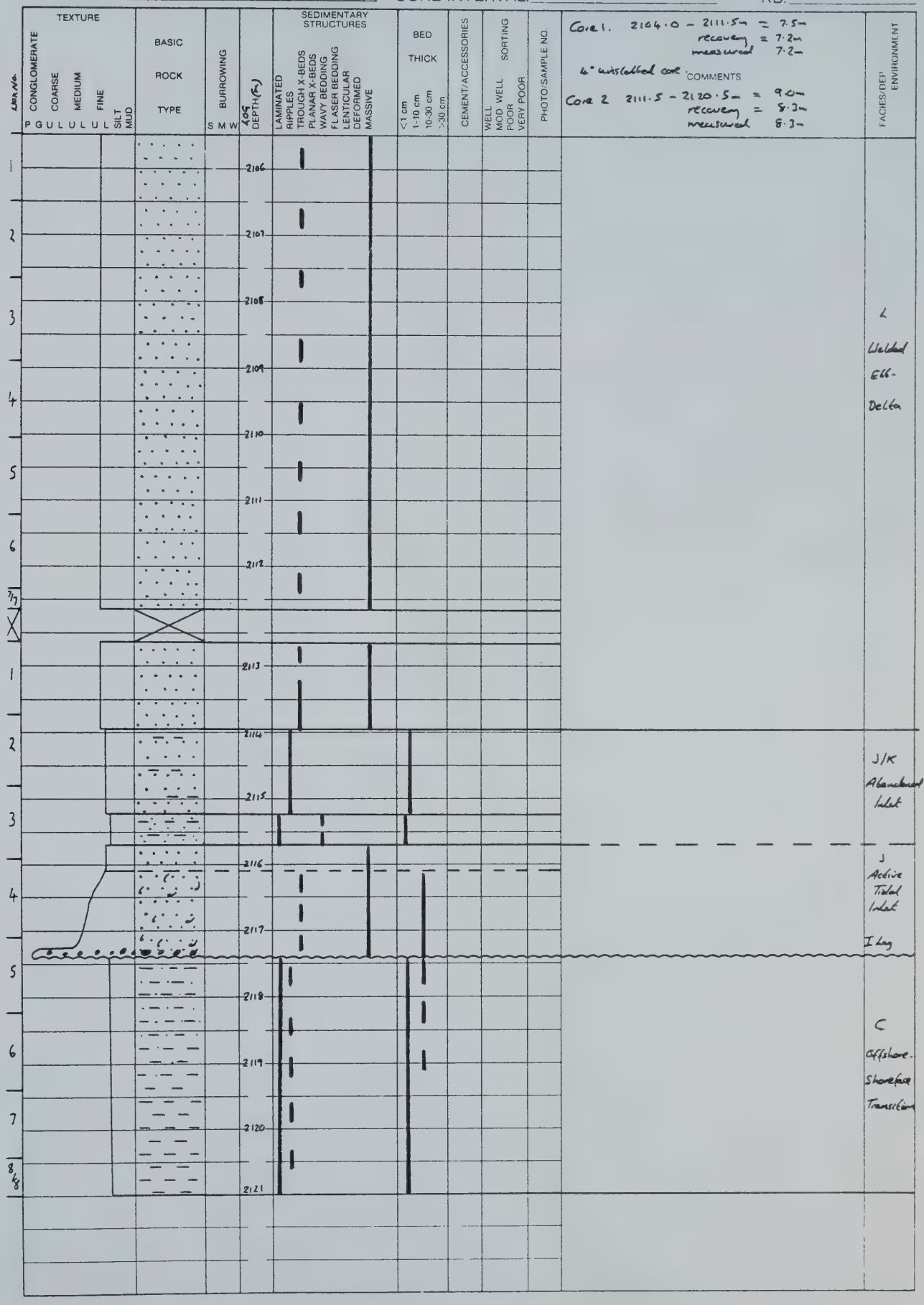

WELL NAME: PCP et al Dimsdale FORMATION: DATE:

LOCATION: 6-11-72-7-W6 CORE INTERVAL: KB:

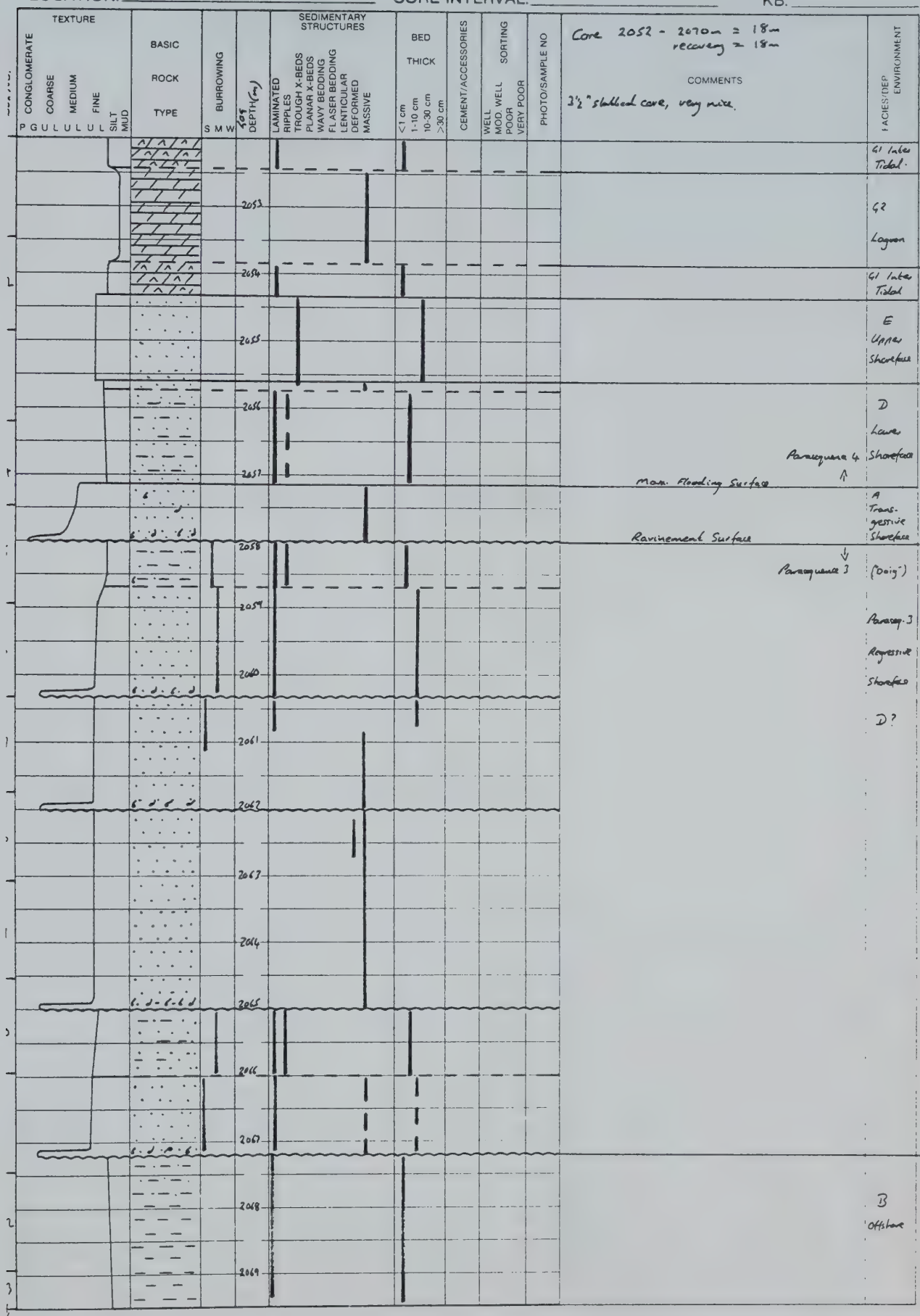

WELL NAME: PCP et al Wembley FORMATION: DATE:

LOCATION: 6-16-72-7-W6 CORE INTERVAL: KB:

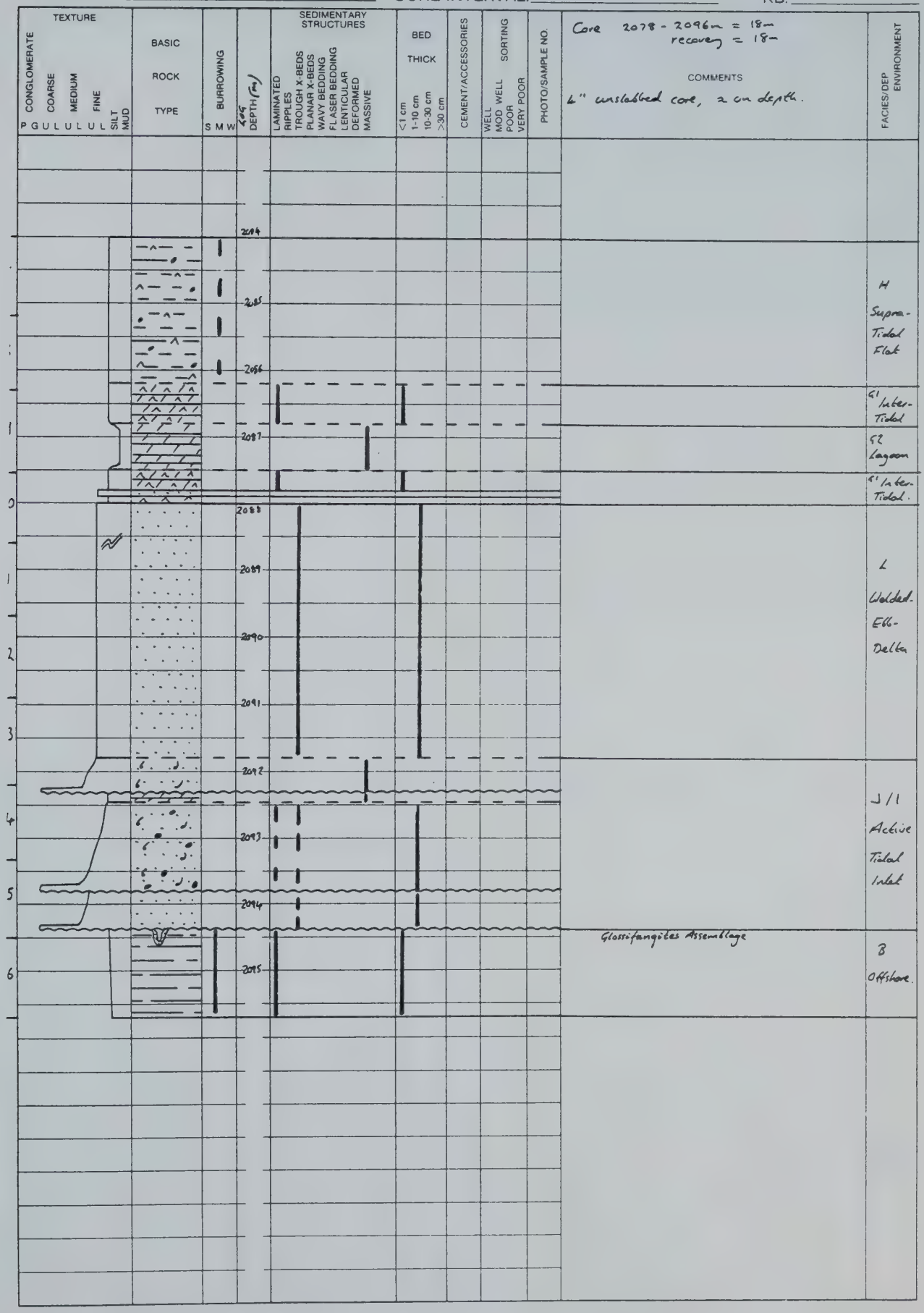

WELL NAME: PCP et al Wembley FORMATION: DATE:

LOCATION: 14-16-72-7-W6 CORE INTERVAL: KB:

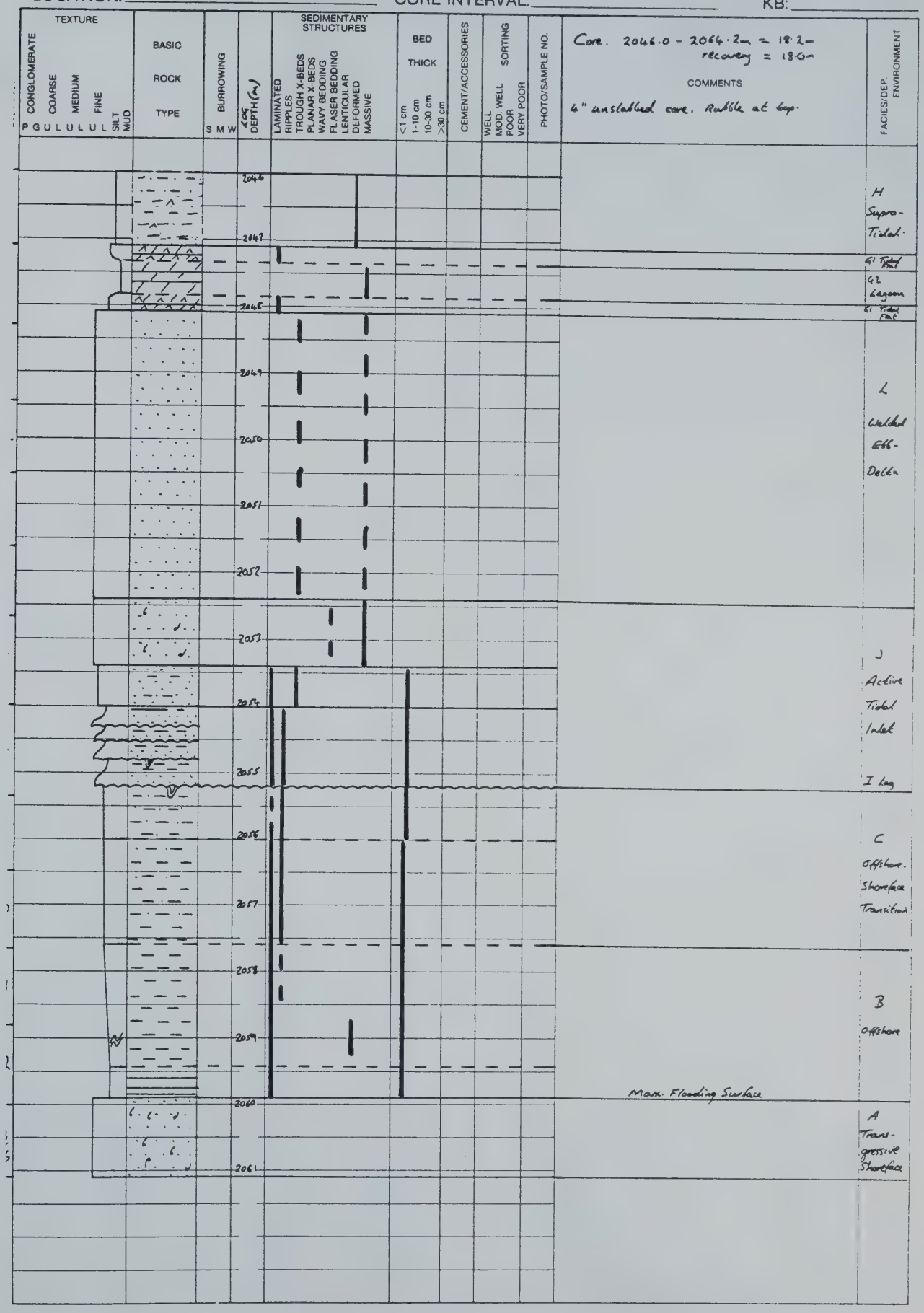

WELL NAME: PCP et al Wembley FORMATION: DATE:

LOCATION: 6-17-72-7-W6 CORE INTERVAL: KB:

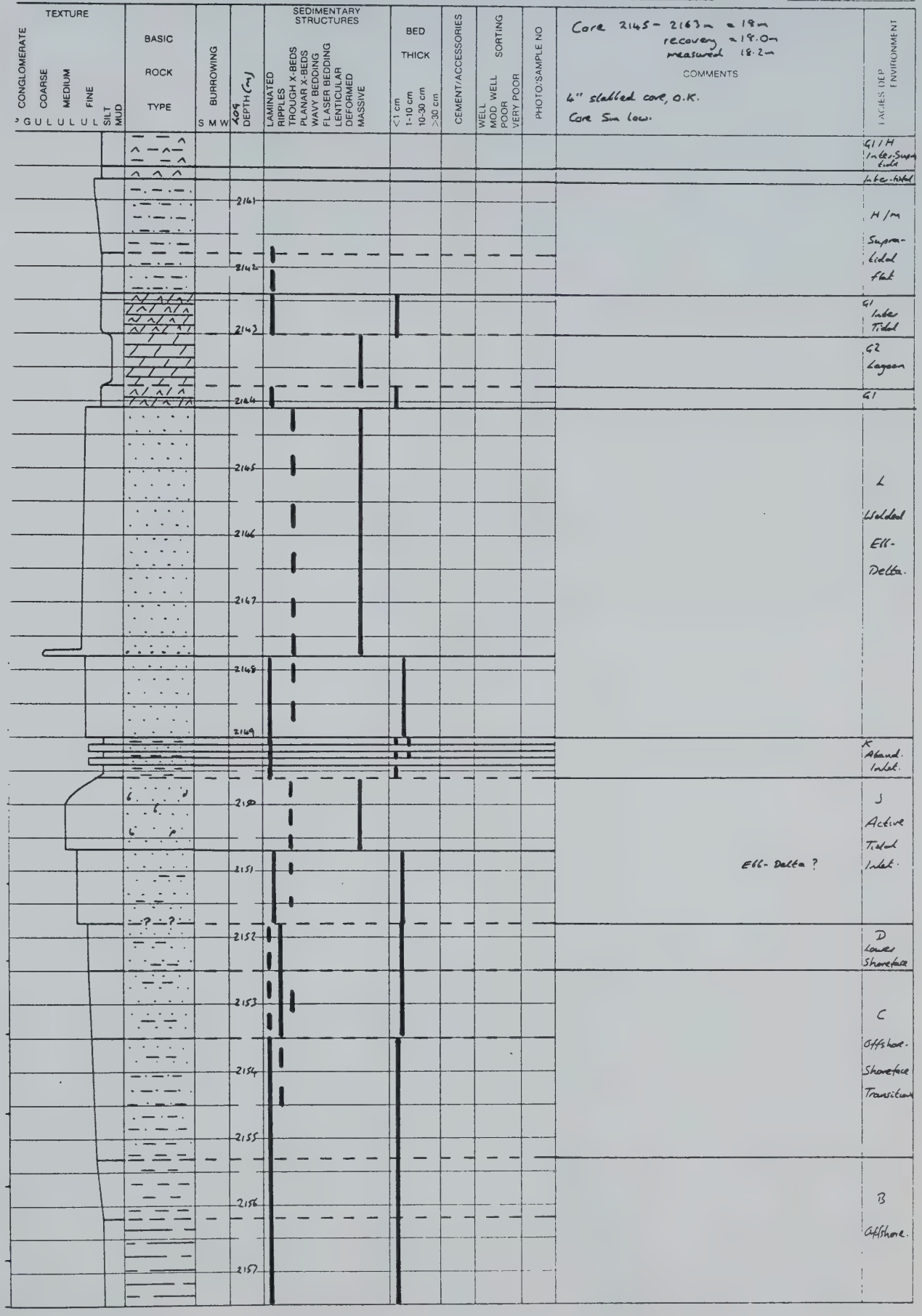

WELL NAME: PCP et al Wembley FORMATION: DATE:

LOCATION: 8-17-72-7-W6 CORE INTERVAL: KB:

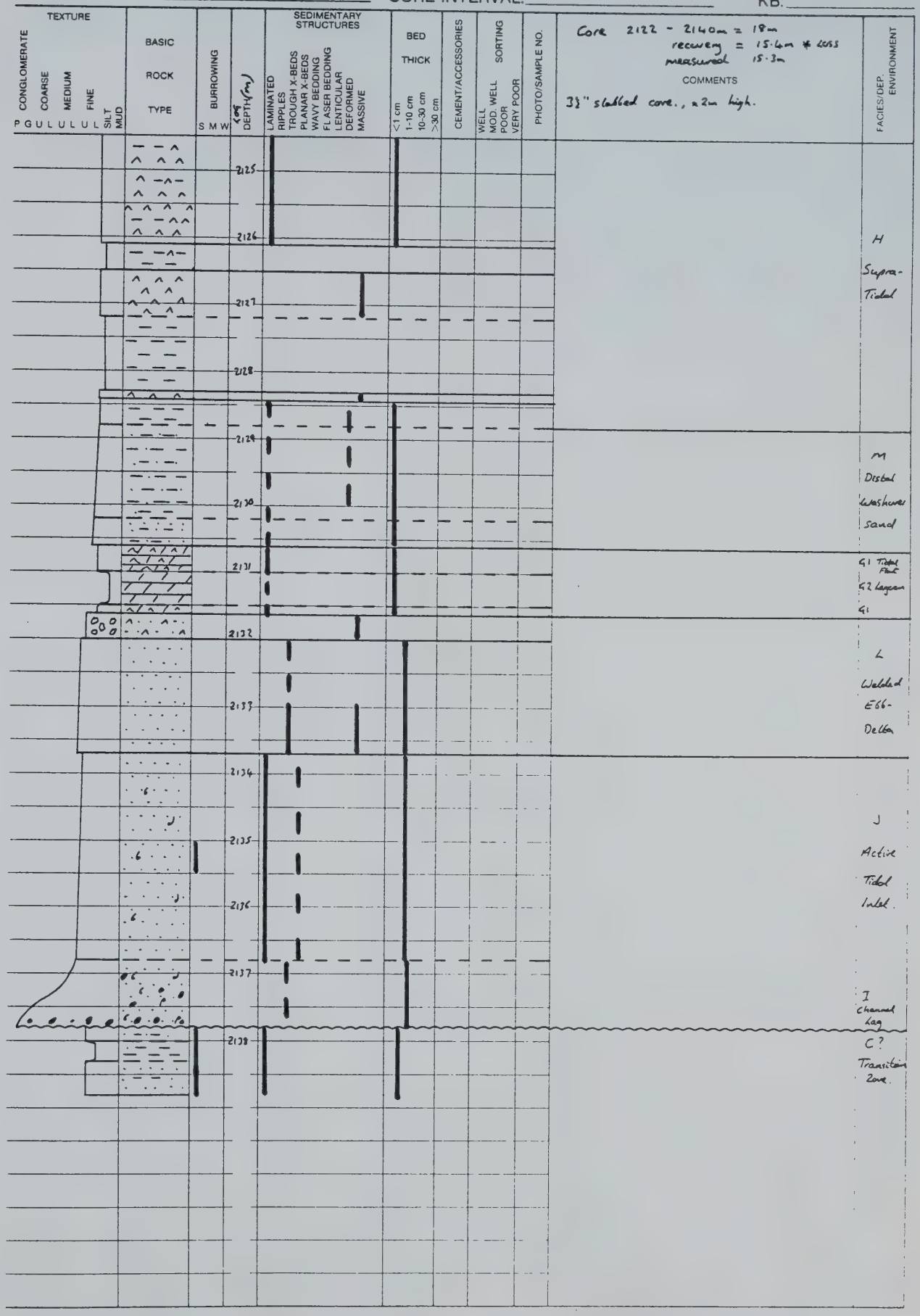

WELL NAME: PCP et al Wembley FORMATION: DATE:

LOCATION: 14-17-72-7-W6 CORE INTERVAL: KB:

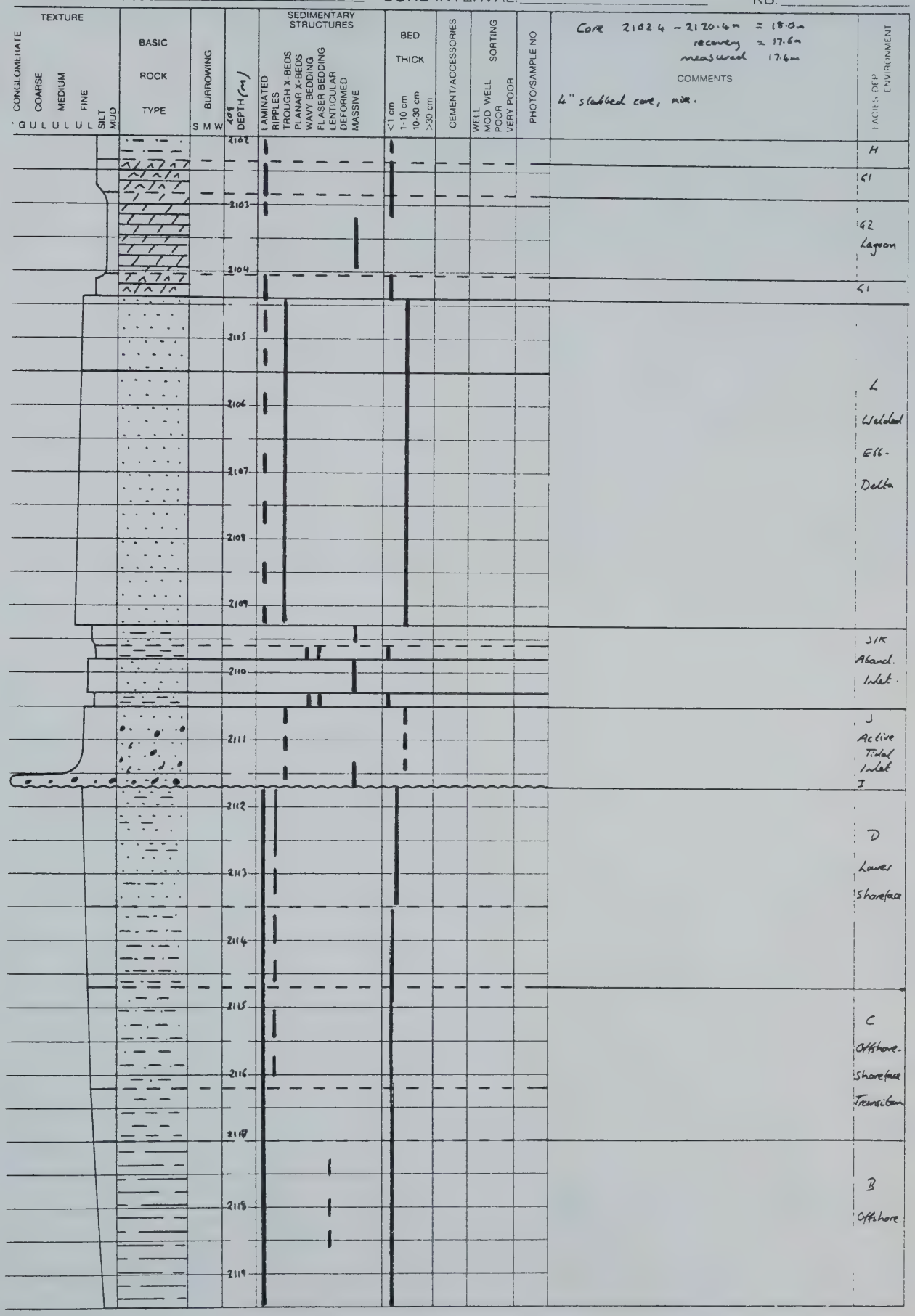

WELL NAME: Shell Wembley FORMATION: DATE:

LOCATION: 16-18-72-7-W6 CORE INTERVAL: KB:

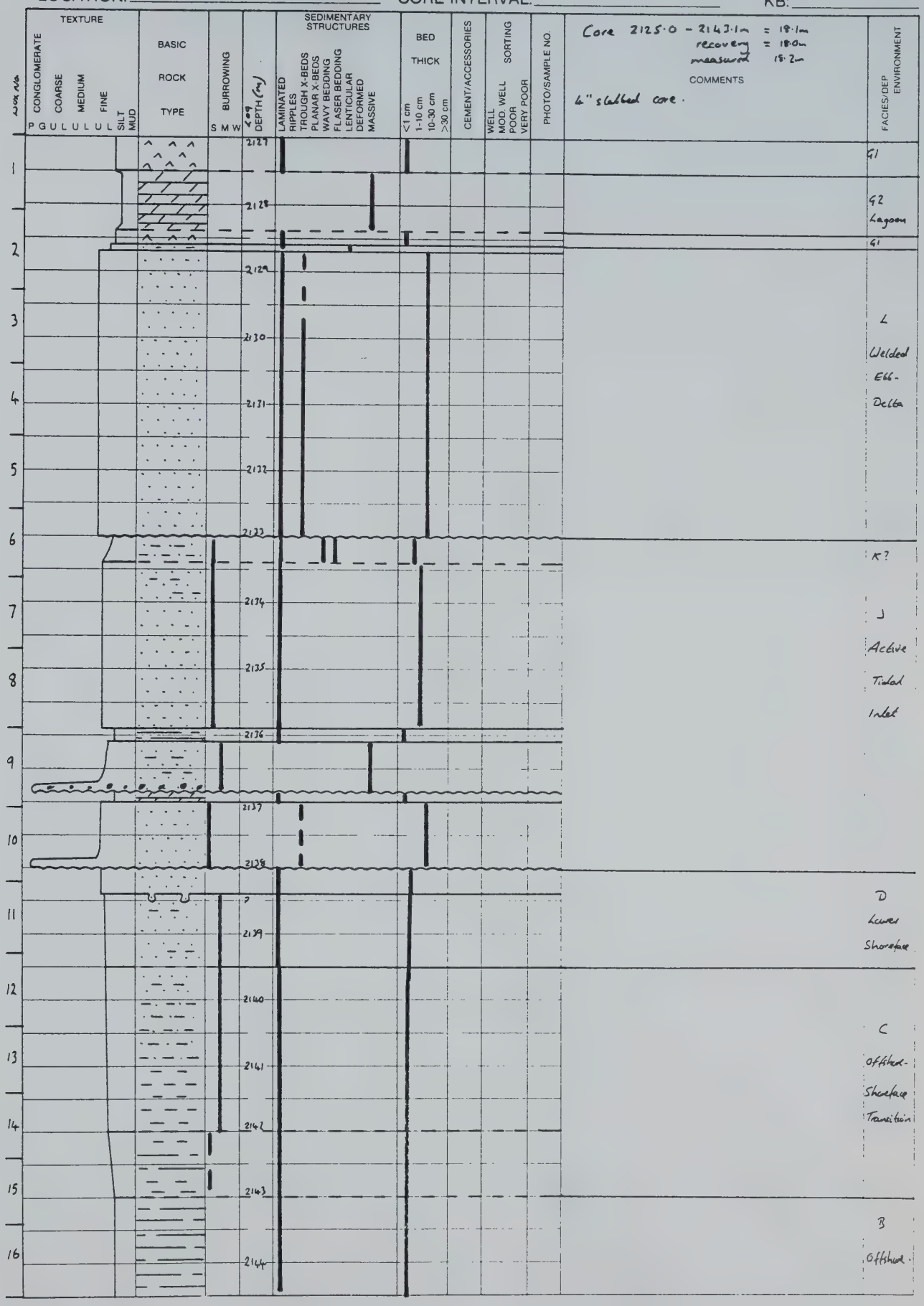

WELL NAME: PCP Wembley FORMATION: DATE:

LOCATION: 8-19-72-7-W6 CORE INTERVAL: KB:

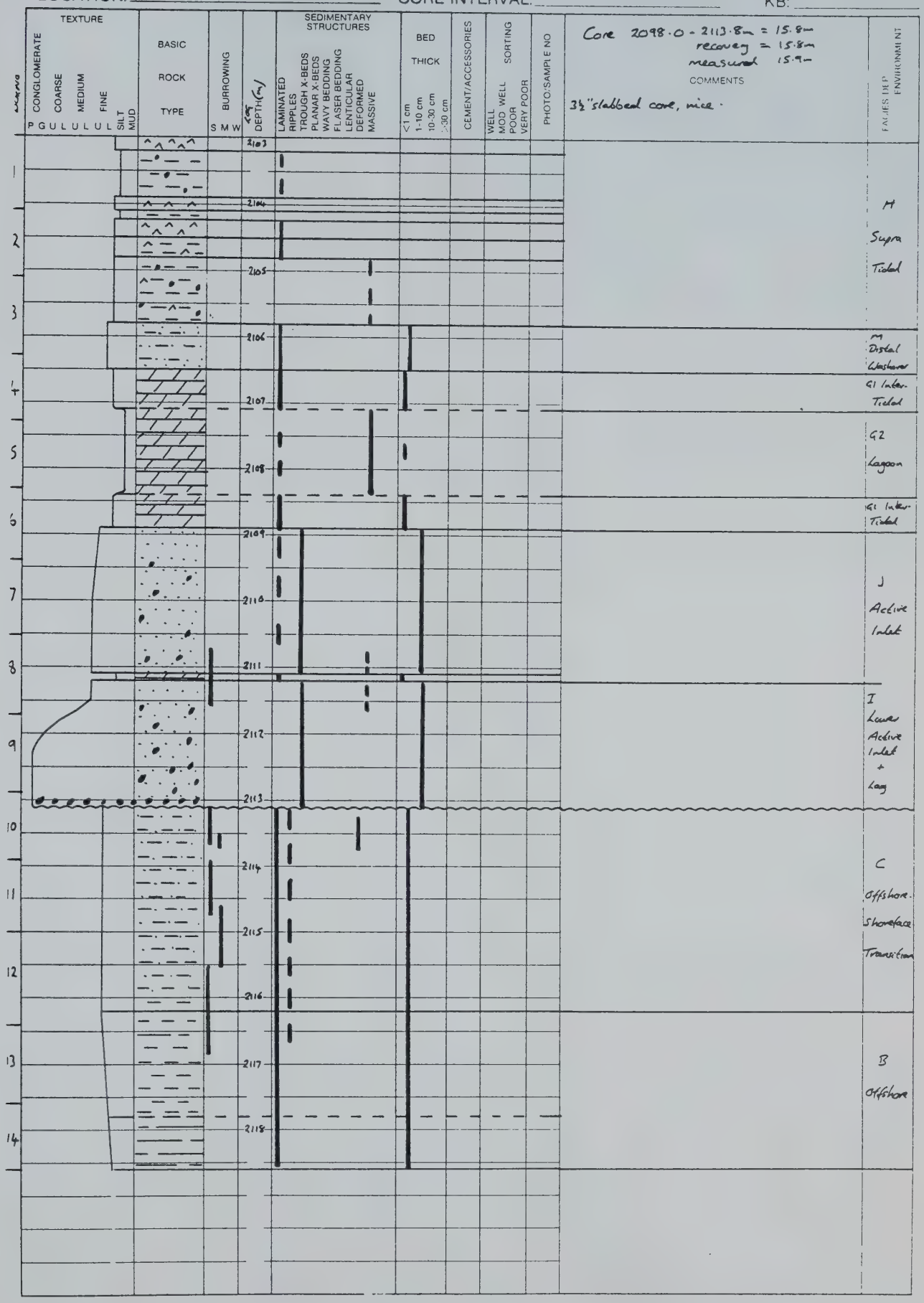

WELL NAME: PCP Beaverlodge FORMATION: DATE:

LOCATION: 14-19-72-7-W6 CORE INTERVAL: KB:

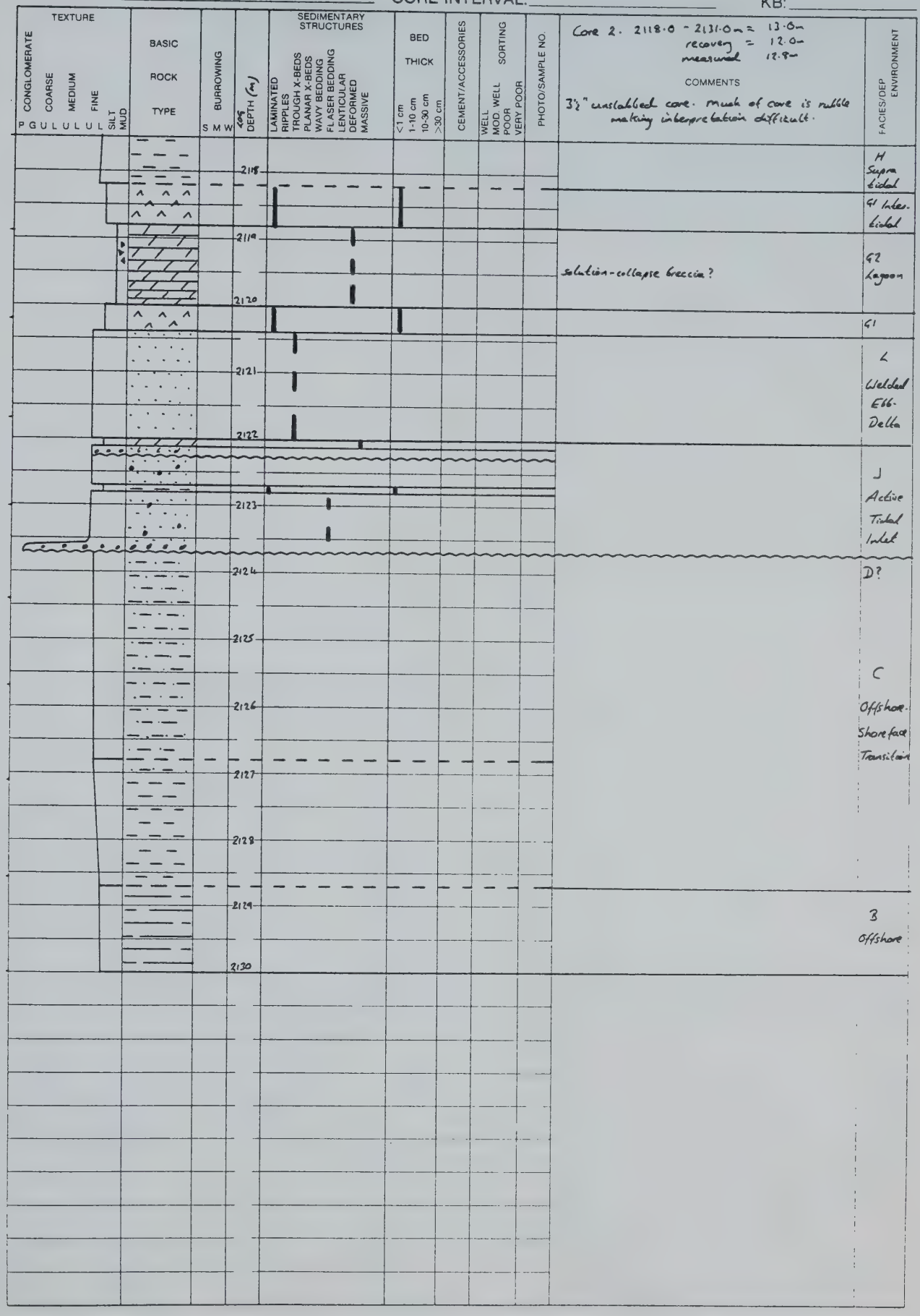

WELL NAME: PCP Wembley FORMATION: DATE:

LOCATION: 16-19-72-7-W6 CORE INTERVAL: KB:

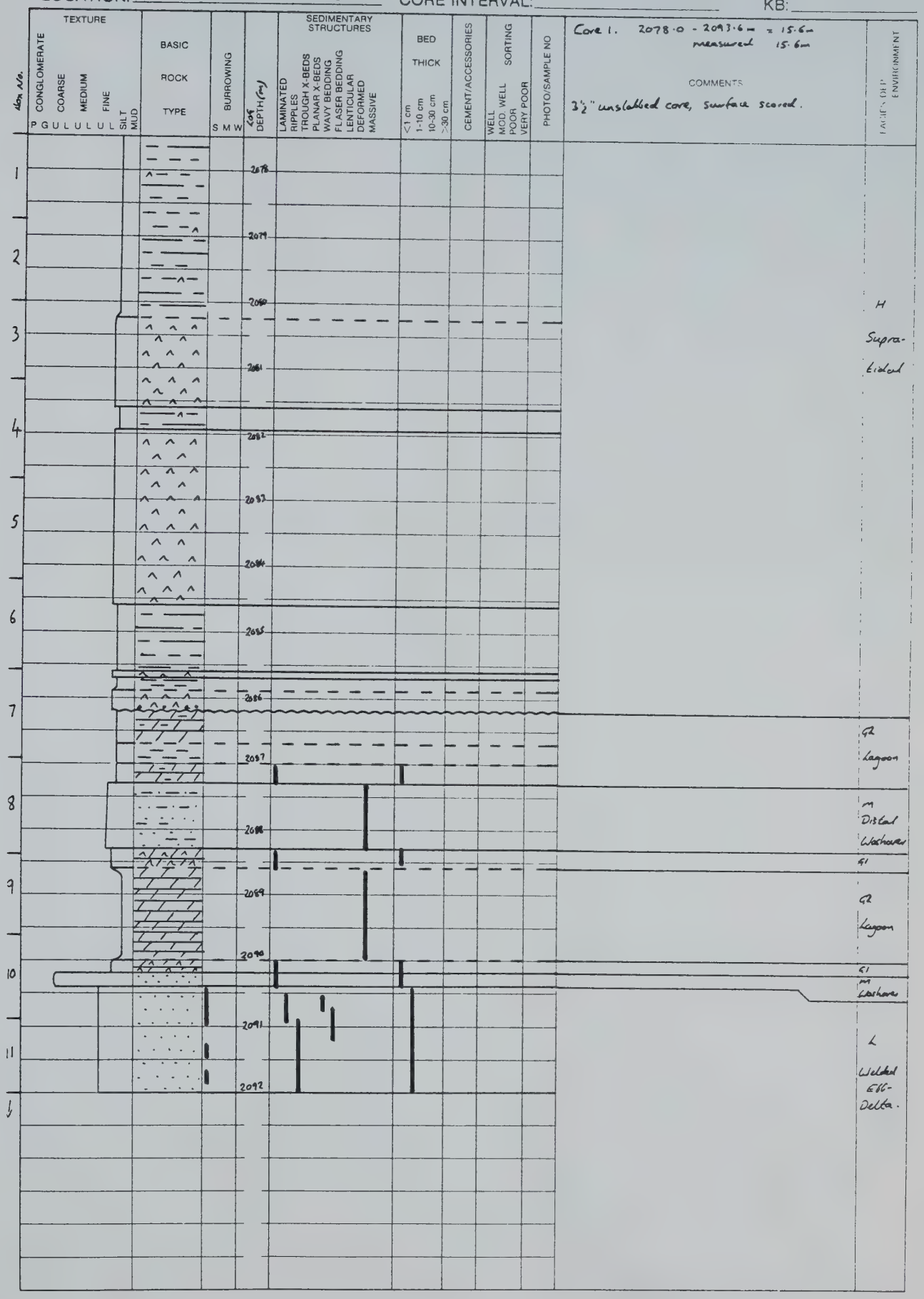

WELL NAME: _____ FORMATION: _____ DATE: _____

LOCATION: 16-19-72-7-W6 (2/2) CORE INTERVAL: _____ KB: _____

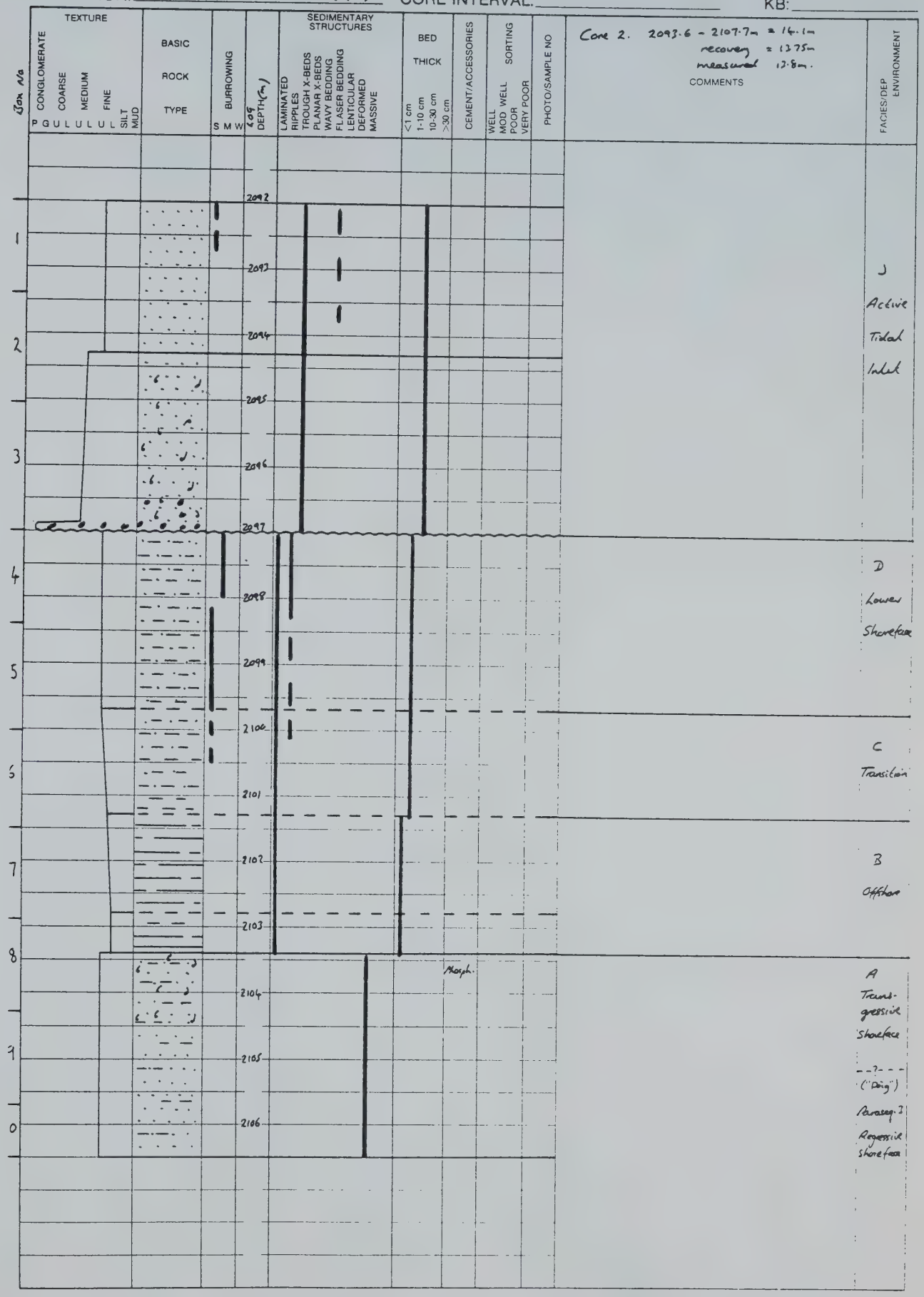

WELL NAME: PCI et al Wembley FORMATION: DATE:

LOCATION: 6-20-72-7-W6 CORE INTERVAL: KB:

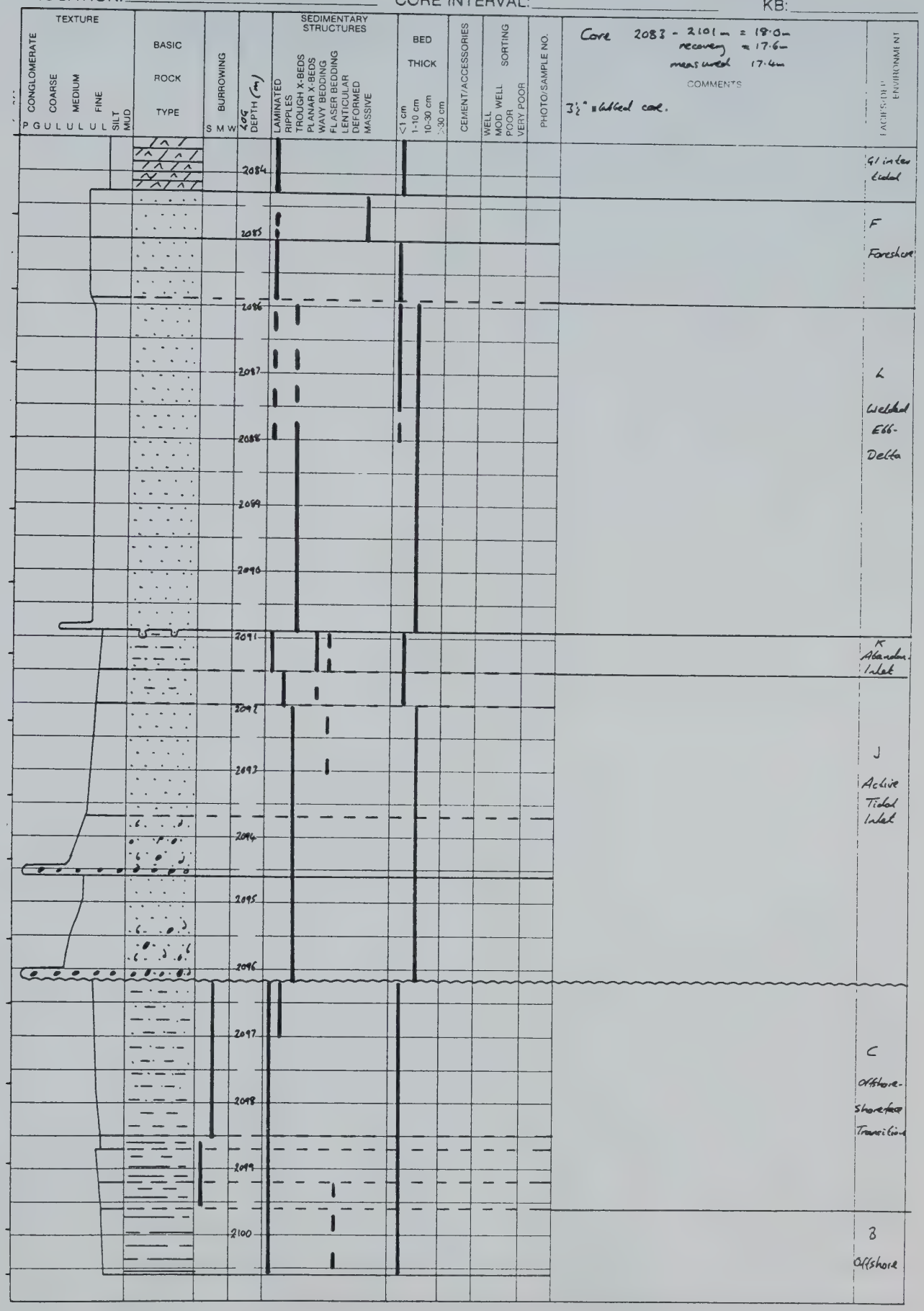

WELL NAME: PCP Wembley FORMATION: DATE:

LOCATION: 8-20-72-7-W6 CORE INTERVAL: KB:

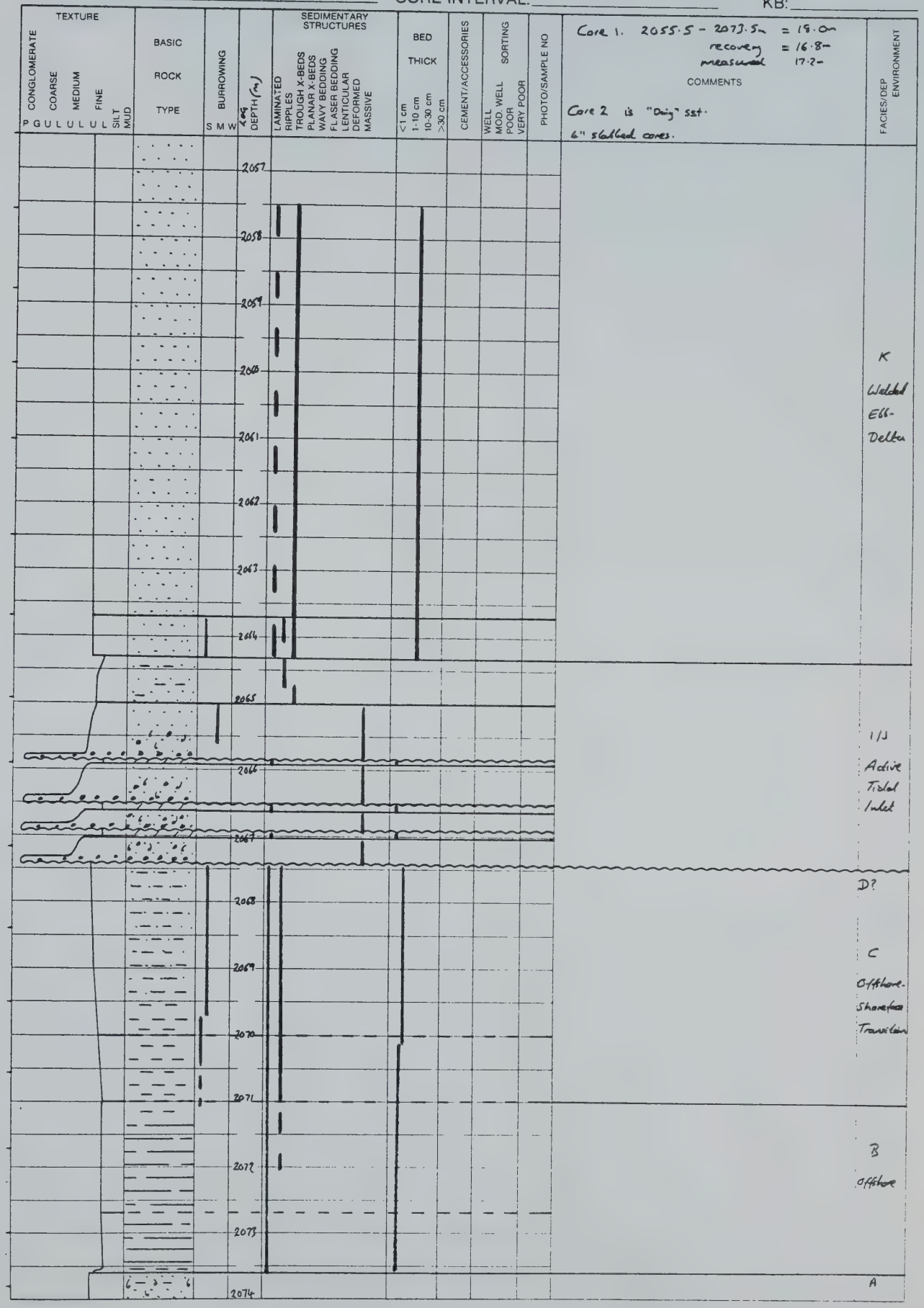

WELL NAME: PCP et al Wembley FORMATION: DATE:

LOCATION: 14-20-72-7-W6 CORE INTERVAL: KB:

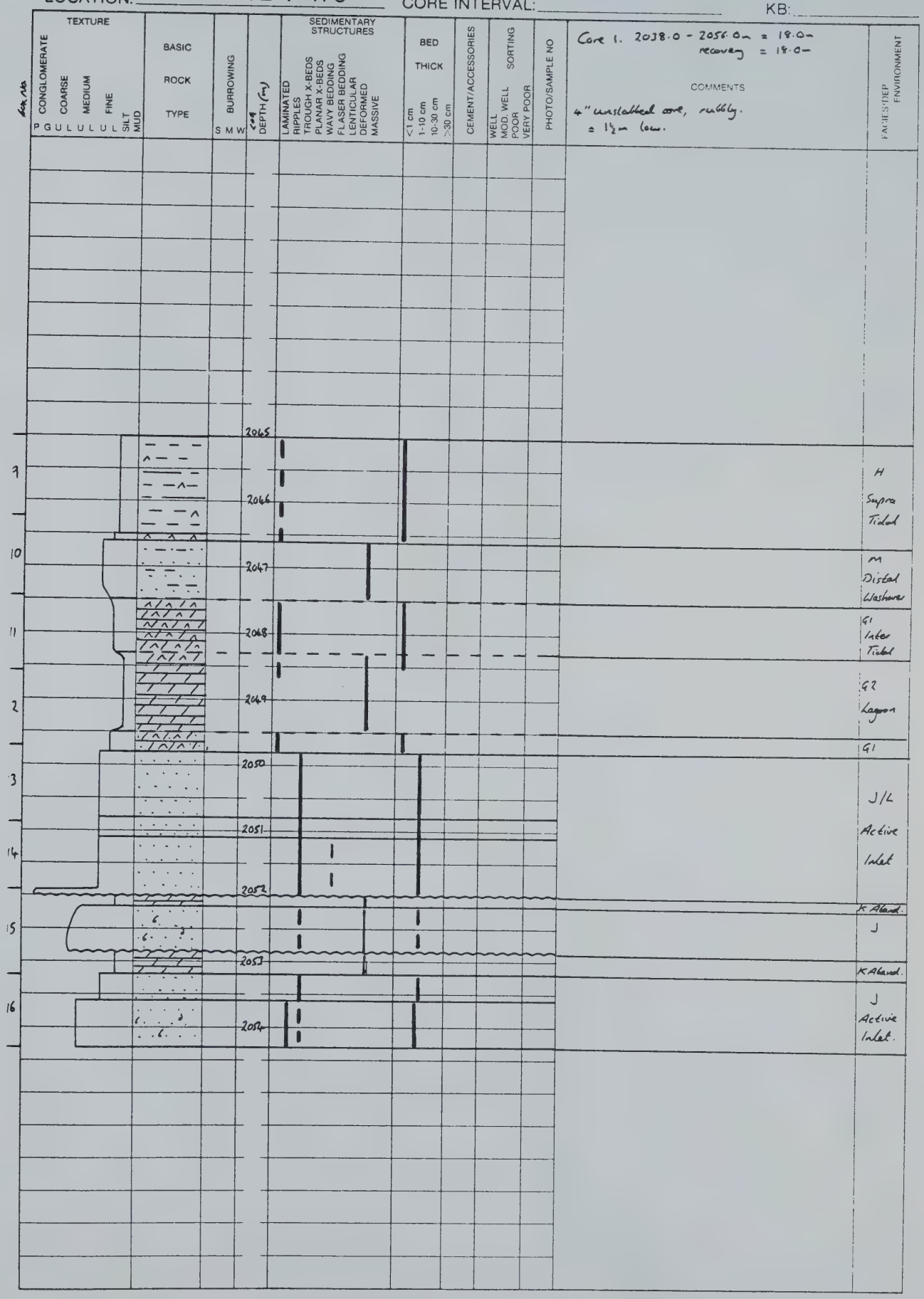

WELL NAME: PCP et al Wembley

FORMATION:

DATE:

LOCATION: 16-20-72-7-W6

CORE INTERVAL:

KB:

TEXTURE (P CONGLOMERATE, G COARSE, U MEDIUM, U FINE, U SILT, U MUD)	BASIC ROCK TYPE	BURROWING (S M W)	DEPTH (m)	SEDIMENTARY STRUCTURES (LAMINATED, RIPPLES, TROUGH X-BEDS, PLANAR X-BEDS, WAVY BEDDING, FLASER BEDDING, LENTICULAR, DEFORMED, MASSIVE)	BED THICK (<1 cm, 1-10 cm, 10-30 cm, >30 cm)	CEMENT/ACCESSORIES	SORTING (WELL, MOD. WELL, POOR, VERY POOR)	PHOTO/SAMPLE NO.	COMMENTS	FACIES/DEP ENVIRONMENT
									Core 2091.2 - 2110.2m = 19m recovery = 18m 3½" slabbed core	
			2094							
			2095							H Supra-tidal
			2096							G1 Inter tidal
			2097							G2 Lagoon
			2098							
			2099							
			2100							L
			2101							Welded Egg-Delta
			2102							
			2103							
			2104							
			2105							
			2106							K Abandon Tidal Inlet

WELL NAME: PCP et al Wembley FORMATION: DATE:

LOCATION: 6-21-72-7-W6 CORE INTERVAL: KB:

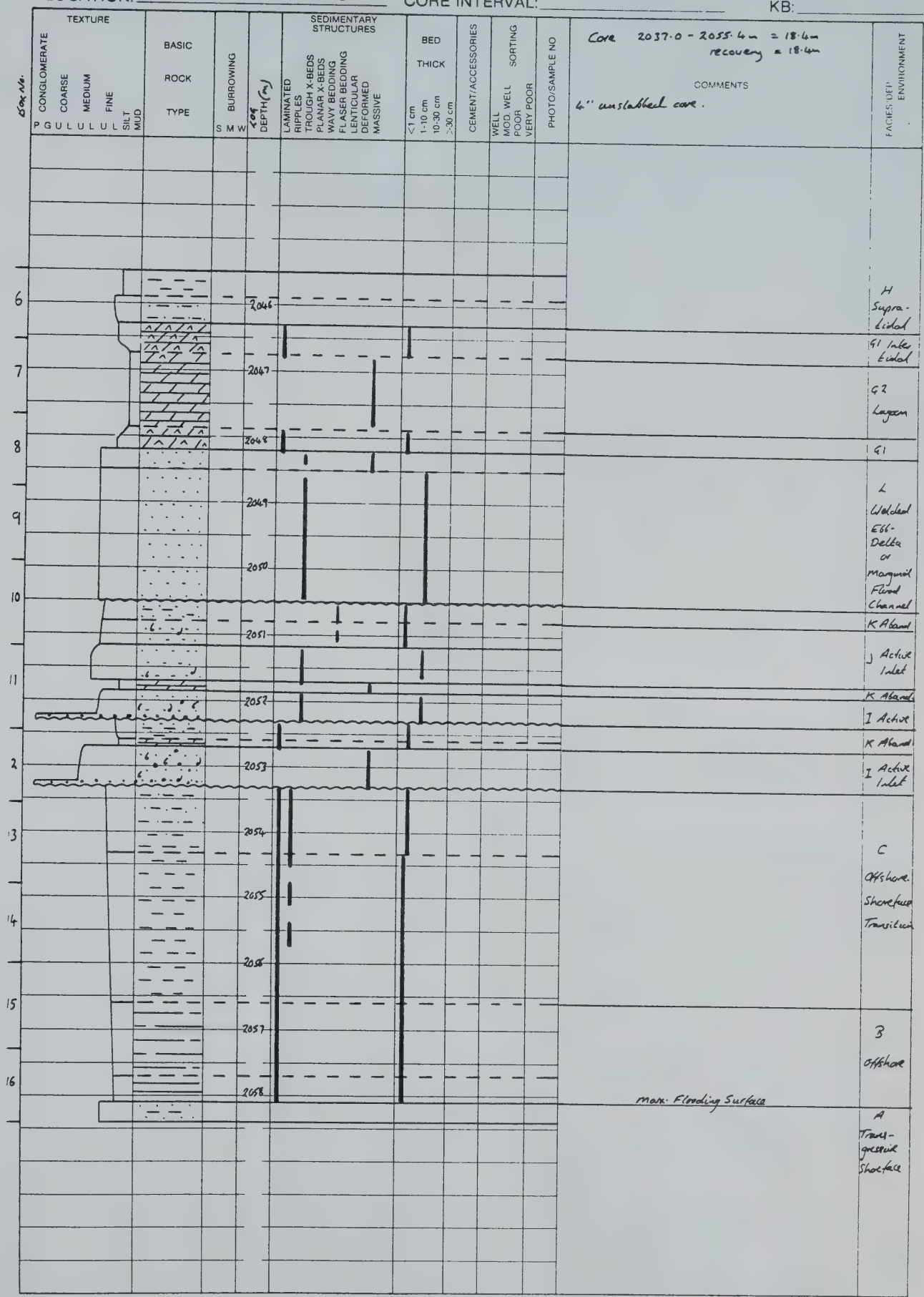

WELL NAME: PCP et al Wembley FORMATION: DATE:

LOCATION: 6-29-72-7-W6 CORE INTERVAL: KB:

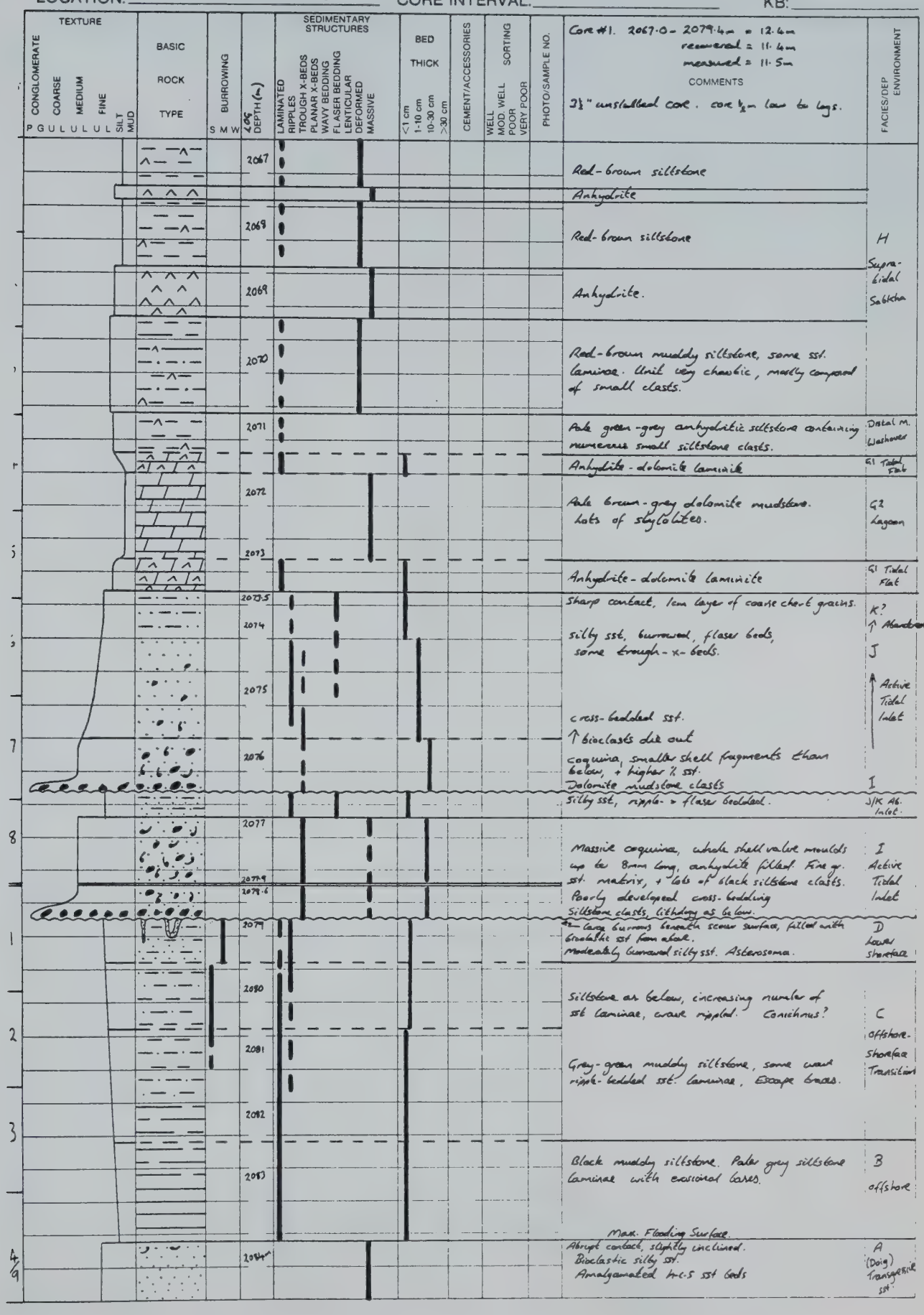

WELL NAME: PCP Wembley

FORMATION:

DATE:

LOCATION: 8-30-72-7-W6

CORE INTERVAL:

KB:

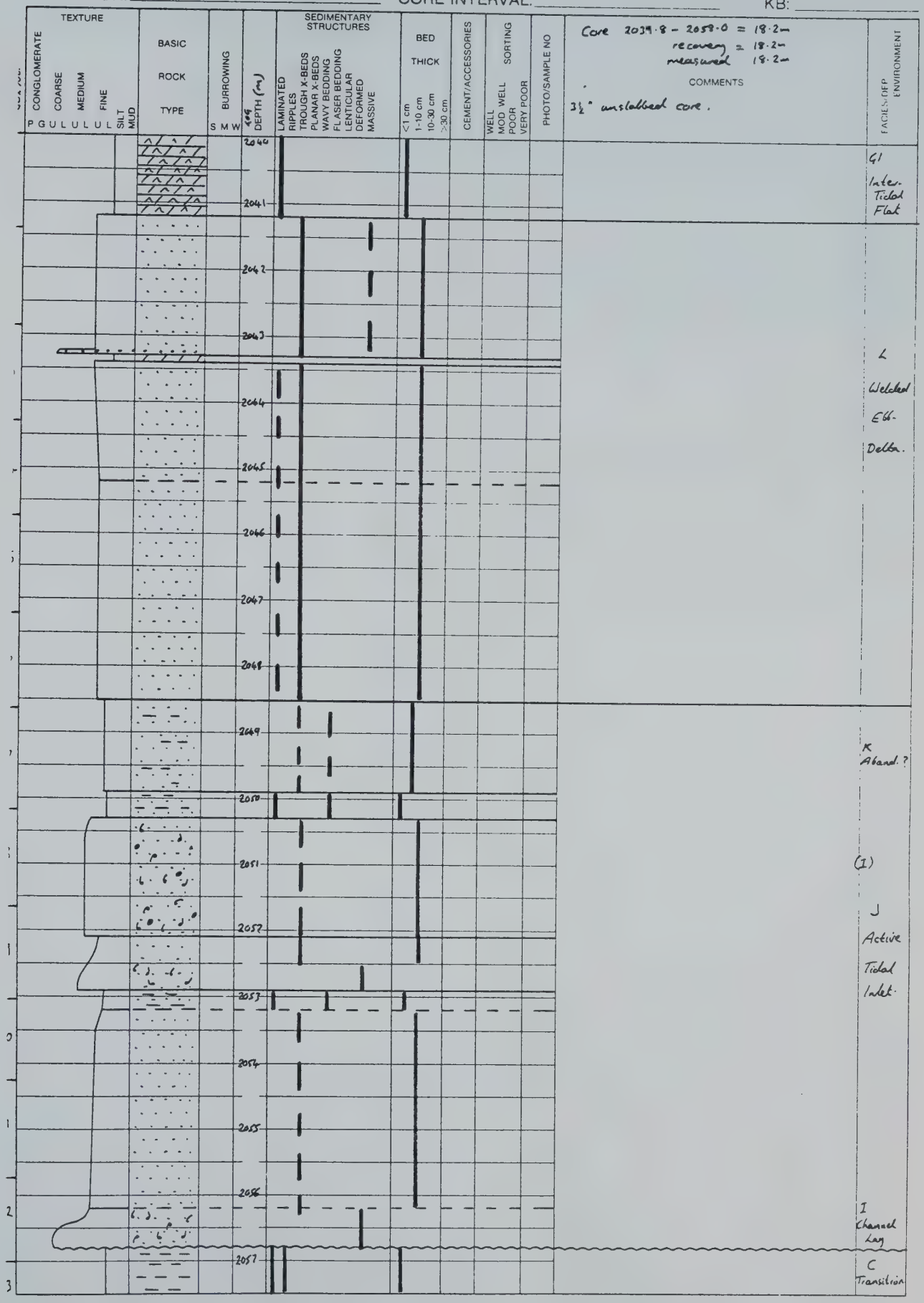

WELL NAME: PCP Wembley FORMATION: DATE:

LOCATION: 14-30-72-7-W6 CORE INTERVAL: KB:

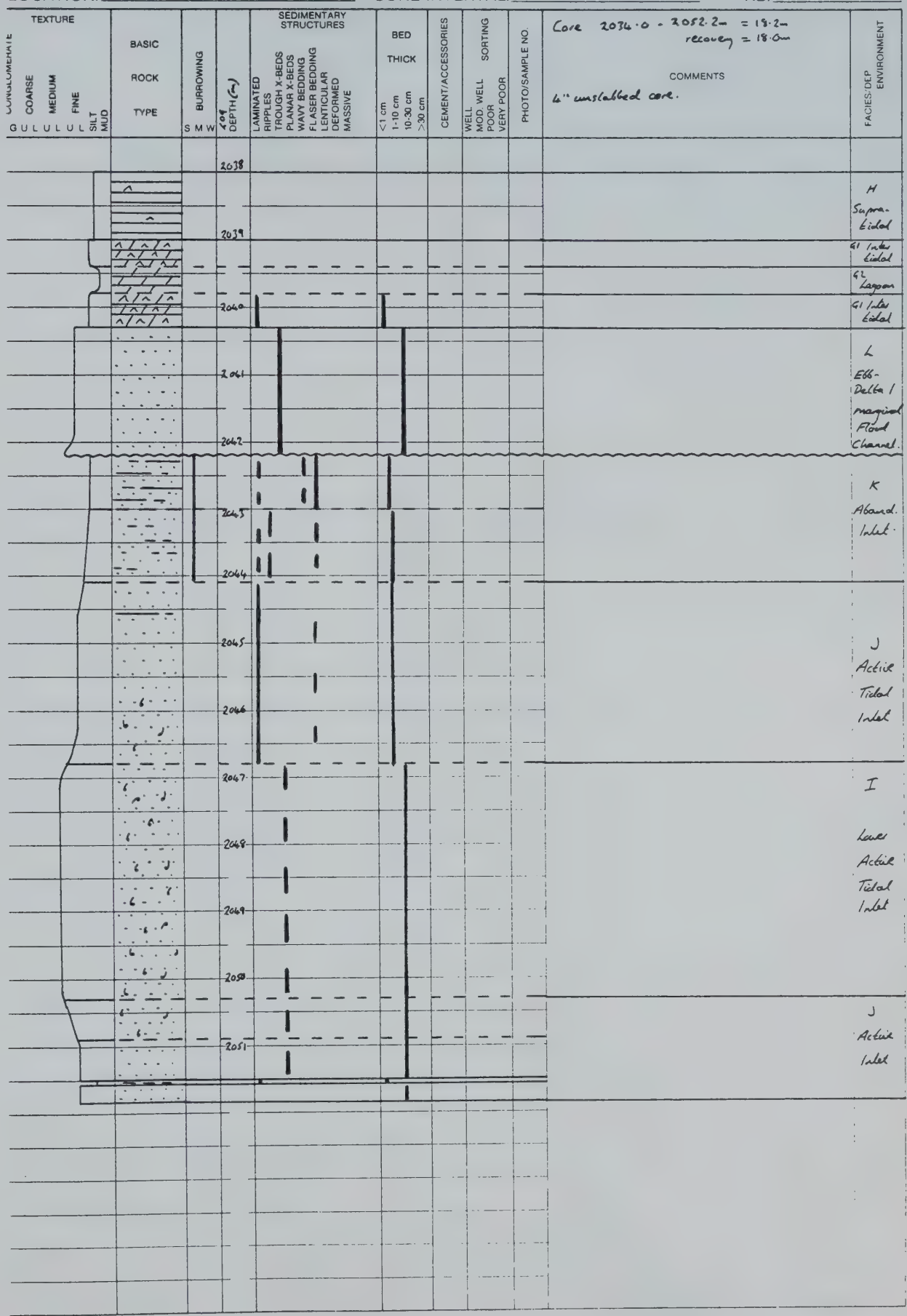

WELL NAME: PCP Wembley FORMATION: DATE:

LOCATION: 16-30-72-7-W6 CORE INTERVAL: KB:

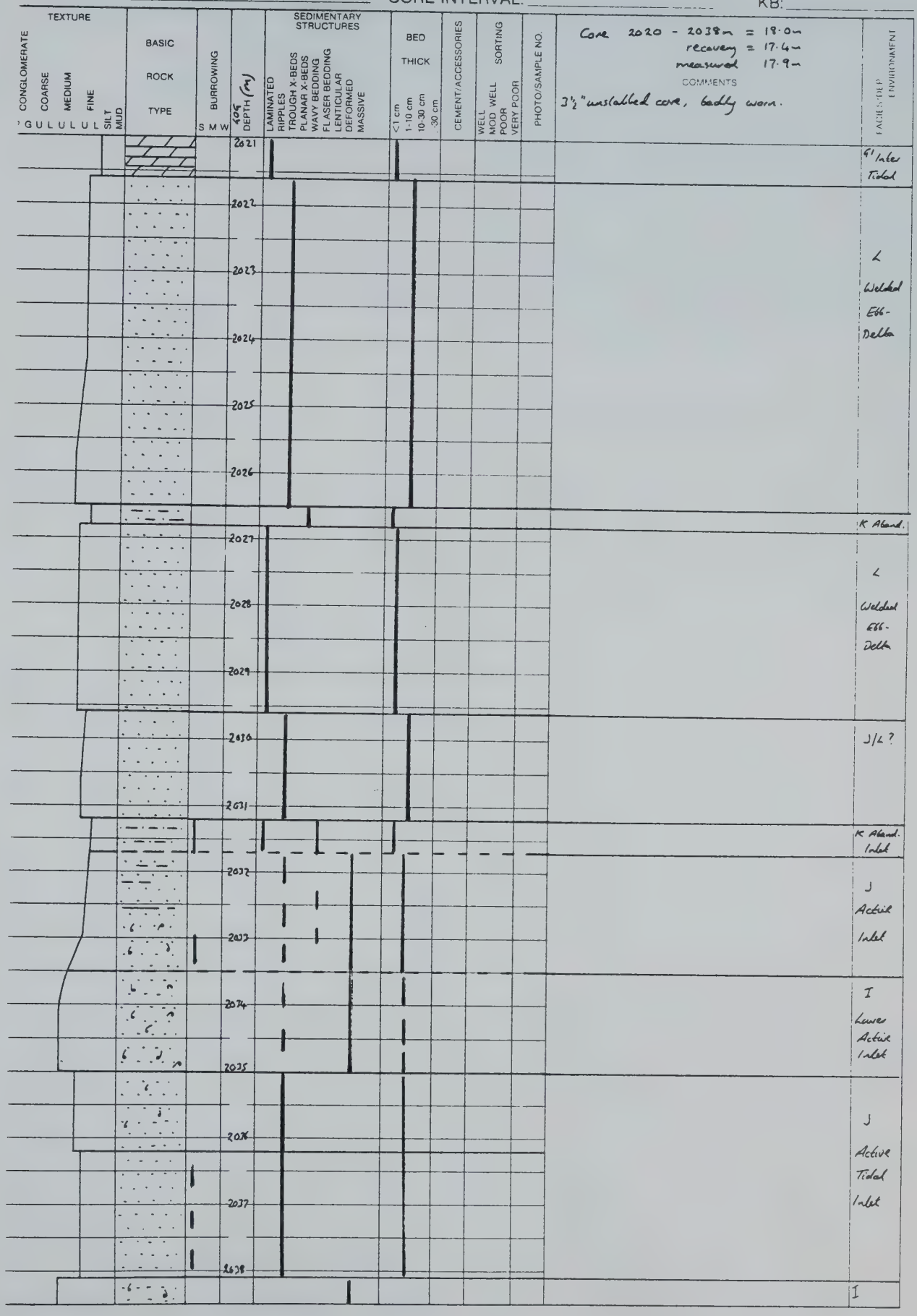

WELL NAME: PCP Grande Prairie FORMATION: DATE:

LOCATION: 6-31-72-7-W6 CORE INTERVAL: KB:

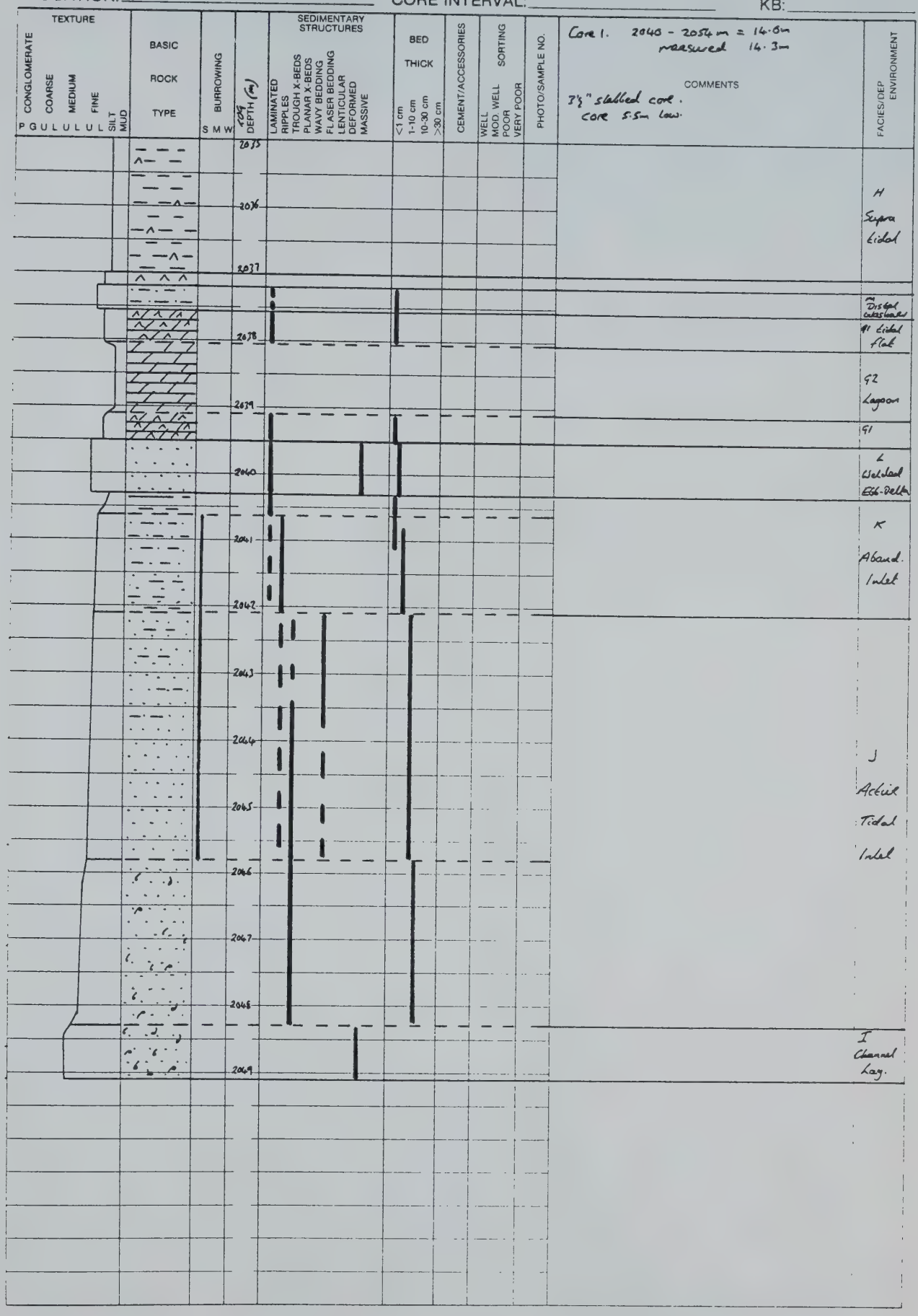

WELL NAME: _____ FORMATION: _____ DATE: _____

LOCATION: 6-31-72-7-W6 (2/2) CORE INTERVAL: _____ KB: _____

Core 2. 2054.0 - 2064.7m = 10.7m

TEXTURE (CONGLOMERATE, COARSE, MEDIUM, FINE, SILT, MUD; P G U L U L U L)	BASIC ROCK TYPE	BURROWING (S M W)	KOG DEPTH (m)	SEDIMENTARY STRUCTURES (LAMINATED, RIPPLES, TROUGH X-BEDS, PLANAR X-BEDS, WAVY BEDDING, FLASER BEDDING, LENTICULAR, DEFORMED, MASSIVE)	BED THICK (<1 cm, 1-10 cm, 10-30 cm, >30 cm)	CEMENT/ACCESSORIES	SORTING (WELL, MOD. WELL, POOR, VERY POOR)	PHOTO/SAMPLE NO	COMMENTS	FACIES DEP ENVIRONMENT
			Core loss? ≈ 2m							
			2052							B Offshore
			2053							
			2054						Maximum Flooding Surface.	
			2055							("Dolly") A Trans-gressive Shoreface
			2056							
			2057							
			2058							

WELL NAME: PCP Esso Wembley FORMATION: DATE:

LOCATION: 6-32-72-7-W6 CORE INTERVAL: KB:

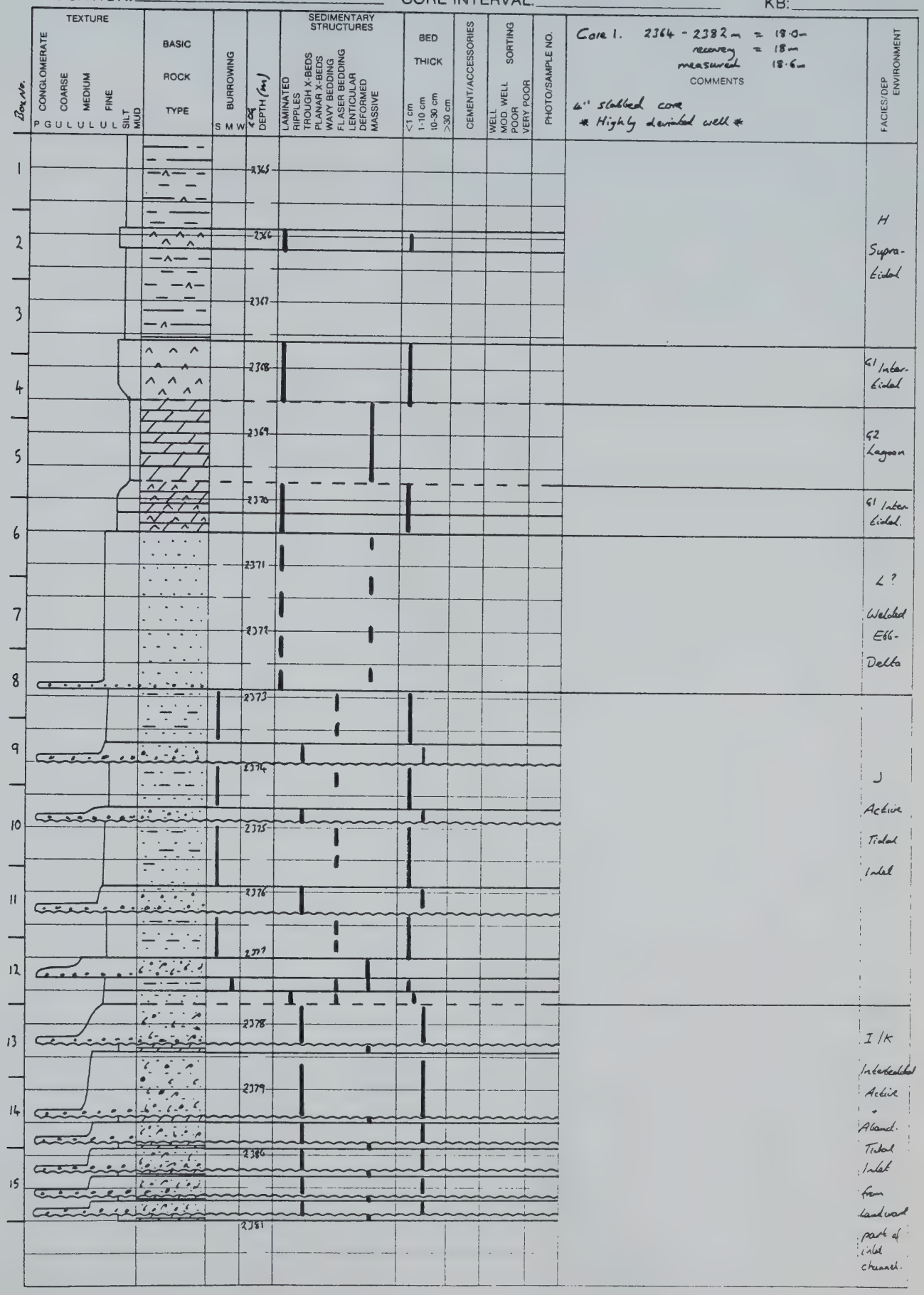

WELL NAME: _____ FORMATION: _____ DATE: _____

LOCATION: 6-32-72-7-W6 (2/2) CORE INTERVAL: _____ KB: _____

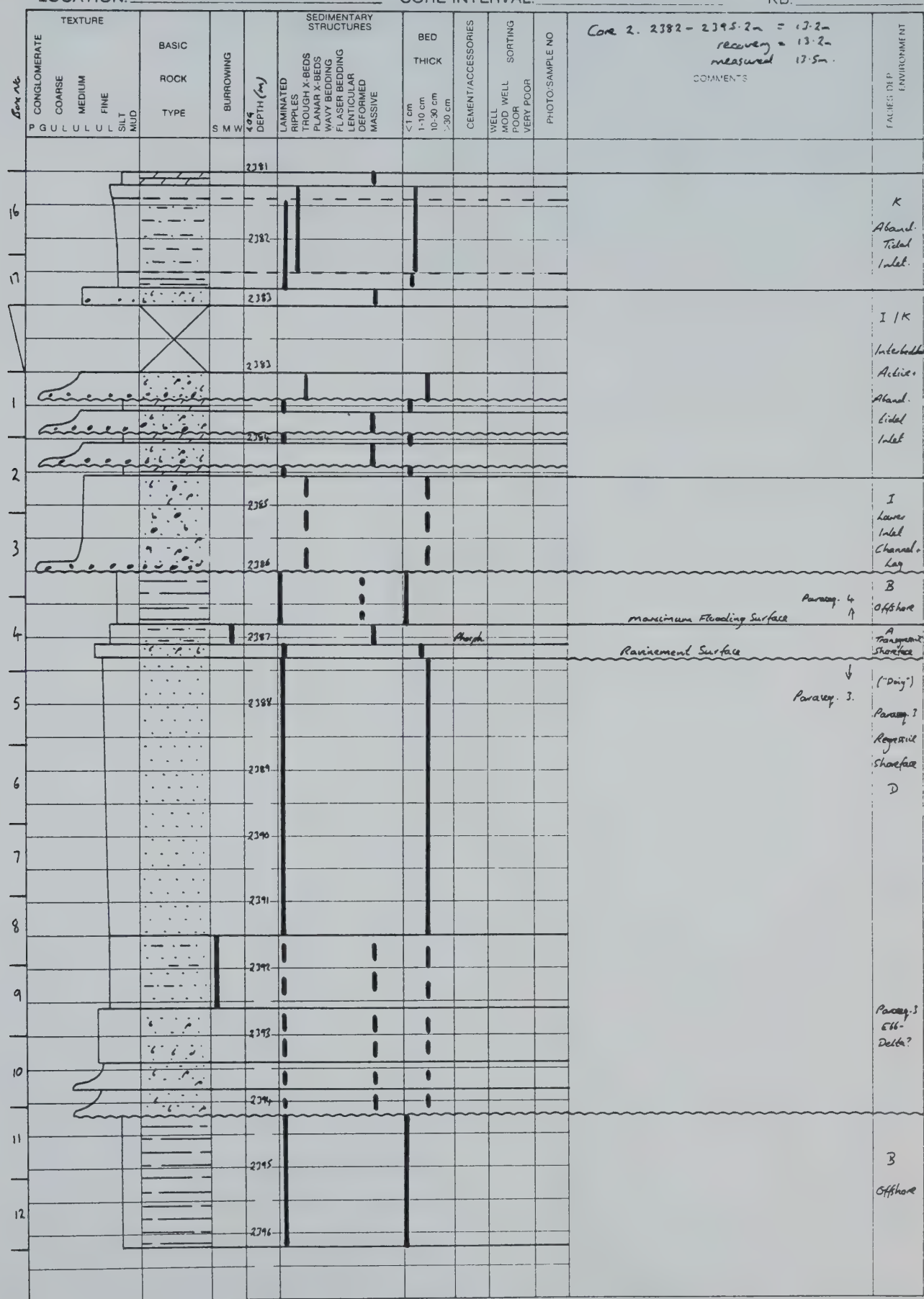

WELL NAME: PCP Wembley FORMATION: DATE:

LOCATION: 6-34-72-7-W6 CORE INTERVAL: KB:

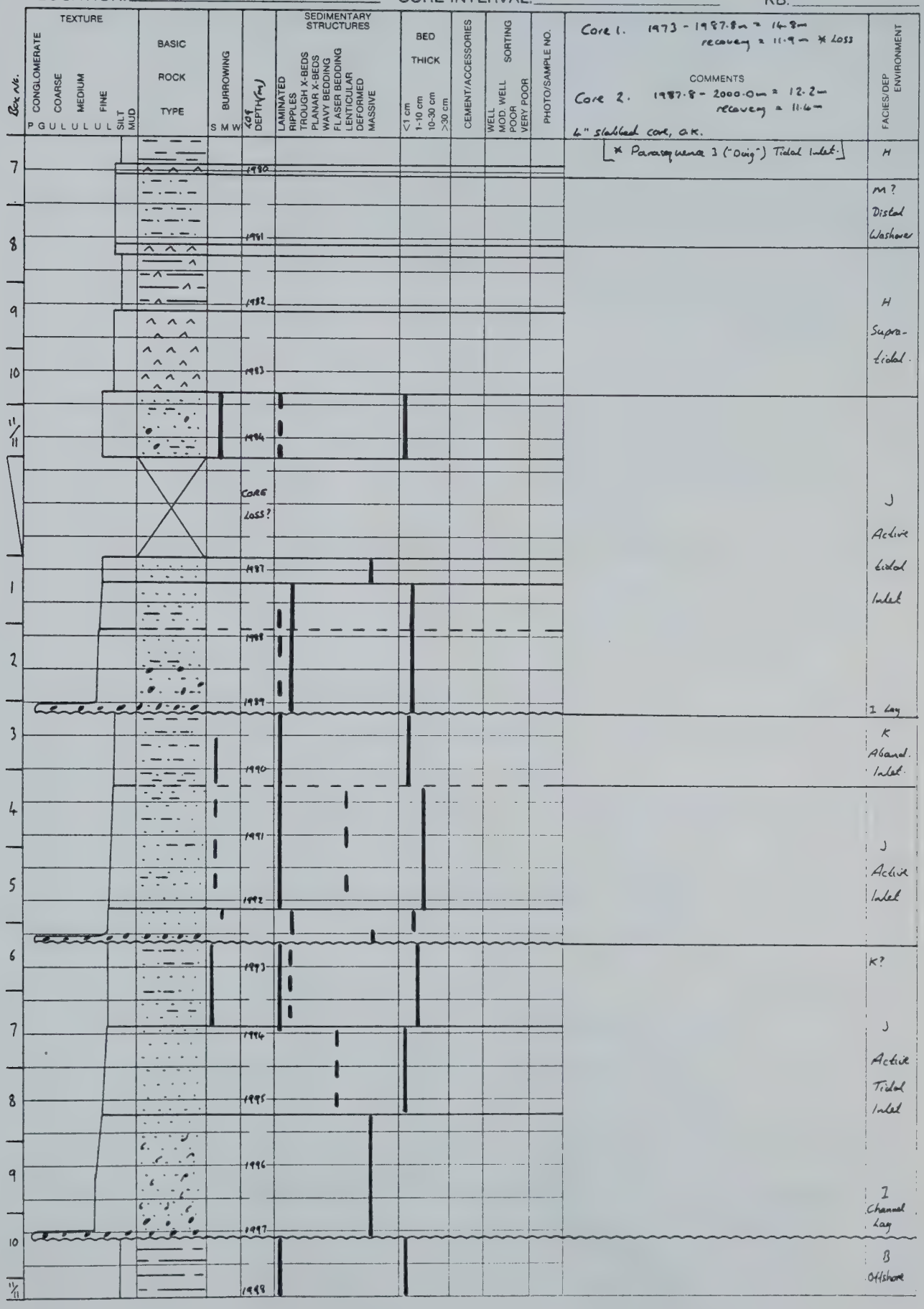

WELL NAME: Colonial Wembley FORMATION: DATE:

LOCATION: 6-4-72-8-W6 CORE INTERVAL: KB:

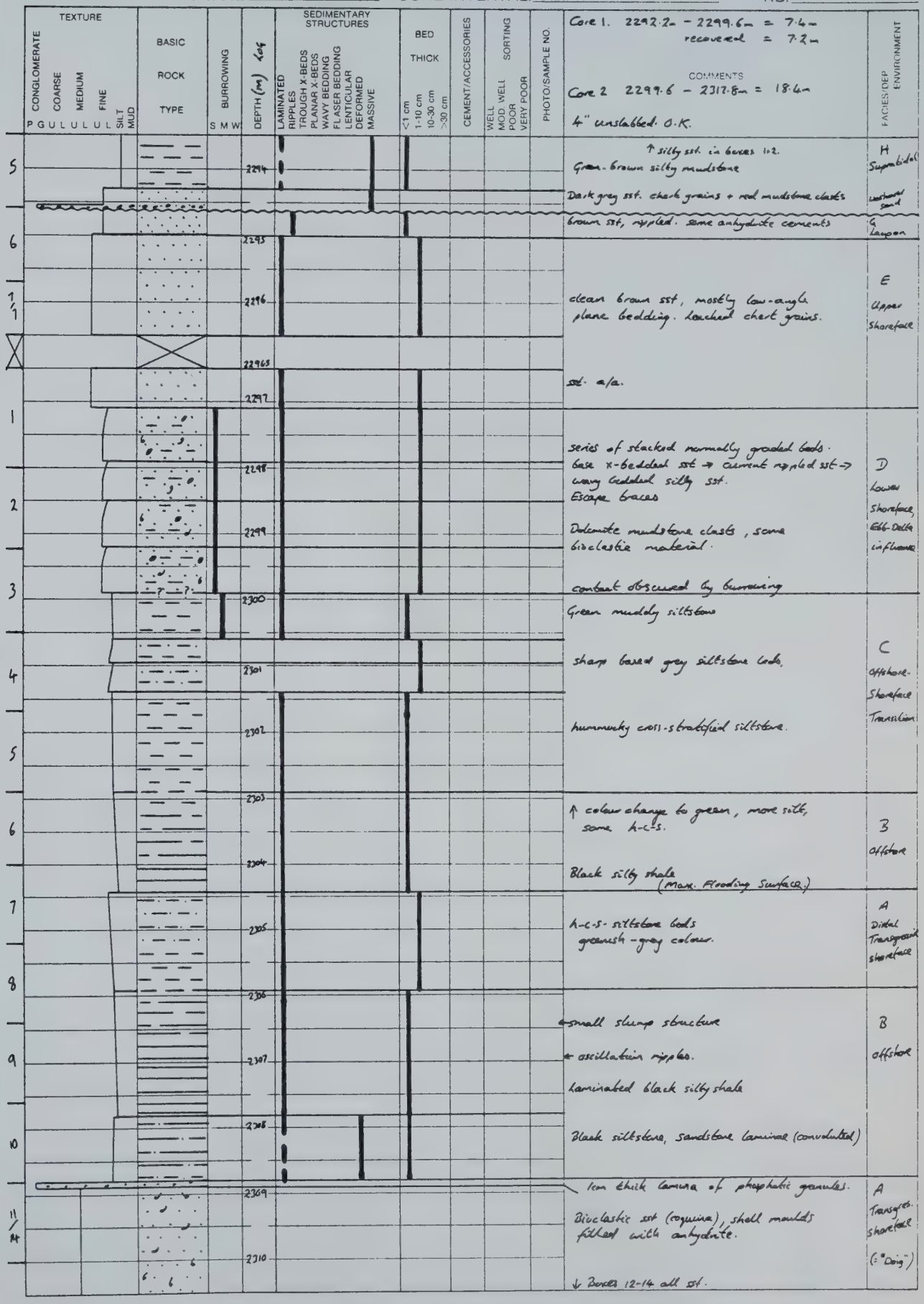

WELL NAME: Colonial Wembley FORMATION: DATE:

LOCATION: 8-9-72-8-W6 CORE INTERVAL: KB:

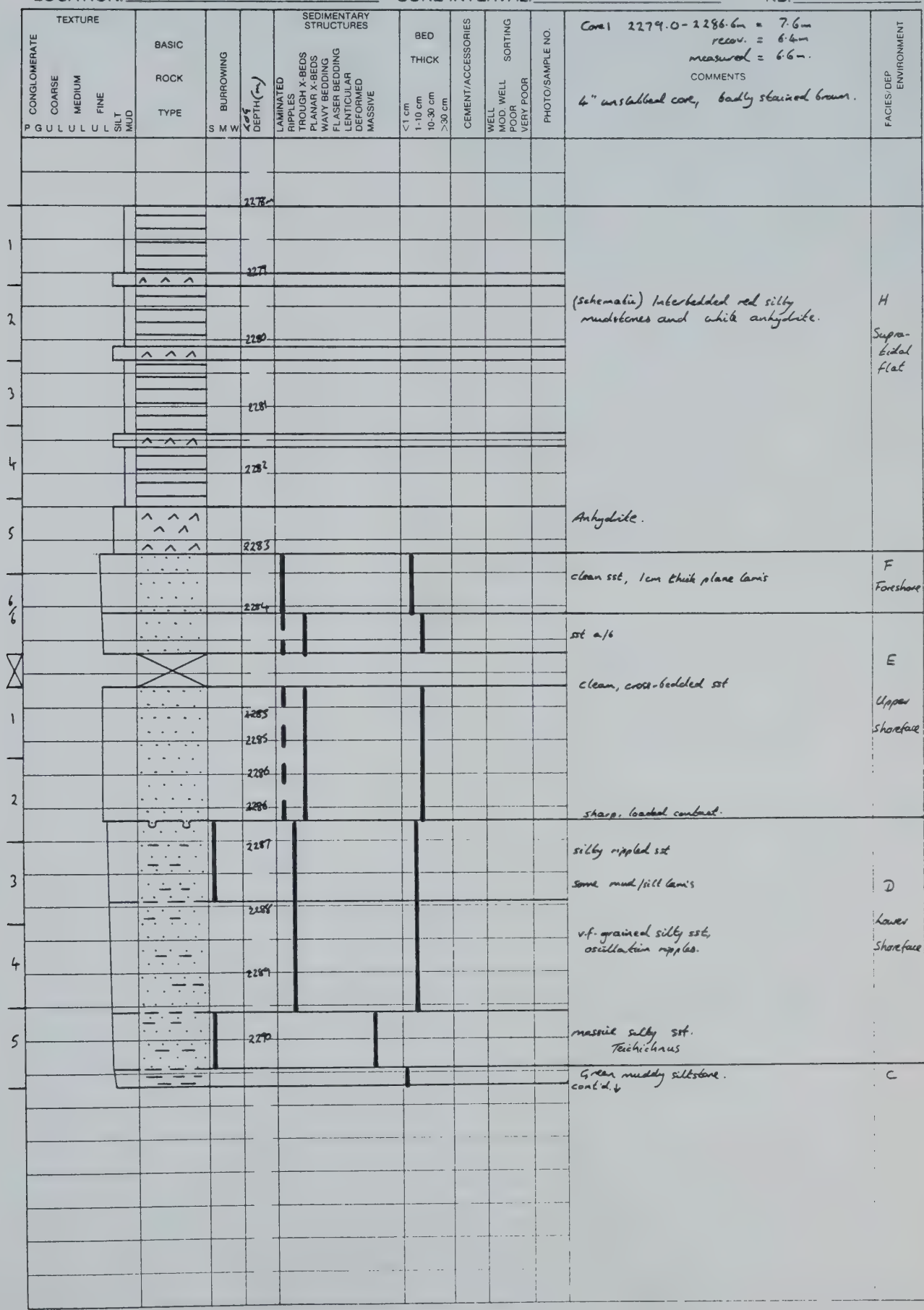

WELL NAME: (2/2) FORMATION: DATE:

LOCATION: 8-9-72-8-W6 CORE INTERVAL: KB:

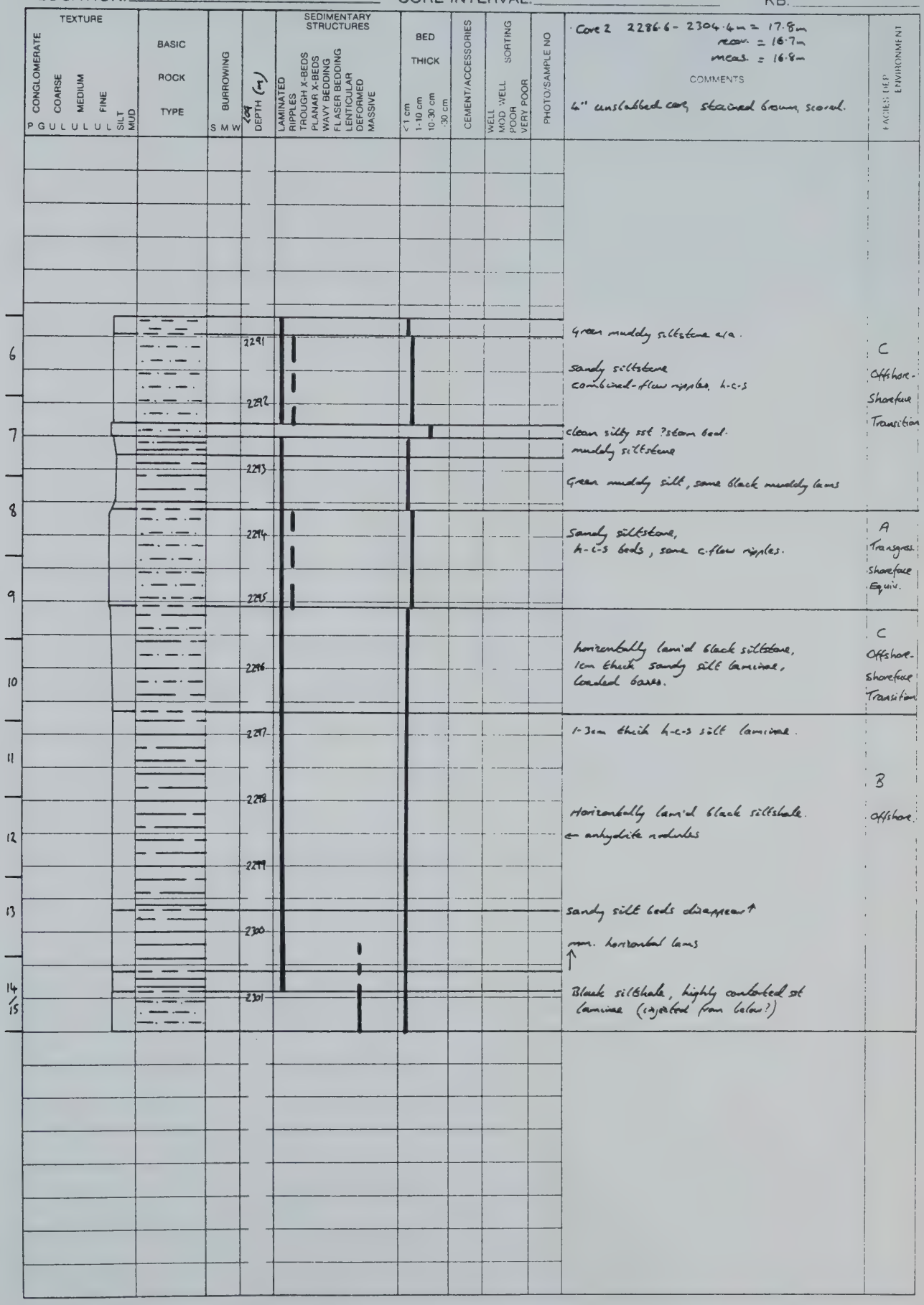

WELL NAME: Shell Wembley FORMATION: DATE:

LOCATION: 14-11-72-8-W6 CORE INTERVAL: KB:

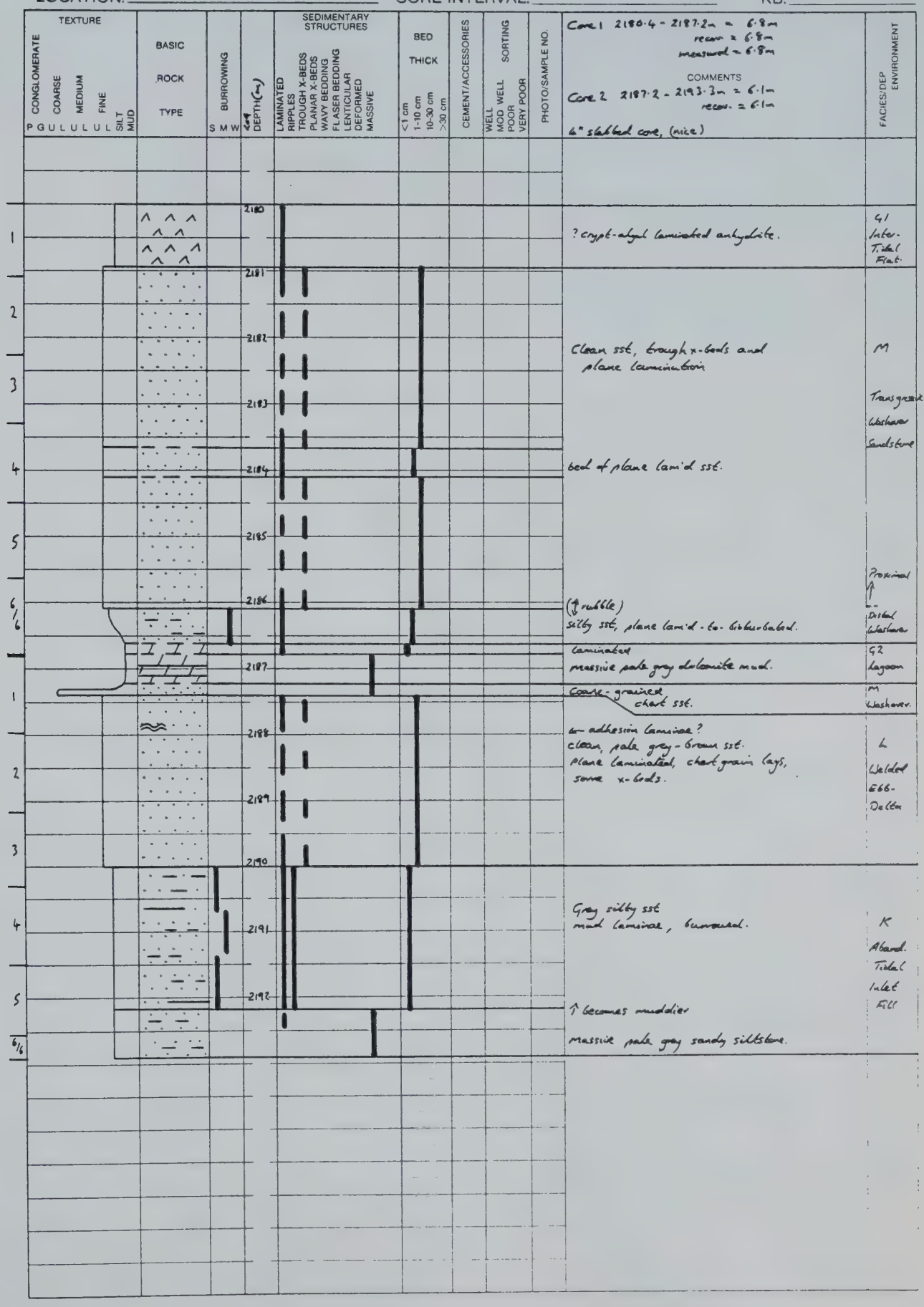

WELL NAME: Dome et al Wembley FORMATION: DATE:

LOCATION: 8-12-72-8-W6 CORE INTERVAL: KB:

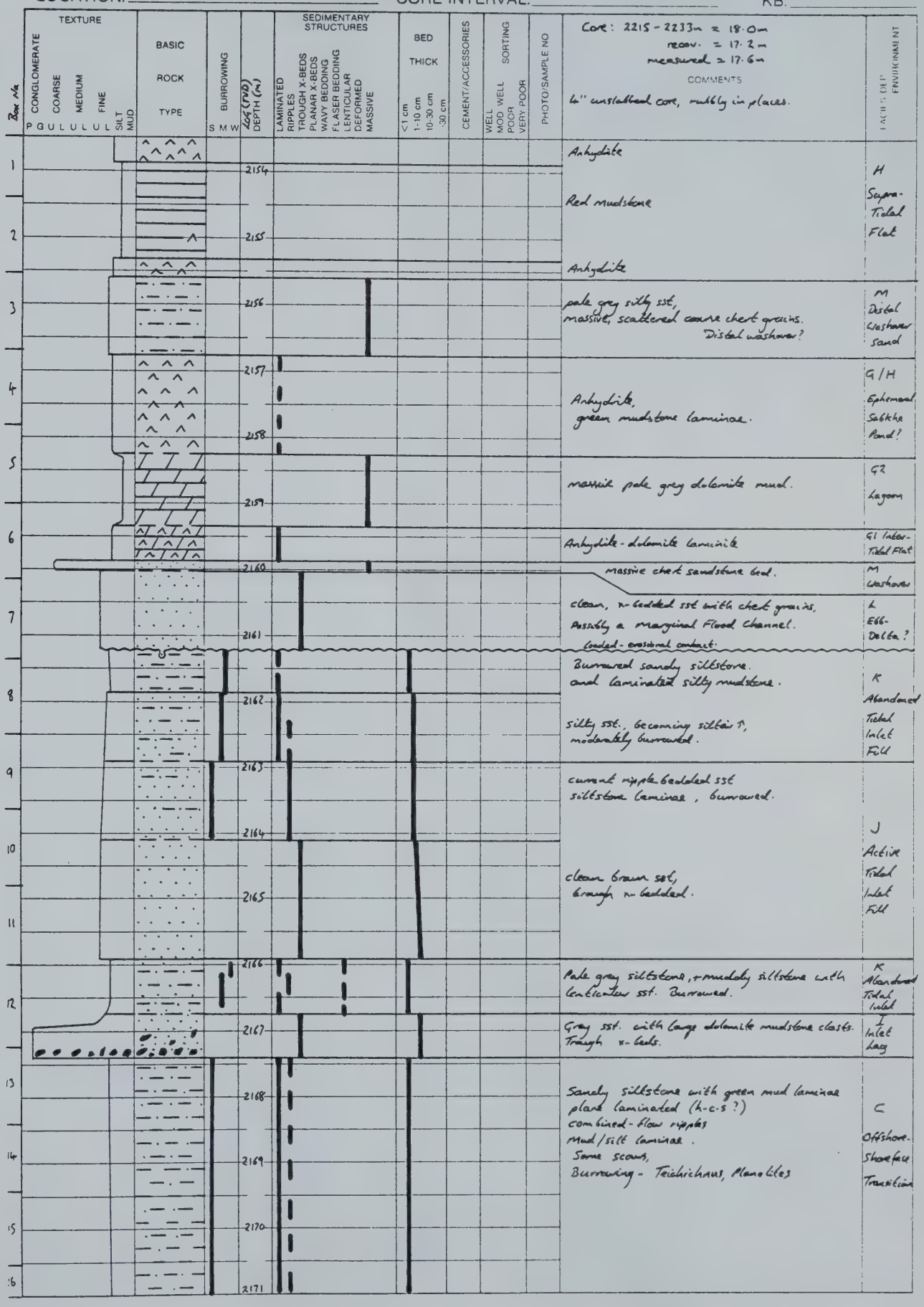

WELL NAME: Shell Wembley 5-13-72-8-W6 FORMATION: DATE:

LOCATION: CORE INTERVAL: KB:

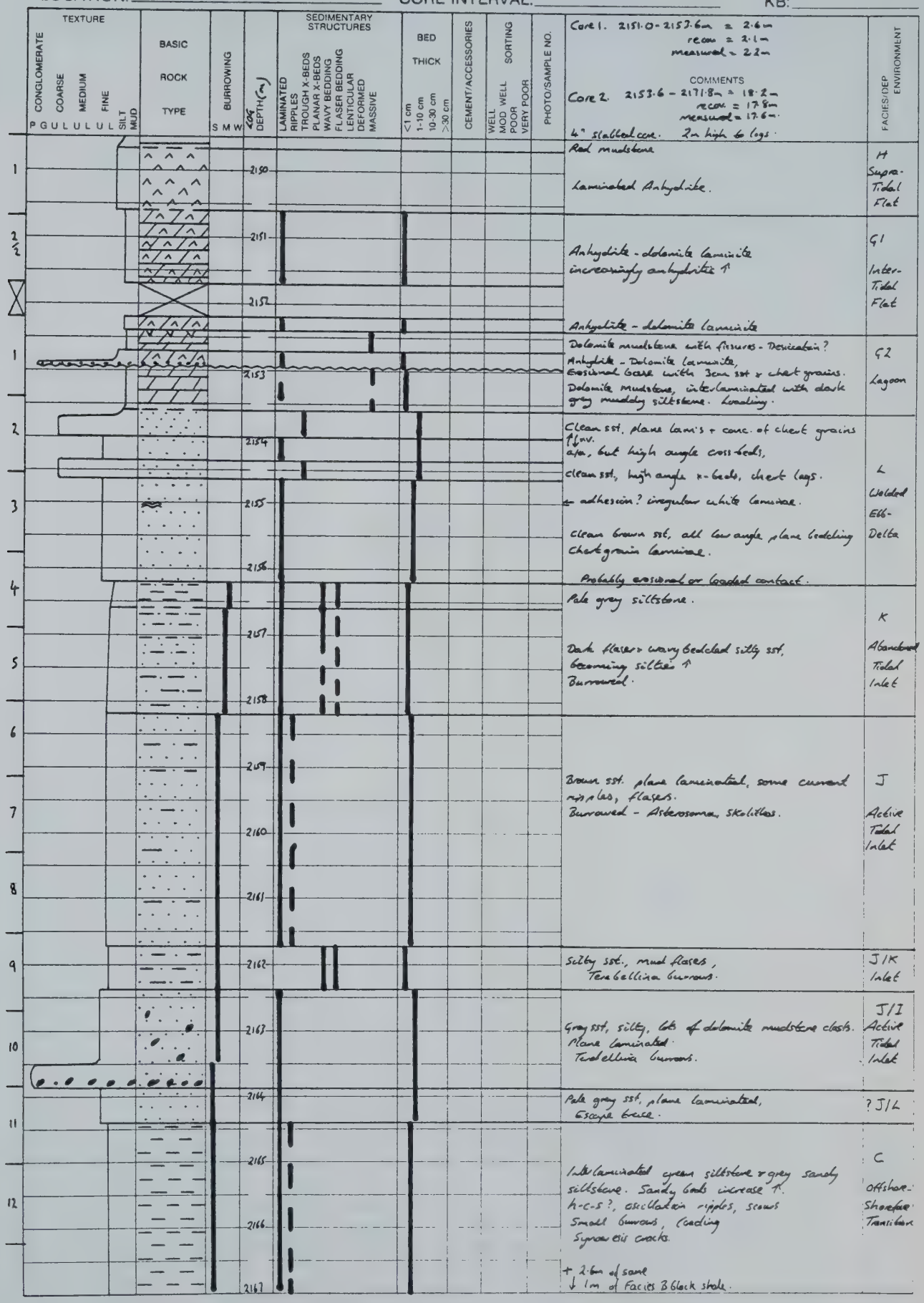

WELL NAME: Shell Wembley FORMATION: DATE:

LOCATION: 8-13-72-8-W6 CORE INTERVAL: KB:

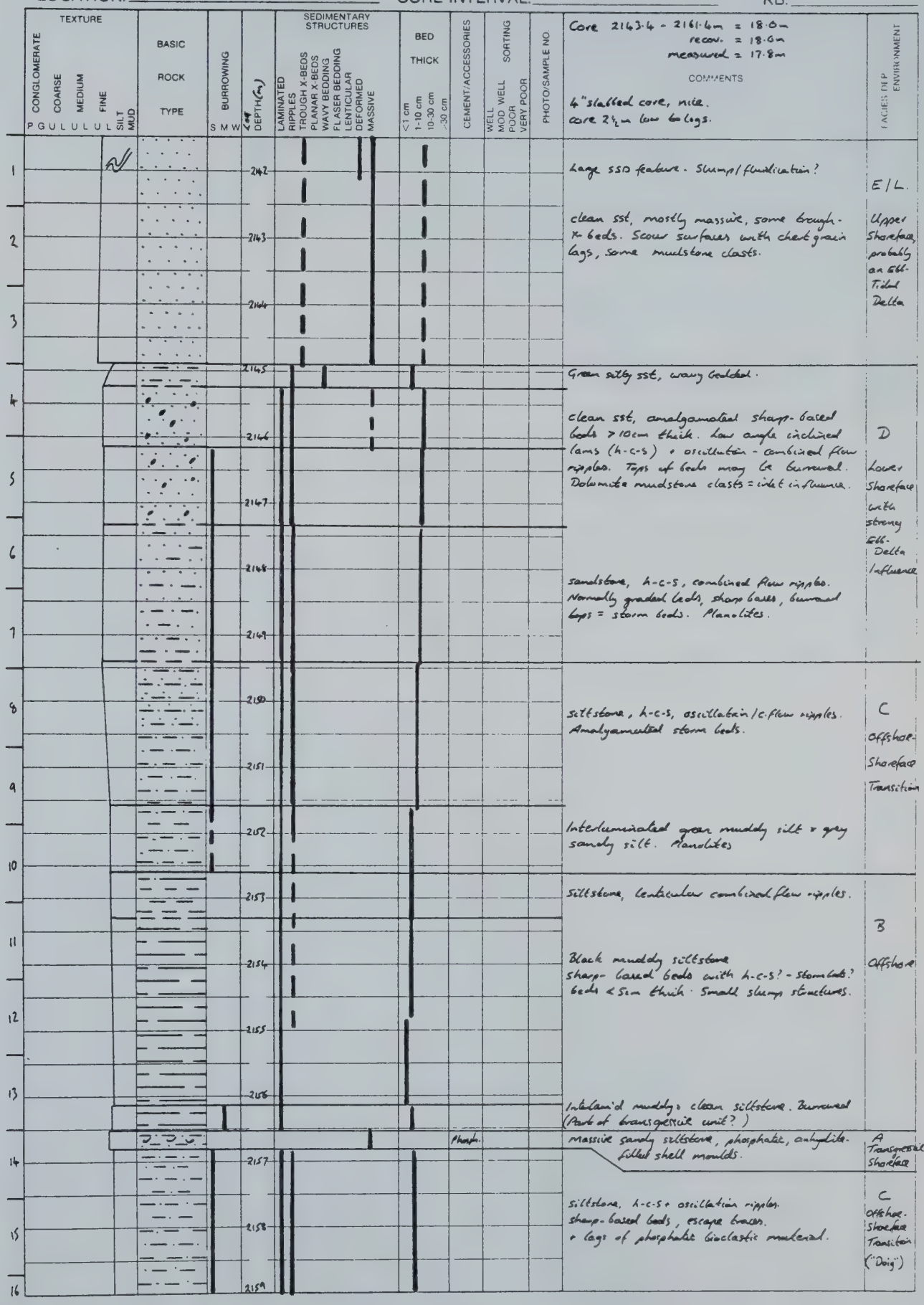

WELL NAME: Shell Wembley FORMATION: DATE:

LOCATION: 6-14-72-8-W6 CORE INTERVAL: KB:

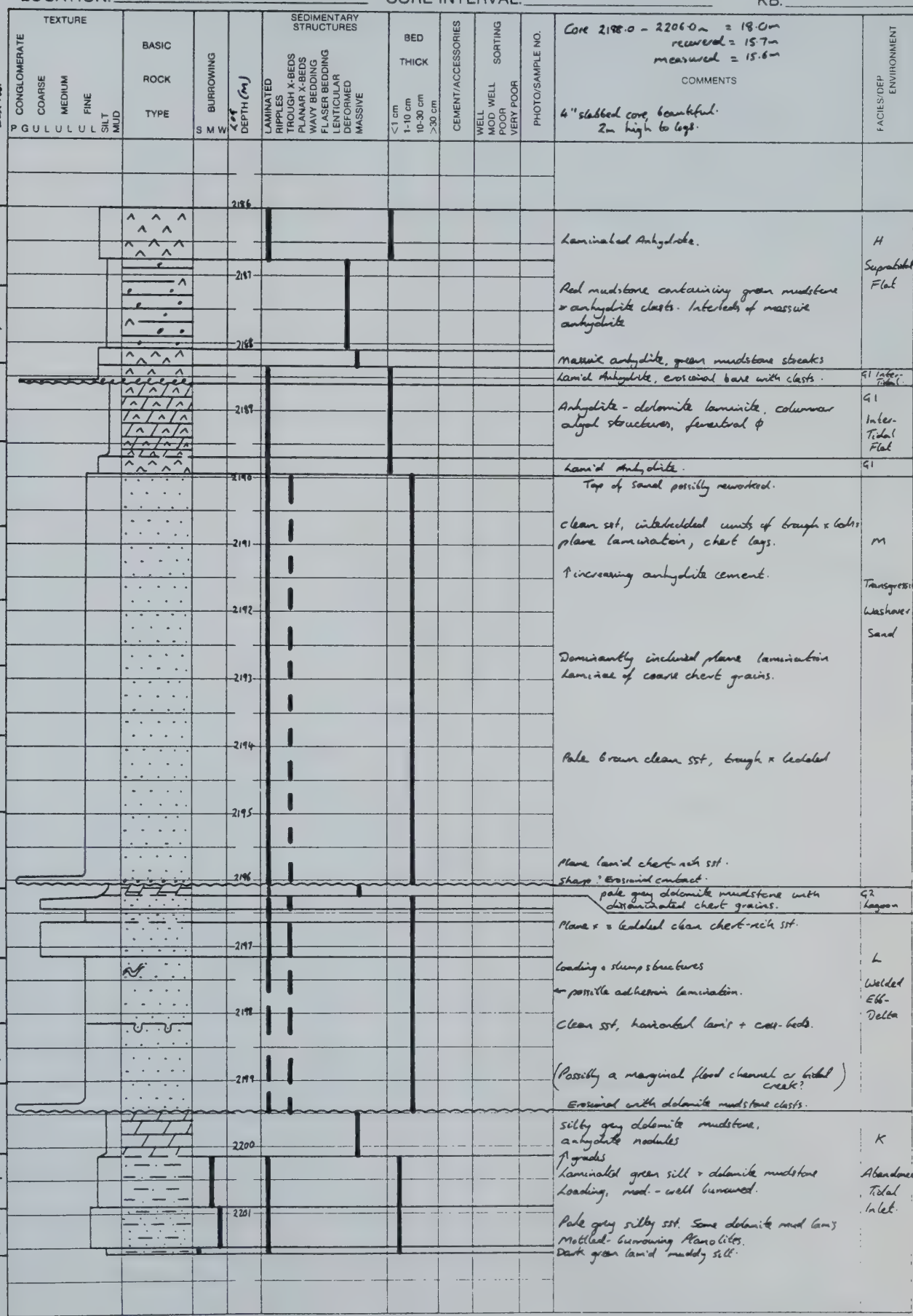

WELL NAME: Shell Wembley FORMATION: DATE:

LOCATION: 16-15-72-8-W6 CORE INTERVAL: KB:

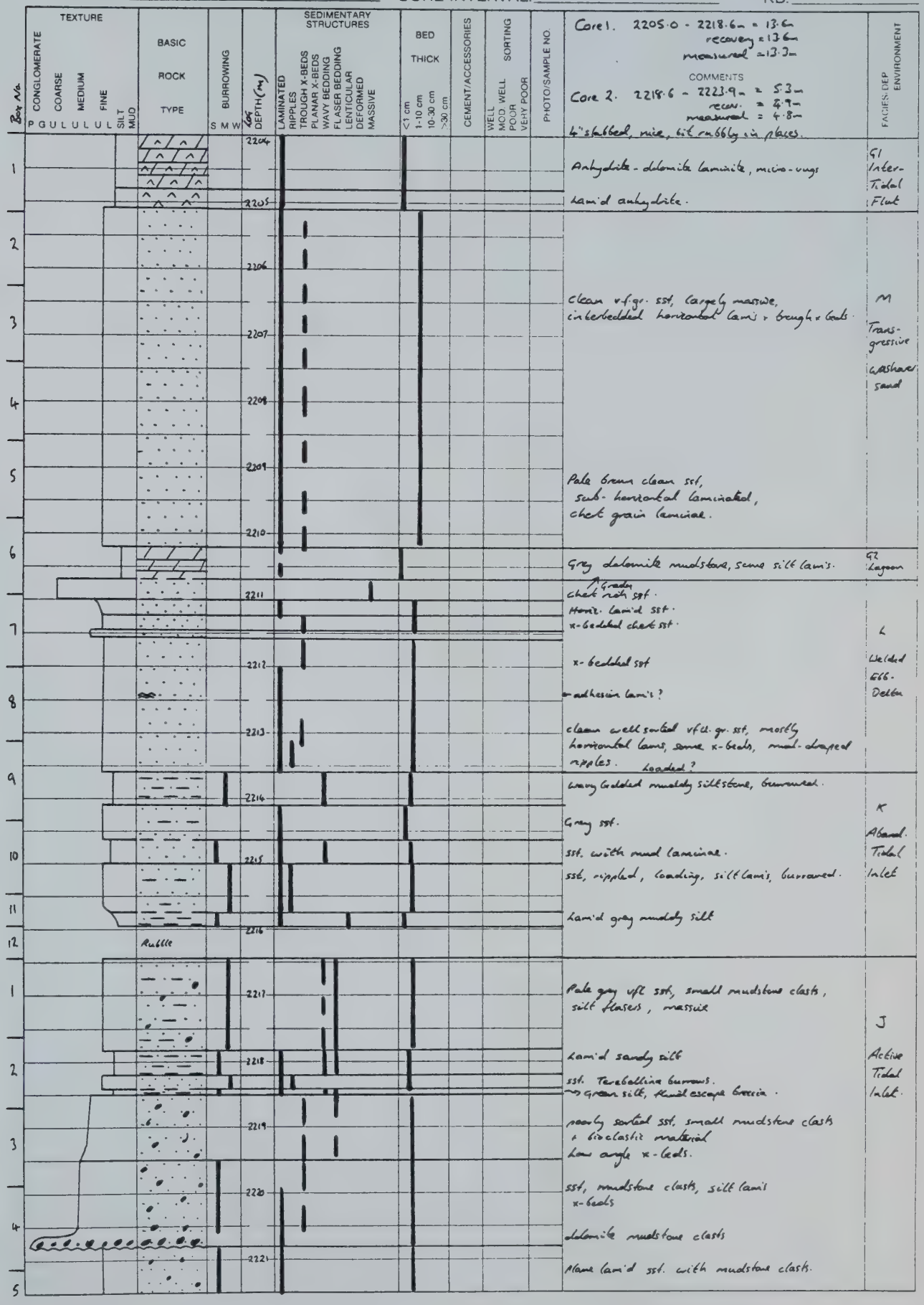

WELL NAME: Shell Wembley FORMATION: DATE:

LOCATION: 6-16-72-8-W6 CORE INTERVAL: KB:

Core 2281·0 - 2287·0m = 6m
Recovery = 6m
Measured = 5·9m.

3½" slabbed core, o.k.

Box No.	TEXTURE (CONGLOMERATE, COARSE, MEDIUM, FINE, SILT, MUD)	BASIC ROCK TYPE	BURROWING (S M W)	DEPTH (m)	SEDIMENTARY STRUCTURES (LAMINATED, RIPPLES, TROUGH X-BEDS, PLANAR X-BEDS, WAVY BEDDING, FLASER BEDDING, LENTICULAR, DEFORMED, MASSIVE)	BED THICK (<1 cm, 1-10 cm, 10-30 cm, >30 cm)	CEMENT/ACCESSORIES	WELL SORTING (MOD. WELL, POOR, VERY POOR)	PHOTO/SAMPLE NO.	COMMENTS	FACIES/DEP ENVIRONMENT
				2281						vfu clean sst. massive	D
1										vfu-L clean sst. some plane lams, mostly massive. Green mudstone lams near base.	Lower Shoreface
				2282						Well burrowed silty sst.	
2				2283						Interlam'd silty sst & muddy siltstone.	—?— C
				2284						Plane lam'd vfl silty sst, escape traces = h-c-s. Thin green mudstone laminae. Massive / burrowed areas. Planolites, Palaeophycus, ? Asterosoma.	Offshore Shoreface Transition
3				2285						Interlam'd grey sandy siltstone & green muddy silt. Plane lams (h-c-s), combined flow ripples, loading. Large Planolites burrows.	
4				2286							
5											

WELL NAME: Total Wembley FORMATION: DATE:

LOCATION: 6-21-72-8-W6 CORE INTERVAL: KB:

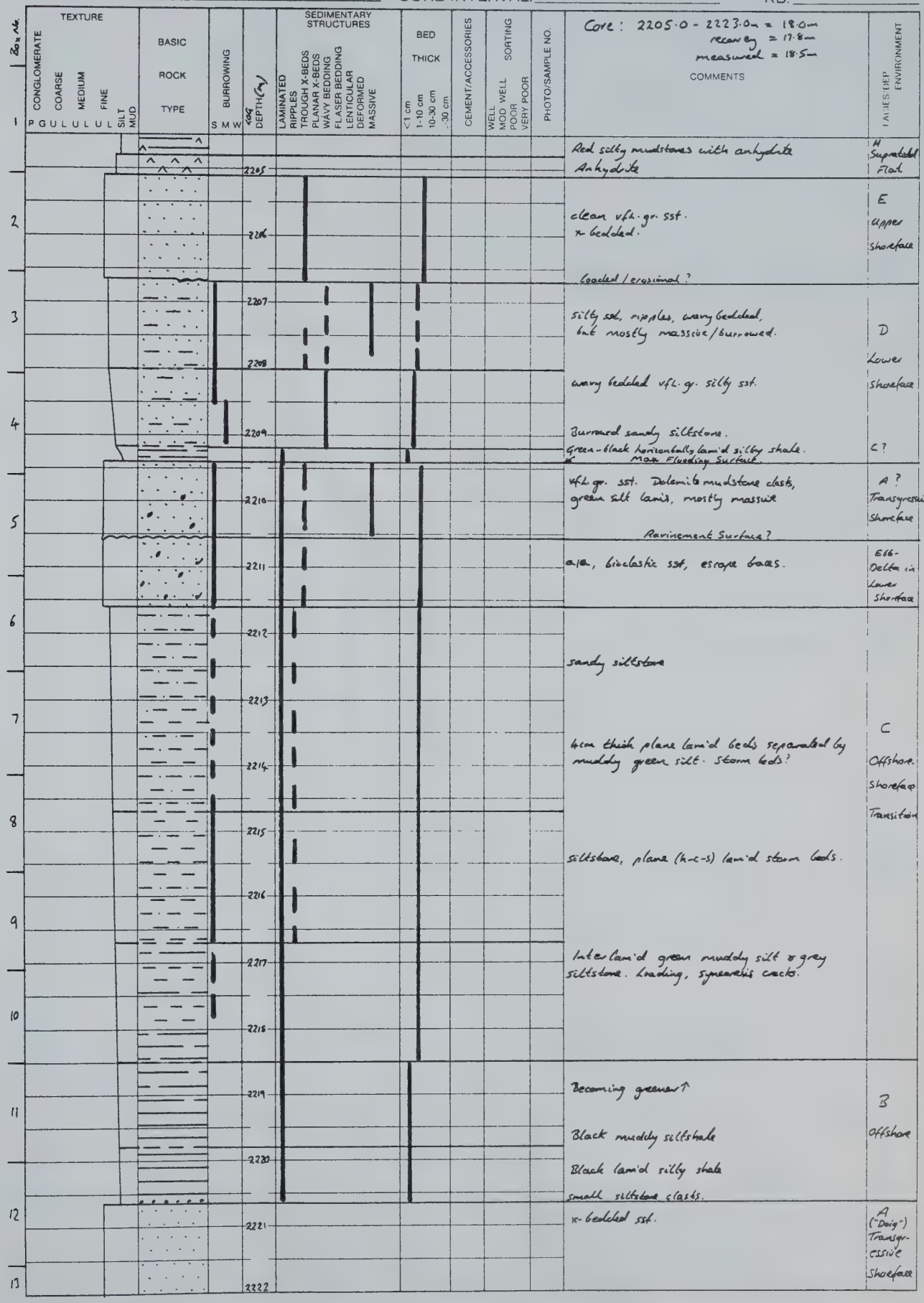

WELL NAME: Total Wembley FORMATION: DATE:

LOCATION: 16-21-72-8-W6 CORE INTERVAL: KB:

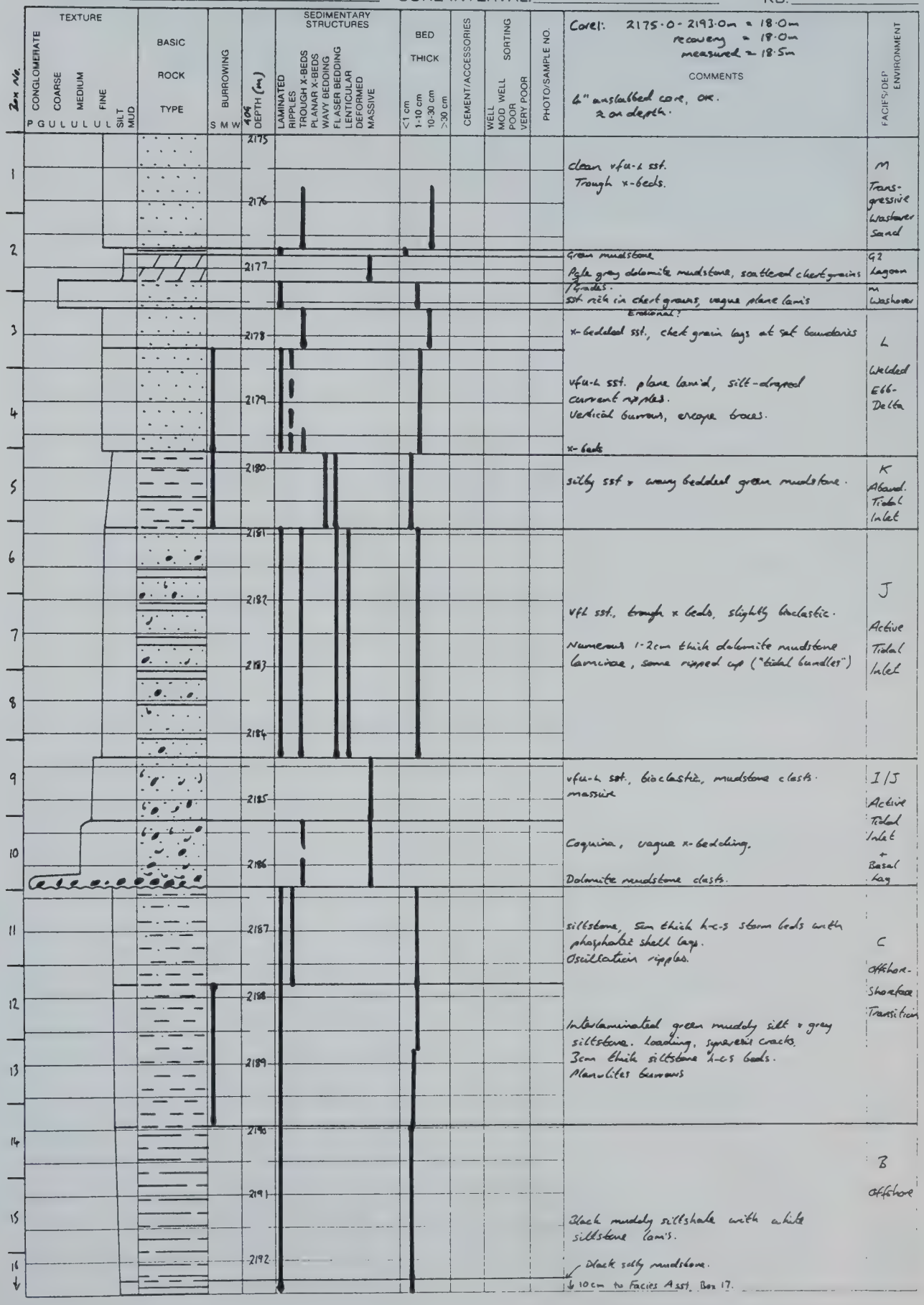

WELL NAME: Total et al Wembley FORMATION: DATE:

LOCATION: 6-22-72-8-W6 CORE INTERVAL: KB:

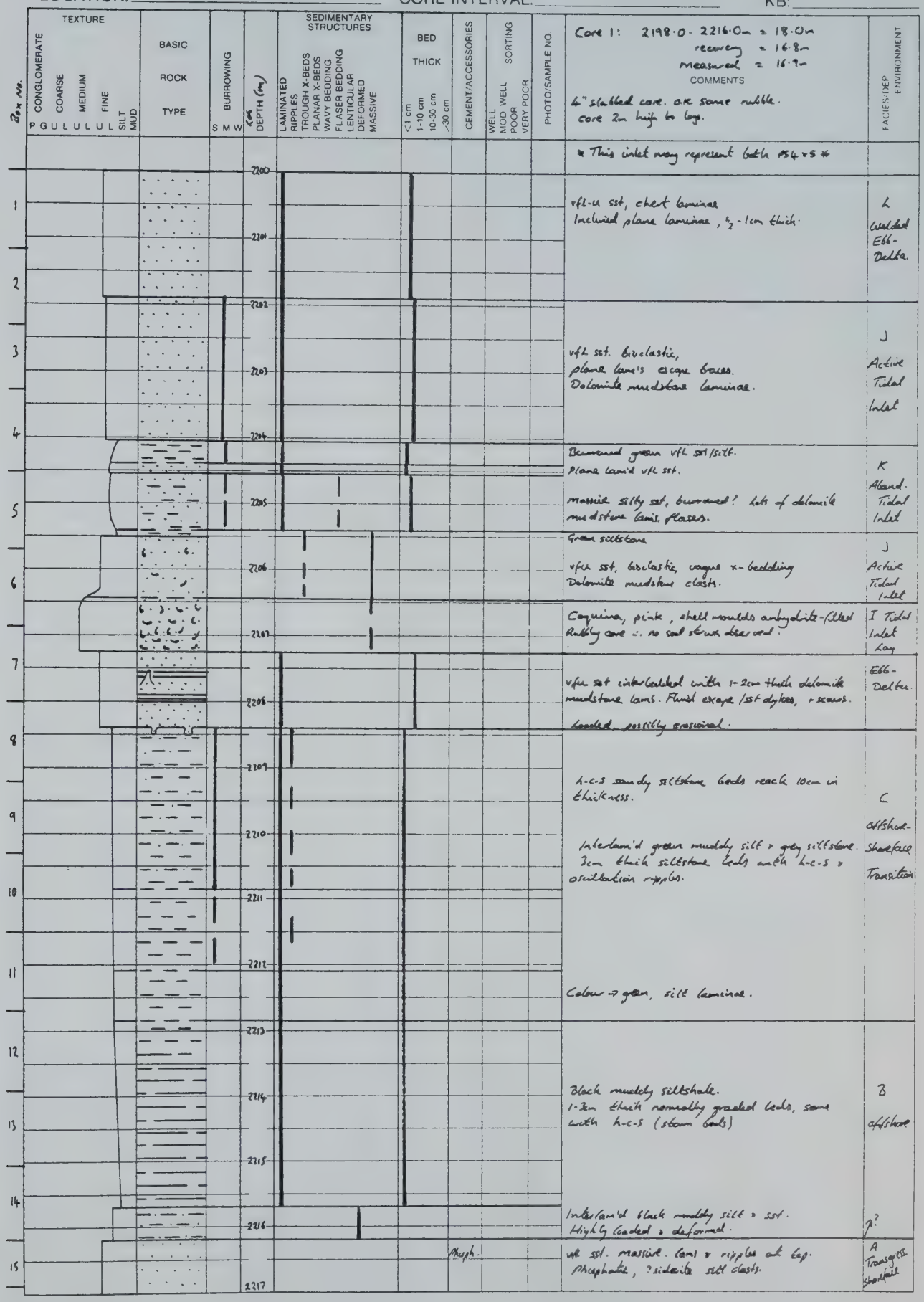

WELL NAME: Total et al Wembley FORMATION: DATE:

LOCATION: 8-22-72-8-W6 CORE INTERVAL: KB:

Core 1. 2180.0 – 2198.0 m = 18.0 m
recovery = 17.6 m
measured = 17.6 m

Zone no.	TEXTURE: CONGLOMERATE (P)	COARSE (G)	MEDIUM (U)	FINE (L)	FINE (U)	SILT (L)	MUD (U)	BASIC ROCK TYPE	BURROWING: S	M	W	Core DEPTH (m)	SEDIMENTARY STRUCTURES: LAMINATED	RIPPLES	TROUGH X-BEDS	PLANAR X-BEDS	WAVY BEDDING	FLASER BEDDING	LENTICULAR	DEFORMED	MASSIVE	BED THICK: <1 cm	1-10 cm	10-30 cm	>30 cm	CEMENT/ACCESSORIES	WELL SORTING: MOD. WELL	POOR	VERY POOR	PHOTO/SAMPLE NO.	COMMENTS	FACIES/DEP ENVIRONMENT
1												2179																				
2												2180																			vfu. clean sst, plane laminated, some cross-bed sets. laminae of coarse chert grains.	M Trans-gressive Washover Sand
3												2181																				
4												2182																				
												2183																				
5																															Concentration of chert grains. Dolomite mudstone	G2 Lagoon
																															coarse grained chert sst.	M Washover
6												2184																			vfu-u. sst. plane laminated, cross-beds, chert grain lags.	L Welded Ebb-Delta
7												2185																				
												2186																				
8												2187																			vfu. brown-grey silty sst., silt laminae, current ripples, horizontal laminae.	J/K
9												2188																				
10												2189																				J Active Tidal Inlet
11												2190																			vfu-L sst, slightly bioclastic, vague x-beds	
												2191																				
12												2192																			vfu sst with chert grains. x-beds.	
13												2193																			vfu sst; small dolomite mudstone clasts bioclastic, possible plane laminae.	
14												2194																				J/I

WELL NAME: (2/2) FORMATION: DATE:

LOCATION: 8-22-72-8-W6 CORE INTERVAL: KB:

Box no.	TEXTURE: CONGLOMERATE / COARSE / MEDIUM / FINE / SILT / MUD (P G U L U L U L)	BASIC ROCK TYPE	BURROWING (S M W)	DEPTH (m)	SEDIMENTARY STRUCTURES: LAMINATED / RIPPLES / TROUGH X-BEDS / PLANAR X-BEDS / WAVY BEDDING / FLASER BEDDING / LENTICULAR / DEFORMED / MASSIVE	BED THICK: <1 cm / 1-10 cm / 10-30 cm / >30 cm	CEMENT/ACCESSORIES	SORTING: WELL / MOD WELL / POOR / VERY POOR	PHOTO/SAMPLE NO.	COMMENTS (Core 2. 2198.0 – 2216.4m = 18.4m; recovery = 18.4m; measured = 12m; 4" slabbed core, otherwise)	FACIES/DEP ENVIRONMENT
15				2195						Pale gray vf. sst, bioclastic.	J Active Tidal Inlet
16				2196						vfu. sst, large dolomite mudstone clasts.	I Tidal Inlet Lag.
1				2197						a/b, increasing sand content. Storm beds up to 8cm thick.	
2				2198							C Offshore Shoreface Transition
3				2199							
4				2200						Interlaminated muddy or sandy siltstone. Plane lam'd, pyrite, syneresis cracks, planolites burrows. Loading.	
5				2201			Pyrite				
6				2202							
7				2203						much siltier than typical facies B. Lam'd, lenticular ripples. A-C-S.?	B Offshore
8				2204						sst laminae, slumping.	
9				2205						Interlam'd black silt & sst.	
10				2206			Phosph. Anhydrite			vf. sst, bioclastic, phosphatic. Anhydrite cement.	A Transgressive Shoreface ("Daly")
11				2207							
				2208							

WELL NAME: Total et al Wembley FORMATION: DATE:

LOCATION: 14-22-72-8-W6 CORE INTERVAL: KB:

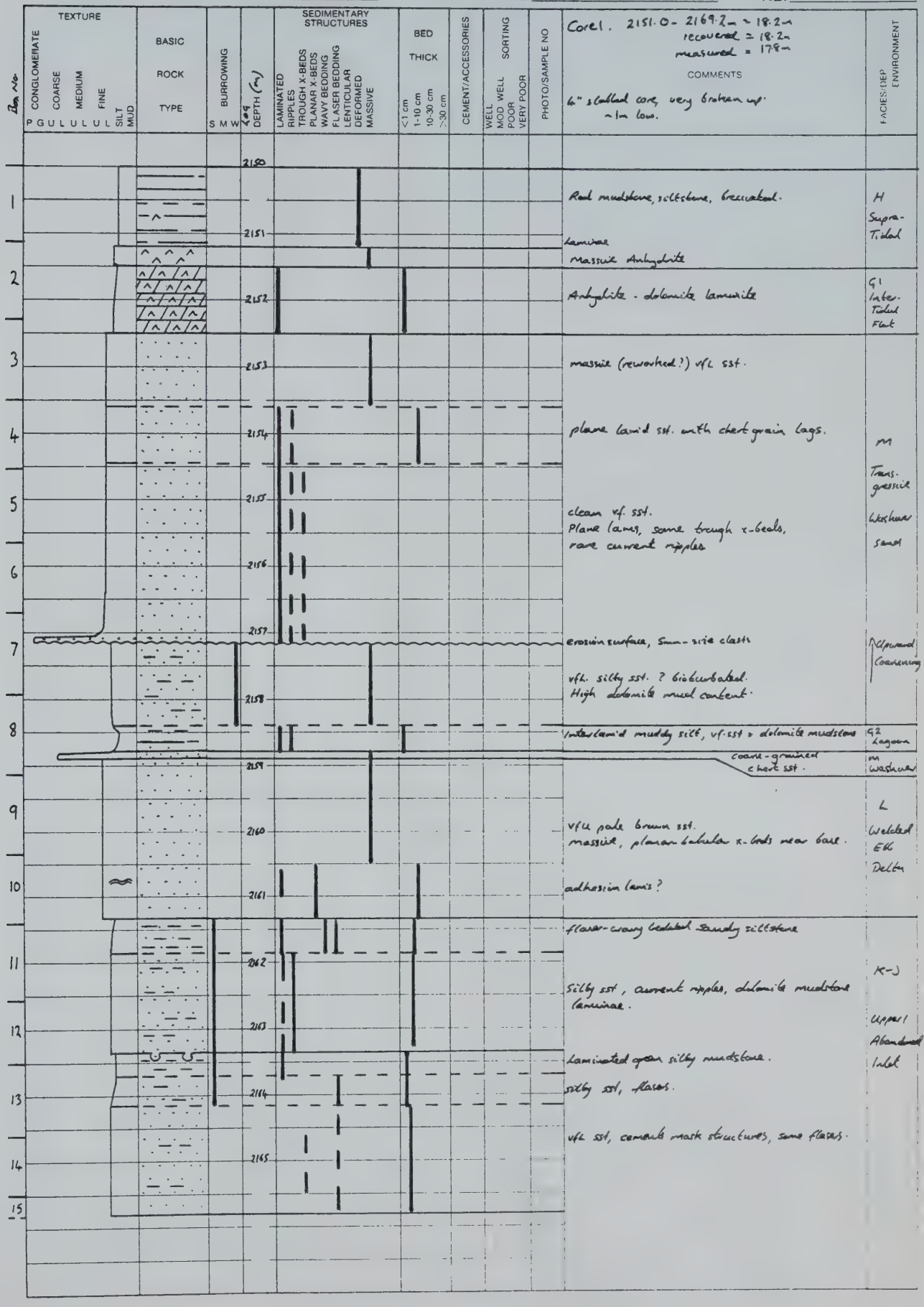

WELL NAME: (2/2) FORMATION: DATE:

LOCATION: 14-22-72-8-W6 CORE INTERVAL: KB:

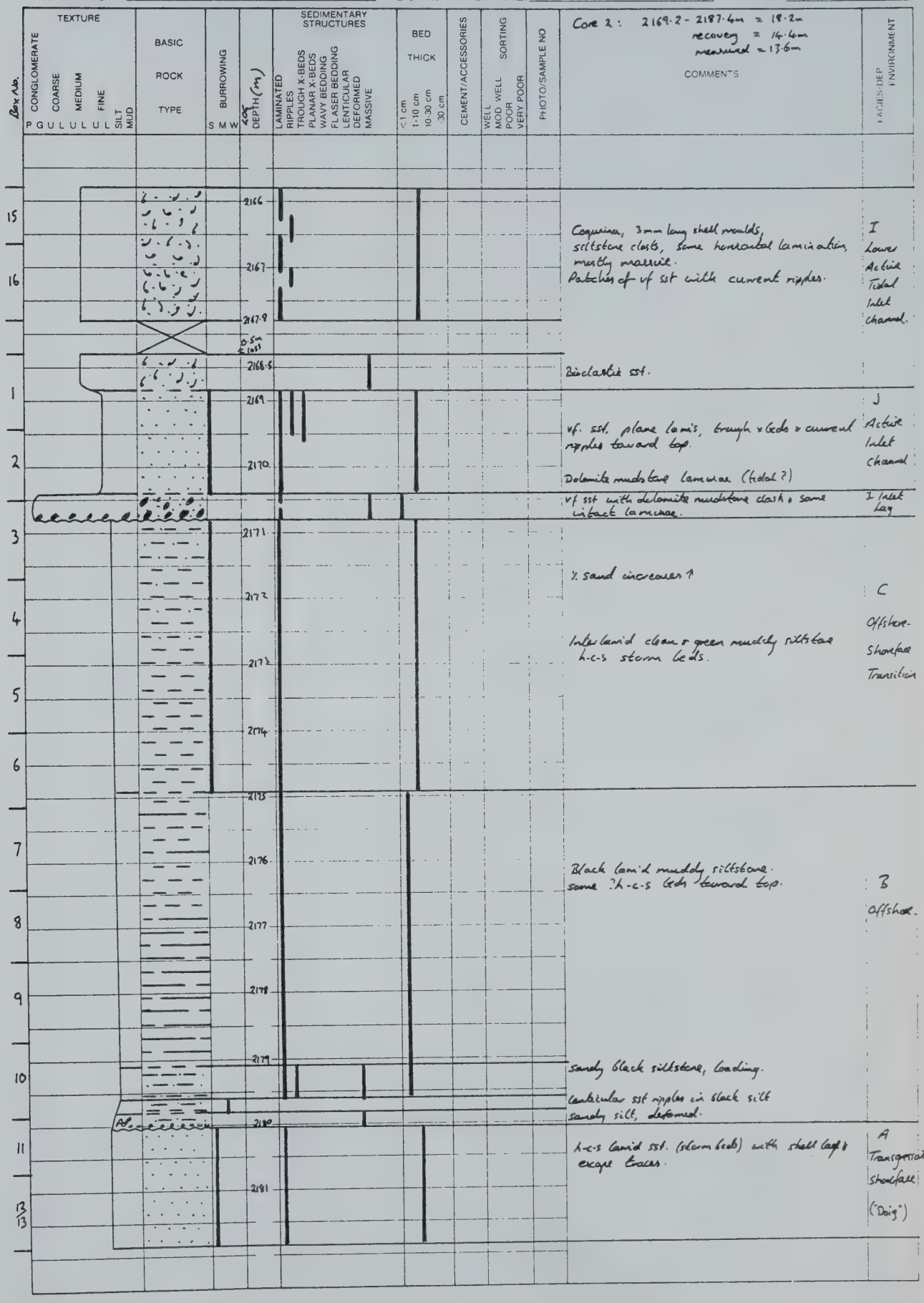

WELL NAME: Total et al Wembley FORMATION: DATE:

LOCATION: 16-22-72-8-W6 CORE INTERVAL: KB:

Core: 2150.0 - 2168.0m = 18.0m
recovery = 16.5m
measured = 16.0m

COMMENTS: 4" unslabbed core, ok. ≈ on depth.

Box no.	TEXTURE: CONGLOMERATE (P)	COARSE (G)	MEDIUM (U)	FINE (L)	SILT (U)	MUD (L)	BASIC ROCK TYPE	BURROWING (S M W)	DEPTH (m)	SEDIMENTARY STRUCTURES: LAMINATED	RIPPLES	TROUGH X-BEDS	PLANAR X-BEDS	WAVY BEDDING	FLASER BEDDING	LENTICULAR	DEFORMED	MASSIVE	BED THICK: <1 cm	1-10 cm	10-30 cm	>30 cm	CEMENT/ACCESSORIES	SORTING: WELL	MOD. WELL	POOR	VERY POOR	PHOTO/SAMPLE NO.	COMMENTS	FACIES/DEP ENVIRONMENT
1									2151																				white anhydrite, faintly laminated	
									2152																					
2																													Red mudstone	H Supra-tidal Sabkha
									2153																				Anhydrite a/a	
3									2154																				red mudstone, anhydritic	
4																													lam'd white anhydrite.	
									2155																				sharp undulatory contact.	
5									2156																				Fl sst, planar laminae	M Trans-gressive Washover
																													Loaded, possibly burrowed contact.	
																													Grey dolomite mudstone, some darker silt lams. chert grains from later	G2 lagoon
6									2157																				ch chert sst, plane lams, possibly ripples.	M Washover
7									2158																				Fl clean sst, small black siltstone clasts planar-tabular & trough x beds throughout.	L Marginal Fluvial Channel of Est. Delta
																													concentration of chert grains	
8									2159																				Silty sst, current ripples, flaser beds, some escape traces. Increasingly burrowed ↑ Some dolomite mud clasts.	K Abandon. Inlet.
9									2160																					
									2161																				Plane lam'd green silty shale.	
10									2162																				silty sst a/b, current ripples.	
																													Bed of ?bioclast bioclastic sst.	
11									2163																					J Active Tidal Inlet
12									2164																				Brown-grey sst, plane laminated, silty drapes (tidal?), escape traces. Climbing ripples } = rapid sedimentation; fluctuating. + some low angle x beds.	
13									2165																					
14									2166																				Bioclastic sst, anhydrite-cemented.	
																													vf sst, dolomite mudstone clasts, silt lams, some ripples.	
15									2167																				Bioclastic sst, dolomite mudstone clasts.	I/J

WELL NAME: Total et al Wembley FORMATION: DATE:

LOCATION: 6-23-72-8-W6 CORE INTERVAL: KB:

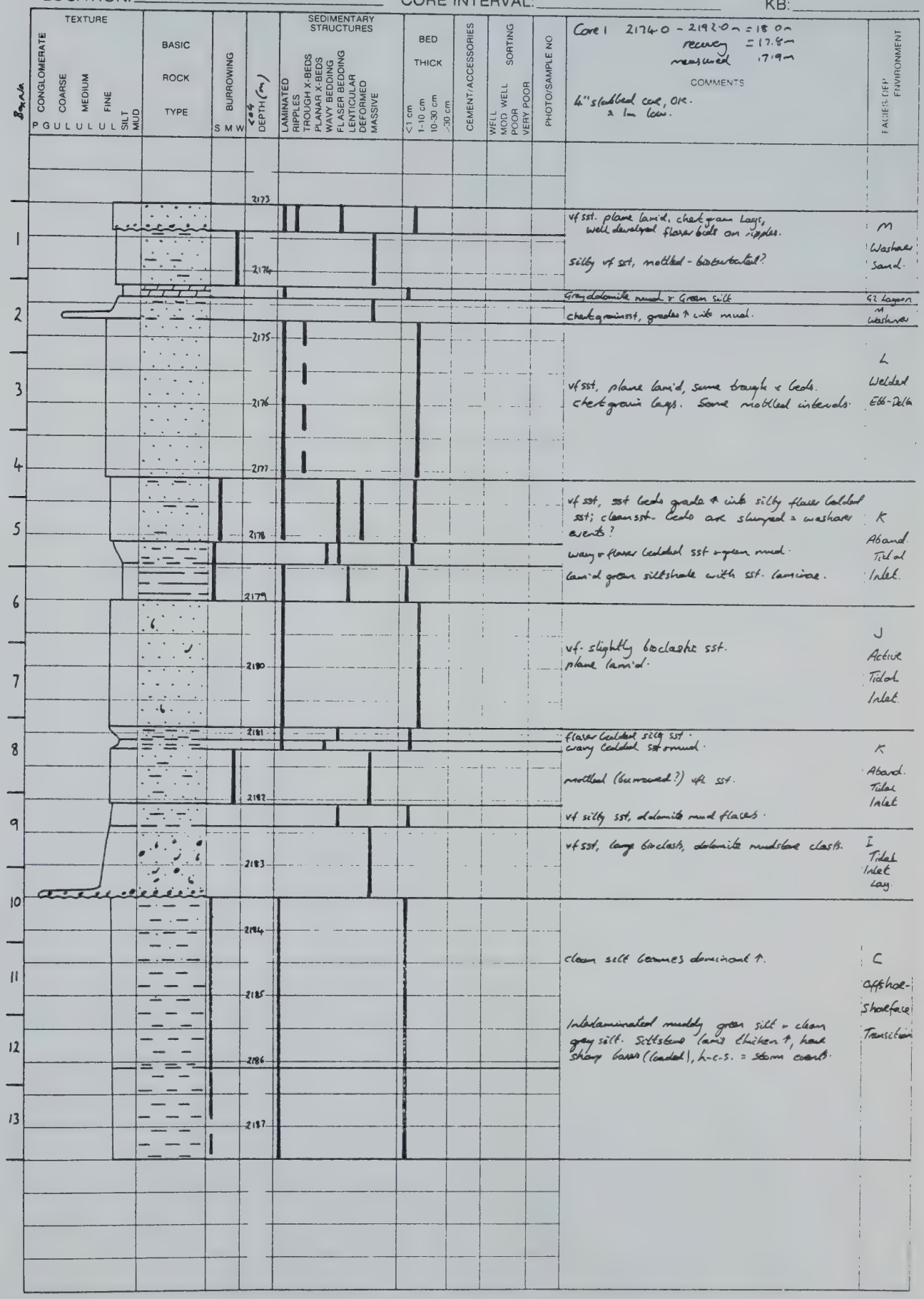

WELL NAME: (2/2)

LOCATION: 6-23-72-8-W6

FORMATION:

CORE INTERVAL:

DATE:

KB:

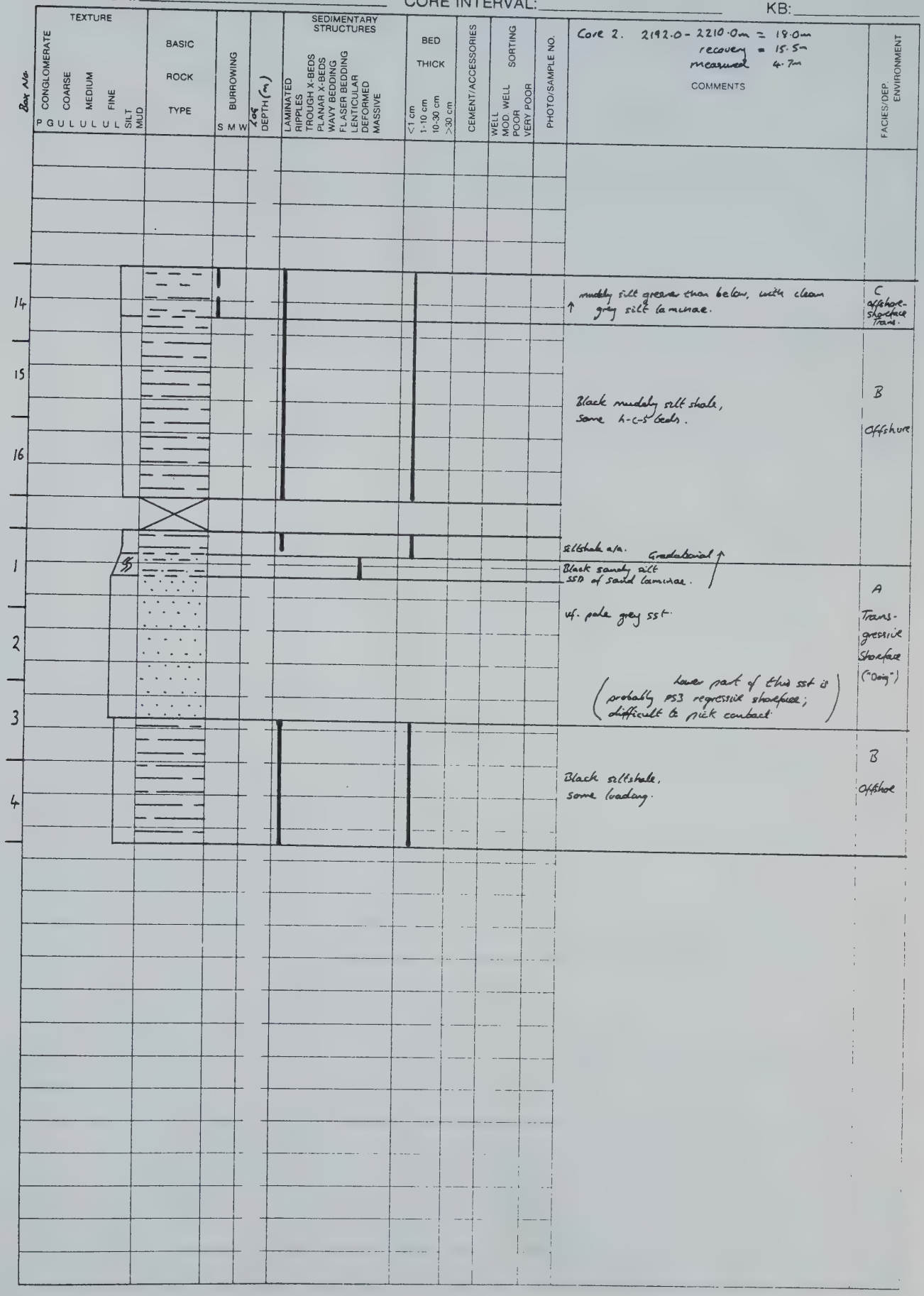

WELL NAME: Total et al Wembley FORMATION: DATE:

LOCATION: 8-23-72-8-W6 CORE INTERVAL: KB:

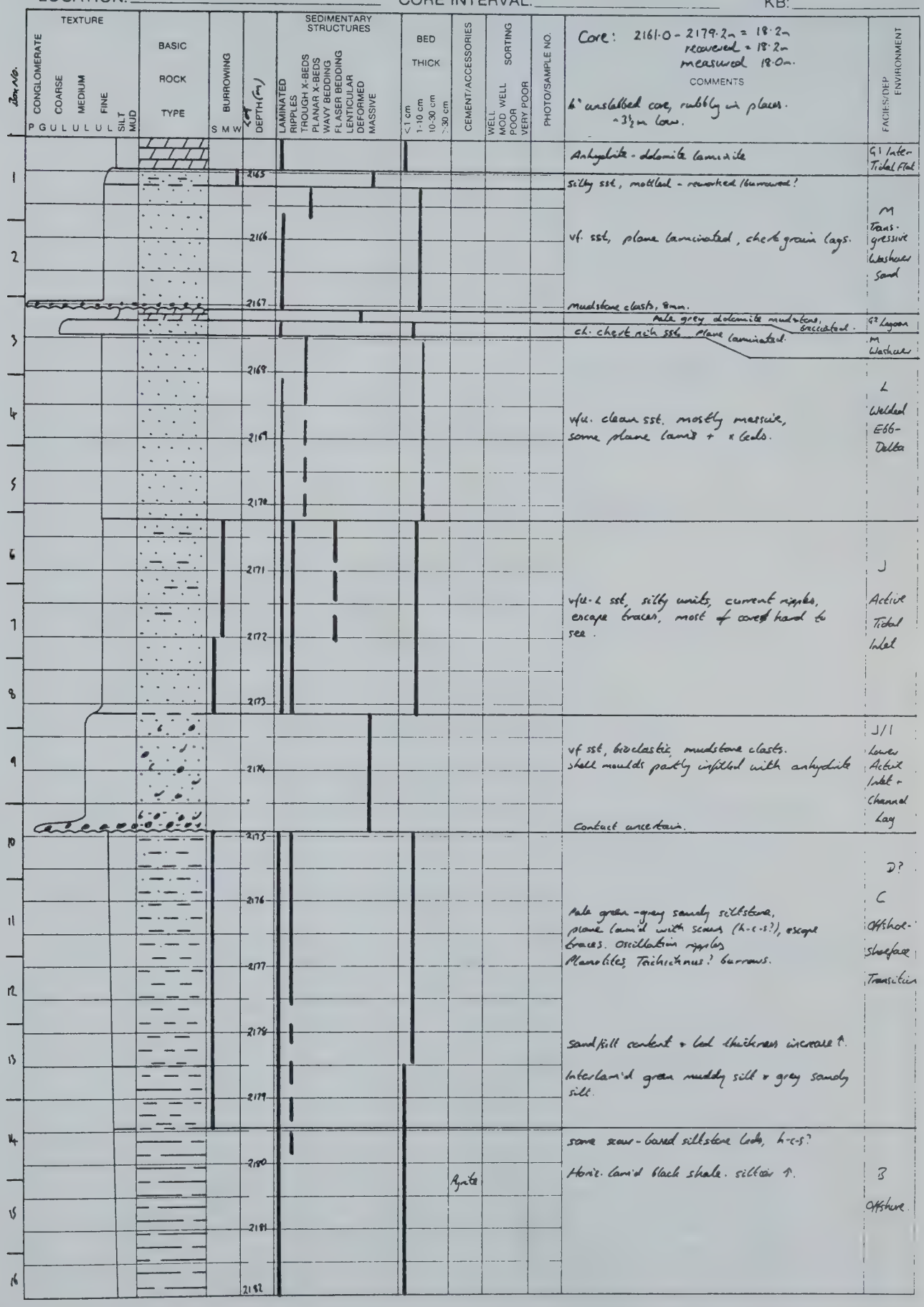

WELL NAME: Total et al Wembley FORMATION: DATE:

LOCATION: 16-23-72-8-W6 CORE INTERVAL: KB:

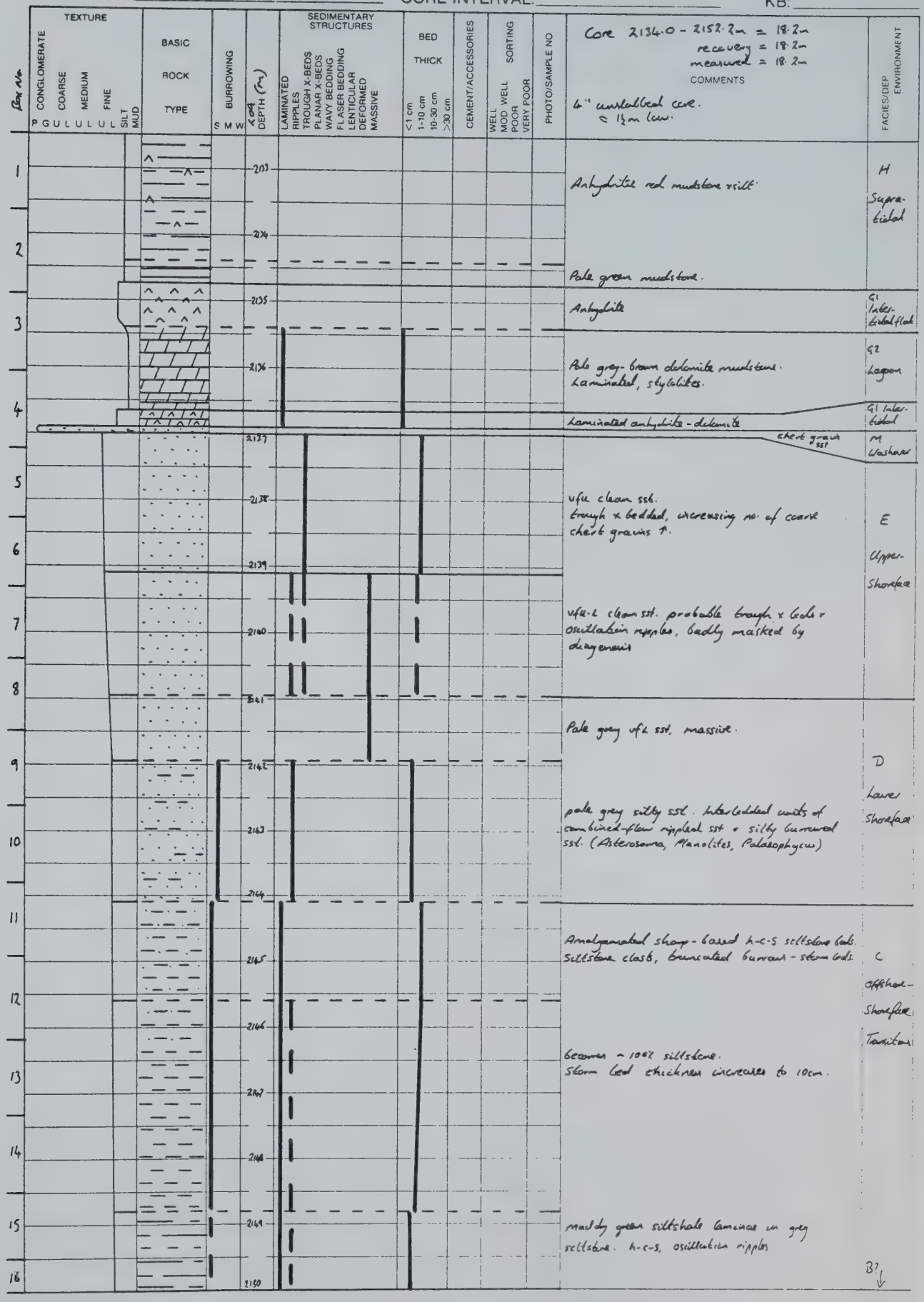

WELL NAME: PCP Beaverlodge FORMATION: DATE:

LOCATION: 11-24-72-8-W6 CORE INTERVAL: KB:

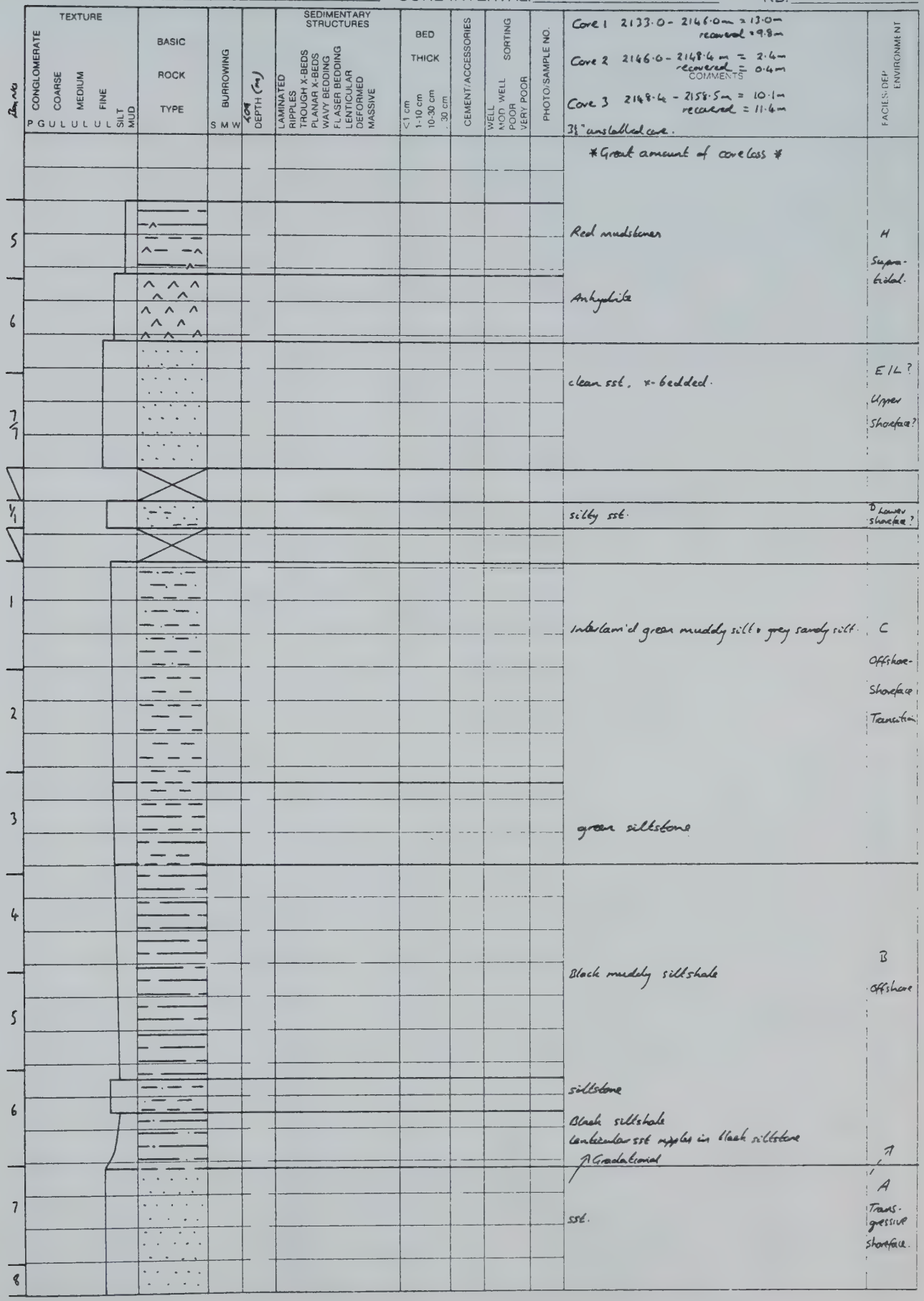

WELL NAME: PCP Beaverlodge FORMATION: DATE:

LOCATION: 11-25-72-8-W6 CORE INTERVAL: KB:

Box no	TEXTURE (CONGLOMERATE, COARSE, MEDIUM, FINE, SILT, MUD)	BASIC ROCK TYPE	BURROWING (S M W)	Core DEPTH (m)	SEDIMENTARY STRUCTURES (LAMINATED, RIPPLES, TROUGH X-BEDS, PLANAR X-BEDS, WAVY BEDDING, FLASER BEDDING, LENTICULAR, DEFORMED, MASSIVE)	BED THICK (<1 cm, 1-10 cm, 10-30 cm, >30 cm)	CEMENT/ACCESSORIES	SORTING (WELL, MOD. WELL, POOR, VERY POOR)	PHOTO/SAMPLE NO	COMMENTS	FACIES/DEP ENVIRONMENT
										Core 1 2113.5 - 2122.0m = 8.5m recovered = 7.22m very rubbly, 4" slabbed core, Core 2 2122.0 - 2138.3m = 16.3m recovered = 15.8m measured = 15.2m	
3				2115						laminated anhydrite	G1 Inter tidal flat
				2116						sst with chert grains & silt clasts.	
4										silty dolomite mudstone.	G2 Lagoon
										chert-rich sst, vague low angle x-beds.	Washover? F foreshore
5				2117							
				2118							
6				2119						clean uf. x-bedded sst. laminae of chert grains.	L E66-Delta
7				2120							
1				2121						clean, x-bedded sst.	
2				2122							
3				2123						bioclastic sst, planar tabular x-beds, some silt laminae (tidal?) stolithos burrow	I/J Inlet E66 Channel
4				2124						current rippled uf. sst.	
5				2125						mudstone, syneresis cracks filled with sst from above. Teichichnus burrow.	
6				2126						uf sst in beds 10-20cm thick of h-c-s? / plane lam's with small dolomite mudstone clasts + escape traces. + phosphatic bioclasts. large oscillation ripples ?	E66-Delta (Shoal) in lower Shoreface?
7				2127							
8				2128							
9				2129						muddy siltstones Asterosoma, Planolites, Rosselia, stolithos, Teichichnus burrows	C/D? Offshore-Shoreface transition
10				2130						↓ 5.5m facies C + B	

WELL NAME: PCP Wembley FORMATION: DATE:

LOCATION: 16-25-72-8-W6 CORE INTERVAL: KB:

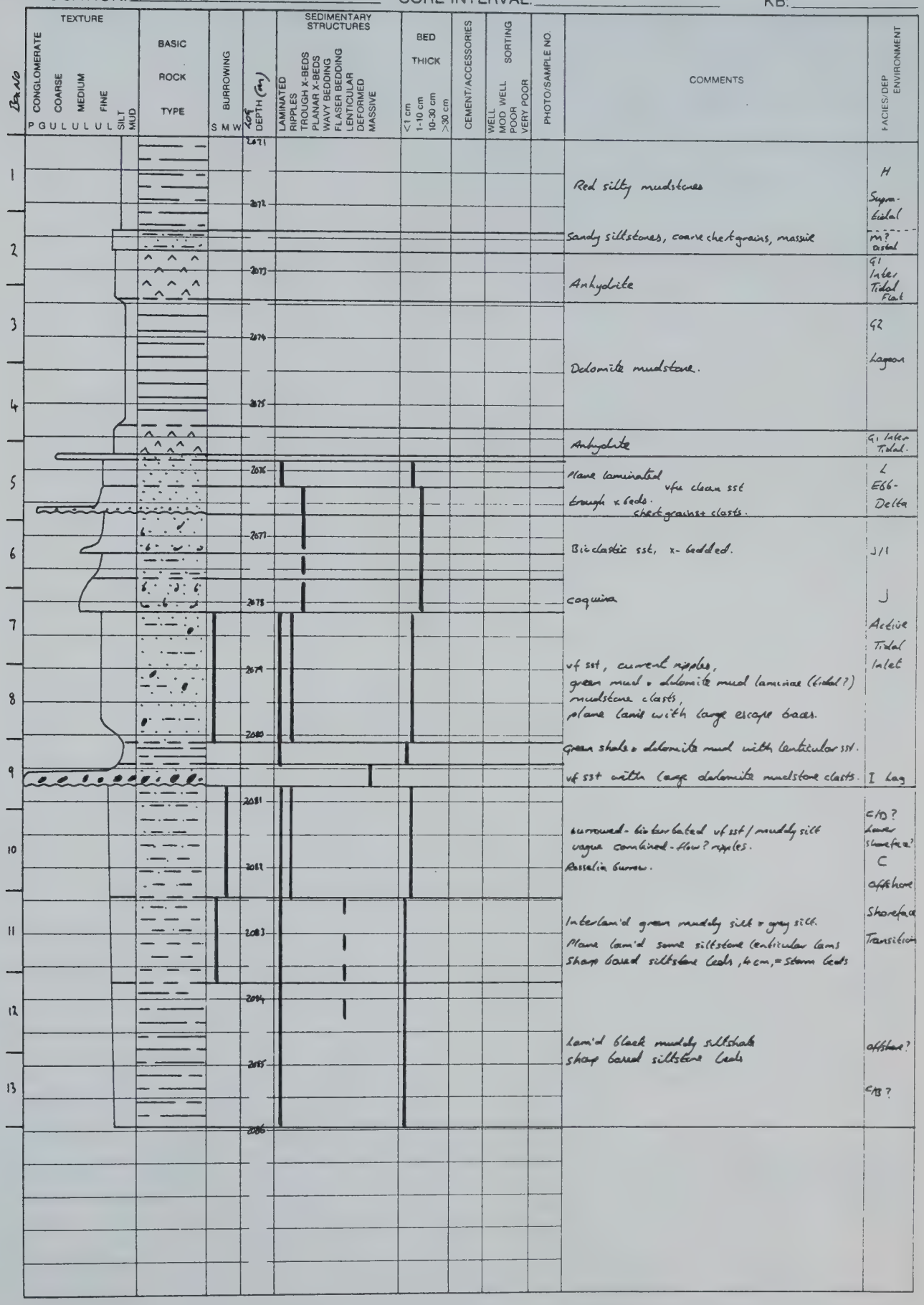

WELL NAME: Total et al Wembley FORMATION: DATE:

LOCATION: 6-26-72-8-W6 CORE INTERVAL: KB:

Core 2165.0 - 2183.0m = 18.0m
recovery = 14.1m
measured 14.5m

Box No.	TEXTURE (CONGLOMERATE, COARSE, MEDIUM, FINE, SILT, MUD)	BASIC ROCK TYPE	BURROWING (S M W)	Log DEPTH (m)	SEDIMENTARY STRUCTURES (LAMINATED, RIPPLES, TROUGH X-BEDS, PLANAR X-BEDS, WAVY BEDDING, FLASER BEDDING, LENTICULAR, DEFORMED, MASSIVE)	BED THICK (<1 cm, 1-10 cm, 10-30 cm, >30 cm)	CEMENT/ACCESSORIES	SORTING (WELL, MOD. WELL, POOR, VERY POOR)	PHOTO/SAMPLE NO.	COMMENTS	FACIES/DEP ENVIRONMENT
										4" unslabbed core, scored + difficult to describe * 1m high * Deviated well *	
										E66 - Tidal Delta Sequence.	
1				2066						Red silty mudstone	H Supra-tidal
2				2067 2068						laminated anhydrite	G1/H Inter-tidal
3										chert rich rippled sst. massive grey dolomite mudstone	G2 Lagoon
4				2069						cL chert rich sst. ?cross-bedded. Interbedding ↑	m? F Foreshore
5 6 7				2070 2071 2072 2073 2074						vf - fu. upward-coarsening clean sst, cross-bedded.	E/L Upper Shoreface of Welded E66-Delta.
8 9				2075 2076						vf sst, clean, trough x-beds, some flaser beds.	"D" E66-Delta in Lower Shoreface
10				2077						↑ trough x-beds appear	
11 12				2078 2079						vf sst, silt lam's/flasers, small dolomite mudstone clasts. Planolites burrows	
13				2080						vf sst, trough x beds, dolomite mudstone clasts.	I E66-Channel.

WELL NAME: PCP Wembley FORMATION: DATE:

LOCATION: 8-26-72-8-W6 CORE INTERVAL: KB:

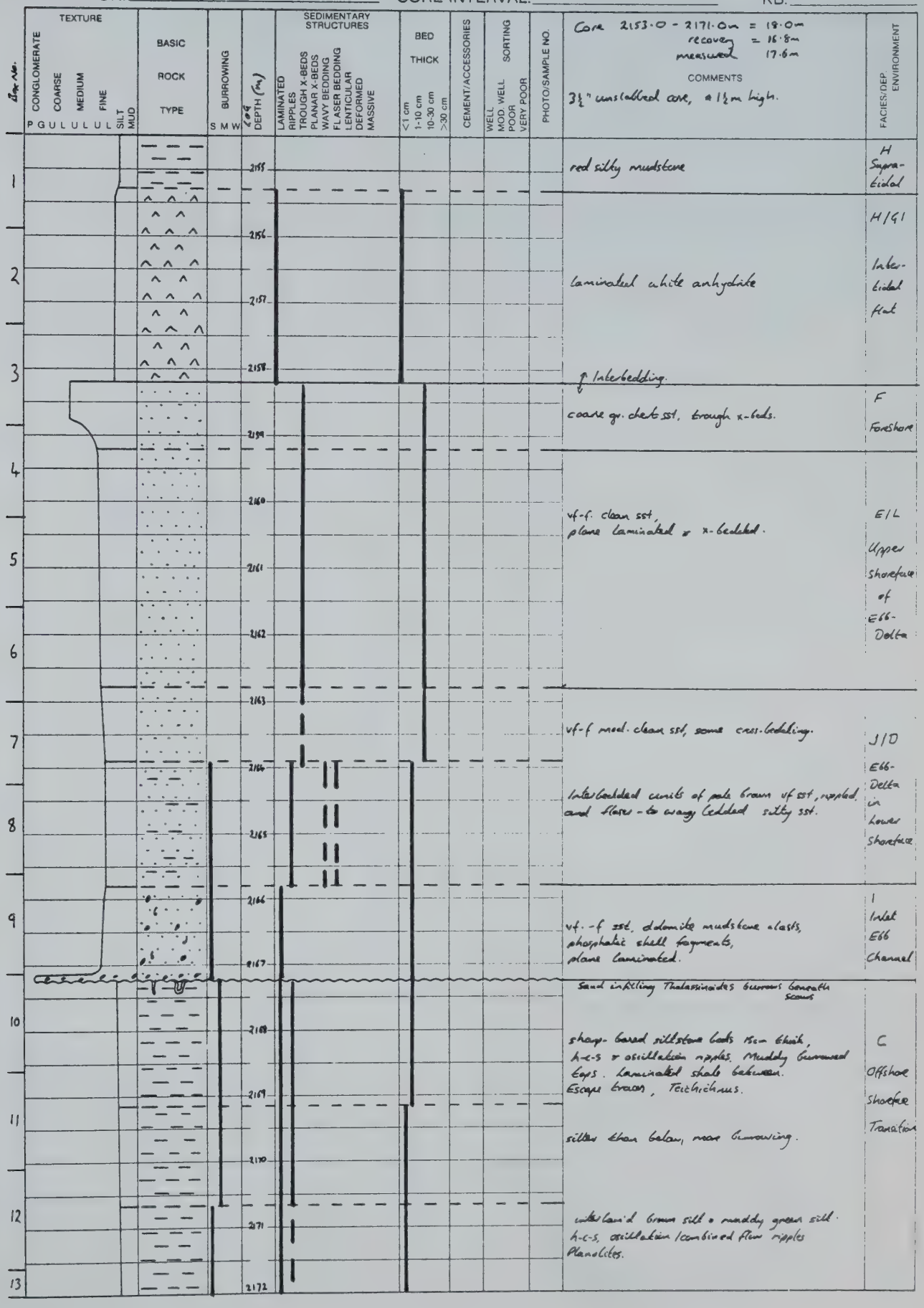

WELL NAME: Total et al Wembley FORMATION: DATE:

LOCATION: 11-26-72-8-W6 CORE INTERVAL: KB:

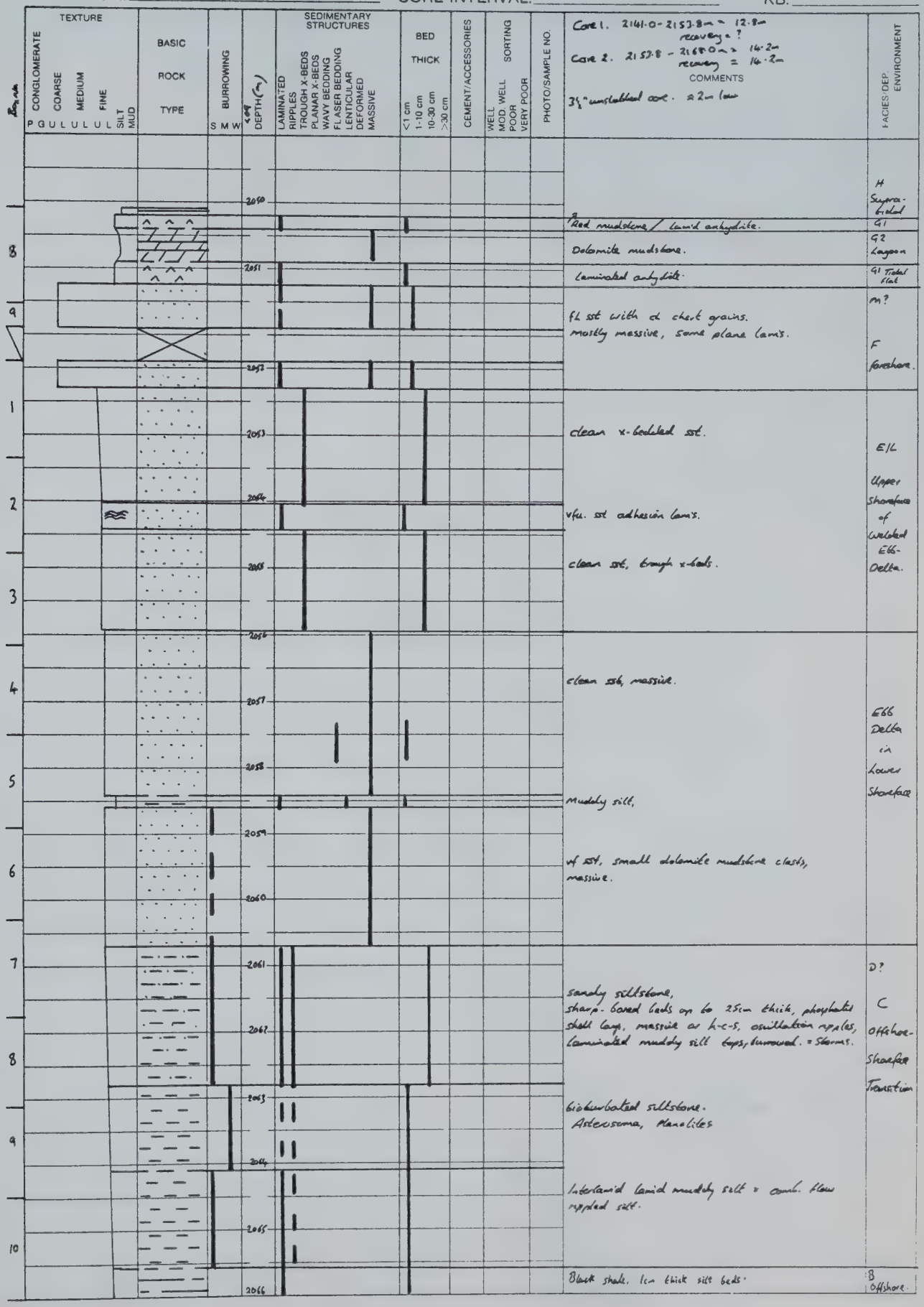

WELL NAME: PCP Beaverlodge FORMATION: DATE:

LOCATION: 16-26-72-8-W6 CORE INTERVAL: KB:

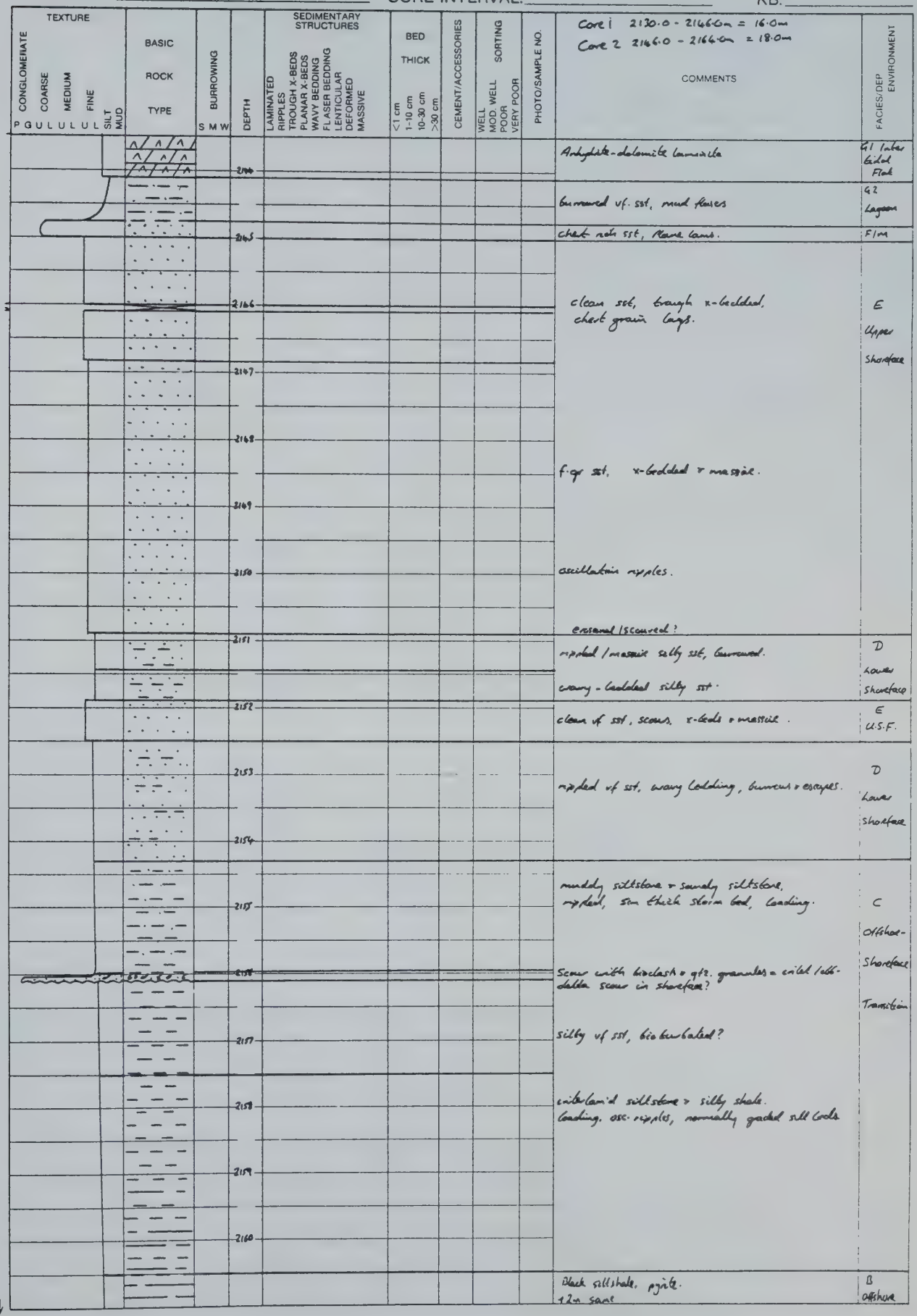

WELL NAME: Total et al Wembley FORMATION: DATE:

LOCATION: 6-27-72-8-W6 CORE INTERVAL: KB:

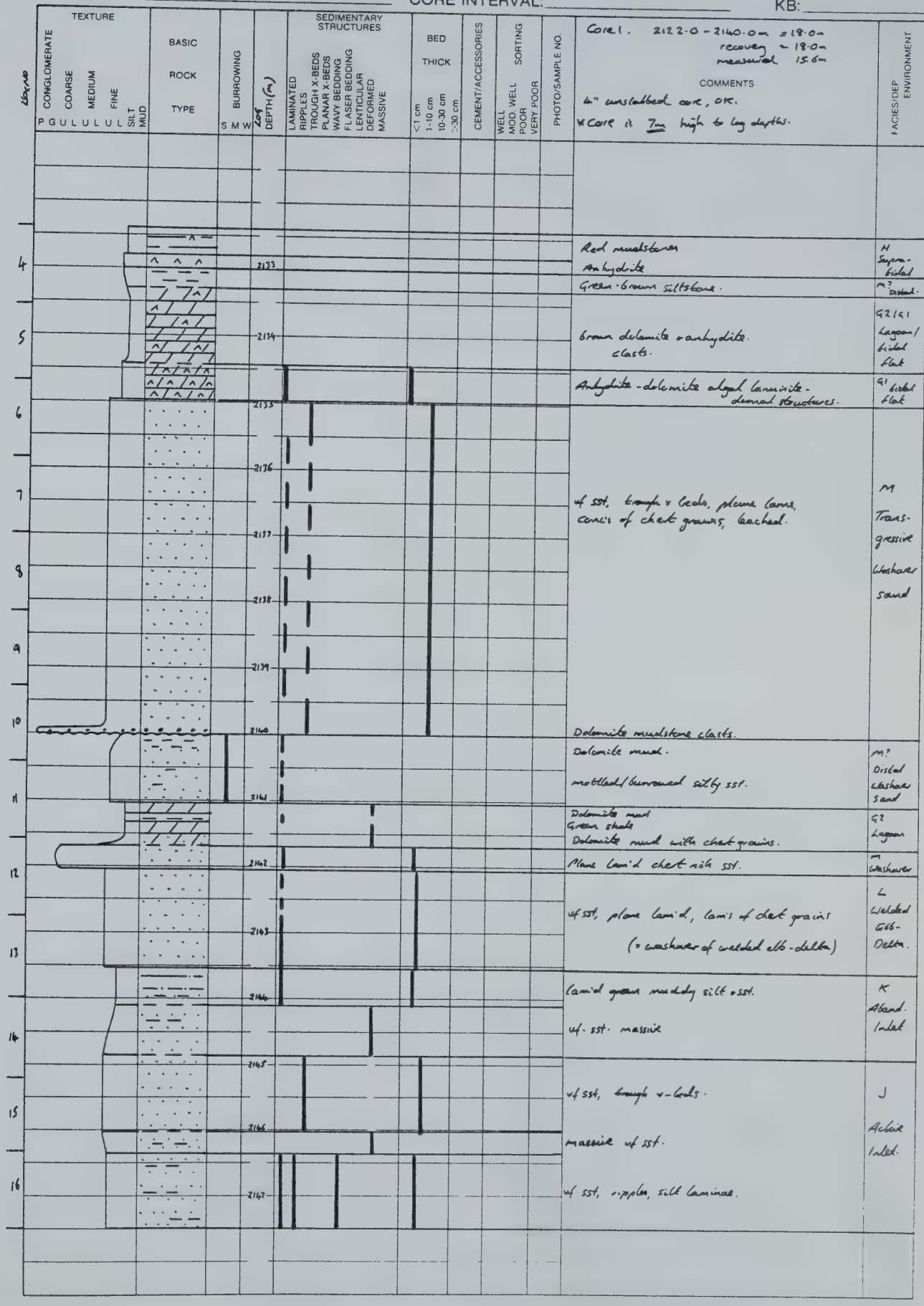

WELL NAME: (2/2) FORMATION: DATE:

LOCATION: 6-27-72-8-W6 CORE INTERVAL: KB:

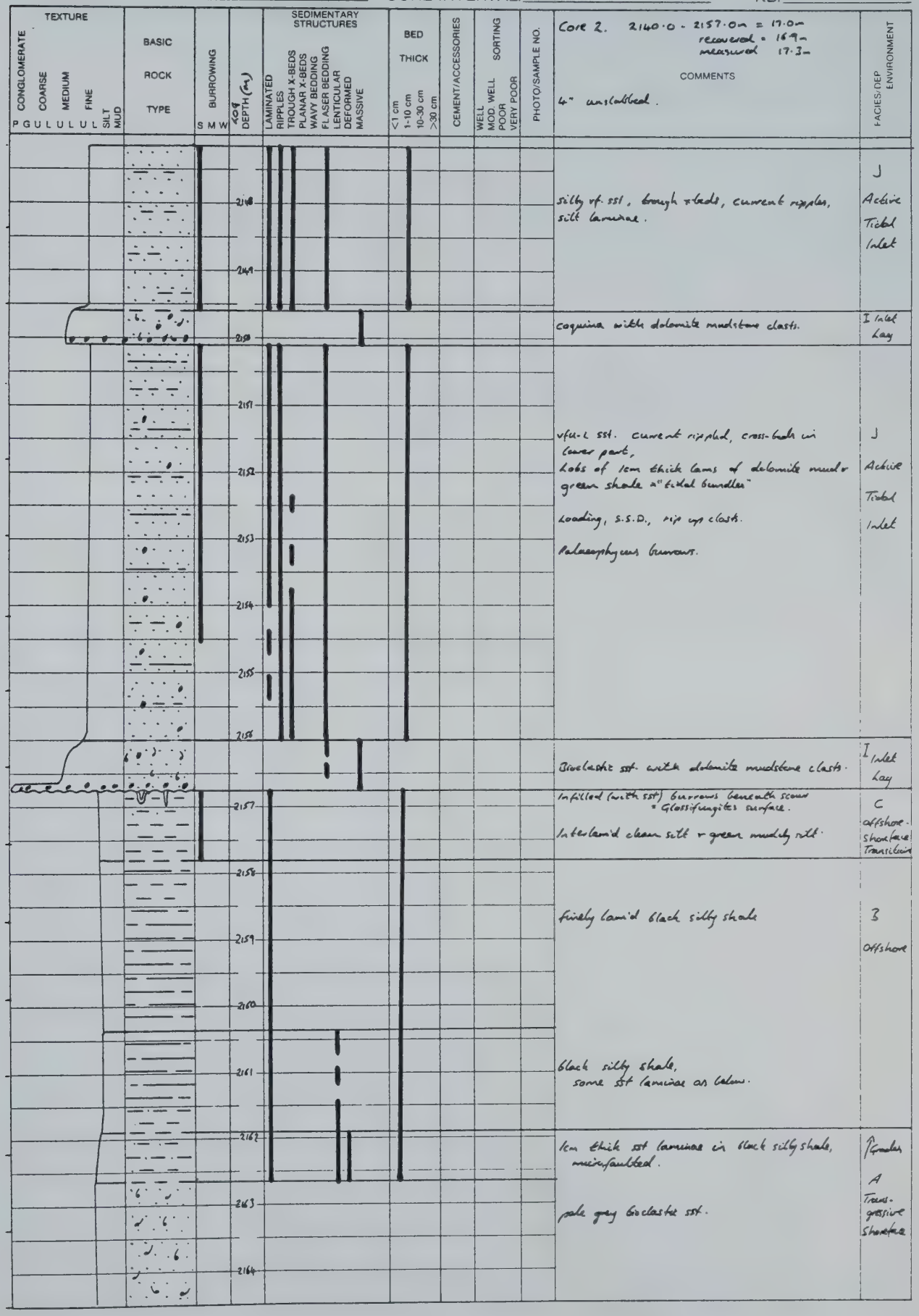

WELL NAME: Total et al Wembley FORMATION: DATE:

LOCATION: 8-27-72-8-W6 CORE INTERVAL: KB:

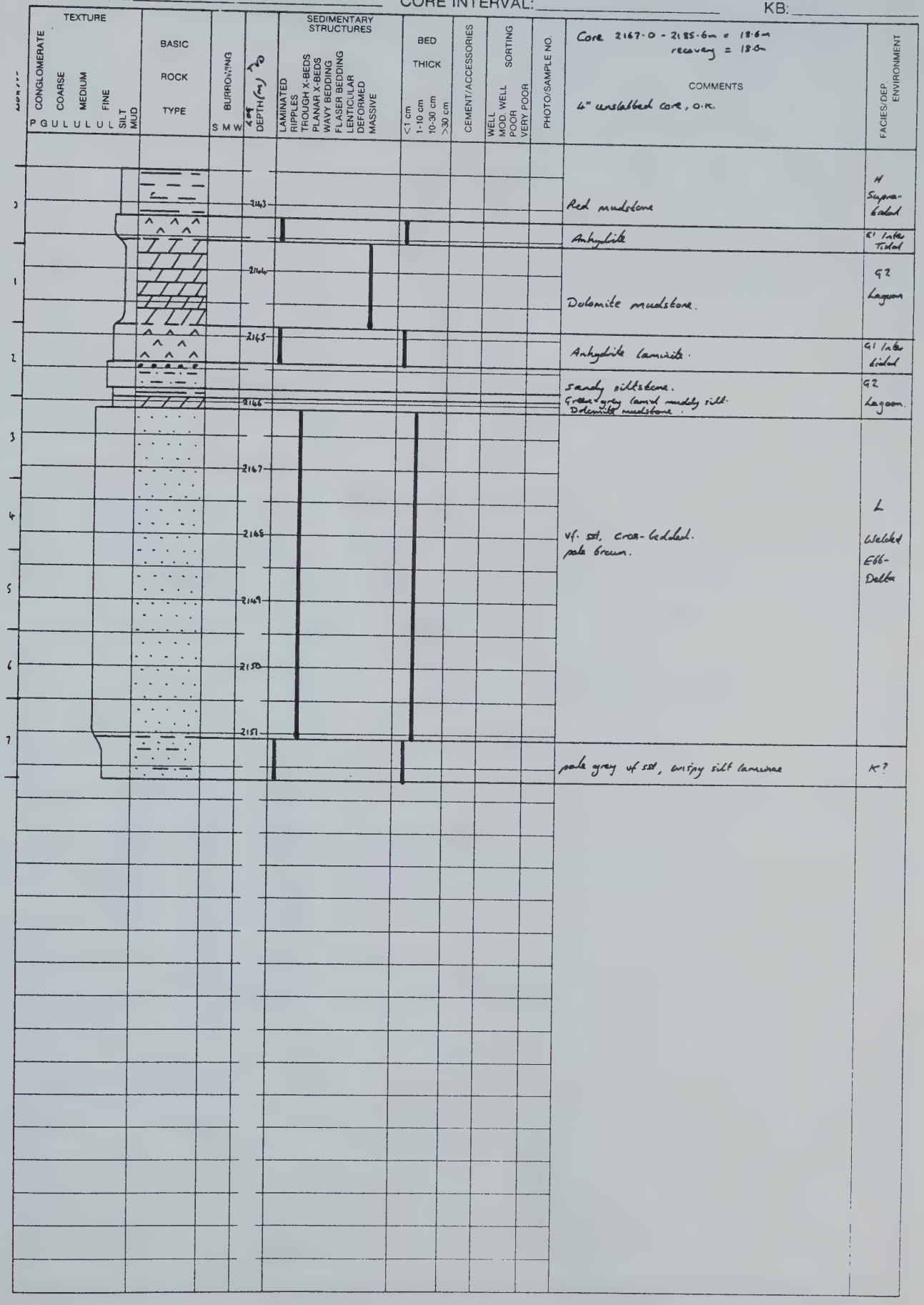

WELL NAME: Total et al Wembley FORMATION: DATE:

LOCATION: 14-27-72-8-W6 CORE INTERVAL: KB:

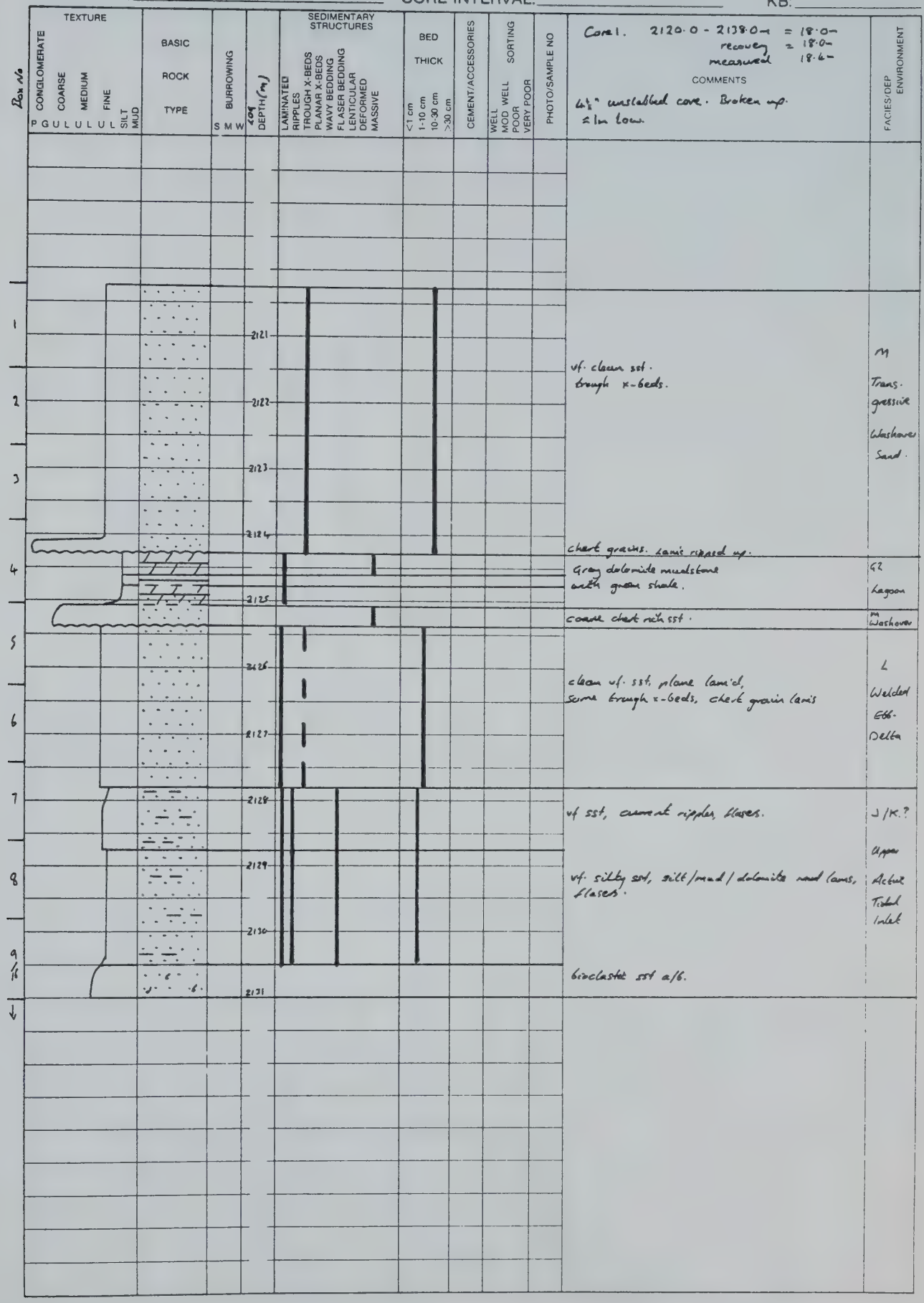

WELL NAME: (2/2) FORMATION: DATE:

LOCATION: 14-27-72-8-W6 CORE INTERVAL: KB:

Core 2 2138.0 - 2146.0m = 8.0m
recovery = 7.75m
measured 4.9m.

Box no.	TEXTURE (CONGLOMERATE, COARSE, MEDIUM, FINE, SILT, MUD)	BASIC ROCK TYPE	BURROWING (S M W)	DEPTH (m)	SEDIMENTARY STRUCTURES (LAMINATED, RIPPLES, TROUGH X-BEDS, PLANAR X-BEDS, WAVY BEDDING, FLASER BEDDING, LENTICULAR, DEFORMED, MASSIVE)	BED THICK (<1 cm, 1-10 cm, 10-30 cm, >30 cm)	CEMENT/ACCESSORIES	SORTING (WELL, MOD WELL, POOR, VERY POOR)	PHOTO/SAMPLE NO.	COMMENTS	FACIES/DEP ENVIRONMENT
10				2131 – 2132						Bioclastic sst with dolomite mud clasts.	J/I Active Tidal Inlet.
11				2133						vf. sst, current ripples, some trough x-beds, siltstone lamis & drapes (tidal?)	J Active Tidal Inlet
12				2134							
13				2135						Bioclastic sst with silt lamis, flasers trough x-beds, mud clasts.	I/J Active Tidal Inlet
14				2136							
15				2137						bioclastic sst, massive / x-bedded, mud clasts. Dolomite mudstone	I Inlet Lag
16/16				2138						Green-grey siltstone	C?
1				2139						Black muddy siltshale, siltstone beds, sharp bases, normally graded, increase in no. & thickness ↑.	B Offshore
2				2140							
3				2141						black siltshale with siltstone lamis - lenticular ripples, loading, microfaulting.	
4				2142			Phosph.			bioclastic sst. with black phosphatic granules. h-c-s storm beds.	A Transgressive Shoreface
				2143							

WELL NAME: Total et al Wembley FORMATION: DATE:

LOCATION: 16-27-72-8-W6 CORE INTERVAL: KB:

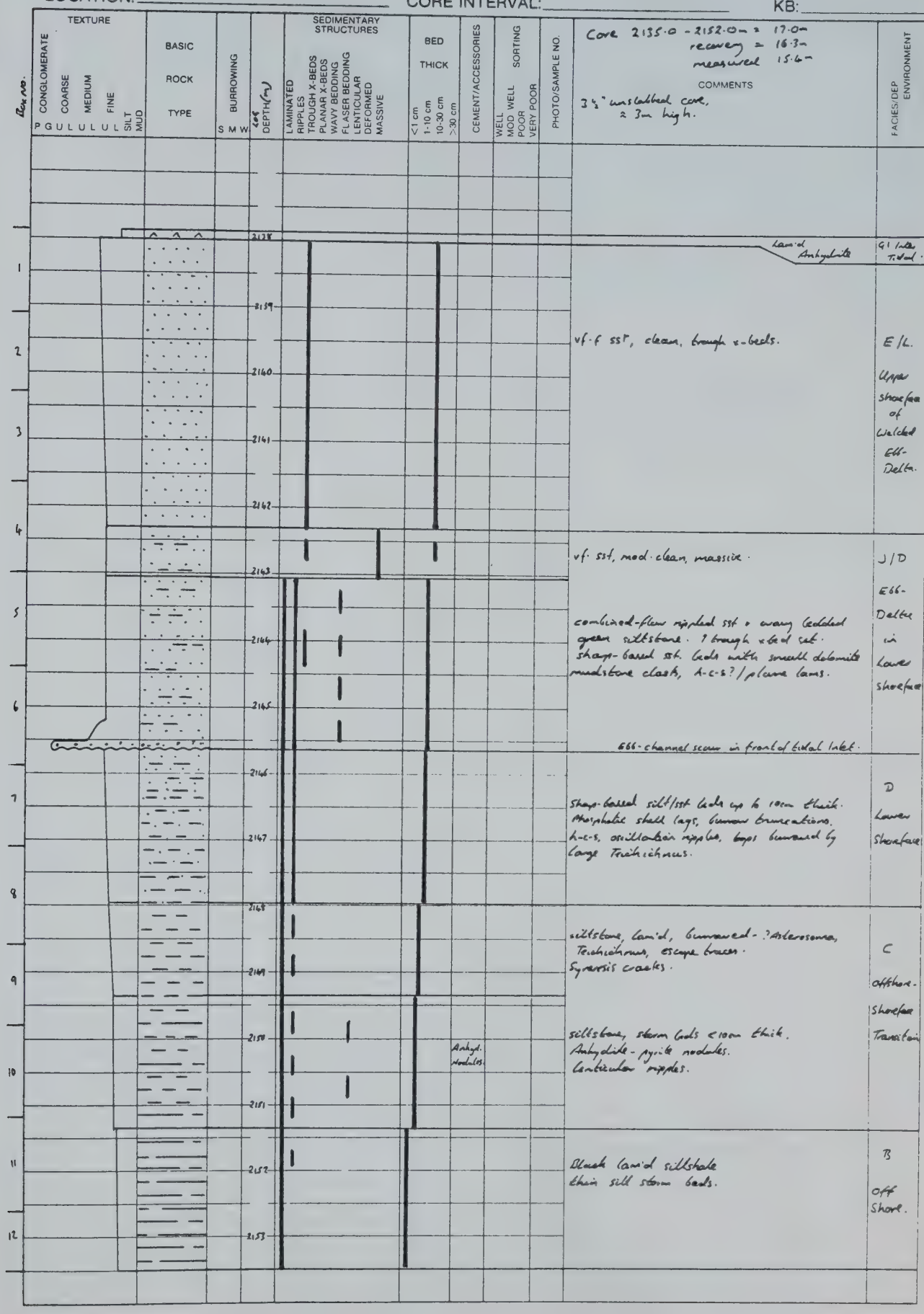

WELL NAME: Total Wembley FORMATION: DATE:

LOCATION: 4-28-72-8-W6 CORE INTERVAL: KB:

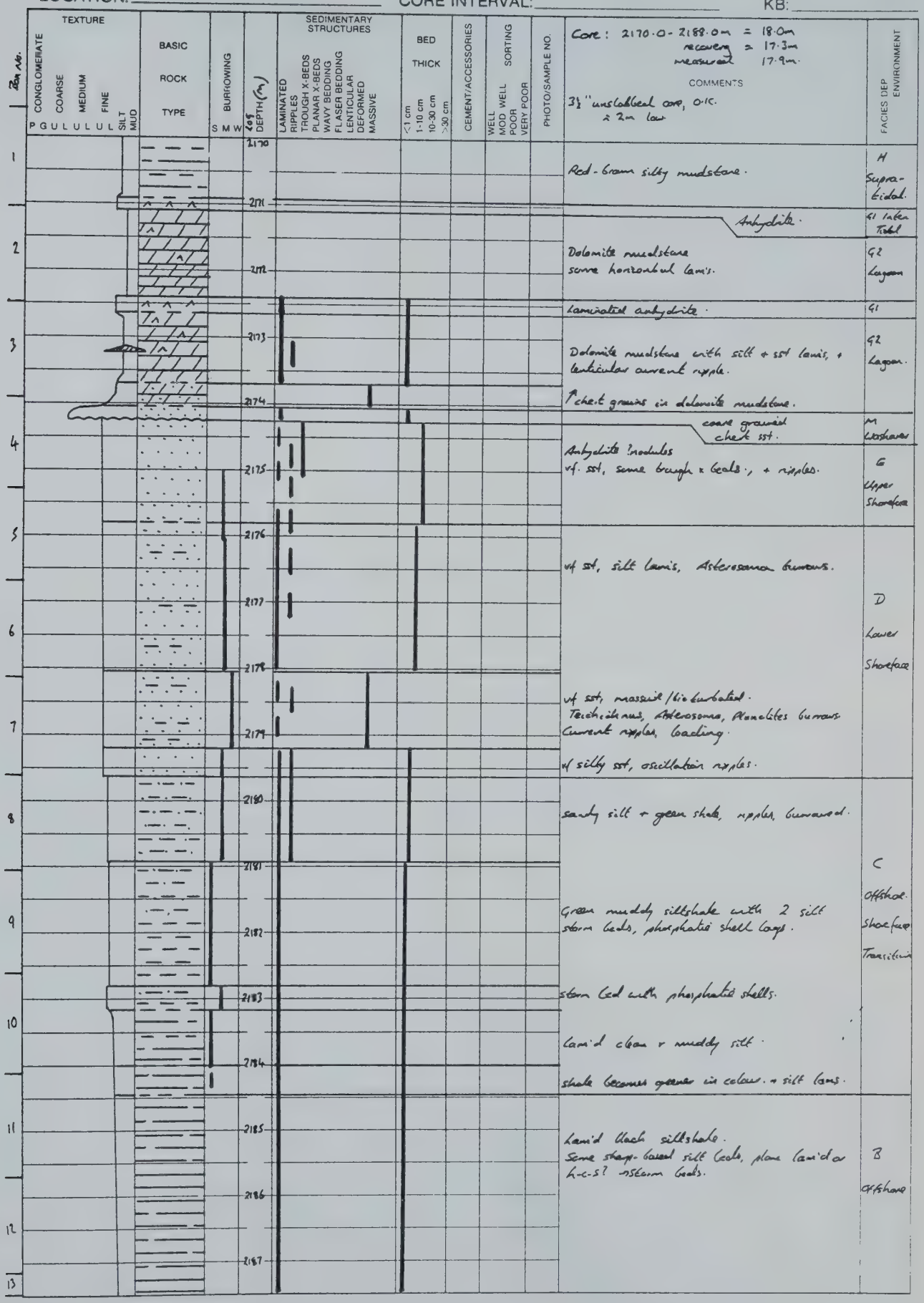

WELL NAME: Total Wembley FORMATION: DATE:

LOCATION: 6-28-72-8-W6 CORE INTERVAL: KB:

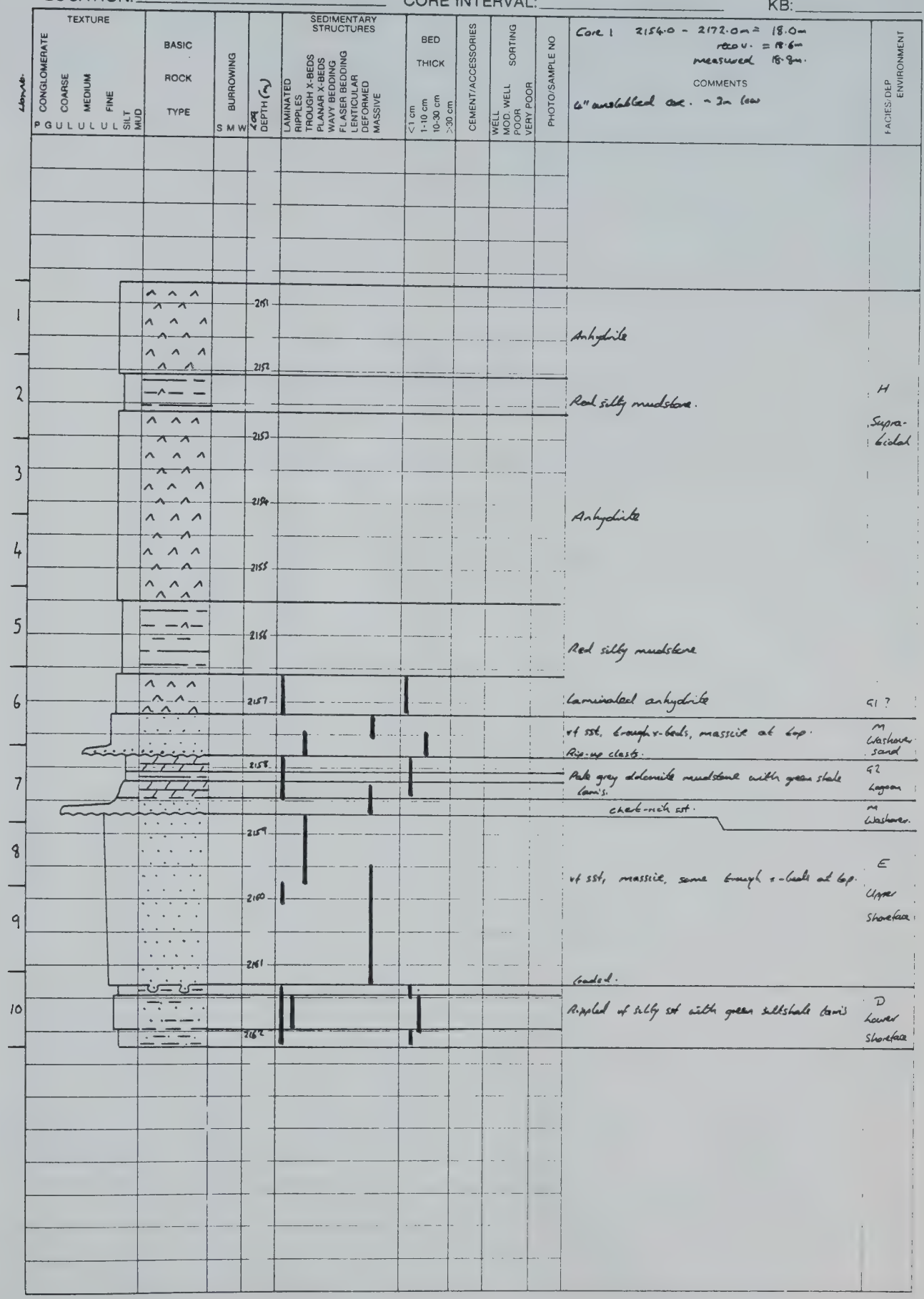

WELL NAME: (2/2) FORMATION: DATE:

LOCATION: 6-28-72-8-W6 CORE INTERVAL: KB:

Core No.	TEXTURE (CONGLOMERATE, COARSE, MEDIUM, FINE, SILT, MUD)	BASIC ROCK TYPE	BURROWING (S M W)	Log DEPTH (m)	SEDIMENTARY STRUCTURES (LAMINATED, RIPPLES, TROUGH X-BEDS, PLANAR X-BEDS, WAVY BEDDING, FLASER BEDDING, LENTICULAR, DEFORMED, MASSIVE)	BED THICK (<1 cm, 1-10 cm, 10-30 cm, >30 cm)	CEMENT/ACCESSORIES	SORTING (WELL, MOD. WELL, POOR, VERY POOR)	PHOTO/SAMPLE NO	COMMENTS	FACIES/DEP ENVIRONMENT
										Core 2 2177.0 - 2195.0m = 18.0m recovered = 17.2m measured = 4.6m. * 5m not cored between cores 1 & 2 *.	
11				2163						ss to siltstone. slightly bioclastic ss, dolomite mudstone clasts Teichichnus.	A? Transgressive Shoreface.
12				2164						Plane lam's, mudstone clasts, comb flow ripples.	Seq. 5↑
13				2165						plane lam'd siltstone beds up to 15cm thick (h-c-s?), escape traces.	C Offshore Shoreface Transition
14				2166							
				2167							
15				2168						← phosphatic brachiopod fragments in storm bed.	
										green muddy silt.	
16				2169						interlaminated silt & green muddy silt. loading, clean silt lams.	
				↑ 5m ↓							
1										vf silty ss.	("Doig") Parasequence 3 Shoreface ss
2											
3											
4											

WELL NAME: Total Wembley FORMATION: DATE:

LOCATION: 8-28-72-8-W6 CORE INTERVAL: KB:

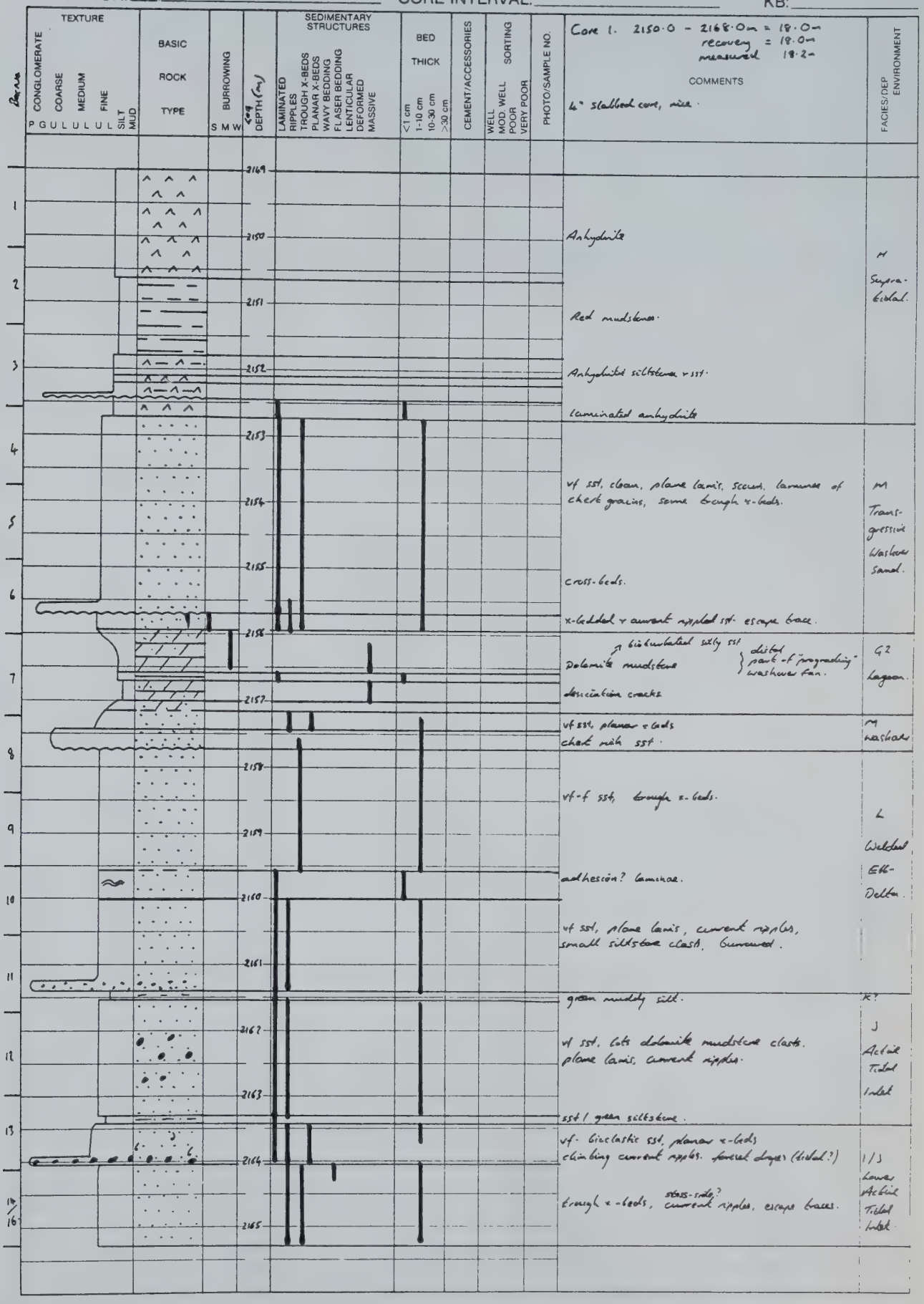

WELL NAME: (2/2) FORMATION: DATE:

LOCATION: 8-28-72-8-W6 CORE INTERVAL: KB:

Core 2. 2168.0 - 2186.0m = 18.0m
recovery = 18.0m
measured 8m

Depth (m)	Comments	Facies/Dep Environment
15	Interbedded bioclastic sst + dolomite mudstone (tidal?) stylolites	I Tidal Inlet Lag/Fill
16		C Offshore.
1	Interlam'd green muddy silt + grey silt with sharp-based, normally graded silt. Gds. oscillation ripples.	Shoreface Transition
2		
3		B Offshore
4	Lam'd black siltshale. Some h-c-s at top.	
5		
6	small ? climbing current ripples of sst in black siltshale.	A/B Grades.
7	Pale grey vf. sst; bioclastic	A Transgressive Shoreface

Depth (m): 2166, 2167, 2168, 2169, 2170, 2171, 2172, 2173, 2174, 2175

WELL NAME: Total Wembley FORMATION: DATE:

LOCATION: 14-28-72-8-W6 CORE INTERVAL: KB:

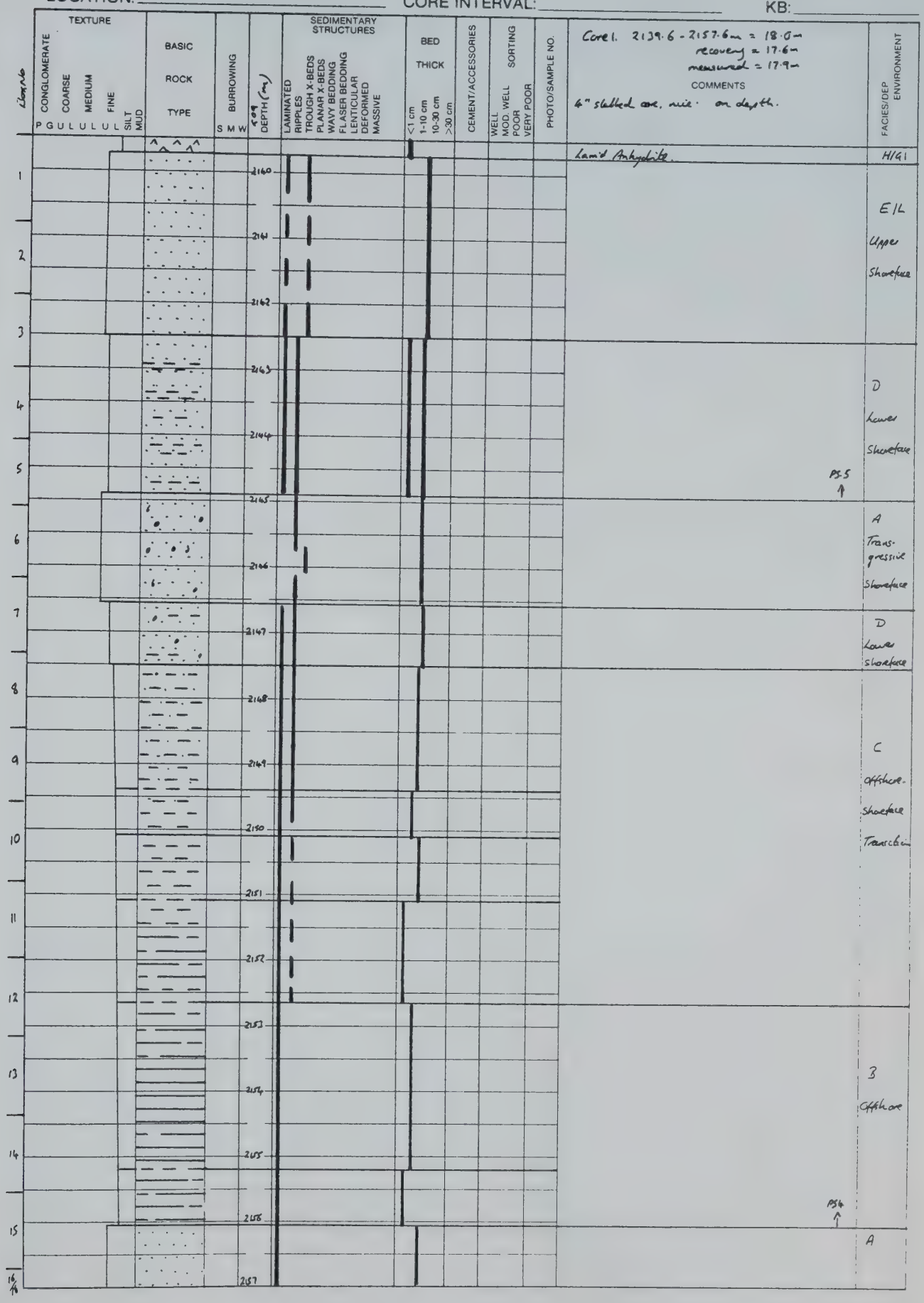

WELL NAME: Total Wembley FORMATION: DATE:

LOCATION: 16-28-72-8-W6 CORE INTERVAL: KB:

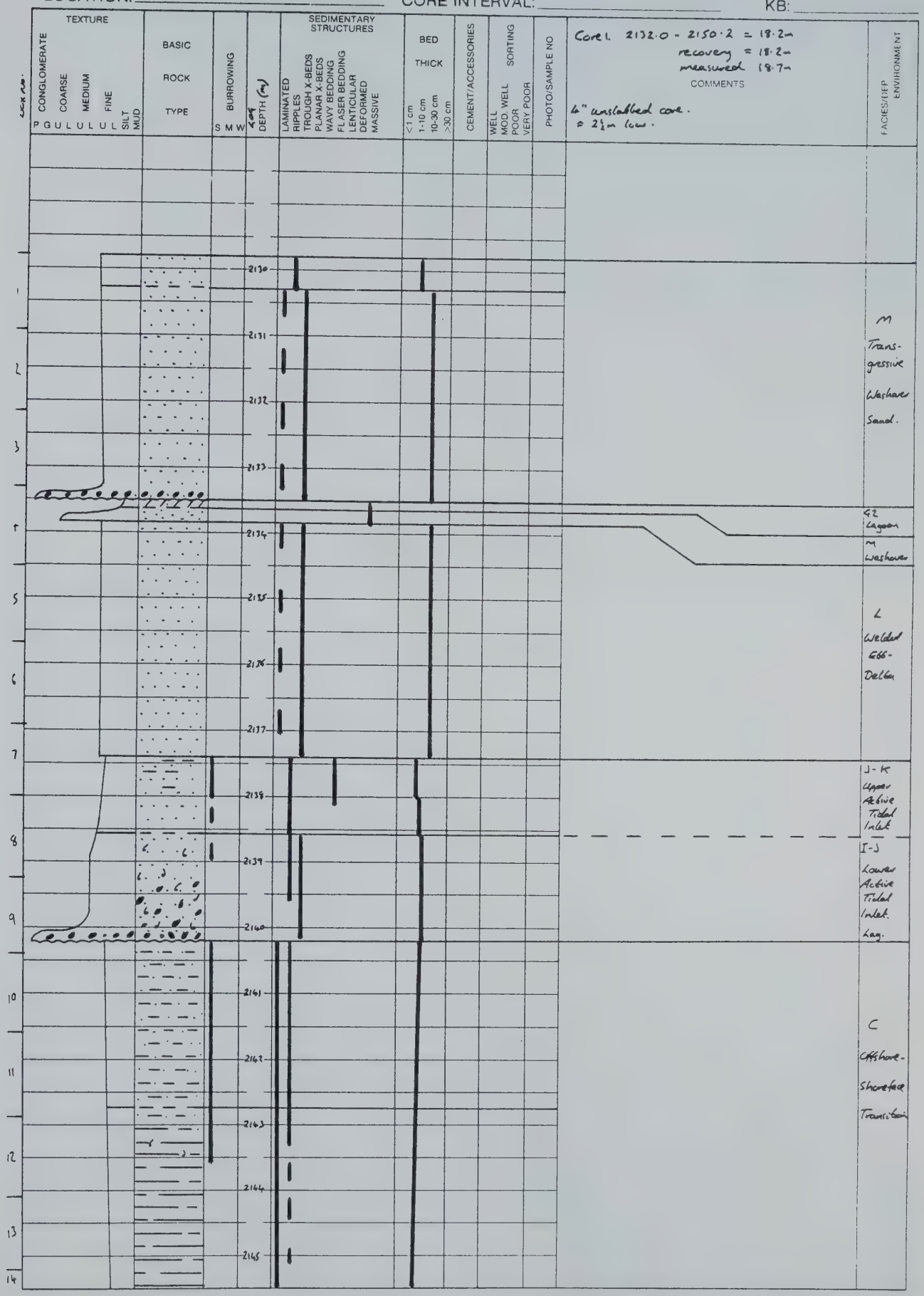

WELL NAME: Total Wembley FORMATION: DATE:

LOCATION: 16-29-72-8-W6 CORE INTERVAL: KB:

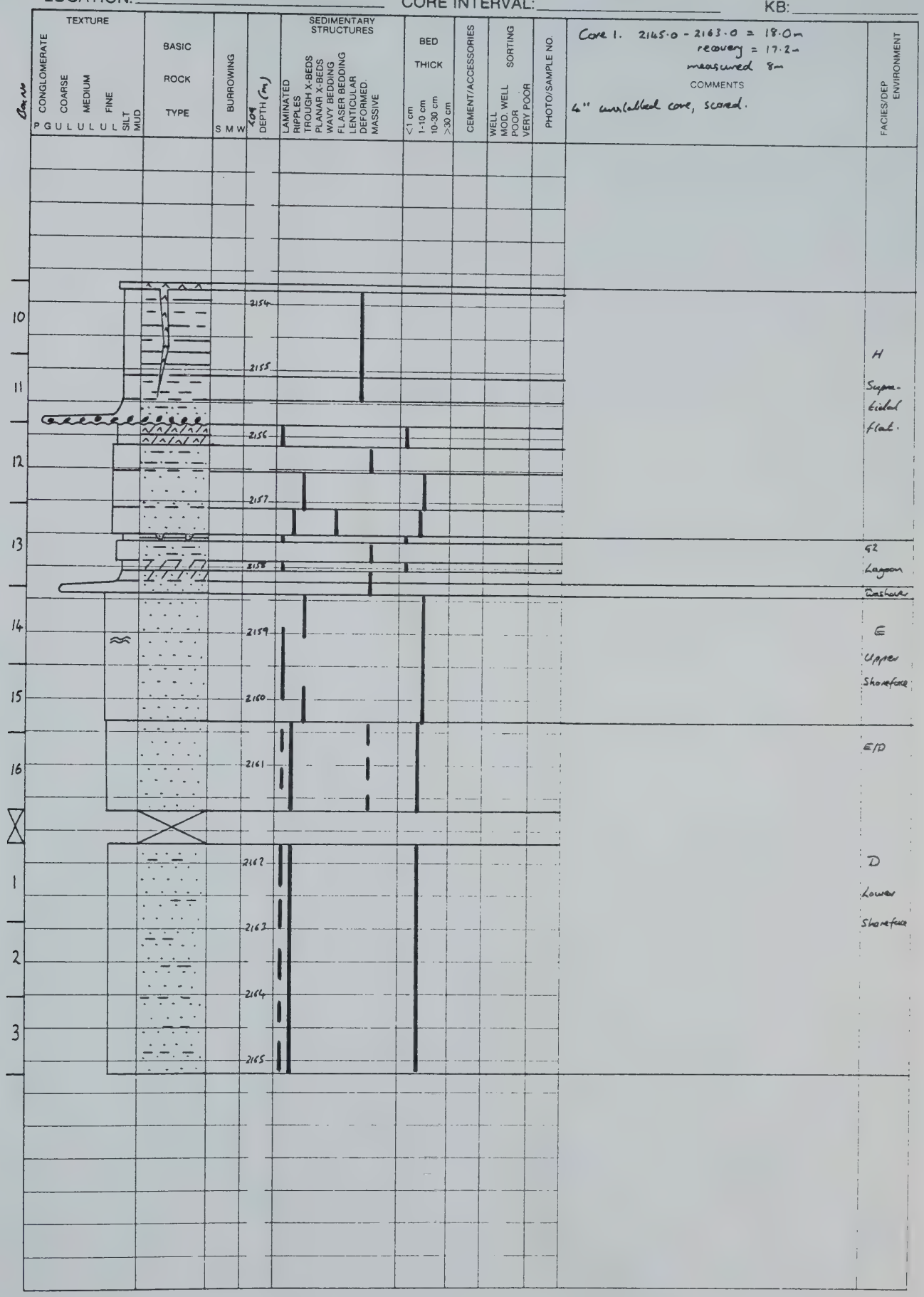

WELL NAME: (2/2) FORMATION: DATE:

LOCATION: 16-29-72-8-W6 CORE INTERVAL: KB:

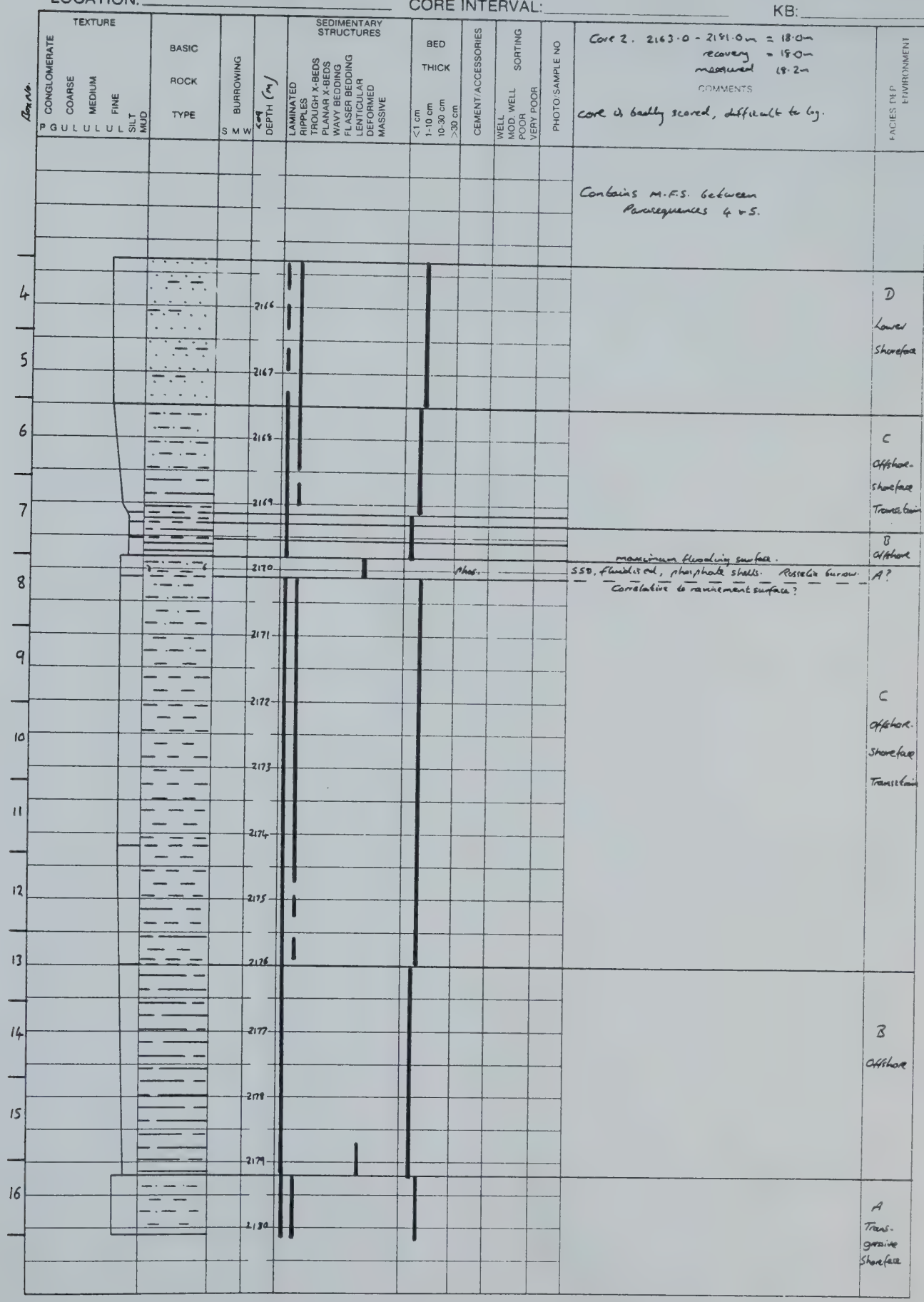

WELL NAME: Total Wembley FORMATION: DATE:

LOCATION: 16-30-72-8-W6 CORE INTERVAL: KB:

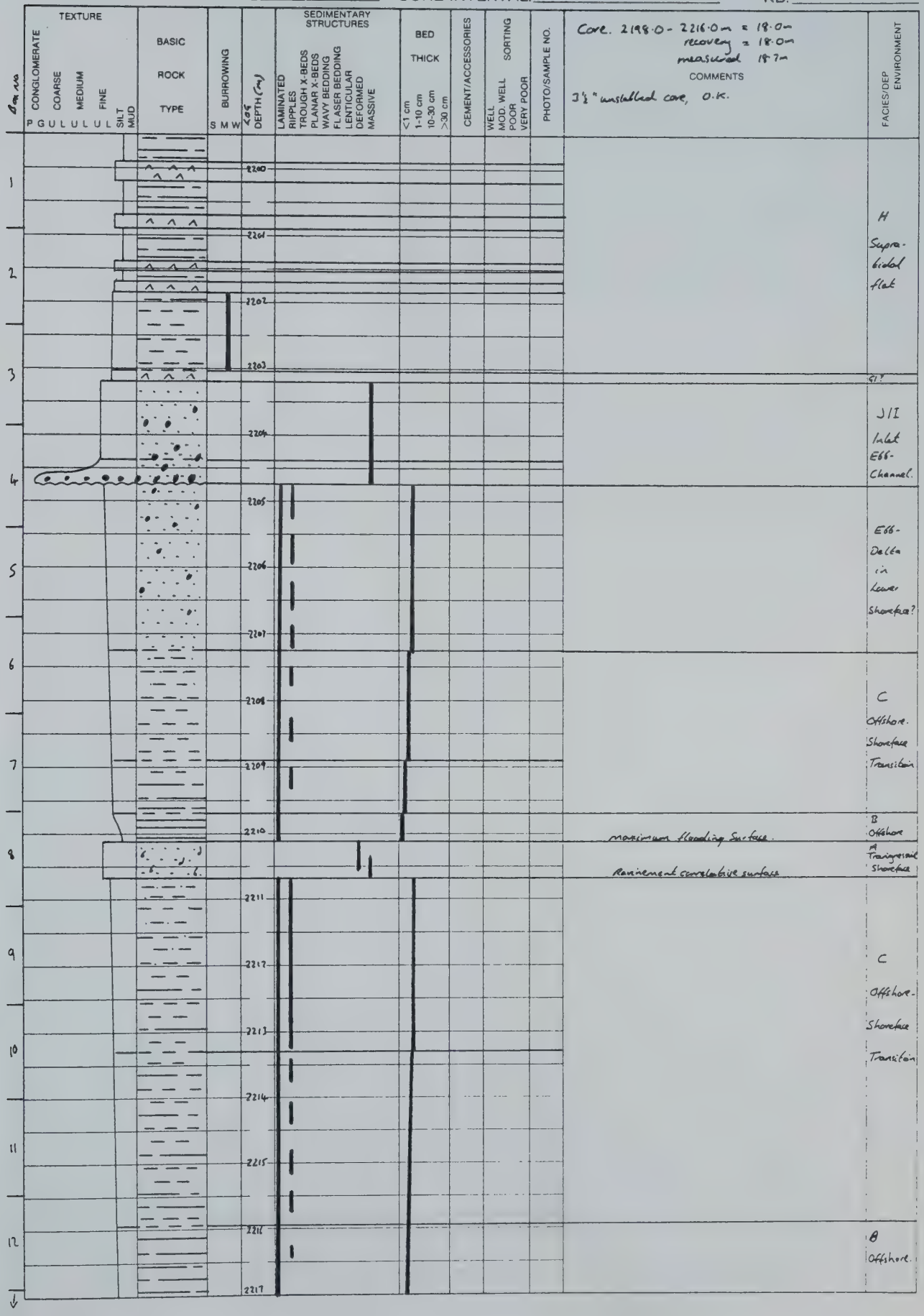

WELL NAME: Coseka et al Wembley FORMATION: DATE:

LOCATION: 16-31-72-8-W6 CORE INTERVAL: KB:

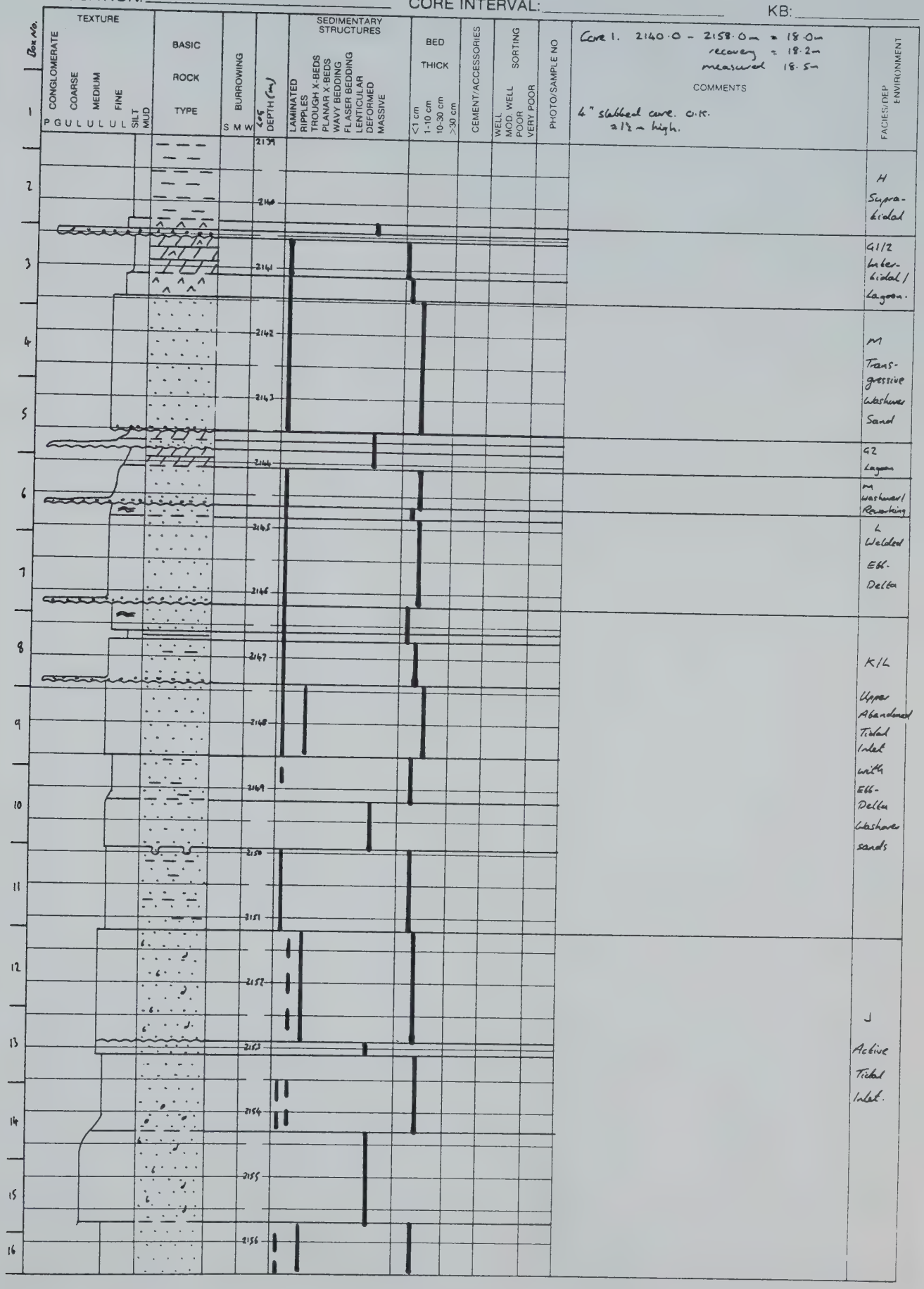

WELL NAME: Petrorep etal Wembley FORMATION: DATE:

LOCATION: 6-32-72-8-W6 CORE INTERVAL: KB:

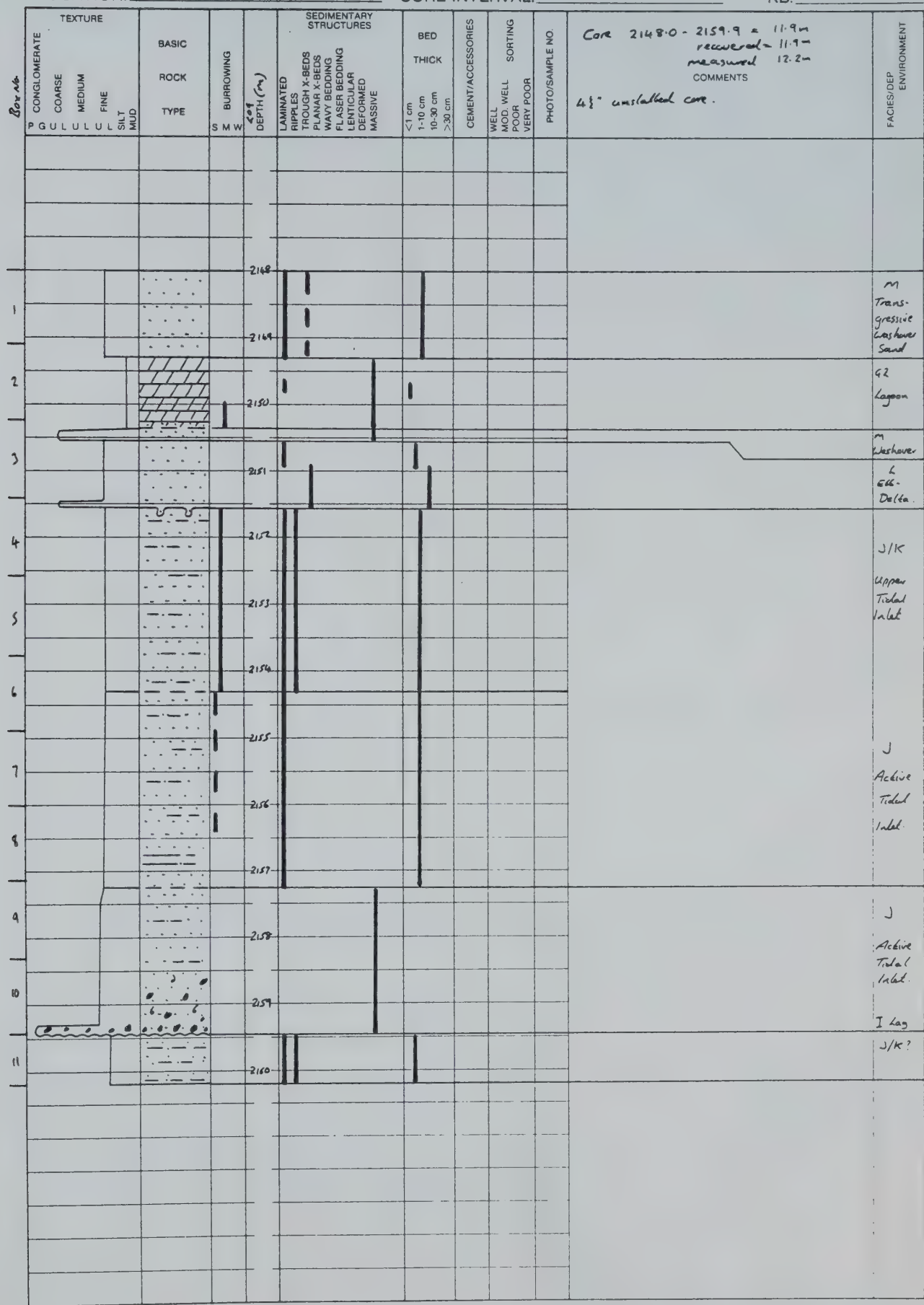

WELL NAME: Total Wembley FORMATION: DATE:

LOCATION: 10-32-72-8-W6 CORE INTERVAL: KB:

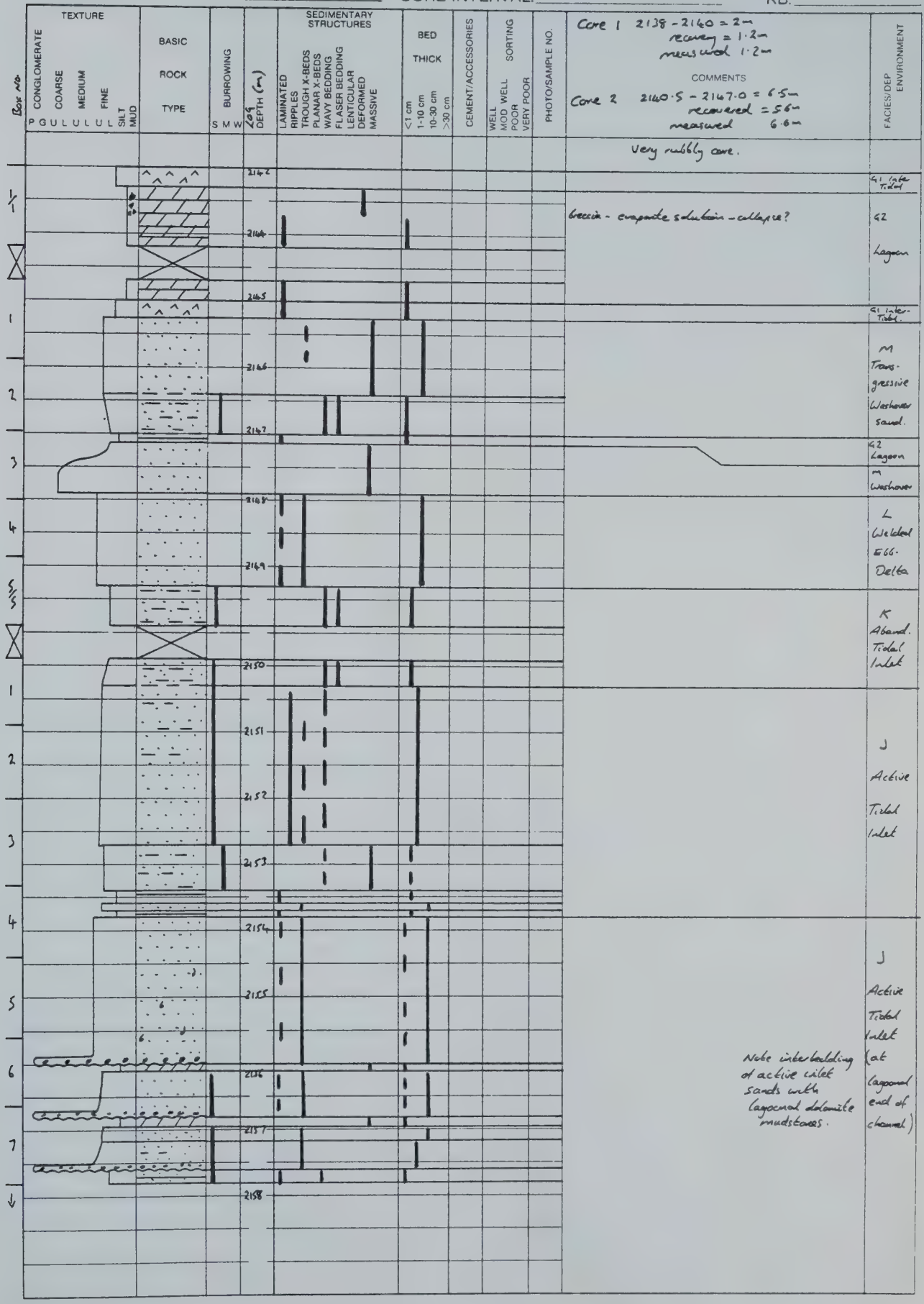

WELL NAME: (2/2) FORMATION: DATE:

LOCATION: 10-32-72-8-W6 CORE INTERVAL: KB:

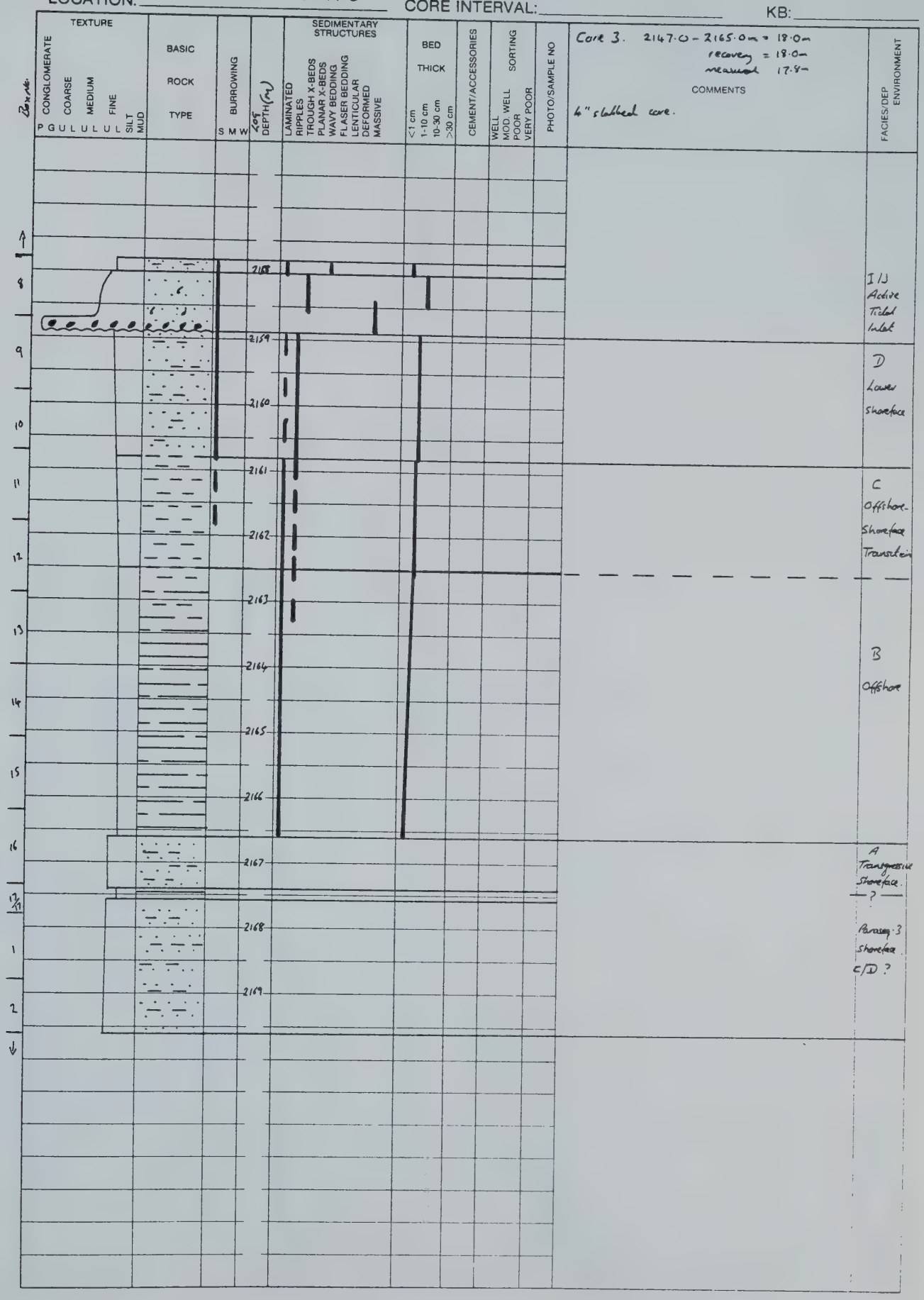

WELL NAME: Total Wembley

LOCATION: 6-33-72-8-W6

FORMATION:

CORE INTERVAL:

DATE:

KB:

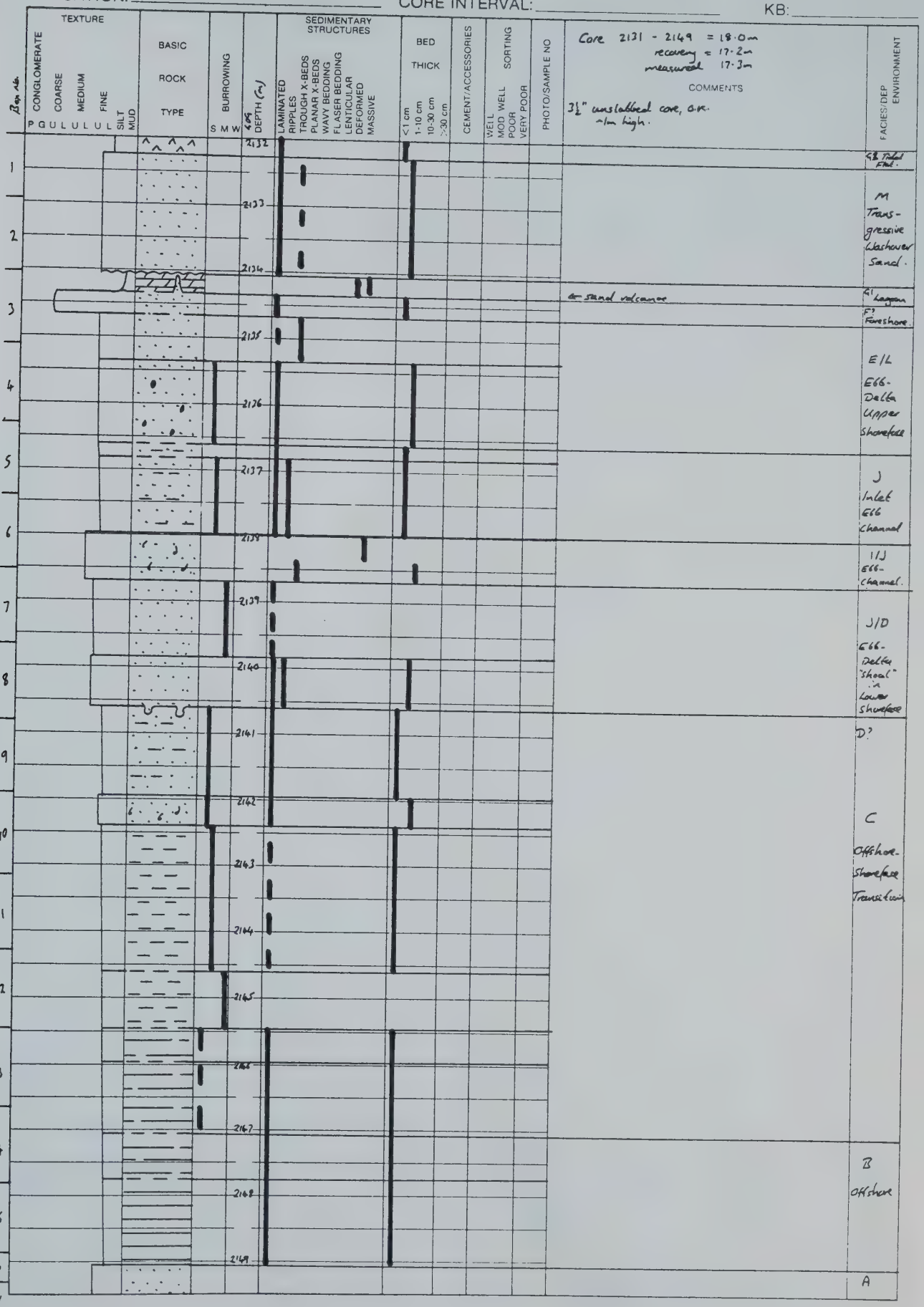

WELL NAME: Total Wembley FORMATION: DATE:

LOCATION: 8-33-72-8-W6 CORE INTERVAL: KB:

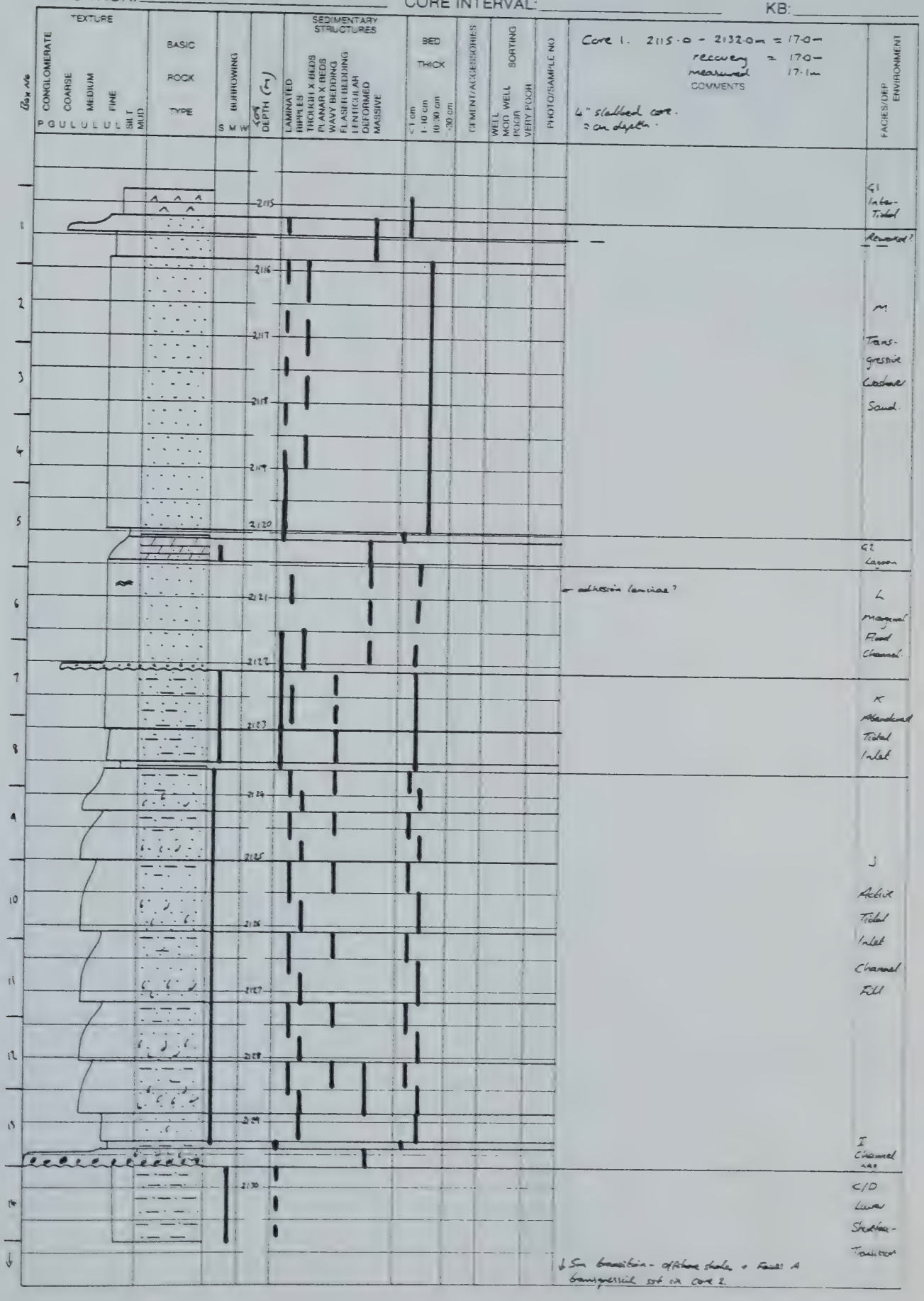

WELL NAME: Total et al Wembley

LOCATION: 14-33-72-8-W6

FORMATION:

CORE INTERVAL:

DATE:

KB:

Box No.	TEXTURE: CONGLOMERATE (P G)	COARSE (U L)	MEDIUM (U L)	FINE (U L)	SILT (U L)	MUD	BASIC ROCK TYPE	BURROWING (S M W)	DEPTH (m)	SEDIMENTARY STRUCTURES: LAMINATED	RIPPLES	TROUGH X-BEDS	PLANAR X-BEDS	WAVY BEDDING	FLASER BEDDING	LENTICULAR	DEFORMED	MASSIVE	BED THICK: <1 cm	1-10 cm	10-30 cm	>30 cm	CEMENT/ACCESSORIES	SORTING: WELL	MOD WELL	POOR	VERY POOR	PHOTO/SAMPLE NO.	COMMENTS	FACIES DIP ENVIRONMENT
																												Core 1. 2115.0 - 2121.8m = 6.8m recovery = 6.8m measured 7.1m		
																												COMMENTS		
																												Core 2 2121.8 - 2130.6m = 8.8m recovered = 8.7m measured 8.9m	4½' unsalbled core.	
1									2115																					J?
2									2116																					J/K Aband. Tidal Inlet.
3									2117																					
4									2118																					J
									2119																					
5																														
									2120																					
6																														
									2121																					
7																														
																														J
1									2122																					Active Tidal Inlet.
									2123																					
2																														
									2124																					
3																														
									2125																					
4																														
									2126																					
5																														I-J.
									2127																					
																														I Tidal Inlet Channel Lag.
6									2128																			* Inlet scour has removed all 154 shoreface deposits & rests directly on 153.	("Dain")	
																														Parasequence 3
7									2129																					Thick sand.
8									2130																					
Core 3 ↓																														

WELL NAME: Total et al Wembley FORMATION: DATE:

LOCATION: 16-33-72-8-W6 CORE INTERVAL: KB:

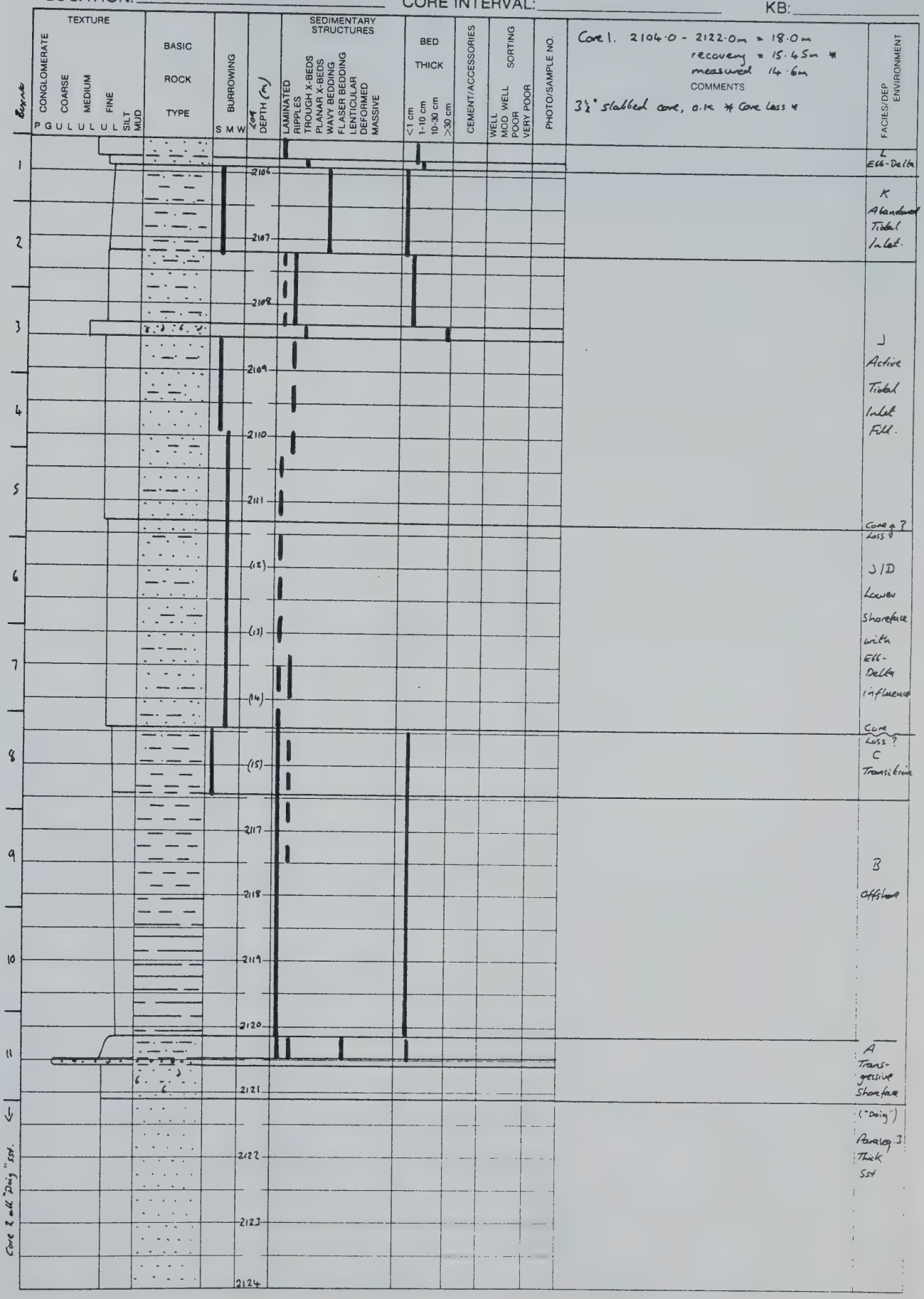

WELL NAME: Total et al Wembley FORMATION: DATE:

LOCATION: 6-34-72-8-W6 CORE INTERVAL: KB:

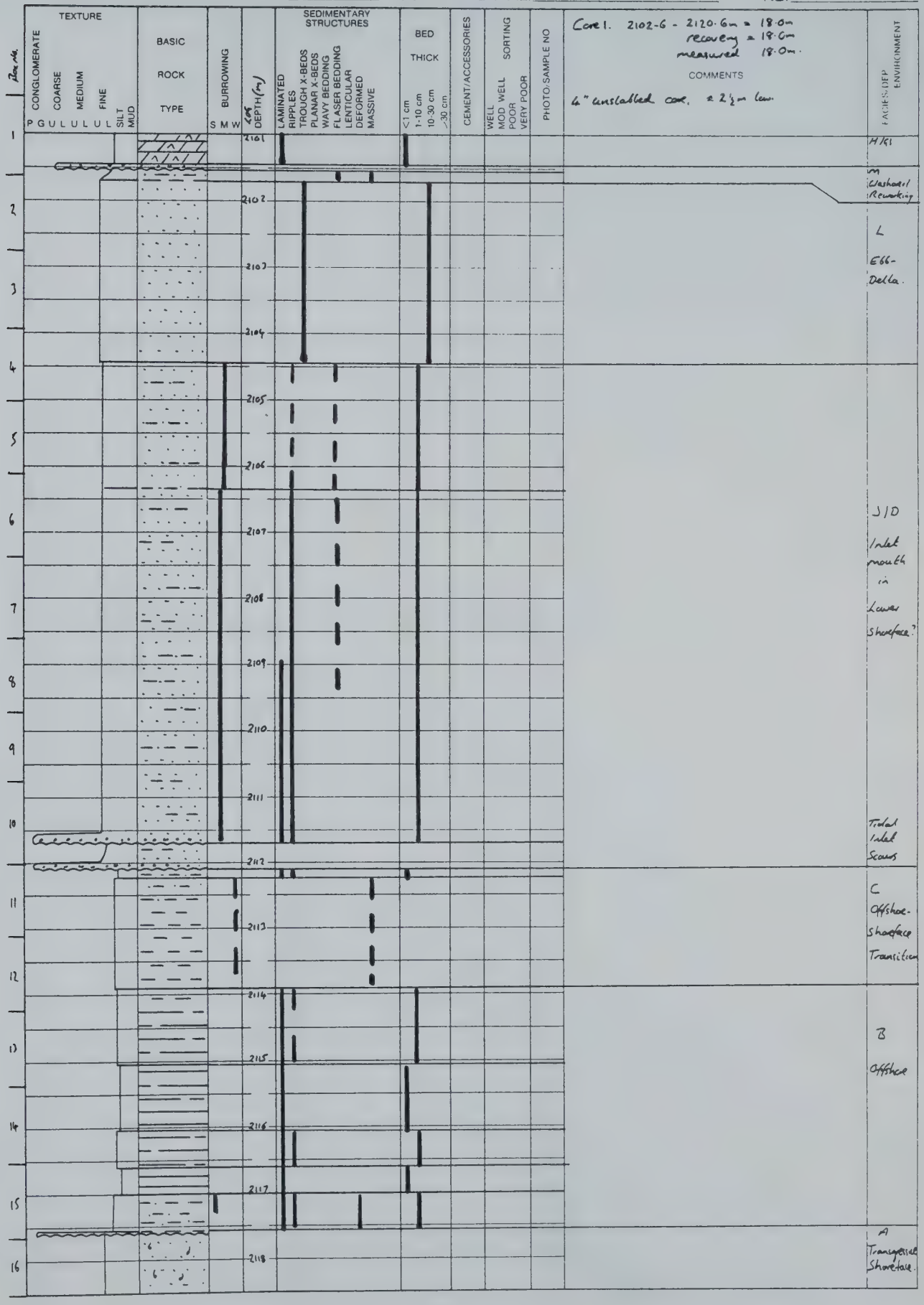

WELL NAME: Total et al Wembley FORMATION: DATE:

LOCATION: 7-34-72-8-W6 CORE INTERVAL: KB:

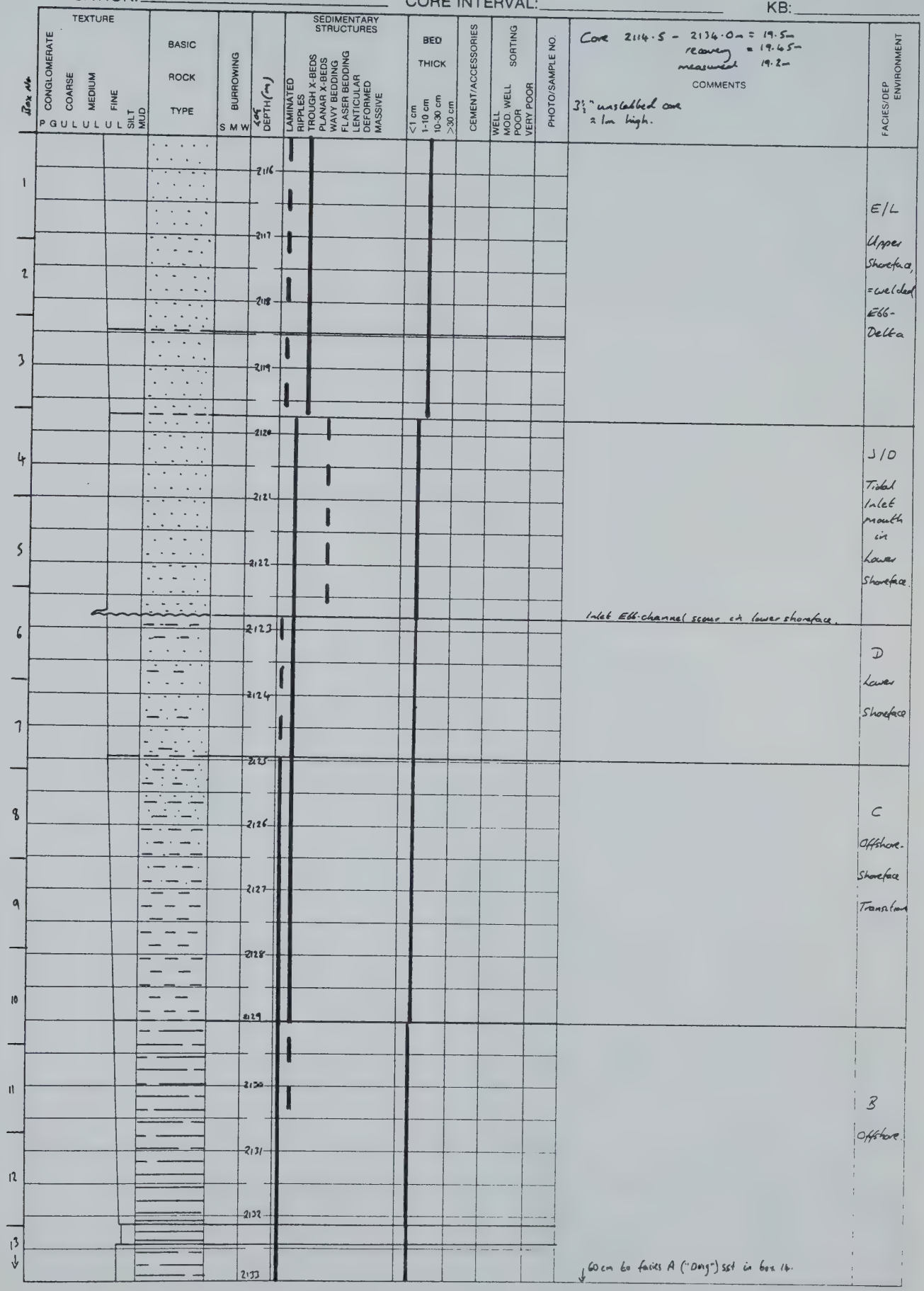

WELL NAME: Total et al Wembley FORMATION: DATE:

LOCATION: 16-34-72-8-W6 CORE INTERVAL: KB:

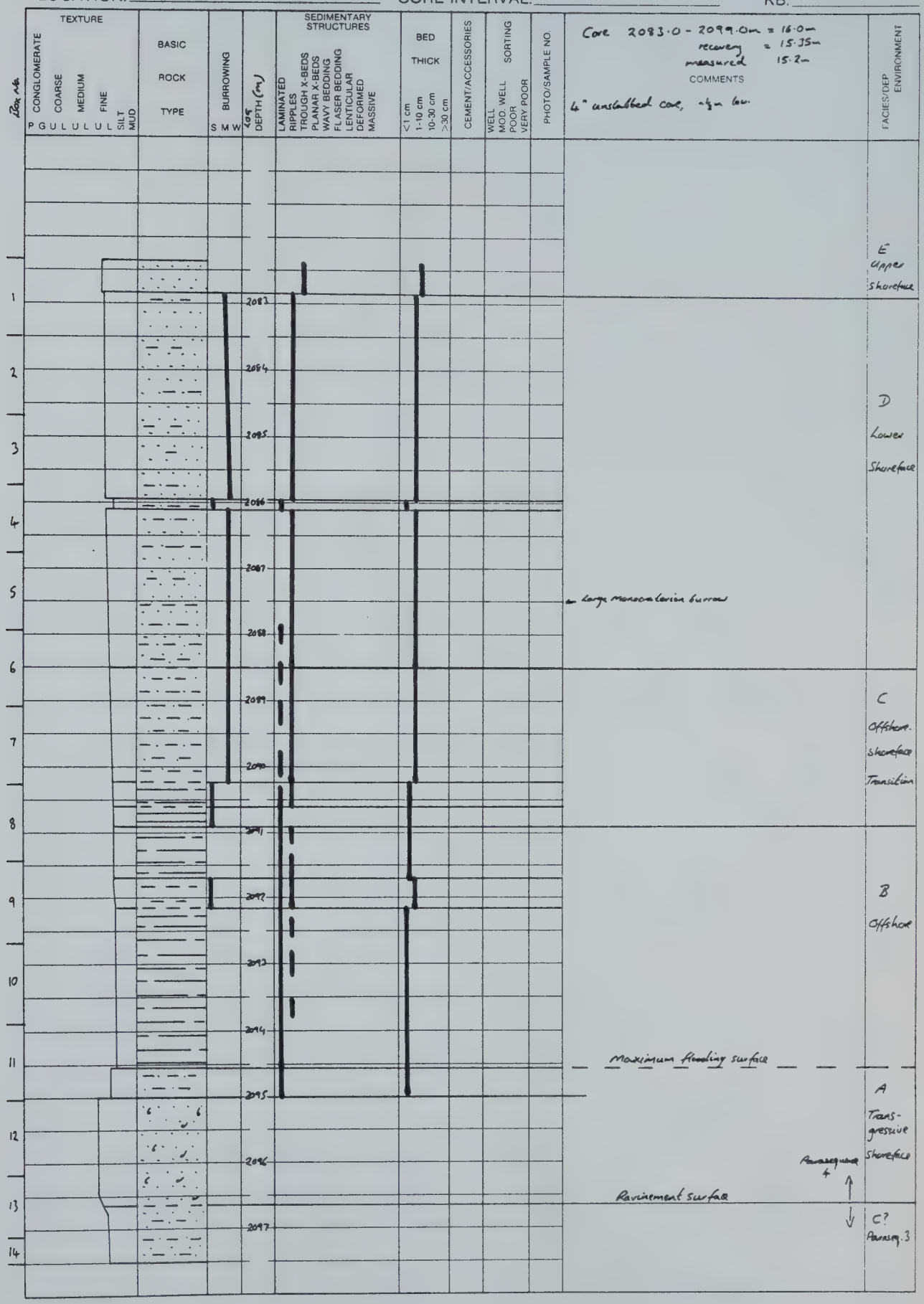

WELL NAME: Total et al Wembley FORMATION: DATE:

LOCATION: 6-35-72-8-W6 CORE INTERVAL: KB:

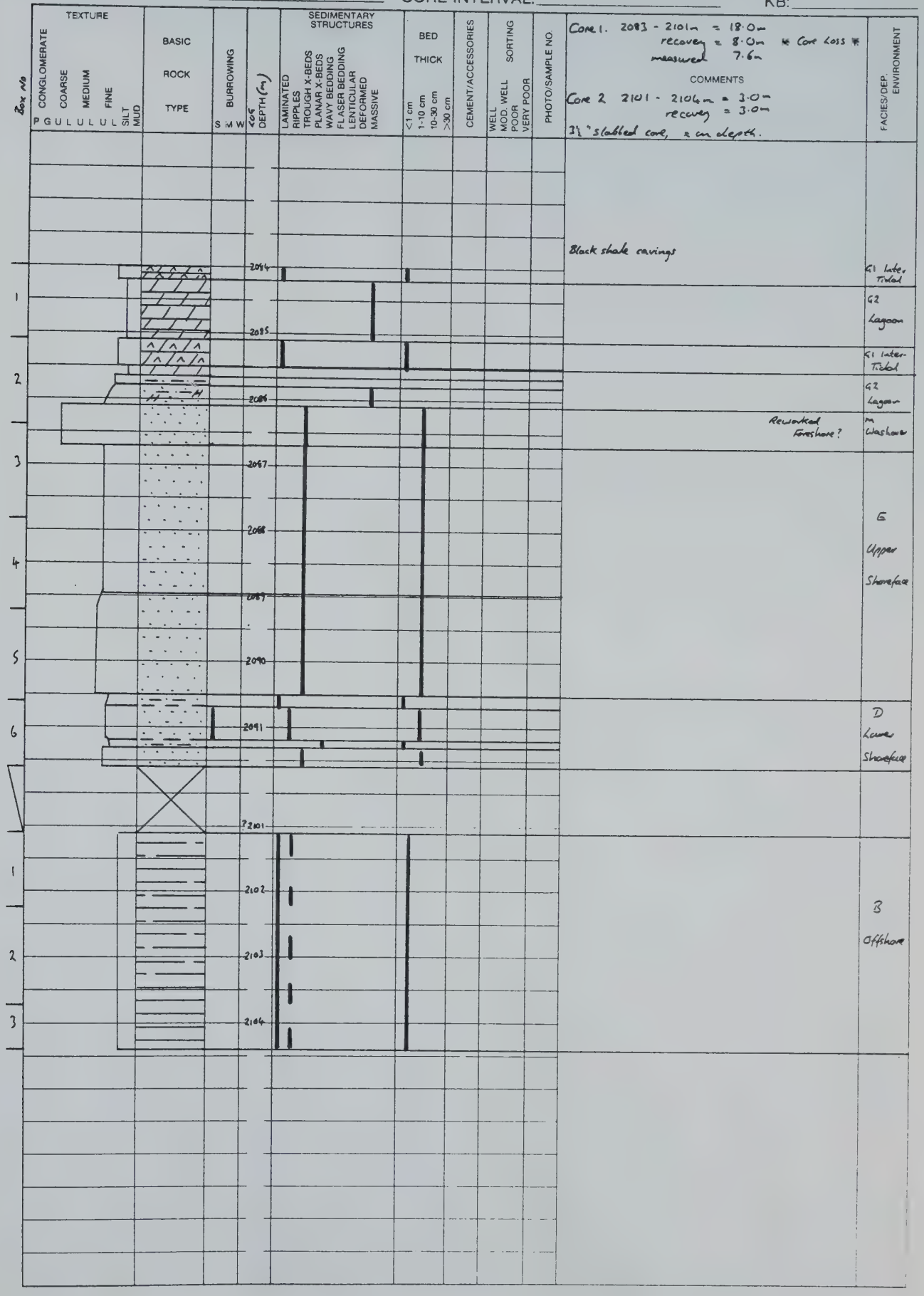

WELL NAME: Total et al Wembley FORMATION: DATE:

LOCATION: 8-35-72-8-W6 CORE INTERVAL: KB:

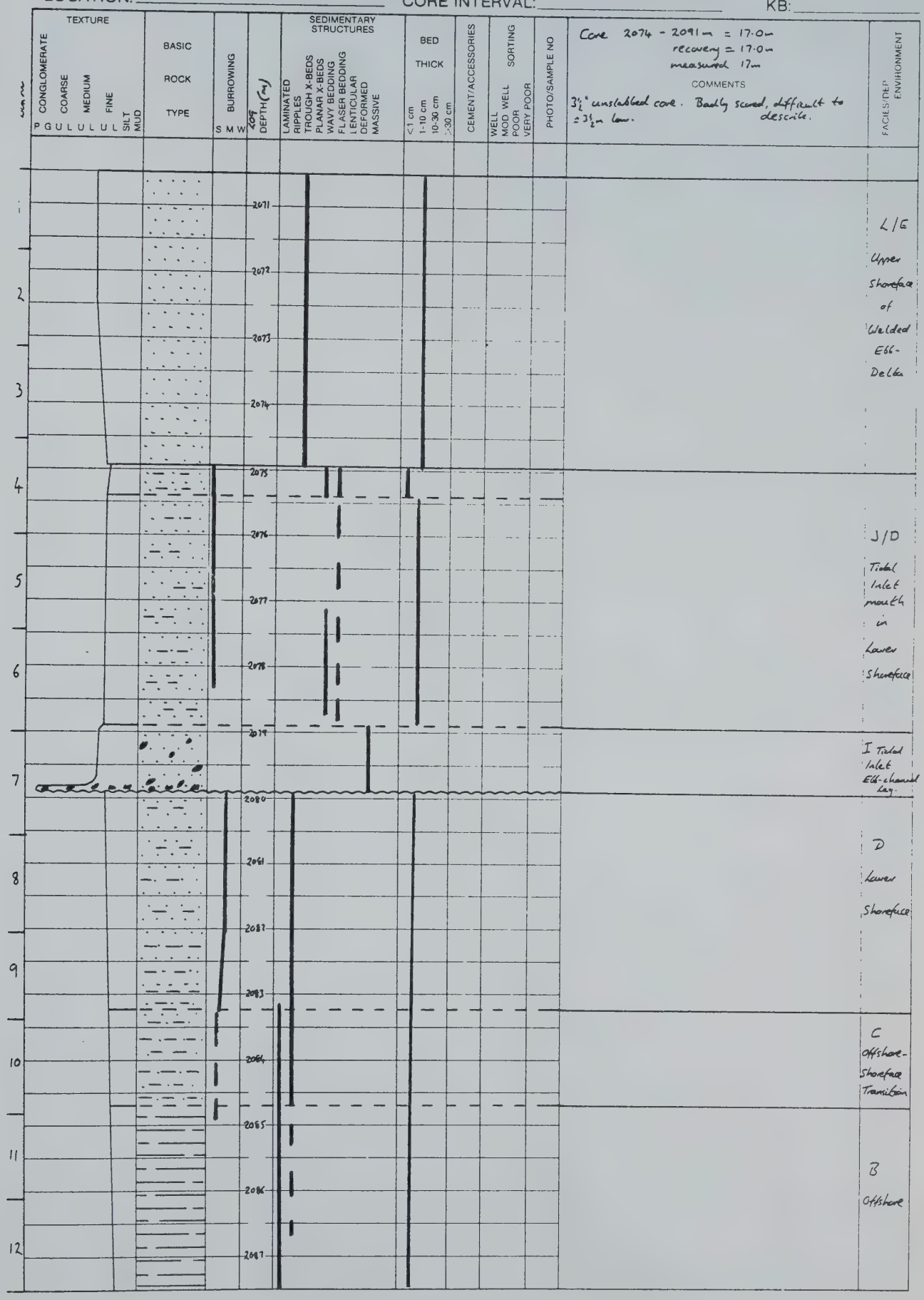

WELL NAME: Total et al Wembley FORMATION: DATE:

LOCATION: 10-35-72-8-W6 CORE INTERVAL: KB:

Core 1. 2055.0 - 2072.9m = 17.9m
recovery = 17.9m

3½" partly slabbed core.

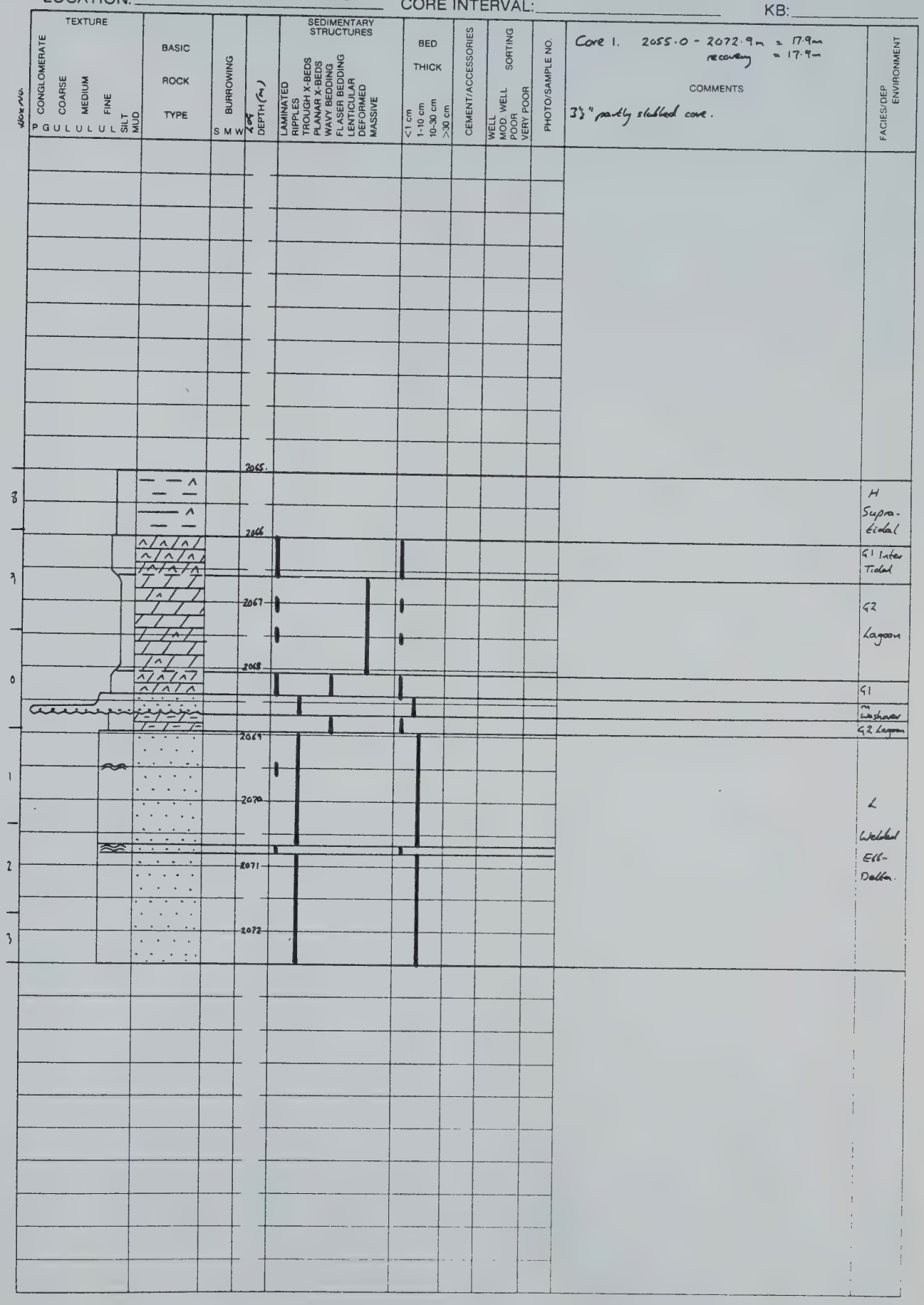

WELL NAME: (2/2) FORMATION: DATE:

LOCATION: 10-35-72-8-W6 CORE INTERVAL: KB:

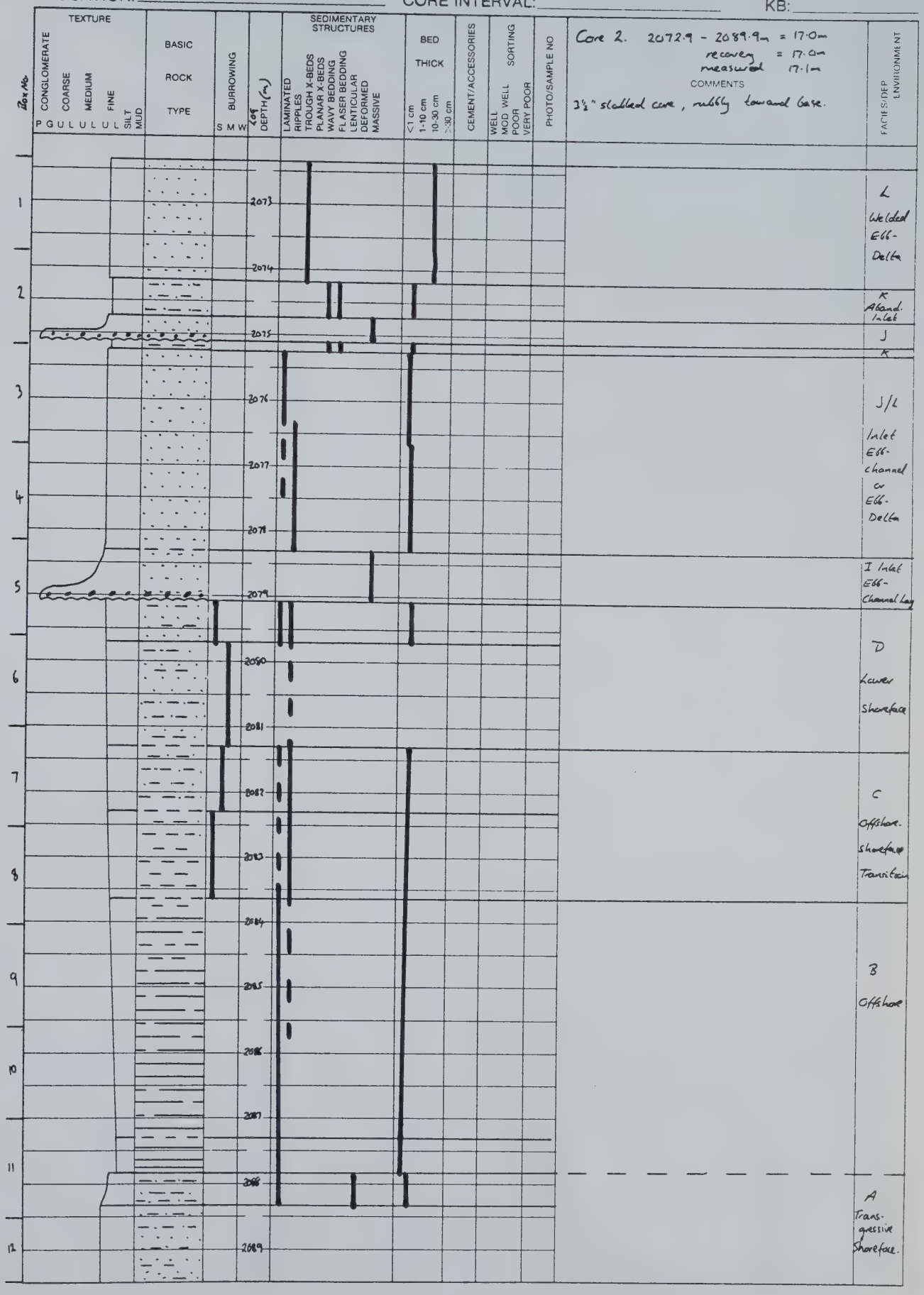

WELL NAME: PCP Wembley FORMATION: DATE:

LOCATION: 6-36-72-8-W6 CORE INTERVAL: KB:

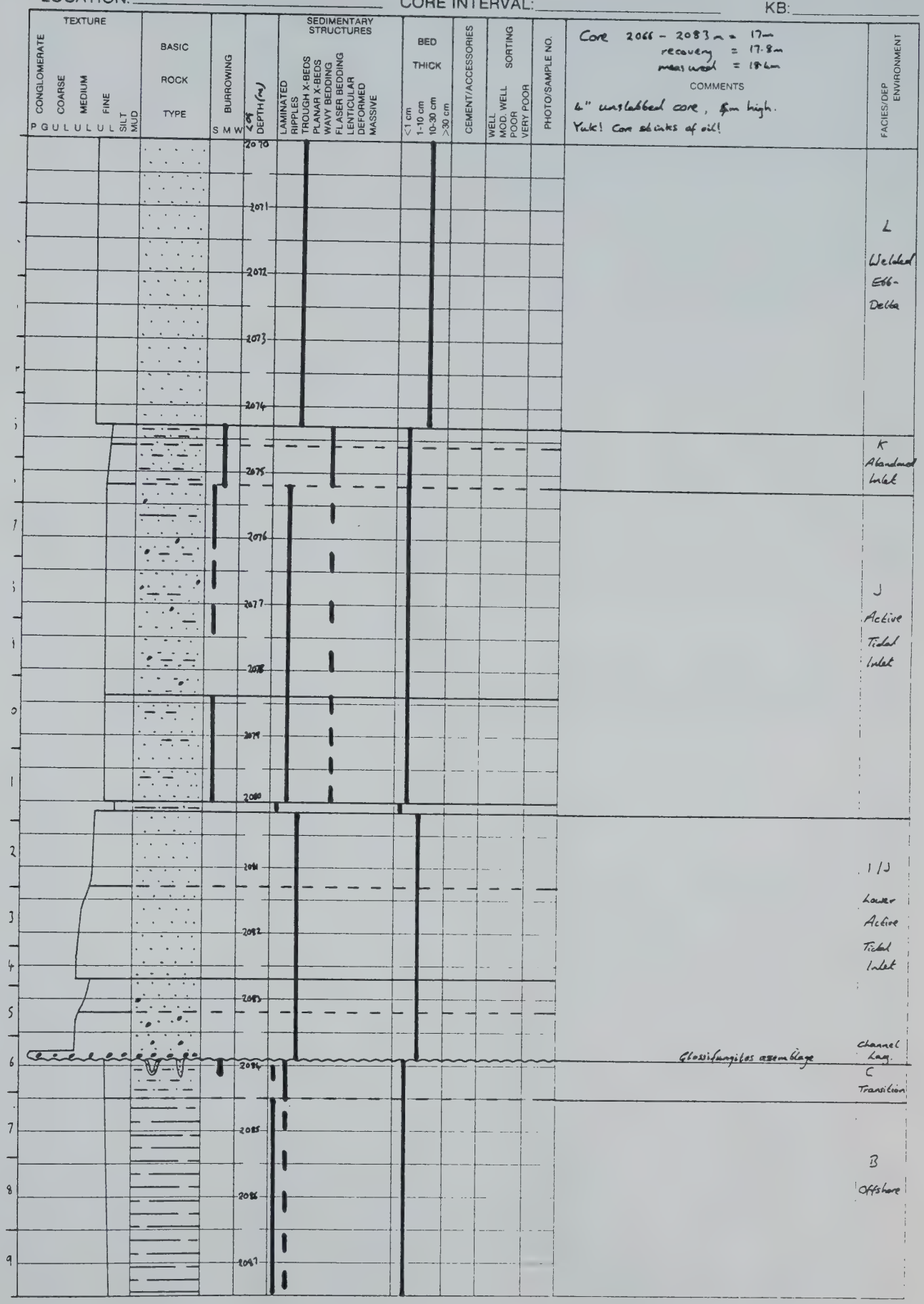

WELL NAME: PCP Wembley FORMATION: DATE:

LOCATION: 7-36-72-8-W6 CORE INTERVAL: KB:

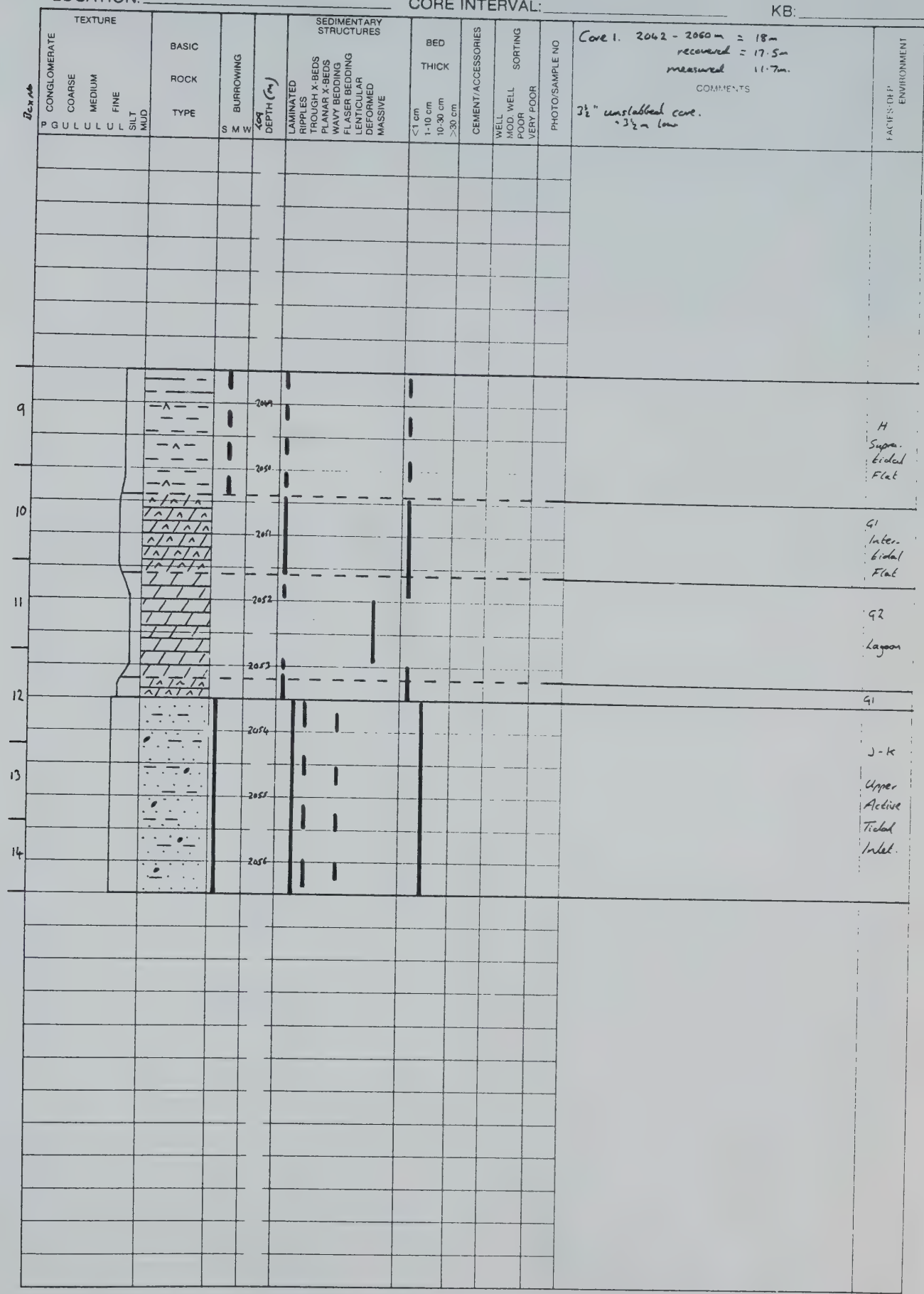

WELL NAME: (2/2)

LOCATION: 7-36-72-8-W6

FORMATION:

CORE INTERVAL:

DATE:

KB:

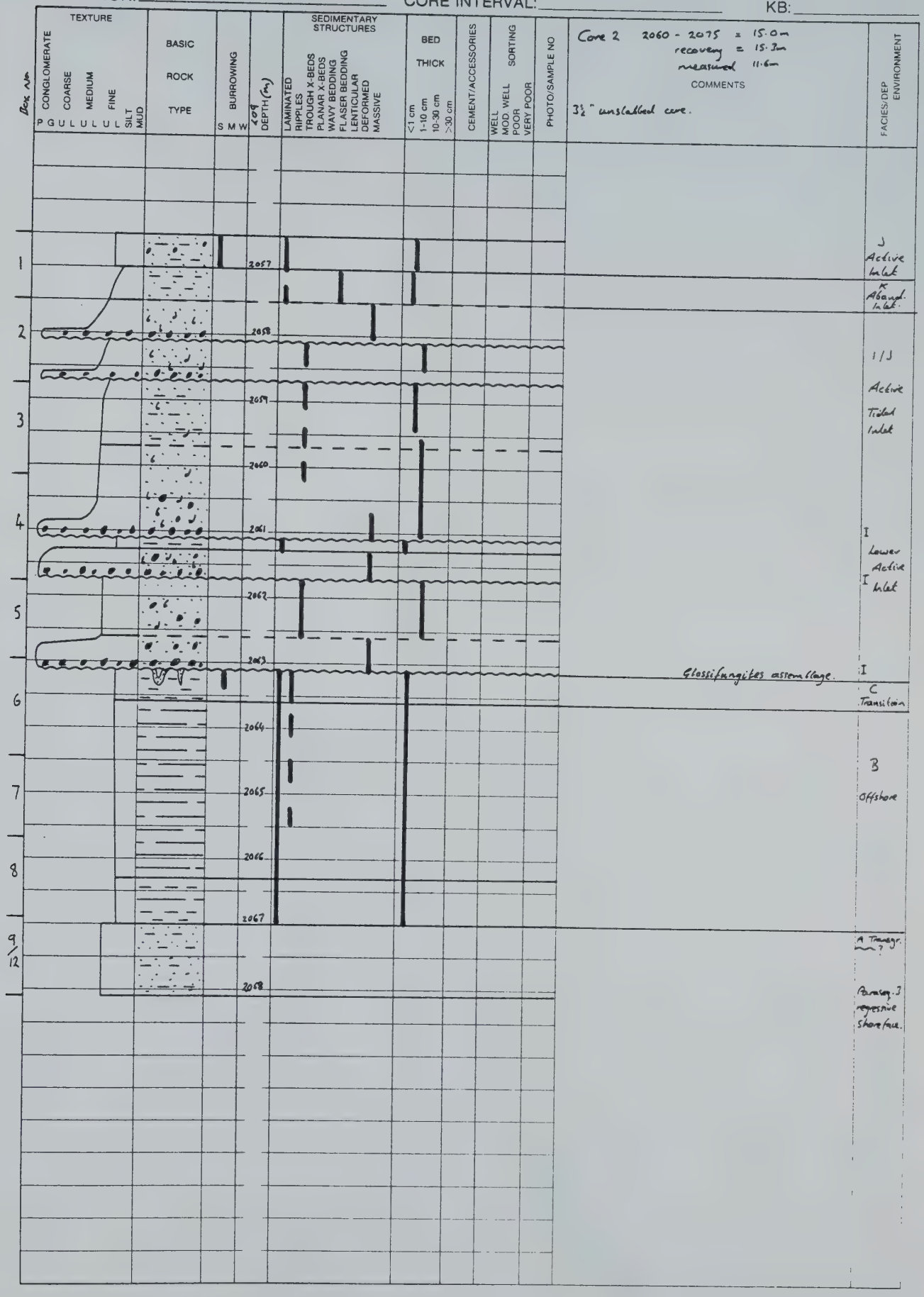

WELL NAME: PCP Beaverlodge FORMATION: DATE:

LOCATION: 11-36-72-8-W6 CORE INTERVAL: KB:

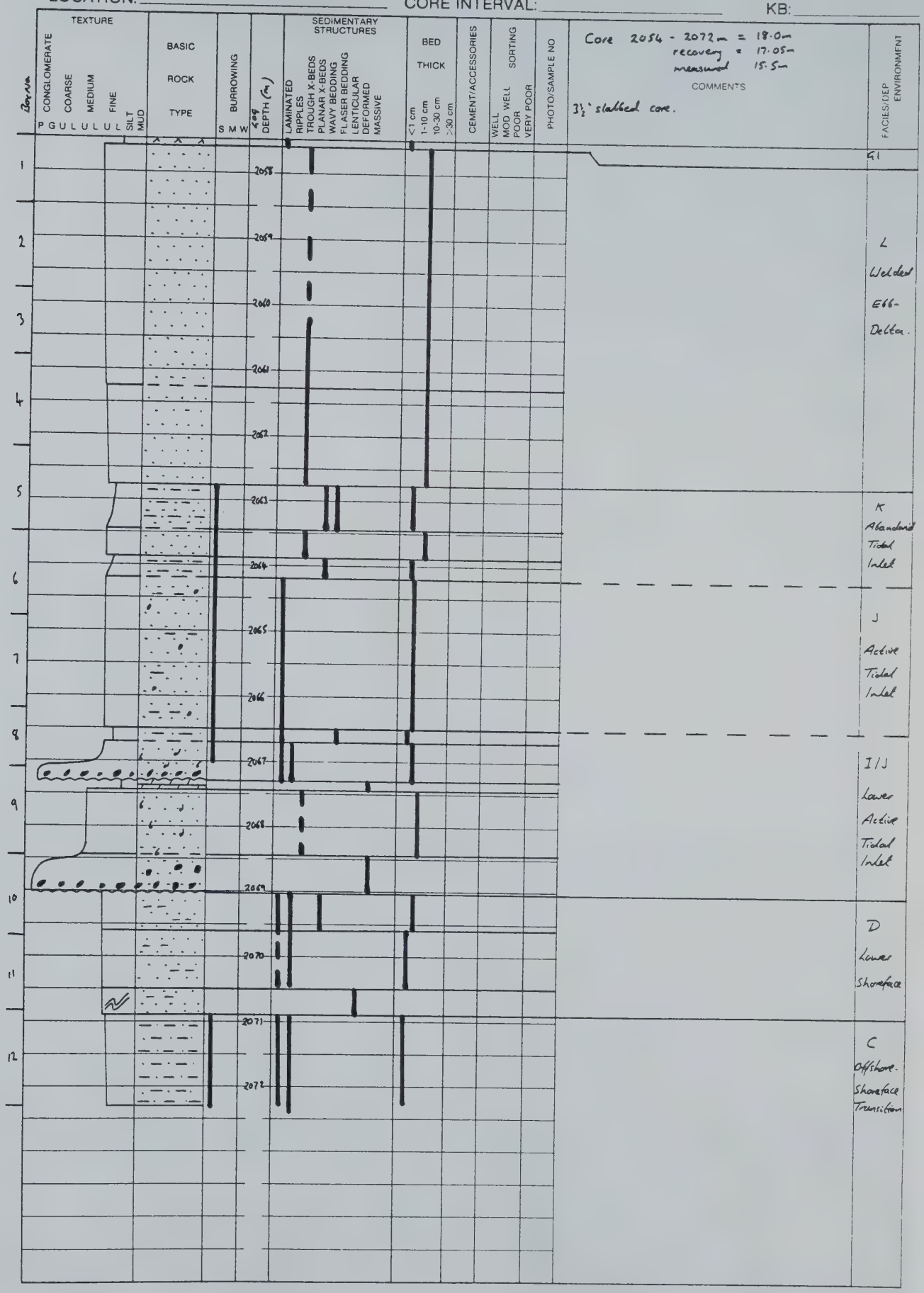

WELL NAME: PCP Wembley FORMATION: DATE:

LOCATION: 16-36-72-8-W6 CORE INTERVAL: KB:

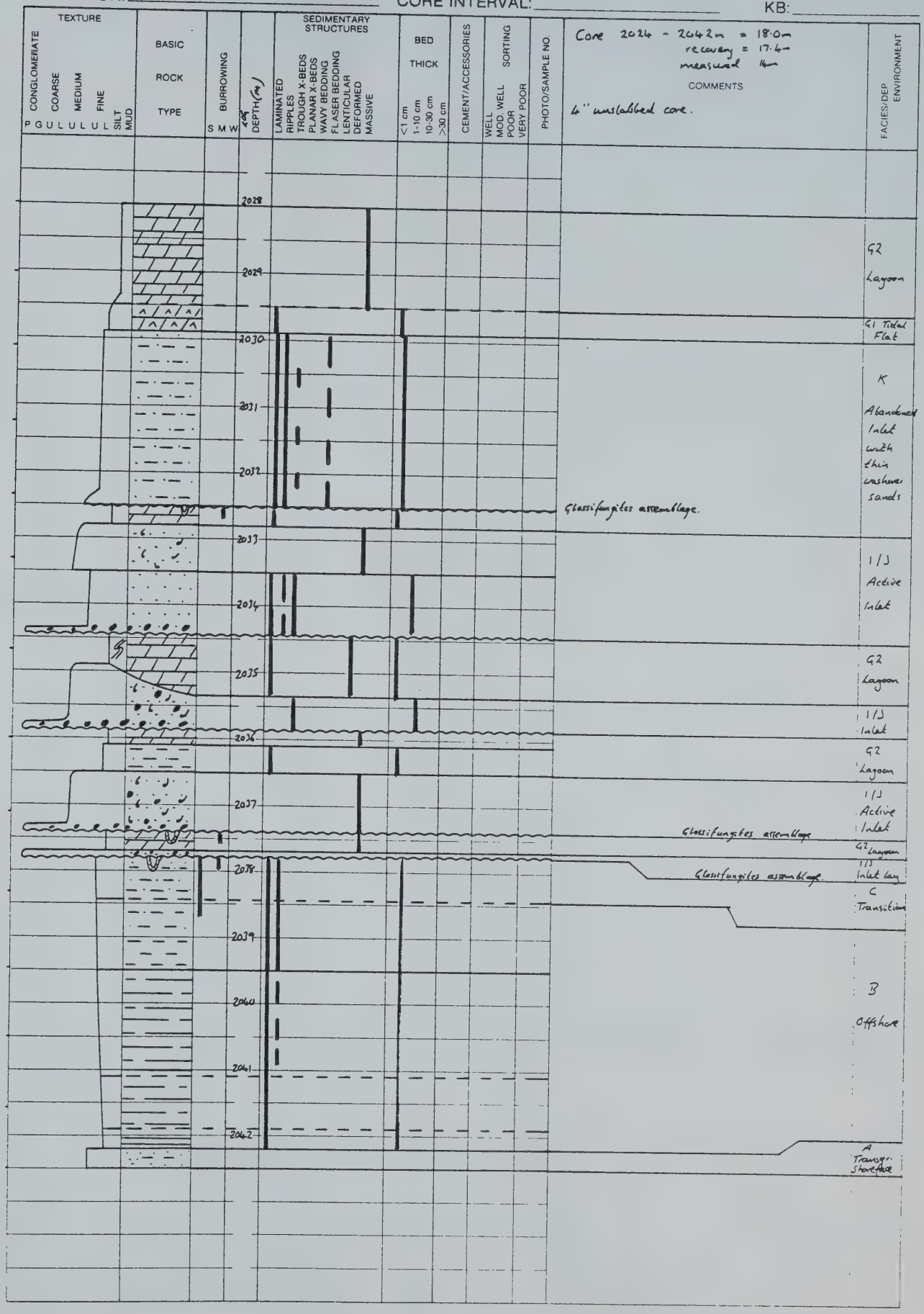

WELL NAME: Dome et al Albright 8-1-72-9-W6 FORMATION: DATE:

LOCATION: CORE INTERVAL: KB:

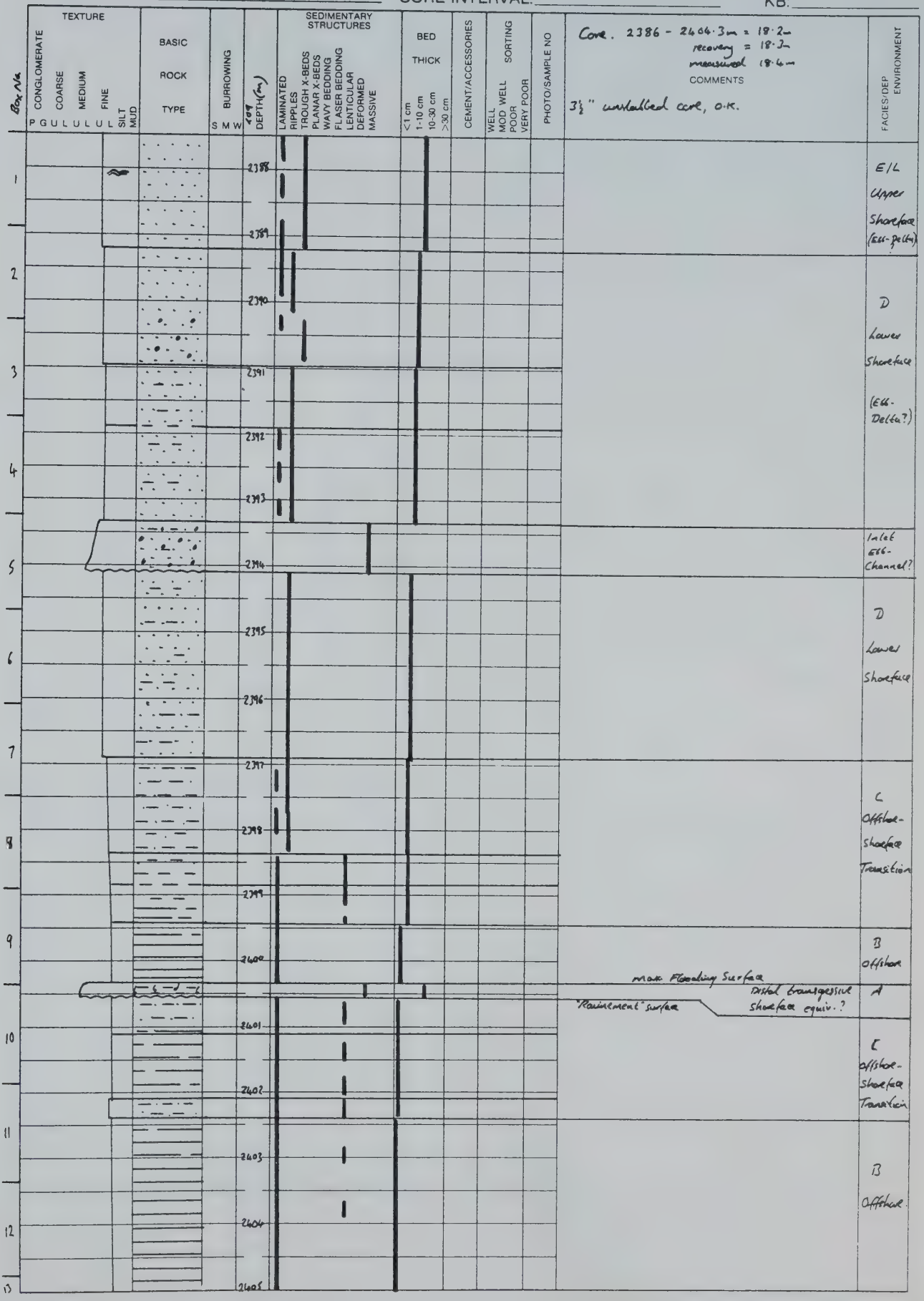

WELL NAME: Amoco Beaverlodge 10-35-72-9-W6 FORMATION: DATE:

LOCATION: CORE INTERVAL: KB:

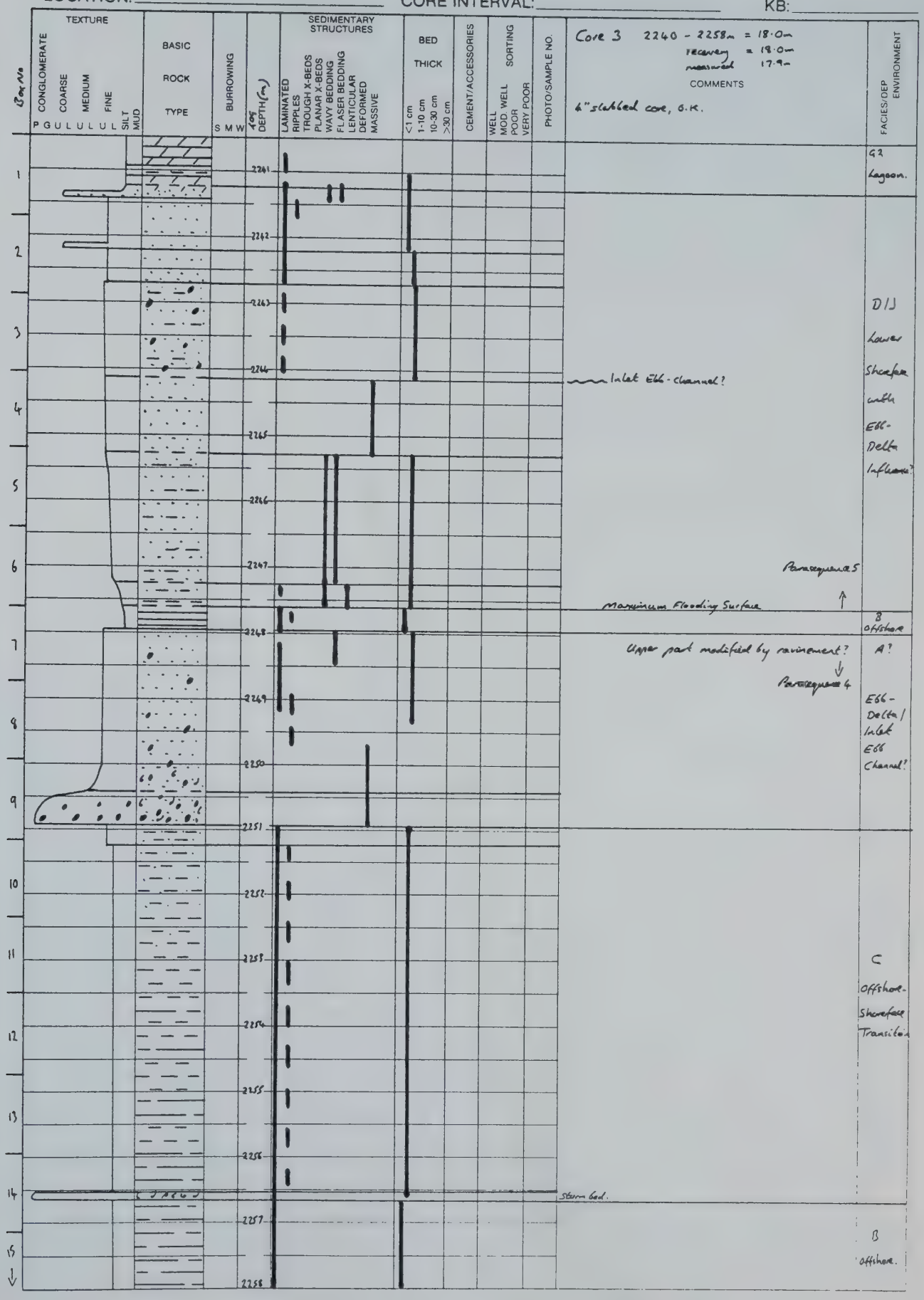

WELL NAME: PCP Esso Wembley 6-6-73-7-W6 FORMATION: DATE:

LOCATION: CORE INTERVAL: KB:

Box No	TEXTURE (P CONGLOMERATE, G COARSE, U MEDIUM, U FINE, U SILT, U MUD)	BASIC ROCK TYPE	BURROWING (S M W)	Core DEPTH (m)	SEDIMENTARY STRUCTURES (LAMINATED, RIPPLES, TROUGH X-BEDS, PLANAR X-BEDS, WAVY BEDDING, FLASER BEDDING, LENTICULAR, DEFORMED, MASSIVE)	BED THICK (<1 cm, 1-10 cm, 10-30 cm, >30 cm)	CEMENT/ACCESSORIES	SORTING (WELL, MOD. WELL, POOR, VERY POOR)	PHOTO/SAMPLE NO.	COMMENTS	FACIES/DEP ENVIRONMENT
										Core 1. 1996.0 - 2006.4m = 10.4m recovery = 9.65m Core 2. 2006.4 - 2015m = 8.6m recovery = 7.65m 4" slabbed core.	
5				1997							H Supra tidal
				1998							
6				1999							G' Inter tidal
7				2000							L Welded Ebb-Delta
8				2001							
9											
				2002							
1				2003							
2				2004							K Aband. Inlet
3				2005							J Active Inlet
4											
				2006							
5				2007							J/I Lower Active Tidal Inlet
6											
				2008							
7											
				2009							
8											C Transition Zone

WELL NAME: Dome et al Bear Lake 6-8-73-7-W6 FORMATION: DATE:

LOCATION: CORE INTERVAL: KB:

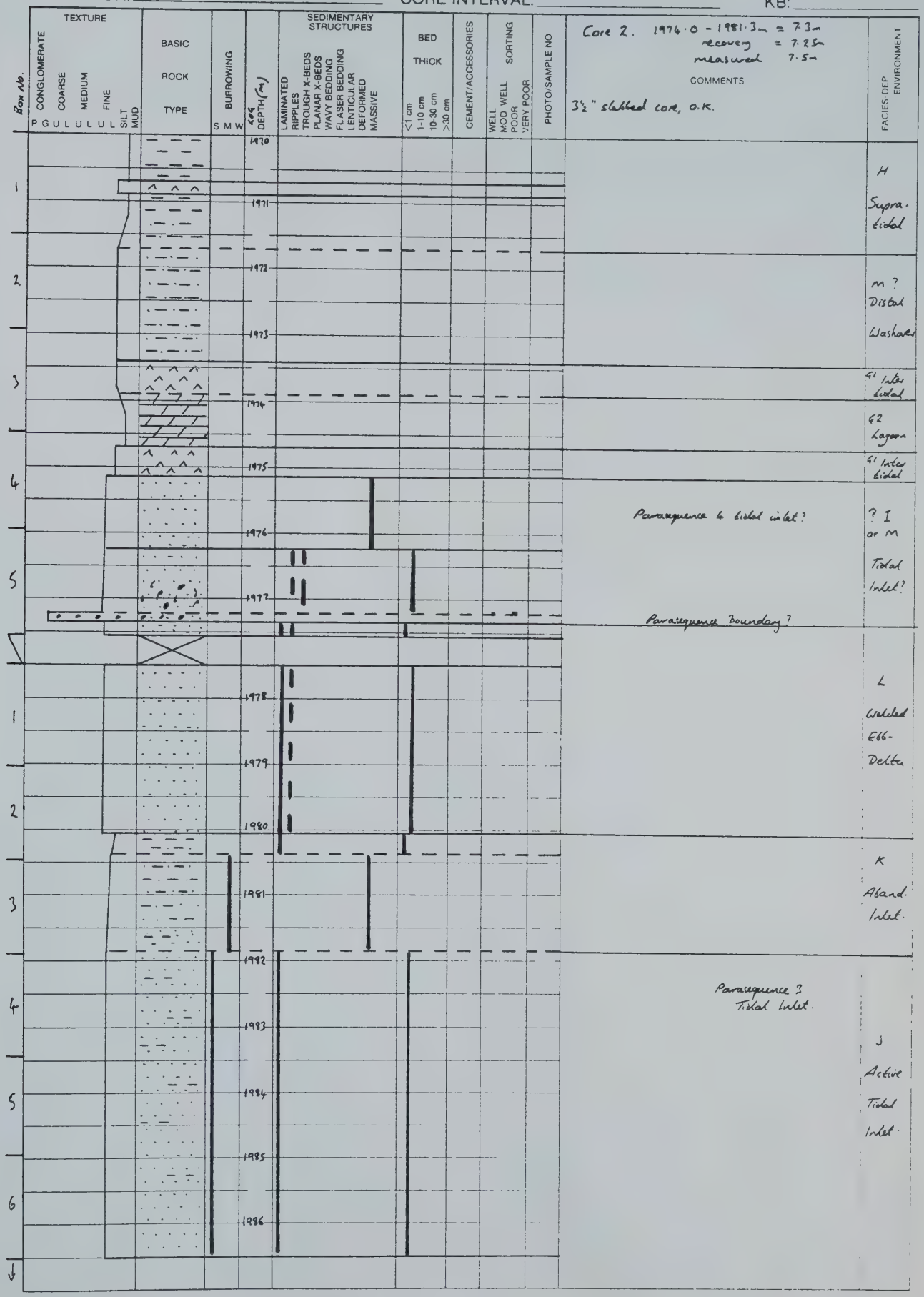

WELL NAME: (2/2) 6-8-73-7-W6 FORMATION: DATE:

LOCATION: CORE INTERVAL: KB:

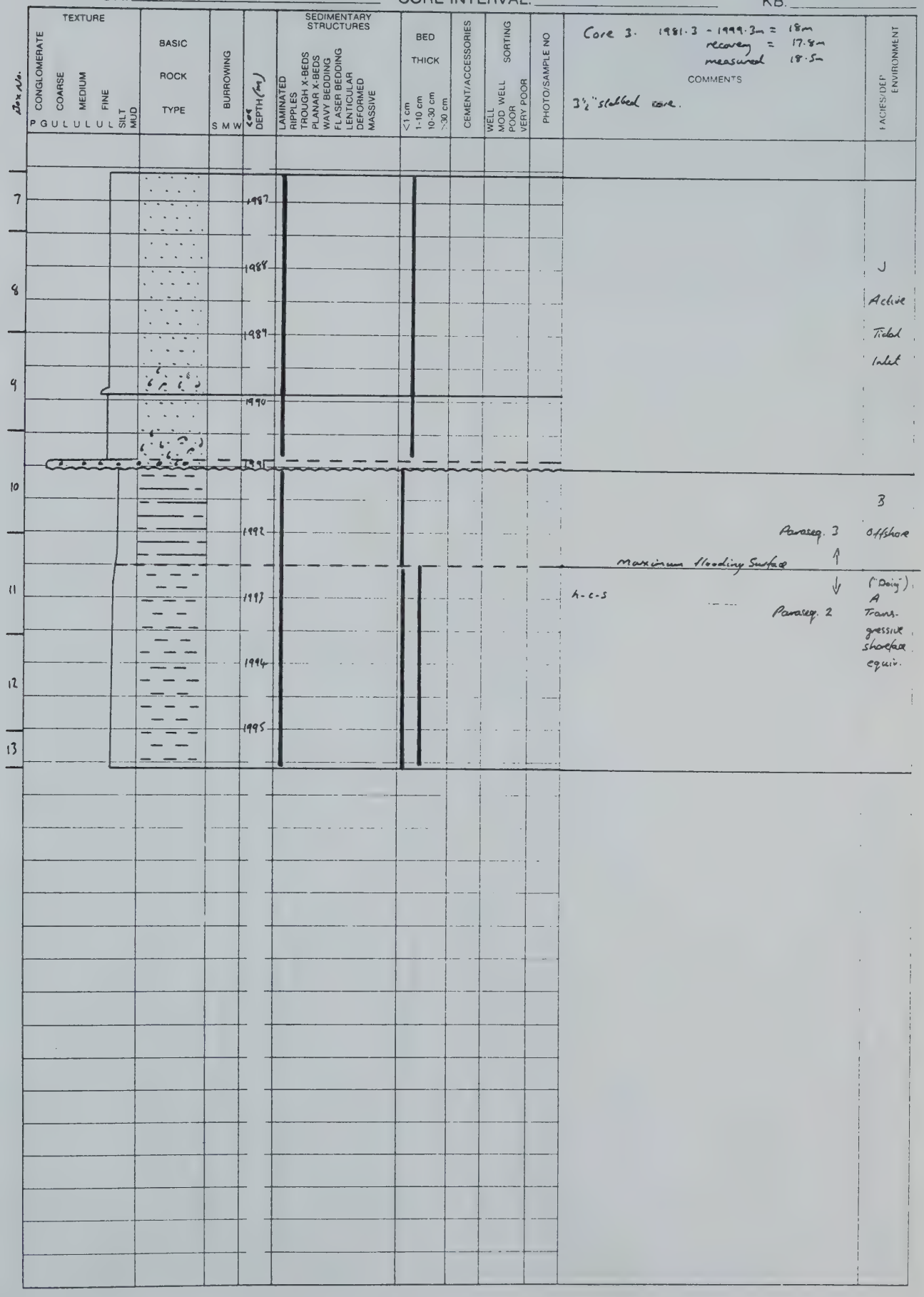

WELL NAME: PCP Esso Wembley 102/10-18-73-7-W6 FORMATION: DATE:

LOCATION: CORE INTERVAL: KB:

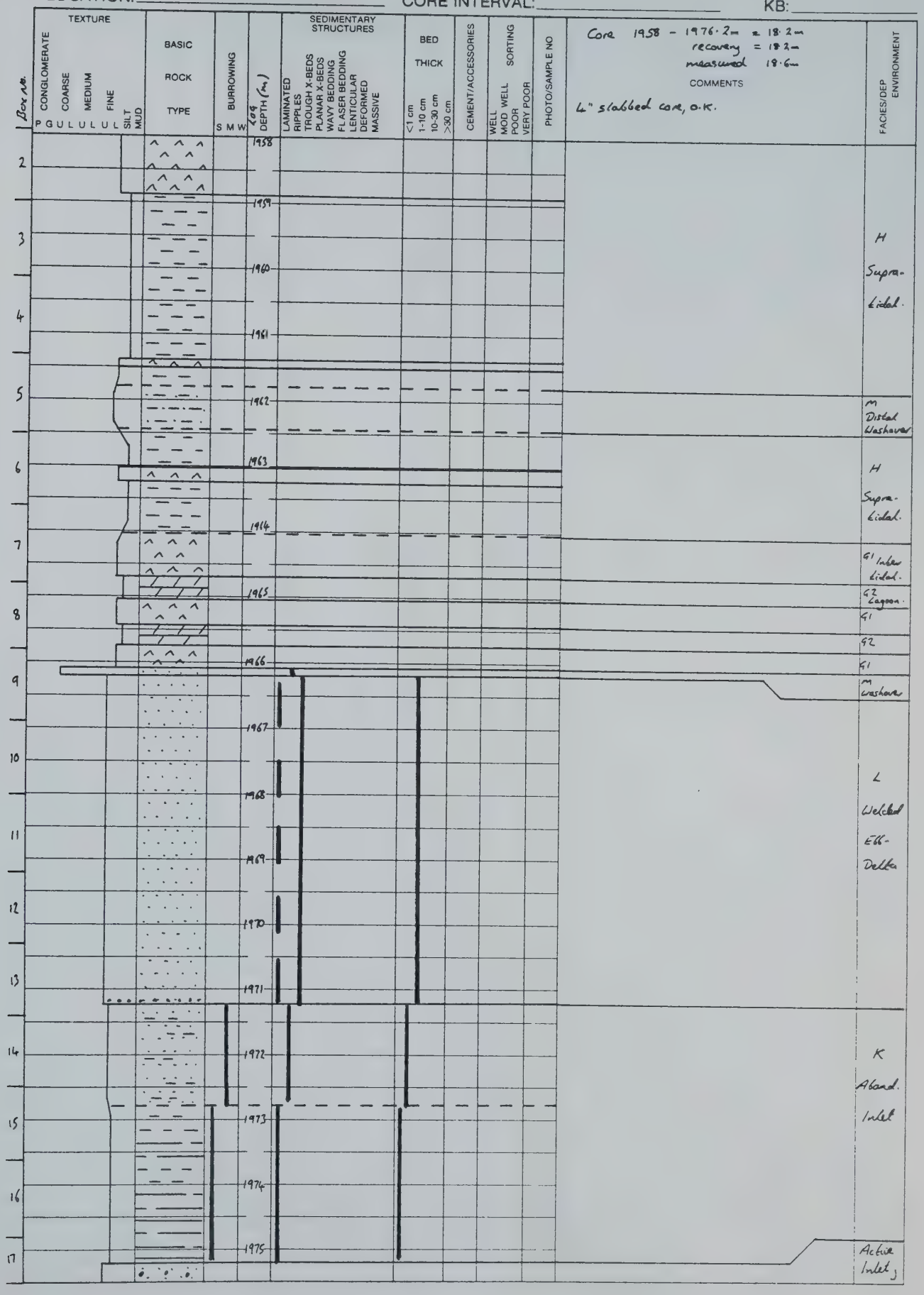

WELL NAME: Huber et al Grande Prairie 14-22-73-7-W6 FORMATION: DATE:

LOCATION: CORE INTERVAL: KB:

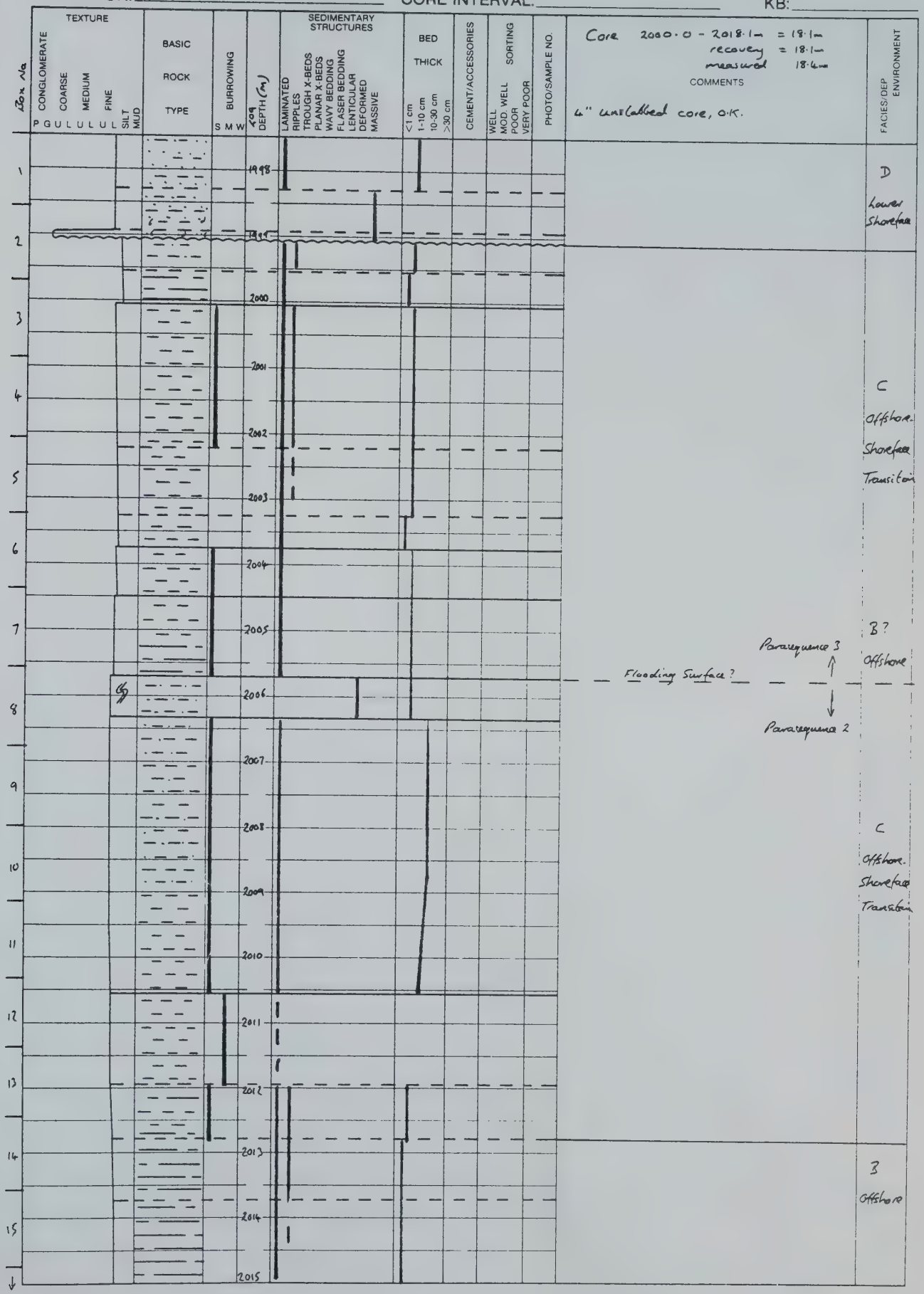

WELL NAME: PCP Esso Beaverlodge FORMATION: DATE:

LOCATION: 7-1-73-8-W6 CORE INTERVAL: KB:

Core. 2014.0 - 2032.0m = 18.0m
recovery = 12.5m *Loss
measured 13.3m

very rubbley core.

Box No.	TEXTURE: CONGLOMERATE (P G)	COARSE (U L)	MEDIUM (U L)	FINE (U L)	SILT (U L)	MUD	BASIC ROCK TYPE	BURROWING (S M W)	log DEPTH (m)	SEDIMENTARY STRUCTURES: LAMINATED, RIPPLES, TROUGH X-BEDS, PLANAR X-BEDS, WAVY BEDDING, FLASER BEDDING, LENTICULAR, DEFORMED, MASSIVE	BED THICK: <1 cm, 1-10 cm, 10-30 cm, >30 cm	CEMENT/ACCESSORIES	SORTING: WELL, MOD. WELL, POOR, VERY POOR	PHOTO/SAMPLE NO.	COMMENTS	FACIES/DEP ENVIRONMENT
																H Supra tidal
5																G1 Inter tidal
6																G2 Lagoon
7									2020							G1 Inter tidal
																K Aband. Inlet
8																I/J
9																Lower Active Tidal Inlet
10																
11									2030							B Offshore

WELL NAME: PCP Esso Wembley FORMATION: DATE:

LOCATION: 6-2-73-8-W6 CORE INTERVAL: KB:

Core 1. 2042 - 2060 m = 18m
recovery = 17.9m
measured 17.7m

3½" unslabbed core.

Box no.	TEXTURE: CONGLOMERATE (P G) / COARSE (U L) / MEDIUM (U L) / FINE (U L) / SILT (U L) / MUD	BASIC ROCK TYPE	BURROWING (S M W)	log DEPTH (m)	SEDIMENTARY STRUCTURES: LAMINATED / RIPPLES / TROUGH X-BEDS / PLANAR X-BEDS / WAVY BEDDING / FLASER BEDDING / LENTICULAR / DEFORMED / MASSIVE	BED THICK: <1 cm / 1-10 cm / 10-30 cm / >30 cm	CEMENT/ACCESSORIES	SORTING: WELL / MOD WELL / POOR / VERY POOR	PHOTO/SAMPLE NO.	COMMENTS	FACIES/DEP ENVIRONMENT
1				2040							H Supra tidal
				2041							
2				2042							G1 ?
											m/L ? Washover
3				2043							G2 Lagoon
				2044							L Welded Ebb-Delta.
4				2045						Adhesion Laminae ?	
5				2046							
				2047							

WELL NAME: _____ FORMATION: _____ DATE: _____

LOCATION: 6-2-73-8-W6 (2/2) CORE INTERVAL: _____ KB: _____

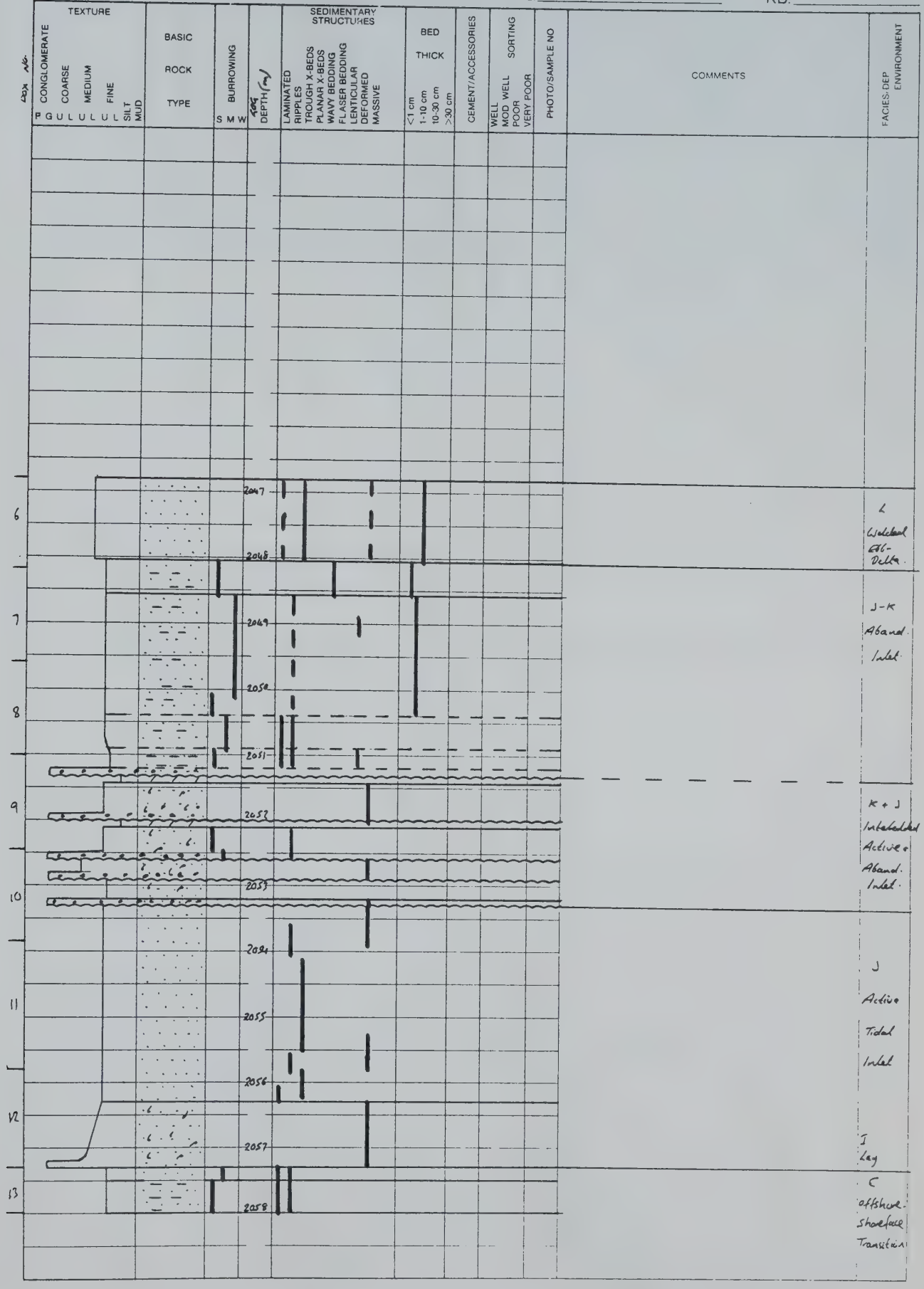

WELL NAME: PCP Esso Wembley FORMATION: DATE:

LOCATION: 14-2-73-8-W6 CORE INTERVAL: KB:

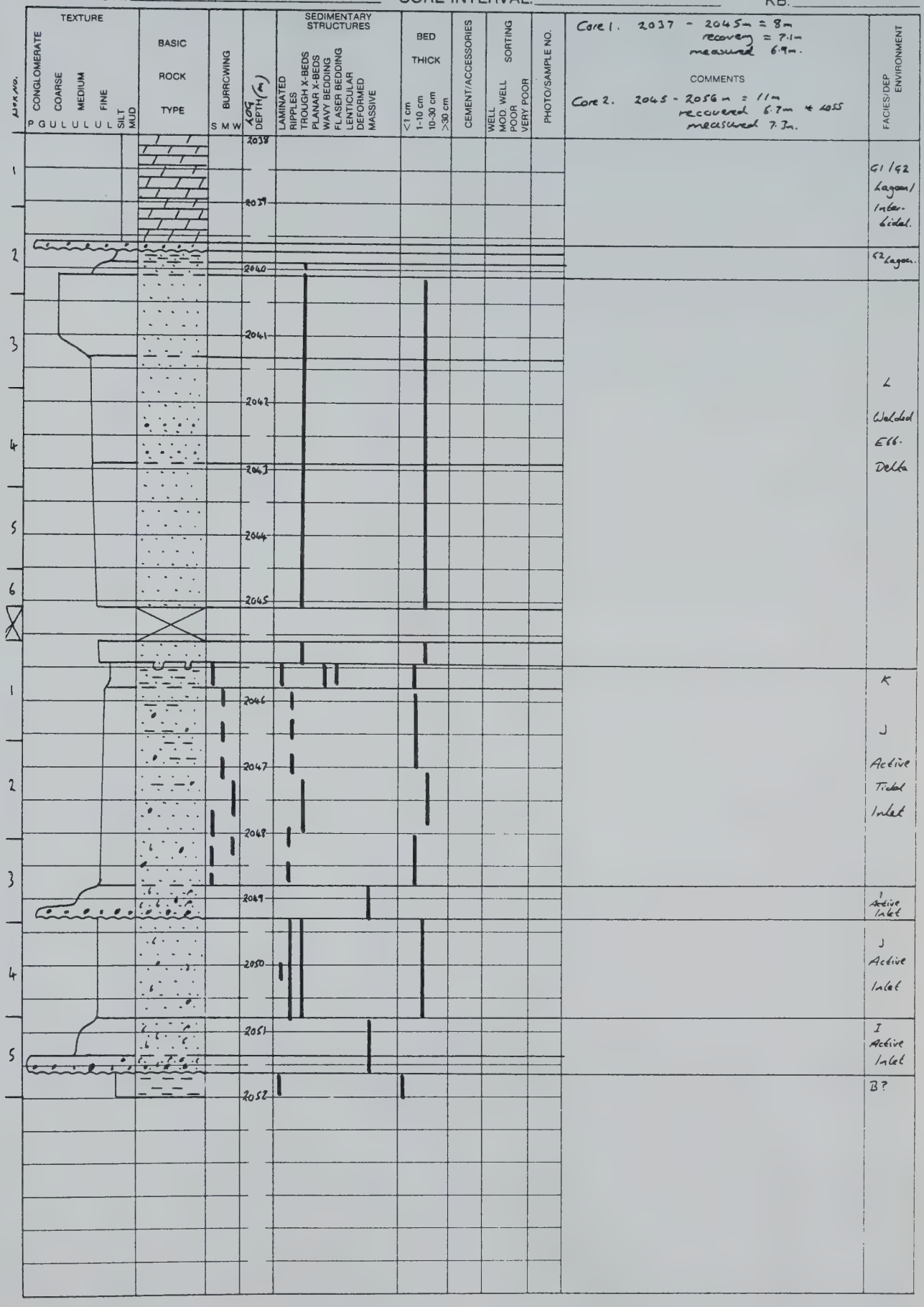

WELL NAME: PCP Esso Wembley 16-2-73-8-W6 FORMATION: DATE:

LOCATION: CORE INTERVAL: KB:

TEXTURE (CONGLOMERATE, COARSE, MEDIUM, FINE, SILT, MUD)	BASIC ROCK TYPE	BURROWING (S M W)	DEPTH (m)	SEDIMENTARY STRUCTURES (LAMINATED, RIPPLES, TROUGH X-BEDS, PLANAR X-BEDS, WAVY BEDDING, FLASER BEDDING, LENTICULAR, DEFORMED, MASSIVE)	BED THICK (<1 cm, 1-10 cm, 10-30 cm, >30 cm)	CEMENT/ACCESSORIES	SORTING (WELL, MOD. WELL, POOR, VERY POOR)	PHOTO/SAMPLE NO	COMMENTS	FACIES/DEP ENVIRONMENT
									Core 2020 - 2038m = 18m recovery = 16.7m measured 16.8m	
									4" slabbed core, ≈ 2m high.	
			2022							H Supra-tidal
			2023							
			2024							G1 Inter-tidal
			2025							
			2026							M Washover
										G2 Lagoon.
			2027							L Welded Ebb-Delta.

WELL NAME: _____ FORMATION: _____ DATE: _____

LOCATION: 16-2-73-8-W6 (2/2) CORE INTERVAL: _____ KB: _____

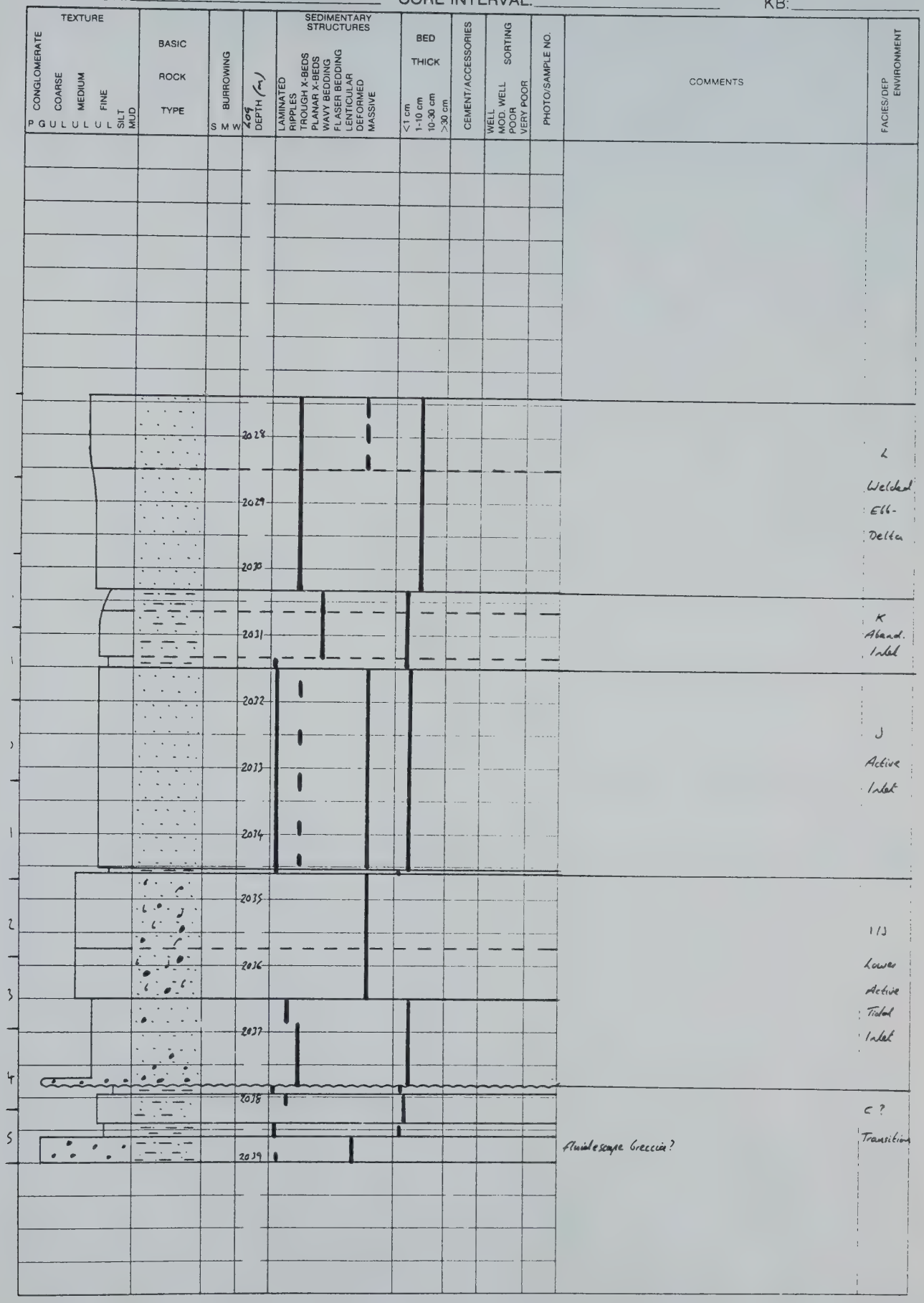

WELL NAME: Total et al Wembley FORMATION: DATE:

LOCATION: 7-3-73-8-W6 CORE INTERVAL: KB:

Box No	TEXTURE: CONGLOMERATE (P)	COARSE (G)	MEDIUM (U)	FINE (L)	SILT (U)	MUD (L)	BASIC ROCK TYPE	BURROWING: S	M	W	DEPTH (m)	SEDIMENTARY STRUCTURES: LAMINATED	RIPPLES	TROUGH X-BEDS	PLANAR X-BEDS	WAVY BEDDING	FLASER BEDDING	LENTICULAR	DEFORMED	MASSIVE	BED THICK: <1 cm	1-10 cm	10-30 cm	>30 cm	CEMENT/ACCESSORIES	SORTING: WELL	MOD WELL	POOR	VERY POOR	PHOTO/SAMPLE NO.	COMMENTS	FACIES/DEP ENVIRONMENT
																															Core 1. 2072.0 - 2090.2m = 18.2m recovery = 18.0m	
																															COMMENTS: 3½" partly slabbed core.	
7											2085																					H Supra tidal.
											2086																					
8																																
											2087																					
9											2088																					
											2089																					m Washover
10																																G2 Lagoon
											2090																					L Welded Ebb-Delta.
11											2091																					
											2092																					
12											2093																					
13/13											2094																					

WELL NAME: _____ FORMATION: _____ DATE: _____

LOCATION: 7-3-73-8-W6 (2/2) CORE INTERVAL: _____ KB: _____

TEXTURE (CONGLOMERATE, COARSE, MEDIUM, FINE, SILT, MUD)	BASIC ROCK TYPE	BURROWING (S M W)	DEPTH (m)	SEDIMENTARY STRUCTURES (LAMINATED, RIPPLES, TROUGH X-BEDS, PLANAR X-BEDS, WAVY BEDDING, FLASER BEDDING, LENTICULAR, DEFORMED, MASSIVE)	BED THICK (<1 cm, 1-10 cm, 10-30 cm, >30 cm)	CEMENT/ACCESSORIES	SORTING (WELL, MOD. WELL, POOR, VERY POOR)	PHOTO/SAMPLE NO.	COMMENTS	FACIES/DEP ENVIRONMENT
									Core 2. 2090.2 - 2101.0m = 10.8m recovery measured = 8.1m 8.3m	
									3½" unslabbed core.	

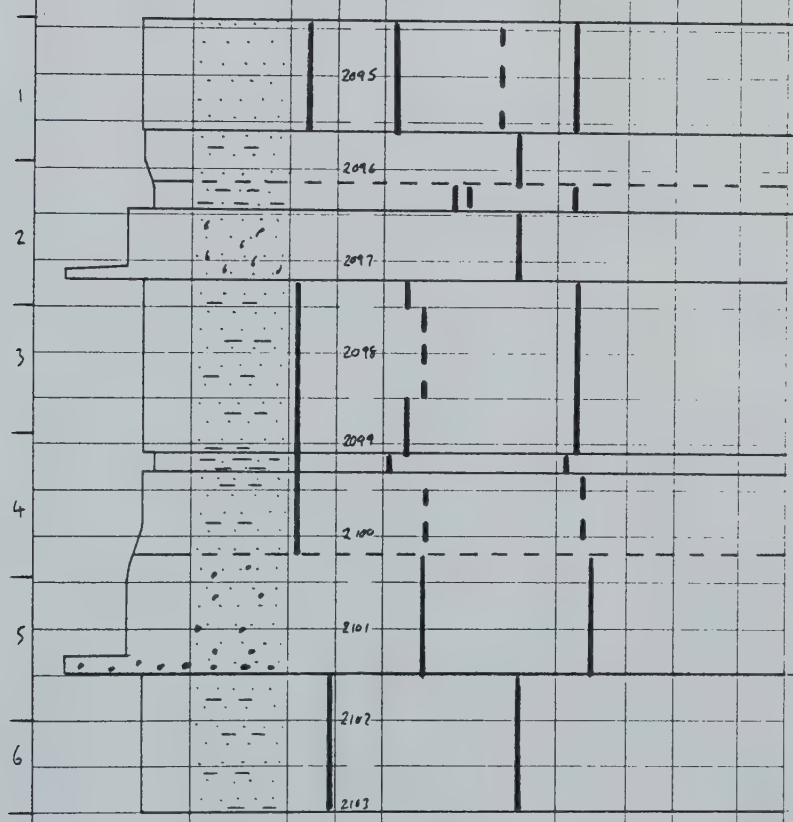

L Welded Ebb-Delta

K Aband. Inlet

J Active Tidal Inlet

I Lag

D Lower Shoreface

WELL NAME: Total et al Wembley FORMATION: DATE:

LOCATION: 14-3-73-8-W6 CORE INTERVAL: KB:

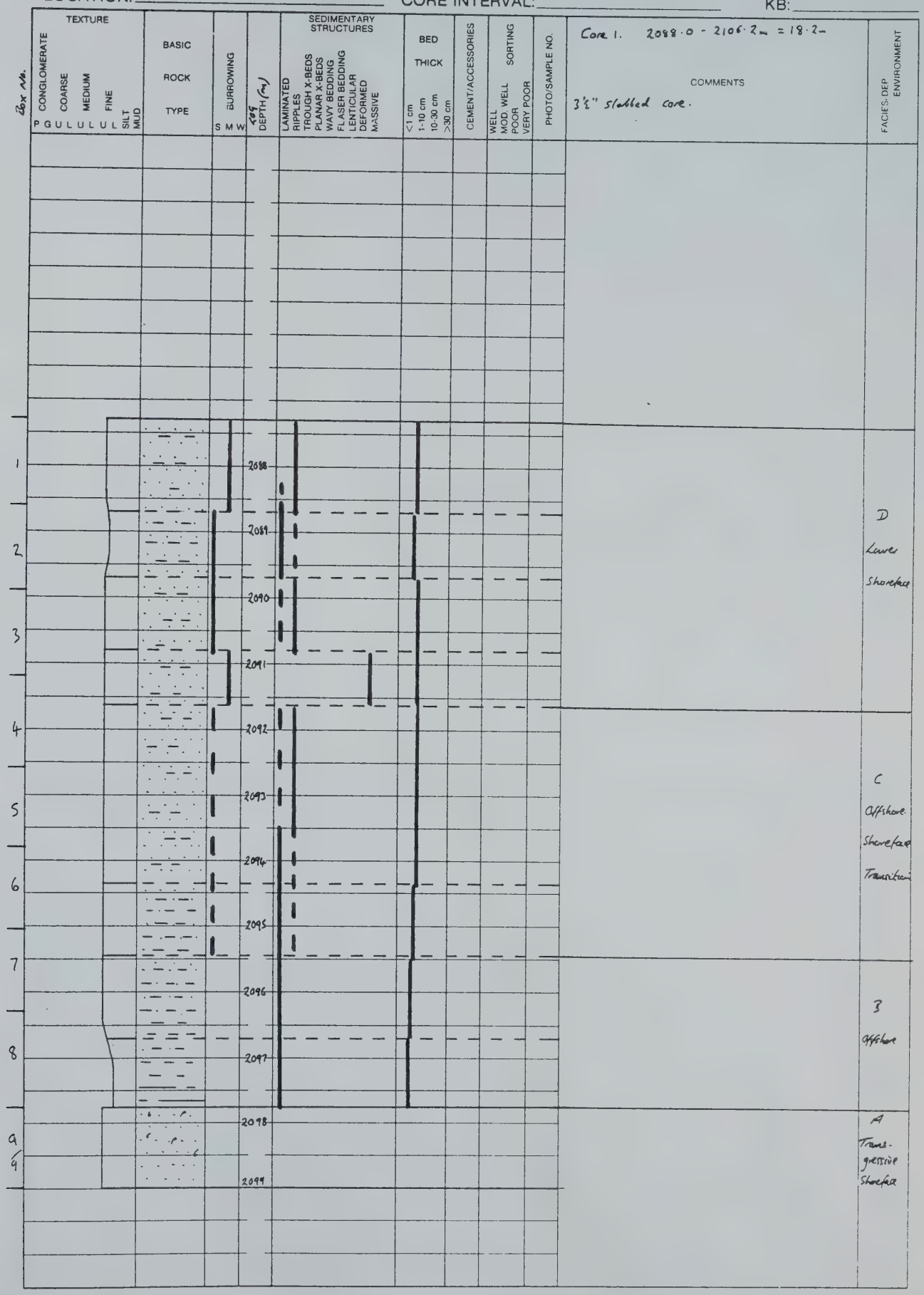

WELL NAME: Total et al Wembley FORMATION: DATE:

LOCATION: 6-4-73-8-W6 CORE INTERVAL: KB:

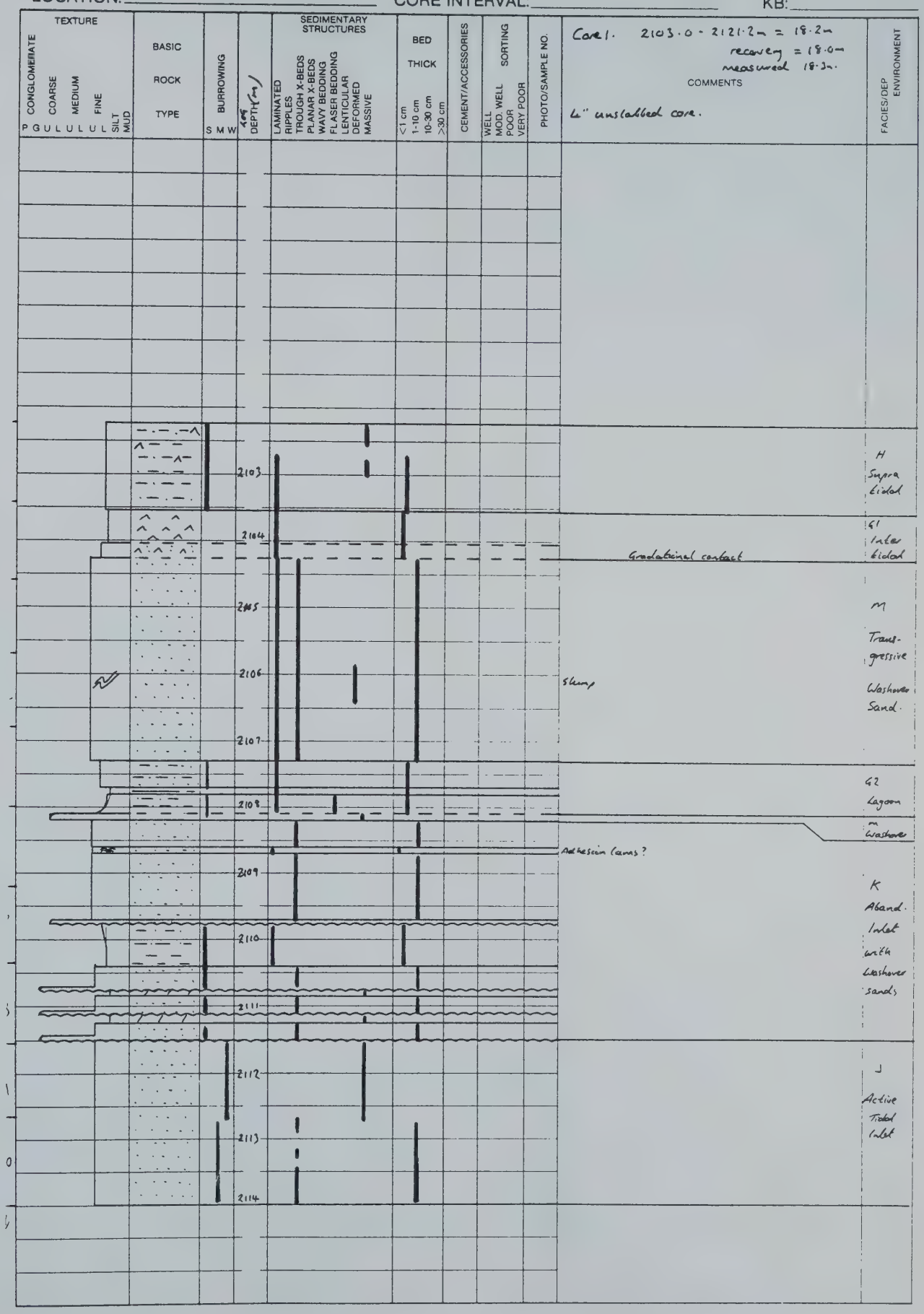

WELL NAME: _____ FORMATION: _____ DATE: _____

LOCATION: 6-4-73-8-W6 (2/2) CORE INTERVAL: _____ KB: _____

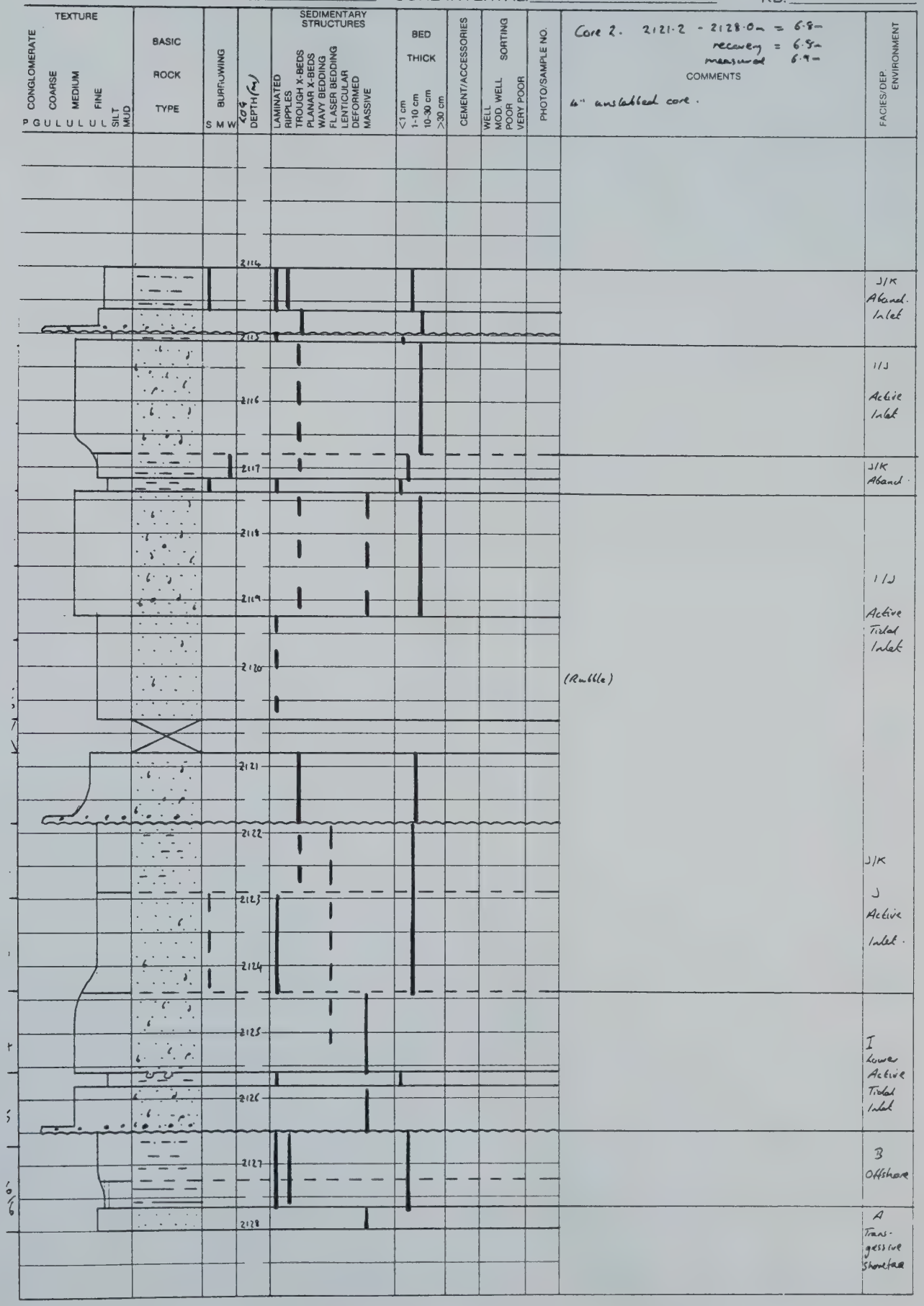

WELL NAME: Total et al Wembley

LOCATION: 8-4-73-8-W6

FORMATION:

DATE:

CORE INTERVAL:

KB:

TEXTURE: CONGLOMERATE (P)	COARSE (G)	MEDIUM (U)	FINE (L)	SILT (U)	MUD (L)	BASIC ROCK TYPE	BURROWING: S	M	W	DEPTH (m)	SEDIMENTARY STRUCTURES: LAMINATED	RIPPLES	TROUGH X-BEDS	PLANAR X-BEDS	WAVY BEDDING	FLASER BEDDING	LENTICULAR	DEFORMED	MASSIVE	BED THICK: <1 cm	1-10 cm	10-30 cm	>30 cm	CEMENT/ACCESSORIES	WELL SORTING: WELL	MOD. WELL	POOR	VERY POOR	PHOTO/SAMPLE NO.	COMMENTS	FACIES/DEP ENVIRONMENT
																														Core 1. 2101 - 2119 m = 18 m recovery = 17.3 m. 3½" slabbed core.	

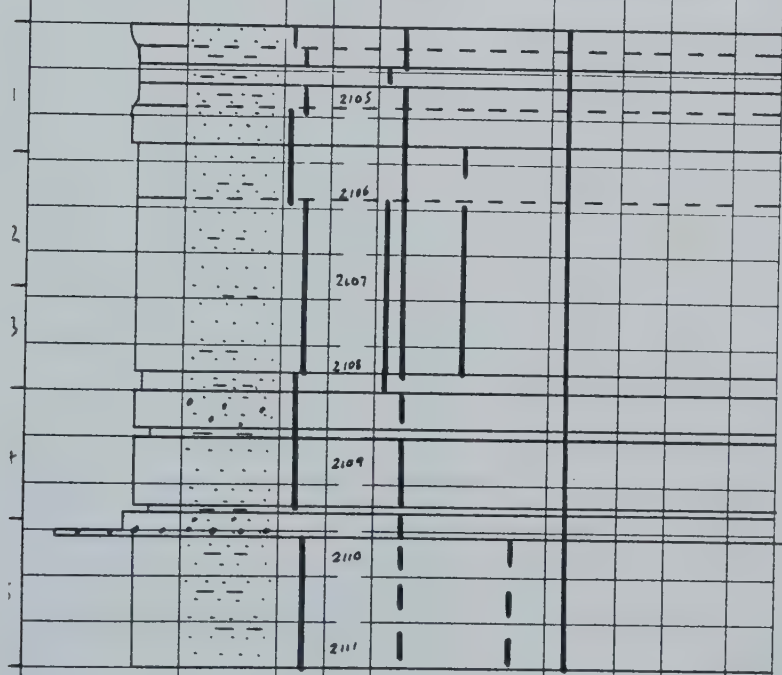

Upper Inlet S/L.

J Tidal Inlet Ebb-Channel.

I Lag

D Lower Shoreface

WELL NAME: _____ FORMATION: _____ DATE: _____

LOCATION: 8-4-73-8-W6 (2/2) CORE INTERVAL: _____ KB: _____

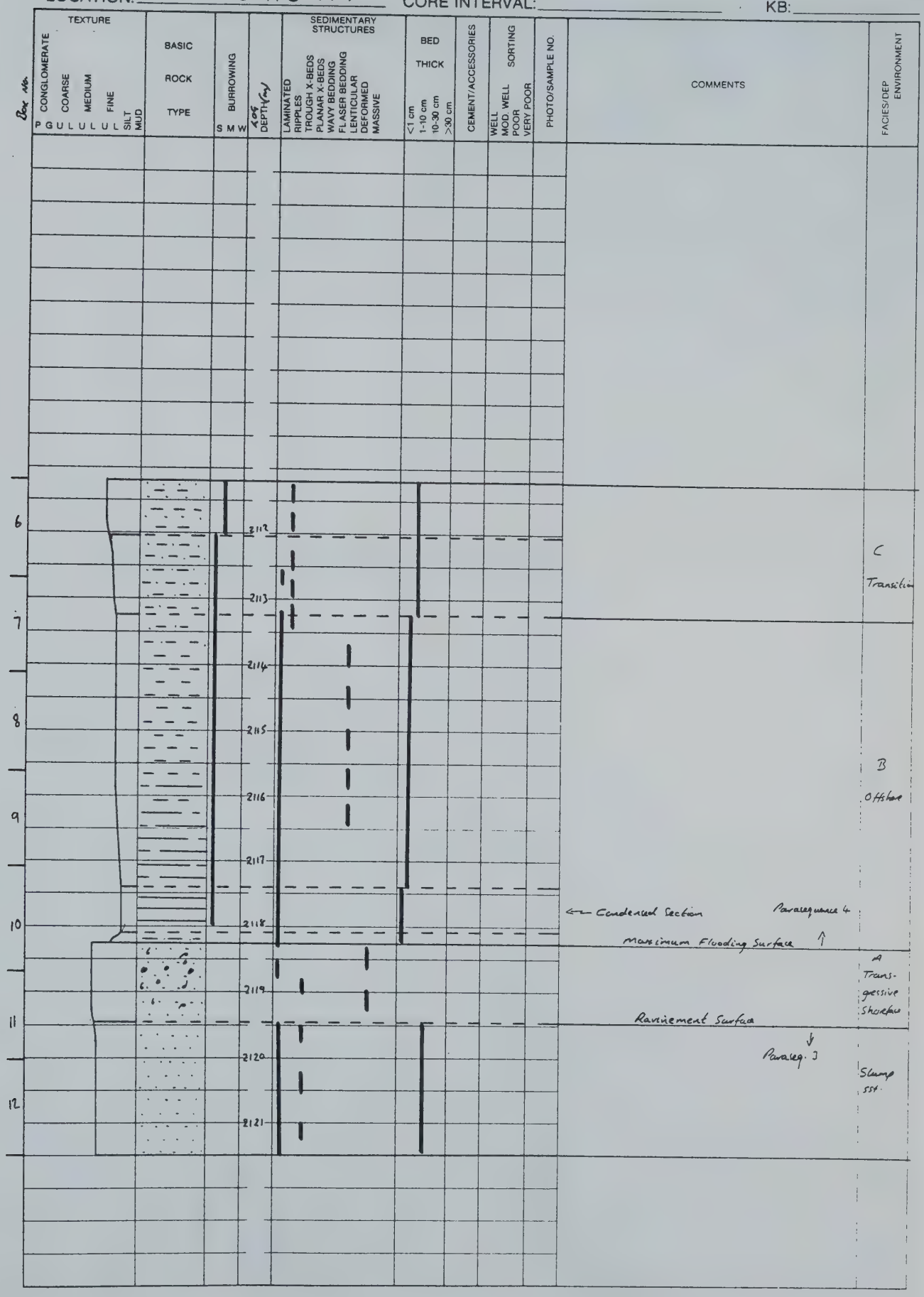

WELL NAME: Total et al Wembley FORMATION: DATE:

LOCATION: 13-4-73-8-W6 CORE INTERVAL: KB:

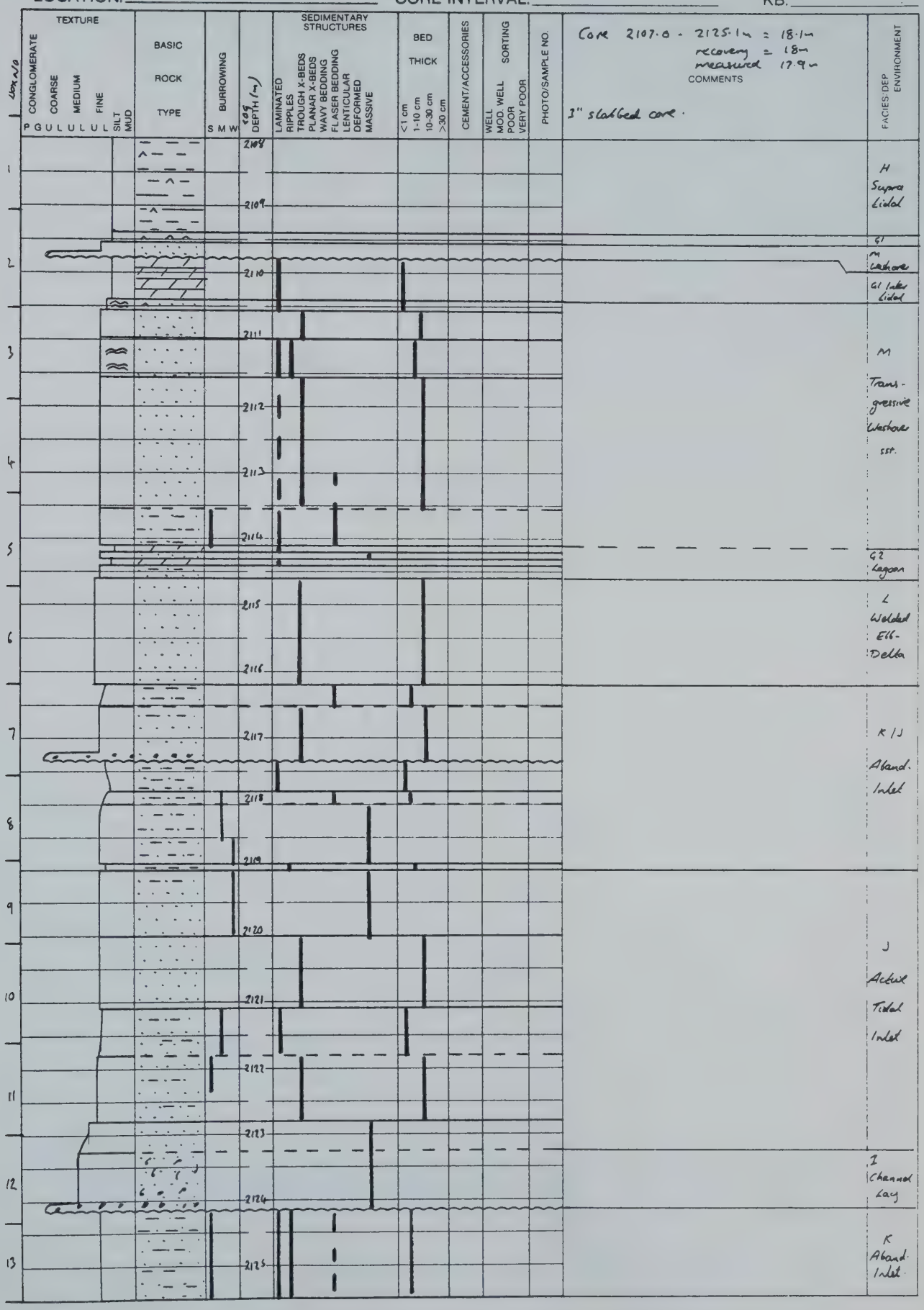

WELL NAME: Total et al Wembley 6-5-73-8-W6 FORMATION: DATE:

LOCATION: CORE INTERVAL: KB:

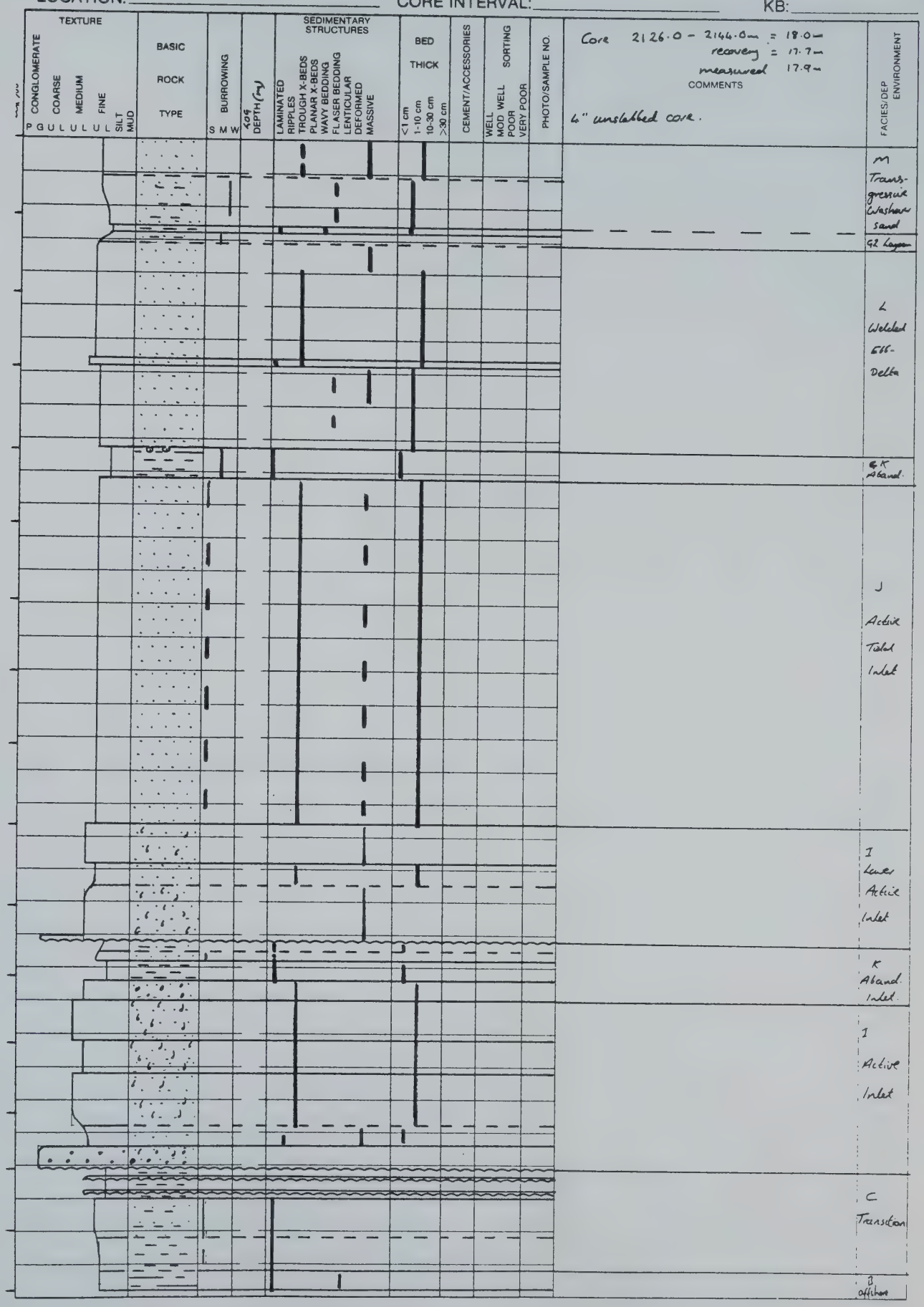

WELL NAME: Total et al Wembley FORMATION: DATE:

LOCATION: 7-5-73-8-W6 CORE INTERVAL: KB:

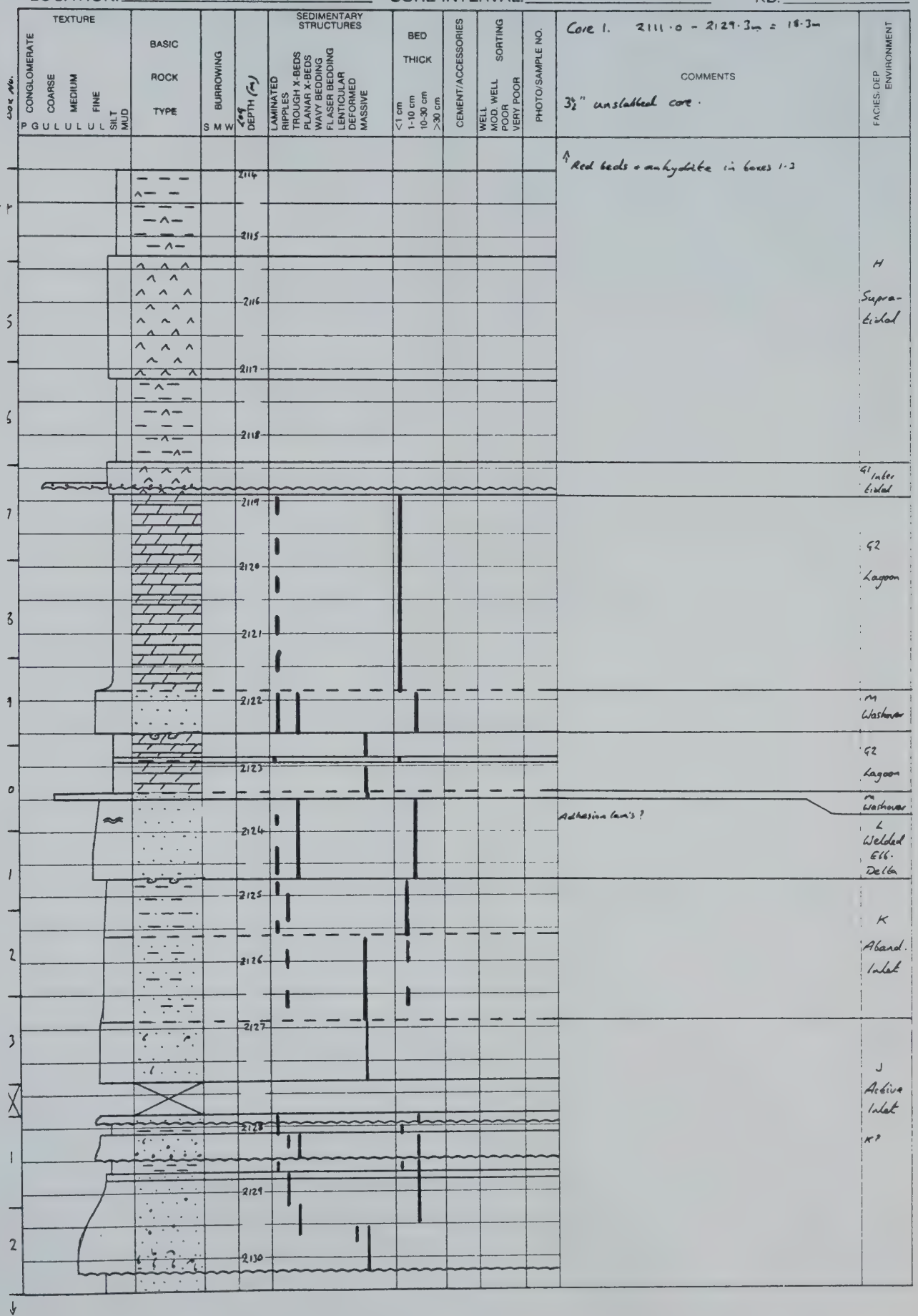

WELL NAME: _____ FORMATION: _____ DATE: _____

LOCATION: 7-5-73-8-W6 (2/2) CORE INTERVAL: _____ KB: _____

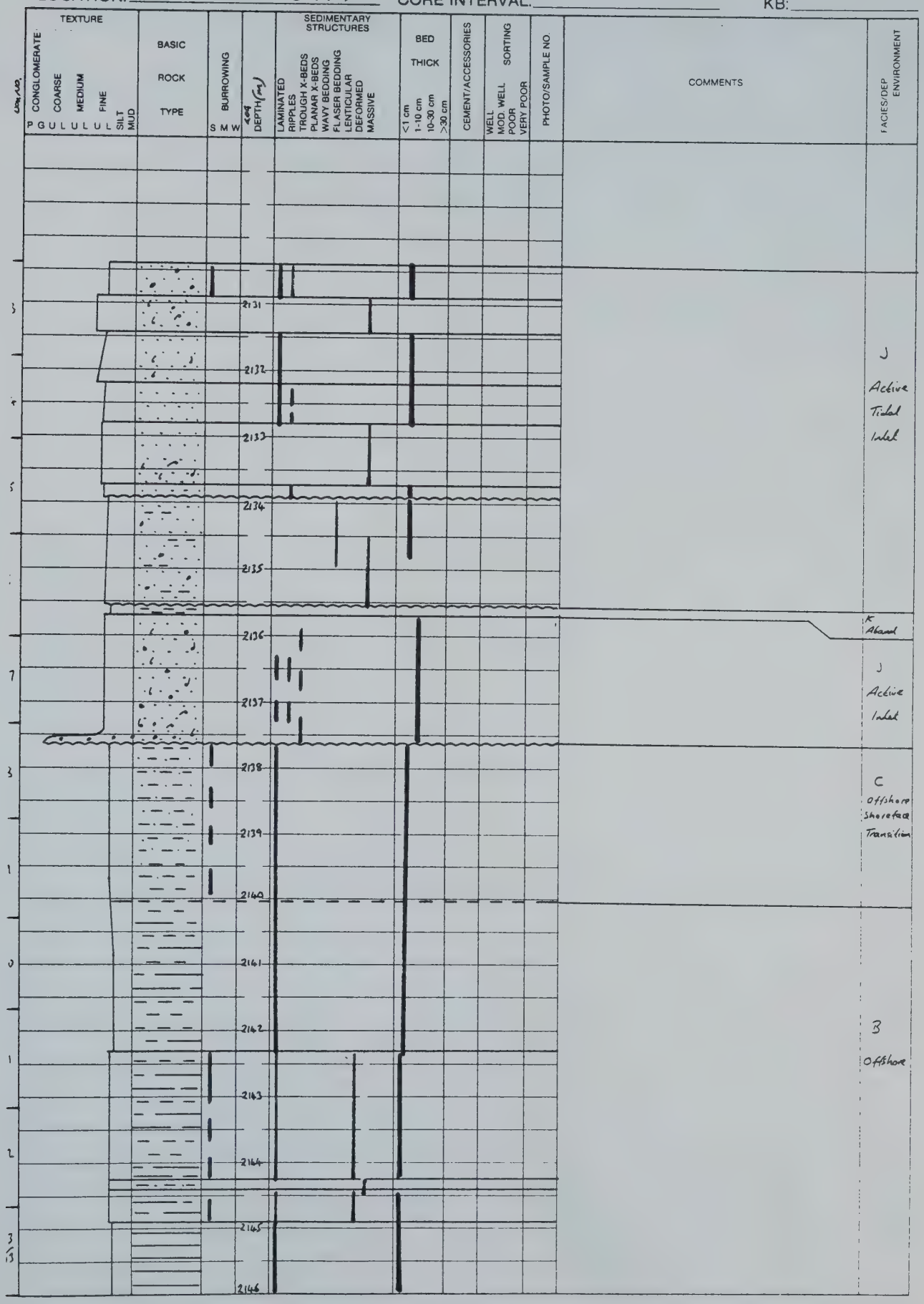

WELL NAME: Total et al Wembley FORMATION: DATE:

LOCATION: 16-5-73-8-W6 CORE INTERVAL: KB:

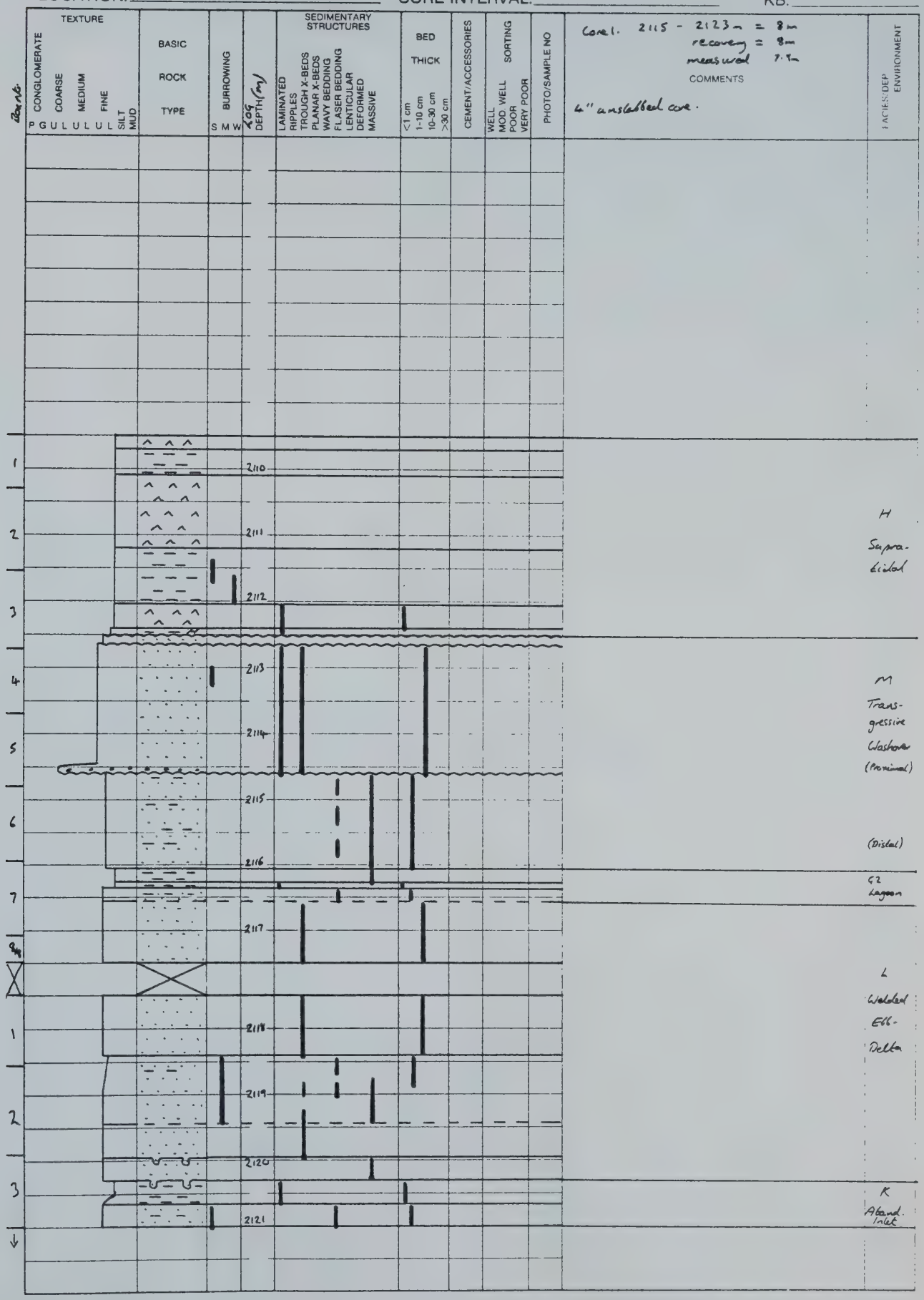

WELL NAME: _____ FORMATION: _____ DATE: _____

LOCATION: 16-5-73-8-W6 (2/2) CORE INTERVAL: _____ KB: _____

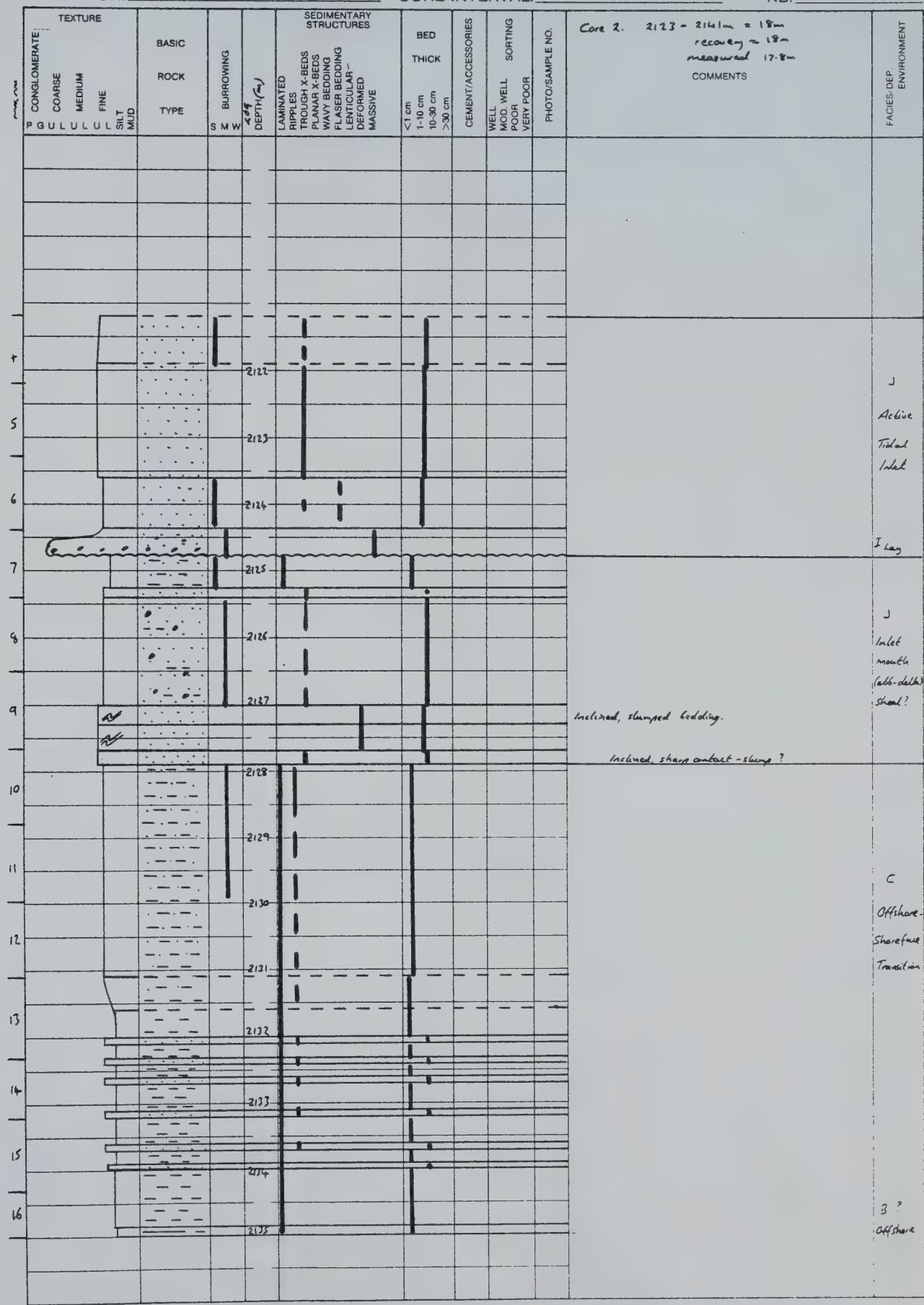

WELL NAME: Total et al Wembley FORMATION: DATE:

LOCATION: 8-6-73-8-W6 CORE INTERVAL: KB:

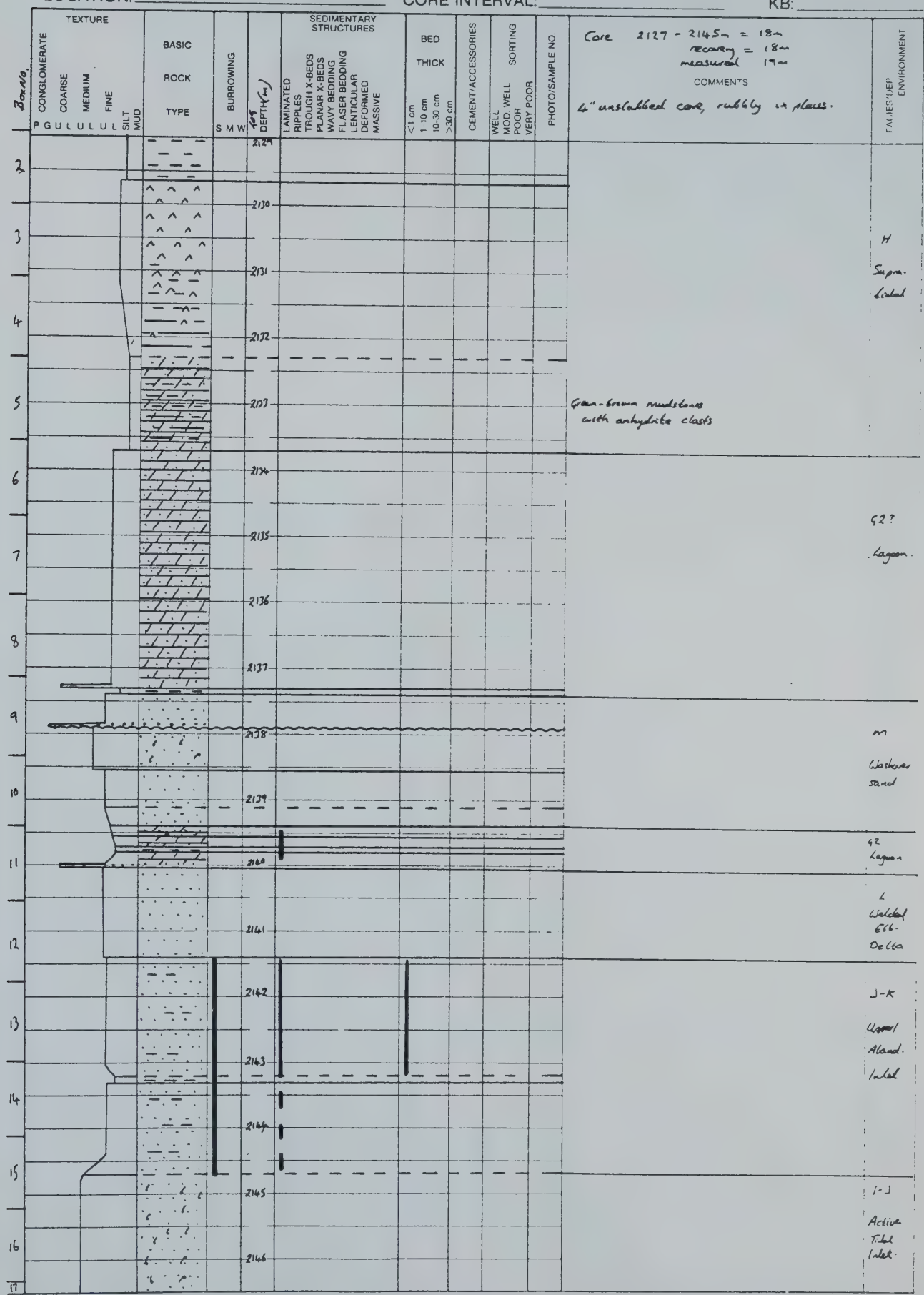

WELL NAME: Total et al Wembley FORMATION: DATE:

LOCATION: 14-6-73-8-W6 CORE INTERVAL: KB:

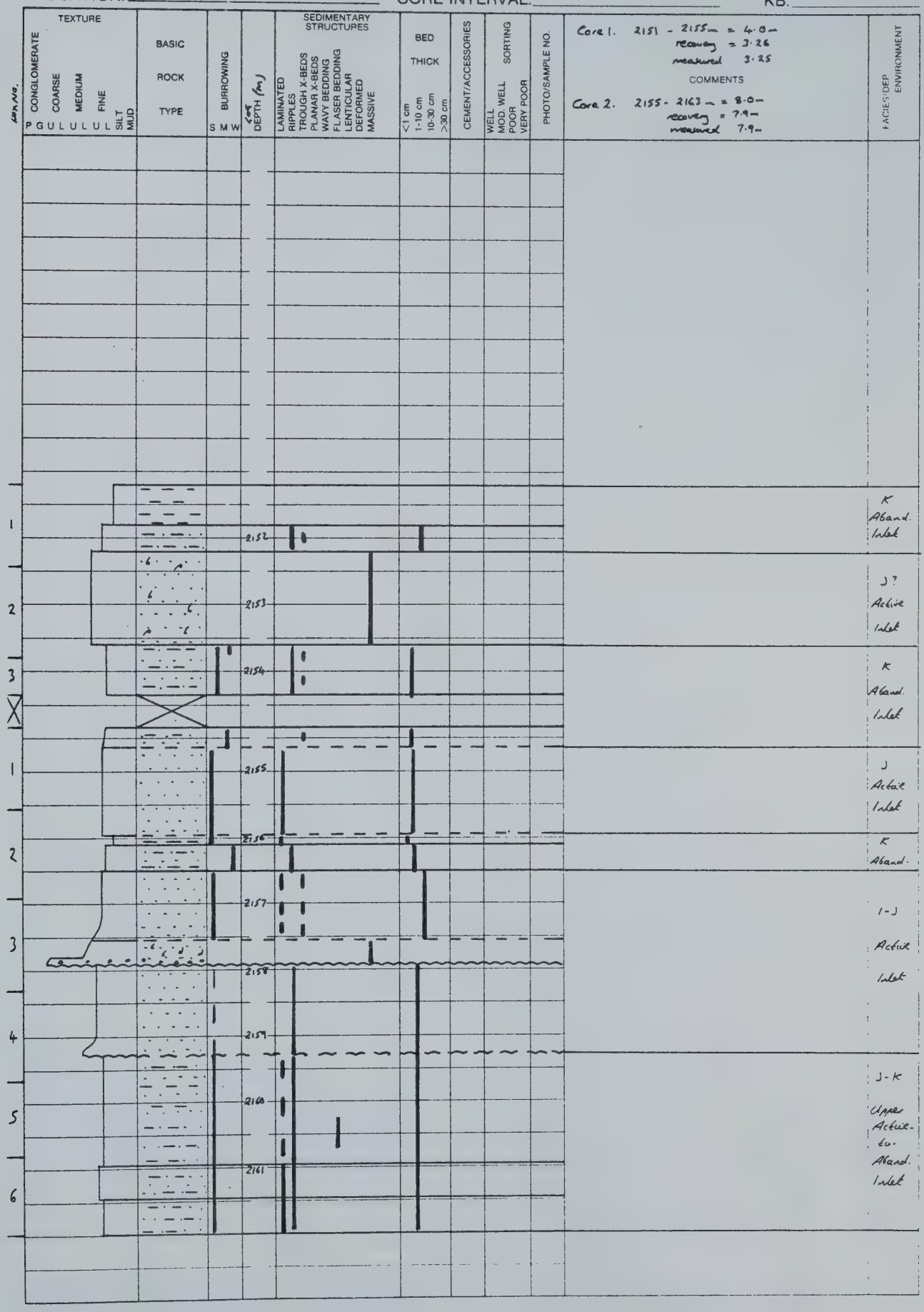

WELL NAME: Total et al Wembley FORMATION: DATE:

LOCATION: 5-8-73-8-W6 CORE INTERVAL: KB:

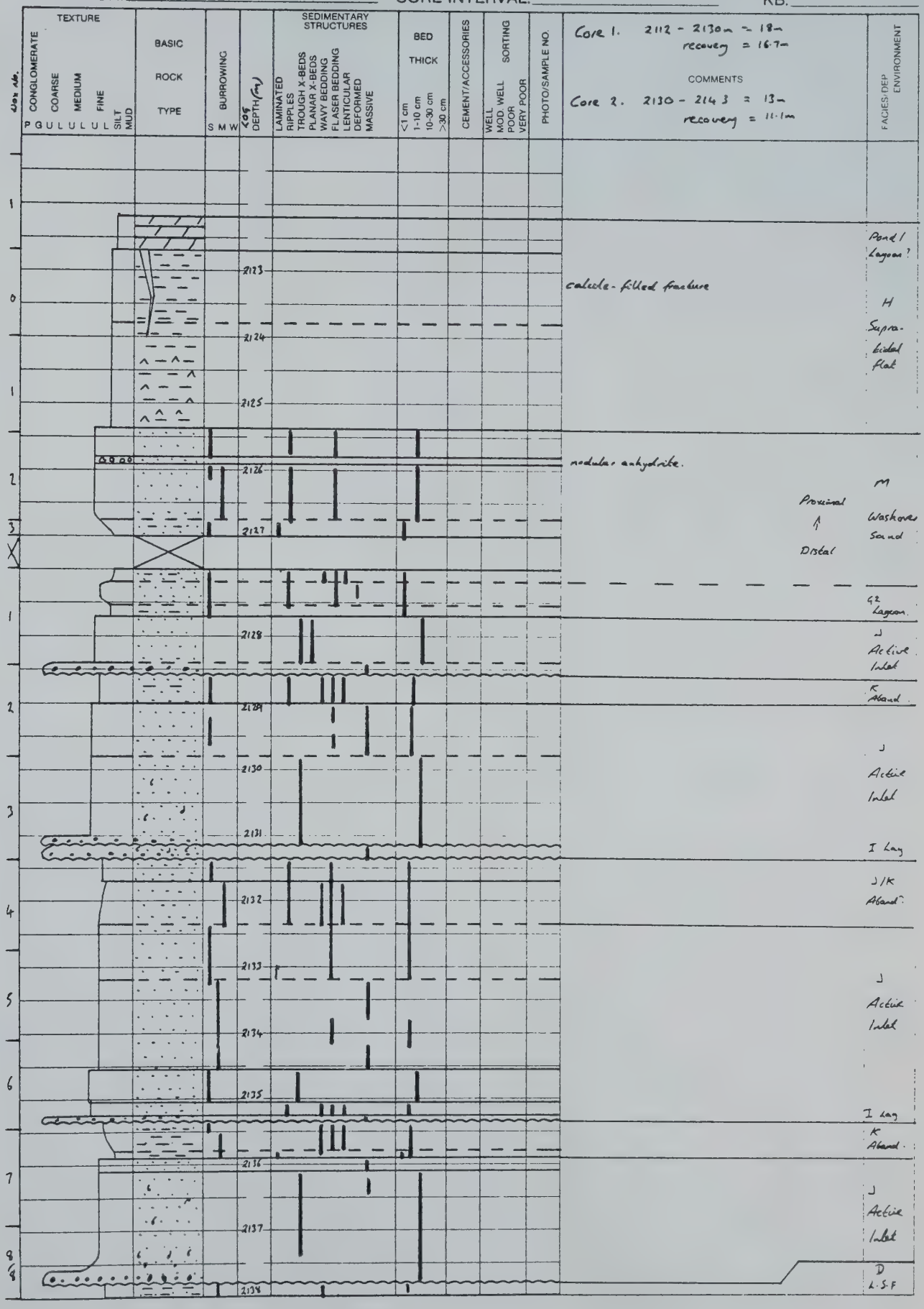

WELL NAME: Total et al Wembley 8-8-73-8-W6 FORMATION: DATE:

LOCATION: CORE INTERVAL: KB:

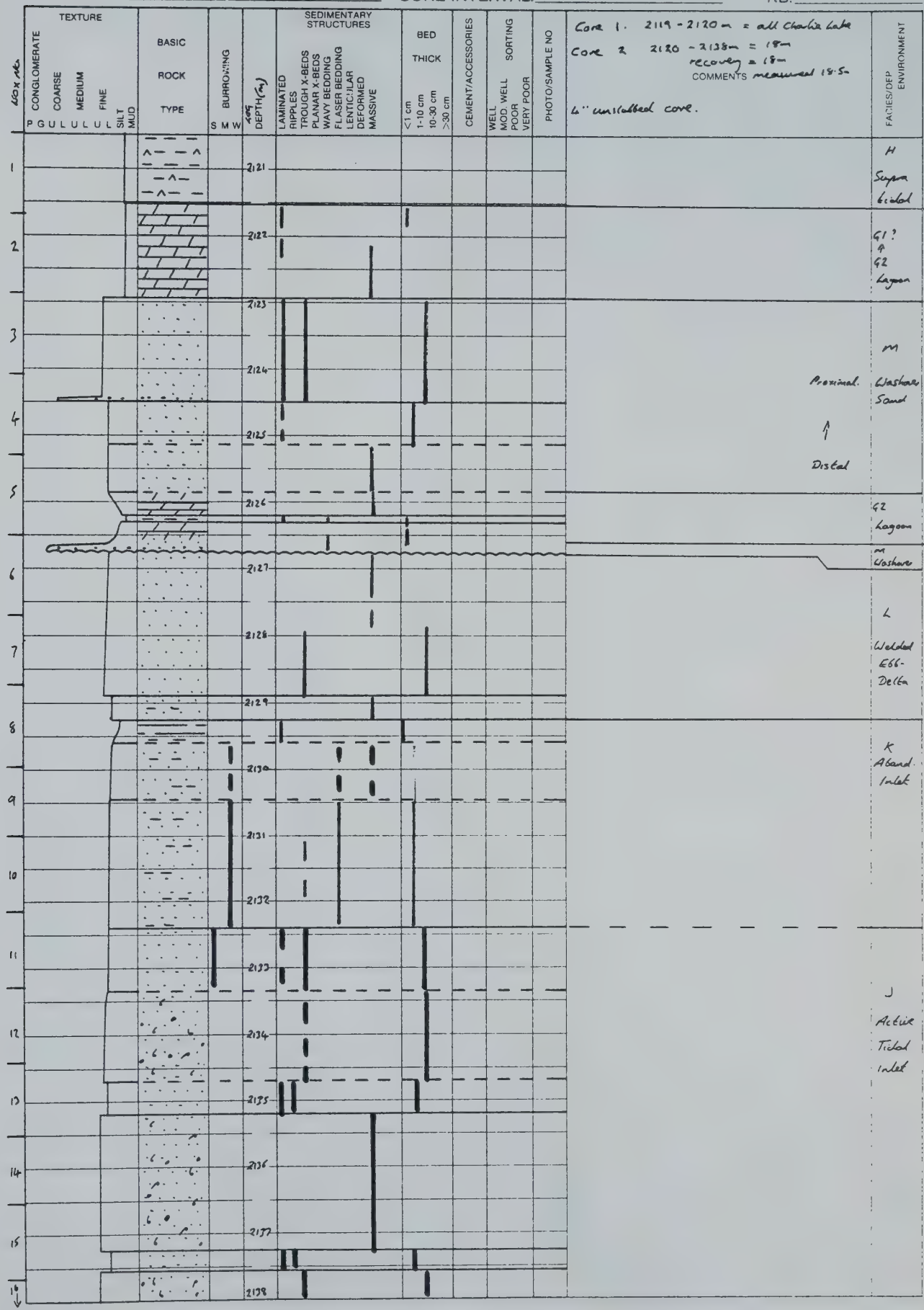

WELL NAME: Total et al Wembley 14-8-73-8-W6 FORMATION: DATE:

LOCATION: CORE INTERVAL: KB:

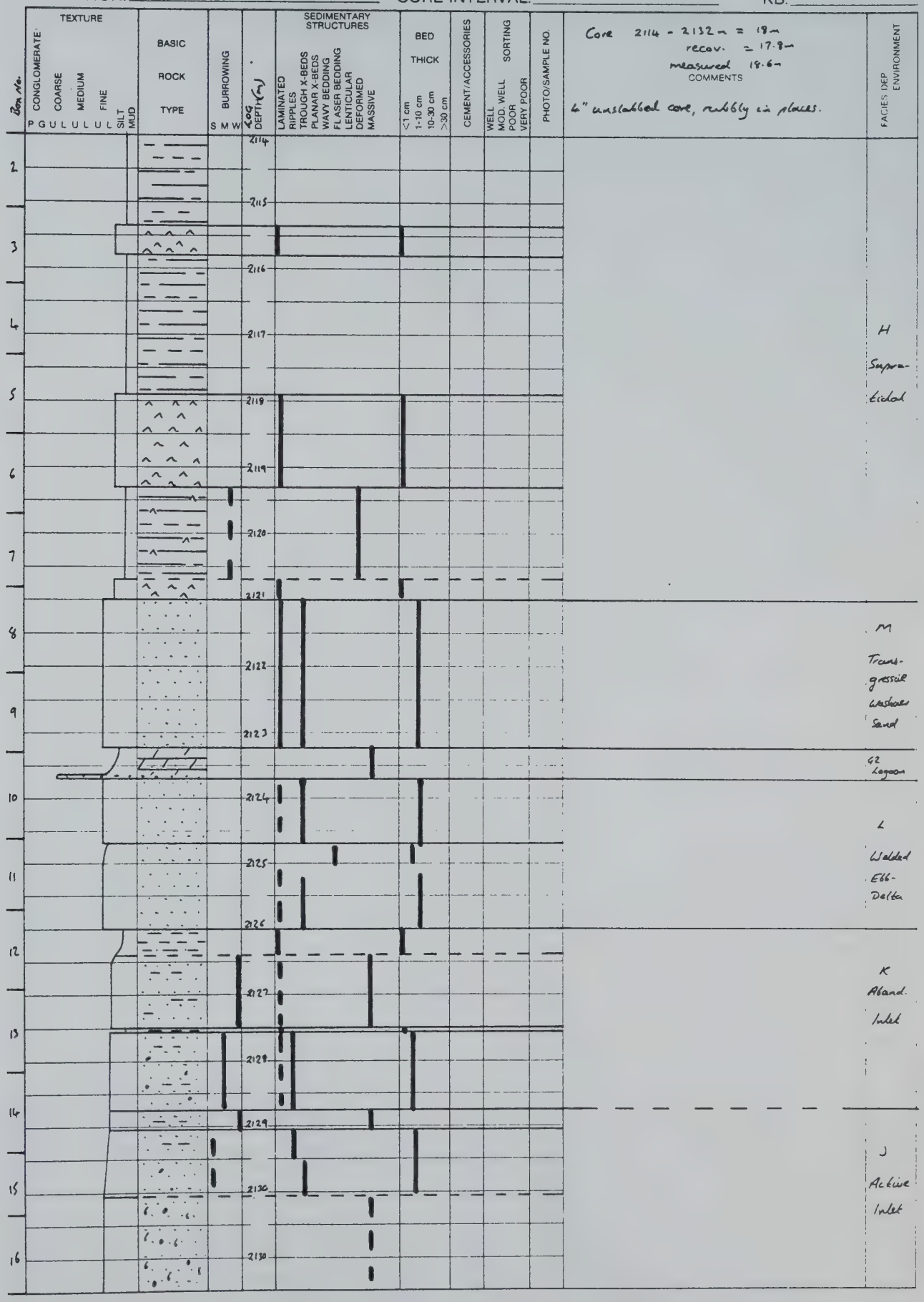

WELL NAME: Total et al Wembley 16-8-73-8-W6 FORMATION: DATE:

LOCATION: CORE INTERVAL: KB:

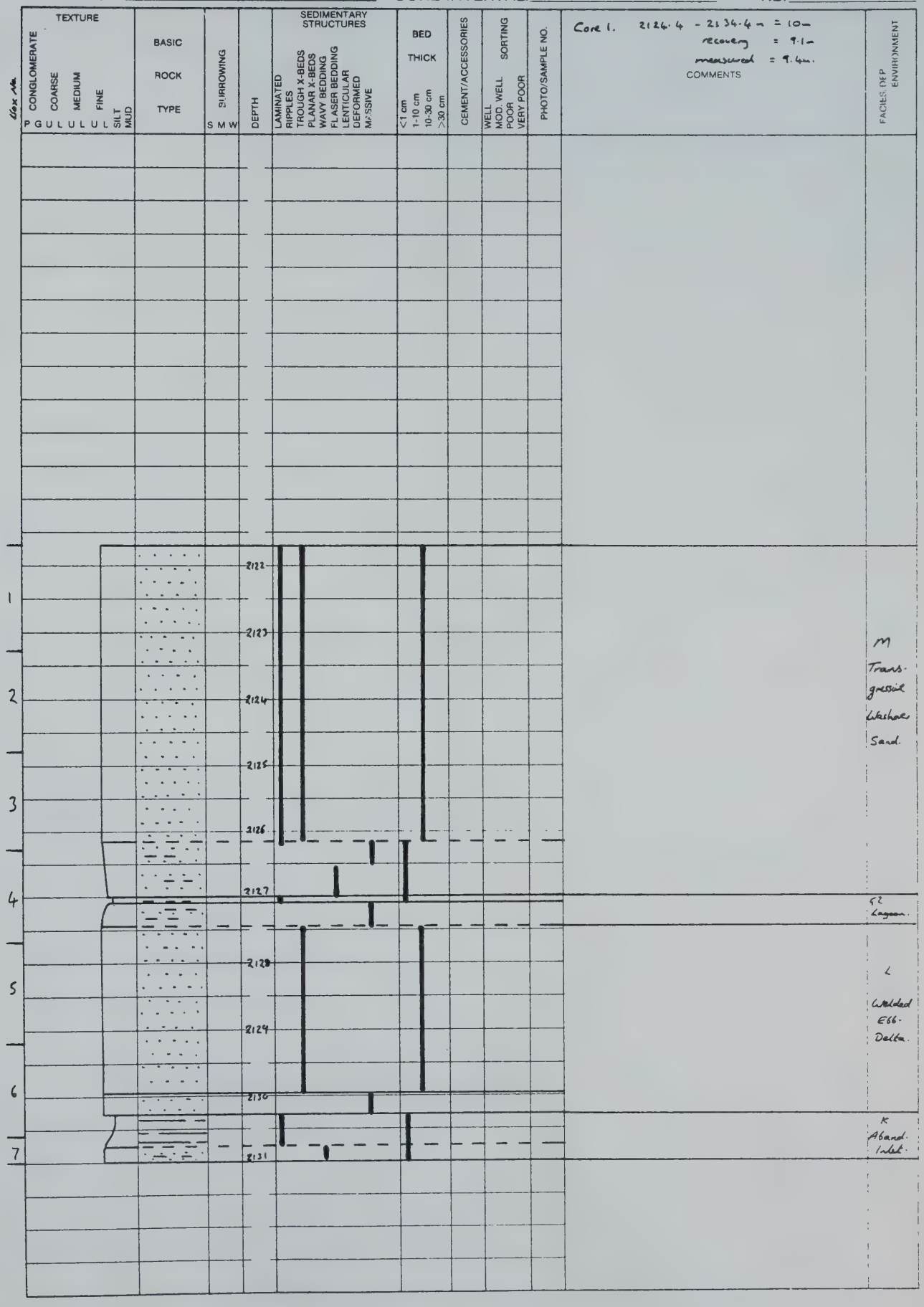

WELL NAME: _____ FORMATION: _____ DATE: _____

LOCATION: 16-8-73-8-W6 (2/2) CORE INTERVAL: _____ KB: _____

TEXTURE (CONGLOMERATE, COARSE, MEDIUM, FINE, SILT, MUD; P G U L U L U L)	BASIC ROCK TYPE	BURROWING (S M W)	log DEPTH (m)	SEDIMENTARY STRUCTURES (LAMINATED, RIPPLES, TROUGH X-BEDS, PLANAR X-BEDS, WAVY BEDDING, FLASER BEDDING, LENTICULAR, DEFORMED, MASSIVE)	BED THICK (<1 cm, 1-10 cm, 10-30 cm, >30 cm)	CEMENT/ACCESSORIES	SORTING (WELL, MOD. WELL, POOR, VERY POOR)	PHOTO/SAMPLE NO.	Core 2. 2134.4 - 2143m = 8.6m recovery = 8.6m measured 8.8m. COMMENTS	FACIES DEP ENVIRONMENT

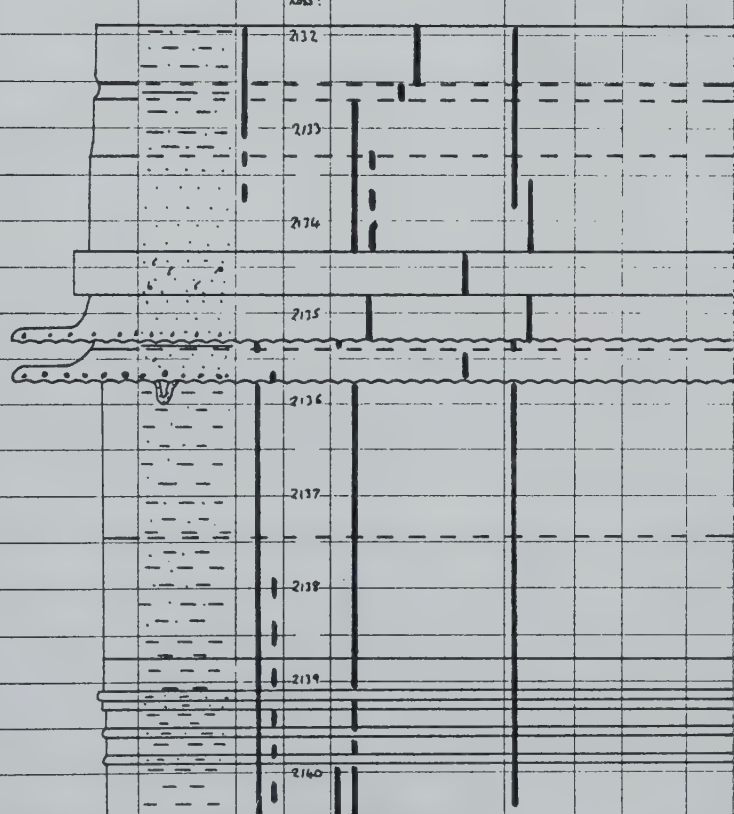

J-K Upper 1 Aband. Inlet

I-J Active Tidal Inlet.

C Offshore Shoreface Transition

WELL NAME: Total et al Wembley 6-9-73-8-W6 FORMATION: DATE:

LOCATION: CORE INTERVAL: KB:

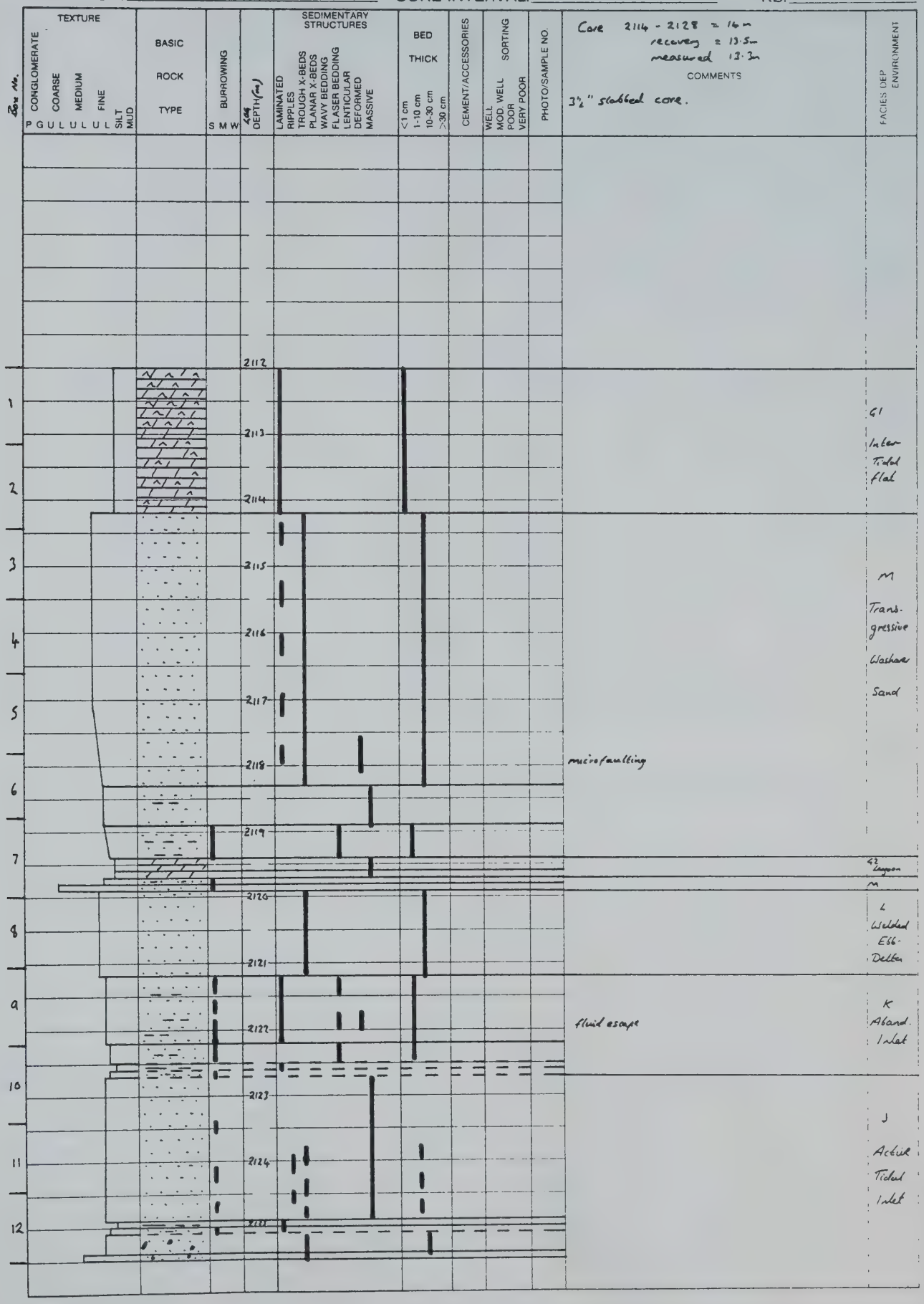

WELL NAME: Total et al Wembley FORMATION: DATE:

LOCATION: 7-9-73-8-W6 CORE INTERVAL: KB:

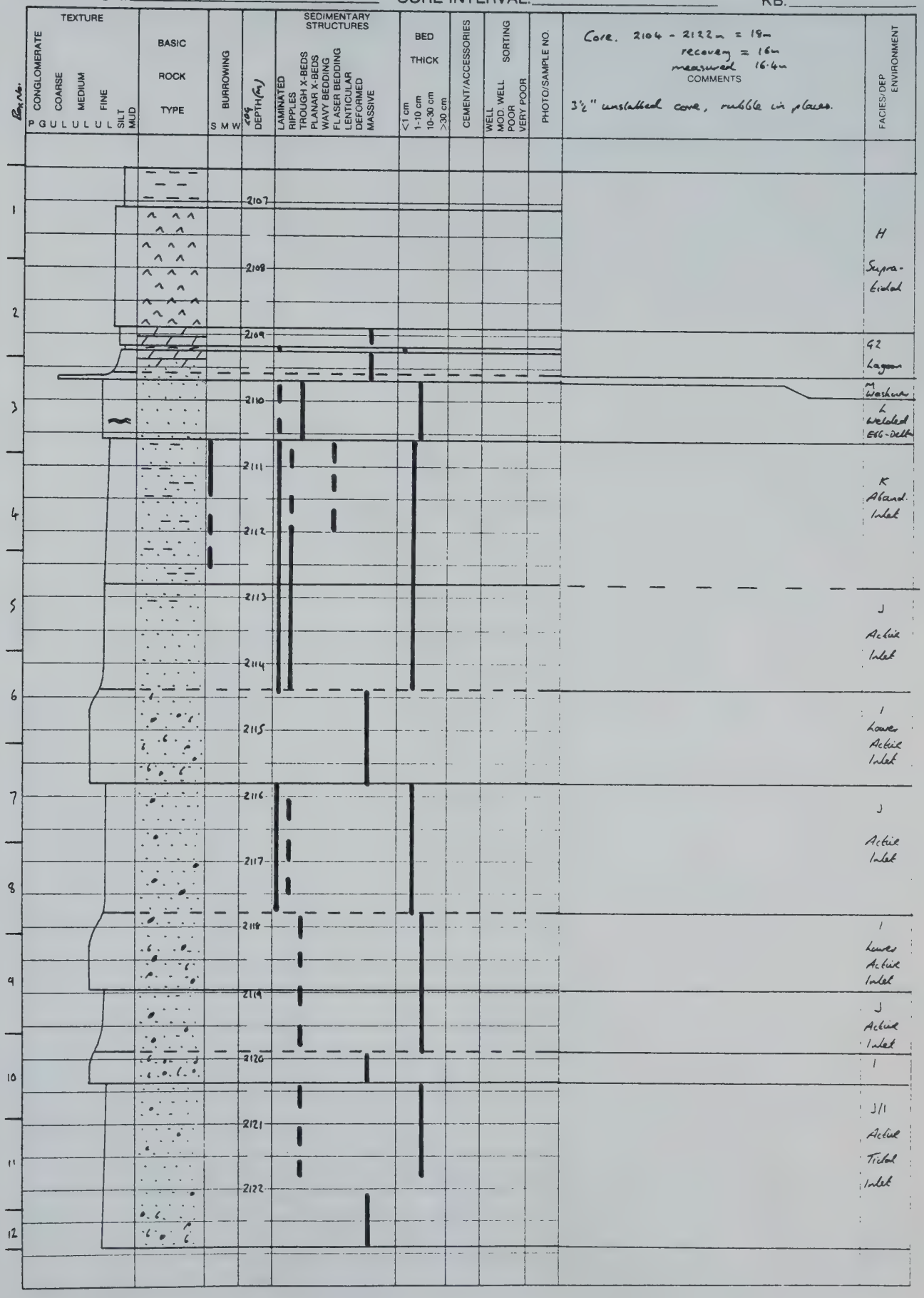

WELL NAME: Total et al Wembley FORMATION: DATE:

LOCATION: 1-10-73-8-W6 CORE INTERVAL: KB:

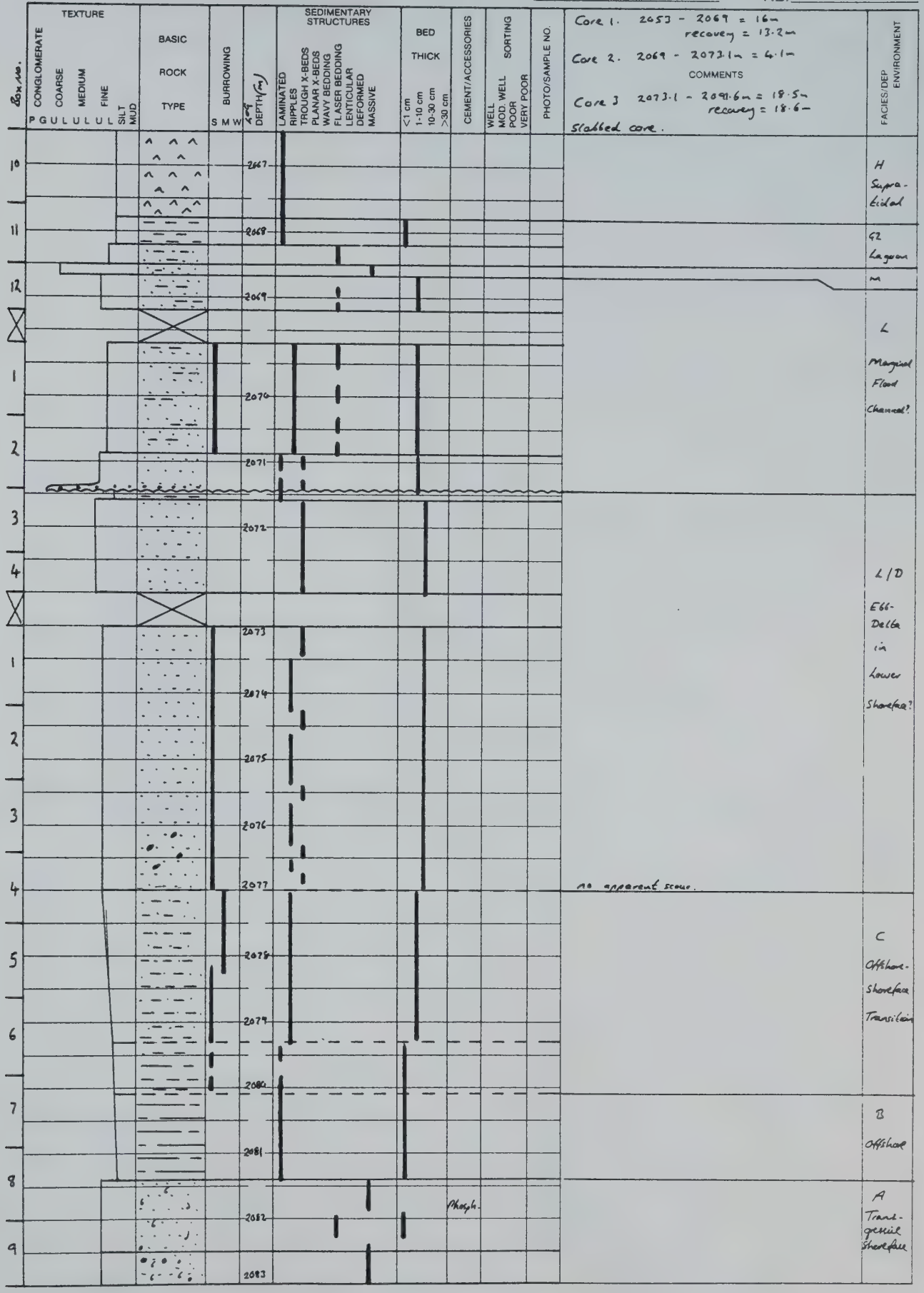

WELL NAME: Total et al Wembley 6-10-73-8-W6 FORMATION: DATE:

LOCATION: CORE INTERVAL: KB:

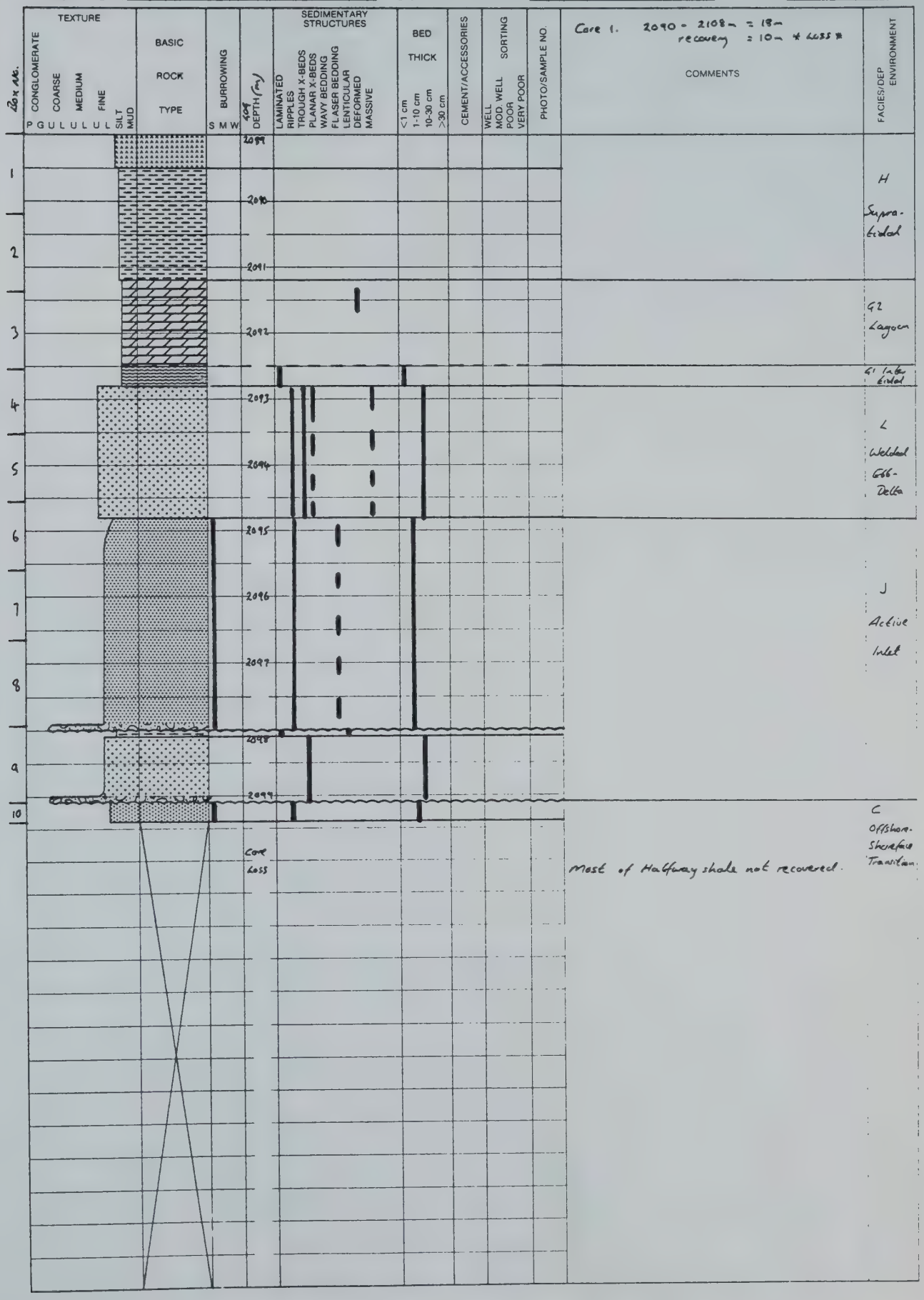

WELL NAME: _____ FORMATION: _____ DATE: _____

LOCATION: 6-10-73-8-W6 (2/2) CORE INTERVAL: _____ KB: _____

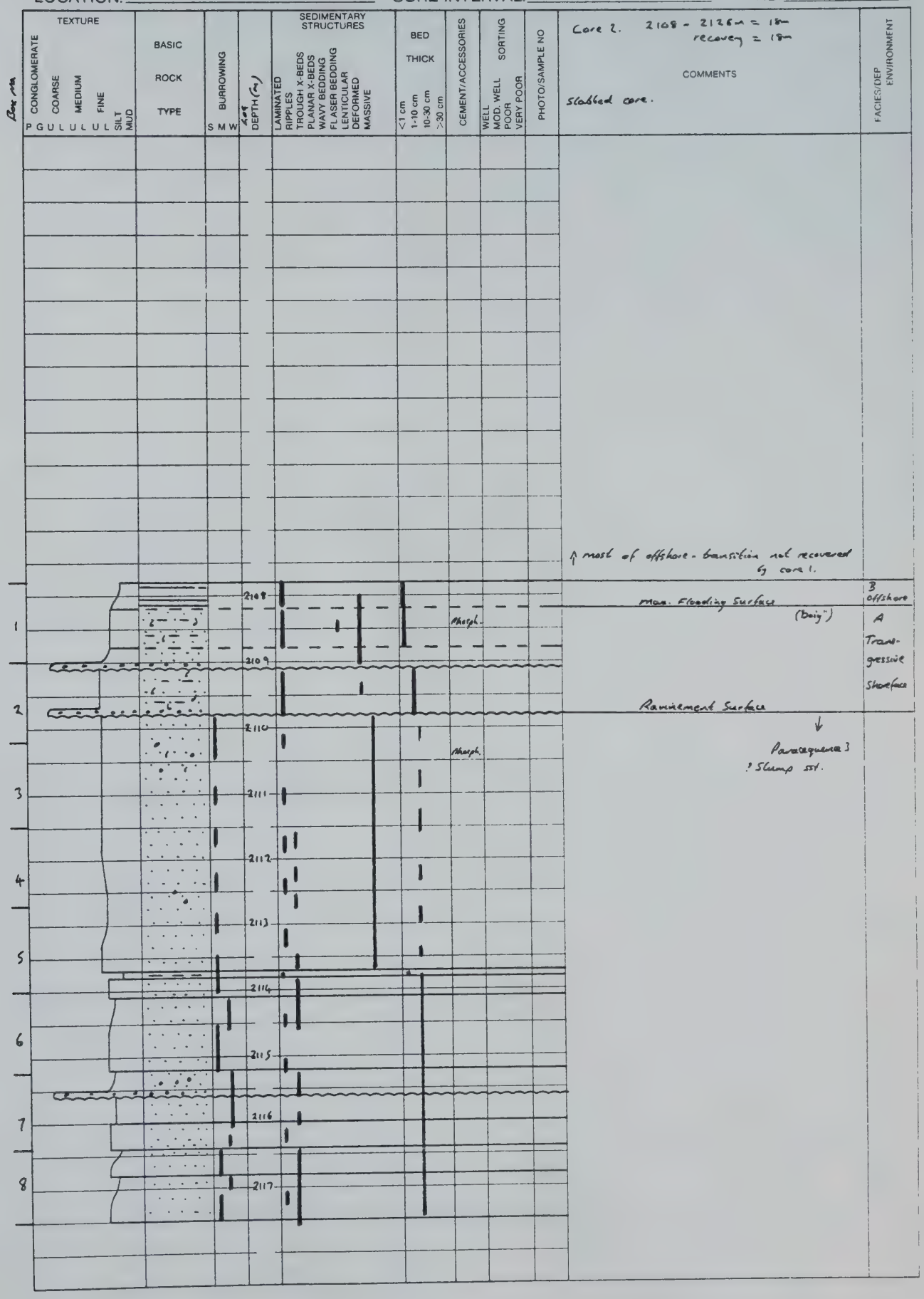

WELL NAME: PCP Esso Beaverlodge FORMATION: DATE:

LOCATION: 6-11-73-8-W6 CORE INTERVAL: KB:

Core 2015 - 2028.4 m = 13.4 m
recovery = 11.5 m
measured 11.5 m

3½" unslabbed core.

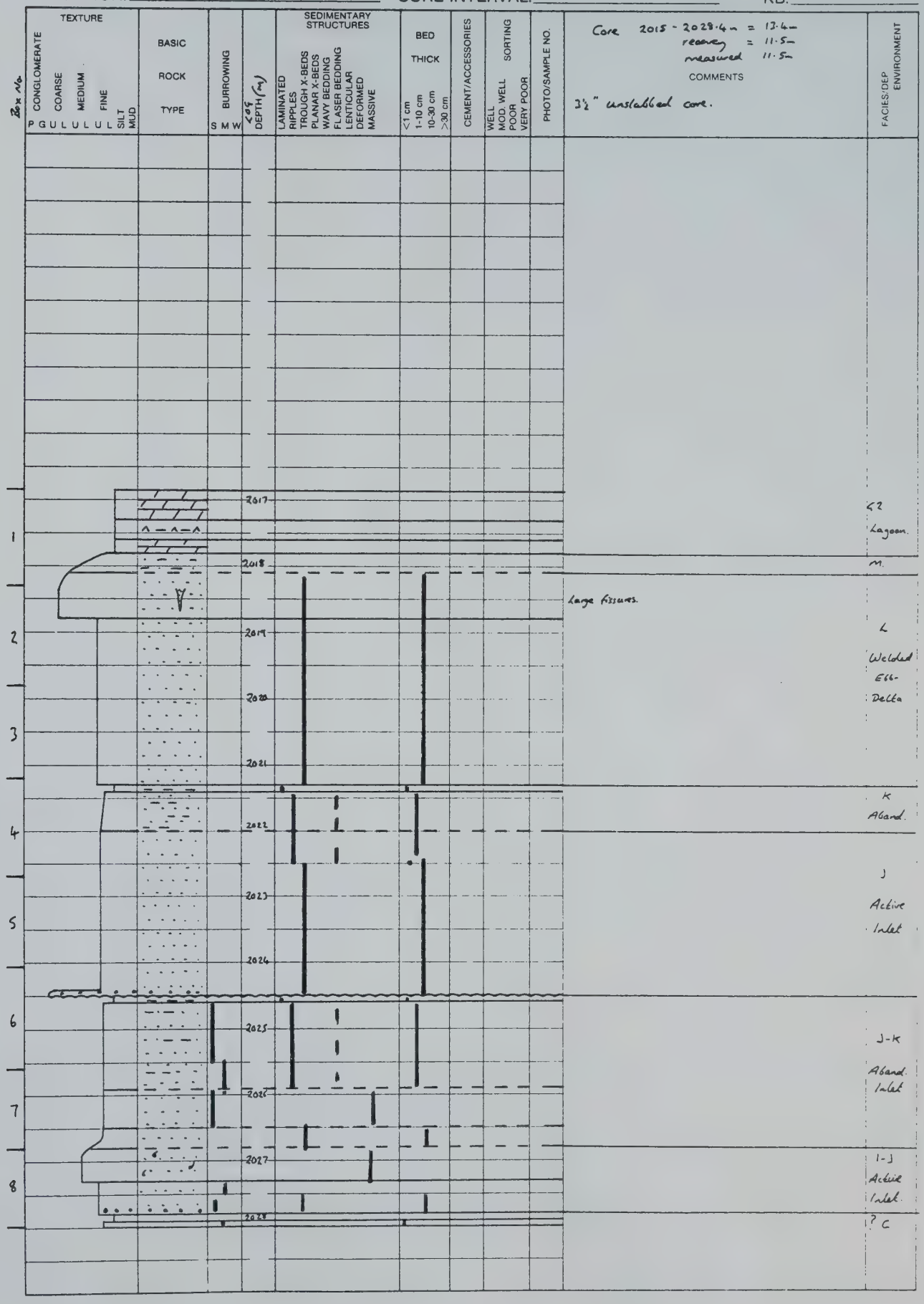

WELL NAME: PCP Esso Wembley FORMATION: DATE:

LOCATION: 6-12-73-8-W6 CORE INTERVAL: KB:

Box no.	TEXTURE (CONGLOMERATE, COARSE, MEDIUM, FINE, SILT, MUD)	BASIC ROCK TYPE	BURROWING (S M W)	DEPTH (m)	SEDIMENTARY STRUCTURES (LAMINATED, RIPPLES, TROUGH X-BEDS, PLANAR X-BEDS, WAVY BEDDING, FLASER BEDDING, LENTICULAR, DEFORMED, MASSIVE)	BED THICK (<1 cm, 1-10 cm, 10-30 cm, >30 cm)	CEMENT/ACCESSORIES	SORTING (WELL, MOD. WELL, POOR, VERY POOR)	PHOTO/SAMPLE NO.	COMMENTS	FACIES DEP ENVIRONMENT
										Core 2002.1 - 2020.2m = 18.1m recovery = 18.1m measured 18.1m 4" slabbed core.	
1				2003							L Welded Ell-Delta
2				2004							
3				2005							
4				2006							K Aband. Inlet
				2007							

WELL NAME: _____ FORMATION: _____ DATE: _____

LOCATION: 6-12-73-8-W6 (2/2) CORE INTERVAL: _____ KB: _____

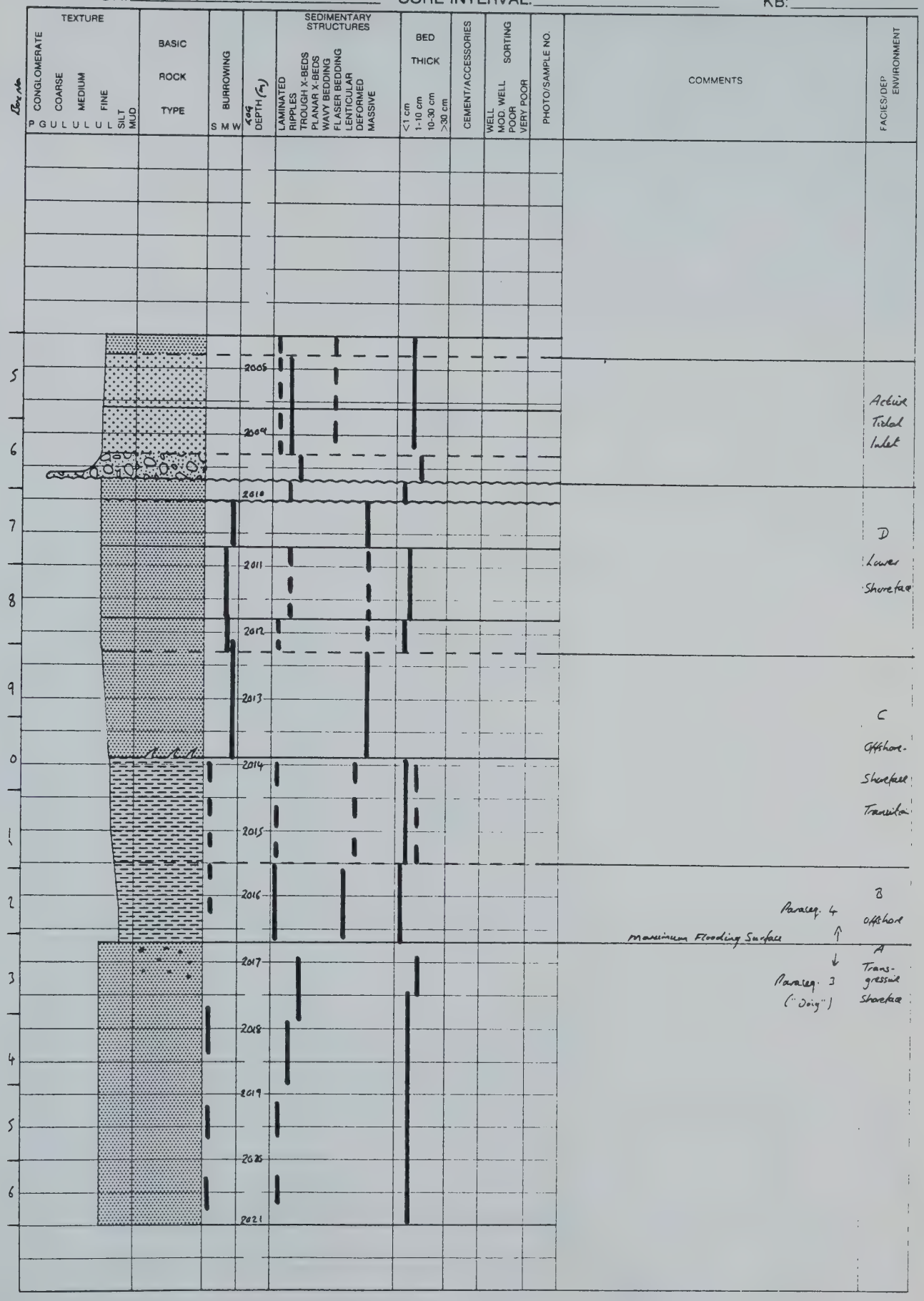

WELL NAME: PCP Esso Wembley 2-14-73-8-W6 FORMATION: DATE:

LOCATION: CORE INTERVAL: KB:

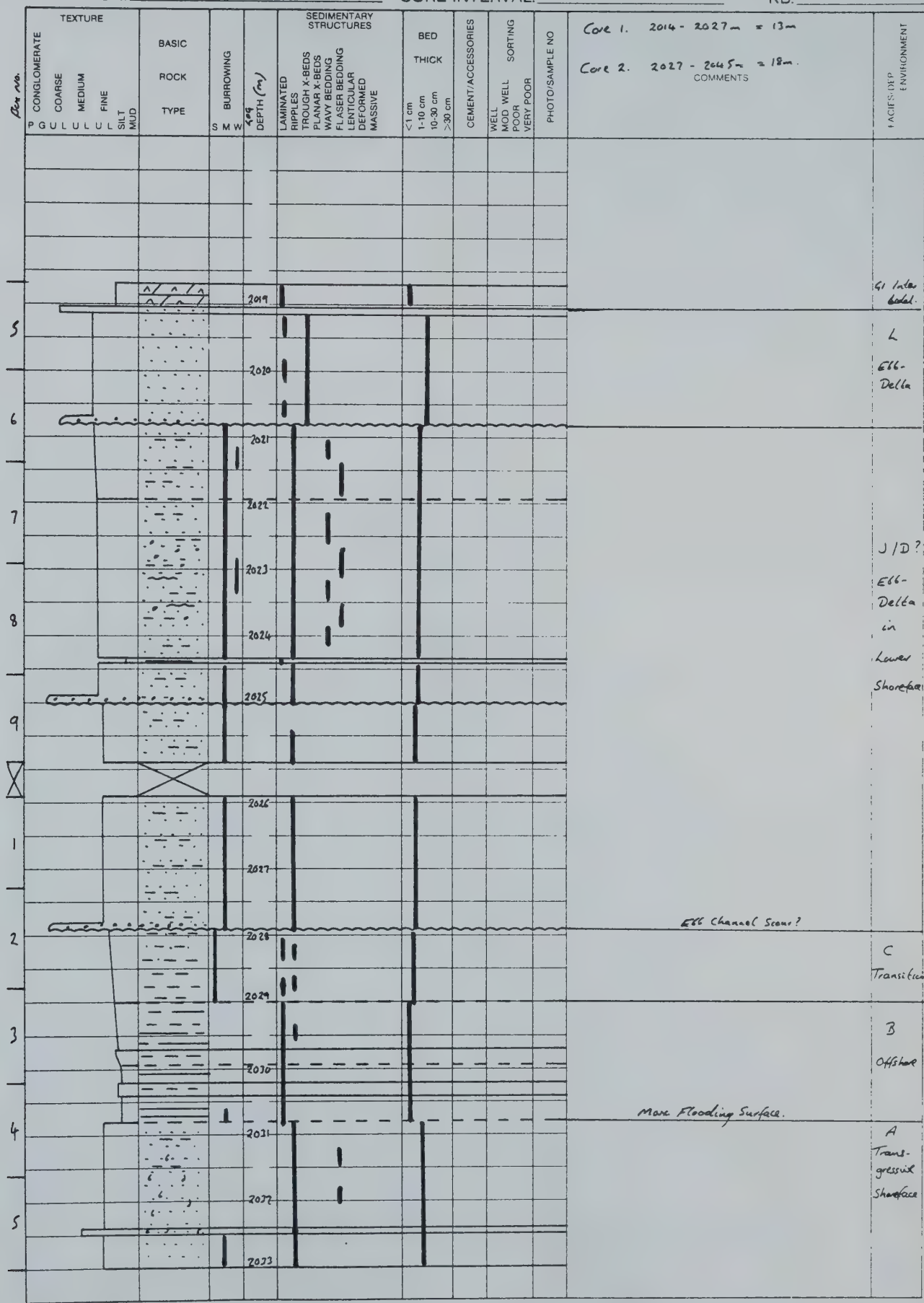

WELL NAME: Dome et al La Glace 7-15-73-8-W6 FORMATION: DATE:

LOCATION: CORE INTERVAL: KB:

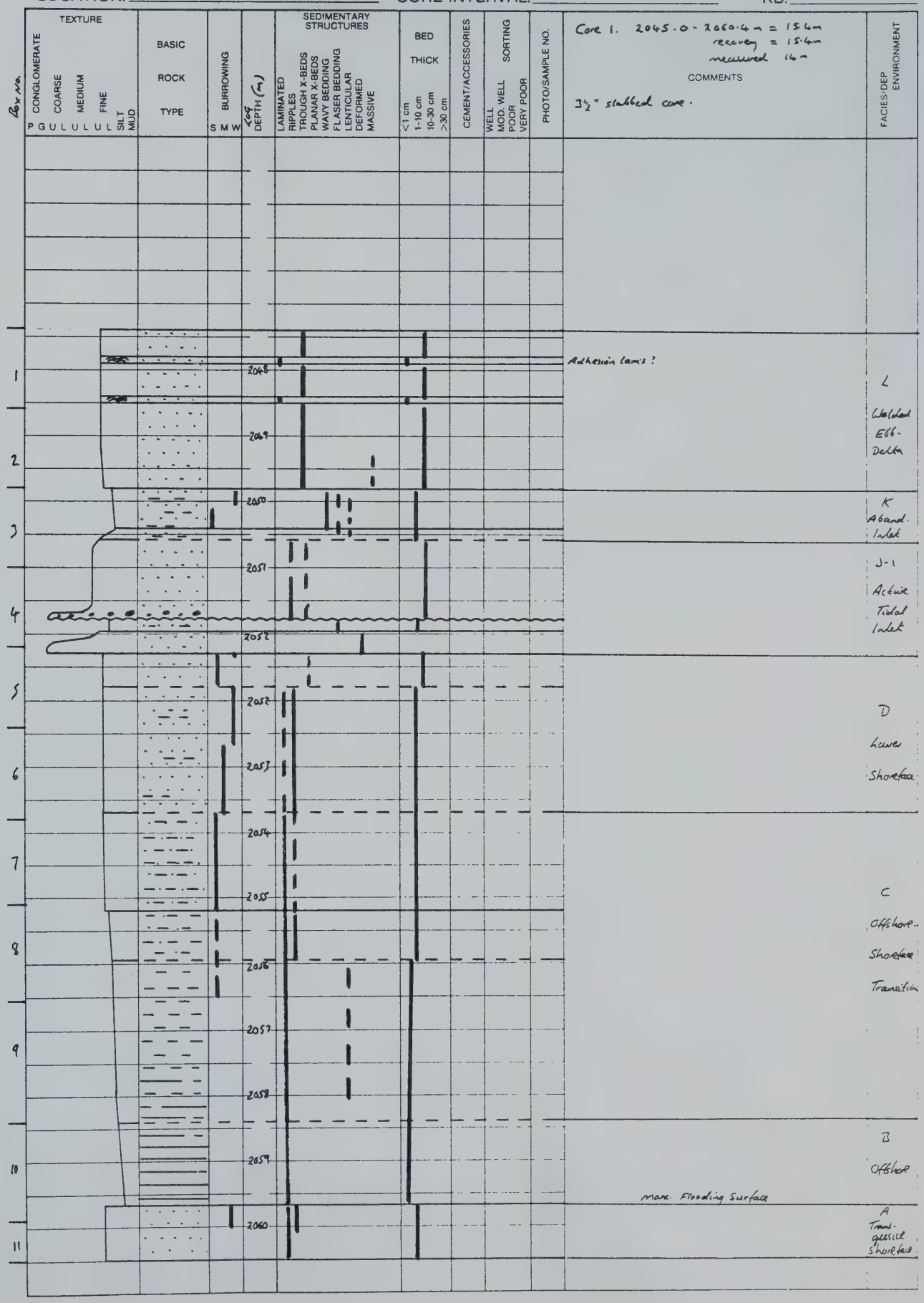

WELL NAME: Dome et al Wembley 6-16-73-8-W6 FORMATION: DATE:

LOCATION: CORE INTERVAL: KB:

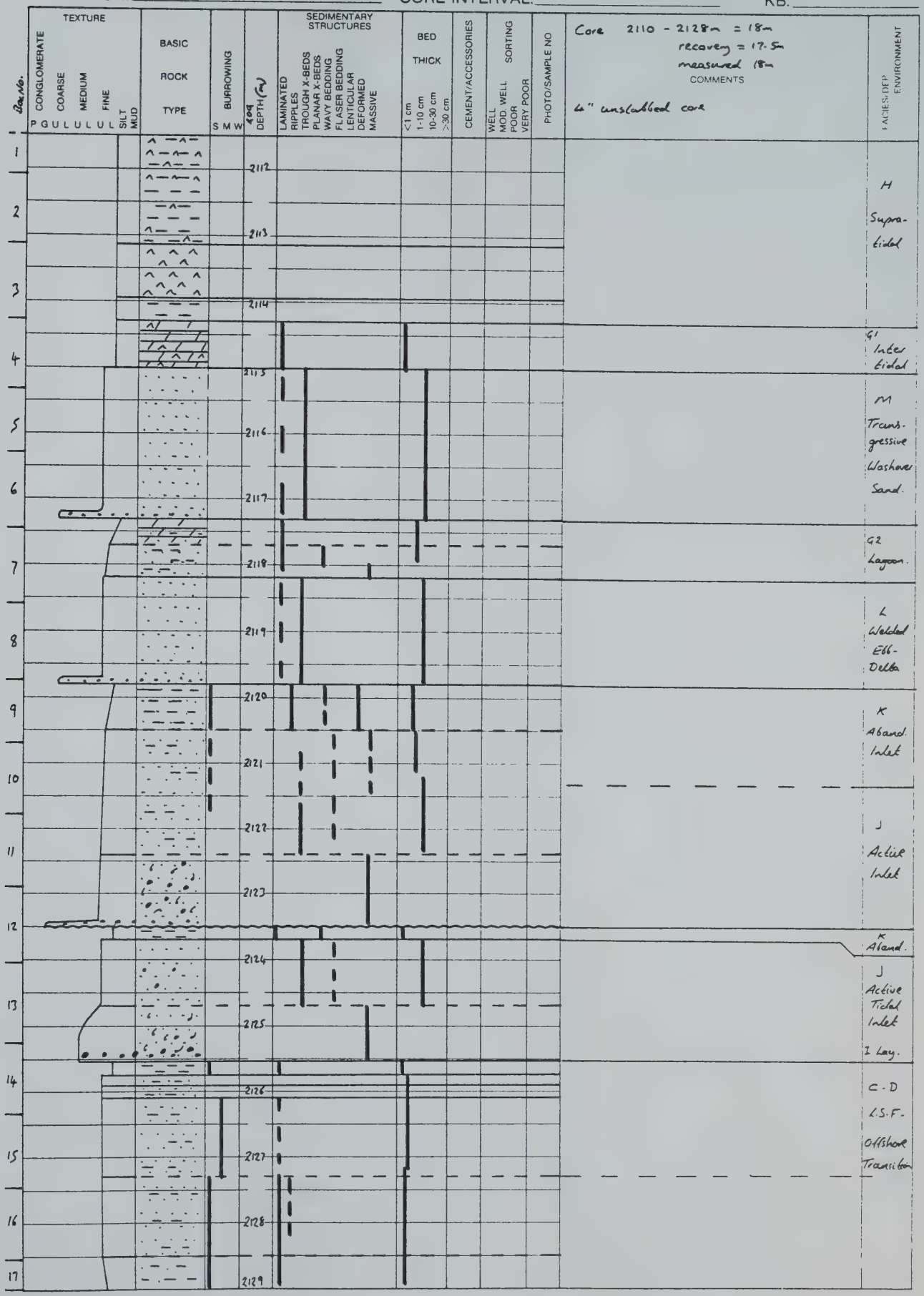

WELL NAME: Dome et al Wembley FORMATION: DATE:

LOCATION: 6-17-73-8-W6 CORE INTERVAL: KB:

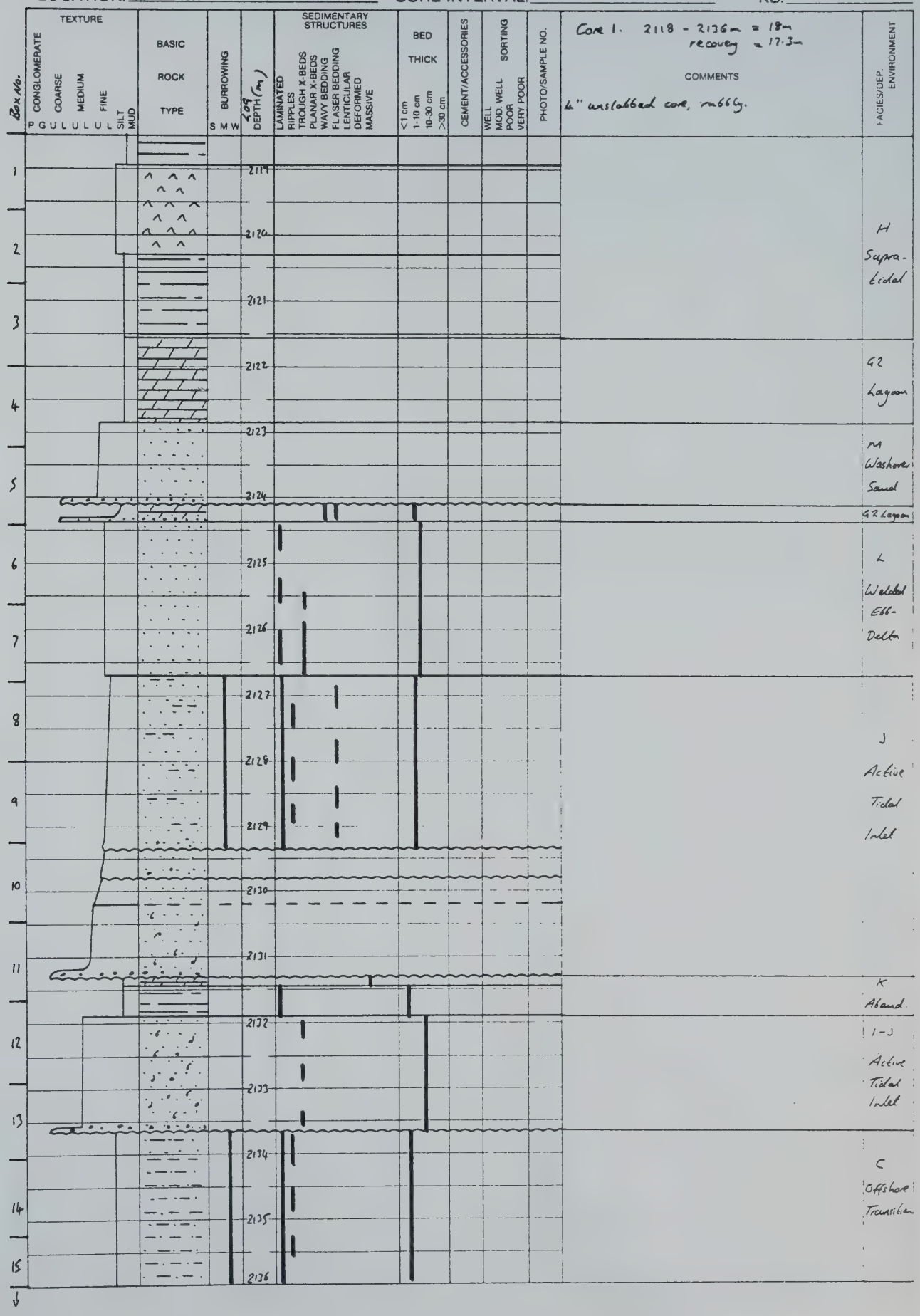

WELL NAME: Dome La Glace FORMATION: DATE:

LOCATION: 9-17-73-8-W6 CORE INTERVAL: KB:

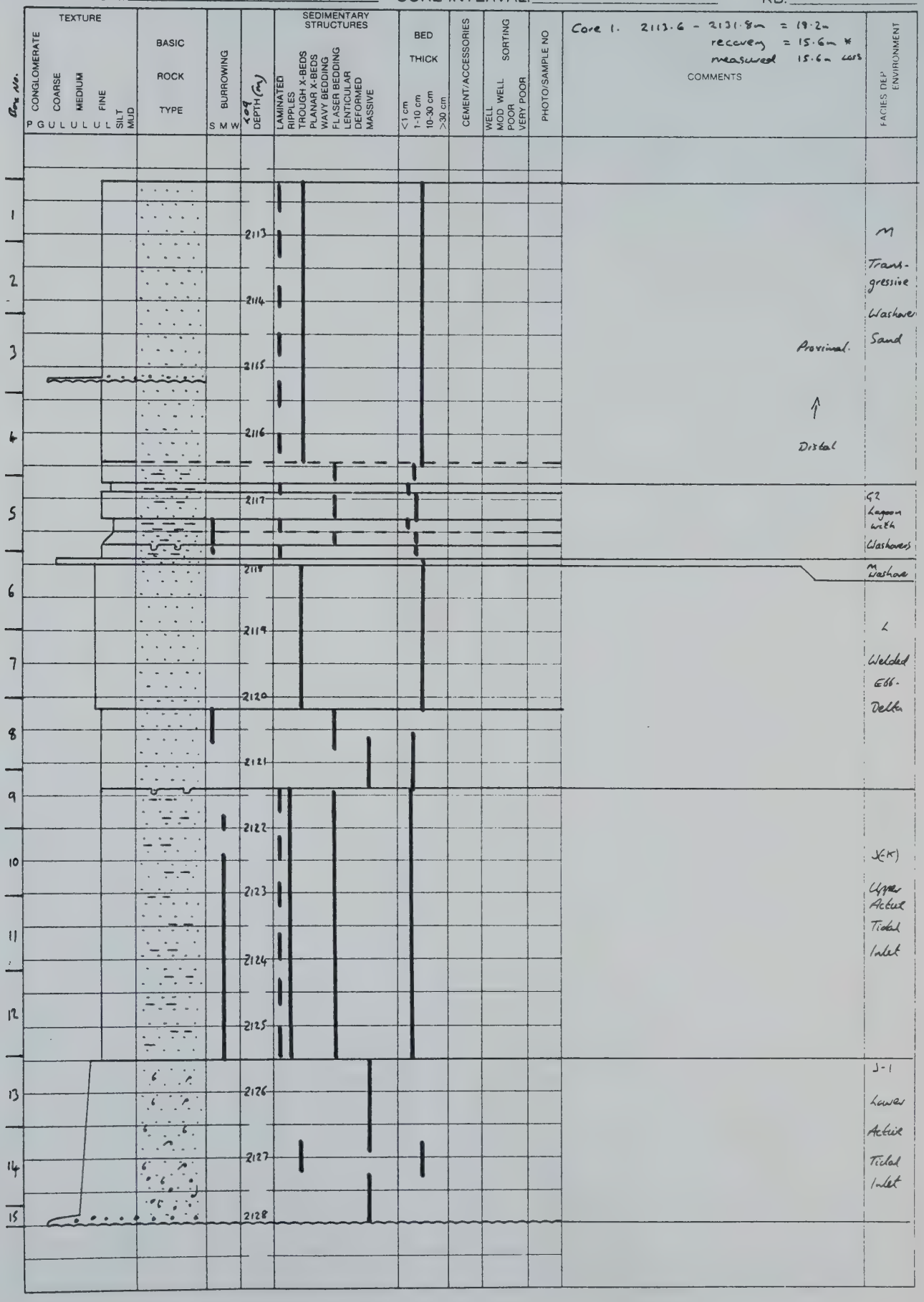

WELL NAME: _____ FORMATION: _____ DATE: _____

LOCATION: 9-17-73-8-W6 (2/2) CORE INTERVAL: _____ KB: _____

Core 2. 2132.0 - 2139.5m = 7.5m
recovery = 7.45m

Box No	TEXTURE: CONGLOMERATE (P G) / COARSE (U L) / MEDIUM (U L) / FINE (U L) / SILT (L) / MUD	BASIC ROCK TYPE	BURROWING (S M W)	Log DEPTH (m)	SEDIMENTARY STRUCTURES: LAMINATED / RIPPLES / TROUGH X-BEDS / PLANAR X-BEDS / WAVY BEDDING / FLASER BEDDING / LENTICULAR / DEFORMED / MASSIVE	BED THICK: <1 cm / 1-10 cm / 10-30 cm / >30 cm	CEMENT/ACCESSORIES	SORTING: WELL / MOD. WELL / POOR / VERY POOR	PHOTO/SAMPLE NO.	COMMENTS	FACIES/DEP ENVIRONMENT
1				2129							C Offshore-Transition
2				2130							
3				2131							
4				2132							B Offshore
5				2133							
6				2134							
				2135							

WELL NAME: Dome et al La Glace FORMATION: DATE:

LOCATION: 11-18-73-8-W6 CORE INTERVAL: KB:

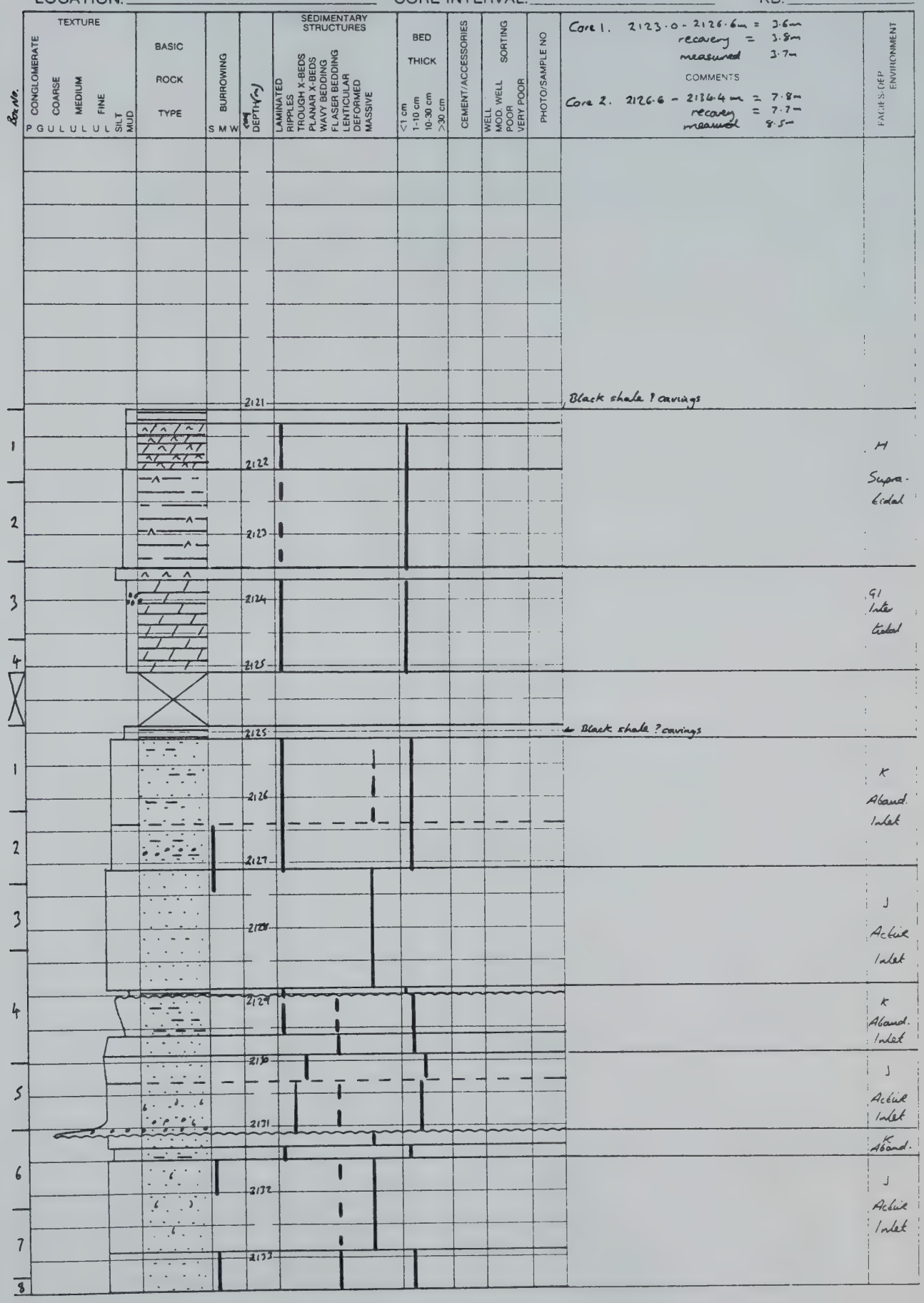

WELL NAME: _____ FORMATION: _____ DATE: _____

LOCATION: 11-18-73-8-W6 (2/2) CORE INTERVAL: _____ KB: _____

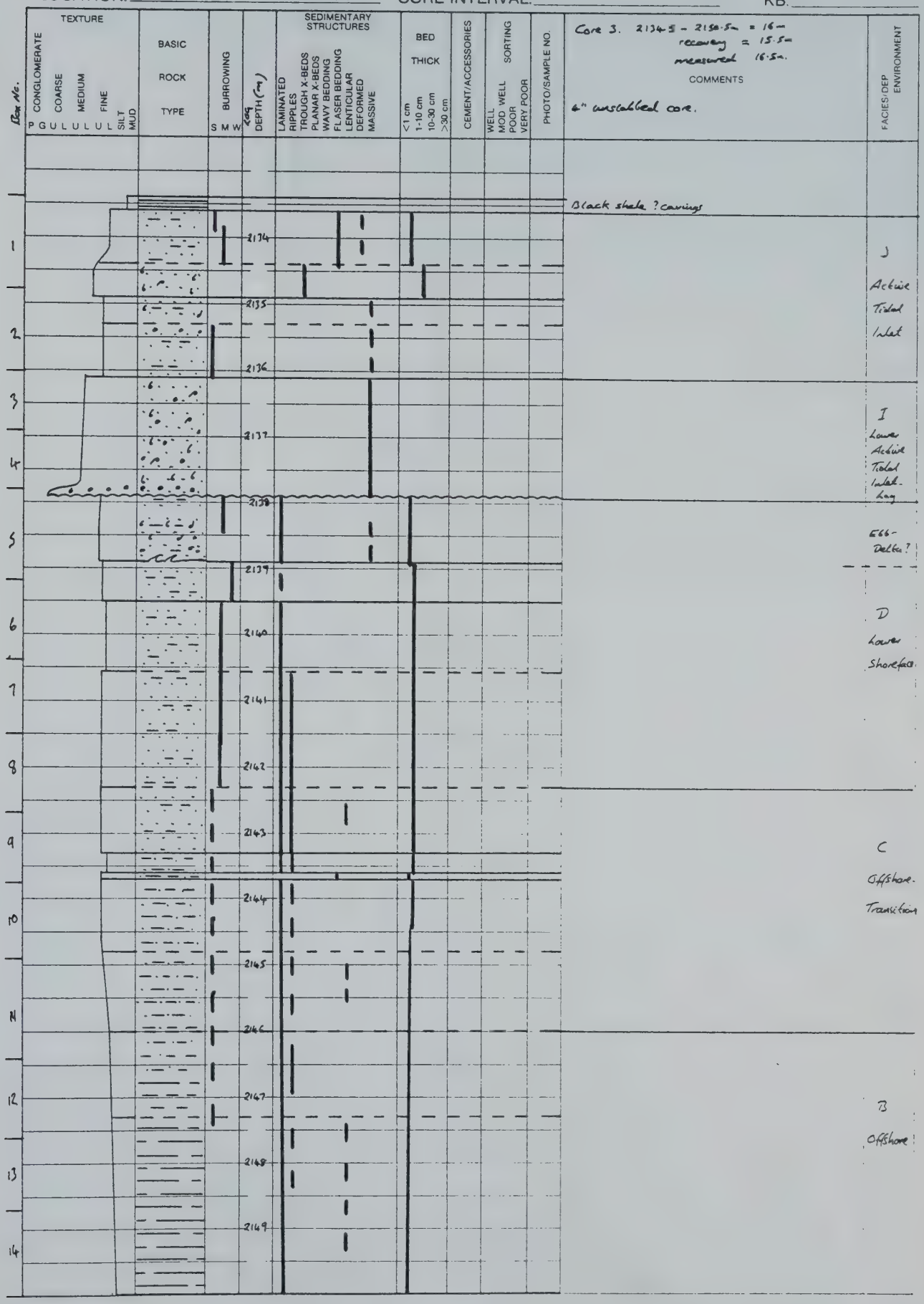

WELL NAME: Dome et al Wembley 8-19-73-8-W6 FORMATION: DATE:

LOCATION: CORE INTERVAL: KB:

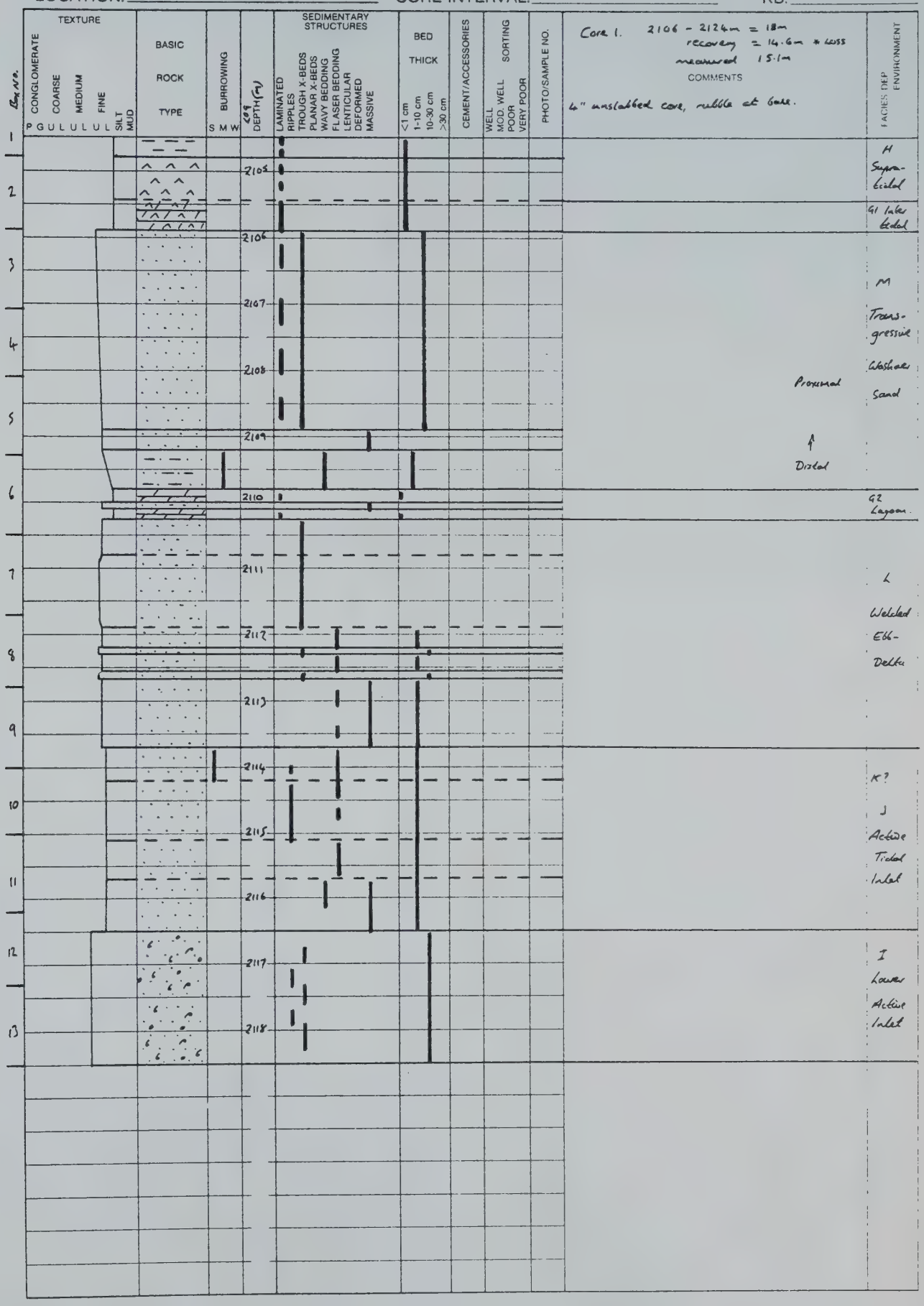

WELL NAME: Dome et al Wembley 14-19-73-8-W6 FORMATION: DATE:

LOCATION: CORE INTERVAL: KB:

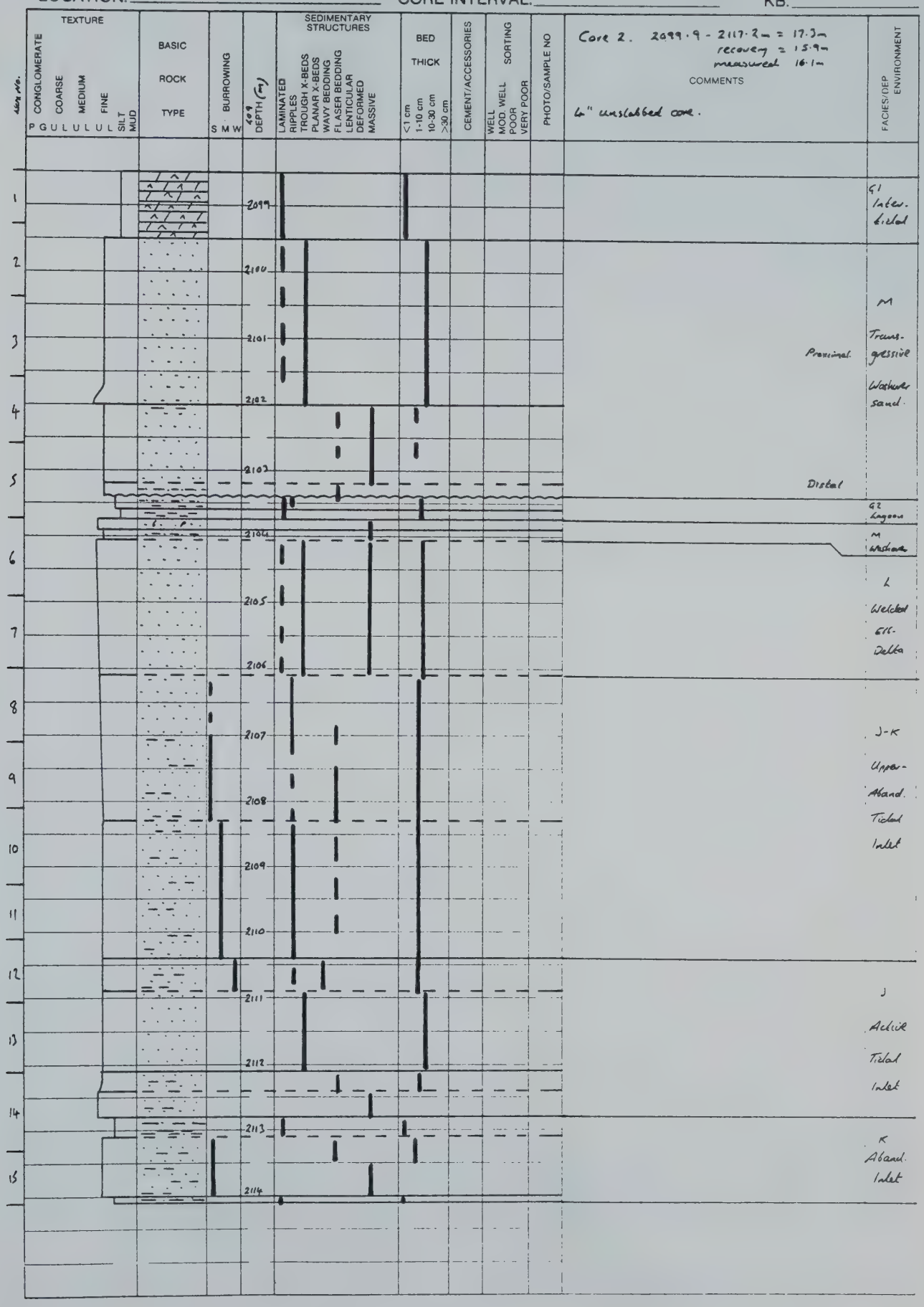

WELL NAME: Dome et al Wembley FORMATION: DATE:

LOCATION: 6-20-73-8-W6 CORE INTERVAL: KB:

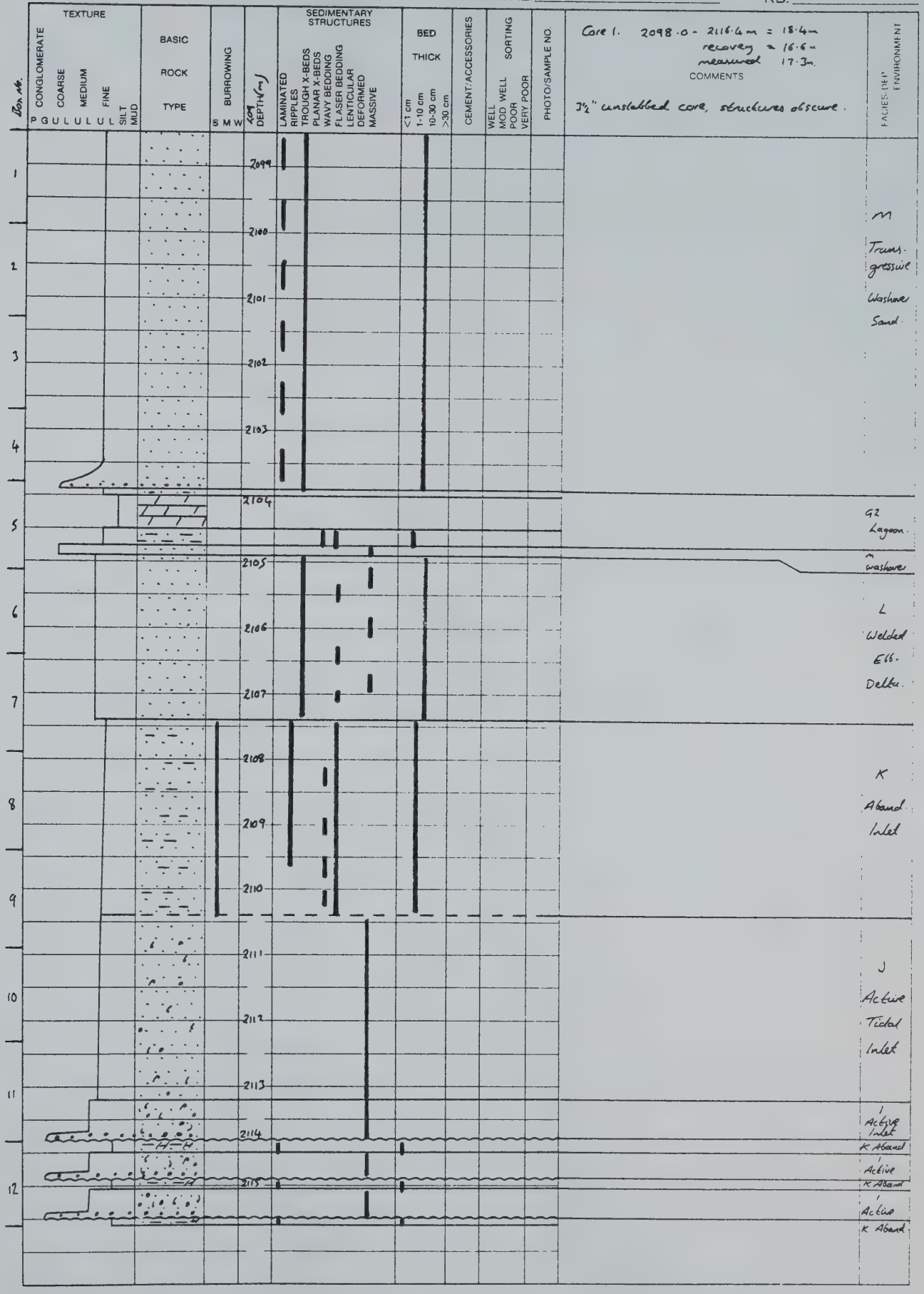

WELL NAME: Dome et al Wembley 6-21-73-8-W6 FORMATION: DATE:

LOCATION: CORE INTERVAL: KB:

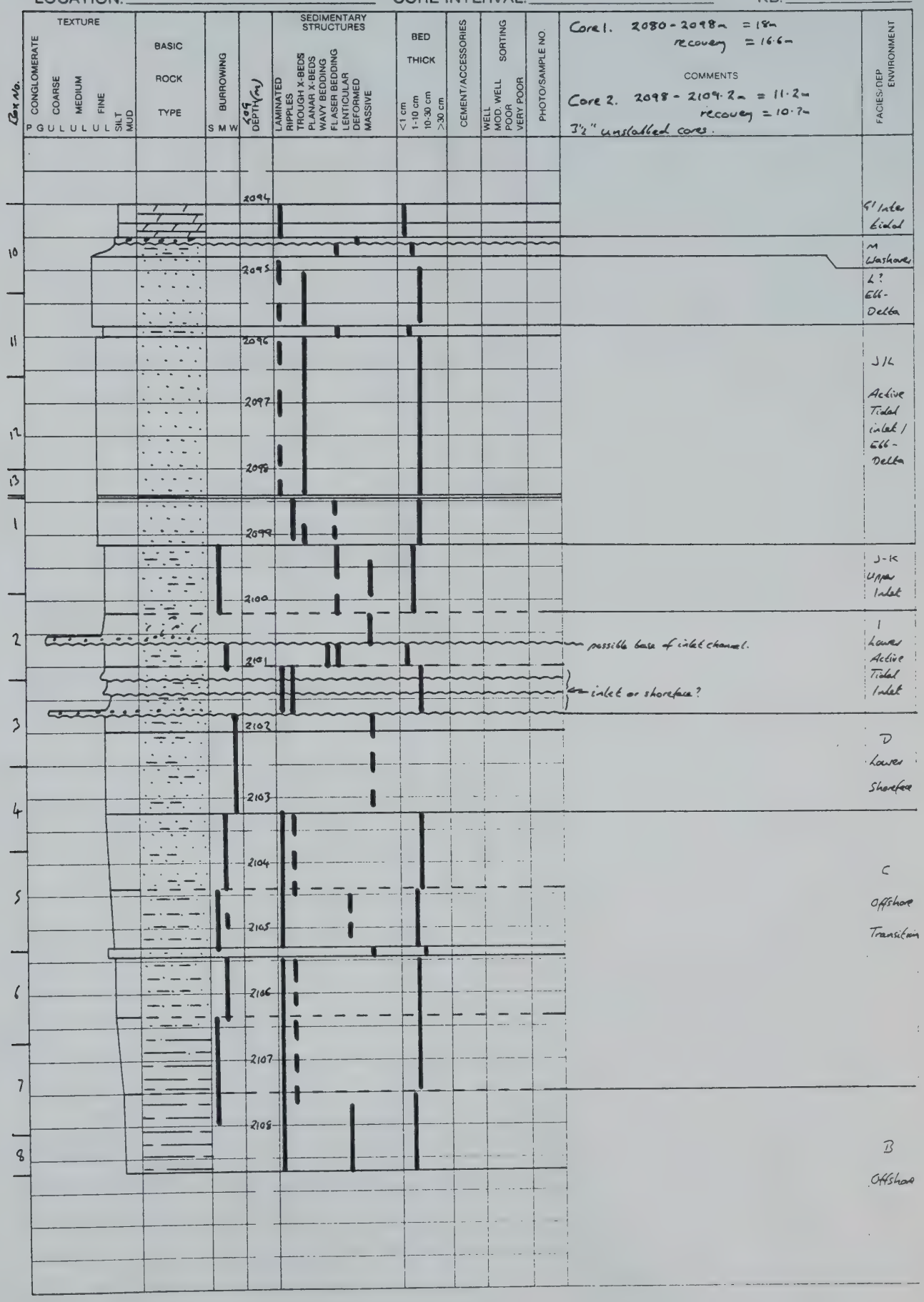

WELL NAME: Dome et al La Glace FORMATION: DATE:

LOCATION: 6-22-73-8-W6 CORE INTERVAL: KB:

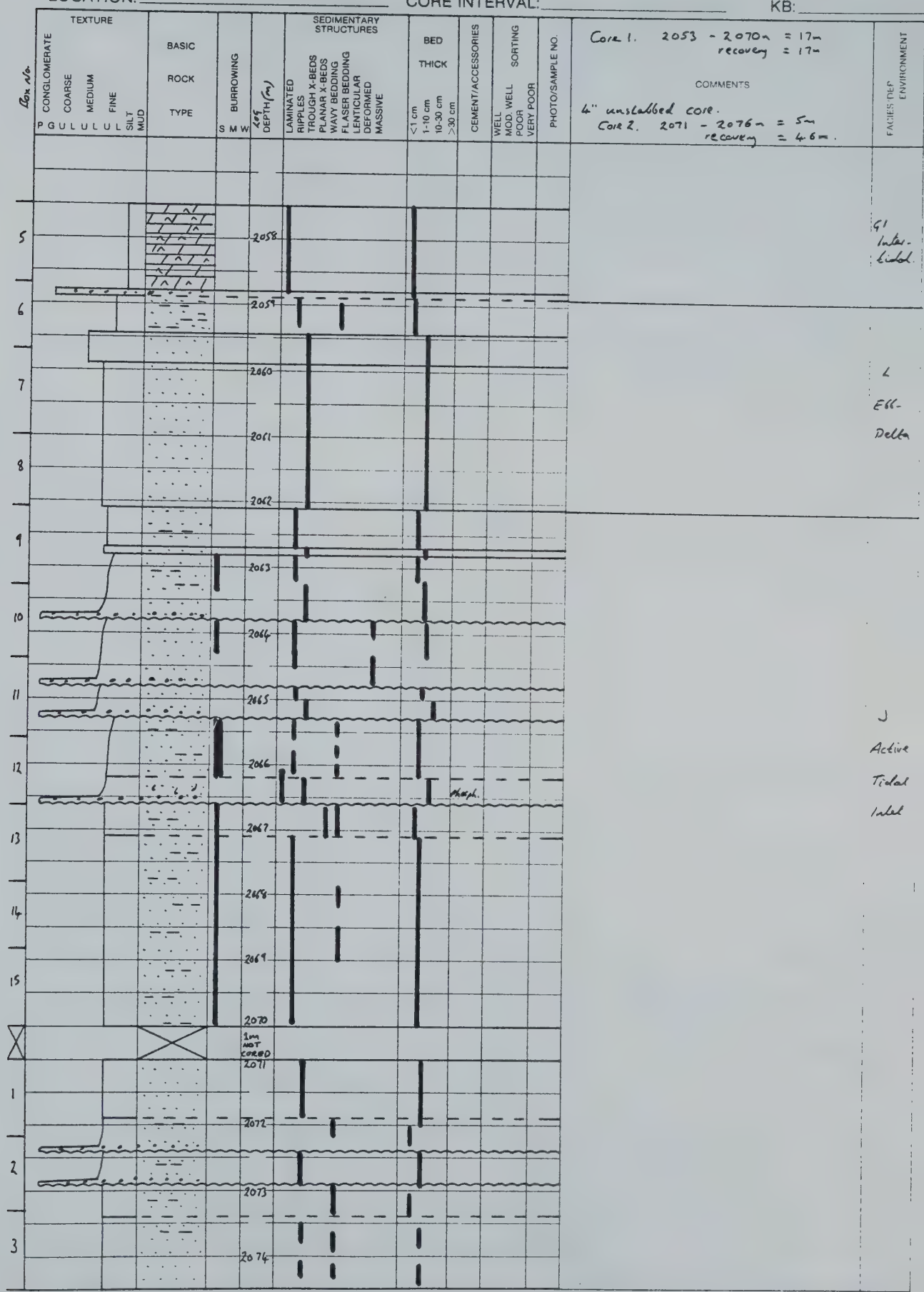

WELL NAME: _____ FORMATION: _____ DATE: _____

LOCATION: 6-22-73-8-W6 (2/2) CORE INTERVAL: _____ KB: _____

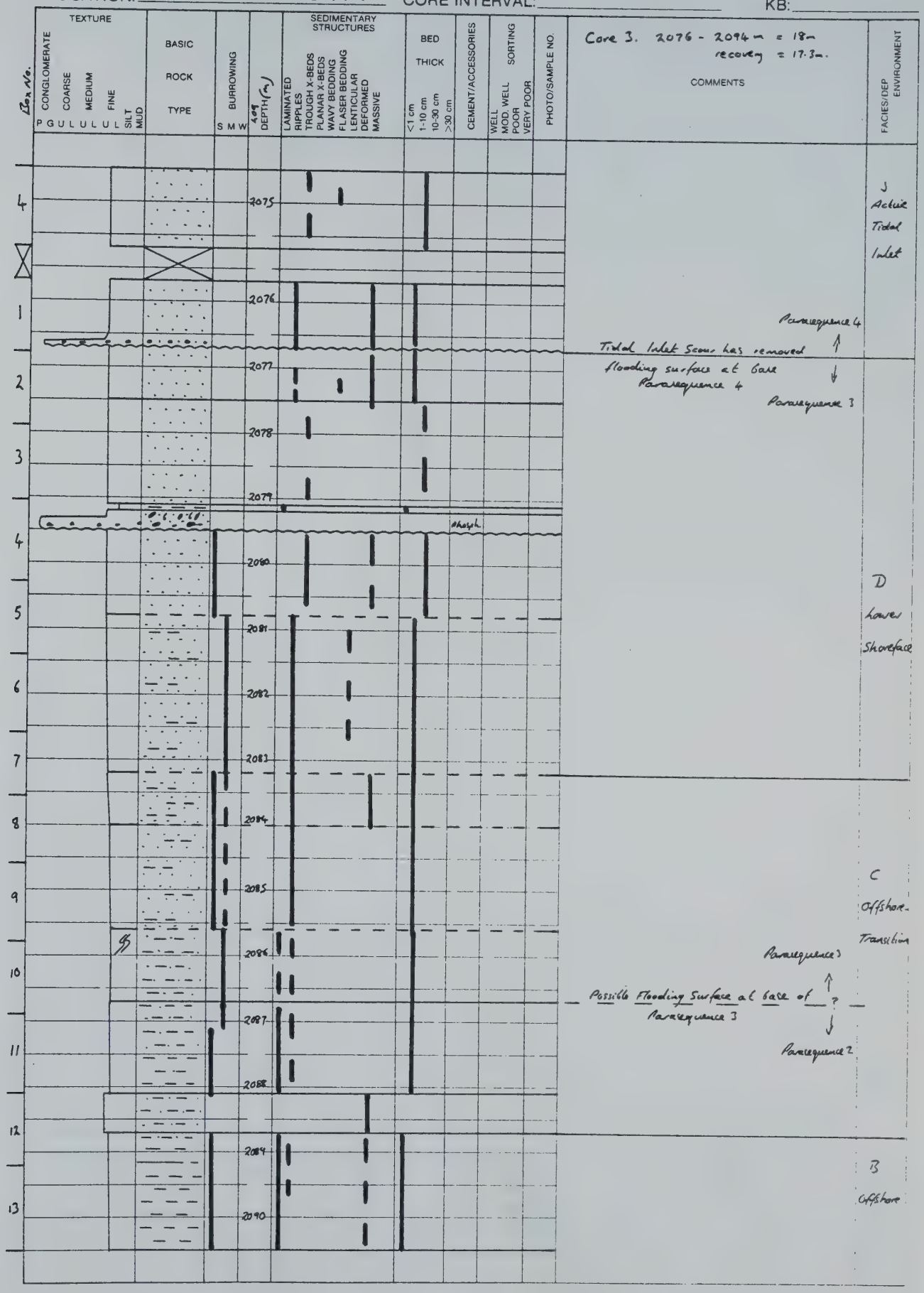

WELL NAME: PCP Esso Wembley FORMATION: DATE:

LOCATION: 16-23-73-8-W6 CORE INTERVAL: KB:

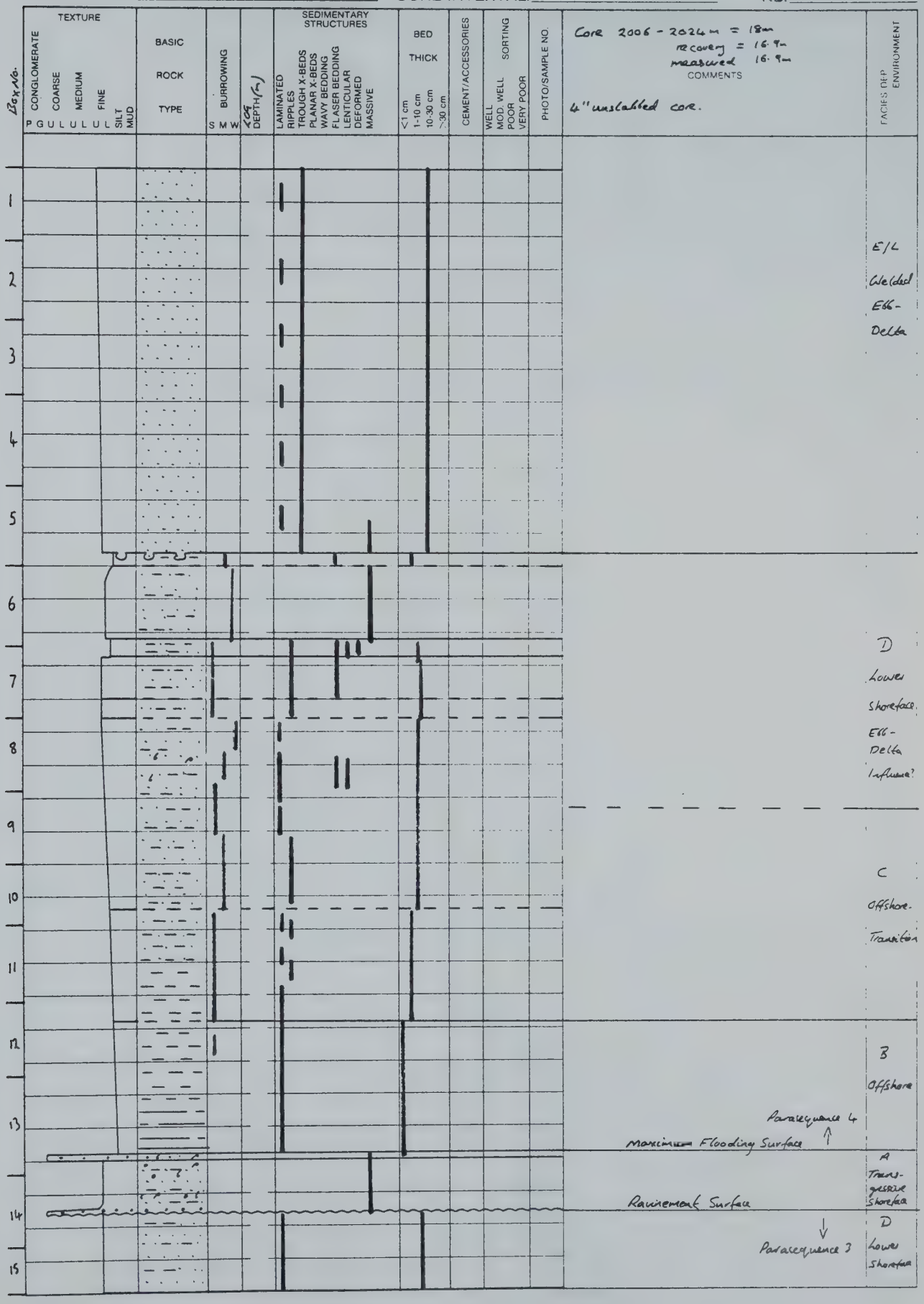

WELL NAME: Ladd et al Wembley 4-24-73-8-W6 FORMATION: DATE:

LOCATION: CORE INTERVAL: KB:

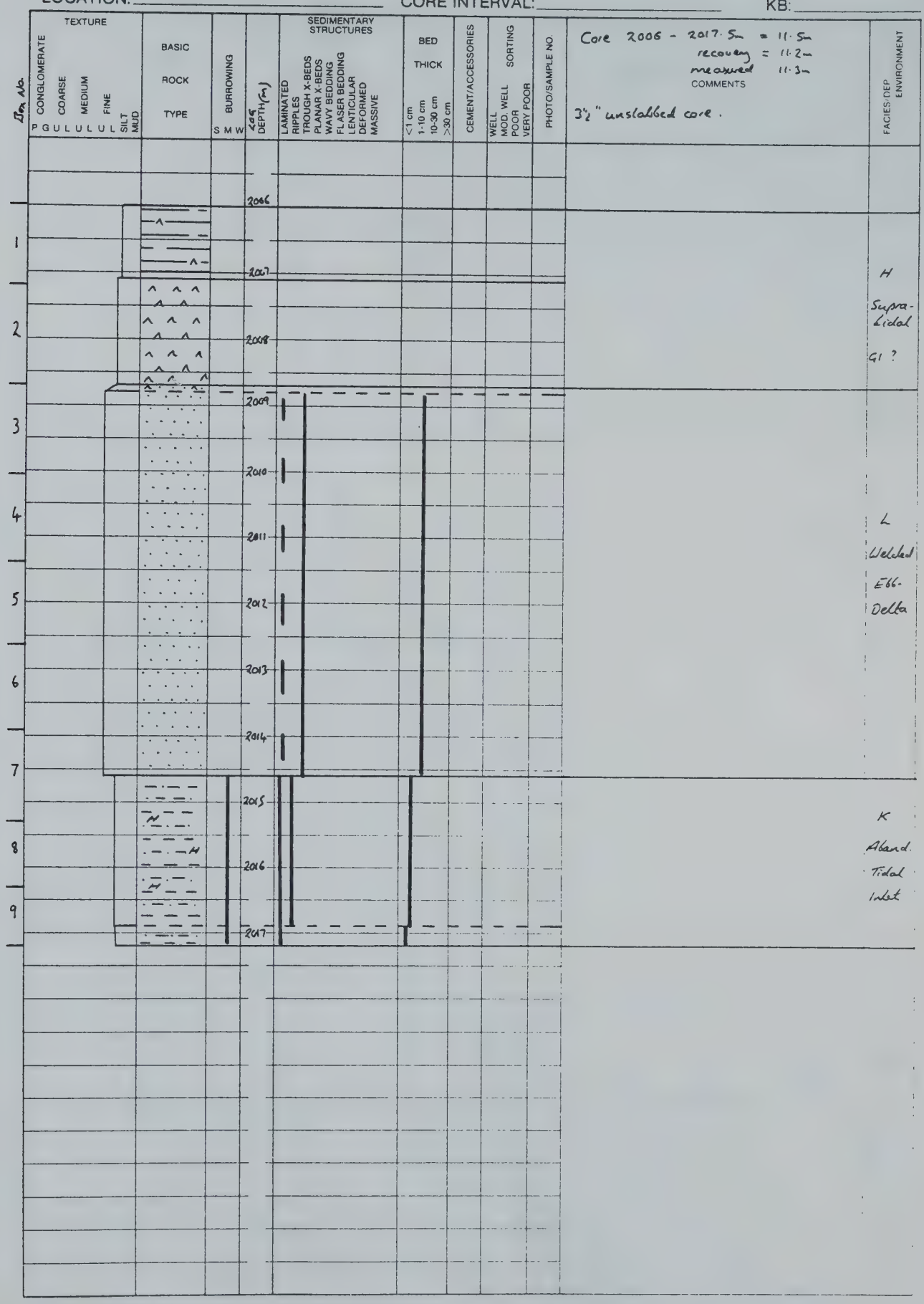

WELL NAME: PCP Esso Wembley FORMATION: DATE:

LOCATION: 10-26-73-8-W6 CORE INTERVAL: KB:

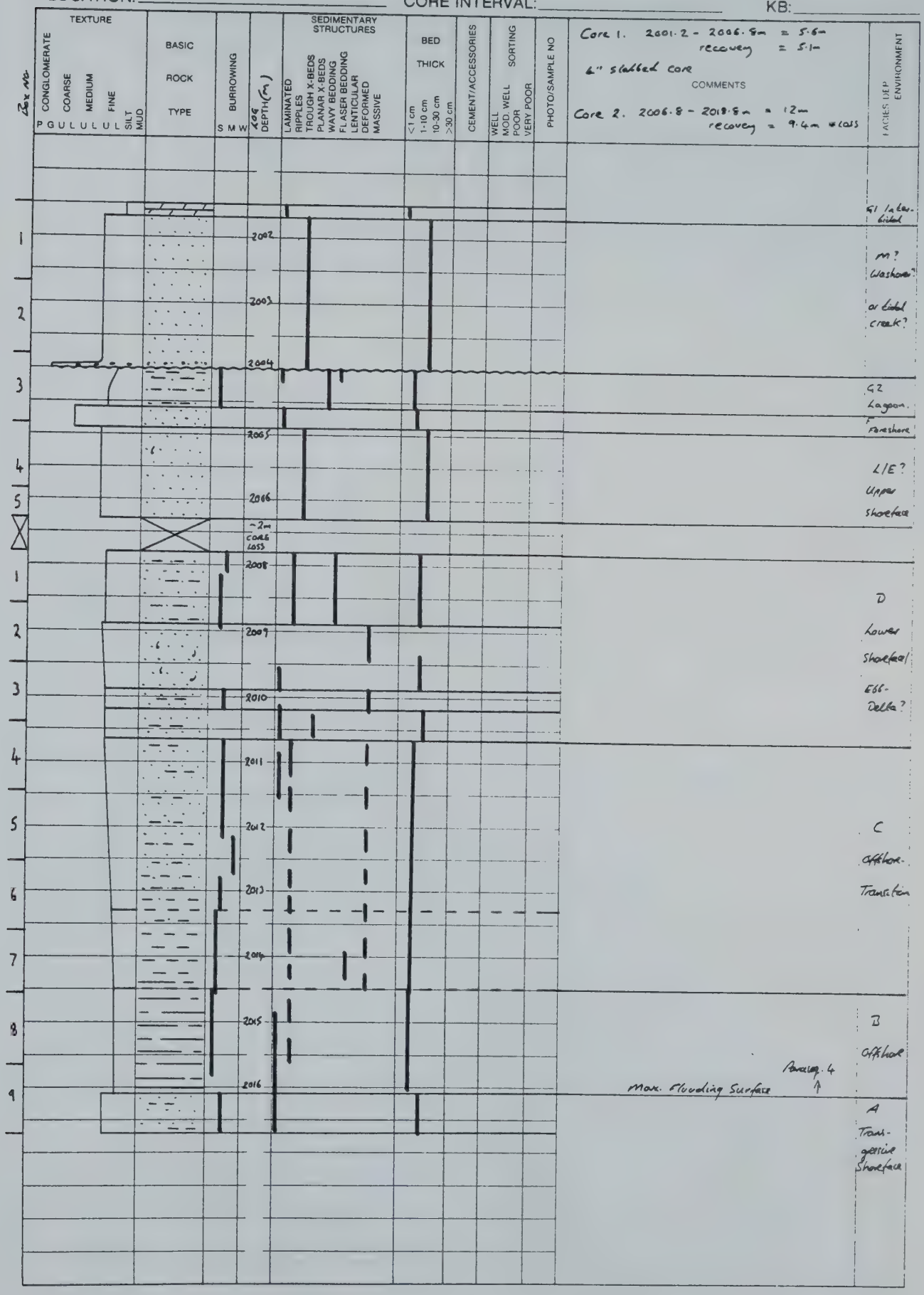

WELL NAME: Dome et al Wembley 6-28-73-8-W6 FORMATION: DATE:

LOCATION: CORE INTERVAL: KB:

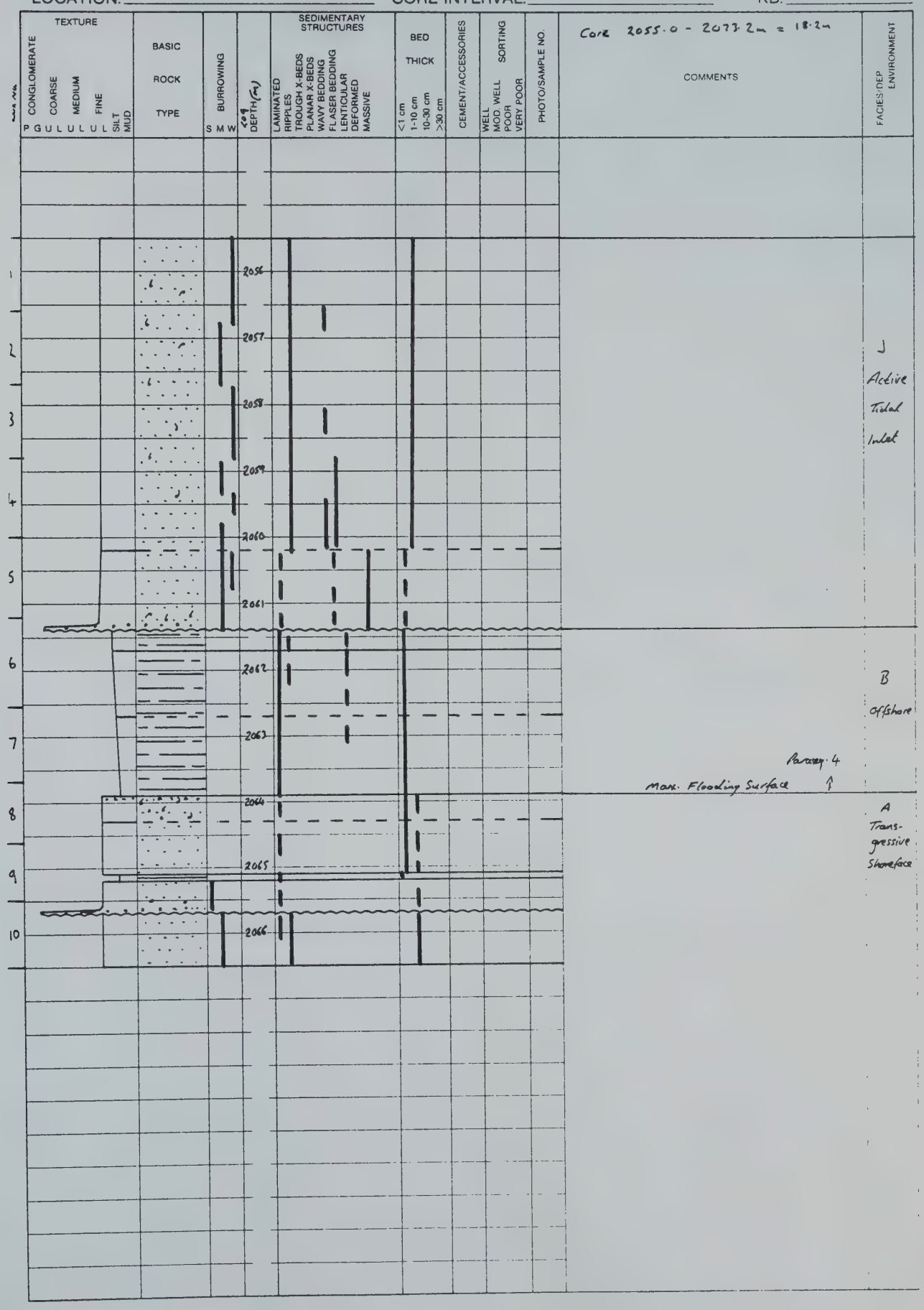

WELL NAME: Chiefco et al La Glace FORMATION: DATE:

LOCATION: 10-31-73-8-W6 CORE INTERVAL: KB:

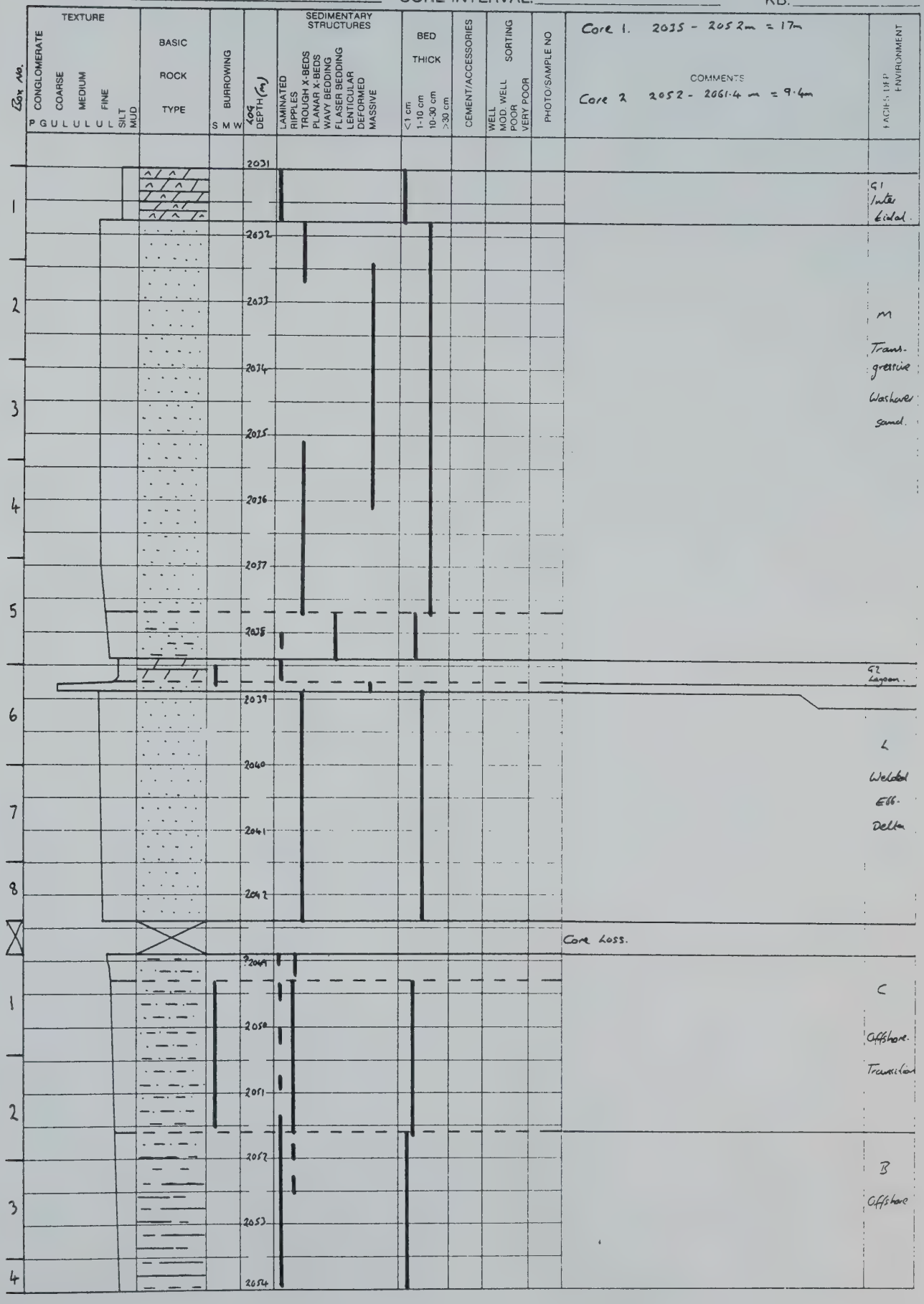

WELL NAME: _____ FORMATION: _____ DATE: _____

LOCATION: 10-31-73-8-W6 (2/2) CORE INTERVAL: _____ KB: _____

Core 3. 2061.4 - 2079.4m = 18m

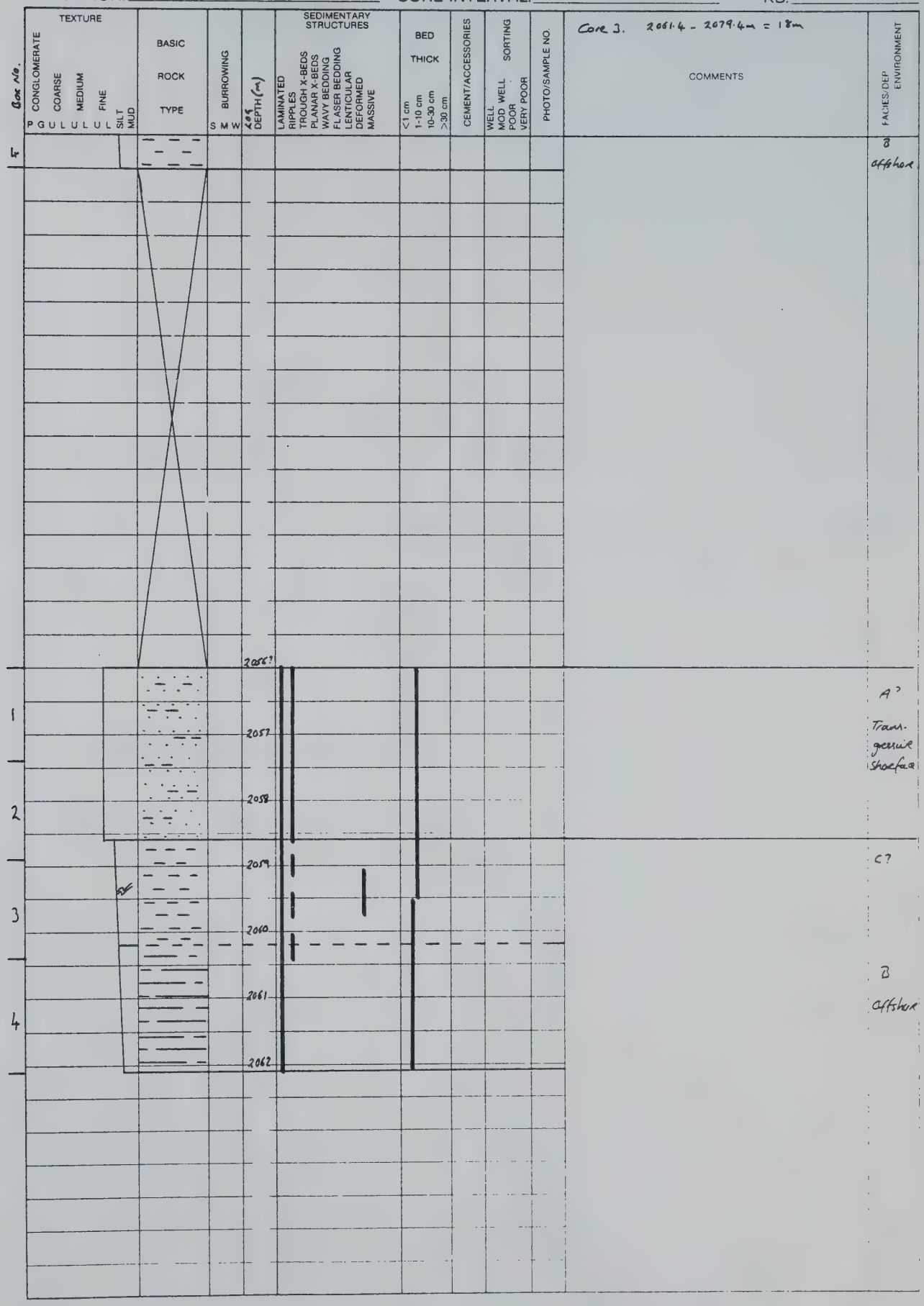

WELL NAME: Amoco Hythe 6-13-73-9-W6 FORMATION: DATE:

LOCATION: CORE INTERVAL: KB:

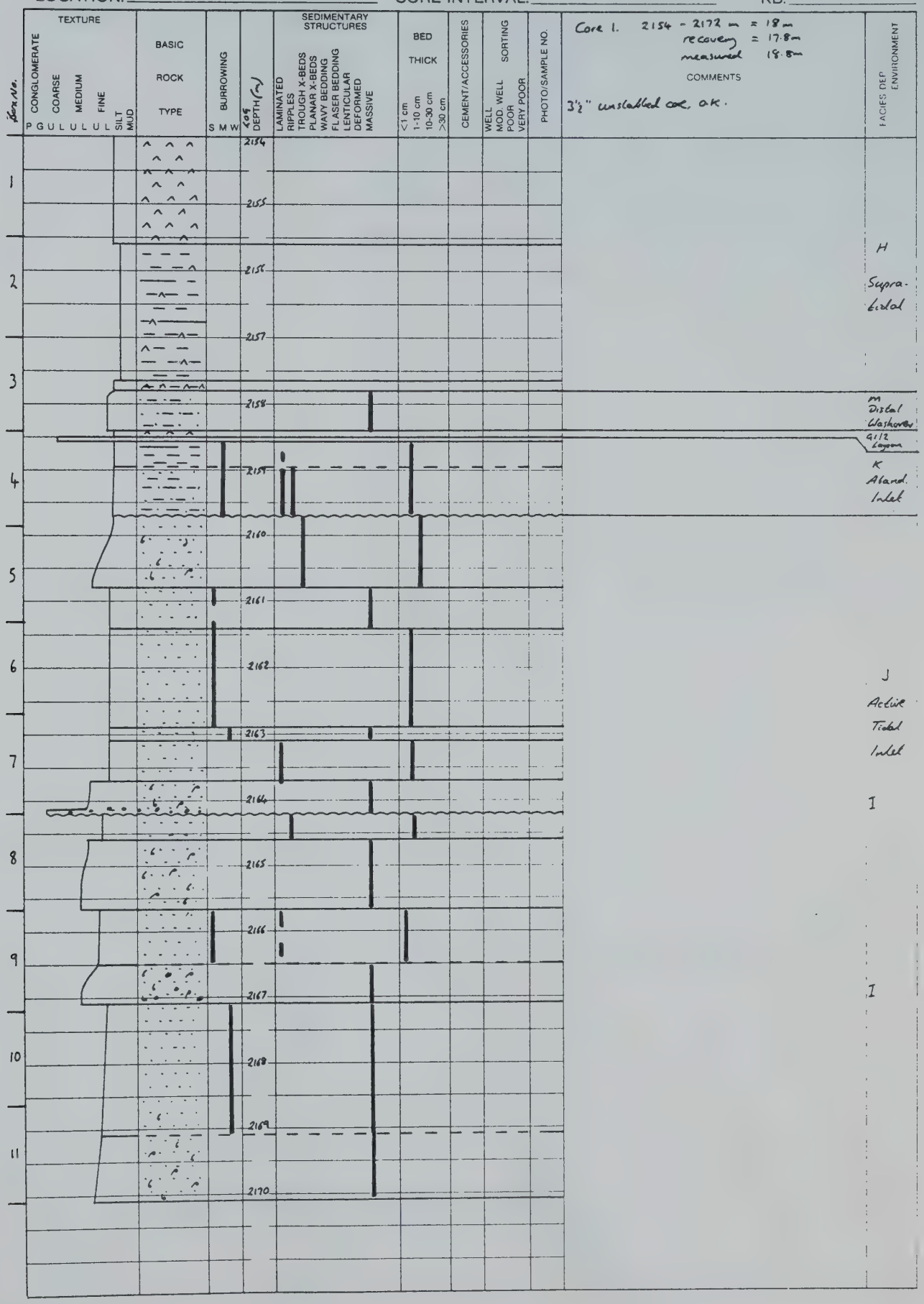

WELL NAME: (2/2) 6-13-73-9-W6 FORMATION: DATE:

LOCATION: CORE INTERVAL: KB:

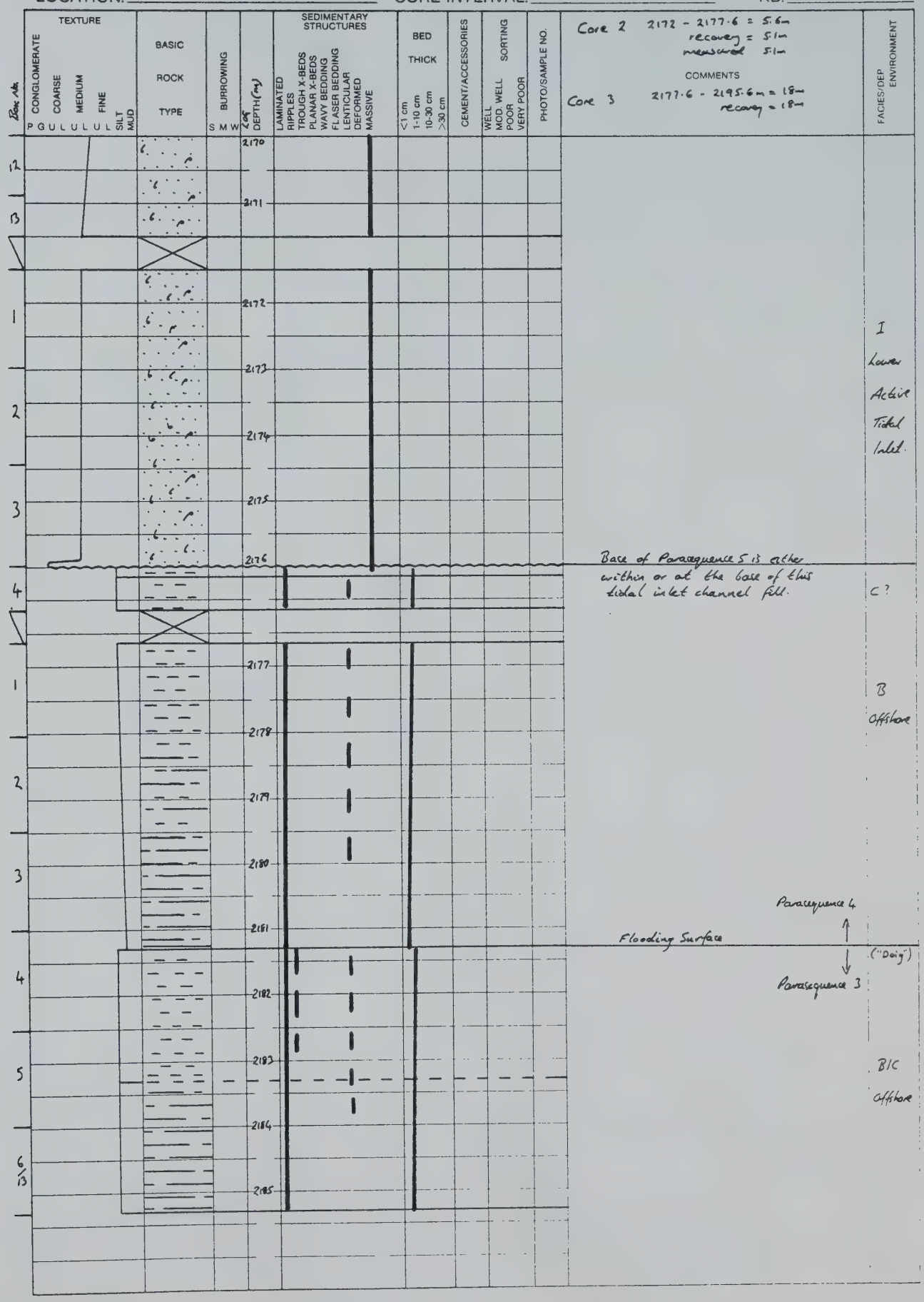

WELL NAME: Total Hythe 8-23-73-9-W6 FORMATION: DATE:

LOCATION: CORE INTERVAL: KB:

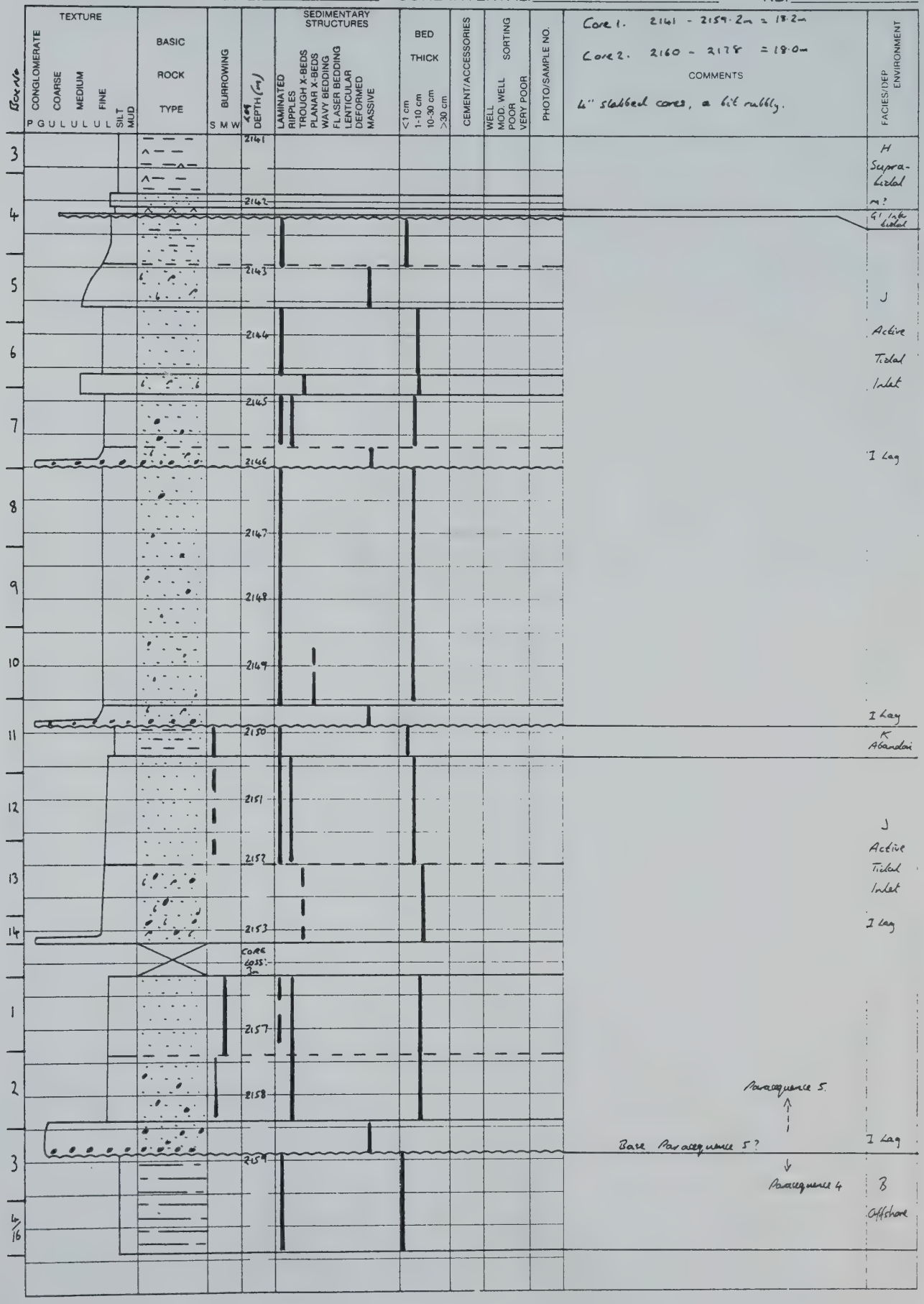

WELL NAME: Dome et al Sexsmith 6-1-74-7-W6 FORMATION: DATE:

LOCATION: CORE INTERVAL: KB:

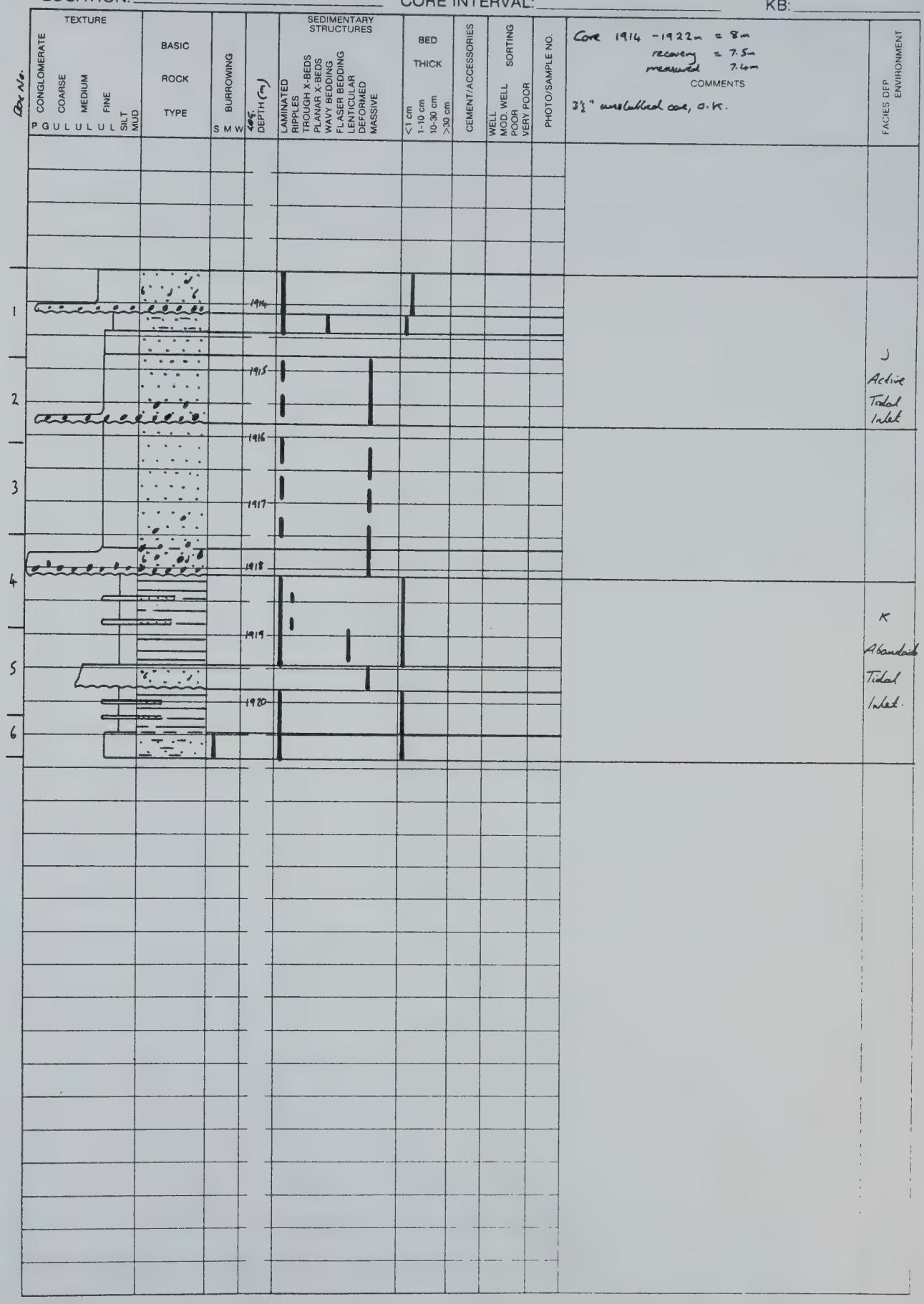

WELL NAME: Chiefco et al La Glace 15-7-74-8-W6 FORMATION: DATE:

LOCATION: CORE INTERVAL: KB:

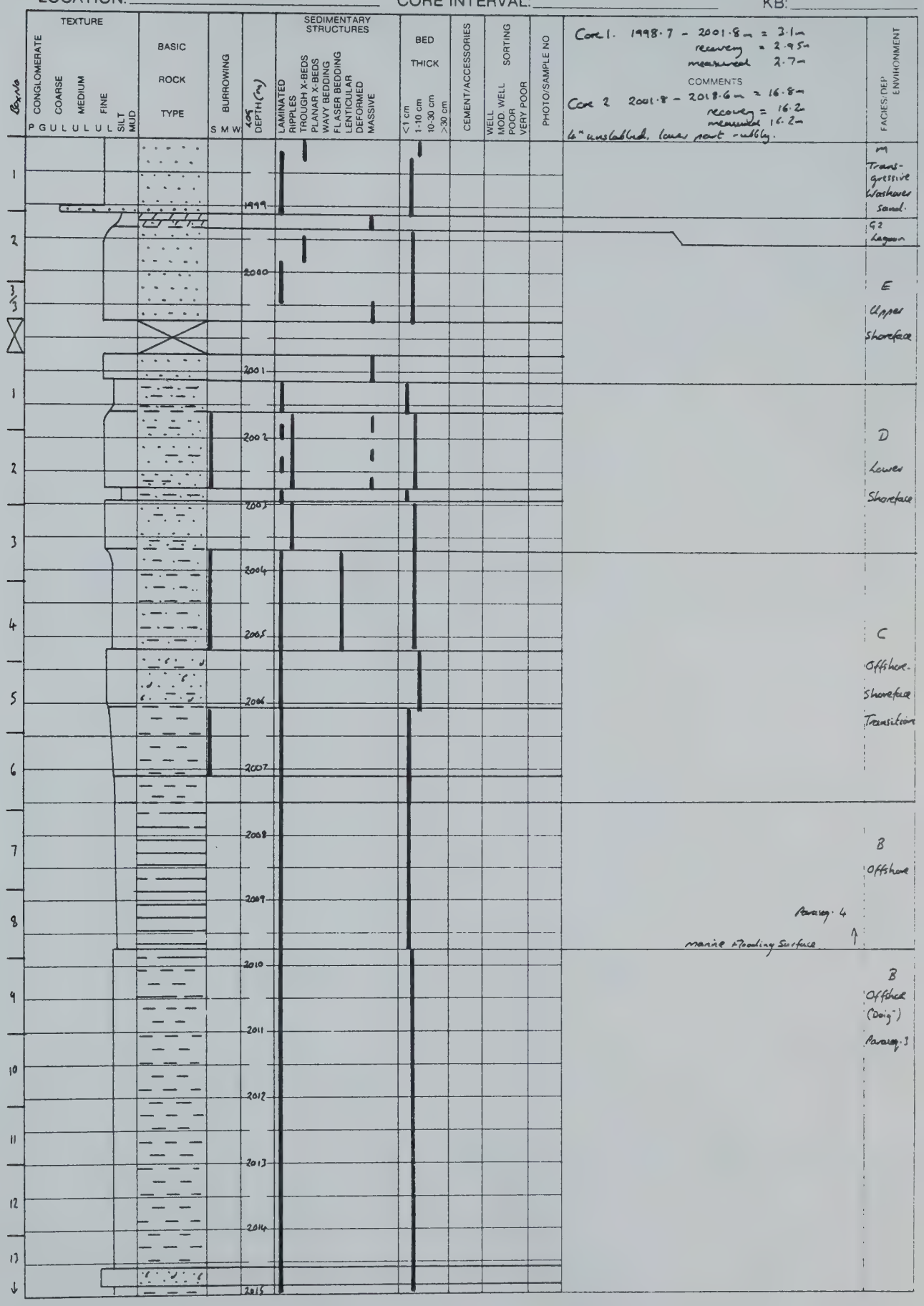

WELL NAME: Esso Valhalla 6-8-74-8-W6 FORMATION: DATE:

LOCATION: CORE INTERVAL: KB:

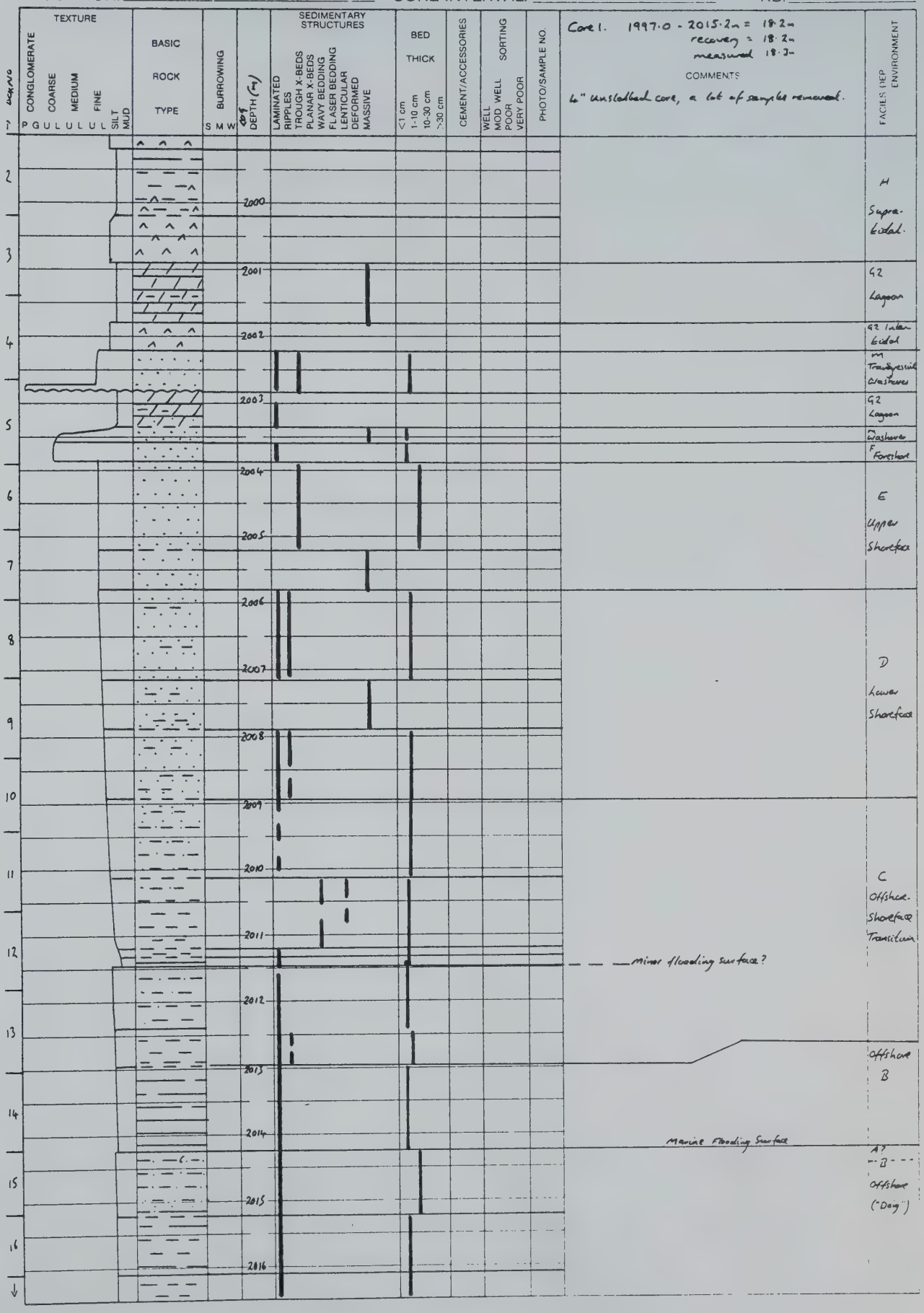

WELL NAME: Dome et al Valhalla 10-12-74-9-W6 FORMATION: DATE:

LOCATION: CORE INTERVAL: KB:

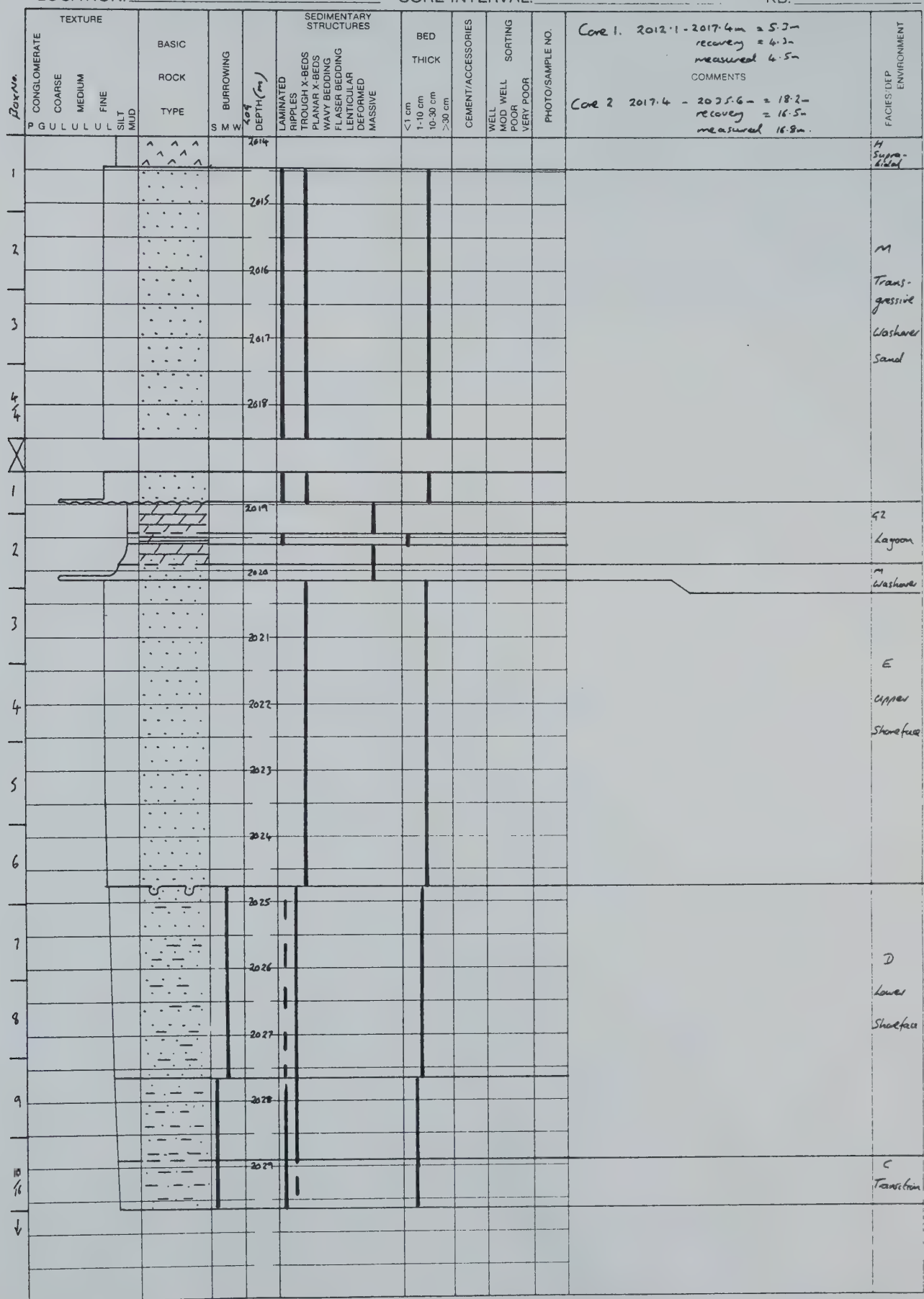

WELL NAME: (2/2) FORMATION: DATE:

LOCATION: 10-12-74-9-W6 CORE INTERVAL: KB:

Box No	TEXTURE: CONGLOMERATE (P G) / COARSE (U L) / MEDIUM (U L) / FINE (U L) / SILT / MUD	BASIC ROCK TYPE	BURROWING (S M W)	Log DEPTH (m)	SEDIMENTARY STRUCTURES: LAMINATED / RIPPLES / TROUGH X-BEDS / PLANAR X-BEDS / WAVY BEDDING / FLASER BEDDING / LENTICULAR / DEFORMED / MASSIVE	BED THICK: <1 cm / 1-10 cm / 10-30 cm / >30 cm	CEMENT/ACCESSORIES	SORTING: WELL / MOD. WELL / POOR / VERY POOR	PHOTO/SAMPLE NO	COMMENTS	FACIES/DEP ENVIRONMENT
										6" unslabbed core, #1 rubbly at top.	
11				2030							C
				2031							Offshore.
12				2032							Shoreface Transition
13				2033							
14				2034							B
15				2035							Offshore
16											

WELL NAME: Dome Sulpetro Valhalla 6-14-74-9-W6 FORMATION: DATE:

LOCATION: CORE INTERVAL: KB:

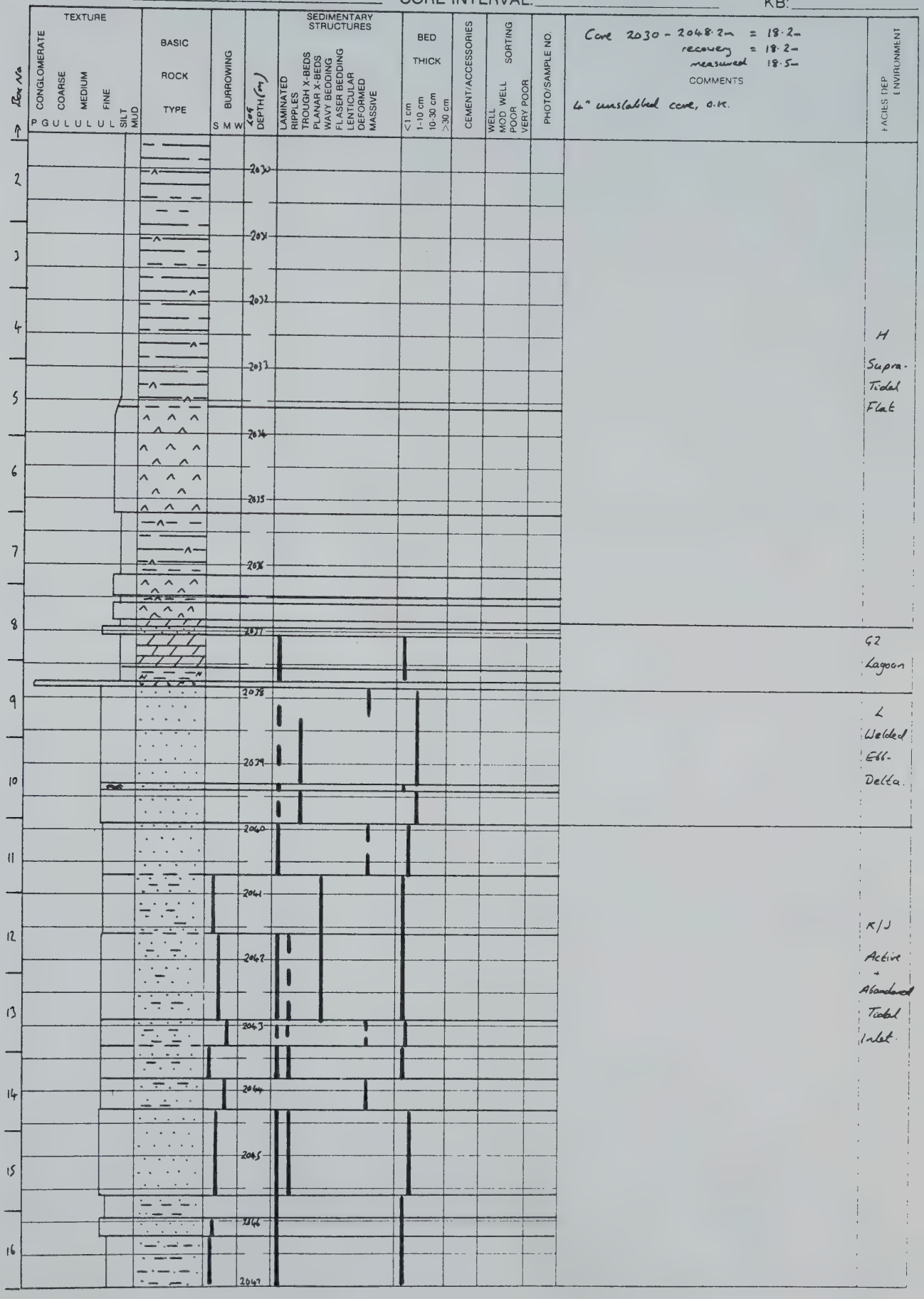

WELL NAME: Mesa Sulpetro Valhalla 10-22-74-9-W6 FORMATION: DATE:

LOCATION: CORE INTERVAL: KB:

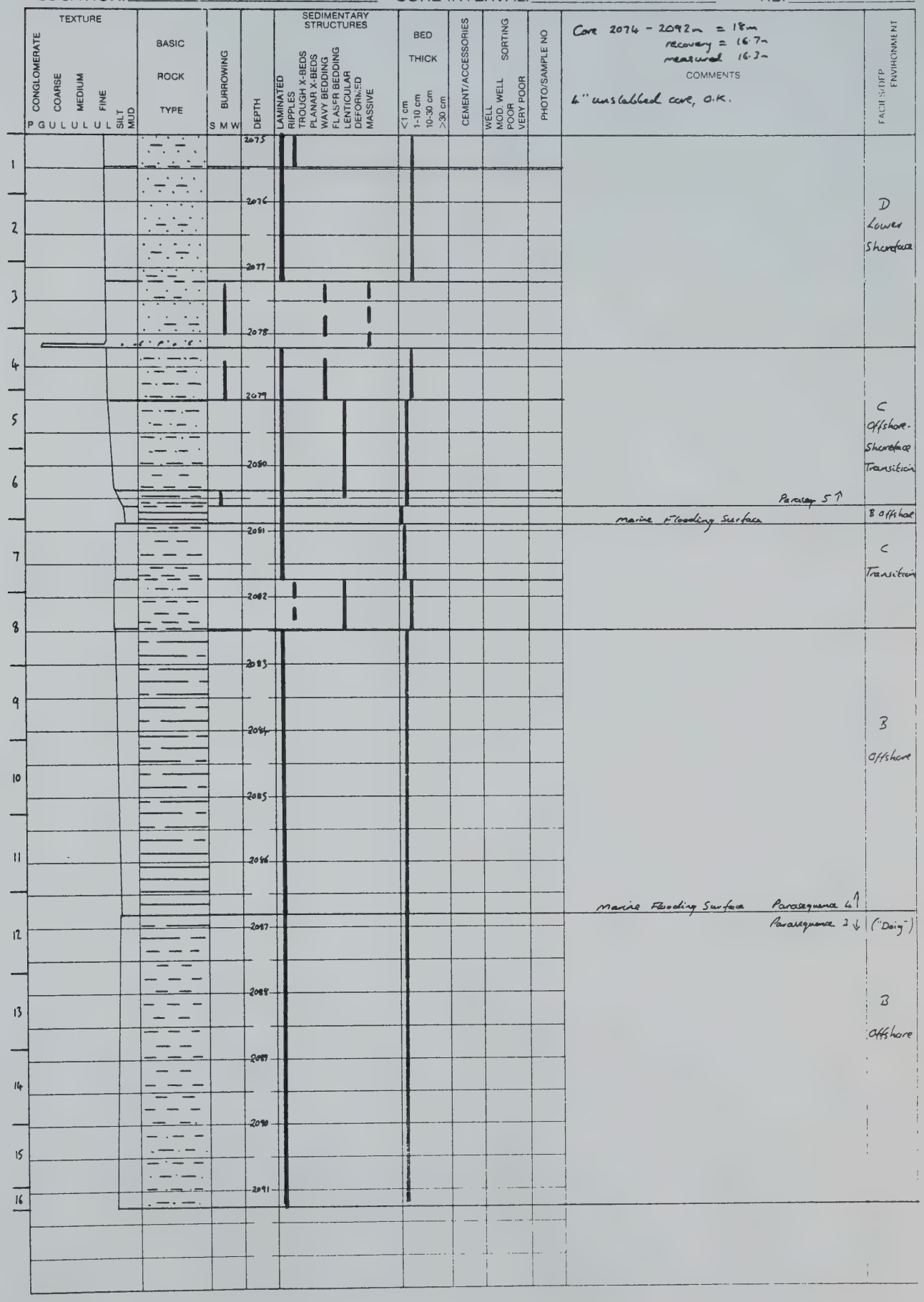

WELL NAME: Dome et al Valhalla 5-24-74-9-W6 FORMATION: DATE:

LOCATION: CORE INTERVAL: KB:

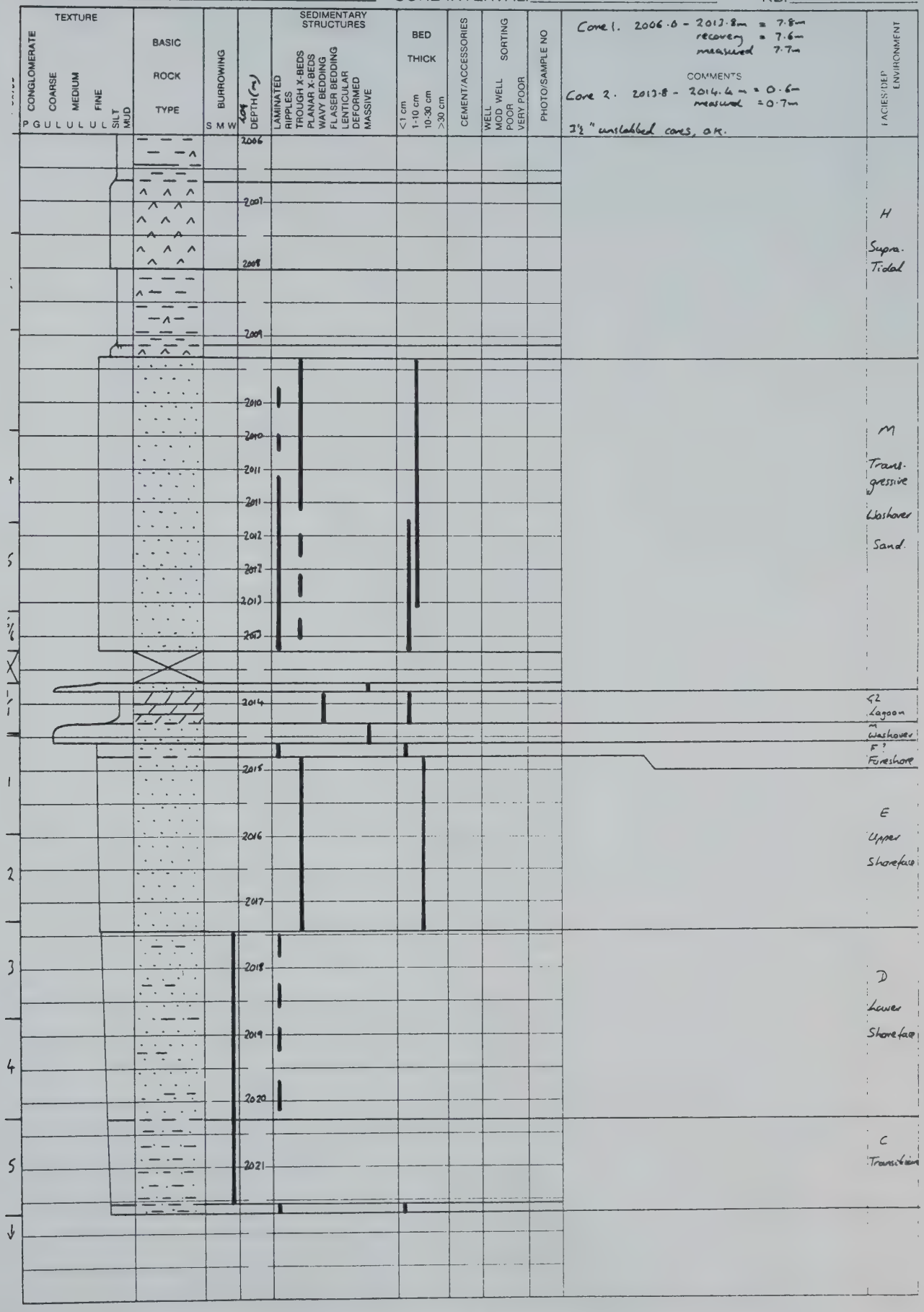

WELL NAME: (2/2) 5-24-74-9-W6 FORMATION: DATE:

LOCATION: CORE INTERVAL: KB:

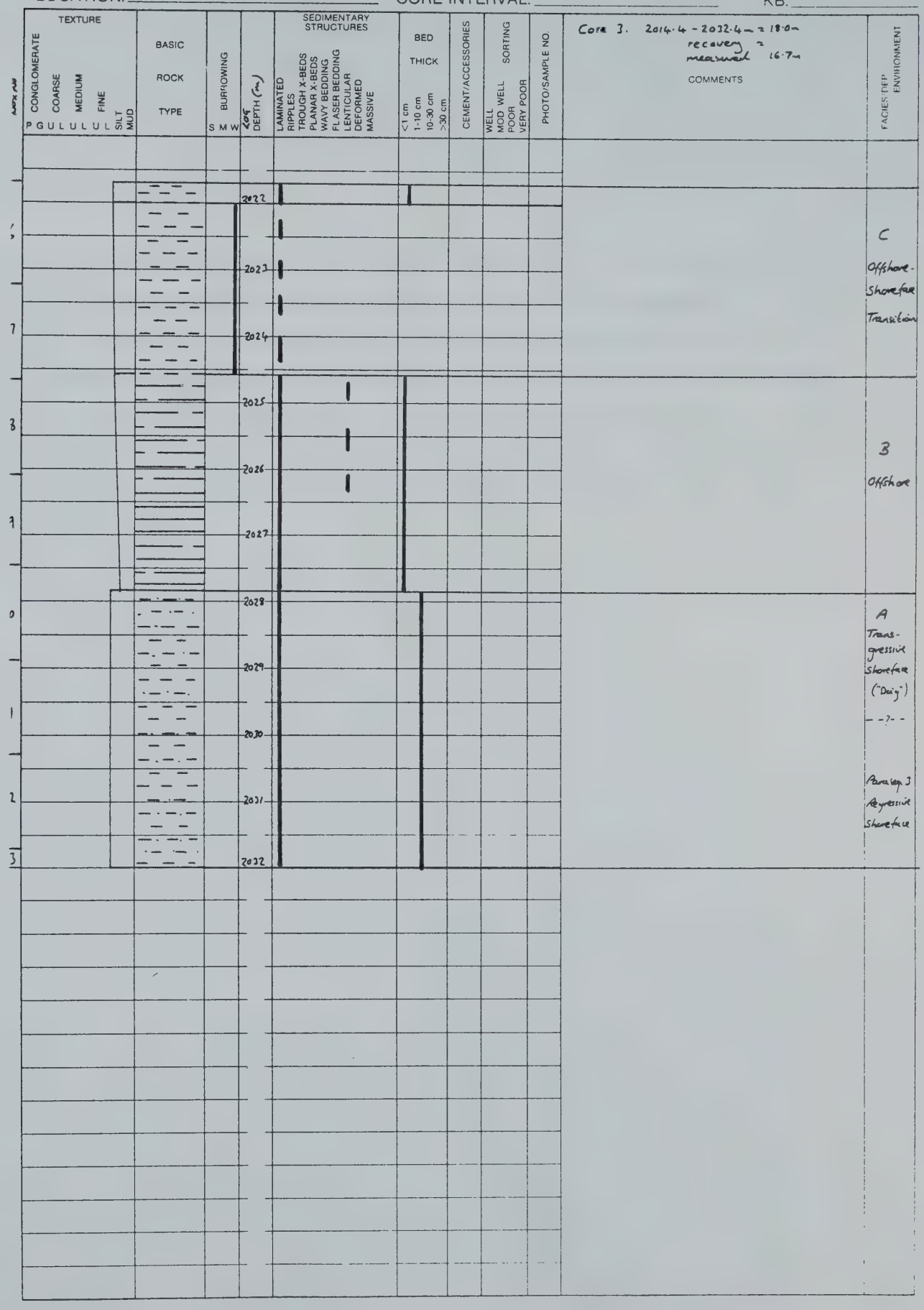

APPENDIX B.

Appendix B contains Kelly Bushing Elevation of each well together with well log depths (in metres) of each marine flooding surface (parasequence boundary) identified in each well in the study area. These depths were used to make structure maps of the five marine flooding surfaces in the Middle Triassic section and isopach maps of the parasequences. The entry "NP" indicates that a particular flooding surface was not identified in the well, either because the well does not penetrate deep enough or it lies outside the depositional limit of the flooding event.

In the case of parasequences 4 and 5 (PS 1 and PS 5), it was not always possible to identify correlative marine flooding surfaces within the coastal plain deposits of the lower Charlie Lake Formation. To facilitate the construction of isopach maps of these parasequences where the upper bounding flooding surface cannot be accurately identified, an additional column labelled "Top PS 4/5" is included. This represents the top of the sandstones in the parasequence (ie. the base of the Charlie Lake Formation) and therefore excludes 1-3 m of associated backbarrier and coastal plain deposits from the true parasequence thickness.

WELL LOCATION	KBE (M)	Top Montney	Base PS1	Base PS2	Base PS3	Base PS4	Top PS4	Base PS5	Top PS5
100/10-08-71-07 W6	705.90	NP	2280.00	2268.00	2255.00	2230.00	2215.00	NP	NP
100/14-11-71-07 W6	684.40	NP	NP	NP	NP	2154.00	NP	NP	NP
100/09-12-71-07 W6	686.10	2187.00	2169.00	2155.00	NP	2121.00	NP	NP	NP
100/07-15-71-07 W6	689.20	NP	2199.00	2187.00	2175.00	2152.50	NP	NP	NP
100/15-15-71-07 W6	693.80	NP	NP	NP	NP	2163.00	NP	NP	NP
100/14-22-71-07 W6	709.40	NP	NP	2180.00	2173.50	2146.00	NP	NP	NP
100/06-24-71-07 W6	681.90	NP	2155.00	2141.00	2132.00	2108.50	2098.00	NP	NP
100/08-25-71-07 W6	669.40	NP	NP	2118.00	2108.00	2087.00	2081.00	NP	NP
100/06-27-71-07 W6	751.40	NP	2226.00	2211.00	2202.00	2178.00	2163.50	NP	NP
100/08-28-71-07 W6	750.00	NP	2238.50	2225.00	2216.00	2191.00	2177.00	NP	NP
100/14-28-71-07 W6	731.20	NP	NP	2212.00	2203.00	2178.00	2164.00	2163.00	2162.00
100/07-31-71-07 W6	749.50	NP	2290.00	2276.00	2267.00	2242.00	NP	NP	2222.00
100/10-03-71-08 W6	704.30	2354.00	2342.00	2334.00	2327.00	2295.00	NP	2289.00	2275.00
100/16-04-71-08 W6	705.50	2357.50	2346.00	2338.00	2333.00	2302.00	NP	2292.00	2285.00
100/06-12-71-08 W6	706.60	2303.00	2289.00	2278.00	2266.00	2238.00	NP	2226.00	2220.00
100/08-17-71-08 W6	721.00	2392.00	2382.50	2372.00	2369.00	2335.00	NP	2327.00	2316.00
102/06-25-71-08 W6	729.50	2303.00	2287.00	2274.00	2267.00	2237.00	NP	2225.00	2217.00
100/14-28-71-08 W6	756.40	2389.00	2375.00	2362.00	2357.00	2298.00	NP	NP	NP
100/08-30-71-08 W6	770.20	2432.00	2421.50	2410.50	2403.50	2375.00	NP	2366.00	2345.00
100/06-31-71-08 W6	790.20	2438.00	2426.00	2416.00	2411.00	2389.00	NP	2380.00	2367.00
100/11-34-71-08 W6	756.70	2358.00	2342.00	2328.00	2321.50	2291.50	NP	NP	2273.00
100/14-05-71-09 W6	691.30	2513.50	2497.00	2492.00	2489.00	2475.00	NP	2471.00	2448.00
100/06-10-71-09 W6	717.30	2502.00	2486.00	2481.00	2477.00	2464.00	NP	2458.00	2435.00
100/14-12-71-09 W6	738.20	2469.00	2454.00	2446.00	2443.00	2423.00	NP	2415.00	2389.00
100/06-25-71-09 W6	778.70	2464.00	2454.00	2444.00	2436.00	2411.00	NP	2399.00	2387.00
100/06-27-71-09 W6	773.60	2501.00	2490.00	2480.00	2476.00	2454.00	NP	2441.00	2417.00
100/06-28-71-09 W6	756.90	2498.00	2486.00	2476.00	2474.00	2454.00	NP	2440.00	2414.00
100/08-32-71-09 W6	766.50	NP	NP	NP	NP	2454.00	NP	2434.00	2410.00
100/06-03-72-07 W6	670.70	2163.50	2150.00	2134.50	2124.00	2101.50	2092.00	NP	NP
100/14-04-72-07 W6	690.60	NP	NP	NP	2139.00	2116.00	2104.00	NP	NP
100/10-05-72-07 W6	735.80	2242.00	2227.00	2212.00	2202.00	2179.00	2169.00	2168.00	2166.50

WELL LOCATION	KBE (M)	Top Montney	Base PS1	Base PS2	Base PS3	Base PS4	Top PS4	Base PS5	Top PS5
100/06-06-72-07 W6	721.20	NP	NP	NP	NP	2196.50	2180.00	2178.00	2172.50
100/06-07-72-07 W6	718.30	NP	NP	NP	NP	2168.50	2150.00	2149.00	2148.00
100/14-07-72-07 W6	721.60	NP	NP	NP	2182.00	2161.00	2141.00	NP	NP
100/06-08-72-07 W6	733.60	2232.50	2218.00	2201.50	2191.00	2169.50	2156.50	NP	NP
100/08-08-72-07 W6	711.50	NP	NP	NP	NP	2142.00	2129.50	2128.50	2121.00
100/14-08-72-07 W6	731.90	NP	NP	2195.00	2184.50	2164.00	2151.00	NP	NP
100/16-08-72-07 W6	719.40	NP	NP	NP	NP	2152.00	2137.50	NP	NP
100/06-09-72-07 W6	700.60	NP	NP	2159.50	2149.00	2127.50	2112.00	NP	NP
100/08-09-72-07 W6	680.20	NP	NP	2129.50	2119.00	2097.50	2080.00	NP	NP
100/14-09-72-07 W6	705.40	NP	NP	2156.00	2145.00	2124.50	2105.00	NP	NP
100/16-09-72-07 W6	688.40	NP	NP	2130.50	2119.50	2100.00	2089.00	NP	NP
100/16-10-72-07 W6	677.00	2118.50	2104.00	2087.50	2074.50	2055.00	2047.50	NP	NP
100/06-11-72-07 W6	684.50	NP	2107.00	2091.00	2077.50	2057.00	2051.00	NP	NP
100/06-16-72-07 W6	693.80	NP	2147.00	2131.00	2119.00	2100.00	2088.50	2086.00	2085.00
100/07-16-72-07 W6	685.00	2151.00	2135.50	2118.00	2106.00	2087.00	2077.00	NP	NP
100/14-16-72-07 W6	672.70	2126.00	2108.50	2091.50	2079.00	2060.00	2047.50	NP	NP
100/06-17-72-07 W6	736.40	NP	2206.00	2189.50	2179.00	2159.00	2145.00	2142.00	2141.00
100/08-17-72-07 W6	726.70	NP	NP	2176.00	2165.00	2145.50	2132.00	2130.00	2129.00
100/14-17-72-07 W6	704.60	NP	NP	2150.50	2139.00	2120.50	2105.50	2102.50	2102.00
100/16-17-72-07 W6	685.60	NP	2135.00	2118.00	2106.00	2088.50	2076.00	NP	NP
100/10-18-72-07 W6	749.80	NP	2226.00	2209.50	2198.50	2179.50	2164.50	NP	NP
100/14-18-72-07 W6	725.60	NP	2196.00	2180.00	2169.00	2150.00	2137.00	NP	NP
100/16-18-72-07 W6	722.40	NP	NP	2175.50	2164.00	2145.00	2128.00	NP	NP
100/06-19-72-07 W6	718.70	NP	2180.50	2164.00	2153.00	2134.50	2122.50	NP	NP
100/08-19-72-07 W6	708.20	NP	2166.00	2149.00	2137.50	2119.00	2106.00	2103.00	2102.00
100/14-19-72-07 W6	721.20	2197.00	2179.00	2161.50	2150.50	2132.50	2121.00	2119.00	2118.00
100/16-19-72-07 W6	700.50	NP	2150.00	2132.00	2120.50	2103.00	2090.00	2087.00	2086.00
100/06-20-72-07 W6	695.70	NP	2150.00	2132.50	2120.50	2103.00	2083.50	NP	NP
100/08-20-72-07 W6	679.10	2139.00	2121.00	2103.50	2091.00	2074.00	2054.50	NP	NP
100/14-20-72-07 W6	671.00	NP	2109.00	2091.00	2079.00	2062.00	2050.00	2046.50	2045.50
100/16-20-72-07 W6	672.90	NP	2105.50	2088.00	2074.00	2058.00	2038.50	2036.00	2035.50

WELL LOCATION	KBE (M)	Top Montney	Base PS1	Base PS2	Base PS3	Base PS4	Top PS4	Base PS5	Top PS5
100/06-21-72-07 W6	672.00	NP	2106.00	2089.00	2076.00	2058.00	2048.00	2046.50	2046.00
100/06-22-72-07 W6	670.00	NP	NP	2062.00	2045.00	2023.00	2021.00	NP	NP
100/07-27-72-07 W6	675.70	NP	2054.00	2036.00	2014.50	NP	NP	NP	NP
100/06-29-72-07 W6	670.70	NP	2101.00	2084.00	2070.00	2054.00	2041.00	2038.00	2036.50
100/08-29-72-07 W6	674.70	NP	2092.00	2074.00	2060.00	2045.00	2026.00	NP	NP
100/06-30-72-07 W6	707.10	NP	NP	2133.50	2121.50	2104.50	2091.00	NP	NP
100/08-30-72-07 W6	680.10	NP	2106.00	2089.50	2076.50	2060.50	2043.00	2042.50	2040.50
100/14-30-72-07 W6	678.80	NP	2103.00	2085.50	2072.00	2056.50	2040.00	NP	NP
100/16-30-72-07 W6	671.20	NP	2089.50	2072.00	2058.50	2043.00	2026.50	2025.50	2021.00
100/06-31-72-07 W6	681.80	NP	2100.00	2082.50	2068.50	2054.00	2041.00	2037.00	2036.50
100/08-31-72-07 W6	671.20	NP	2080.50	2063.00	2048.00	2034.00	2012.00	NP	NP
100/14-31-72-07 W6	681.80	NP	2090.00	2073.00	2058.00	2045.50	2025.00	NP	NP
100/06-32-72-07 W6	670.80	NP	2078.00	2060.00	2042.00	2030.00	2016.00	NP	NP
100/06-34-72-07 W6	680.40	NP	2041.50	2023.00	1999.50	1983.00	1982.00	NP	NP
100/14-36-72-07 W6	685.40	NP	NP	2021.00	1998.00	NP	NP	NP	NP
100/06-04-72-08 W6	794.90	2395.00	2379.00	2368.00	2363.00	2309.00	NP	2300.00	2295.00
100/14-08-72-08 W6	799.50	2391.00	2371.50	2359.00	2353.00	2323.00	NP	2315.00	2305.00
100/05-09-72-08 W6	839.40	NP	NP	NP	NP	NP	NP	NP	NP
102/05-09-72-08 W6	837.60	NP	2415.00	2402.00	2394.00	2343.00	NP	2338.00	2328.00
100/08-09-72-08 W6	804.70	2378.50	2359.00	2346.00	2339.00	2300.00	NP	2292.00	2282.00
100/14-11-72-08 W6	728.80	2272.50	2255.00	2240.00	2230.00	2207.00	2187.00	2186.00	2181.00
100/08-12-72-08 W6	720.00	NP	2224.00	2209.00	2199.00	2176.00	2160.00	2156.00	2155.00
100/05-13-72-08 W6	721.70	NP	NP	NP	NP	2174.00	2154.00	2152.00	2151.50
100/08-13-72-08 W6	718.10	NP	2203.50	2187.00	2177.00	2157.00	2141.00	NP	NP
100/14-13-72-08 W6	732.60	NP	NP	NP	NP	2172.00	2158.00	2157.00	2156.00
100/06-14-72-08 W6	747.50	NP	NP	2249.00	2239.00	2218.00	2197.50	2196.00	2191.00
100/08-14-72-08 W6	729.80	NP	NP	NP	NP	2191.00	2169.50	2168.50	2167.00
100/14-14-72-08 W6	754.00	NP	NP	NP	2243.50	2223.00	2201.00	2200.00	2196.50
100/16-14-72-08 W6	735.70	NP	NP	2224.00	2213.50	2194.00	2173.00	2172.00	2170.50
100/06-15-72-08 W6	784.50	2335.00	2316.50	2302.00	2293.00	2268.00	NP	2257.00	2248.00
100/08-15-72-08 W6	756.10	NP	NP	NP	NP	2229.50	2210.00	2209.00	2203.50

WELL LOCATION	KBE (M)	Top Montney	Base PS1	Base PS2	Base PS3	Base PS4	Top PS4	Base PS5	Top PS5
100/16-15-72-08 W6	765.10	2297.00	2278.00	2263.00	2253.00	2232.00	2211.00	2210.00	2205.00
100/06-16-72-08 W6	803.10	NP	2361.00	2347.00	2339.00	2292.00	NP	2285.00	2277.00
100/07-16-72-08 W6	788.50	2353.00	2323.50	2320.00	2312.00	2270.00	NP	2261.00	2251.50
100/10-17-72-08 W6	793.70	2363.00	2342.00	2329.00	2322.00	2295.00	NP	2285.50	2272.00
100/16-20-72-08 W6	752.60	2298.50	2278.00	2265.00	2257.00	2232.00	NP	2225.00	2211.00
100/06-21-72-08 W6	759.50	NP	2283.00	2268.00	2260.00	2220.50	NP	2212.00	2205.00
100/16-21-72-08 W6	751.30	NP	NP	NP	2231.00	2193.00	2177.50	2177.00	2175.00
100/06-22-72-08 W6	769.60	NP	2275.00	2259.50	2246.00	2216.50	NP	NP	2199.50
100/08-22-72-08 W6	751.00	NP	2251.50	2236.00	2225.50	2205.00	2184.00	2183.00	2177.50
100/14-22-72-08 W6	732.60	2246.00	2226.00	2211.00	2201.00	2178.50	2159.00	2158.50	2153.00
100/16-22-72-08 W6	730.40	NP	2223.50	2208.50	2198.00	2175.00	2157.00	2156.00	2154.50
100/06-23-72-08 W6	745.60	2260.00	2241.00	2225.00	2214.50	2192.00	2175.00	2174.00	2173.50
100/08-23-72-08 W6	740.90	2251.00	2232.50	2216.00	2205.00	2183.00	2167.00	2168.50	2165.00
100/14-23-72-08 W6	730.50	2233.00	2213.00	2198.00	2187.00	2165.00	2148.00	NP	NP
100/16-23-72-08 W6	721.60	2220.00	2201.50	2184.50	2173.00	2155.00	2137.00	NP	NP
100/06-24-72-08 W6	739.70	NP	2221.00	2205.00	2194.00	2175.50	2159.00	NP	NP
100/11-24-72-08 W6	738.50	2225.00	2206.00	2189.00	2179.00	2157.00	2143.50	NP	NP
100/06-25-72-08 W6	735.60	NP	NP	2180.00	2168.00	2151.00	2135.00	NP	NP
100/11-25-72-08 W6	722.80	NP	2181.00	2164.00	2152.50	2135.00	2116.00	NP	NP
100/16-25-72-08 W6	694.00	NP	2132.00	2115.00	2102.00	2087.00	2076.00	2072.00	2171.50
100/06-26-72-08 W6	737.00	NP	NP	NP	NP	NP	NP	NP	NP
100/08-26-72-08 W6	747.20	NP	2223.00	2206.00	2195.00	2177.50	2157.50	NP	NP
100/11-26-72-08 W6	739.60	NP	2216.50	2201.00	2190.00	2172.00	2152.00	NP	NP
100/16-26-72-08 W6	741.60	NP	2211.00	2194.00	2183.00	2165.00	2145.00	NP	NP
100/06-27-72-08 W6	719.20	NP	2208.00	2193.00	2183.00	2162.00	2141.50	2140.00	2135.00
100/08-27-72-08 W6	729.90	NP	NP	2196.00	2185.00	2164.00	2146.00	2145.00	2144.50
100/14-27-72-08 W6	714.10	NP	NP	2182.50	2173.50	2142.00	2125.50	2124.00	2120.00
100/16-27-72-08 W6	728.10	NP	NP	2193.00	2182.00	2155.00	2138.00	NP	NP
100/03-28-72-08 W6	744.00	NP	NP	NP	NP	NP	NP	NP	NP
100/04-28-72-08 W6	743.70	NP	2250.00	2235.00	2227.00	2187.50	NP	2179.00	2174.00
100/06-28-72-08 W6	738.80	2253.00	2233.00	2218.50	2210.00	2172.50	NP	2162.00	2158.00

WELL LOCATION	KBE (M)	Top Montney	Base PS1	Base PS2	Base PS3	Base PS4	Top PS4	Base PS5	Top PS5
100/08-28-72-08 W6	738.40	2251.00	2230.00	2216.00	2207.50	2174.00	2157.00	2156.00	2152.50
100/14-28-72-08 W6	730.60	NP	2218.00	2204.00	2194.00	2156.00	NP	2147.00	2140.00
100/16-28-72-08 W6	728.20	2230.00	2209.50	2194.00	2183.50	2149.00	2134.00	2133.00	2129.50
100/16-29-72-08 W6	729.40	2245.00	2223.50	2209.00	2201.50	2179.00	NP	2170.00	2158.00
100/16-30-72-08 W6	748.30	2285.00	2263.00	2251.50	2245.50	2219.00	NP	2210.00	2202.00
100/14-31-72-08 W6		NP	NP	NP	NP	NP	NP	NP	NP
100/16-31-72-08 W6	722.50	NP	NP	NP	NP	2170.50	2145.00	2143.50	2141.00
100/06-32-72-08 W6	722.40	NP	NP	NP	NP	2172.50	2149.50	2148.50	2146.50
100/10-32-72-08 W6	722.00	NP	NP	NP	NP	2170.00	2147.00	NP	NP
100/14-32-72-08 W6	720.60	NP	NP	2191.00	2183.50	2161.50	2140.00	2138.50	2134.40
100/06-33-72-08 W6	727.80	NP	2212.00	2197.00	2186.50	2149.50	2135.00	2134.00	2132.50
100/08-33-72-08 W6	718.00	NP	2195.00	2181.00	2173.00	2136.50	2121.00	2120.00	2116.00
100/14-33-72-08 W6	716.00	NP	2187.00	2172.00	2159.50	2128.00	2112.00	NP	NP
100/16-33-72-08 W6	707.00	NP	NP	2165.00	2157.00	2120.50	2105.00	2104.00	2102.00
100/06-34-72-08 W6	705.10	NP	2178.00	2163.00	2152.00	2117.50	2102.00	NP	NP
100/07-34-72-08 W6	710.80	NP	2182.00	2166.00	2154.50	2133.50	2115.00	NP	NP
100/14-34-72-08 W6	700.40	NP	2161.00	2145.00	2134.00	2107.00	2090.00	NP	NP
100/16-34-72-08 W6	696.40	2172.00	2152.00	2137.50	2128.50	2095.50	2080.00	NP	NP
100/06-35-72-08 W6	694.00	NP	2151.00	2134.50	2123.00	2106.00	2086.00	NP	NP
100/08-35-72-08 W6	693.40	2154.00	2134.00	2117.00	2105.00	2089.00	2070.00	NP	NP
100/10-35-72-08 W6	689.20	NP	2132.50	2116.00	2104.00	2088.00	2069.00	NP	NP
100/14-35-72-08 W6	690.00	2150.00	2129.00	2112.50	2101.00	2084.00	2065.50	NP	NP
100/06-36-72-08 W6	695.50	2153.00	2133.00	2116.50	2104.00	2088.50	2067.00	NP	NP
100/07-36-72-08 W6	688.20	2132.00	2112.00	2095.00	2081.50	2067.00	2054.00	NP	NP
100/11-36-72-08 W6	689.50	NP	2119.00	2103.00	2089.50	2074.50	2055.00	NP	NP
100/16-36-72-08 W6	675.40	NP	2087.00	2070.00	2055.50	2042.00	2030.00	NP	NP
100/08-01-72-09 W6	836.50	2471.00	2457.00	2447.00	2442.50	2417.00	NP	2409.00	2386.50
100/14-02-72-09 W6	933.60	NP	2568.50	2558.50	2555.00	2534.00	NP	2522.00	2500.00
100/06-08-72-09 W6	775.70	2503.00	2491.00	2481.00	2478.00	2460.00	NP	2455.00	NP
100/10-13-72-09 W6	825.40	NP	NP	NP	NP	NP	NP	NP	NP
100/11-29-72-09 W6	775.30	2430.00	2408.00	2401.00	2398.00	NP	NP	NP	NP

WELL LOCATION	KBE (M)	Top Montney	Base PS1	Base PS2	Base PS3	Base PS4	Top PS4	Base PS5	Top PS5
100/10-35-72-09 W6	762.00	NP	2307.00	2297.00	2294.00	2267.00	NP	2251.00	2241.50
100/16-36-72-09 W6	742.00	NP	2260.00	2248.00	2243.00	2217.00	NP	2208.50	2199.00
100/06-02-73-07 W6	685.80	NP	2023.00	2004.00	1980.00	NP	NP	NP	NP
100/11-03-73-07 W6	680.40	2037.00	2019.00	2000.50	1977.00	NP	NP	NP	NP
100/06-06-73-07 W6	688.70	2081.00	2061.00	2043.00	2025.00	2010.00	1998.00	NP	NP
100/01-07-73-07 W6	672.90	NP	NP	NP	2002.00	1981.00	1977.50	NP	NP
100/06-08-73-07 W6	672.70	2054.00	2035.00	2017.00	1994.00	1978.00	1975.00	NP	NP
100/06-15-73-07 W6	701.20	2040.00	2023.00	2004.50	1983.00	NP	NP	NP	NP
100/16-15-73-07 W6	720.50	NP	NP	NP	1999.00	NP	NP	NP	NP
100/10-18-73-07 W6	671.80	NP	NP	NP	NP	NP	NP	NP	NP
102/10-18-73-07 W6	672.20	NP	NP	2007.00	1984.00	1963.00	1962.00	NP	NP
100/11-20-73-07 W6	713.10	2047.00	2030.00	2013.00	1991.00	NP	NP	NP	NP
100/06-21-73-07 W6	726.10	NP	NP	2018.00	1997.00	NP	NP	NP	NP
100/14-22-73-07 W6	740.30	2060.00	2044.00	2025.00	2006.00	NP	NP	NP	NP
100/06-24-73-07 W6	738.40	NP	2023.50	2000.00	1981.00	NP	NP	NP	NP
100/06-30-73-07 W6	713.90	2046.00	2029.00	2011.00	1991.00	NP	NP	NP	NP
100/07-01-73-08 W6	676.00	NP	2081.00	2064.00	2046.00	2035.00	2020.00	NP	NP
100/06-02-73-08 W6	681.80	NP	2108.00	2091.00	2078.00	2062.50	2043.50	2042.00	2041.00
100/07-02-73-08 W6	684.00	NP	2106.50	2090.00	2075.00	2062.00	2041.00	2039.00	2038.00
100/14-02-73-08 W6	678.00	NP	2103.00	2087.00	2073.50	2058.50	2039.00	NP	NP
100/16-02-73-08 W6	676.60	NP	2091.00	2074.00	2060.00	2045.50	2027.00	2026.00	2025.50
100/06-03-73-08 W6	712.70	NP	NP	2150.00	2141.00	2109.00	2092.50	2092.00	2091.00
100/07-03-73-08 W6	702.70	NP	2156.00	2139.00	2128.00	2109.00	2090.00	2089.00	2087.00
100/14-03-73-08 W6	717.40	NP	2155.00	2139.50	2127.00	2098.50	2083.00	NP	NP
100/16-03-73-08 W6	696.20	NP	NP	NP	NP	NP	NP	NP	NP
100/06-04-73-08 W6	713.20	NP	NP	NP	NP	NP	2107.50	2106.50	2104.00
100/08-04-73-08 W6	710.70	NP	2175.00	2160.00	2148.00	2117.50	2102.00	2101.00	2100.00
100/13-04-73-08 W6	719.70	NP	2181.00	2166.00	2157.50	2134.00	2114.00	2113.50	2110.00
100/15-04-73-08 W6	719.30	NP	NP	NP	2155.00	2127.00	2111.00	2108.00	2102.50
100/06-05-73-08 W6	717.10	NP	2194.00	2180.00	2173.00	2151.50	2128.50	2127.50	2124.50
100/07-05-73-08 W6	715.40	NP	2189.00	2175.00	2167.00	2146.50	2123.00	2122.00	2121.00

WELL LOCATION	KBE (M)	Top Montney	Base PS1	Base PS2	Base PS3	Base PS4	Top PS4	Base PS5	Top PS5
100/16-05-73-08 W6	724.70	NP	NP	NP	NP	2142.00	2121.00	2120.00	2117.00
100/08-06-73-08 W6	721.60	NP	NP	NP	NP	2163.50	2140.00	2139.00	2133.50
100/14-06-73-08 W6	726.40	NP	2211.00	2198.50	2192.50	2170.00	NP	2162.00	2152.00
100/16-06-73-08 W6	720.90	NP	NP	NP	NP	2155.00	NP	2145.00	2136.00
100/05-08-73-08 W6	729.30	NP	NP	NP	NP	2146.50	2128.00	2127.00	2125.50
100/08-08-73-08 W6	737.80	NP	NP	2176.50	2165.00	2147.50	2126.00	2125.00	2122.00
100/14-08-73-08 W6	739.50	NP	NP	NP	2163.00	2141.00	2124.00	2123.00	2121.00
100/16-08-73-08 W6	751.90	NP	2191.00	2176.00	2163.00	2148.00	2127.50	2126.50	2121.00
100/06-09-73-08 W6	739.00	NP	NP	NP	NP	NP	NP	2118.00	2114.00
100/07-09-73-08 W6	736.00	NP	NP	2165.00	2153.50	2128.00	2110.00	NP	NP
100/14-09-73-08 W6	NP	NP	NP	NP	NP	NP	NP	NP	NP
100/01-10-73-08 W6	706.20	2153.00	2132.00	2116.00	2102.00	2082.00	2065.00	2064.00	2063.00
100/06-10-73-08 W6	733.40	NP	2162.00	2148.00	2136.50	2108.00	2092.00	NP	NP
100/06-11-73-08 W6	677.10	NP	2085.50	2069.00	2051.50	2035.00	2018.50	NP	NP
100/06-12-73-08 W6	679.50	2085.50	2065.00	2048.00	2030.00	2017.50	2002.50	NP	NP
100/02-14-73-08 W6	698.20	NP	2081.00	2065.50	2048.00	2030.50	2018.00	NP	NP
100/07-15-73-08 W6	703.00	2132.00	2109.00	2094.00	2075.00	2059.00	2043.50	NP	NP
100/06-16-73-08 W6	764.00	NP	2182.00	2168.00	2153.50	2133.00	2118.50	2117.00	2115.00
100/06-17-73-08 W6	752.70	NP	2187.00	2174.00	2161.00	2145.50	2125.00	2124.00	2122.50
100/09-17-73-08 W6	756.90	NP	2178.00	2164.50	2150.00	2135.50	2118.50	2117.00	2111.50
100/11-18-73-08 W6	740.10	NP	2190.00	2177.00	2170.00	2149.00	2127.00	2126.00	2124.50
100/08-19-73-08 W6	749.70	NP	NP	NP	NP	2130.00	2110.50	2109.50	2106.00
100/14-19-73-08 W6	751.00	NP	NP	2152.00	2139.00	2124.00	2104.00	2103.00	2099.50
100/06-20-73-08 W6	753.90	2191.00	2166.00	2152.50	2136.50	2124.50	2105.00	2104.00	2098.00
100/06-21-73-08 W6	759.30	2181.00	2156.50	2143.00	2124.00	2111.00	2095.00	2094.00	2093.00
100/06-22-73-08 W6	733.30	NP	2123.00	2108.50	2087.00	2080.00	2059.00	NP	NP
100/16-23-73-08 W6	721.40	NP	2071.00	2054.50	2033.00	2021.00	2005.00	NP	NP
100/04-24-73-08 W6	712.10	NP	2073.00	2056.50	2035.00	2024.00	2009.00	NP	NP
100/10-26-73-08 W6	733.00	NP	2063.50	2048.00	2028.00	2016.00	2005.00	NP	NP
100/06-28-73-08 W6	743.50	NP	2109.00	2096.00	2076.00	2064.00	2050.50	NP	NP
100/06-29-73-08 W6	764.40	NP	2165.00	2152.00	2133.00	2123.00	2105.00	2104.00	2099.50

WELL LOCATION	KBE (M)	Top Montney	Base PS1	Base PS2	Base PS3	Base PS4	Top PS4	Base PS5	Top PS5
100/10-31-73-08 W6	730.00	2124.00	2098.00	2086.00	2067.50	2055.50	2039.00	2038.00	2032.50
100/07-32-73-08 W6	747.00	2133.00	2108.00	2094.00	2072.00	2061.50	2046.00	2045.50	2042.00
100/14-34-73-08 W6	725.40	NP	NP	NP	NP	NP	NP	NP	NP
100/16-36-73-08 W6	739.10	2051.00	2031.00	2014.50	1998.00	NP	NP	NP	NP
100/14-02-73-09 W6	750.70	NP	2287.00	2275.50	2269.00	2247.00	NP	2237.00	2218.00
100/08-11-73-09 W6	742.90	NP	2249.00	2237.00	2229.00	2209.00	NP	2200.00	2182.00
100/06-12-73-09 W6	735.20	NP	2225.00	2213.00	2202.00	2185.00	NP	2175.00	2162.00
100/06-13-73-09 W6	745.90	NP	2221.00	2210.00	2200.00	2181.00	NP	NP	2158.00
100/14-14-73-09 W6	751.50	NP	2231.50	2221.00	2209.00	2193.00	NP	NP	2161.00
100/06-15-73-09 W6	758.60	NP	2291.00	2281.00	2274.00	2255.00	NP	2237.00	2225.00
100/14-16-73-09 W6	777.20	2340.00	2314.00	2305.00	2302.00	2281.00	NP	NP	NP
100/14-17-73-09 W6	774.00	2355.00	2329.00	2321.00	2318.00	2298.00	NP	2278.00	2258.00
100/06-20-73-09 W6	782.30	NP	2319.00	2311.00	2308.00	2288.00	NP	2273.00	2249.00
100/06-21-73-09 W6	775.80	NP	NP	2282.00	2278.00	2258.00	NP	2250.00	2226.00
100/08-21-73-09 W6	774.80	2304.00	2277.00	2268.00	2262.00	2242.00	NP	2233.00	2210.00
100/14-22-73-09 W6	752.30	NP	2229.00	2220.00	2211.00	2192.50	NP	2183.00	2163.00
100/08-23-73-09 W6	743.60	2229.00	2202.00	2192.00	2180.00	2163.00	NP	NP	2142.00
100/05-28-73-09 W6	765.90	NP	2254.00	2246.00	2242.00	2222.00	NP	2214.00	2186.00
100/10-30-73-09 W6	747.90	NP	NP	2254.00	2252.00	2232.00	NP	2210.00	2195.00
100/06-34-73-09 W6	735.10	NP	2186.00	2176.00	2167.00	2148.00	NP	2136.00	2121.00
100/06-01-74-07 W6	734.00	NP	NP	NP	NP	NP	NP	NP	NP
100/03-03-74-07 W6	740.40	2006.50	1991.50	1967.00	1949.00	NP	NP	NP	NP
100/06-04-74-07 W6	739.70	NP	2002.00	1979.00	NP	NP	NP	NP	NP
100/16-10-74-07 W6	734.10	1976.50	1958.00	1929.00	NP	NP	NP	NP	NP
100/10-11-74-07 W6	749.60	1976.00	1959.00	1927.00	NP	NP	NP	NP	NP
100/06-14-74-07 W6	760.00	1968.00	1951.00	1918.50	NP	NP	NP	NP	NP
100/14-15-74-07 W6	752.90	1978.50	1961.50	1930.00	NP	NP	NP	NP	NP
100/16-16-74-07 W6	758.10	1986.00	1969.00	1939.00	NP	NP	NP	NP	NP
100/02-17-74-07 W6	766.80	2025.00	2007.00	1983.00	1965.00	NP	NP	NP	NP
100/13-17-74-07 W6	789.70	2034.50	2015.50	1992.00	1983.00	NP	NP	NP	NP
100/11-18-74-07 W6	798.40	NP	2026.00	2008.00	1991.00	NP	NP	NP	NP

WELL LOCATION	KBE (M)	Top Montney	Base PS1	Base PS2	Base PS3	Base PS4	Top PS4	Base PS5	Top PS5
100/14-20-74-07 W6	771.50	2011.00	1990.00	1963.00	1949.00	NP	NP	NP	NP
100/08-23-74-07 W6	766.80	NP	1939.00	1905.00	NP	NP	NP	NP	NP
100/07-30-74-07 W6	785.30	2023.50	2001.00	1975.00	1968.50	NP	NP	NP	NP
100/06-32-74-07 W6	832.40	2045.00	2022.00	1991.00	NP	NP	NP	NP	NP
100/06-33-74-07 W6	825.20	2025.00	2003.00	1971.00	NP	NP	NP	NP	NP
100/06-34-74-07 W6	842.20	NP	NP	NP	NP	NP	NP	NP	NP
100/04-01-74-08 W6	749.80	NP	2048.00	2032.00	2015.00	NP	NP	NP	NP
100/10-03-74-08 W6	724.10	2045.00	2022.00	2008.00	1991.00	1977.00	1970.00	NP	NP
100/08-06-74-08 W6	727.50	2106.50	2080.00	2068.00	NP	2024.00	2010.50	2009.50	2006.00
100/11-06-74-08 W6	729.10	2117.00	2089.00	2077.00	NP	2046.00	2029.00	2028.00	2021.00
100/16-06-74-08 W6	726.90	2101.00	2072.00	2060.00	NP	2018.00	2002.00	NP	NP
100/08-07-74-08 W6	727.00	NP	NP	NP	NP	2005.50	1991.00	NP	NP
100/14-07-74-08 W6	732.50	2094.00	2065.50	2054.00	NP	2014.00	2002.00	2001.00	1999.00
100/15-07-74-08 W6	732.70	2090.00	2064.00	2052.00	NP	2010.00	2000.00	1999.00	1996.50
100/06-08-74-08 W6	738.30	2085.00	2058.00	2046.00	2024.00	2015.00	2003.50	2002.50	2002.00
100/06-11-74-08 W6	747.20	NP	2031.00	2016.00	1999.00	NP	NP	NP	NP
100/10-11-74-08 W6	755.00	NP	NP	NP	NP	NP	NP	NP	NP
100/06-12-74-08 W6	755.40	2049.00	2030.00	2013.00	1995.00	NP	NP	NP	NP
100/14-12-74-08 W6	753.20	NP	NP	NP	NP	NP	NP	NP	NP
100/11-13-74-08 W6	771.10	NP	NP	NP	NP	NP	NP	NP	NP
100/06-18-74-08 W6	739.60	2091.00	2062.00	NP	NP	2003.00	1991.00	NP	NP
102/14-18-74-08 W6	738.70	2079.00	2052.00	2042.00	NP	1997.00	1988.50	1987.00	1986.00
100/16-18-74-08 W6	737.90	2072.00	2044.50	2034.00	NP	1987.00	1980.00	NP	NP
100/06-19-74-08 W6	745.30	2072.00	2041.00	2030.50	NP	1984.00	1976.00	NP	NP
100/10-22-74-08 W6	765.50	NP	NP	NP	NP	NP	NP	NP	NP
100/06-25-74-08 W6	797.90	2044.00	2020.00	1996.00	NP	NP	NP	NP	NP
100/11-26-74-08 W6	764.70	2006.00	1980.00	1959.00	1947.00	NP	NP	NP	NP
100/06-28-74-08 W6	740.80	NP	1995.00	1983.50	1955.00	NP	NP	NP	NP
100/10-29-74-08 W6	756.20	NP	NP	NP	NP	NP	NP	NP	NP
100/06-31-74-08 W6	778.40	2074.00	2041.50	2032.00	NP	1993.00	1985.00	NP	NP
100/08-32-74-08 W6	782.90	NP	NP	NP	NP	NP	NP	NP	NP

WELL LOCATION	KBE (M)	Top Montney	Base PS1	Base PS2	Base PS3	Base PS4	Top PS4	Base PS5	Top PS5
100/14-32-74-08 W6	776.50	NP	2014.50	2002.00	1983.00	NP	NP	NP	NP
100/16-32-74-08 W6	773.00	NP	NP	NP	NP	NP	NP	NP	NP
100/08-33-74-08 W6	761.30	NP	1978.00	1960.00	1939.00	NP	NP	NP	NP
100/05-35-74-08 W6	759.20	NP	NP	NP	NP	NP	NP	NP	NP
100/06-06-74-09 W6	733.30	NP	2217.00	2210.00	2205.00	2188.00	NP	2176.00	2151.00
100/10-07-74-09 W6	737.30	NP	2173.00	2167.00	2159.00	2142.00	NP	2134.00	2119.00
100/10-12-74-09 W6	727.00	2108.50	2077.00	2066.50	2046.00	2035.00	2019.00	2018.00	2013.00
100/06-13-74-09 W6	744.60	2114.50	2084.00	2073.50	NP	2042.00	2026.00	2025.00	2020.00
100/06-14-74-09 W6	744.70	2127.00	2094.00	2085.00	2069.00	2054.00	NP	2049.00	2038.00
100/08-17-74-09 W6	748.20	NP	NP	NP	2134.00	2118.00	NP	2112.00	2096.00
100/14-19-74-09 W6	753.10	NP	NP	2144.00	NP	2116.00	NP	2110.00	2094.00
100/07-21-74-09 W6	757.90	NP	2123.00	2116.50	NP	2087.00	NP	2079.00	2065.00
100/10-22-74-09 W6	785.20	NP	2123.00	2118.00	2104.00	2086.00	NP	2081.50	2071.00
100/05-24-74-09 W6	751.00	NP	NP	NP	NP	2028.00	2015.00	2014.00	1010.00
100/11-26-74-09 W6	799.80	NP	NP	NP	NP	2065.00	2051.50	2050.00	2047.00
100/06-27-74-09 W6	796.00	NP	NP	2119.00	2104.00	2087.00	NP	2084.00	2069.00
100/14-29-74-09 W6	755.30	NP	NP	NP	NP	2069.00	NP	2065.00	2048.00
100/09-30-74-09 W6	761.40	NP	NP	2131.00	NP	2100.00	NP	2095.00	2078.00
100/06-31-74-09 W6	768.40	NP	NP	NP	NP	2089.00	NP	2082.50	2074.00
100/06-35-74-09 W6	800.90	NP	NP	NP	NP	2050.00	2038.00	2037.00	2032.00
100/08-36-74-09 W6	771.00	2079.00	2046.00	2037.50	NP	1995.00	2087.00	NP	NP

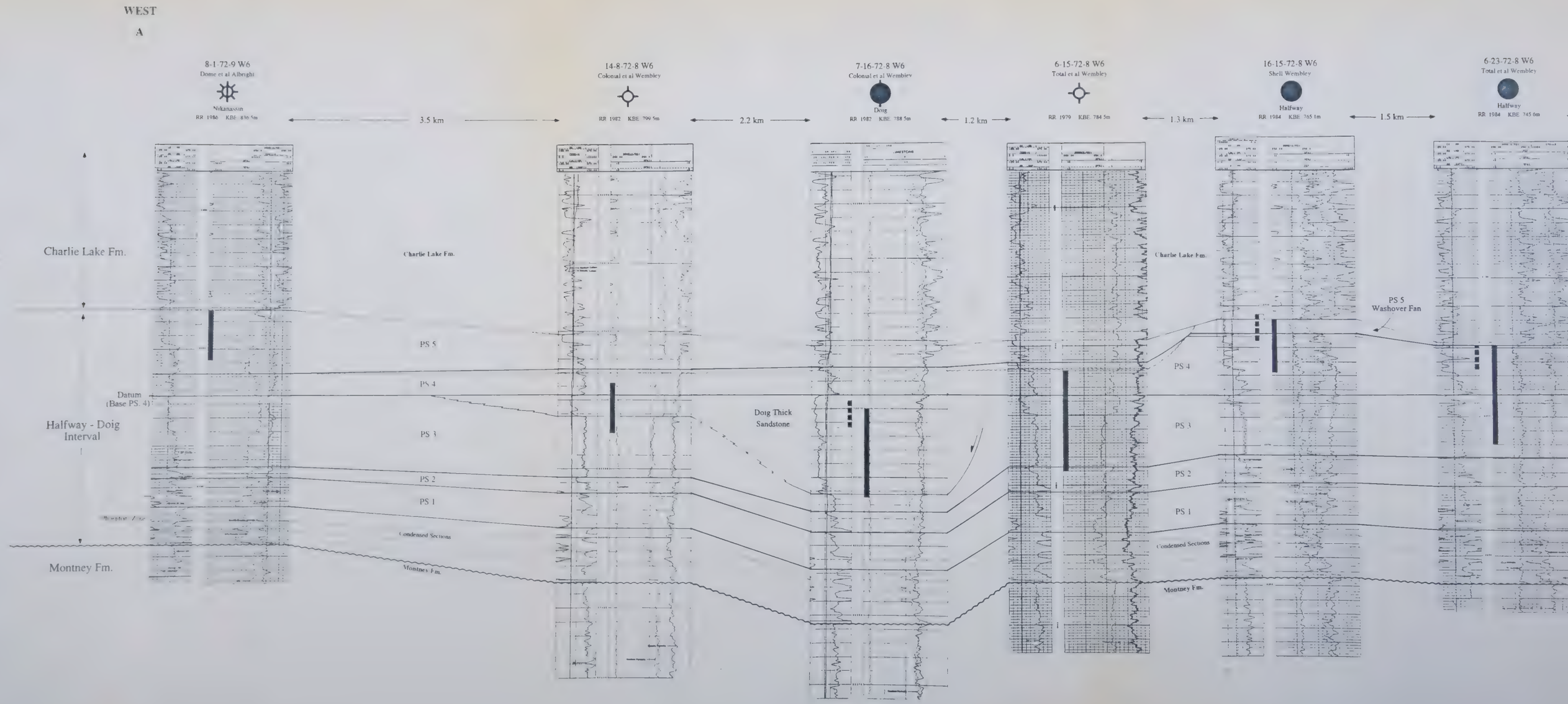
WEST
A
8-1-72-9 W6
Dome et al Albright
Nikanassin
RR 1986 KBE 836.5m
3.5 km
14-8-72-8 W6
Colonial et al Wembley
RR 1982 KBE 799.5m
2.2 km
7-16-72-8 W6
Colonial et al Wembley
Doig
RR 1982 KBE 788.5m
1.2 km
6-15-72-8 W6
Total et al Wembley
RR 1979 KBE 784.5m
1.3 km
16-15-72-8 W6
Shell Wembley
Halfway
RR 1984 KBE 765.1m
1.5 km
6-23-72-8 W6
Total et al Wembley
Halfway
RR 1984 KBE 745.6m
Charlie Lake Fm.
Charlie Lake Fm.
Charlie Lake Fm.
PS 5
PS 4
Datum
(Base PS. 4)
Halfway - Doig
Interval
PS 3
PS 2
PS 1
Condensed Sections
Montney Fm.
Montney Fm.
Doig Thick
Sandstone
PS 5
Washover Fan
PS 4
PS 3
PS 2
PS 1
Condensed Sections
Montney Fm.

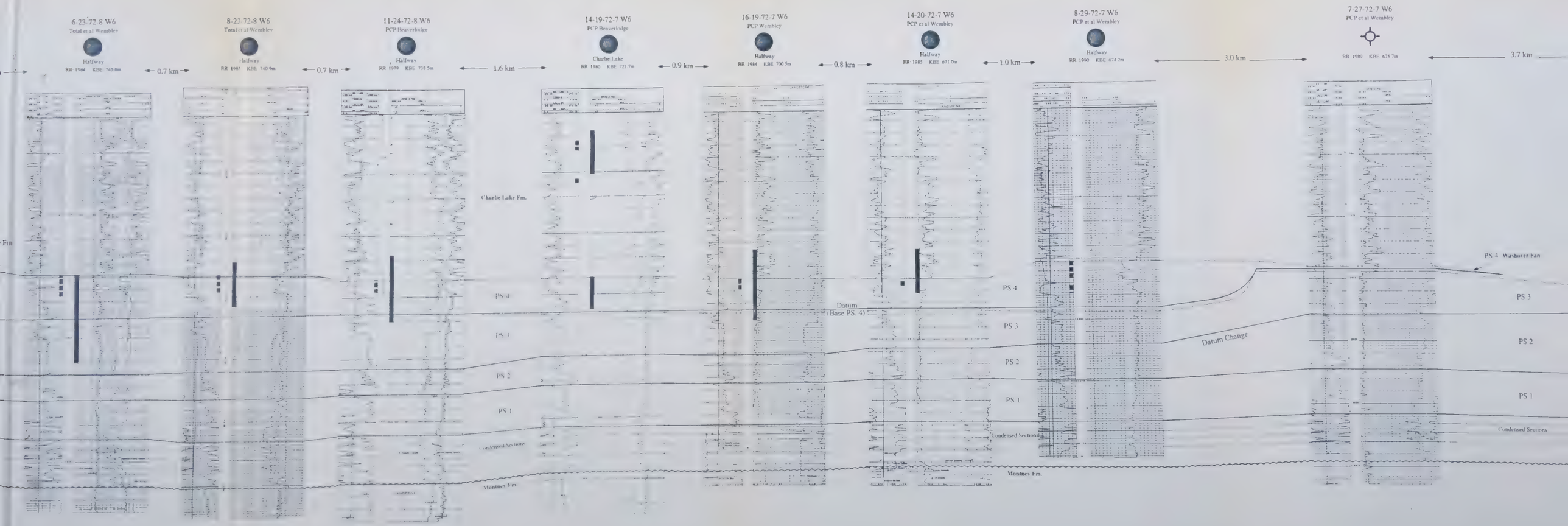
6-23-72-8 W6
Total et al Wembley
Halfway
RR 1984 KBE 745.6m
0.7 km
8-23-72-8 W6
Total et al Wembley
Halfway
RR 1981 KBE 740.9m
0.7 km
11-24-72-8 W6
PCP Beaverlodge
Halfway
RR 1979 KBE 738.5m
1.6 km
14-19-72-7 W6
PCP Beaverlodge
Charlie Lake
RR 1980 KBE 721.7m
0.9 km
16-19-72-7 W6
PCP Wembley
Halfway
RR 1984 KBE 700.5m
0.8 km
14-20-72-7 W6
PCP et al Wembley
Halfway
RR 1985 KBE 671.0m
1.0 km
8-29-72-7 W6
PCP et al Wembley
Halfway
RR 1990 KBE 674.2m
3.0 km
7-27-72-7 W6
PCP et al Wembley
RR 1989 KBE 675.7m
3.7 km
Charlie Lake Fm.
PS 4
PS 3
PS 2
PS 1
Condensed Sections
Montney Fm.
Datum
(Base PS. 4)
Datum Change
PS 4 Washover Fan

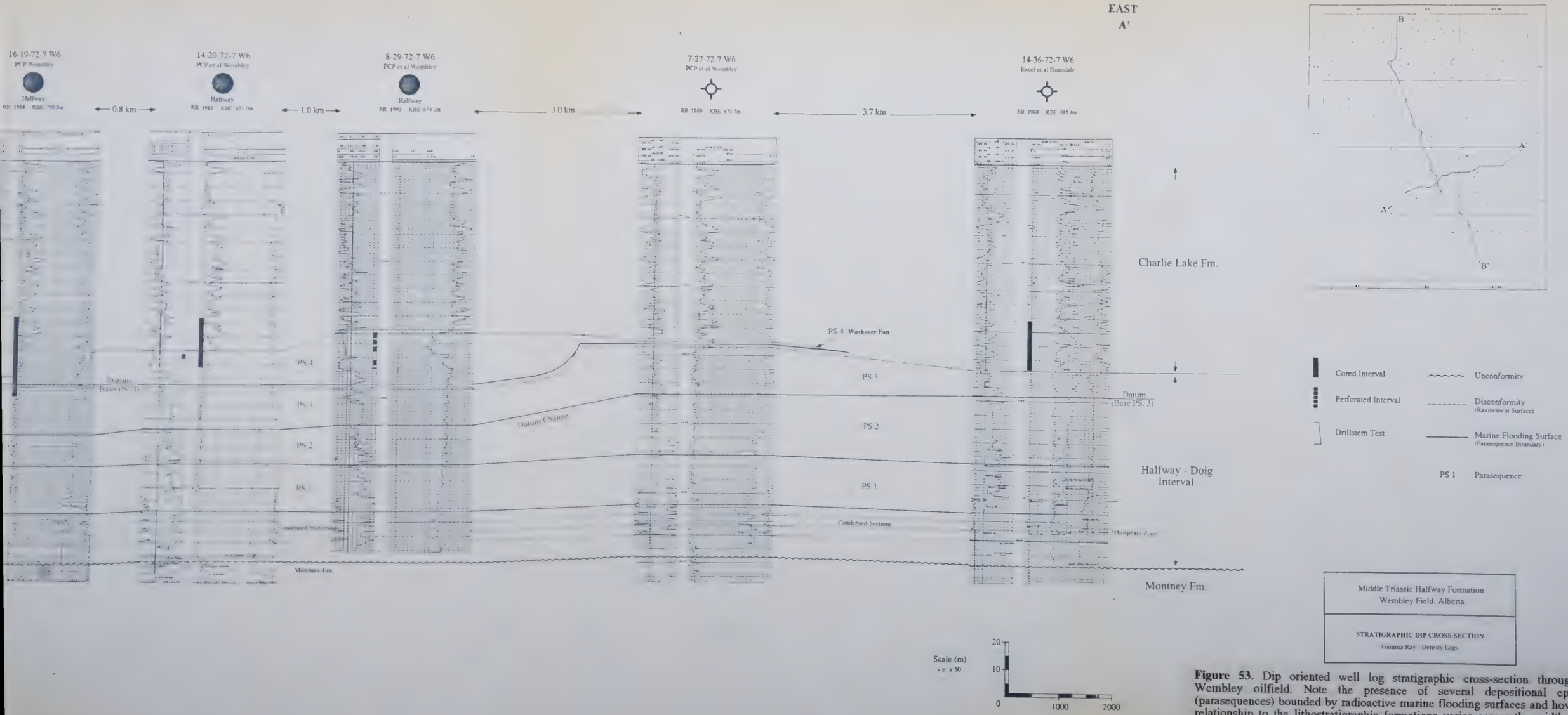

Figure 53. Dip oriented well log stratigraphic cross-section through the Wembley oilfield. Note the presence of several depositional episodes (parasequences) bounded by radioactive marine flooding surfaces and how their relationship to the lithostratigraphic formations varies across the width of the section.

NORTH

B

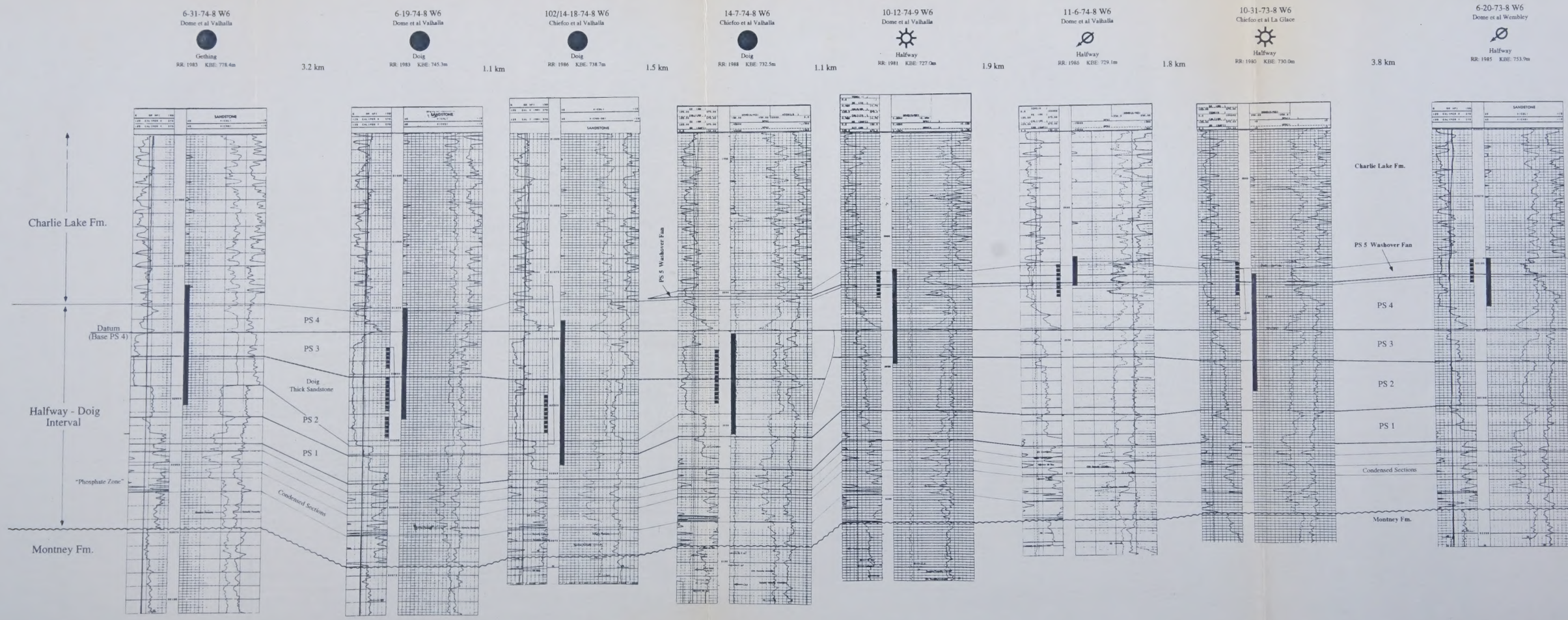
6-31-74-8 W6
Dome et al Valhalla
Gething
RR: 1983 KBE: 778.4m
3.2 km
6-19-74-8 W6
Dome et al Valhalla
Doig
RR: 1983 KBE: 745.3m
1.1 km
102/14-18-74-8 W6
Chiefco et al Valhalla
Doig
RR: 1986 KBE: 738.7m
1.5 km
14-7-74-8 W6
Chiefco et al Valhalla
Doig
RR: 1988 KBE: 732.5m
1.1 km
10-12-74-9 W6
Dome et al Valhalla
Halfway
RR: 1981 KBE: 727.0m
1.9 km
11-6-74-8 W6
Dome et al Valhalla
Halfway
RR: 1986 KBE: 729.1m
1.8 km
10-31-73-8 W6
Chiefco et al La Glace
Halfway
RR: 1980 KBE: 730.0m
3.8 km
6-20-73-8 W6
Dome et al Wembley
Halfway
RR: 1985 KBE: 753.9m
Charlie Lake Fm.
Datum
(Base PS 4)
Halfway - Doig
Interval
"Phosphate Zone"
Montney Fm.
PS 4
PS 3
Doig
Thick Sandstone
PS 2
PS 1
Condensed Sections
PS 5 Washover Fan
Charlie Lake Fm.
PS 5 Washover Fan
PS 4
PS 3
PS 2
PS 1
Condensed Sections
Montney Fm.

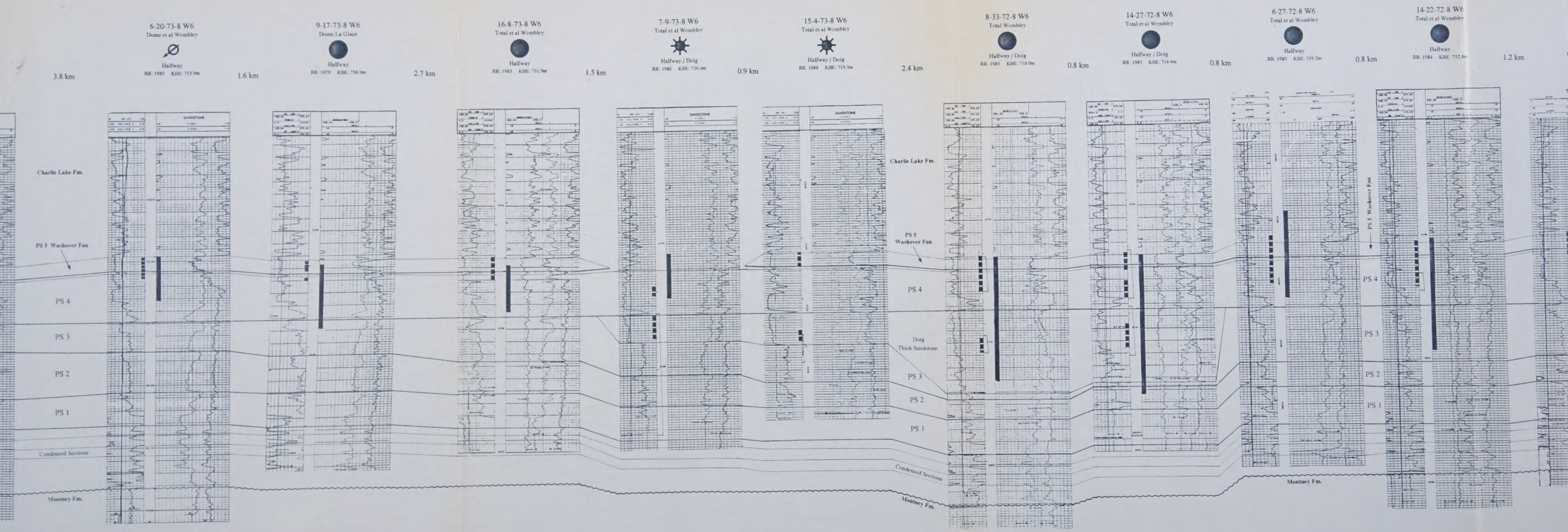
6-20-73-8 W6
Dome et al Wembley
Halfway
RR: 1985 KBE: 753.9m
3.8 km
9-17-73-8 W6
Dome La Glace
Halfway
RR: 1979 KBE: 756.9m
1.6 km
16-8-73-8 W6
Total et al Wembley
Halfway
RR: 1983 KBE: 751.9m
2.7 km
7-9-73-8 W6
Total et al Wembley
Halfway / Doig
RR: 1980 KBE: 736.0m
1.5 km
15-4-73-8 W6
Total et al Wembley
Halfway / Doig
RR: 1988 KBE: 719.3m
0.9 km
8-33-72-8 W6
Total Wembley
Halfway / Doig
RR: 1983 KBE: 718.0m
2.4 km
14-27-72-8 W6
Total et al Wembley
Halfway / Doig
RR: 1983 KBE: 714.4m
0.8 km
6-27-72-8 W6
Total et al Wembley
Halfway
RR: 1983 KBE: 719.2m
0.8 km
14-22-72-8 W6
Total et al Wembley
Halfway
RR: 1984 KBE: 732.6m
1.2 km
SANDSTONE
Charlie Lake Fm.
PS 5 Washover Fan
PS 4
PS 3
PS 2
PS 1
Condensed Sections
Montney Fm.
Doig Thick Sandstone

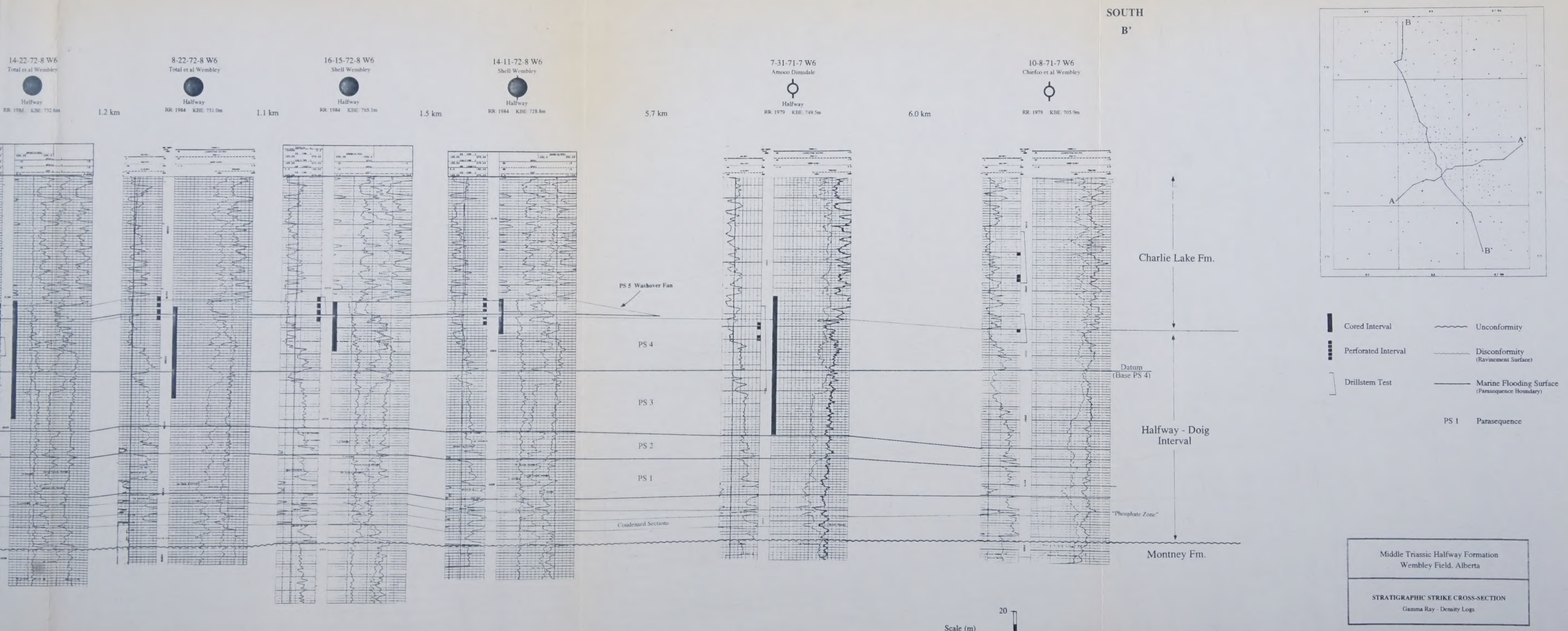

Figure 59. Strike oriented well log stratigraphic cross-section through the Middle Triassic section of the Wembley oilfield. Note the lateral variation in parasequence thickness and the different ages of the thick "Doig" sandstone bodies in the Valhalla and Wembley fields.

EAST
A'

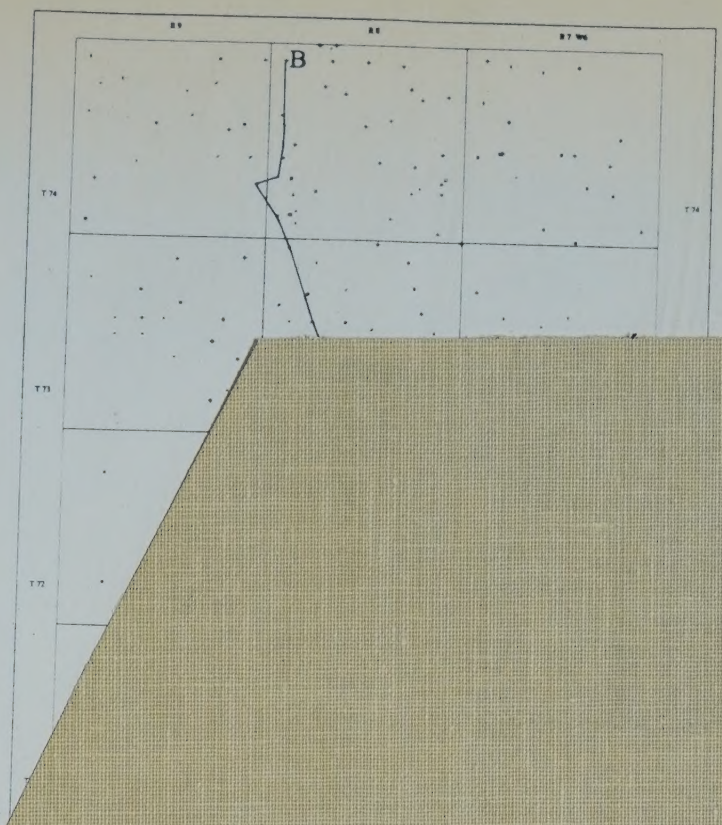

Charlie Lake Fm.

Datum
Base PS. 3)

Halfway - Doig
Interval

hosphate Zone"

Montney Fm.

Figure 5
Wembley
(parasequ
relationsh
section.